UNIVERSITY OF SHEFFIELD

Department of Civil and Structural Engineering

THE BEHAVIOUR OF STEEL AND COMPOSITE BEAM-TO-COLUMN CONNECTIONS IN FIRE

by

Khalifa Saif Al-Jabri

A thesis submitted in partial fulfilment of the requirement for the Degree of Doctor of Philosophy

December 1999

ABSTRACT

Recent fire tests on the Cardington full-scale test frame and observations from real fires have demonstrated the significance of connections in fire, when they can have beneficial effects on the survival time of the structure. The lack of experimental data on the behaviour of steel and composite connections in fire means that this is insufficiently addressed in current design codes and also limits the effective use of numerical models. However, recent experimental tests on small-scale specimens have shown that it is possible to derive accurately the moment-rotation relationships at elevated temperature and have established the principles by which this could be achieved.

In order to extend the scope to include further parameters, five series of tests have been carried out in a portable connection furnace at the Building Research Establishment. The test series includes flush and flexible end-plate bare-steel connections, and flexible end-plate composite connections. The testing procedure and the resulting behaviour are described. The fire test temperature profiles across the connections are detailed and the connection failure mechanisms are discussed. From the test results, moment-rotation-temperature curves for different connection types are derived. The degradation of connection characteristics is compared with that of structural steel. The experimental behaviour is also compared with the results obtained from an existing finite element analysis developed to model connection response in fire conditions.

The experimentally derived connection characteristics have been incorporated within a parametric study of a typical sub-frame, to study the effect of connection type, end-plate thickness, concrete strength, load ratio, and connection temperature. Analysis is extended to a three-dimensional sub-frame.

The patterns of behaviour observed in the connection tests is compared with that of the connections in the large-scale fire tests on the composite building at BRE's Cardington laboratory.

Based on knowledge about the behaviour of connections at elevated temperature, a component-based model is developed for the elevated temperature response for flexible end-plate connections, both as bare-steel and composite. This is based on the response of constitutive parts of connection. The model is easy to use, and capable of modelling the entire non-linear range of connection behaviour. The predicted response is compared with that recorded experimentally.

TABLE OF CONTENTS

LIST OF FIGURES

LIST OF TABLES

ACKNOWLEDGEMENTS

The author expresses his sincere thanks to Dr. Ian Burgess and Prof. Roger Plank for their supervision and support during this research project. The financial support of the Government of the Sultanate of Oman (Sultan Qaboos University) and the Department of the Environment under a Partners in Technology Award are gratefully acknowledged.

My special thanks to Tom Lennon and David Moore and staff at the Building Research Establishment for their advice, comment and continued commitment of time and resources in the development of experimental program. Also Dr. Timothy Liu is thanked for his co-operation. The beams and column sections from which test specimens were fabricated were generously provided by British Steel plc.

Finally I would like to express my sincere thanks and gratitude to all members of my family for their patience, encouragement and support especially to my wife and children: *Fatima* and *Saif*, who 'ran away' when I was in real need of them.

DECLARATION

Except where specific reference has been made to the work of others, this thesis is the result of my own work. No part of it has been submitted to any other University for a degree, diploma or other qualification.

Khalifa Al-Jabri

1 INTRODUCTION AND CONNECTION BEHAVIOUR

1.1 GENERAL INTRODUCTION

Steel has become one of the most popular construction materials for both low and high rise buildings, and its structural properties such as high strength and ductility, offer distinct advantages when compared with concrete[1]. Fast erection speed, long spans, elegance and adaptability are other features which make steel a popular structural material. In 1997 nearly 58% of all multi-storey structures and some 95% of the frames for single storey industrial buildings in the UK were steel framed[2].

Steel however is seriously affected by fire, losing strength and stiffness leading to large deformations and often collapse. This has highlighted the need to understand the behaviour of structural elements in fire conditions. Interest in the elevated temperature performance of building elements started in the late nineteenth century[3] following major structural failures resulting from fire. Research then was focused on devising new materials and methods to protect the structural members from reaching the critical failure temperature and thus enhancing their performance during the required fire duration. This has resulted in different forms of fire insulating materials for coating, painting, spraying or encasing structural members. Until recently this was the common method for protecting the structure from high temperatures. However, the application of protection materials increases the overall cost of the structure by up to 30%[4]. Also there are secondary costs associated with time delays because the application of fire protection may hinder the progress of construction[5]. This offsets many of the advantages associated with steel-framed construction.

From an engineering point of view it is more logical to design the structure to withstand fire without protection rather than designing the structure for normal condition and then applying protection. Therefore in recent years there has been much interest in understanding the response of different structural elements under fire conditions either in isolation or as a part of a more complete structure. This facilitates the development of new engineering methods of analysis and design taking into account any inherent fire resistance of the structural steel, reducing protection costs and construction time, and simplifying the construction process[6]. This has caused the cost of protection material to be cut by half[7] and the market share of steel framed construction in the UK to double from under 30% to over 60% since the early 1980's[8].

Beam-to-column connections are one of the structural elements which were found to be of great significance in enhancing structural behaviour at ambient temperature and even more at elevated temperatures. Observations from a damaged structure[9] confirm that connections have a considerable effect on the survival time of structural members in fire through their ability to redistribute forces. In order to take advantage of this it is necessary to assess the influence of connection rigidity on the response of structural members. This may then lead to improvements in design methods as well as providing raw data for developing numerical models. If the fire protection to beams could be reduced or eliminated, for example by relying on the inherent continuity of steelwork connections, estimated savings of up to £75 million annually could be made throughout Europe[10].

1.2 SEMI-RIGID BEAM-TO-COLUMN CONNECTIONS

The word 'connection' refers to the structural steel components which mechanically fasten the members within the structure. Such components include the bolts, end-plate, web and flanges of beams and columns. Traditionally the design of steel framed structures assumes that the actual behaviour between the beam and the column is either rigid (implying complete rotational continuity) or pinned (implying no moment resistance)[4,11]. However studies have revealed that in reality the actual connection behaviour exhibits characteristics over a wide spectrum between these two limits. For instance most connections regarded as pinned possess some rotational stiffness whilst rigid connections display some flexibility. Therefore, it might be more rational to categorise most connections as "semi-rigid" with pinned and rigid considered as extreme cases. Incorporating 'semi-rigid' connections in the design of steel framed structures has the benefit of transferring moments from the beams to the supporting columns leading to lighter beams. The effect of connection rigidity on the beam response is shown in Fig. 1.1.

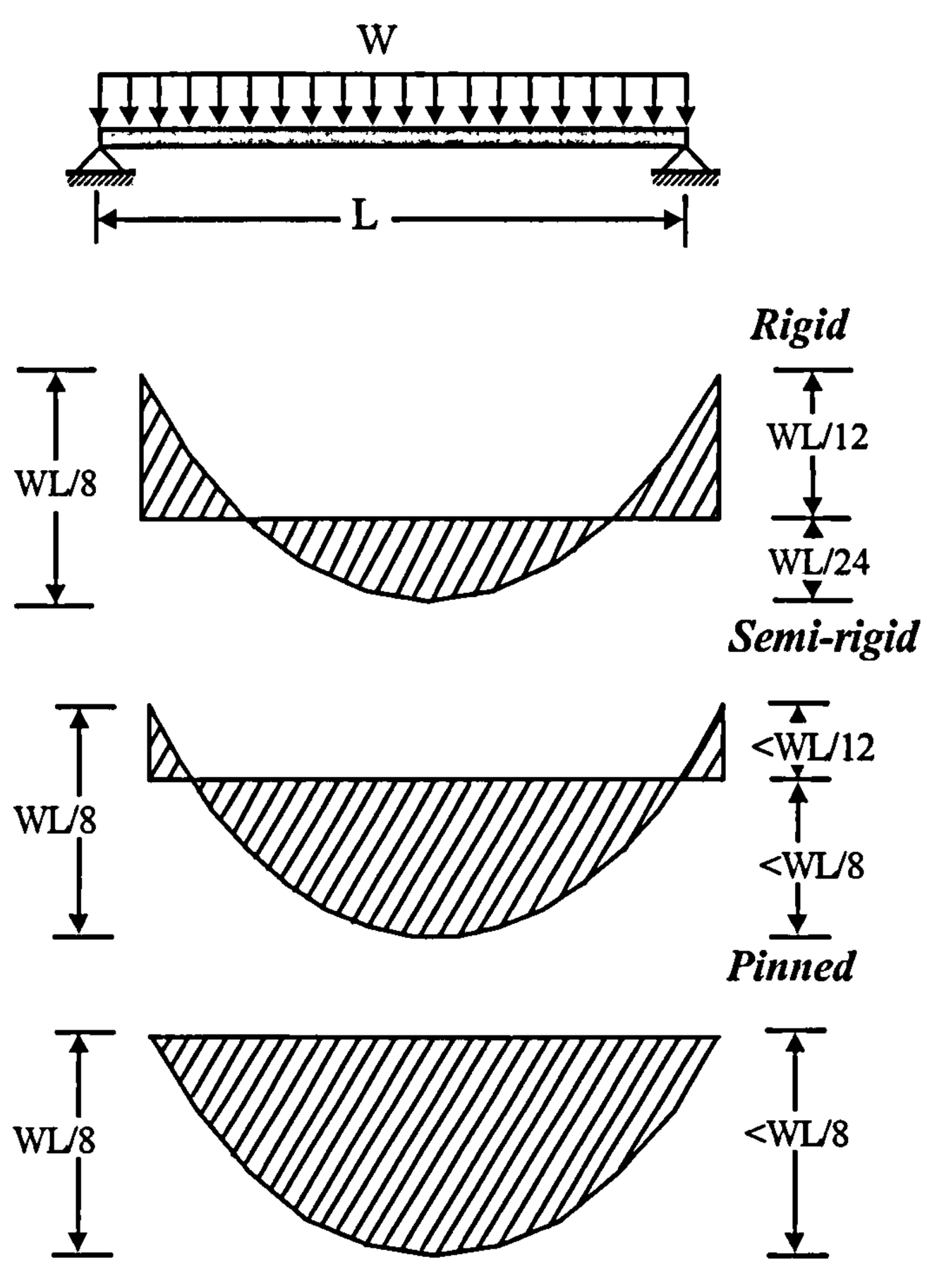

Figure 1.1: Effect of Connection Characteristics on Beam Behaviour

The primary function of a connection is to facilitate transfer of forces and moments between the individual structural members. These forces can take different forms, which may include, in the case of beam-to-column connections, bending moments, shearing and axial forces and torsion. The rotational behaviour of the connections is the

most important parameter that determines the properties of the beam-to-column connections and can have a significant influence on the structural frame response[12]. Other forces may be assumed to have an insignificant effect on the frame behaviour since the axial and shearing deformations have only a small influence in comparison with the rotational deformation. The basic requirement for a connection is to have sufficient strength and stiffness to transmit forces safely between elements within the structure. All connection components should be able to resist the applied loads and possess adequate stiffness to prevent excessive deformation and slip.

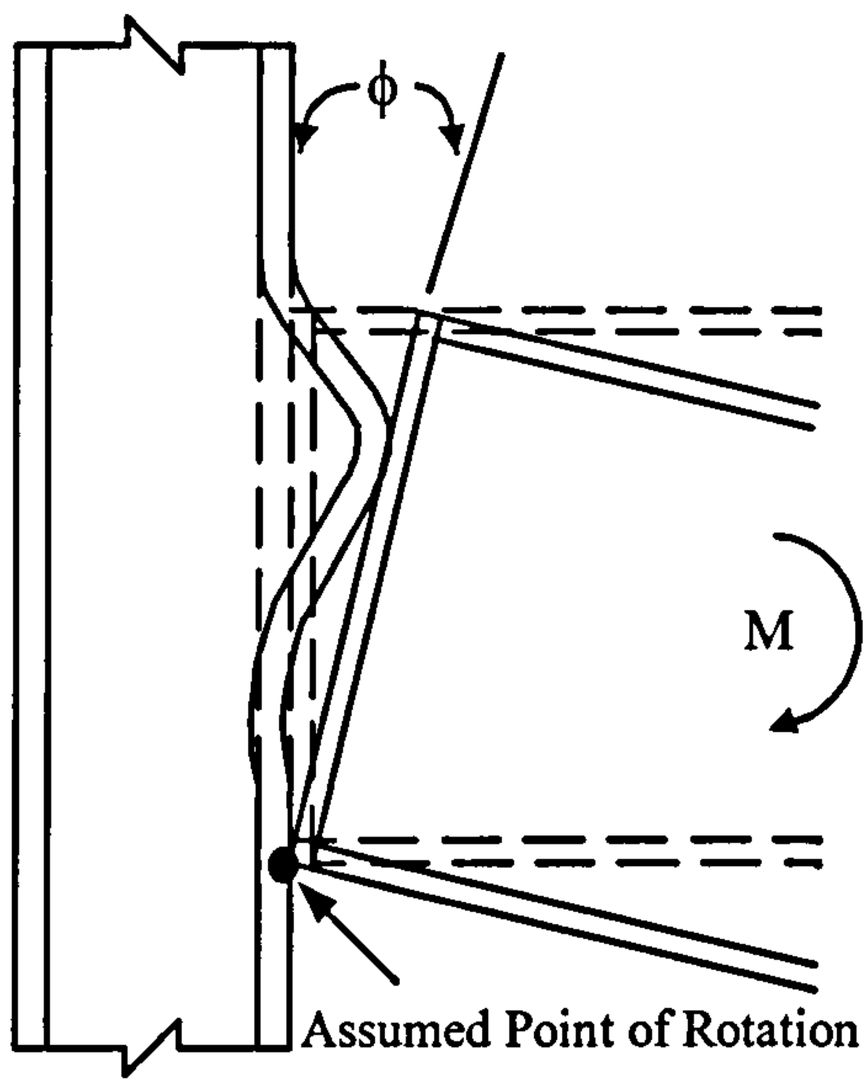

Figure 1.2: Rotational Deformation of a Connection

The rotational characteristics of a connection are usually represented by a moment-rotation relationship. When loads are applied to the connection, a moment *'M'* is induced causing the connection to undergo a rotation *'ϕ'*. This rotation is the change in the angle of the end of the beam and the mating column face as shown in Fig. 1.2. By establishing the moment-rotation characteristics of a connection, the main properties such as strength and stiffness are defined. Experimental testing[13] is the most reliable method of determining accurately connection moment-rotation characteristics.

Various forms of connection are commonly used in the construction industry, the most popular being end-plate, fin-plate, and cleated connections. Selecting suitable and cost effective connections is a complicated decision governed by many factors. Some of these include fabrication costs, ease of transportation and fitting, the capability of the connection to resist the applied loads and the erection time. End-plate connections include extended, flush and flexible end plates, whilst cleated connections include flange cleats, web cleats and a combination of these. The characteristics of these connections can vary considerably from almost pinned to nearly rigid. Depending on the basic use of the connections, they may be further sub-divided into the following categories:

- Moment connections which are designed to resist both bending moments and shear forces; they are mainly used in large span portal frames and in low rise buildings but rarely used in modern high rise commercial buildings.

- Simple shear-resisting pinned connections are widely used in modern steel and composite framed multi-storey buildings in which lateral forces are resisted by vertical bracing and shear walls. This avoids the complexities associated with semi-rigid design and difficulties in defining the moment-rotation behaviour of the connections[14].

Fig. 1.3 illustrates the most popular connections together with an indication of their moment-rotation characteristics.

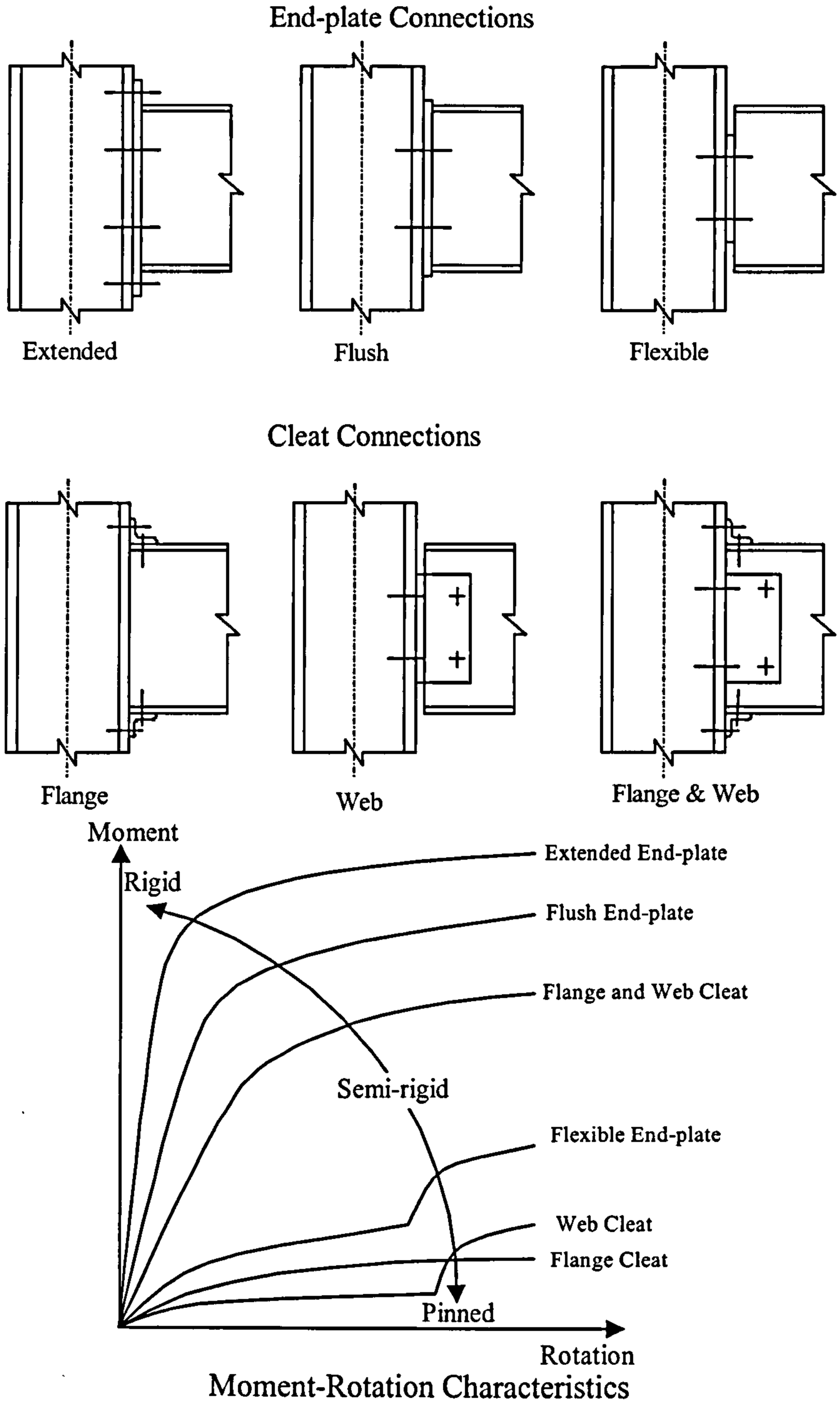

Figure 1.3: Connection Types and Their Moment-Rotation Characteristics

The mechanical properties of the connection are enhanced by casting a concrete slab over the connected beams and connections. The resulting system can be described as a composite construction. In order to ensure that the composite system performs satisfactorily, no slip should be allowed at the interface between the connection and the concrete slab. This can be achieved by the use of shear studs which are welded or shot fired to the steel beam and embedded in the concrete slab. Composite construction offers enhanced stiffness and higher strength allowing the use of shallower sections and so reducing the height of the structure. This can lead to further savings, for example in the cost of cladding, or the provision of more space for services. It has been estimated that savings in steel when using composite construction could reach up to 50% compared with the use of non-composite systems[15,16].

The most important factors that determine the rigidity of common types of connection are summarised as follows:

1. Depth and length of the connected beams;
2. Type and size of fasteners;
3. Whether connected to a column web or column flange;
4. Physical properties of end-plates, members and fastener materials;
5. Beam and column contact during deformation;
6. Position of end-plate (in some connection types);
7. Size of the composite slab;
8. No. of shear connectors and the degree of interaction;

Developing an understanding of connection response is complicated by the wide variety of connection types. However there have been recent moves towards standardisation of the design and detailing of connections[17]. Connection tests can be cumbersome, expensive and time consuming. Some research has therefore been directed towards developing numerical methods for predicting connection response, using test results for validation. These methods range from extrapolation from existing test results to sophisticated finite element analysis as well as models based on the component method concept.

1.3 BEHAVIOUR OF CONNECTIONS AT ELEVATED TEMPERATURES

Modern steel and composite framed buildings are normally designed with simple shear resisting connections and lateral forces are resisted by vertical bracing and shear walls. At ambient temperature, even simple connections can resist significant moments, albeit at large deformations. Recent fire tests on the Cardington full-scale test frame[18] and observations from real fires[9] have demonstrated the significance of connections in fire in improving the survival time of the structure. In fire, beams are allowed to deform significantly more than under normal conditions provided that they maintain sufficient load-carrying capacity. The forces generated from the heated beams are transferred to the adjacent cold structures via the connections, leading to an enhancement in the beam performance in fire as illustrated in Fig. 1.4.

Also, connections tend to heat up slower than the material within the span of the beam due to their relative massivity and shielded location. This allows the development of

higher moments within the connections leading to a reduction in the effective load ratio and hence the amount of fire protection required.

BS5950: Part 8[19] gives no guidance on the design of beam-to-column connections under fire conditions, assuming the connection to have the same properties as used in the design at ambient temperature. That is a connection, which is assumed to be pinned at ambient temperature is assumed to behave in a similar manner at elevated temperatures.

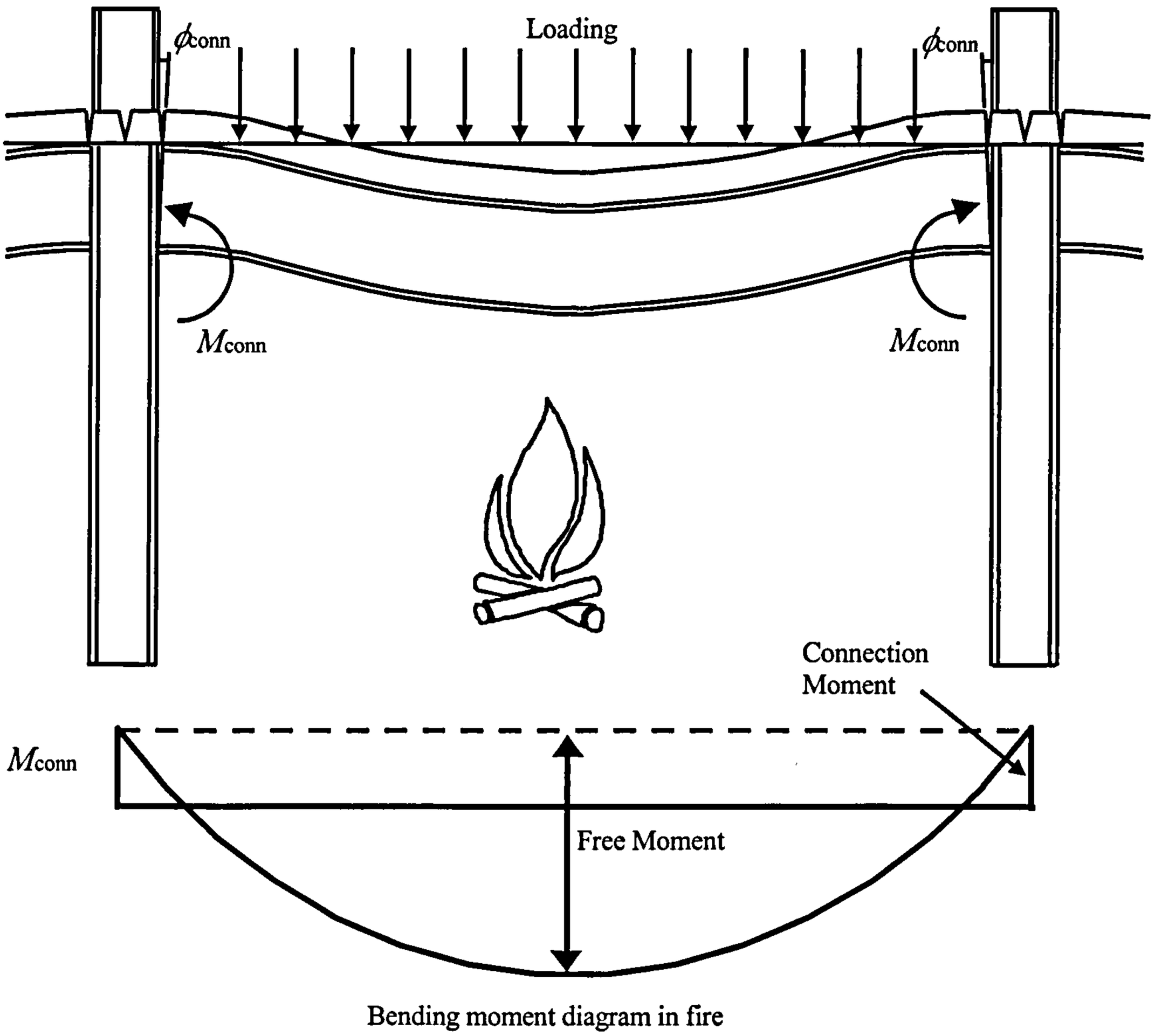

Bending moment diagram in fire

Figure 1.4: Behaviour of Beam in Fire Conditions

1.4 DEVELOPMENTS IN RESEARCH INTO THE BEHAVIOUR OF BARE STEEL AND COMPOSITE BEAM-TO-COLUMN CONNECTIONS AT AMBIENT AND ELEVATED TEMPERATURES

In 1917 connection behaviour was first studied by Wilson and Moore[20] who carried out tests to establish the rigidity of riveted joints in steel structures. Research into connection behaviour progressed slowly until the early 1970's when the potential benefit of connection rigidity in framed structures was realised[21]. In 1983, Jones *et al* [22] reviewed the available test data obtained by many researchers concerning the performance of semi-rigid connections and pointed out the need for further

investigations into the effect of semi-rigid end restraint on the behaviour of individual beam-column members and complete frames.

Since then extensive experimental work, literature reviews and data banks have been published by Nethercot[23,24], Anderson *et al.*[25], Davison *et al*[26,27], Chen[28,29], Chen and Kishi[30,31,32], Xia and Nethercot[33], Aggarwal[34] and Xiao *et al*[35]. A number of books have also been publised[36,37,38] reviewing the recent advances in the performance of various types of structural connections and their influence on the behaviour of isolated structural elements as well as complete structural frames. These advances have resulted in considerable improvements in design codes.

The current UK code for steel design, BS 5950: Part 1[39] provides general guidelines to ensure that the connection satisfies the ultimate limit state design criteria without defining any method for determining the connection stiffness or capacity. However in the European Code, EC3[40] the connection response is considered in much more detail and presented in Annex J. The 'component' approach is adopted in which the behaviour of each component of the connection is determined individually. The overall connection response is then determined by superimposing the behaviour of these components.

To take advantage of the more recent developments in connection design, a number of connection design guides have recently been published dealing with the design of simple[41,42], moment[43] and composite connections[44]. These guides provide a simplified design procedure covering the various forms of connection which are widely used in practice.

In recent years there have been many investigations into the behaviour of structural members at elevated temperatures either in isolation or as part of a frame. Nevertheless, very few studies have been reported on the elevated temperature performance of steel and composite beam-to-column connections. This is mainly due to the high expense associated with connection testing and limitations of existing furnaces. The first experimental fire tests on connections were conducted by CTICM[45] in 1976 with six connection types ranging from "flexible" to "rigid". The primary purpose of these tests was to investigate the performance of high strength bolts at elevated temperatures, and no indication of the performance of the connections was reported. Although a concrete slab was cast over the top flange of the beam to provide a heat sink, composite action was not taken into account. The results suggested that the gross deformation of the other elements preceded failure of the bolts. Two tests were carried out by British Steel in 1982[46] on a "rigid" moment resisting connection. Despite the limited results obtained, it was concluded that connection elements can suffer significant deformation in fire.

The first tests to measure the behaviour of beam-to-column connections at elevated temperatures were carried out by Lawson[47]. The aim of the programme was to develop a design approach for steel beams taking the rotational restraint provided by the connections into consideration. Five of these tests were on non-composite beams, two on composite beams and one on a shelf angle floor beam. Three types of typical connections were studied. These were an extended end-plate, a flush end-plate and a double sided web cleat. The tests demonstrated the robustness of these connections in fire and showed that significant moments (up to two thirds of their ambient temperature

design moment capacity) could be sustained in fire conditions. Lawson noted that the bolts were not susceptible to premature failure, and that the rotation of the connections in all tests exceeded 6° which is consistent with the deflection of beams in standard fire tests. In addition, he suggested that composite action in fire contributed to an enhanced moment capacity of connections which could be estimated by adding the moment capacities of the bare-steel connection and the reinforced concrete slab. Lawson proposed simple rules for designing simply supported beams in fire taking into account the moment transferred via connections in fire conditions[48]. However the tests results provided insufficient data to describe the moment-rotation characteristics of the connections.

The most recent connection tests have been conducted by Leston-Jones *et al.*[49,50,51,52] to develop moment-rotation relationships for flush end-plate connections at elevated temperatures. Eleven tests were carried out on small-scale specimens, including two tests at ambient temperature, for both bare-steel and composite connections. It was observed that both the stiffness and moment capacity of the connection decreased with increasing temperature with a significant reduction in capacity for temperatures in the range of 500°C to 600°C. For the first time, a number of moment-rotation curves at different temperatures were derived, describing the full connection response at elevated temperature.

Studying connection behaviour at elevated temperature is much more complicated than at ambient temperature. This is largely because a number of tests must be conducted, either isothermally or anisothermally, on identical specimens in order to define the moment-rotation-temperature characteristics. Unfortunately, the majority of the experimental tests performed so far have been conducted on single specimens under transient state conditions and this does not give a full description of connection behaviour as required for the numerical analysis of framed structures.

1.5 SCOPE OF RESEARCH

In recent years significant developments have been made in analysing the behaviour of steel-framed structures at elevated temperatures. These have demonstrated the significance of connections in enhancing the performance of structures under fire conditions. The current lack of experimental data on the behaviour of connections means that this is not properly addressed in current design codes. It also limits the effective use of numerical models, since the degradation of the connections at elevated temperatures has to be based on empirical relationships postulated either from ambient temperature tests or from very small amount of elevated temperature data. However, recent experimental tests on small-scale specimens[52] have shown that it is possible to derive accurately moment-rotation relationships at elevated temperatures.

The main aim of this study is to establish full moment-rotation-temperature characteristics for typical bare-steel and composite connections, and to investigate the influence of connection characteristics on frame behaviour at elevated temperatures. The connections studied have been selected as being typical of those used in the UK[53] and designed as simple shear-resisting connections. Part of the work presented in this thesis follows on from the programme of tests conducted by Leston-Jones[52] who developed an experimental methodology for structural furnace testing of beam-to-

column connections, and conducted a series of tests on small flush end-plate joints. Leston-Jones investigated the behaviour of connections within the lower range of available section sizes (254x102UB22 connected to a 152x152UC23 by a full-depth end-plate connection) using both bare-steel and composite specimens. The present work extends the scope to study the influence of parameters such member size, and connection type, and investigates different failure mechanisms. In total twenty tests in five different configurations have been conducted so that a series of load levels can be applied for each detail. The configurations tested include three which were typical of those used in the experimental composite-framed building at Cardington in which a series of large-scale fire tests was performed during 1995 and 1996.

The results from such tests will be of great value to other researchers, especially those developing numerical modelling approaches to the behaviour of steel and composite structures in fire. Also it will allow direct comparison between the behaviour of connections when tested in isolation with those forming part of a structure. Therefore it is necessary to understand the elevated temperature response by means of testing over the complete moment-rotation-temperature range. The primary goal of this investigation is to derive characteristics for typical connections and not to devise joints that are capable of improving the structural response of frames under fire conditions.

1.6 THESIS LAYOUT

The thesis consists of eight chapters as described below:

The first part of Chapter 2 reviews briefly the stages of fire growth and the building fire regulations. The second part considers the effect of elevated temperature on the mechanical properties of the structural materials and connecting elements which are widely used in the construction of steel frames including structural steel, concrete, bolts, reinforcing steel and shear connectors.

Chapter 3 describes the test procedure and results for three series of tests conducted to establish the moment-rotation-temperature relationships for two flush and one flexible end-plate bare-steel connections. The temperature profile across the connection, its behaviour and the observed failure modes of the connections are discussed.

Chapter 4 describes two more series of tests conducted on flexible end-plate composite connections typical to those used in the Cardington Large Building Testing Facility (LBTF). As for bare-steel connection tests the observed failure mechanism of the connections and the temperature profile across the connections are discussed. The enhancement provided by the composite slab on the connection survival is also considered.

Chapter 5 is divided into three sections in which the first section compares the high temperature degradation of the connection properties with those of the basic materials as specified in design codes. The second section deals with the representation of connection characteristics in a form suitable for incorporation within numerical models. The last section reviews finite-element models for connections at both normal and fire conditions. Comparison is made between the experimental connection test results and results obtained from a finite-element model developed at the University of Manchester.

In Chapter 6 parametric studies to investigate the influence of connection characteristics on frame behaviour at elevated temperatures are described. Various parameters were considered such as connection type and end-plate thickness, connection temperature, load ratio and concrete strength. The analyses were carried out utilising existing finite-element software developed at the University of Sheffield[54]. The analysis is extended in the second section to consider a large-scale frame representing the Cardington LBTF. The third section of Chapter 6 compares the behaviour observed in the Cardington full-scale frame with observations from isolated connection tests.

In Chapter 7 a simple component-based model capable of defining the complete range of connection response is presented. Both bare-steel and composite flexible end-plate connections are considered. Comparison is made between the results obtained from the proposed model and those from the connection tests presented in Chapters 3 and 4.

Finally, general conclusions and recommendations for future work are presented in Chapter 8.

2 FIRE ENGINEERING APPROACH AND ELEVATED TEMPERATURE MATERIAL PROPERTIES

Since the discovery of fire mankind realised its power and began to search for sensible ways to minimise its occurrence and the destruction, which it might cause. The risk of fire exists in every building and it is accepted that complete safety from fire is impossible. Fire statistics[55] within the UK reveal that in 1996 there were over 17000 injuries and nearly 800 deaths caused by fire. Beside loss of life, there is an estimated cost of at least £220 million each year in damage to property.

Fire safety regulations for buildings have two main objectives[56]:

- to reduce the loss of life and ensure the safety of the occupants and those in the neighbourhood of building fires;
- to minimise the financial loss both in the property and its neighbourhood.

Fire precautions have been introduced to meet these objectives. These can be classified into two categories as defined in BS4422: Part 5[57]:

- *fire prevention:* 'the concept of preventing the outbreak of fire or reducing the risk of fire spreading and avoiding danger from fire to persons or property'.

- *fire protection:* 'the design features, systems or equipment within a building, to reduce danger to persons and property by detecting, extinguishing or containing fire'. This comprises both *active* and *passive* measures; the former is the process of fire detection and extinction, whilst the latter covers means of escape and structural fire protection, designed to minimise the damage to the structure.

From a structural point of view, 'passive' fire protection is the main concern. Building Regulations[58] specify that, in the event of fire, the structural integrity should be maintained for a certain period. At present the most popular method of providing structural fire protection for steel-framed structures is to use some form of insulating material, with the prime purpose of limiting the temperature of the steel so that adequate strength is retained. However more recent design methods have been proposed for calculating the inherent period of fire resistance of the steel[19,59]. These were developed largely on the basis of experimental studies on isolated members. More recent large-scale fire tests[18] have demonstrated that the fire resistance of whole structures is greater than for isolated elements. Therefore, there is a move to refine existing methods and constructional forms to take advantage of the interaction between members, providing a more rational design approach.

2.1 DEVELOPMENT OF A FIRE

In order to study structural behaviour in fire it is necessary to understand the growth of fire. For fire to occur three components must be present: these are ignition source, fuel source and oxygen which together are called the fire triangle. Fire is a very complicated phenomenon, being governed by the surrounding environment and fuel load. A

compartment fire is generally simplified as having three distinct phases: the ignition (or growth), steady-state combustion and decay (or cooling) phases.

During the early stages of the ignition phase, some combustible materials begin to burn releasing smoke and a small amount of heat. At this stage, the risk to life and property is not very high and active measures such as fire detection devices, fire extinguishers and sprinklers have a vital role. The growth of fire in this phase causes burning of more combustible materials and produces more smoke. Although the fire is still local this causes danger to the occupants and financial losses. At this stage the possibility of structural damage is small although glazing may be shattered.

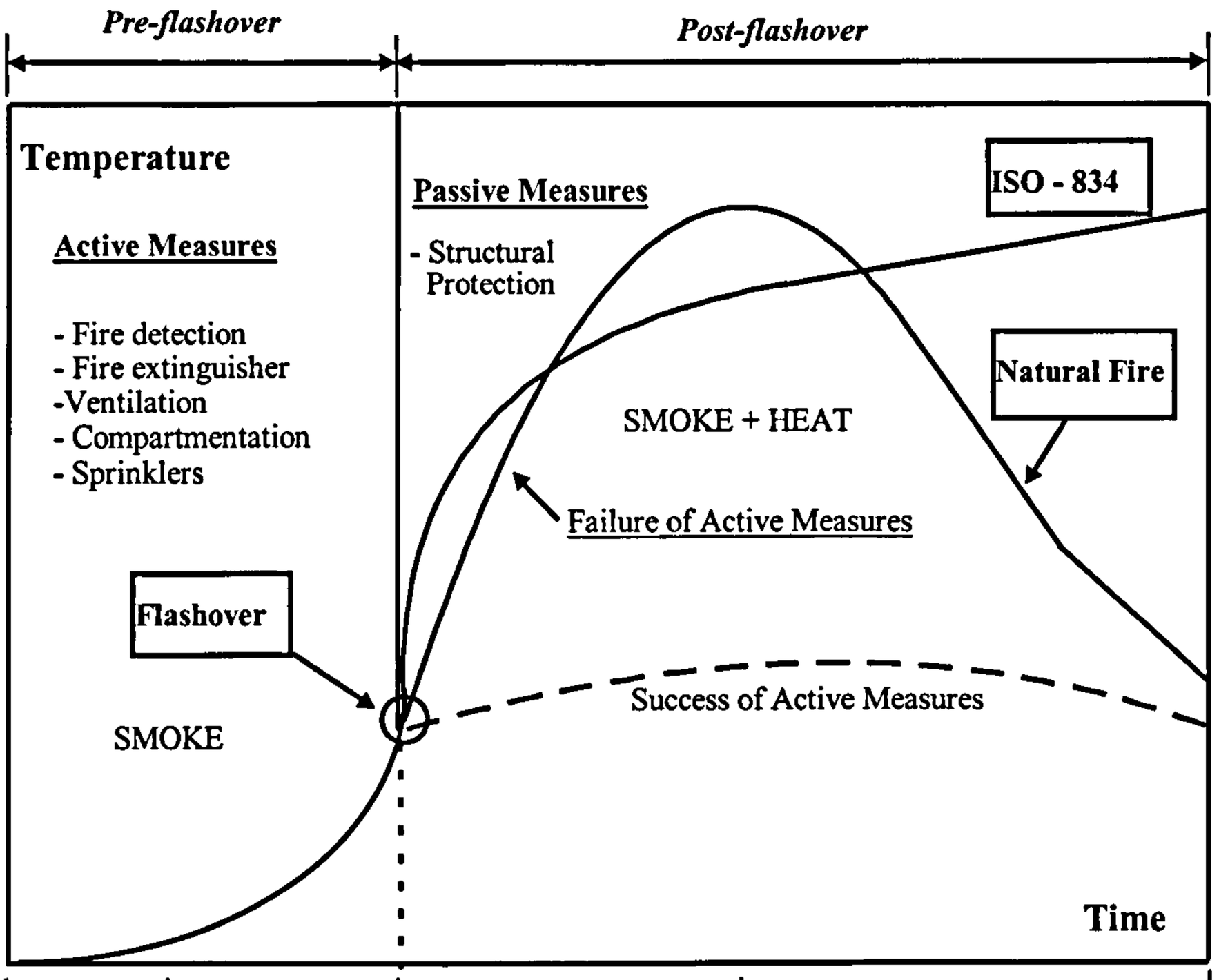

Phase of Fire Growth	Ignition	Smouldering Phase	Heating	Cooling Phase
Phase Governed by	Inflam-ibility	Temp.+Smoke Development	Fire Load Density	Ventilation Conditions

Figure 2.1: Real Fire Development in a Compartment

The transition from a local to a fully developed fire is known as *'flashover'*, the point which separates the ignition state and steady-state combustion. After flashover most of the materials within the compartment are engulfed; the flames reach the ceiling and spread out increasing the surface area of the fire. The onset of flashover may take a long time depending on the ventilation available within the compartment. If there is insufficient ventilation it may not be reached at all due to lack of oxygen. The flashover temperature depends on the combustibility of the material. At steady-state combustion, active measures have no effect in extinguishing the fire and the structural risk of collapse is high unless the structure is protected by passive measures. The temperature within the compartment at this stage is extremely high often in excess of 1000°C depending on the compartment geometry, ventilation and fire load. The fire will

continue to burn at this rate until the fuel begins to run out and the decay phase is entered. An illustration of the real fire phases is shown in Fig. 2.1.

2.2 STANDARD FIRE CURVES

The design data used in solving fire engineering problems and those used in determining the fire resistance of structural elements are normally obtained from testing specimens in special furnaces. Tests are usually conducted under temperature regimes which follow a 'standard fire curve' in which the furnace temperature varies with time in accordance with BS476: Part 20[60] or ISO834[61] as described by the equation:

$$T = T_0 + 345 \log_{10}(8t + 1) \qquad 2.1$$

where,

T and T_0 = temperature in the fire compartment and ambient temperature (°C) respectively;

t = time (minutes).

This relationship is also shown graphically in Fig. 2.2.

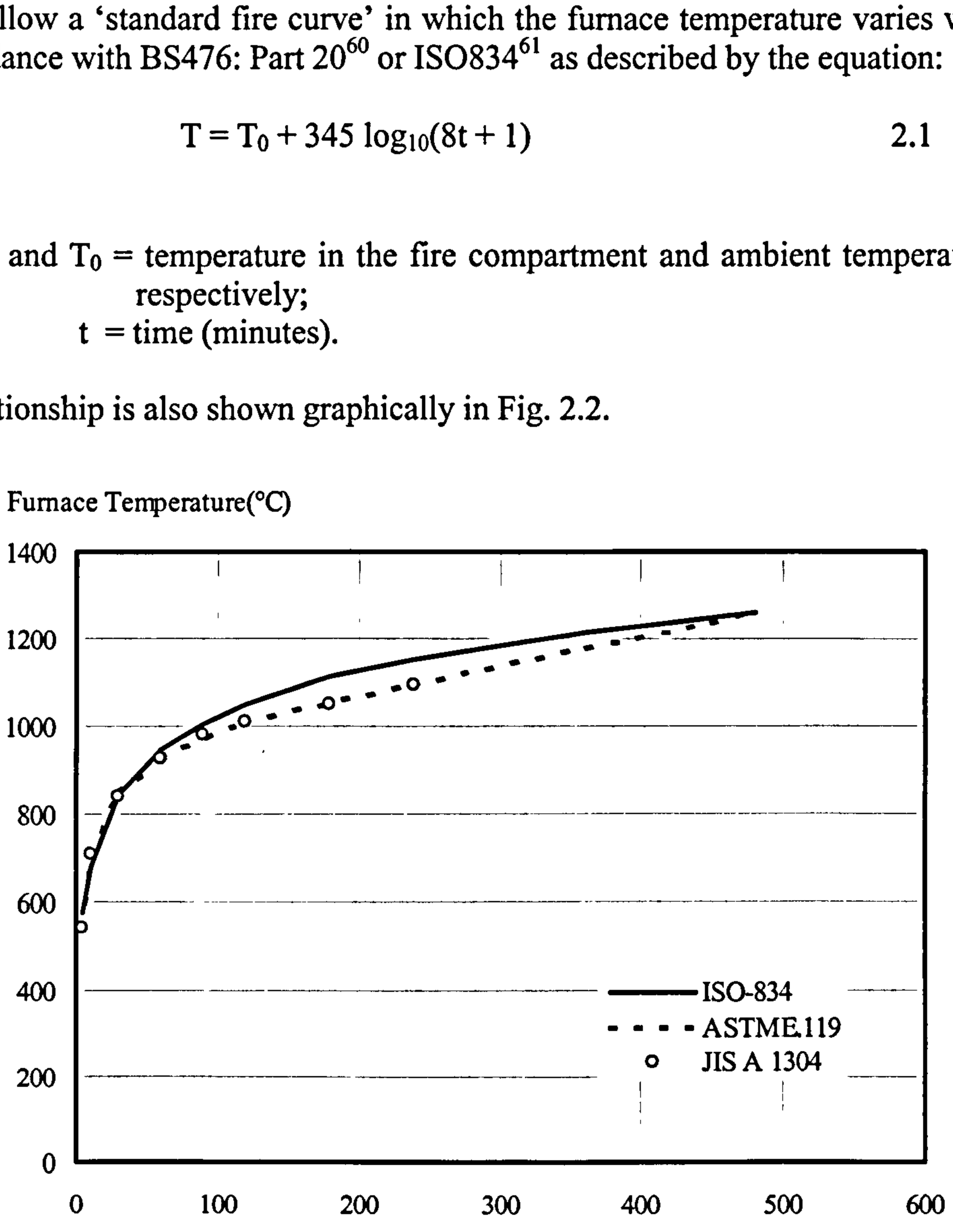

Figure 2.2: Standard Fire Curves

There is some variation in the standard fire curves adopted in different countries, see for example the differences between ISO834, ASTM-E.119[62] and JIS A 1304[63] as shown in Fig. 2.2. Although two furnaces may accurately follow the standard fire curve, the specimen under test may heat up at different rates. This difference may be due to the type of fuel used in the test furnace as well as the type of walls of the furnace and its

general interior geometric features which lead to different convection and radiation conditions and thus effect the heat transfer to the specimen.

It can be seen from Fig. 2.1 that the standard fire curve does not accurately follow the phases of a natural fire, and ignores the growth phase prior to flashover as well as the decay phase. However, it is generally accepted that the standard temperature-time curve does provide a basis for comparison between different fire tests.

2.3 FAILURE CRITERIA IN STANDARD FIRE TESTS

The primary aim of standard fire tests on structural members is to determine the time for which an element can survive without violating any of the specified performance criteria. The temperature regime within the furnace is controlled according to the standard fire curve. The standard test is therefore a means of comparing the performance of one construction with another by maintaining a standard heating environment[64].

Within the UK standard fire tests are conducted according to BS 476[60,65]. Three criteria have been imposed by BS476: Part 21[65] for a load-bearing element of construction:

1. *Stability or load-carrying capacity*: failure of the structural member to support the applied loads in a fire. The stability of the member depends on the temperature it reaches during the fire and is influenced by the following factors:
   (a) The applied load;
   (b) The type and strength of the material at elevated temperature;
   (c) The rate of heating;
   (d) The effect of restraint, continuity and composite action from surrounding structures.

Depending on the member type (beams or columns) different failure criteria are defined as:

(a) Beams: failure is based on maximum deflection and rate of deflection. Failure of the element is assumed not to occur until the deflection exceeds span/30. However deflections in excess of span/30 up to a maximum of span/20 are allowed if the rate of deflection (mm/min.) remains less than $span^2/(9000 \times member\ depth)$. Similar criteria are specified in the European Code[66] but with a limiting deflection of $span^2/(400 \times member\ depth)$ instead of span/20.

(b) Columns: there is no specific deflection limit is defined but the failure occurs when the column fails to support the applied load. Column regain its original length i.e. effects of thermal expansion is exactly balanced by that of material softening.

The fire resistance is reduced by 20% if the element fails to support the load 24 hours later[67].

2. *Integrity:* this refers to the ability of a compartment boundary to sustain fire tightness, preventing the passage of smoke or flame from one compartment to another as a result of breaks or cracks in the wall or floor.

3. *Insulation*: a fire on one side of a compartment wall or floor should not cause combustion of objects on the unexposed side.

In some cases a wall or floor could fail due to insulation or integrity while at the same time still supporting the applied loads. For structural steel elements, it is the stability criterion which is of most importance.

2.4 PROPERTIES OF MATERIALS AT ELEVATED TEMPERATURE

There is a large body of data concerning the degradation of mechanical properties of structural materials at elevated temperature. The rate of degradation of mechanical properties varies significantly between different structural materials[68]. The exact nature of this degradation depends on the chemical and crystalline structure of the material and on the type of manufacturing processes used in forming the structural section. This is discussed in the following sections.

2.4.1 Degradation of Structural Steel

Steel is non-combustible but softens when exposed to fire. The mechanical properties of a material are often expressed in terms of stress-strain characteristics. Much experimental research [68,69,70,71,72,73] has been conducted on structural steels in order to establish their behaviour at elevated temperatures. Special steels have been developed in Japan which have the ability to retain up to two-thirds of their ambient temperature yield stress up to 600°C[74]. These are utilised in certain applications, but the high cost usually restricts their more general use.

The stress-strain characteristics of structural steel at elevated temperature are well established and represented in design codes BS5950: Part 8[19] and EC3: Part 1.2[59] and a typical set of curves for a range of temperatures is shown in Fig. 2.3. The whole stress-strain relationship is usually taken into account when using a finite element analysis. When considering simplified analytical models, on the other hand, it is sufficient to incorporate the main parameters representing the degradation of material properties with temperatures.

Two test methods are commonly used for determining stress-strain characteristics for structural steel at elevated temperature. Transient-state (or anisothermal) tests are carried out by exposing the test specimen to a constant load and increasing temperature. Strain and temperature are measured during the test. Since the test is performed under constant load, a temperature-strain relationship is recorded during the test. Stress-strain curves are derived from a number of curves at different stresses. Steady-state (or isothermal) tests are conducted by heating up unloaded test specimens to a certain temperature and then performing a tensile test. The stress-strain curve is recorded for the specified temperature. Several tests must be carried out at different temperatures in order to establish a family of stress-strain curves at elevated temperature. Both methods have been utilised by Kirby and Preston[71] to determine the mechanical properties for Grade 43A and 50B steels over a temperature range of 20°C to 900°C. They concluded that transient-state tests indicate lower strength than steady-state tests but are more

representative of actual behaviour. Experimental data from these tests have been adopted in BS5950: Part 8[19] and later in EC3: Part 1.2[59] to replace those produced by ECCS[75] which were found to be too conservative.

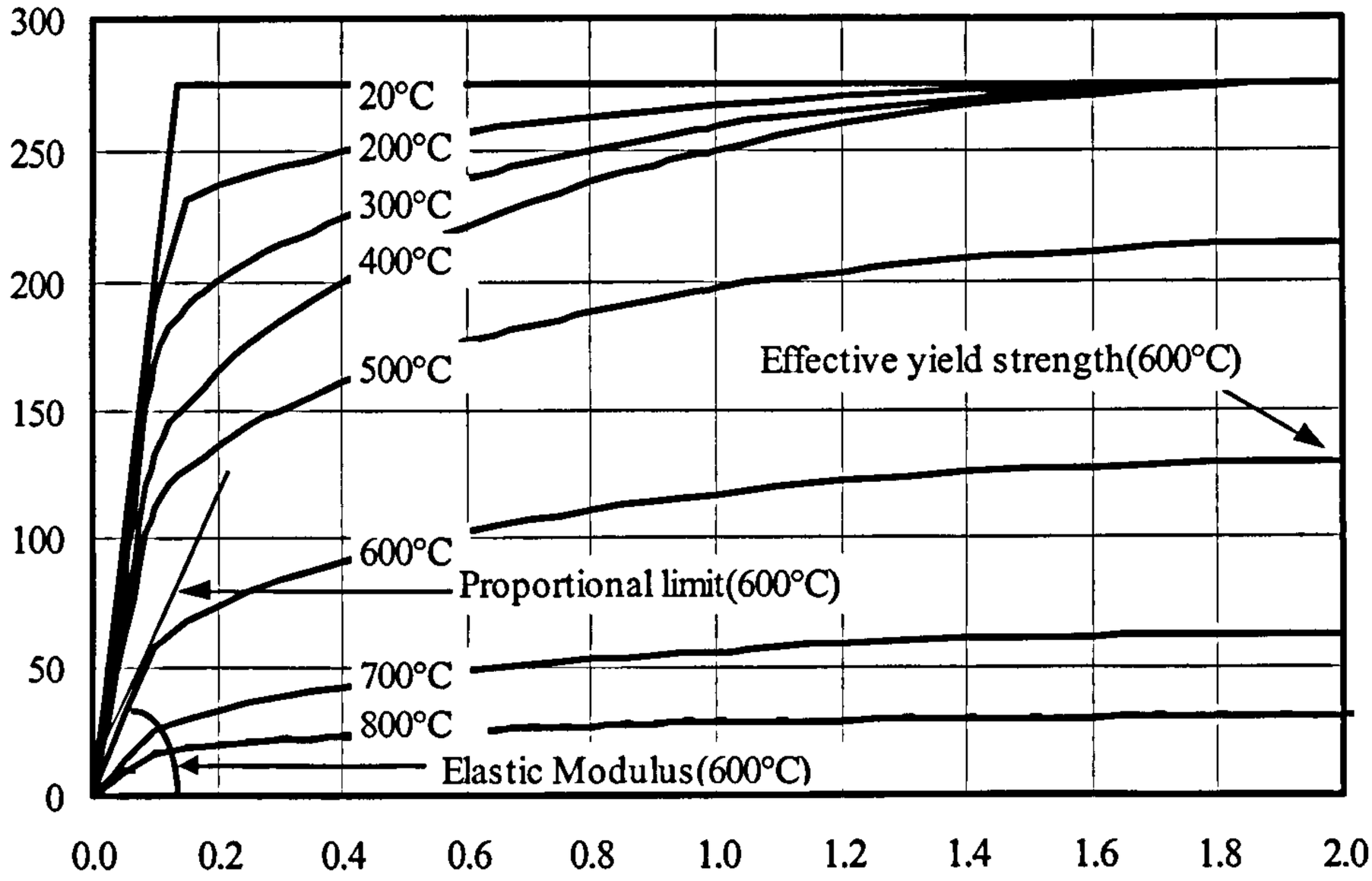

Figure 2.3: Stress-Strain Curves at Increasing Temperatures for S275 Steel (EC3 Curves)

The heating rate can be important due to onset of creep at temperatures above 450°C. This phenomenon of time-dependent deformation at constant load and temperature[76] is difficult to incorporate into time-independent design methods. Therefore experimental investigations have concentrated on practical rates of heating of between 5°C/minute (for well insulated sections) and 20°C/minute (for poorly insulated sections). These relate to limiting temperature of 600°C at failure times of 30 and 120 minutes respectively assuming a linear rate of heating.

2.4.1.1 Degradation of Steel Strength

Design codes have adopted the concept of "Strength Retention Factor" to represent the degradation of material strength at elevated temperature. This is basically the residual strength of the steel at a particular temperature relative to the basic yield strength at room temperature. At ambient temperature, the stress-strain characteristics of steel are approximately bi-linear with a distinct yield plateau. At high temperature, however, the stress-strain curves decrease and loose their bi-linear nature making it difficult to define the exact yield point and elastic modulus (Fig. 2.3). To overcome the problem a limiting strain is specified and the relationship between strength retention factor and temperature will depend on the limit chosen. The design codes BS5950: Part 8 and EC3: Part 1.2 have adopted 0.5%, 1.5% and 2.0% strain limits for the fire limit state. The appropriate limit depends on whether the steel is bare or composite and the strain

limit of any protective material used. In some cases strains as high as 5% may be developed[77].

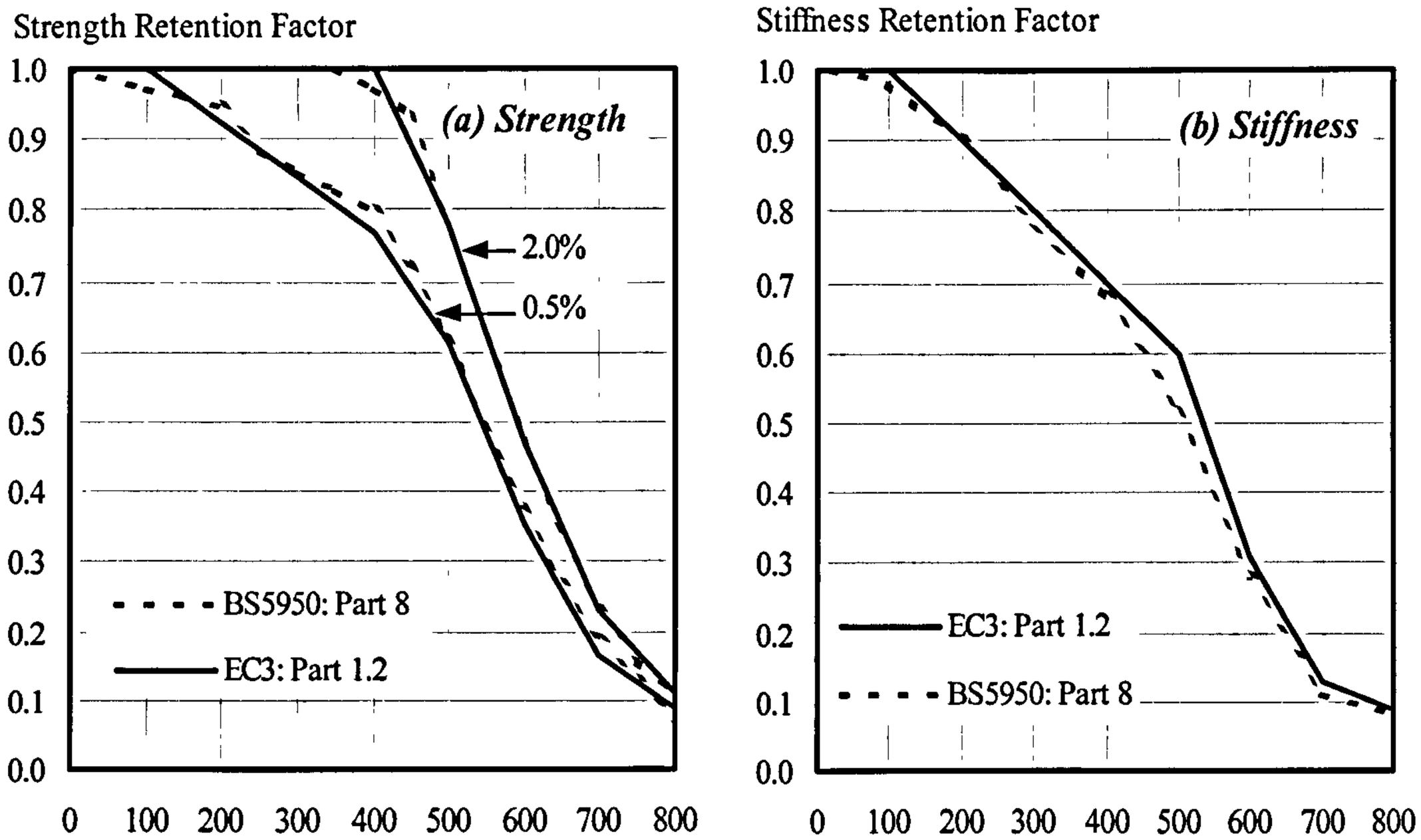

Figure 2.4: Degradation of Strength and Stiffness for Grade 43 Steel with Temperature

The degradation of steel strength for strain limits of 0.5% and 2.0% as considered in both BS5950: Part 8 and EC3: Part 1.2 is shown in Fig. 2.4*(a)*. The same test data is used for both codes which explains the similarity between the two. For steel strength corresponding to 0.5% proof strain there is a gradual decrease in strength up to 400°C beyond which the degradation is much more rapid.

2.4.1.2 Degradation of Steel Stiffness

At ambient temperature the elastic modulus of steel is defined as the slope of the elastic region of the stress-strain curve. At elevated temperature the tangent modulus must be used because of the non-linear nature of the curves. However this depends on the proof strain at which the elastic modulus is measured. Therefore, a bi-linear relationship is usually used with the elastic modulus expressed as function of temperature.

Fig. 2.4*(b)* shows the stiffness retention factor for steel with increasing temperatures as adopted in BS 5950: Part 8 and EC3: Part 1.2. Once again, there is very little difference between the stiffness retention factors adopted in the two.

2.4.1.3 Thermal Expansion of Steel

Most materials expand when heated but at varying rates depending on material type and chemical composition. The rate at which the material expands as a function of temperature is known as the coefficient of thermal expansion, α_s. For steel, this coefficient increases slightly with temperature. BS5950: Part 8 recommends a value of $12x10^{-6}$/°C at ambient temperature and $14x10^{-6}$/°C for temperatures in the range 200 to 600°C. Steel also undergoes a change in the phase diagram at temperatures around 730°C. This causes a significant change in the expansion properties as energy is absorbed and the material develops a denser internal structure. BS5950: Part 8 suggests a formula for calculating the total extension, δ_s from 20°C up to the phase change.

In EC3: Part 1.2 the total extension of steel, δ_s is expressed by the following tri-linear relationships including temperatures beyond the point of phase change:

$$20°C \leq t_s < 750°C$$
$$\delta_s = (0.4x10^{-8} t_s^2 + 1.2x10^{-5} t_s - 2.416x10^{-4}) l \qquad 2.2a$$
$$750°C \leq t_s \leq 860°C$$
$$\delta_s = (1.1x10^{-2}) l \qquad 2.2b$$
$$860°C < t_s \leq 1200°C$$
$$\delta_s = (2.0x10^{-5} t_s - 6.2x10^{-3}) l \qquad 2.2c$$

It may be seen that this relationship is similar to the one recommended by BS5950: Part 8. Moreover, a simplified relationship is adopted for incorporation in simple calculation models. This relationship is constant over the whole range of temperatures and may be given by the following formula:

$$\delta_s = (14x10^{-6} (t_s - 20)) l \qquad 2.2d$$

where,

t_s = temperature of the steel (°C);
l = the original length of the specimen.

Steel density and Poisson's ratio are are considered to be independent of temperature and may be taken as 7850 kg/m^3 and 0.3 respectively.

2.4.2 Degradation of Concrete at Elevated Temperature

Concrete consists mainly of mineral aggregate bound by a matrix of hardened cement paste. The porosity of the paste is high and normally contains a large amount of free water. Studying the behaviour of concrete at elevated temperature is complicated due to the variation in its constituent materials and changes in the properties of any of these will have a direct effect on the concrete behaviour.

Concrete suffers loss of both strength (in tension and compression) and stiffness at high temperatures in a similar manner to steel[78,79,80]. There are several factors affecting the performance of concrete structures in fire. These include: (1) type of aggregate; (2) water content, both absorbed and free; (3) type of cement; and (4) loading conditions.

The free water begins to evaporate at about 100°C causing the modulus of elasticity to reduce by 10-20% while the compressive strength remains the same. At temperatures in excess of 300°C, the concrete paste shrinks due to the loss of the hydration water. This may be accompanied by a little expansion of the aggregate depending on type. A gradual reduction in concrete compressive strength occurs at temperatures between 450°C and 500°C beyond which there is a rapid decrease. At temperatures around 600°C, some types of aggregate especially those containing quartz, undergo a crystalline transformation leading to a significant volume expansion. This may cause cracking and explosive spalling of the cement paste[81]. The initiation of dehydration in the calcium hydroxide and other cement hydration products also causes some deterioration. As the temperature approaches 1000°C, calcium carbonate decomposes and the remaining free and absorbed water is lost reducing the compressive strength to zero. At very high temperatures, in the range of 1200°C to 1700°C the hardened cement paste and aggregates melt [80,82].

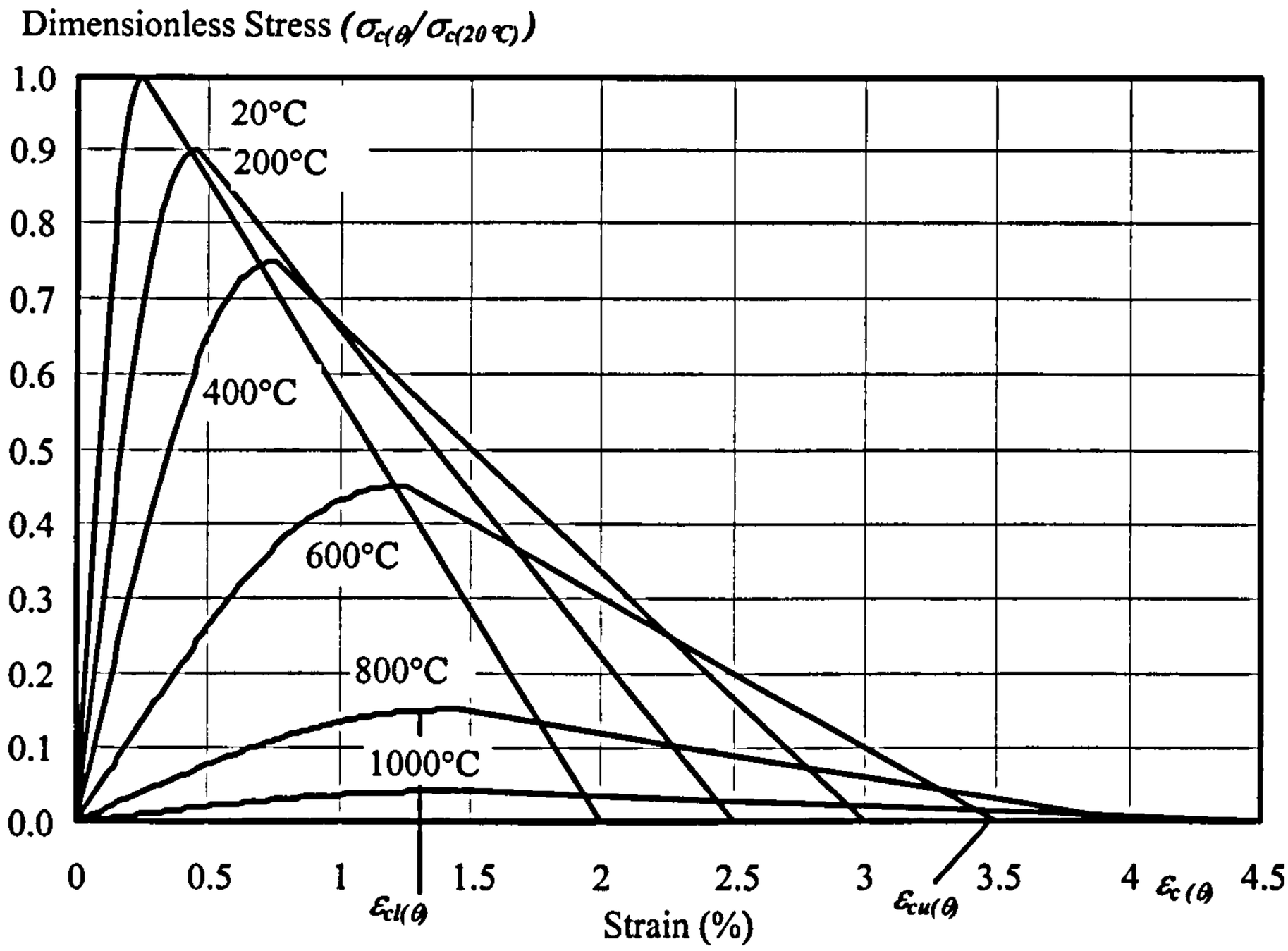

Figure 2.5: Stress-Strain Curves for Concrete with Temperature

The strength and stiffness of the concrete in fire are represented in EC4[83] by stress-strain characteristics at different temperatures. These have been derived from compressive tests conducted on concrete specimens at elevated temperature. The curves for concrete indicate a maximum compressive strength, occurring at strains which gradually increase with temperature, followed by a decreasing branch. This is clearly shown in Fig. 2.5 based on EC4: Part 1.2[83] recommendations for normal-weight and lightweight concrete. It can be seen that at temperatures of approximately 600°C the compressive strength is less than 50% of its value at ambient temperature. It is normally assumed that the tensile strength for all types of concrete is zero.

The strength retention factor according to EC4: Part 1.2[83] for both lightweight and normal-weight concrete is shown in Fig. 2.6. EC4 suggests the use of the lower range of strength values representing the siliceous type to describe the degradation of normal-weight concrete. This assumption may lead to a conservative assessment of the behaviour of other types of normal-weight concrete such as calcareous-aggregate concrete. Despite the fact that lightweight concrete may be produced using different forms of aggregates, EC4: Part 1.2 represents the degradation rate by only a single set of strength retention factors. Consequently, these data might be inappropriate for some types of light-weight concrete. As can be seen the degradation of normal-weight concrete is more rapid than for lightweight concrete.

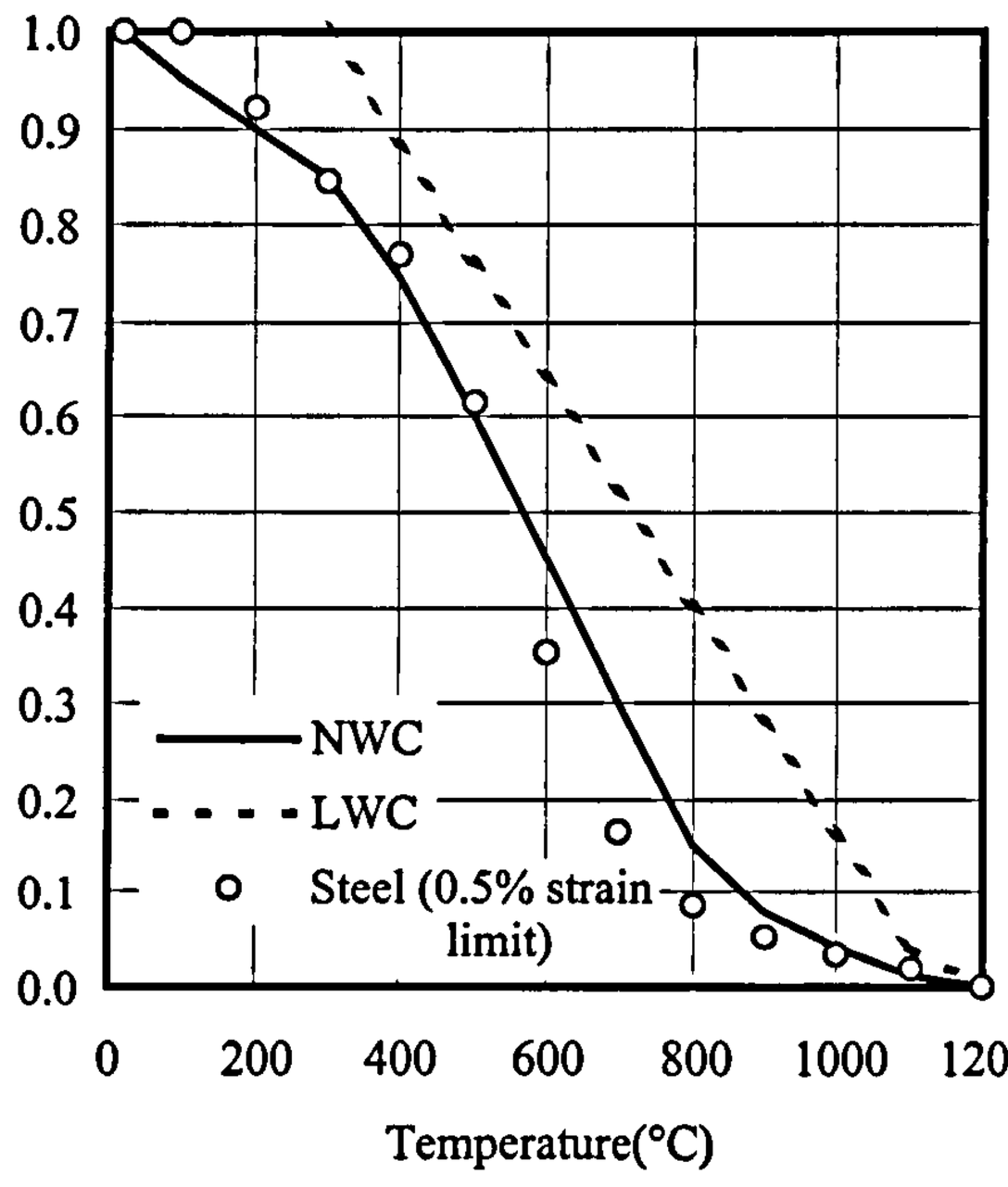

Figure 2.6: Degradation of Concrete Strength at Elevated Temperature According to EC4.

These are consistent with the results obtained by Jau and Wu[84] from a series of tests studying the performance of lightweight concrete panels under fire conditions. It was found that normal-weight concrete has lower residual strength, higher thermal expansion and greater thermal conductivity than lightweight concrete at any temperature. The degradation of the two types is also compared in Fig. 2.6 from which it may be seen that the degradation of structural steel and normal-weight concrete is very similar.

BS 8110: Part 2[85] proposes two formulae for the strength retention factor for both normal-weight and lightweight concrete:

For normal-weight concrete

$350°C<t_c<800°C$

$$SFR = \frac{0.8x(800 - t_c)}{450} + 0.2 \qquad 2.3$$

For lightweight concrete

$500°C<t_c<800°C$

$$SFR = \frac{0.6x(800 - t_c)}{300} + 0.4 \qquad 2.4$$

where,

t_c = concrete temperature

2.4.3 Degradation of Bolts and Weld at Elevated Temperature

Bolts and welds are structural components that connect different structural elements. Unfortunately, little is known about the deterioration of bolts in fire and thus it is insufficiently addressed in design codes. There was little experimental data available when BS5950: Part 8[19] was published and therefore the rate of degradation of bolts is taken as 80% of that for structural steel at 0.5% strain. EC3: Part 1.2[59] gives no recommendations regarding the elevated temperature degradation of bolts.

Although a series of tests has been conducted by Sakumoto *et al.*[86] in Japan to assess the degradation characteristics of bolts at high temperatures, these tests were for fire resistant steel.

In order to determine the deterioration of the bolts in fire a series of tests was conducted by Kirby[87] on Grade 8.8 bolts which are widely used in steel industry. Results obtained showed that the bolts suffer a significant decrease in capacity in the temperature range of 300°C to 700°C. Based on these results the following tri-linear relationship has been proposed describing the degradation of bolt strength at elevated temperature:

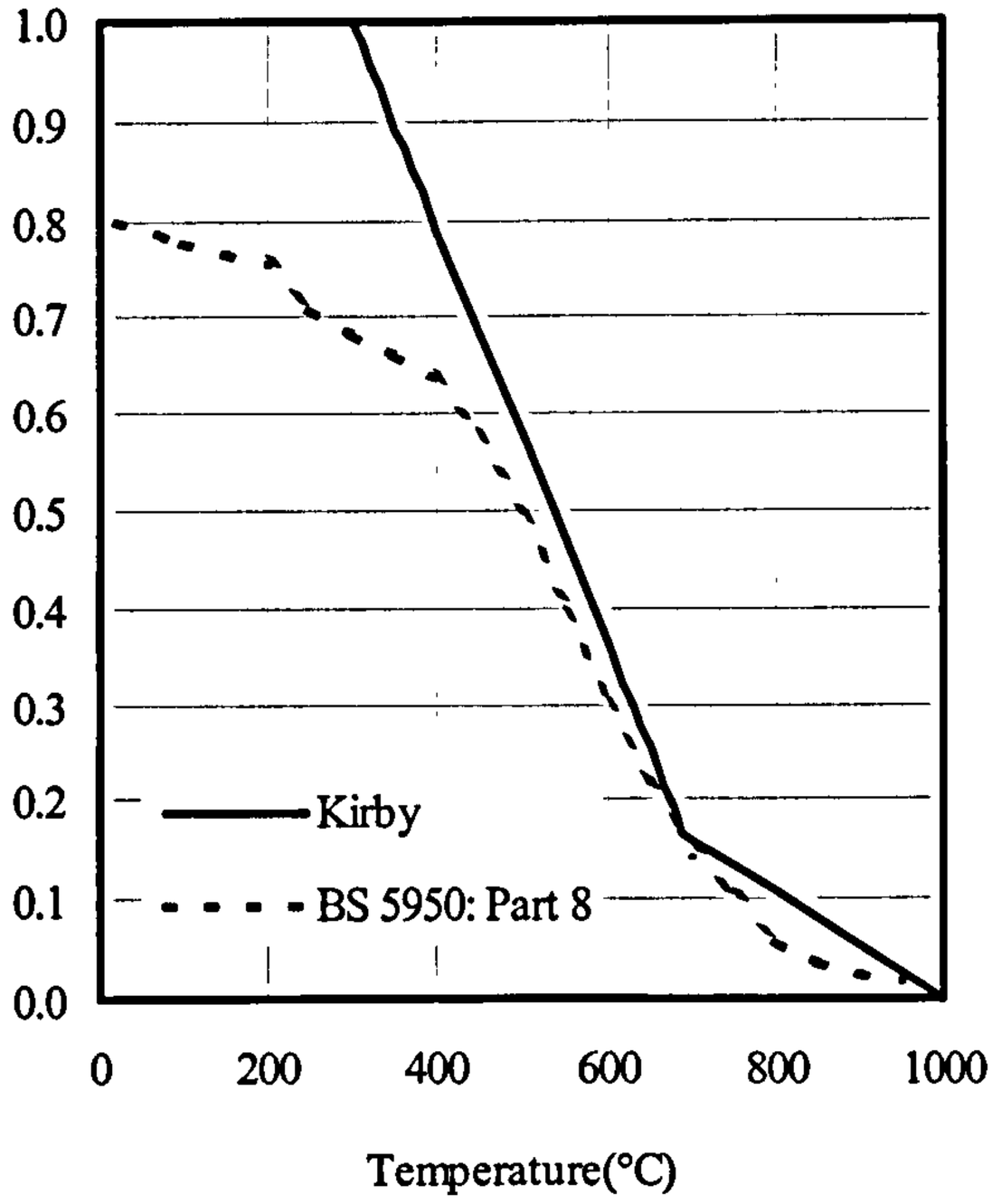

Figure 2.7: Degradation of Bolts at Elevated Temperature

$t_b \leq 300°C$

$SFR = 1.0$ 2.5a

$t_b < 300°C \leq 680°C$

$SFR = 1.0 - (t_b - 300)x2.128x10^{-3}$ 2.5b

$t_b < 680°C \leq 1000°C$

$SFR = 0.17 - (t_b - 680)x5.13x10^{-4}$ 2.5c

where,

t_b = the temperature of the bolt

Kirby found that the present design recommendations are conservative especially at low to intermediate temperatures as shown in Fig. 2.7. Although no recommendations were suggested concerning degradation of other bolt types such as Grade 4.6, it was suggested[87] that they would follow the same trend as Grade 8.8 bolts based on their nominal strength values.

Little data are available concerning the behaviour of welds at elevated temperature. Although studies[88] suggested that the weld capacity reduces sharply in the temperature range 200 to 400°C, but then becomes closer to the strength of parent steel.

2.4.4 Degradation of Reinforcement at Elevated Temperature

Reinforcing steel is used in conjunction with concrete (and composite construction) to provide tensile resistance since concrete is extremely weak in tension. Also steel mesh with nominal steel bars is normally used in composite slabs to control slab cracks. They are normally shielded from heat by the surrounding concrete, keeping them at relatively low temperatures provided that the normal cover is maintained throughout the fire duration.

Holmes *et al.*[89] carried out a series of tests studying the mechanical properties of different types of reinforcing and prestressing steel at high temperatures. Three types of reinforcement: mild steel, cold-worked high yield steel and hot-rolled high yield steel were tested to represent those most commonly used in construction. In order to investigate the effect of reinforcement size three nominal diameters were tested - 8mm, 12mm and 25mm. Tests were performed under steady-state conditions in a specially designed tensile test rig with specimens being heated using a cylindrical tube furnace reaching a maximum operating temperature of 1000°C. The tests provided extensive data for modulus of elasticity, yield and ultimate strengths.

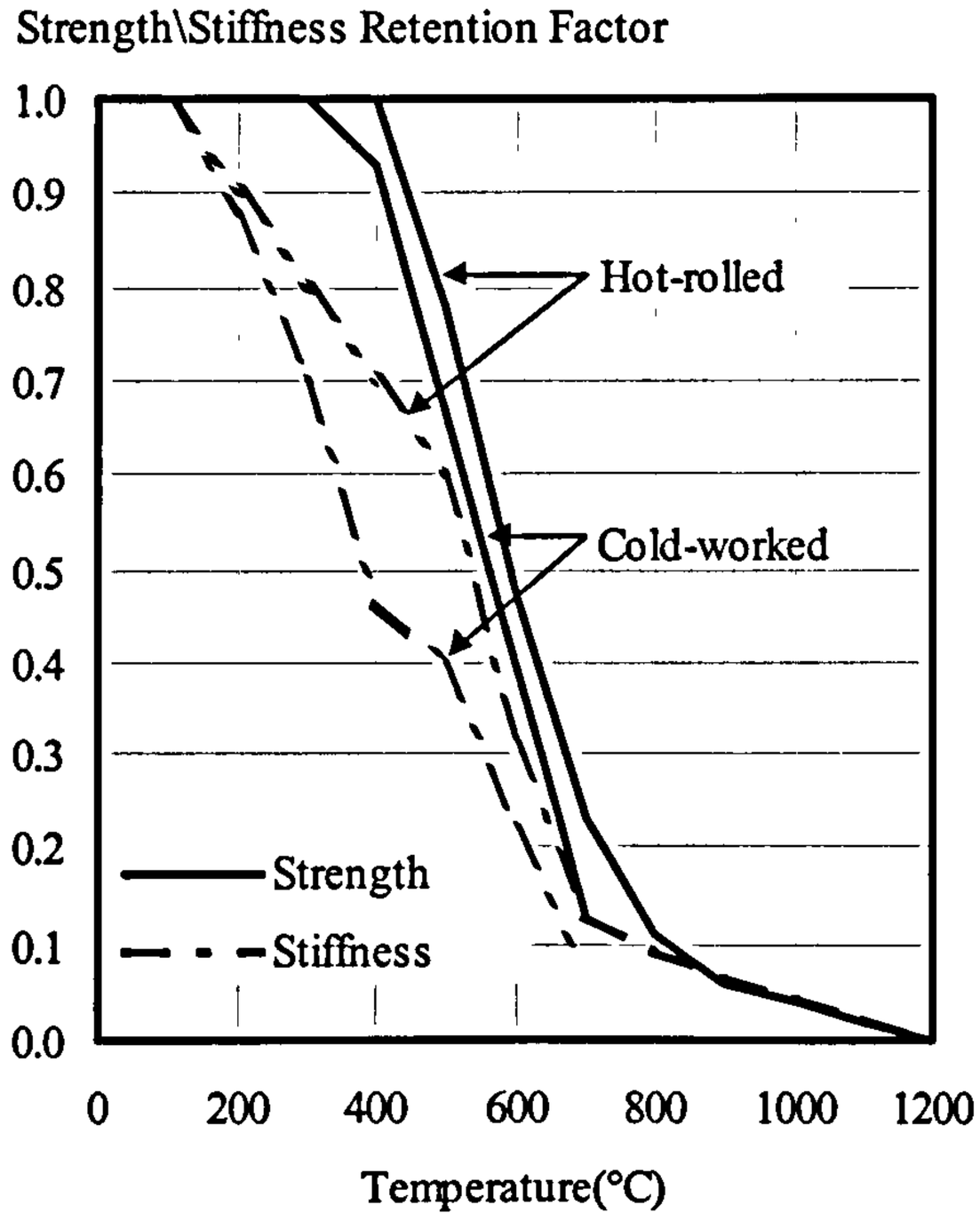

Figure 2.8: Degradation of Hot-rolled and Cold-worked Reinforcements at Elevated Temperature according to EC4

It was found that there was close agreement between the test results and the design curves[90] in the mid-range of temperatures around 400°C to 600°C, whilst the design curves do not form the lower bound limit for temperatures outside this range. Bar size was found to have negligible effect on the reinforcement properties.

EC4 deals with hot-rolled reinforcing bars in a similar manner to structural steel whereas the residual strength of cold-work reinforcing bars reduces more rapidly at elevated temperature than other reinforcing steels. Fig. 2.8 shows a comparison between stiffness and strength retention factors for both hot-rolled and cold-work reinforcing steel.

2.4.5 Degradation of Shear Studs at Elevated Temperature

Shear studs are normally used in composite construction to ensure full interaction between the steel beam and the concrete slab. The stud is electrically welded to the steel member, usually the beam upper flange, and embedded in the concrete slab. It consists of two parts: the shank resisting longitudinal shear and the head which has the main task of resisting the tensile forces perpendicular to the interface.

At elevated temperature the shear studs are largely shielded from the heat and their loss of strength is much lower than that of the steel section. As a result little attention has been given to study their behaviour at high temperatures, although a series of tests was carried out by Twilt and Kruppa[91,92]. These tests were performed for a particular structural arrangement but currently provide the principal source of data. The strength and stiffness retention factors for the shear studs as presented by Twilt and Kruppa are:

Strength Retention Factor

$20°C < t_{ss} \leq 200°C$

$SFR = 1.0$ 2.6a

$200°C < t_{ss} \leq 400°C$

$SFR = 1.150 - 7.5x10^{-4}\ t_{ss}$ 2.6b

$400°C < t_{ss} \leq 800°C$

$SFR = 1.717 - 2.167x10^{-3}\ t_{ss}$ 2.6c

Stiffness Retention Factor

$20°C < t_{ss} \leq 100°C$

$SFR = 1.0$ 2.7a

$100°C < t_{ss} \leq 800°C$

$SFR = 1.445x10^{-(0.0016t_{ss})}$ 2.7b

where,

t_{ss} = shear stud temperature

These expressions suggest that the strength of the shear stud deteriorates gradually at temperatures greater than 200°C, while at temperatures around 400°C there is a rapid reduction in capacity. However, degradation of the stiffness at low temperatures is faster rate than for structural steel which might be related to the type of loading utilised during the tests.

2.5 CONCLUSIONS

Standard tests based on the standard fire curve are not representative of real condition but provide a basis for comparing behaviour of different systems and for design. The influence of elevated temperatures on the mechanical properties of structural materials: steel, concrete, bolts, reinforcements and shear studs is generally well established.

3 ELEVATED TEMPERATURE MOMENT-ROTATION TESTS ON BARE-STEEL CONNECTIONS

3.1 INTRODUCTION

A number of tests have been conducted to establish the moment-rotation relationships for bare steel connections across a range of temperatures following the same methodology adopted by Leston-Jones[52]. The present work extends the scope to study more typical connections with the influence of further parameters considered such as member size, connection type and different failure mechanisms. The intention is to develop a means of using the large body of existing ambient temperature connection data to define high temperature characteristics which can then be used in the numerical modelling of framed-structures in fire. Both flush end-plate and flexible end-plate connections were studied. The experimental programme was carried out by the author in the Structures Laboratory at the Building Research Establishment. The test arrangement, instrumentation, testing procedure and the resulting behaviour are described. The fire test temperature profiles across the connections are detailed and the failure mechanisms are discussed.

3.2 ELEVATED TEMPEATURE BARE-STEEL CONNECTION TESTS

In total eleven tests were conducted divided into three groups. The first series was for a flush end-plate detail with beams and columns within the lower range of available section sizes. Larger section sizes and end-plate details were utilised in the second series in order to give an indication of the effect of member size on connection behaviour. Also the steel used was of higher grade than for the first series. The third series was for a flexible end-plate representative of those used in the eight storey building at Cardington. Section sizes were the same as those used in the second series. The connection types were selected as being those most widely used in current steel framed structures. The test specimens were supplied by British Steel.

In all cases the test specimens consisted of a symmetric cruciform arrangement of a single column 2.7m high with two cantilever beams 1.9m long as shown in Fig 3.1. All specimens were major axis connections i.e. beams connected to the column flanges with mild steel end-plates in Grade 43A. All bolts were tightened to 160Nm by a torque wrench to ensure consistency. A previous study[93] suggests that this is similar to the torque typically achieved from hand tightening.

Unlike ambient temperature connection tests where a single test is sufficient to determine the moment-rotation characteristics, a series of tests has to be conducted in order to establish the corresponding relationships for elevated temperatures. As a result of such tests a family of moment-rotation curves at elevated temperatures for different connections may be generated. For this purpose, the connection tests were conducted by keeping the specimen at a constant load level and increasing the furnace temperature until failure. This method has been shown to provide reliable results and yield adequate data regarding the temperature distribution across the connection depth. Moreover, adopting a constant load with increasing temperature regime reflects the situation in real

building fires. Load levels were based on the calculated moment capacity of the connections so that data could be obtained over the complete range of the connection response. Since the scope of the programme was restricted by the resources available and the number of tests required to establish the elevated temperature connection characteristics, it was not possible to conduct ambient temperature tests.

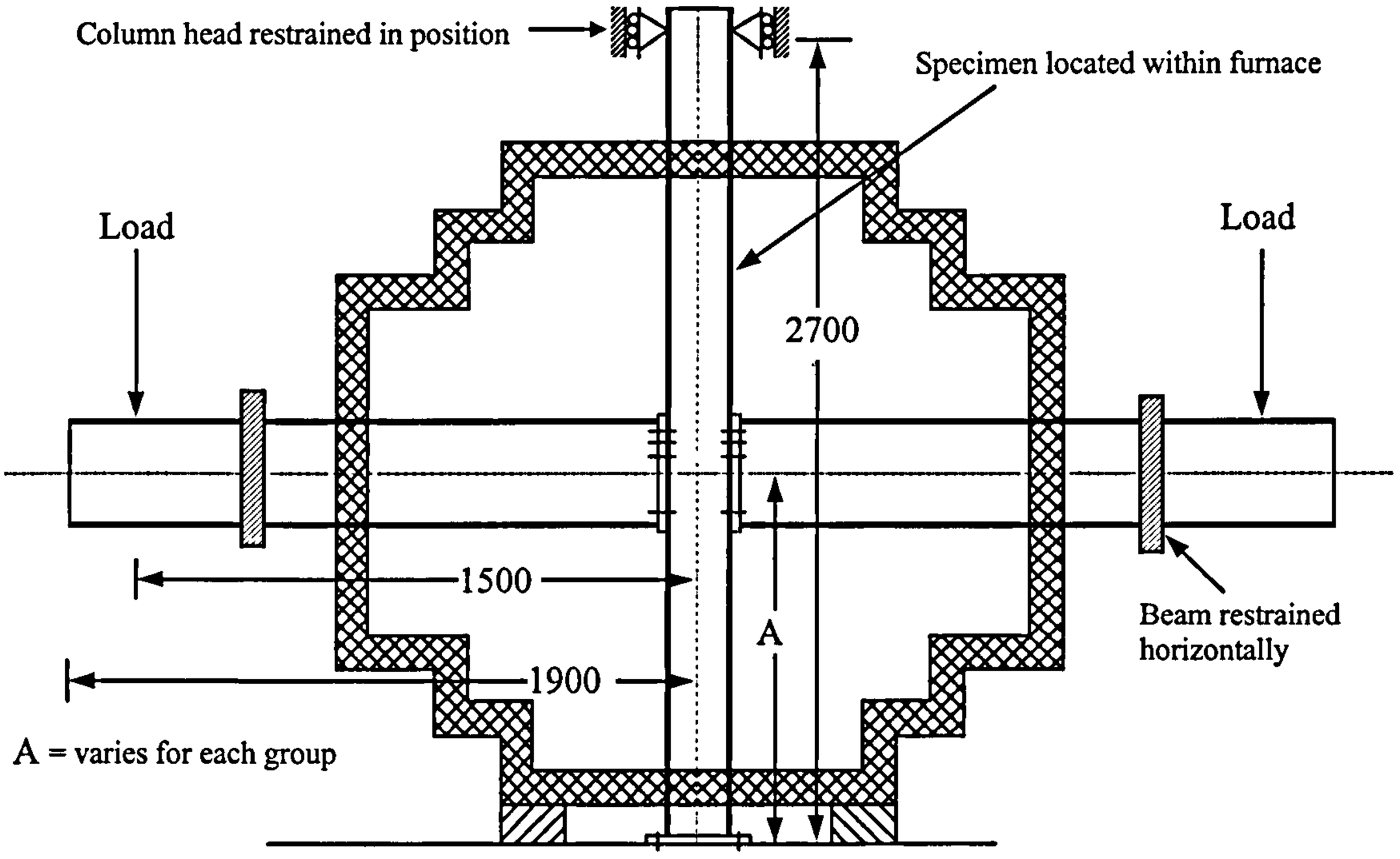

Figure 3.1: Elevated Temperature Test Arrangement

Table 3.1: Material Properties of Steel Sections Used in the Tests

Steel:	*Ultimate Stress (N/mm^2):*	*Yield Stress (N/mm^2):*	*Modulus of Elasticity (kN/mm^2):*
Grade 43	454	322	197
Grade 50	545	412	195

For all specimens, ambient temperature material and geometrical properties were determined for the beam and column sections prior to testing in the furnace. The results are presented in detail in Appendix A and summarised in Table 3.1. It can be seen that the material strength, measured using standard tensile coupon tests, is consistently higher than the nominal values. Measurements carried out to determine the stiffness of the sections revealed consistent values[94] in the range of 190-210 kN/mm^2. Also, it was observed that geometrical properties for the beam and column sections were slightly less than the nominal values due to reductions in flange thickness compared with the nominal figures. Material properties at elevated temperatures were not measured because of the high cost of testing.

3.3 TEST ARRANGEMENT

The cruciform test arrangement shown in Fig. 3.1 was used, as this required a less extensive test rig than the corresponding cantilever arrangement. It also provided an indication of the variability of the nominally identical connections on either side of the column. Tests were performed in a portable junction furnace specially designed for testing connections within a two- or three-dimensional framework. The inner furnace walls were lined with a thick layer of ceramic fibre to facilitate rapid heating using natural gas as the fuel. The furnace uses a tangential firing system in which a high-speed burner is fired into a circular chamber to generate a circulating gas flow, allowing good gas mixing and temperature distribution. A more detailed description of the furnace and its associated control system is given elsewhere[95,96]. Fig. 3.2 shows the general layout of the furnace. A linear temperature ramp achieving 900°C in 90 minutes was adopted, since it had been shown to provide a reasonable representation of the desired temperature profile in previous tests [52].

When the specimens had been positioned within the furnace, the columns were firmly fixed in place at the base, and the top was secured in position but left free to move vertically. The system of lateral column restraint utilised two small-scale angles on either side of the column flange. One leg was secured by bolts to the top of the furnace while the other leg was positioned to prevent any horizontal movement of the column. The column flange and the angle leg were separated by a very small gap, allowing the column to expand freely. Similarly, the beams were only permitted to deflect downwards. Lateral movement, associated with possible lateral torsional buckling of the beams and which would result in premature termination of the test, was prevented by means of horizontal restraint. This restraint system consisted of two small-scale channels positioned on either side of the beams, placed on Rectangular Hollow Section (RHS) and secured in position by bolts passing through the laboratory strong floor. A small gap was left between the beam flanges and the back of the channel to give the beam freedom to move downwards. The furnace and test arrangement are shown in Fig. 3.3.

The furnace doors were made from British Gypsum Glassroc S fire-resistant board and positioned at the point where the beams protruded from the furnace. A slot, corresponding to the width of the flange, allowed for downward movement of the beam. The beams were protected with 50mm thick ceramic fibre blanket to prevent their premature failure, as had happened in previous tests[47]. The connection, column and beam sections within approximately 100mm of the face of the connections were left exposed.

Loads were applied to the beams outside the furnace at a distance of approximately 1500 mm from the centreline of the column web, via Macalloy bars connected through the strong floor of the laboratory to the hydraulic loading system in the basement. The loading arrangement adopted was to maintain a constant moment as the temperature increased.

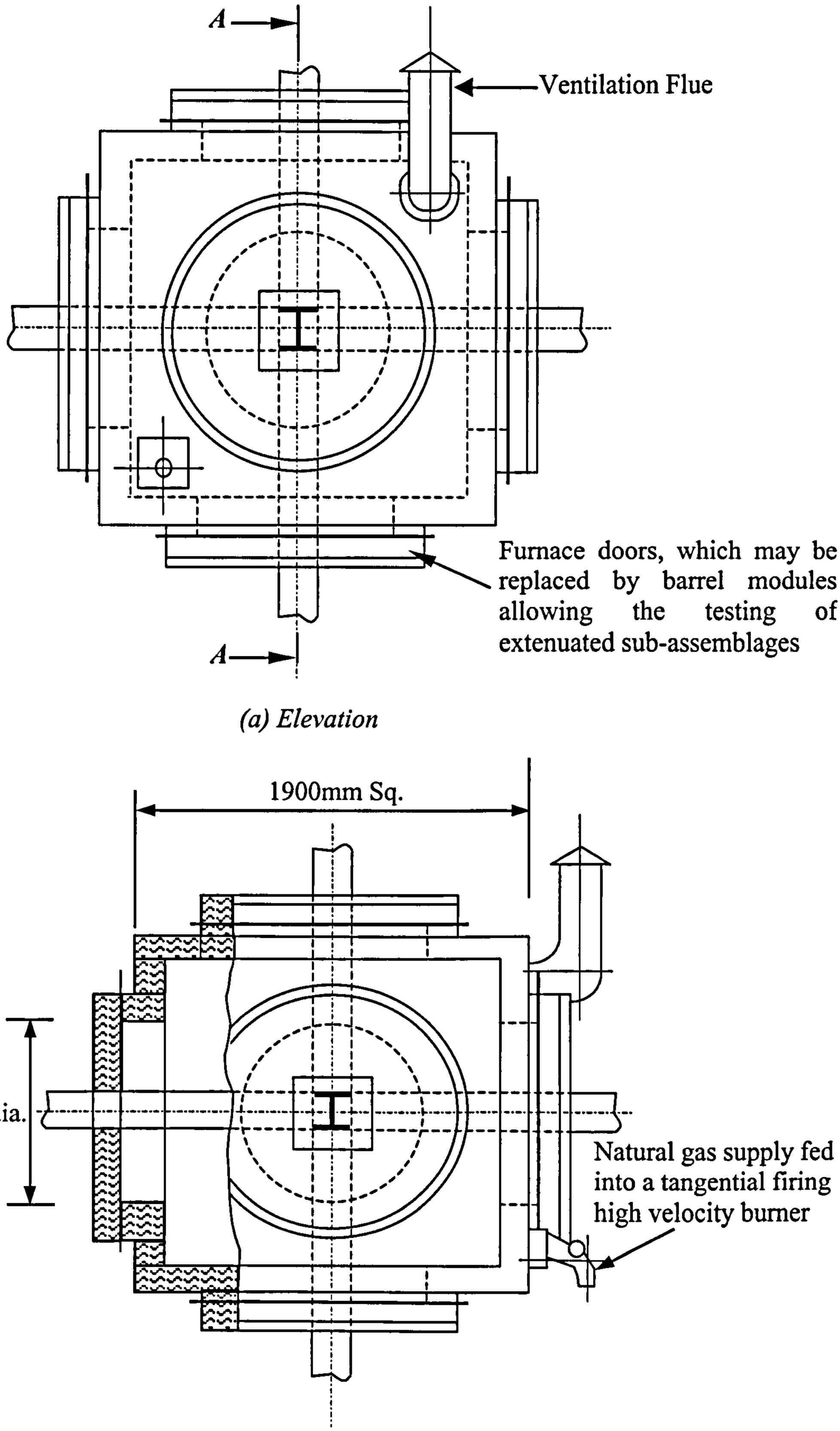

(a) Elevation

(b) Section A - A

Figure 3.2: Junction Furnace Layout

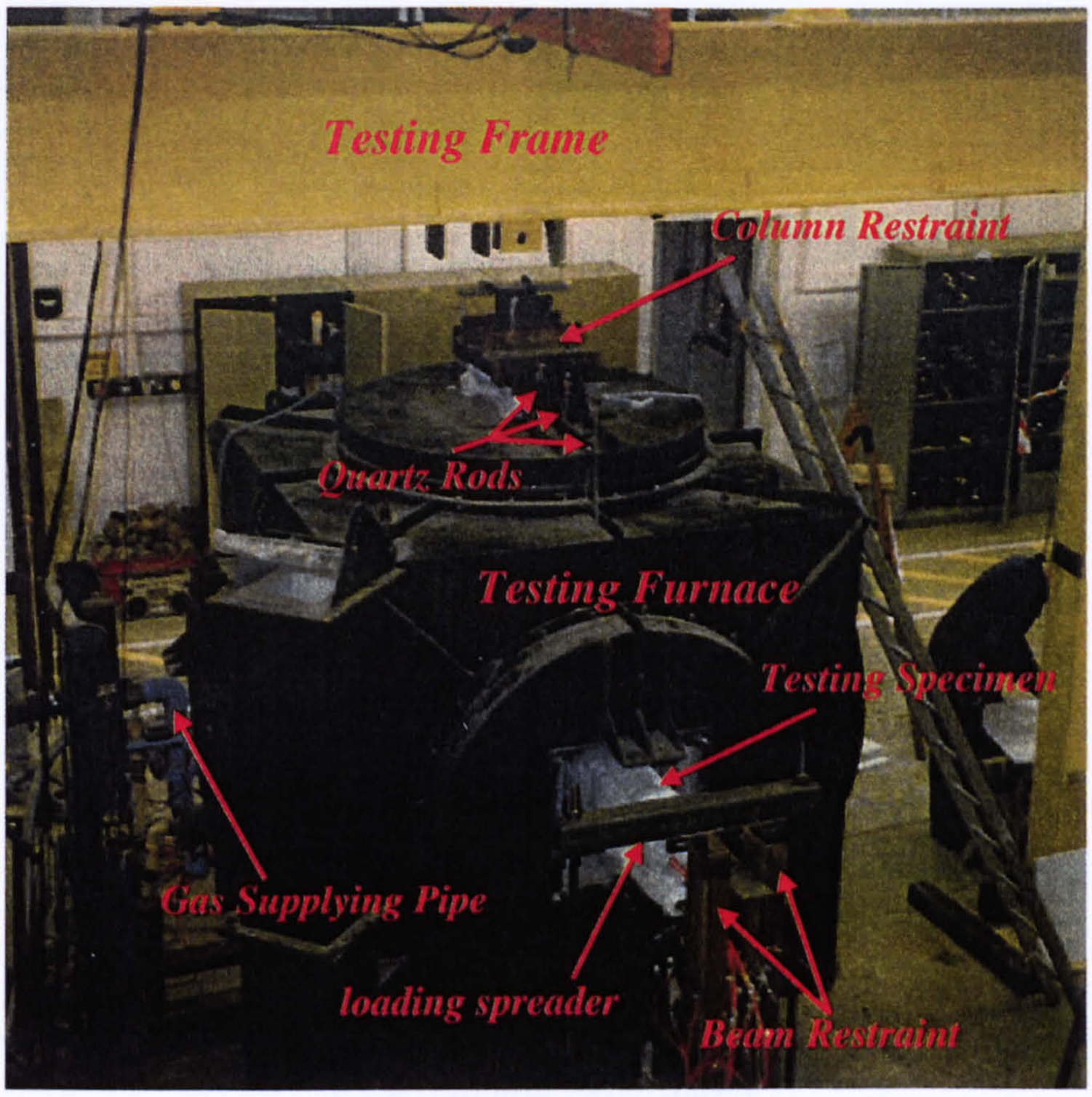

Figure 3.3: Testing Furnace and Elevated Temperature Testing Arrangement

3.4 INSTRUMENTATION

The instrumentation system was designed to capture all the necessary data - rotations, applied loads and temperatures - for determining the elevated temperature characteristics of the connections. The general arrangement of the instrumentation, which included clinometers, displacement transducers, thermocouples and load cells, is illustrated in Fig. 3.4. Both analogue and digital output devices were monitored through an Orion Delta data logger which was in turn controlled through a personal computer. All the data was recorded directly onto the computer's hard disk drive using AXIS software. Unfortunately, it was not possible to process the data while the test was still in progress due to the effort required to analyse the large amount of information.

An effective instrumentation system requires not only the right type of instrumentation, but also that the data is received in a suitable form for subsequent processing. Measurement devices such as clinometers and load cells that involve the use of electronic components were calibrated in the workshop prior to testing. The resulting responses from these were fed directly into the data logger in order to ensure that data obtained from such devices was meaningful. A full description of the calibration procedure and the final results obtained can be found elsewhere[97,98]. The instrumentation used in the experimental programme is illustrated in Fig. 3.5. The exposed beam bottom flange temperature was chosen as the reference for data logging, with channels logged at 50°C steps initially, but refined to 10°C as testing progressed.

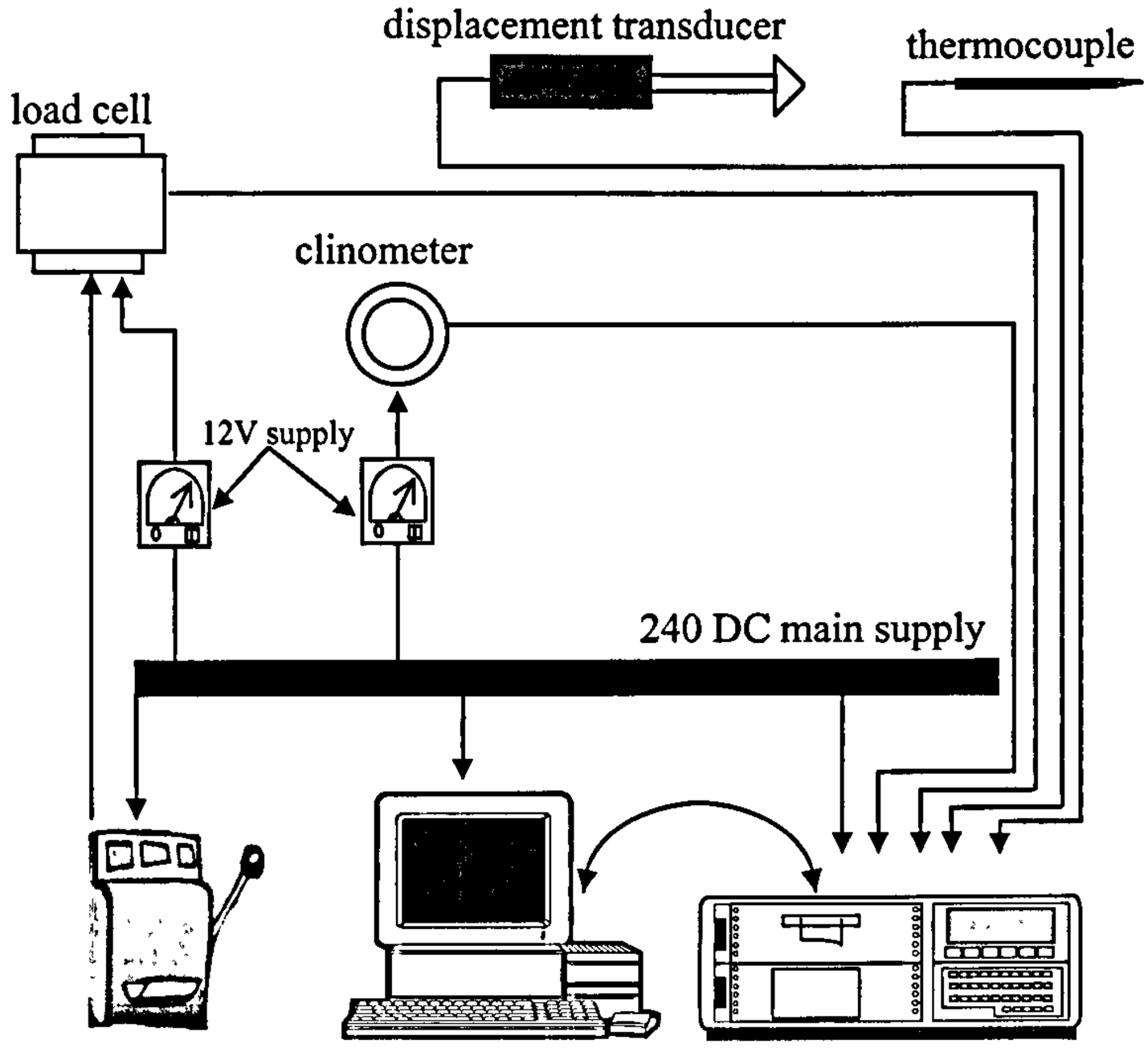

Figure 3.4: Circuit Diagram for the Instrumentation System Adopted for the Experimental Programme

The most common device used to measure the rotational movement of beam-to-column connections is a clinometer. For this purpose one clinometer was attached to each beam at a distance of 250 mm from the face of the column flange and in line with the beam centre-line as shown in Fig. 3.5*(a)*. The main difficulty when using clinometers in elevated temperature tests is that these devices have a maximum operating temperature of approximately 80°C, whereas, the temperature inside the furnace could reach as high as 900°C. They were therefore protected by a purpose-made box constructed from H61 Sindanyo board covered with a layer of insulation. To keep the clinometer temperature as low as possible, cool air was pumped through the box using a compressor. The associated wiring, connections and air piping were also protected by insulation. The option of locating clinometers along the centre-line of the column to measure the deformation was ruled out since it was anticipated that column deformation would be minimal due to the large section size and the lateral restraint provided. The rotation of the connection was therefore calculated from the average rotation of the two beams.

To allow for possible failure of the clinometers during testing, displacement transducers were utilised to provide indirect measurements of rotation and also to describe the displaced shapes of the sections. Four displacement transducers were attached along the length of each beam, three within the furnace and one outside as shown in Fig. 3.5*(b)*. An additional transducer was located at the column head to record its thermal expansion. The transducers recording displacements within the furnace were connected to quartz rods in contact with the specimen whilst the remaining one was attached directly to the beam lower flange. The quartz rods passed through holes in the top of the furnace and attached to the top face of the beam flange by means of high-

temperature cement. Because of the very low thermal conductivity and expansion of the quartz rods, this arrangement allows direct reading of displacements. It has been reported that using displacement measurements results in a maximum error of only approximately 1 millirad. as the connections approach failure[52].

A number of thermocouples were attached to the specimen in drilled holes using high-temperature cement in order to monitor the connection temperature and the thermal gradient across the section. The exact arrangement of the thermocouples varied for the different connections tested, but in general their locations were similar and are shown in Fig. 3.5*(c)* for the second test series. Two additional thermocouples were located in the furnace to record the atmosphere temperature and that of the fire resistant box to monitor the clinometer temperature. Thermocouples were located in the top and bottom flanges of the beam in the exposed and insulated area at distances of 50mm and 300mm respectively from the face of the column flange. Thermocouples were set in the column in a similar pattern. To measure the web temperatures, thermocouples were attached to the middle of the webs of the beams and the column. The temperature of the end-plate was recorded at mid-depth whereas the temperature of the bolts was measured by fixing thermocouples in the heads of the bolts on each side of the connections.

Calibrated compression load cells were used to measure the loads applied to the beams throughout the tests. The loads were applied to the specimen by hydraulic jacks located in the basement underneath the strong floor as shown in Fig. 3.5*(d)*. As loading started, the load cells sense the amount of the load applied to a RHS load spreader located in the laboratory basement. This is connected to Macalloy bars on each side to ensure correct transfer of forces to the beams. The Macalloy bars transmit the forces to a similar RHS load spreader on the top face of the beam. The Macalloy bars pass through the laboratory strong floor and the loading was controlled by means of a manual pressure valve. Prior to each test, several pilot runs were conducted on the instrumentation to ensure that all measuring and monitoring devices were working properly and giving reliable readings.

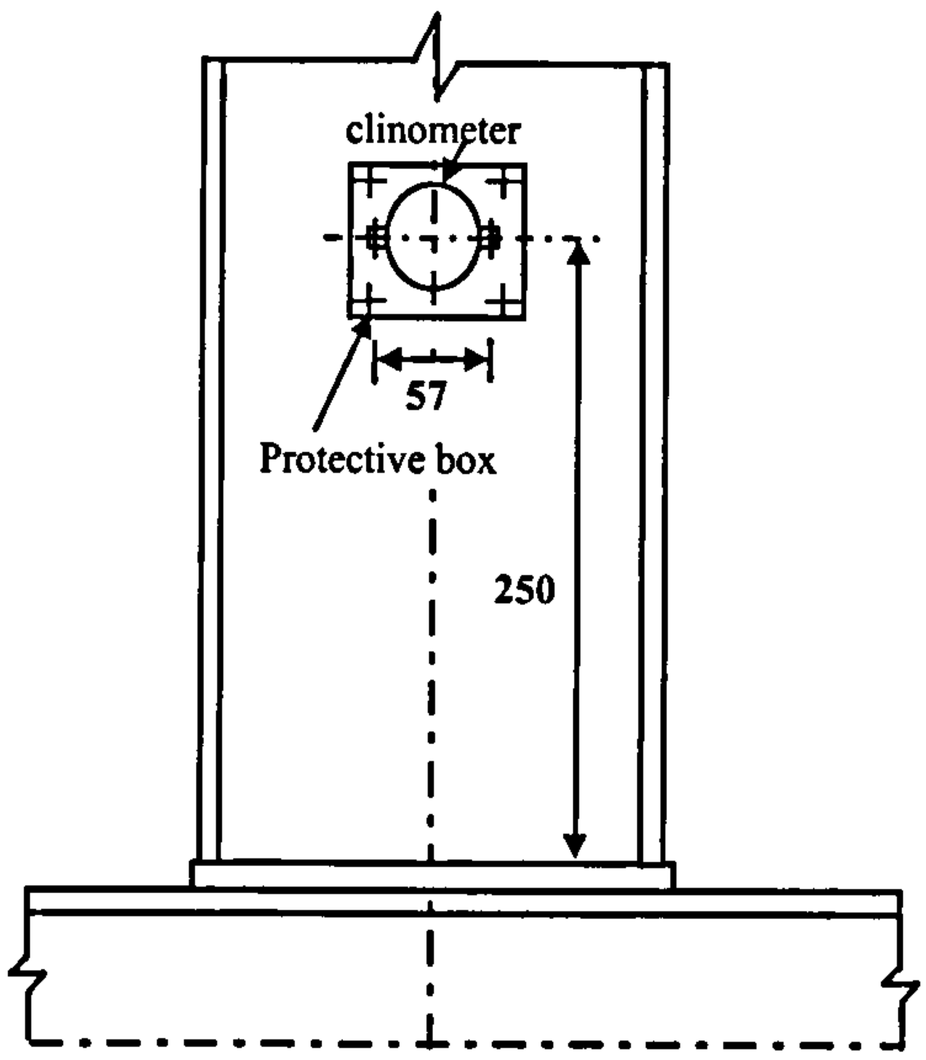

(a) Clinometer

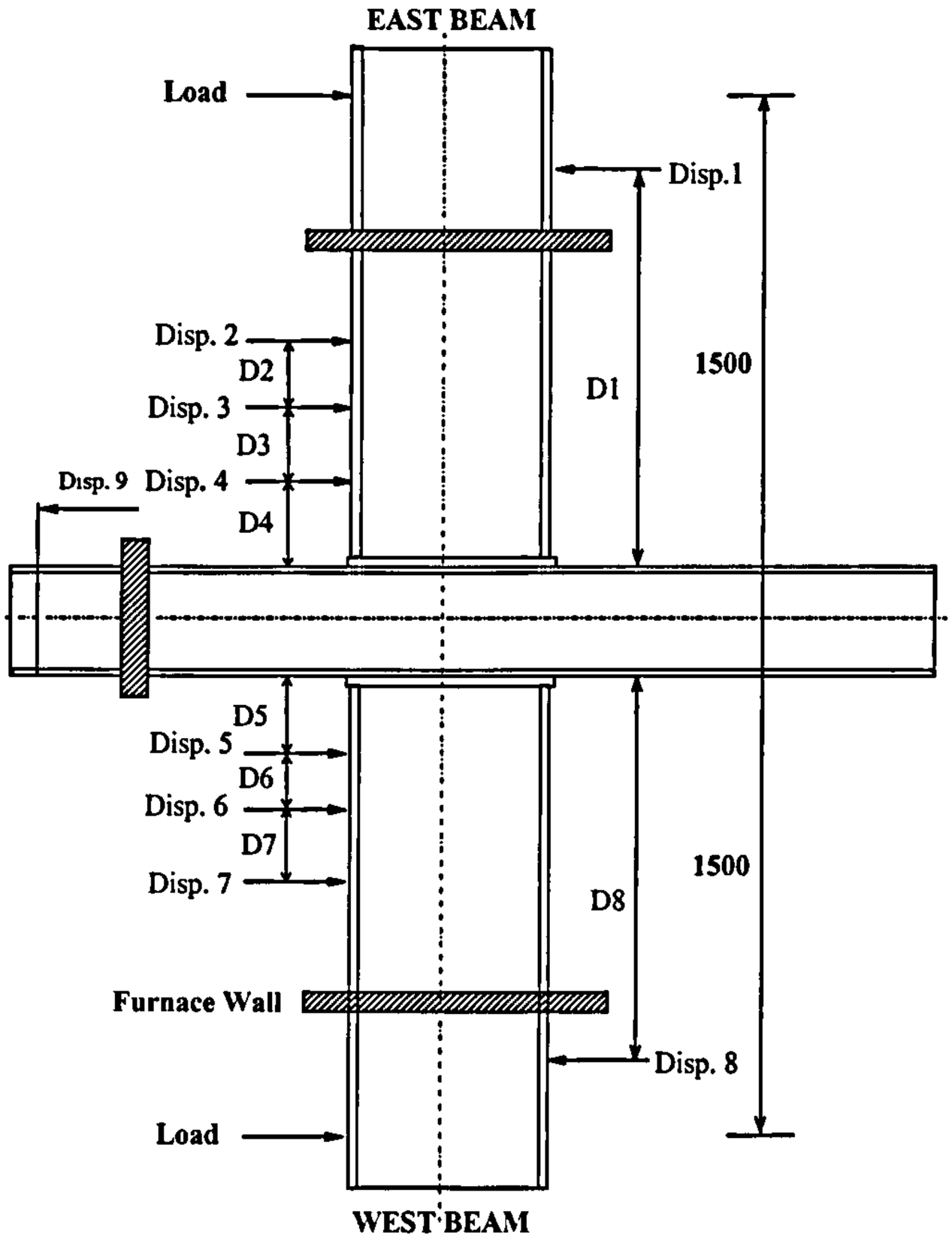

(b) Displacement Transducers

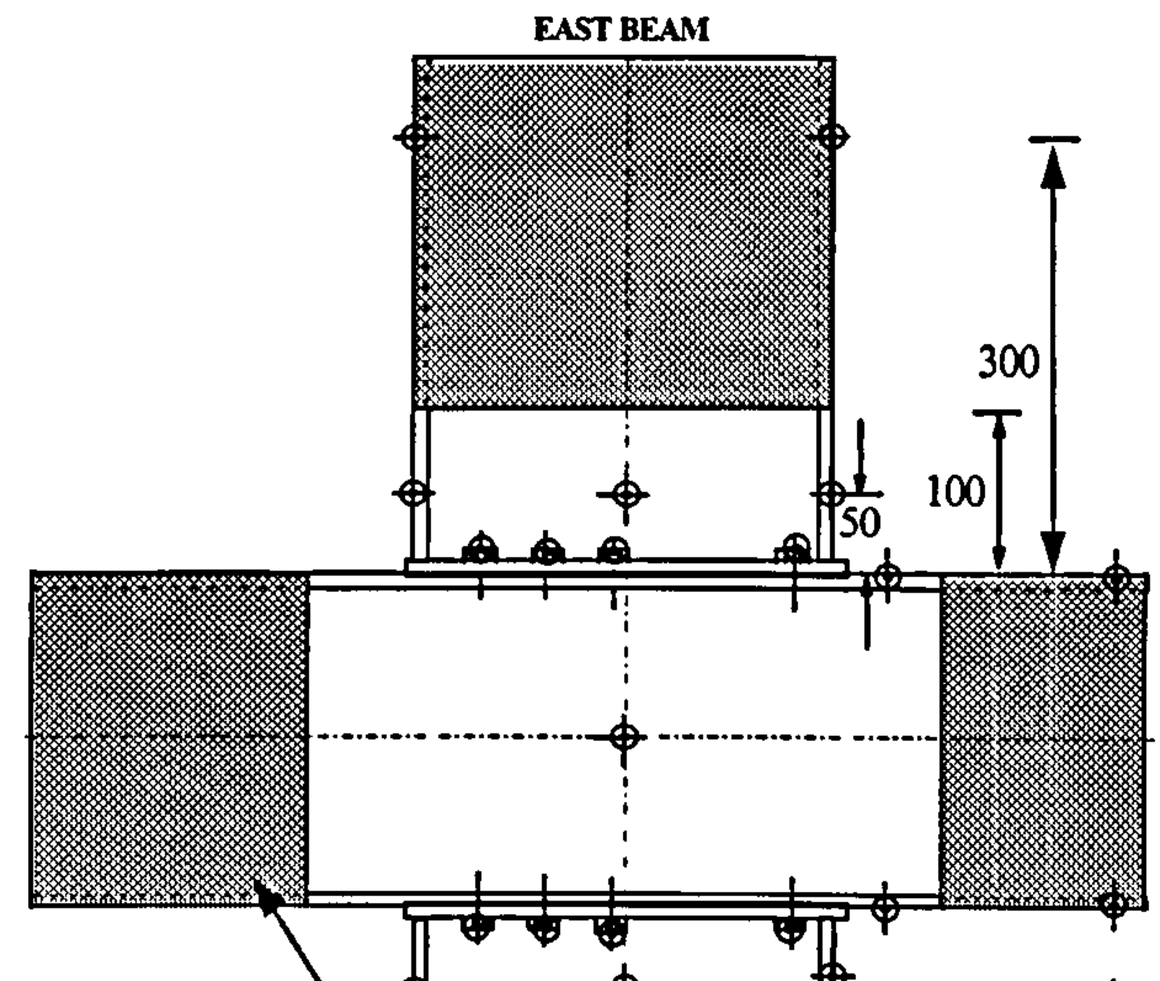

(c) Thermocouples

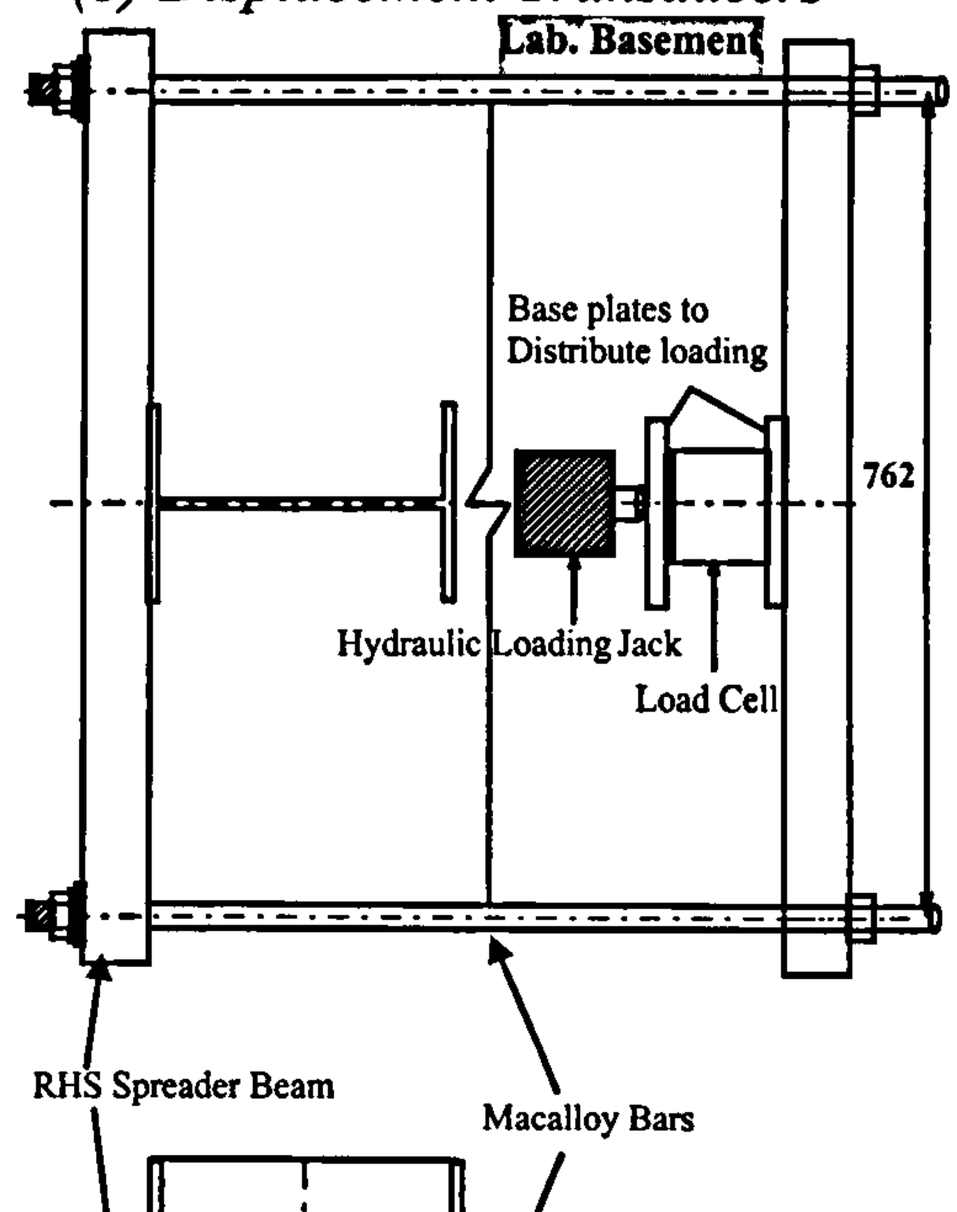

(d) Load Cells

Figure 3.5: Instrumentation Types and Locations

3.5 GENERAL COMMENTS FROM BARE-STEEL CONNECTION FIRE TESTS

The common procedures and observations for all bare-steel connection fire tests can be summarised as follows. Each test started with several pilot runs to ensure that the instrumentation was working properly and progress was carefully monitored throughout the test. For all tests, the connection is deemed to fail when either;

- it reaches post-plastification, which is indicated by progressive rate of rotation at small temperature increments, or;
- one or more of the connection components fail resulting in a rapid drop in the applied load.

In tests involving relatively low levels of loading, despite the efforts to maintain consistent and equal moments in the East and West beams, there was some variation in the level of loading. This occurred as a result of the fluctuation of load cells at small loads.

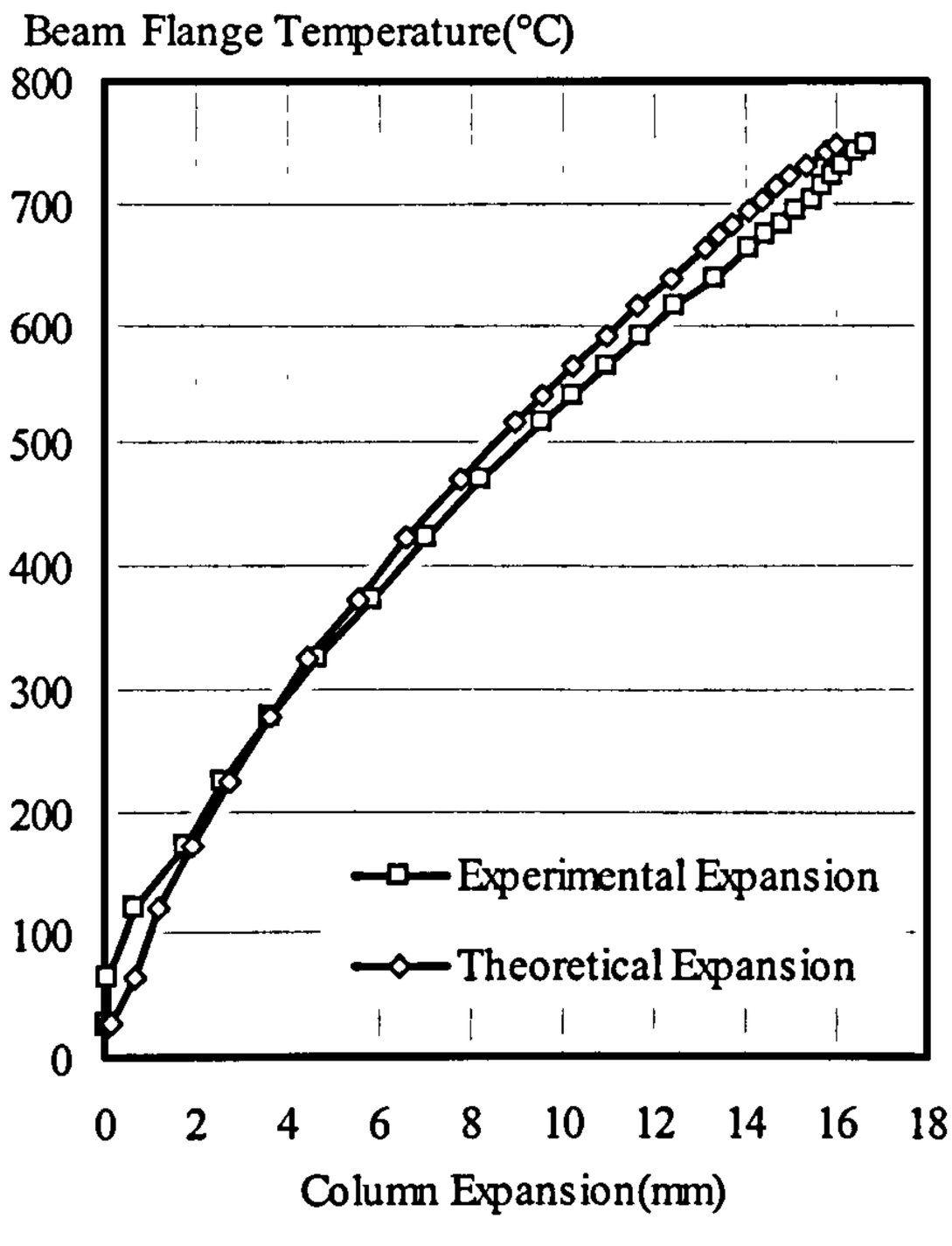

Figure 3.6: Comparison between Experimental and Theoretical Thermal Expansion of the Column

As previously discussed a displacement transducer was positioned in the column head in order to measure the column expansion. The theoretical column expansion was assessed using Eq. 2.2 which describes the thermal expansion of structural steel as presented in Chapter 2. Calculation of the theoretical expansion accounted for the exposed and insulated portions of the column based on thermocouple readings located in the column web and along the insulated and exposed column flanges. Fig. 3.6 shows a comparison between the experimental and theoretical column expansions, indicating very good agreement. Some tests performed previously on a typical arrangement and different end-plate thickness[52] reported a reversal in the experimental column expansion subsequent to the yielding of the connection due to progressive yielding of the column web; such phenomena is not observed in these tests.

As described above, displacement transducers were used as an alternative check on the rotations and to indicate the deformed shape of the beams. In order to obtain accurate rotations from the displacement transducer readings, the beam displacements were subtracted from the corresponding column expansion. Rotations were determined for each displacement, corresponding to its location along the beam, adjusted to allow for column expansion.

Despite the effect of elevated temperatures in causing much greater deflections to the beam than those for normal conditions, analysing the deflections recorded by the

displacement transducers revealed negligible deformation. This is consistent with behaviour observed previously[52] in similar tests, suggesting the importance of protecting the specimen remote from the connection from excessive temperatures. Protection of the arrangement in the vicinity of the connection was essential in order to prevent any failure of the beam prior to connection failure as experienced by Lawson[47].

Apart from a few cases where some thermocouples failed to give sensible recordings of temperature due to lost contact with the element, there was good consistency between the temperature profiles recorded for the East and West sides of the connection, despite the burner being situated on the East side. This demonstrates the ability of the tangential burner to generate adequate gas mixing and provide a uniform temperature within the furnace.

After completion of the test, it was observed that the temperature inside the clinometer protection box tended to rise rapidly, leading to destruction of the clinometers. To avoid this, the furnace doors were removed as quickly as possible immediately after the test with cool air continuously pumped to the box until the clinometer reached a relatively low temperature. Despite this, in some cases the clinometers reached temperatures 90°C higher than their normal operating temperatures but without any sign of malfunction.

3.6 GROUP1: BARE-STEEL FLUSH END-PLATE CONNECTION FIRE TESTS (FB1)

This group consists of two 254x102UB22 beams connected to a 152x152UC23 column by 8mm thick flush end-plates as shown in Fig. 3.7. All steel was Grade 43. Six M16 Grade 8.8 bolts in 18 mm diameter clearance holes were used. The thickness of the end-plate was selected to be representative of current practice[41]. A similar connection detail but with a thicker end-plate (12mm) had been used in previous experimental studies by Leston-Jones[52]. This test series was therefore chosen to provide an indication of the influence of end-plate thickness.

The design strength of the connection was calculated using the method proposed by Horne and Morris[99] based on nominal geometrical and material properties. For flush end-plate connections the connection strength was also assessed according to EC3: Annex J[40]. The relevant parameters include the connection moment capacity and stiffness, end-plate thickness, bearing resistance of the column flange and the expected failure mechanism of the connection. Most of these were assessed using both methods although the connection stiffness was determined according to EC3 only. The predicted failure mode of the connection according to EC3 was end-plate and column flange yielding whilst the Horne and Morris method predicted column flange failure. The calculated moment capacity of the connection based on Horne and Morris and EC3 methods were 22.8kNm and 19kNm respectively, using the nominal material and geometrical properties. The stiffness according to EC3 was 7.5×10^9 Nmm/rad.

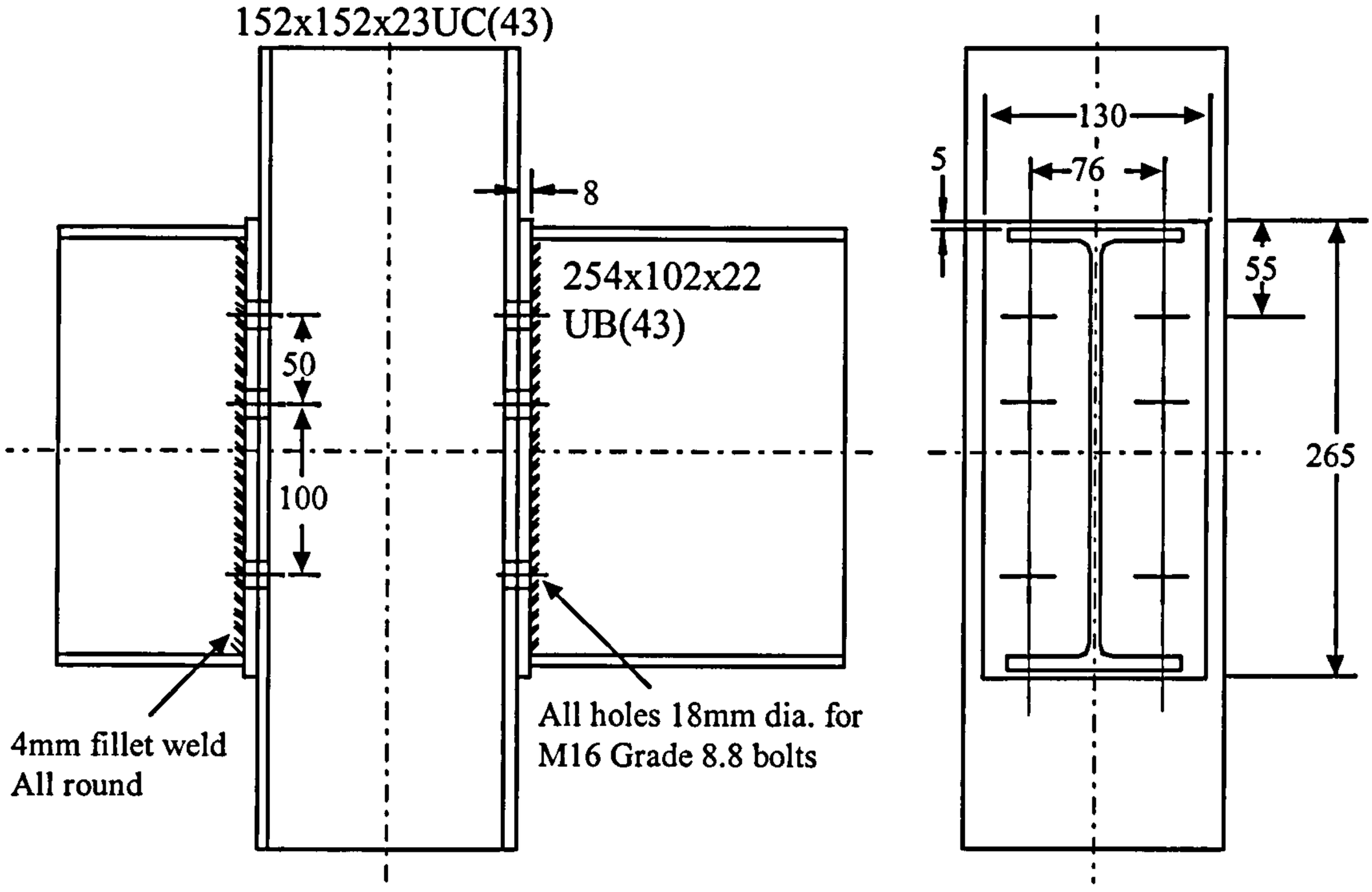

Figure 3.7: Bare-Steel Flush End-Plate Connection Detail (Group 1)

Table 3.2: Group 1: Bare-Steel Flush End-Plate Experimental Programme

Test:	*Moment Level:*	*Applied Moment:*	*Temperature:*	*Comments:*
FB11	$0.2M_{cc}$	4 kNm	10°C/minute	Group 1, Fire Test 1.
FB12	$0.4M_{cc}$	8 kNm	10°C/minute	Group 1, Fire Test 2.
FB13	$0.6M_{cc}$	13 kNm	10°C/minute	Group 1, Fire Test 3.
FB14	$0.8M_{cc}$	17 kNm	10°C/minute	Group 1, Fire Test 4.

M_{cc} = Moment capacity of the connection

In order to obtain an accurate representation of the connection characteristics over a reasonable range of temperatures, four tests were conducted. Load levels were selected based on the calculated moment capacity of the connection and the connection response obtained from the ambient temperature test conducted by Leston-Jones[52] on a similar connection but with thicker end-plate. The loads were applied at a distances of 1423 mm from the face of the column flange. The test programme for this group of tests is summarised in Table 3.2. A description of each test is given below.

3.6.1 General Observations from Group 1 Fire Tests

In all tests conducted in this group the modes of failure were similar in that the top of the end-plate deformed locally, particularly around the top bolt. This was accompanied by deformation of the column flange in the tension zone and buckling of the column web in the compression zone as shown in Fig. 3.8. There was negligible deformation of the beams along their entire length and no distortion of the bolts was observed. There was no sign of slip at the connection interface, demonstrating the efficiency of the bolts

in resisting the applied tension forces and moments, despite the effect of high temperatures in reducing the clamp force of the bolt. This mode of failure was not surprising given the relative dimensions of the end-plate and the unstiffened column flange.

The failure mode observed by Leston-Jones[52] was mainly deformation of the column flange and buckling of the column web without any deformation in the end-plate due to its excessive thickness.

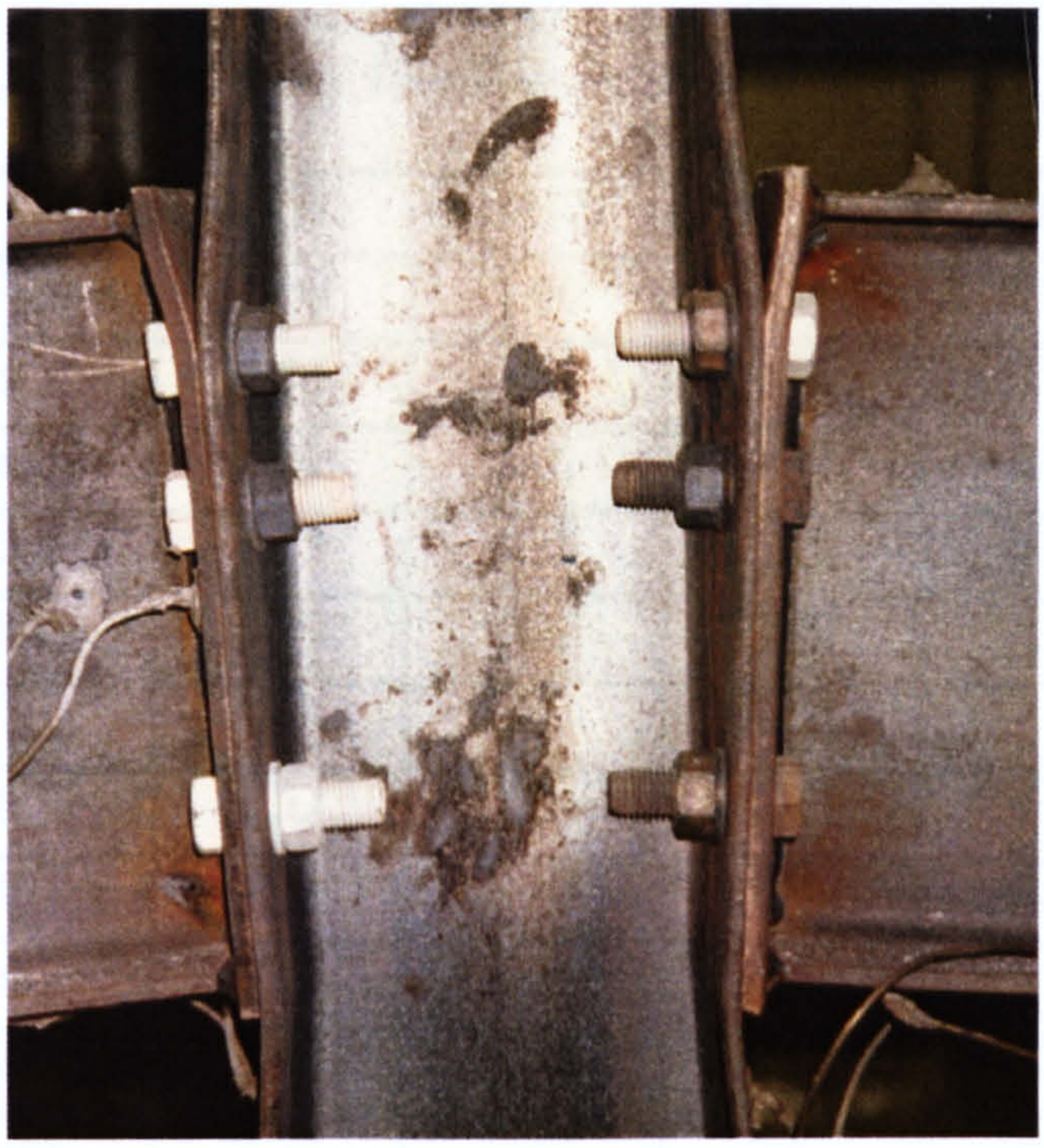

Figure 3.8: Elevated Temperature Connection Failure Mechanism for Group 1

The average relative temperature distributions across the connection are summarised for all tests in Table 3.3. The temperature distribution is presented in non-dimensional form with respect to the exposed beam bottom flange temperature (the reference for the data logging). The average relative temperature profile was determined based on the average thermocouple readings of connection elements for the East and West sides, after ensuring that the readings are consistent. Then, the relative temperature profile for each element is obtained by dividing the element temperatures by the reference temperature (beam bottom flange). The average of these values represents the average relative temperature profile as shown in Table 3.3. Although there was some variation in the relative temperature profile with increasing temperatures, this is not significant with a maximum difference of approximately 15%. In all the tests both the top and bottom flanges of the beam were left unprotected near the connection in order to allow comparison between the temperature attained by the beam top and bottom flanges and to investigate the temperature distribution across the connection depth. It was felt that insulating the beam top flange in the connection region would have negligible influence on the connection response.

It may be seen from Table 3.3 that there is negligible variation in the temperature of the exposed steel with all connection elements showing a similar temperature rise in all tests. Therefore, the connection temperatures can be represented by the average value of the beam top and bottom flange temperatures. The hottest of the connection elements was the column web which was 14% higher than the beam bottom flange temperature. The temperature attained inside the clinometer housing box was approximately 10% of the bottom flange temperature, indicating the efficiency of the cooling system devised to protect the instrument. Also it may be seen that the average atmospheric temperature recorded was approximately 38% higher than the bottom flange temperature.

Table 3.3: Average Relative Temperature Profiles for Group 1 Tests

Element:	*FB11:*	*FB12:*	*FB13:*	*FB14:*	*Average:*
Beam Bottom Flange	1.00	1.00	1.00	1.00	1.00
Beam Web	1.04	1.03	1.06	1.10	1.06
Beam Top Flange	1.02	1.02	1.02	1.01	1.02
Beam Top Flange*	0.43	0.37	0.35	0.37	0.38
Beam Bottom Flange*	0.39	0.37	0.40	0.37	0.38
Top Bolt	1.04	1.01	1.07	1.05	1.04
Middle Bolt	1.02	1.01	1.03	1.05	1.03
Bottom Bolt	1.02	0.98	1.01	1.02	1.01
Column Web	1.10	1.14	1.14	1.16	1.14
Column Flange	1.00	1.03	1.04	1.03	1.03
Column Flange*	0.52	0.47	0.44	0.43	0.47
End-plate	1.03	1.00	1.04	1.03	1.03
Clinometer	-	0.09	0.10	0.10	0.10
Furnace Atmosphere	-	1.43	1.37	1.35	1.38

Note: * identifies insulated thermocouple locations

3.6.2 Group 1: Fire Test 1 (FB11)

A relatively low moment of approximately 4 kNm was applied to the connection in order to obtain results for the connection stiffness in the elastic zone. The results are shown in Fig. 3.9. It may been seen from Fig. 3.9*(a)* that there is a higher moment applied to the West beam than the East beam. The difference remains almost constant up to a temperature of about 500°C when there is some fluctuation in the load cell readings. At temperatures exceeding 700°C, the moments recorded for both beams became variable with a sudden increase in the moment applied to the East beam followed by a gradual reduction whilst there is a rapid reduction in the moment applied to West beam. This occurred towards the end of the test due to the absence of ball seating in the load cells. This resulted in uncontrollable loading with increasing rotations because of the angle of bearing of the loads on the load cells and large

curvature of the loaded beams. Moreover, as the West connection failed, the load applied to the West beam reduced rapidly due to the inability of the connection to resist the applied moment. This was compensated for by a sudden increase in the East beam moment to maintain equilibrium within the specimen. In the subsequent analysis of the results, the average connection moment was used. This was found to be in the range of 4.4 kNm.

As the test progressed it was observed that the temperature inside the clinometer housing boxes increased at a higher rate than expected up to a temperature of about 570°C when the clinometers started to give inaccurate readings. Inspection after the completion of the test revealed that the cables of the clinometers and the air pipes were destroyed during the test due to inadequate insulation. Therefore, measurements of connection rotations had to be based on the readings obtained from the displacement transducers, together with the average clinometer readings before destruction.

Rotations obtained from displacements for the East and West connections are compared in Fig. 3.9*(c)*, from which it can be seen that the East connection was capable of resisting temperature up to 575°C without experiencing any significant rotation. Rotation of the West connection is greater over the complete range of temperatures. This is probably due to the higher level of loading recorded for the West beam throughout the test. However, the difference between the rotations at temperatures exceeding 690°C becomes negligible. There is an approximately linear increase in rotation up to temperatures around 575°C. Beyond this there is a curved knee due to the yielding of one or more components within the connection. At temperatures in excess of 700°C, as the connection approaches failure, the rate of rotation increases rapidly, resulting in a plateau in the connection behaviour. The average rotations recorded by displacement transducers and clinometers (before malfunctioning) are compared in Fig. 3.9*(d)* and are in very good agreement.

3.6.3 Group 1: Fire Test 2 (FB12)

For this test, the loading was increased to provide an applied connection moment of approximately 8 kNm. Results are shown in Fig. 3.10. The test was performed in a similar manner to the first test. Despite serious attempts to maintain consistent load levels over the East and West beams, there was a significant, but almost constant variation in the applied moments throughout the test as shown in Fig. 3.10*(a)* probably for the same reasons as in the first test. The average moment applied to the connections was approximately 8.2 kNm.

Fig. 3.10*(b)* shows rotations of the connection obtained from clinometers. It may be seen that there is a good agreement between the East and West connection despite the difference in the level of loading. Also, there is indiscernible difference between the rotations recorded by displacement transducers as shown in Fig. 3.10*(c)*. From the rotations recorded by both methods, it may be seen that the connection sustains temperatures up to 500°C without undergoing significant rotation. The rotation-temperature response then follows a curved shape as the connection enters a state of plastification and the rotations increase progressively as the connection approaches failure. The failure temperature of the connection is reduced in comparison with the first test due to the increased level of moment applied to the connections.

3.6.4 Group 1: Fire Test 3 (FB13)

A moment of approximately 13 kNm was applied to the connection in the third test. Results obtained from this test summarising the connection response are shown in Fig. 3.11. To avoid the variation in the moment levels applied to the beams observed during the previous two tests, the loading procedure was carefully monitored to ensure all devices were working properly. This resulted in a consistent loading for both connections throughout the test as seen in Fig. 3.11*(a)*. The average recorded moment applied was approximately 13.12 kNm. The failure mode of the connection observed was similar to those in the previous tests.

Rotations recorded from both clinometers are shown in Fig. 3.11*(b)*. It can be seen that there was some slight variation between the response measured for the East and West beams, with the East beam rotating approximately 4 millirads more at ambient temperature. However, the rotations obtained from displacement transducers show good correlation between the two connections as seen in Fig. 3.11*(c)*. Examination of clinometer and displacement devices revealed no problems, suggesting that the asymmetrical behaviour was probably due to rotation of the test arrangement. Fig. 3.11*(d)* compares the average rotations obtained from displacement and clinometer readings, showing reasonable agreement.

3.6.5 Group 1: Fire Test 4 (FB14)

The final elevated temperature test in Group 1 was conducted for a nominal moment of 17 kNm. Fig. 3.12 summarises the connection response obtained from the test. The failure mechanism was similar to that observed in previous tests but the distortions were more pronounced due to the increased load level and resulting deformations at low temperatures. It may be seen from Fig. 3.12*(a)* that the load level for both East and West beams was indiscernible throughout the test. The average moment applied to the connection recorded was approximately 17.1 kNm. Also, it may be seen from Fig. 3.12*(d)* that the connection rotations recorded by clinometers and displacement transducers compare well.

3.6.6 Comparison of Results from Group 1 Elevated Temperature Connection Tests

Initial rotations of the connection under loading at ambient temperature are shown in Fig. 3.13, together with results from an ambient temperature test conducted by Leston-Jones on a similar connection but with a thicker end-plate. It may be seen that the two sets of results are similar but the thinner end plates give a more flexible response.

From these tests the temperature-rotation curves at a number of load levels can be defined, enabling the derivation of a set of moment-rotation curves at increasing temperature. The temperature-rotation relationships obtained are shown in Fig. 3.14, and show a progressive degradation in the strength and stiffness of the connection with increasing temperature and load. The temperature-rotation response presented for the first test was based solely on the average displacement transducer readings, due to failure of clinometer connecting cables at about 570°C giving erratic results for the rest

the of the test. The connection responses for the remaining tests are based on the average clinometer readings since there was negligible difference between rotations obtained from both displacement and clinometer readings. However, there is a slight variation in the ambient temperature response between clinometer rotations recorded for East and West connections in test FB13 which may be attributed to actual rotation of the testing arrangement.

3.7 GROUP 2: BARE-STEEL FLUSH END-PLATE CONNECTION FIRE TESTS (FB2)

The connection detail for Group 2 comprised a pair of 356x171UB51 beams in Grade 50 steel connected to a 254x254UC89, also Grade 50 steel, by 10mm thick flush end-plates with eight M20 Grade 8.8 bolts in 22mm diameter clearance holes as shown in Fig. 3.15. These represent medium-sized sections within the standard range. One of the purposes of these tests was to provide an indication on the influence of member sizes on the performance of steel connections at elevated temperatures.

Both the Horne and Morris method and EC3 design recommendations were used to assess the moment capacity of the connection based on specified material and geometrical properties. The parameters considered in assessing the connection strength were as for the Group 1 connections. The failure mechanism of the connection predicted by the Horne and Morris method was yielding of the end-plate with the column flange and web being sufficiently stiff to resist the applied force in the tension and compression zones without the need to provide stiffeners. The predicted failure mode according to EC3: Annex J was also failure of the end-plate in bending with all other connection components able to resist the applied load. The predicted moment capacity of the connection at ambient temperature was 90 kNm and 141.2 kNm according to EC3 and Horne and Morris respectively. It was expected that the actual moment capacity of the connection would exceed this and therefore the load level for each test was determined on the basis of a connection strength of 140 kNm. In order to achieve an ideal representation of the connection response over the complete loading spectrum, four elevated temperature tests were performed under constant load and increasing temperatures. Loads were applied at 1370mm from the face of the column flange. The test procedure adopted and instrumentation devices used were similar to those described for Group 1, although the load cells were re-calibrated for the new load levels. The test programme is summarised in Table 3.4. Individual tests are described in the sections below.

Table 3.4: Group 2: Bare-Steel Flush End-Plate Experimental Programme

Test:	*Moment Level:*	*Applied Moment:*	*Temperature:*	*Comments:*
FB21	$0.2M_{cc}$	27 kNm	10°C/minute	Group 2, Fire Test 1.
FB22	$0.4M_{cc}$	56 kNm	10°C/minute	Group 2, Fire Test 2.
FB23	$0.6M_{cc}$	82 kNm	10°C/minute	Group 2, Fire Test 3.
FB24	$0.8M_{cc}$	110 kNm	10°C/minute	Group 2, Fire Test 4.

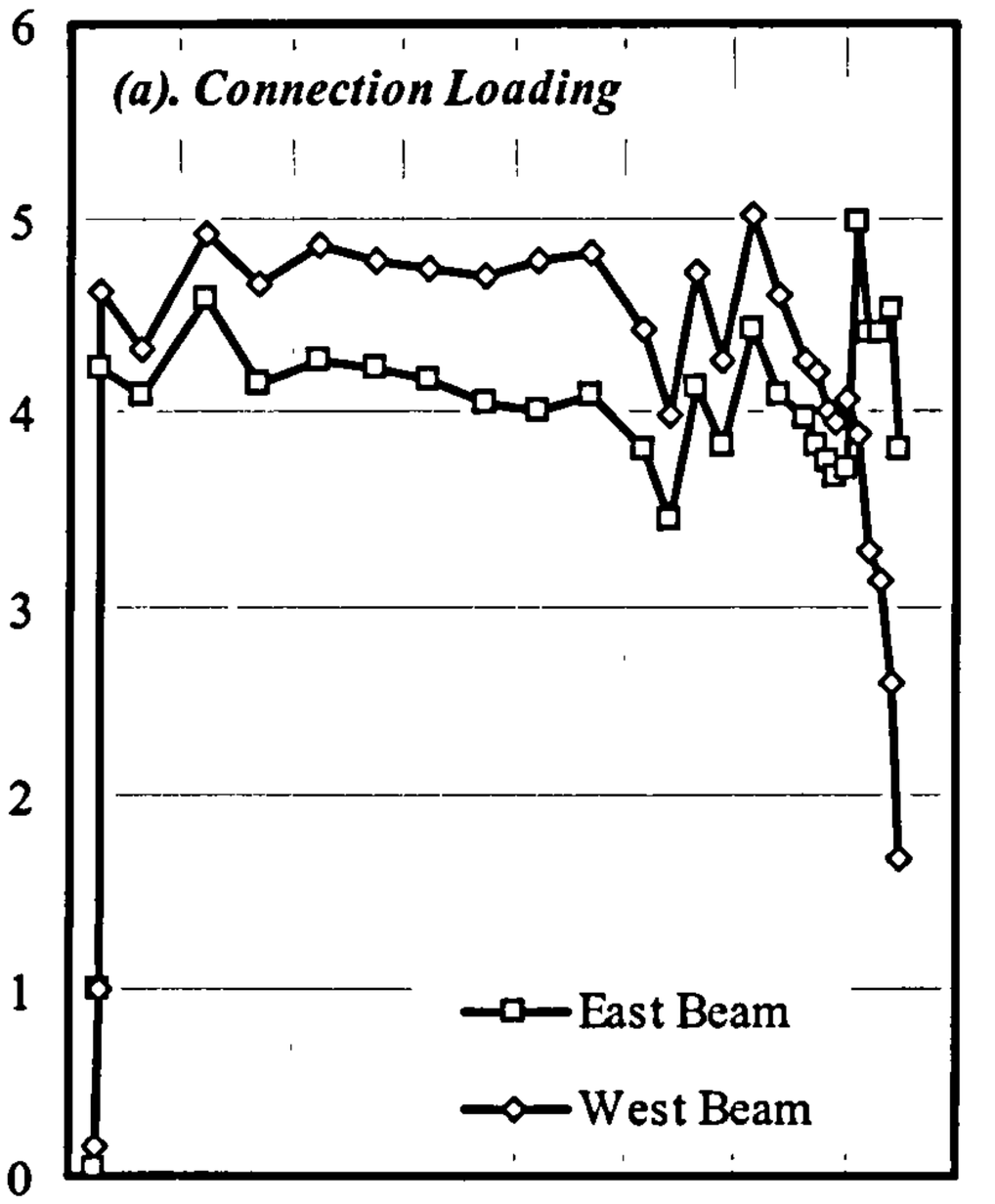

Figure 3.9: Summary of Results from Group 1: Fire Test 1 (FB11)

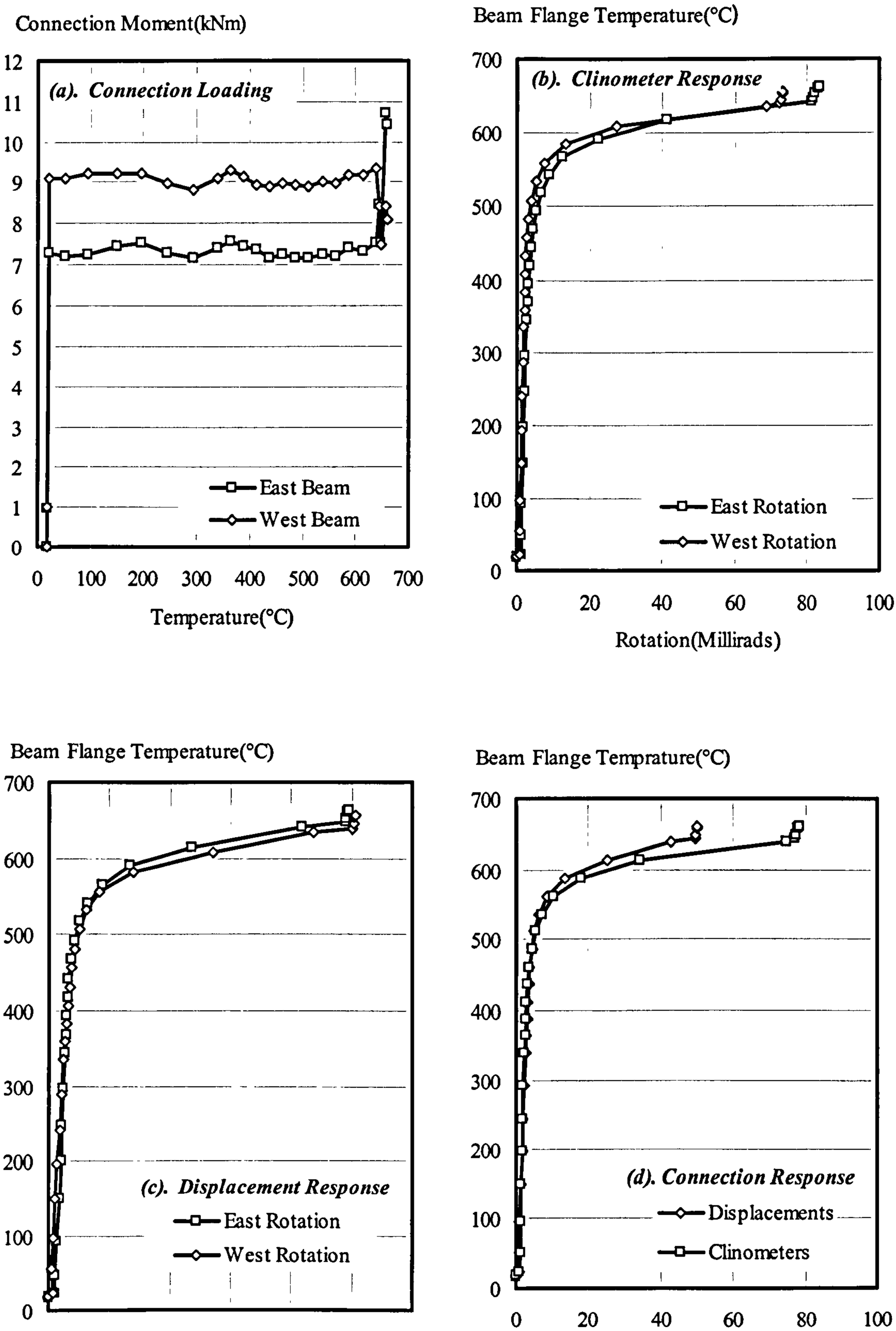

Figure 3.10: Summary of Results from Group 1: Fire Test 2 (FB12)

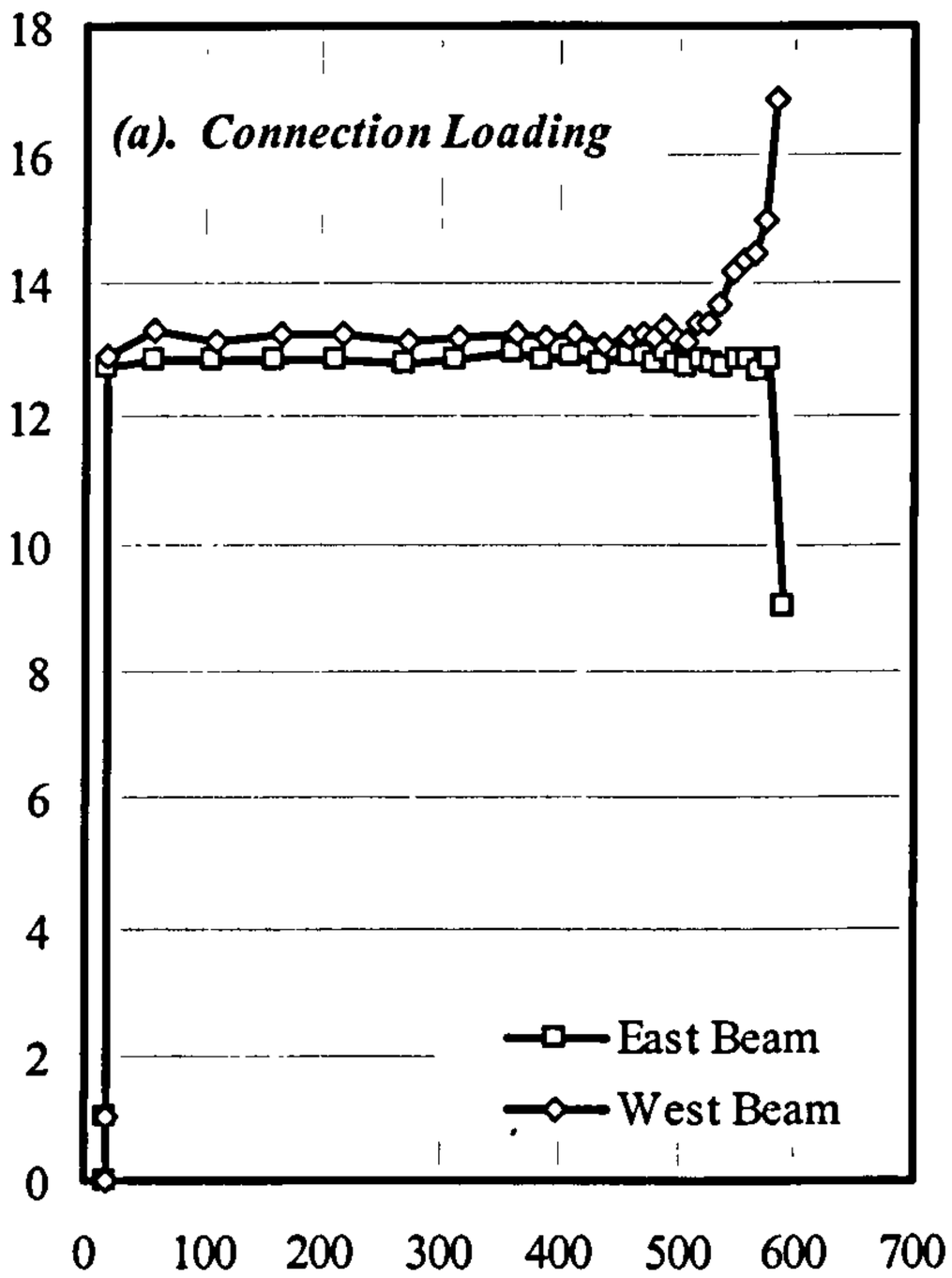

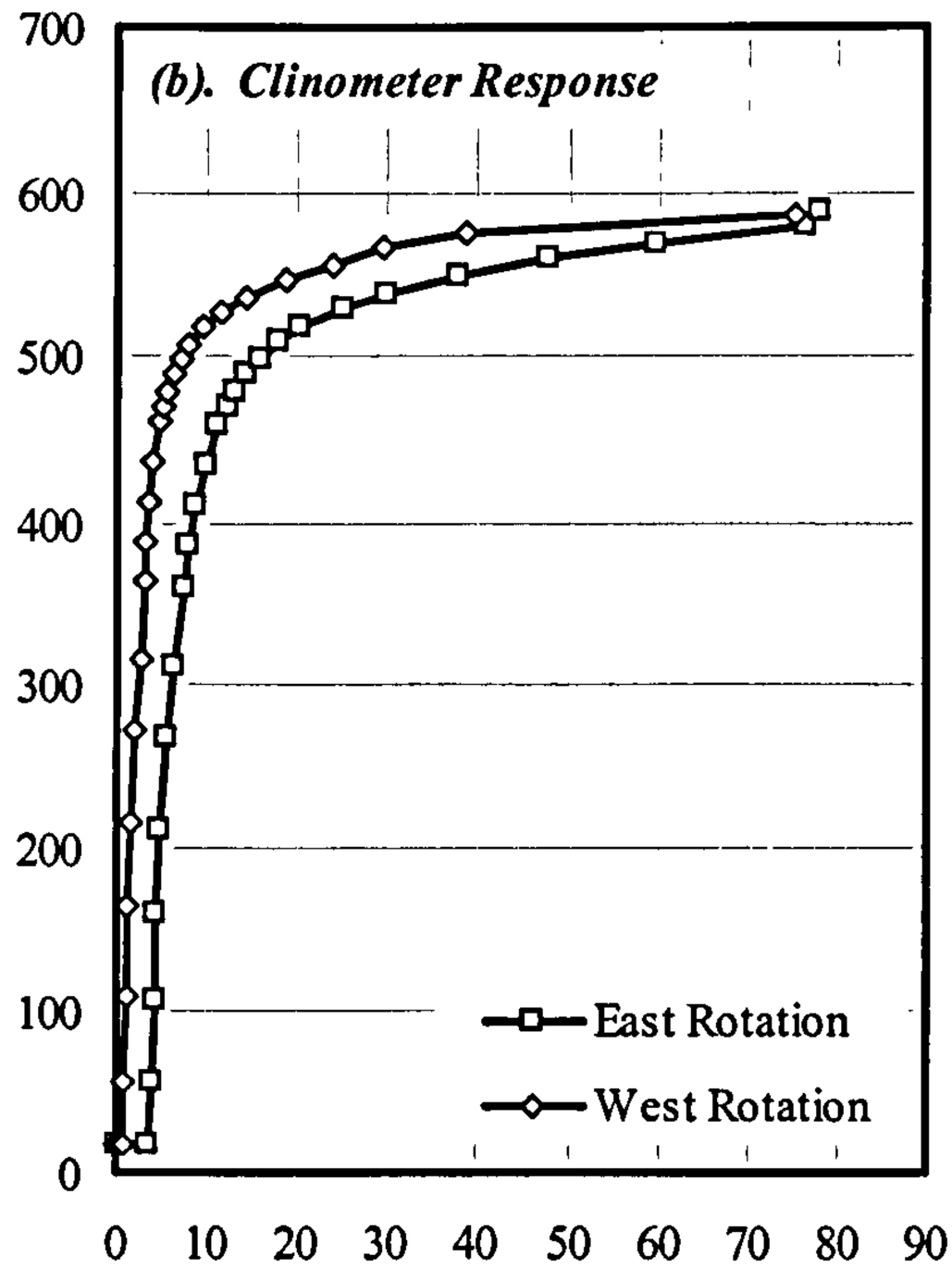

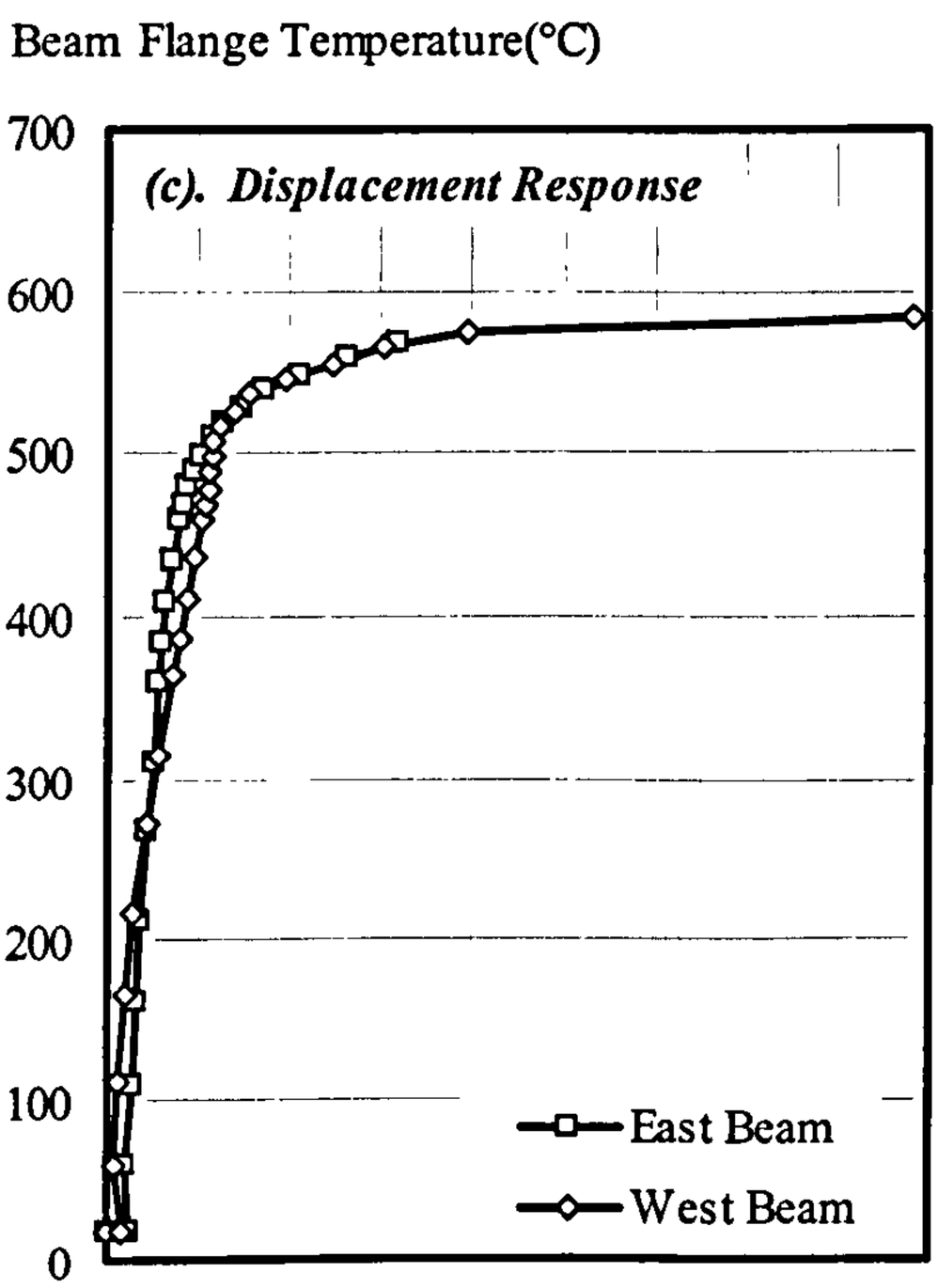

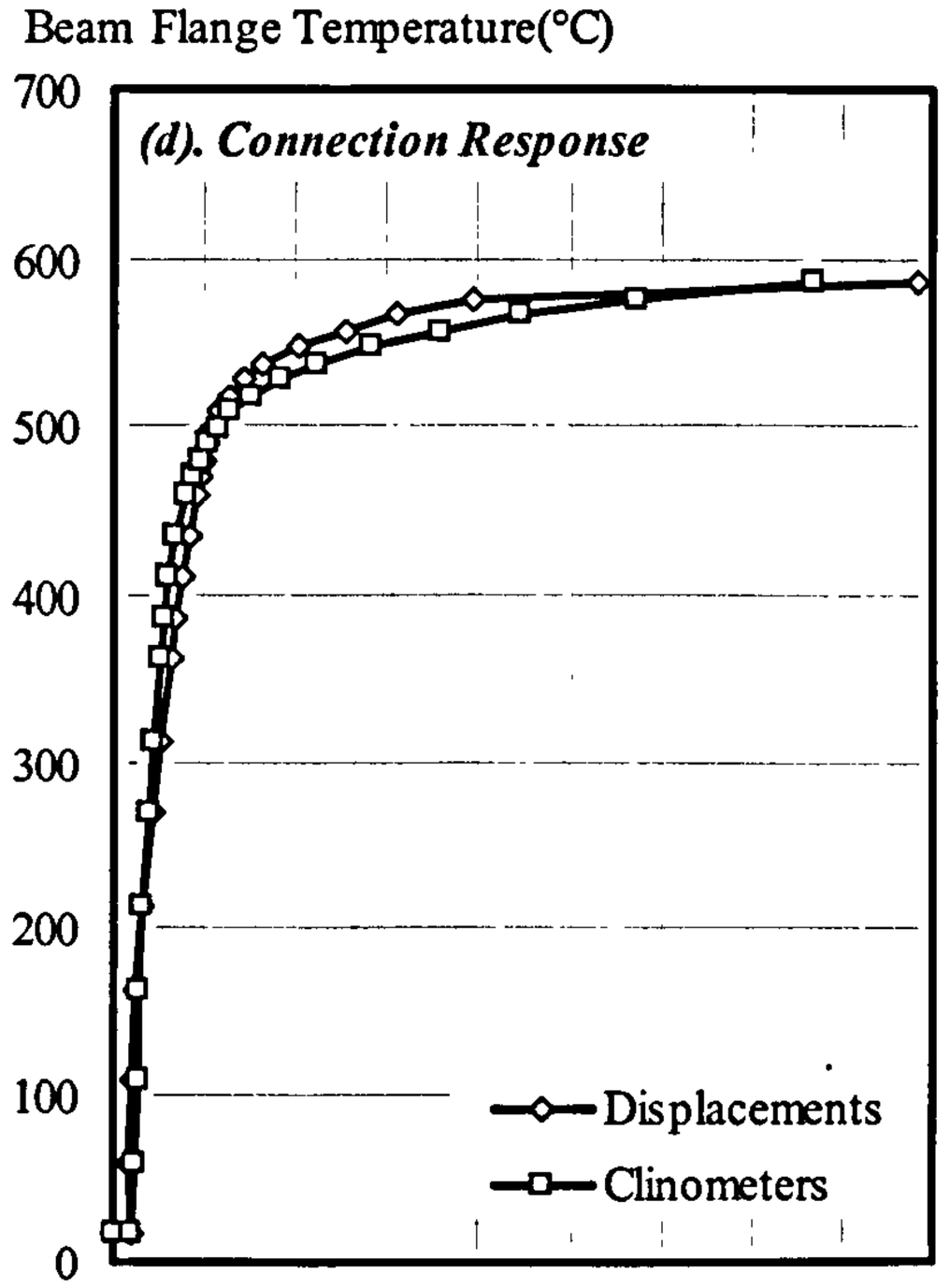

Figure 3.11: Summary of Results from Group 1: Fire Test 3 (FB13)

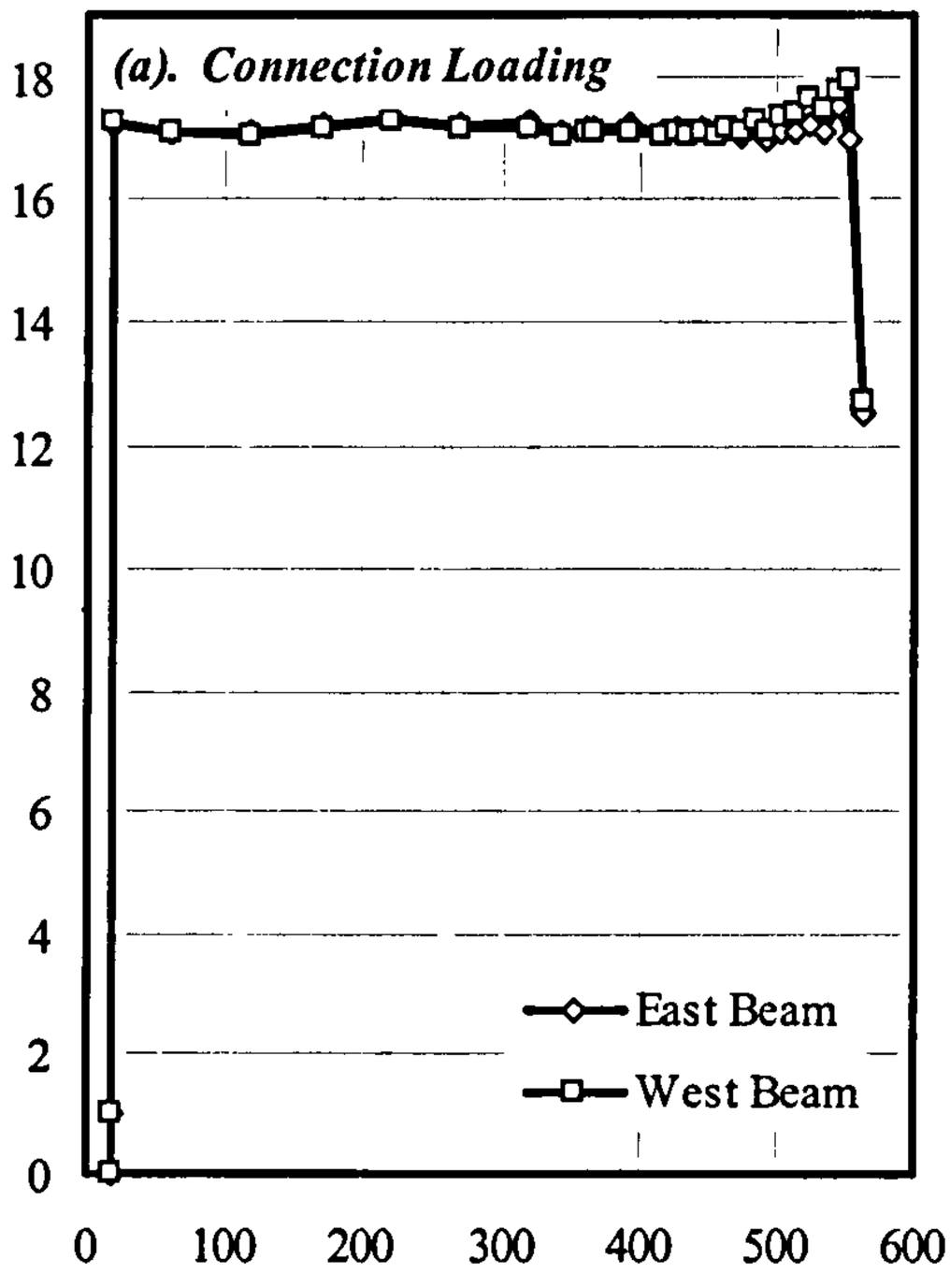

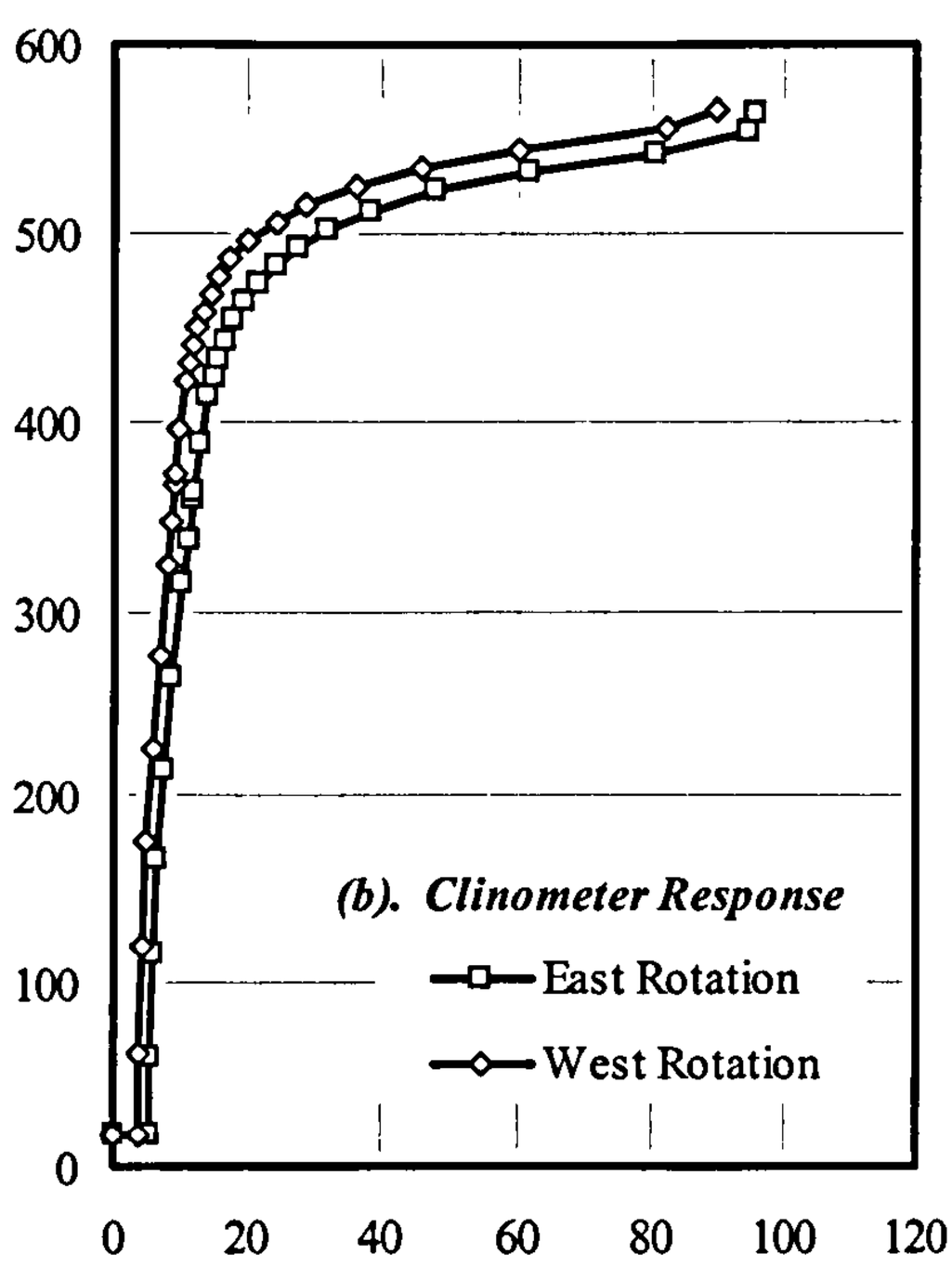

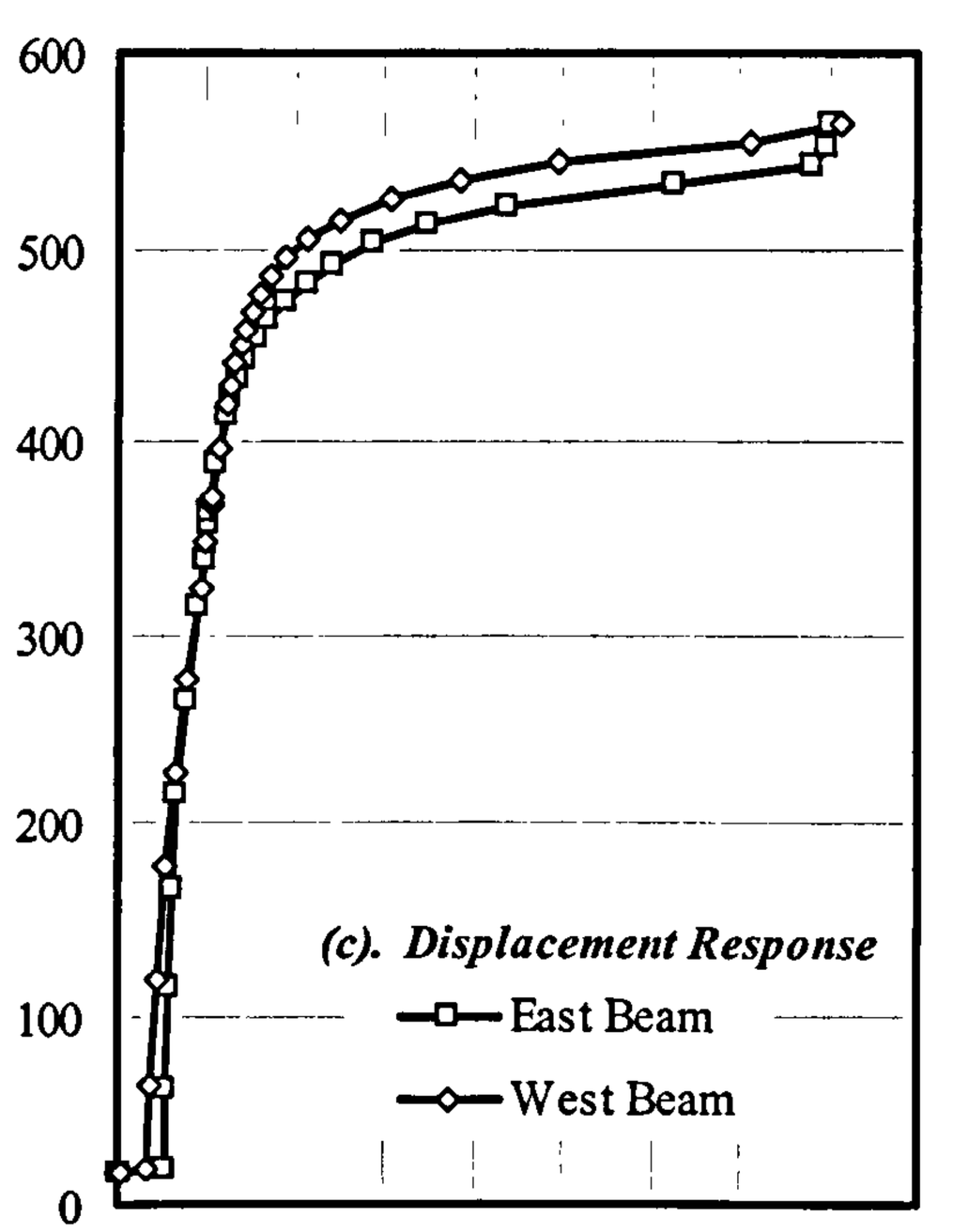

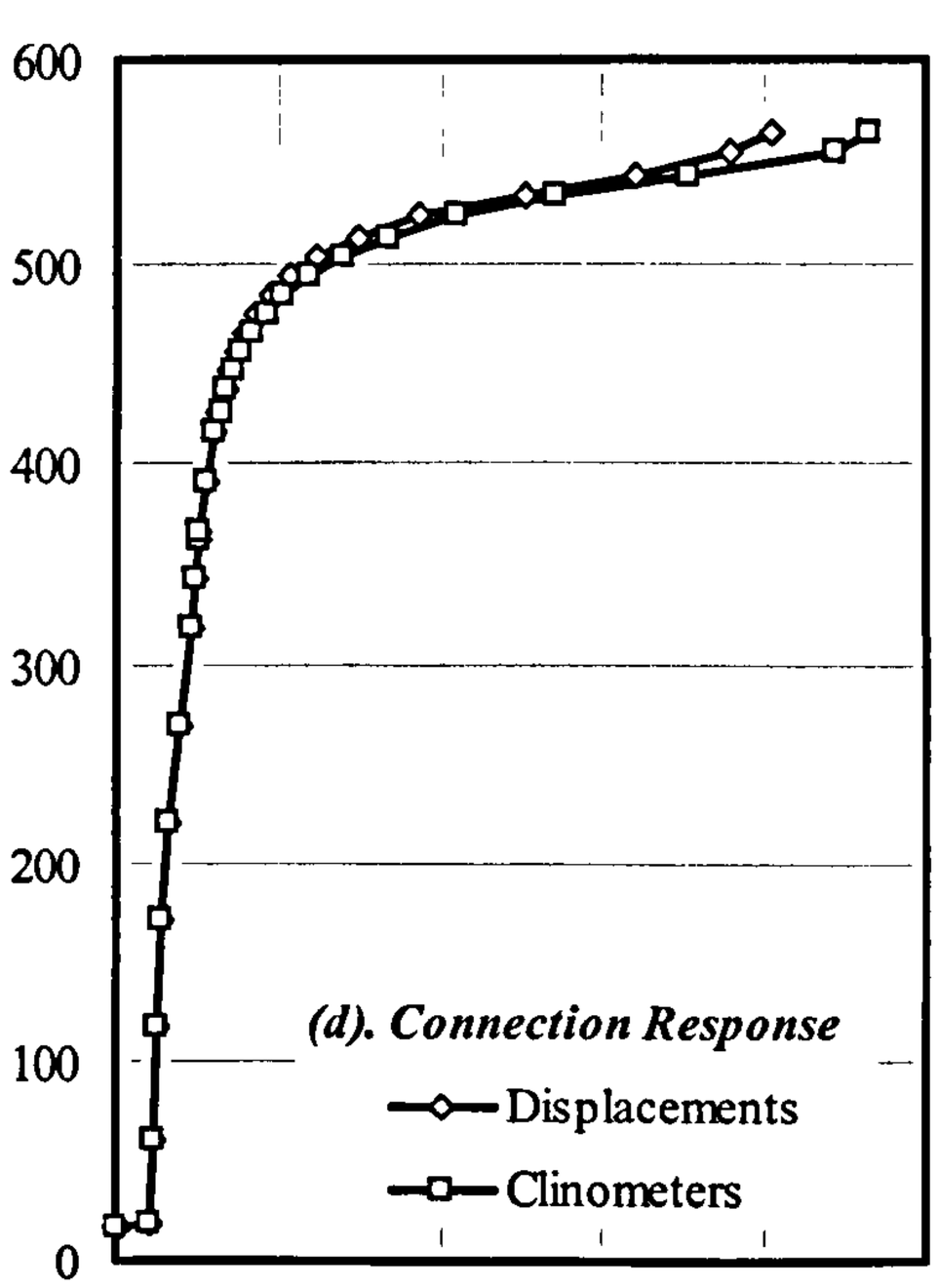

Figure 3.12: Summary of Results from Group 1: Fire Test 4 (FB14)

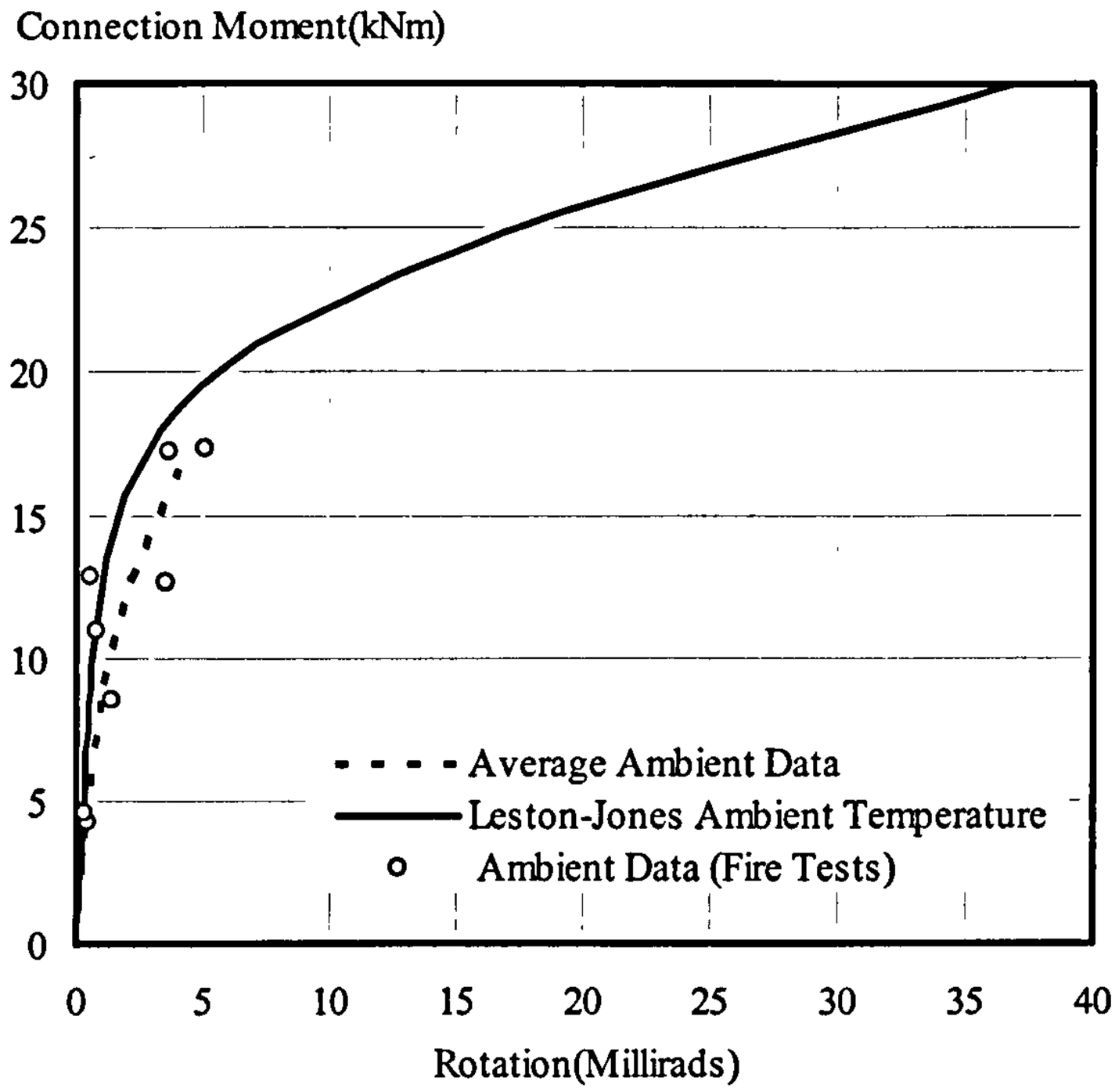

Figure 3.13: Ambient Temperature Response Compared to Ambient Temperature Data from Group 1 Fire Tests

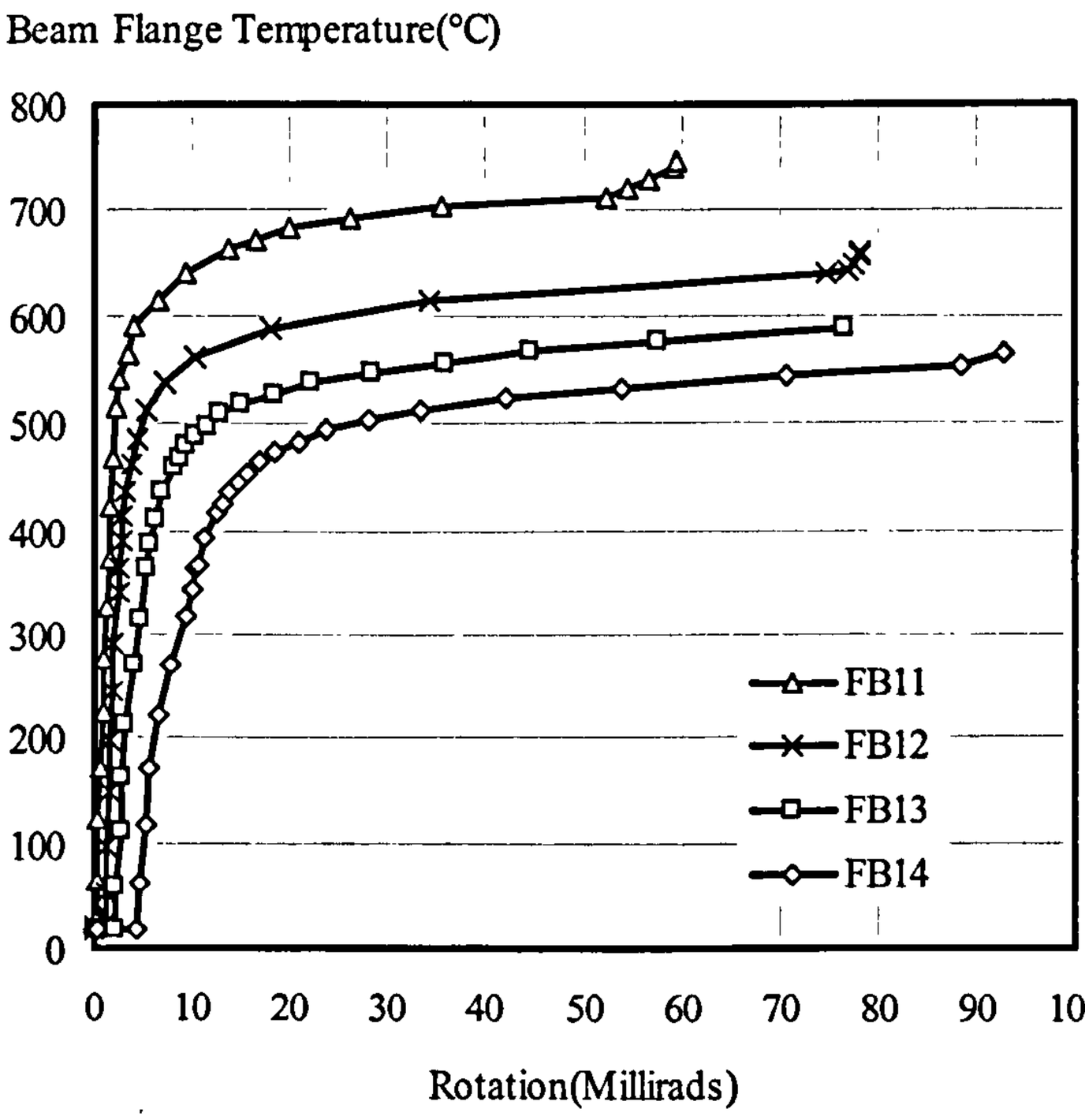

Figure 3.14: Elevated Temperature Connection Response of Group 1 Tests

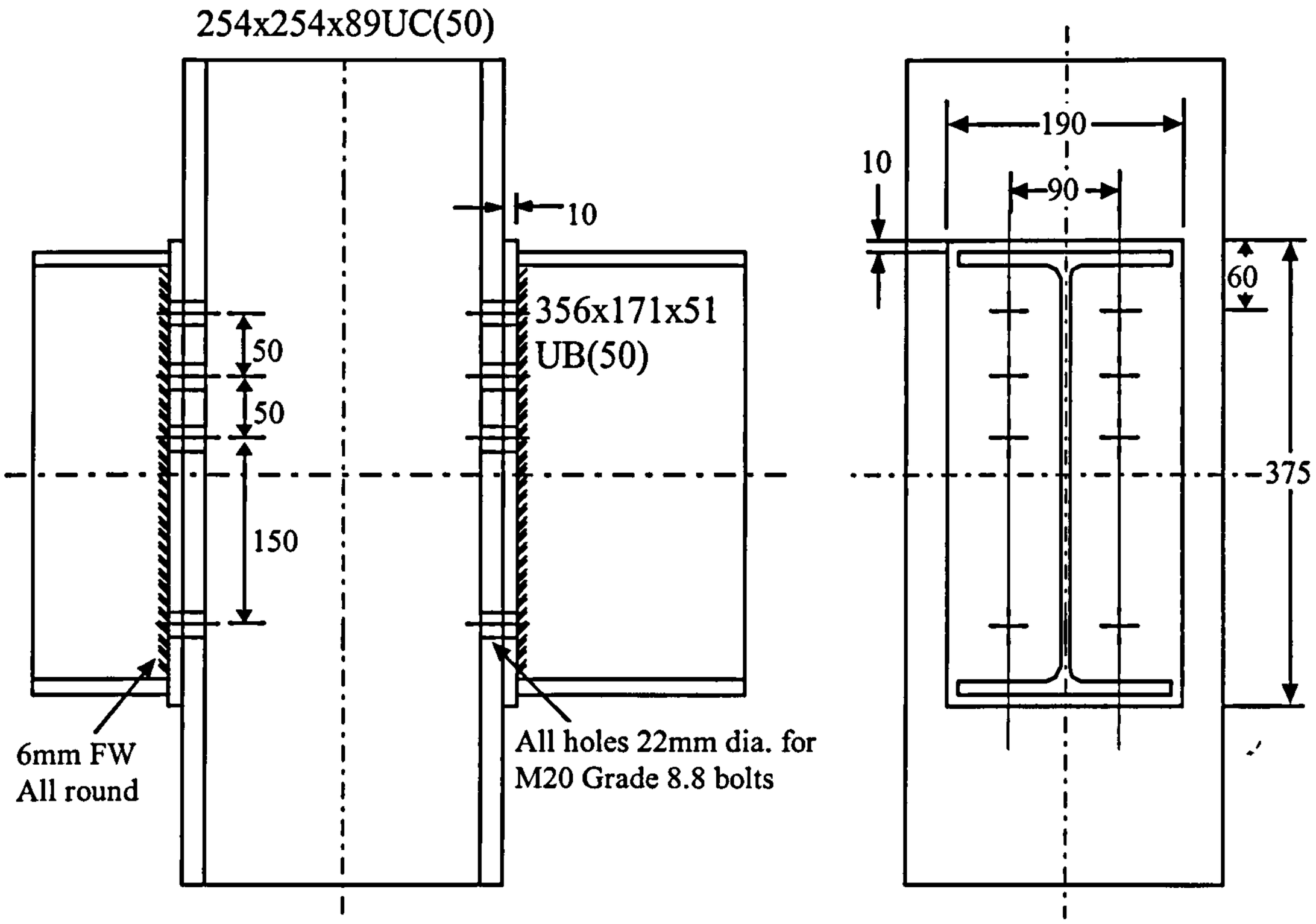

Figure 3.15: Bare-Steel Flush End-Plate Connection Detail (Group 2)

3.7.1 General Observations from Group 2 Fire Tests

Four elevated temperature tests were conducted in the second series on flush end-plate connections with the primary aim of establishing the degradation of the connection characteristics at elevated temperatures by means of moment-rotation-temperature curves. The test arrangement was chosen to be representative of medium-sized connections used in practice.

Consistent failure mechanisms were observed for all of the fire tests conducted under Group 2. In each case a localised deformation developed in the top of the end-plate as shown in Fig. 3.16, without any damage to the beams and the column along their entire lengths. This is different to some extent from the failure mode observed in the Group 1 tests. This is mainly due to the much larger member sizes, whereas the end-plates are only slightly thicker. The mechanism was more apparent as the load level increased. The most unusual aspect was the slipping of the top bolts at the connection interface in the tension zone as illustrated in Fig. 3.16*(b)*. There are two possible reasons for this:

- a low bolt clamp force as a result of insufficient torque applied when tightening the bolts, or
- high temperature softening of the bolts, particularly the top bolts which are in greatest tension, causing a reduction in the clamping force at temperatures in excess of 350°C[86].

Unfortunately it was not possible to confirm the exact cause of this behaviour due to the difficulty in viewing the specimen during testing since it was contained within the furnace. However, it is believed that the first cause is unlikely since all bolts were carefully tightened to 160 Nm by a torque wrench ensuring good consistency typical of

site practice[93]. Such slipping was not experienced in Group 1 tests since the failure of those connections was not concentrated within the top part of the end-plate alone but also involved deformation of the column flange and buckling of the column web.

At high load levels in tests FB23 and FB24, cracks in the end-plate were observed along the toe of the welds which connect the end-plate to the beam. In contrast the welds exhibited exceptional robustness without any sign of cracks. The only deformation observed in the bolts was slipping of the top bolts.

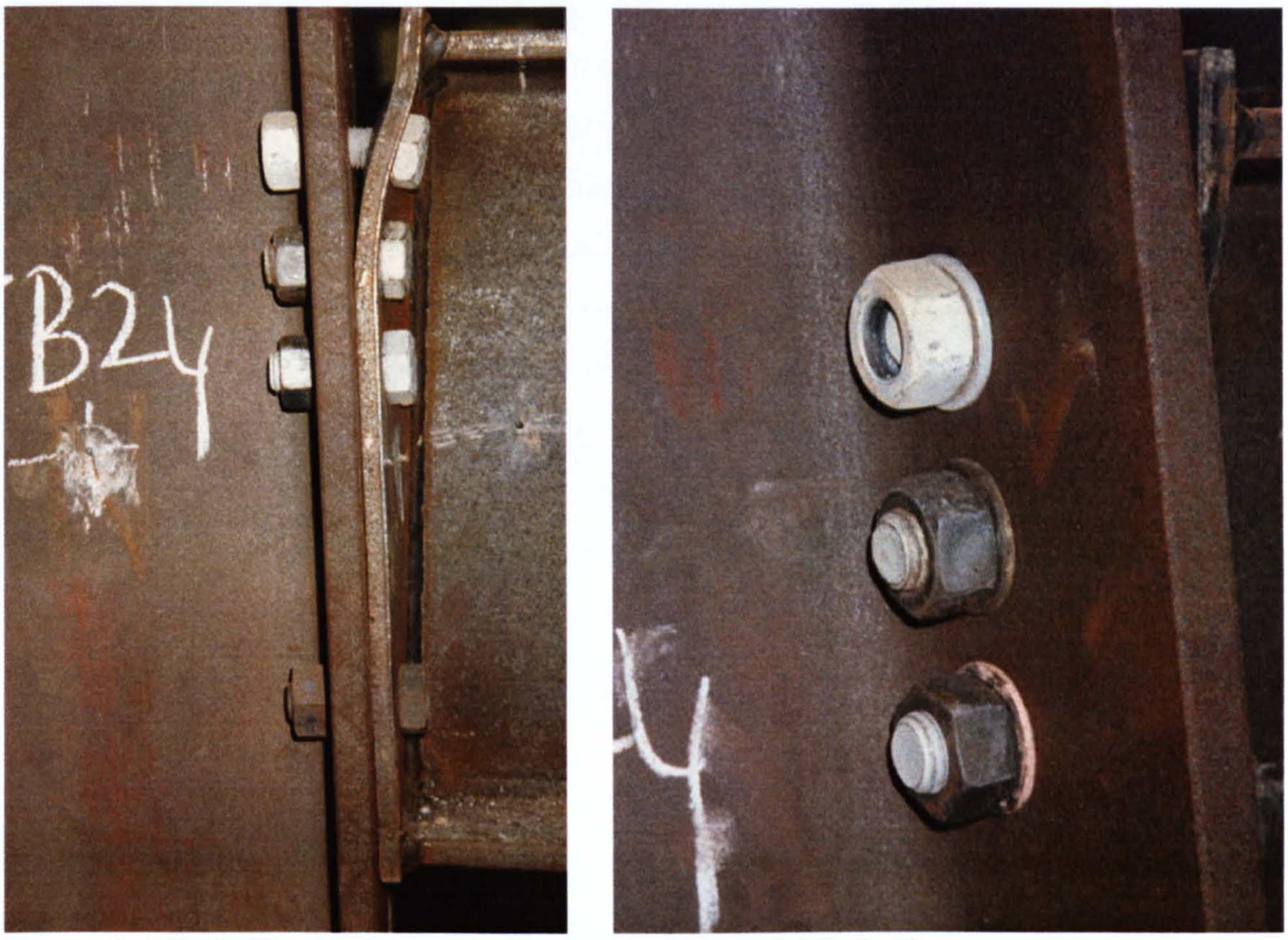

(a) End-plate Deformation *(b) Bolt Slip*

Figure 3.16: Elevated Temperature Connection Failure Mechanism for Group 2

Table 3.5 shows the average relative temperature profiles of the connections. The temperature distribution across the depth of the connection is almost linear. The firing operating system in the furnace was designed to create a uniformly heated environment throughout the furnace with a comparatively slow rate of heating. Once more, the average temperature profile for the four tests is shown as a proportion of the beam bottom flange temperature with the average temperatures of the beam top and bottom flanges being selected to represent the connection temperature. The hottest temperature was in the column web, approximately 21% higher than the beam bottom flange temperature. There was a uniform temperature distribution across the depth of the connection with the beam web temperature being 6% greater than the beam bottom flange. Once again, the temperature achieved within the housing box was 11% of the beam bottom flange whereas the average atmosphere temperature was recorded to be 66% greater than the beam bottom flange temperature.

Table 3.5: Average Relative Temperature Profiles for Group 2 Tests

Element:	*FB21:*	*FB22:*	*FB23:*	*FB24:*	*Average:*
Beam Bottom Flange	1.00	1.00	1.00	1.00	1.00
Beam Web	1.06	1.04	1.10	1.02	1.06
Beam Top Flange	1.03	1.00	1.01	1.02	1.02
Beam Top Flange*	0.47	0.38	0.36	0.43	0.41
Beam Bottom Flange*	0.45	0.37	0.36	0.42	0.40
Top Bolt	1.06	0.97	1.04	0.99	1.02
2nd Row Bolts	1.03	0.96	1.05	0.96	1.00
3rd Row Bolts	1.08	0.97	1.04	0.95	1.01
Bottom Bolt	0.97	0.94	0.97	0.91	0.95
Column Web	1.15	1.20	1.27	1.23	1.21
Column Flange	0.90	0.97	1.00	1.03	0.98
Column Flange*	0.38	0.34	0.36	0.37	0.36
End-plate	1.00	0.99	1.01	0.99	1.00
Clinometer	0.11	0.09	0.09	0.14	0.11
Furnace Atmosphere	1.64	1.61	1.68	1.71	1.66

Note: * identifies insulated thermocouple locations

3.7.2 Group 2: Fire Test 1 (FB21)

The first test in Group 2 was conducted at a comparatively low load level, corresponding to a moment at the connection of approximately 27 kNm. This was applied in two equal increments. Results from the test are shown in Fig. 3.17. It may be seen from Fig. 3.17*(a)* that there is good consistency in the moment level applied to the East and West connections. The average moment was 27.4 kNm.

Rotations recorded by clinometers and displacement transducers are shown in Fig. 3.17*(b)* and 3.17*(c)* respectively showing that the connection is capable of resisting temperatures up to nearly 450°C with little rotation. At temperatures in excess of 450°C there is a curved knee in the temperature-rotation response up to approximately 630°C, indicating yielding of one or more elements within the connection. After that there is a rapid increase in the connection rotation causing a flat plateau in the response prior to failure. Also, it may be seen that there is close agreement between the recorded rotations for the East and West connections. Fig. 3.17*(d)* compares the average connection rotations recorded by clinometers and displacement transducers with indiscernible difference between the two up to temperatures of approximately 600°C. Above this, however, the displacement transducers do suggest a slightly stiffer connection.

3.7.3 Group 2: Fire Test 2 (FB22)

In this test the moment applied to the connection was approximately 56 kNm, applied in four equal increments and the results are summarised in Fig. 3.18. There was a slight decrease in the level of moment applied to both beams with increasing temperature, with a lower moment being applied to the West beam throughout. This may be due to friction on the Macalloy bars as they passed through small holes in the laboratory strong floor. The average connection moment was recorded to be 54.8 kNm. Comparison of the average rotations recorded by clinometers and displacement transducers demonstrates very close correlation with the clinometers predicting slightly higher connection rotation.

3.7.4 Group 2: Fire Test 3 (FB23)

A moment of approximately 82 kNm was applied to the connection in the third test in six equal steps and the test results are summarised in Fig. 3.19. The main purpose behind conducting the initial ambient temperature loading in increments was to establish the connection response at ambient temperature and to compare the results with the average moment-rotation response of the connections utilised in the elevated temperature tests. The average moment applied to the connections was measured as 82.1 kNm. Unfortunately, at the beginning of the test, the column head displacement transducer measuring the column expansion lost contact with the column, leading to erratic readings for the column expansion. This was not discovered until the test was well advanced. Rotations based on displacement measurements were therefore calculated based on the predicted thermal expansion of the column.

The connection response obtained from clinometers and displacement transducers are shown in Figs. 3.19*(b)* and 3.19*(c)* respectively. It may be seen that there is some discrepancy in the response of the East and West beams, with the West beam showing greater rotations at ambient temperature. The average rotations recorded by clinometers and displacement readings are shown in Fig. 3.19*(d)* and compare well.

3.7.5 Group 2: Fire Test 4 (FB24)

The final elevated temperature test in Group 2 was carried out for a moment of 110 kNm, applied in eight increments. The connection response is summarised in Fig. 3.20 and is similar to that of the previous tests, but with further reduction in the connection characteristics with increasing temperatures due to the higher load level applied. The failure mode observed was also similar.

There is very close agreement between the rotations of the East and West connections obtained from clinometers and displacement transducer readings as shown in Figs. 3.20*(b)* and 3.20*(c)* respectively with consistent initial loading. Average rotations recorded by clinometers and displacements transducers compare well as shown in Fig. 3.20*(d)*.

3.7.6 Comparison of Results from Group 2 Elevated Temperature Connection Tests

The initial loading response of the connection for all elevated temperature tests is illustrated in Fig. 3.21. This includes the rotations obtained from clinometers and displacement transducers for both connections together with the average response obtained from all tests. It may be seen that there is good agreement between the rotations of the East and West connections for each test. However, rotations obtained from test FB24 do suggest slightly stiffer connection than FB23 connection. The connection response for test FB23 follows closely the average general connection response obtained from all the elevated temperature tests.

Fig. 3.22 shows the temperature-rotation response for Group 2 tests based on the average clinometer readings for the East and West beams. The tests were performed satisfactorily with close correlation observed between the rotations recorded by both rotation devices. It may be seen that there is a reduction in the connection stiffness with increasing load levels and temperatures with similarity in the response to Group 1 tests. Rotations from displacement transducers for test FB23 were calculated based on the predicted thermal column expansion due to the failure of the transducer that measures the column expansion. The slight discrepancy in the ambient temperature rotation between the East and West connections in test FB23 may be occurred as a result of rotation of the test arrangement.

3.8 GROUP 3: BARE-STEEL FLEXIBLE END-PLATE CONNECTION FIRE TESTS (FLB3)

The specimen detail for this group of tests was identical to that for Group 2 but with a flexible end-plate of reduced thickness - 8mm. The detail was chosen as typical of the connections used in the Cardington full-scale test frame. By comparing with the results of Group 2, the influence of end-plate detail can be assessed. The connection details are illustrated in Fig. 3.23. The end-plate thickness was selected based on recommendations adopted in SCI/BSCA publication: *"Design methods for Joints in Simple Construction Volumes 1*[41] *and 2*[42]*"*.

Due to the lack of design recommendations for flexible connections the moment capacity was calculated by modifying the method proposed by Horne and Morris[99] for flush and extended end-plate connections. The centre of rotation was assumed to be at the lower edge of the end-plate at a distance of 5mm from the edge. The calculated moment capacity of the connection based on the modified Horne and Morris method was found to be 83.76 kNm. An ambient temperature test has been conducted on a similar connection by Boreman *et al.*[100] indicating an ultimate moment capacity of the connection of approximately 100 kNm.

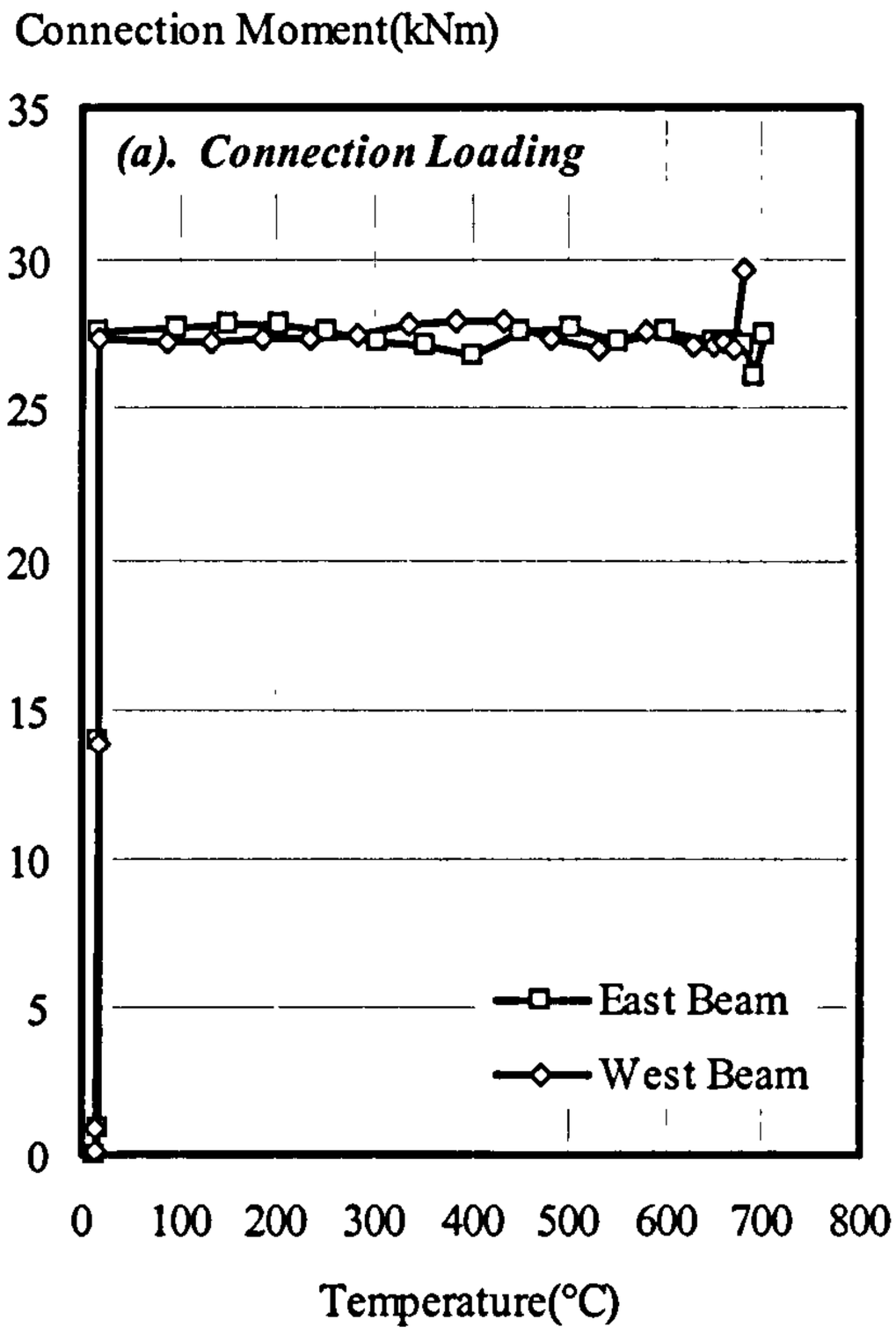

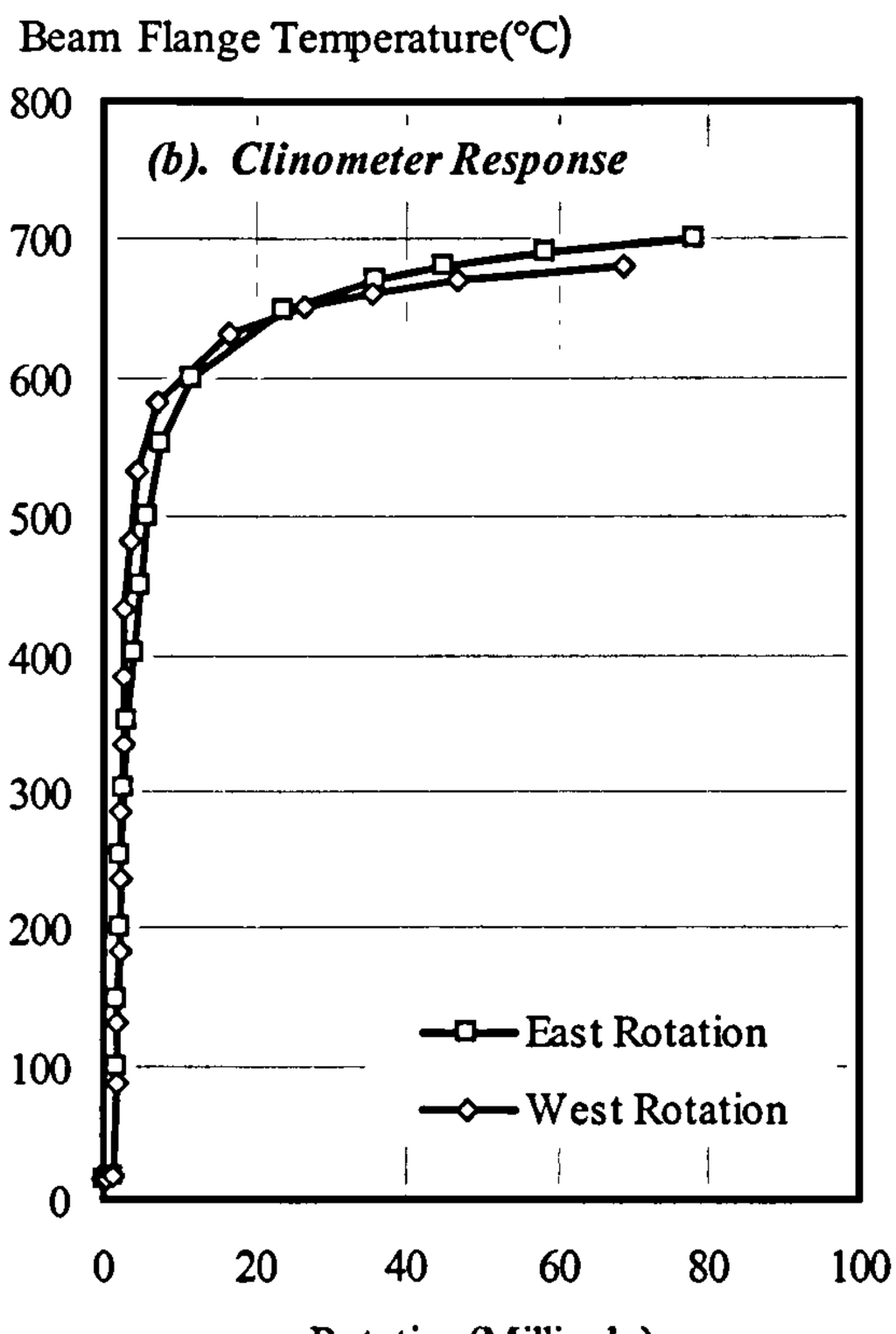

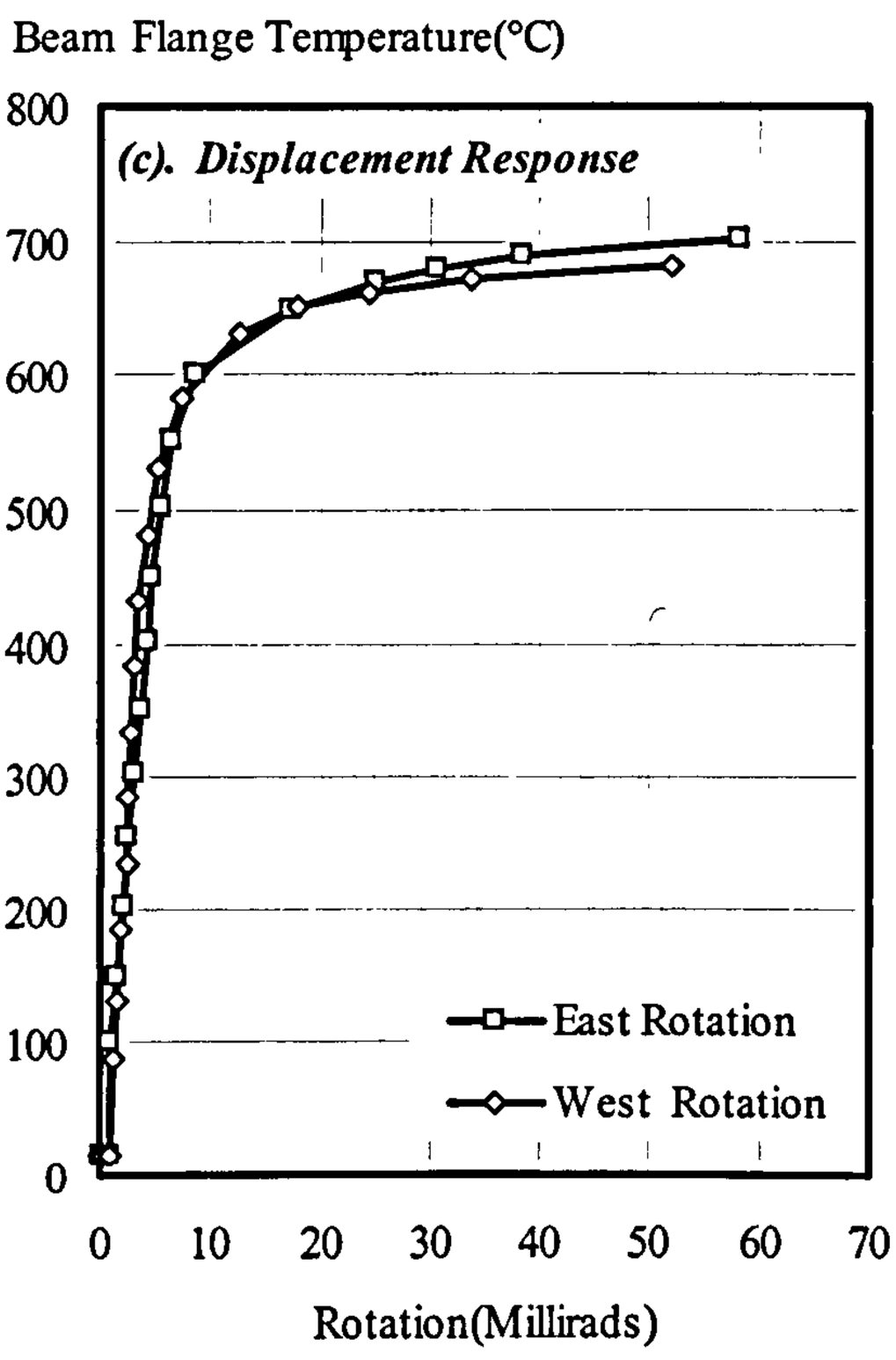

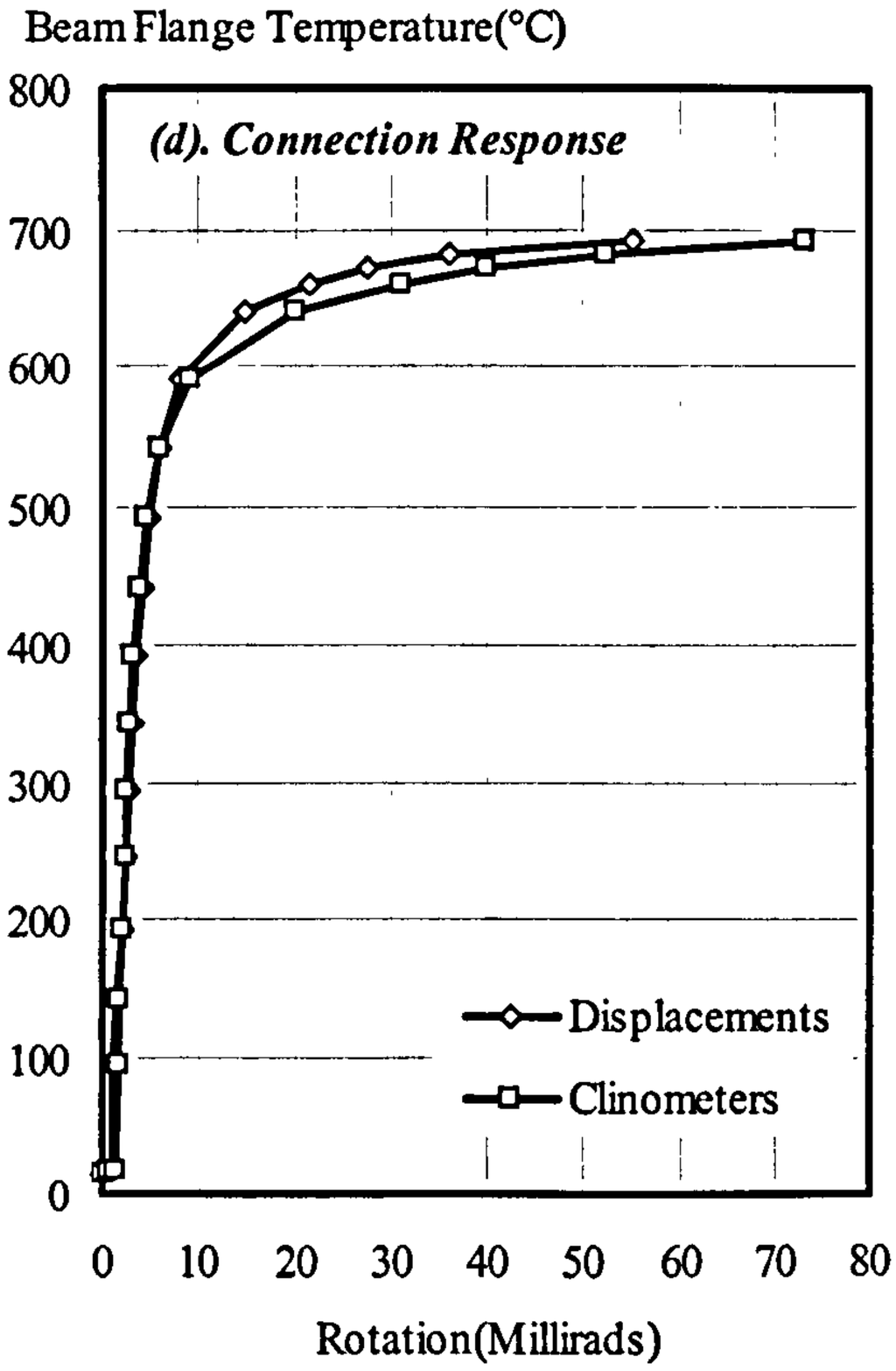

Figure 3.17: Summary of Results from Group 2: Fire Test 1 (FB21)

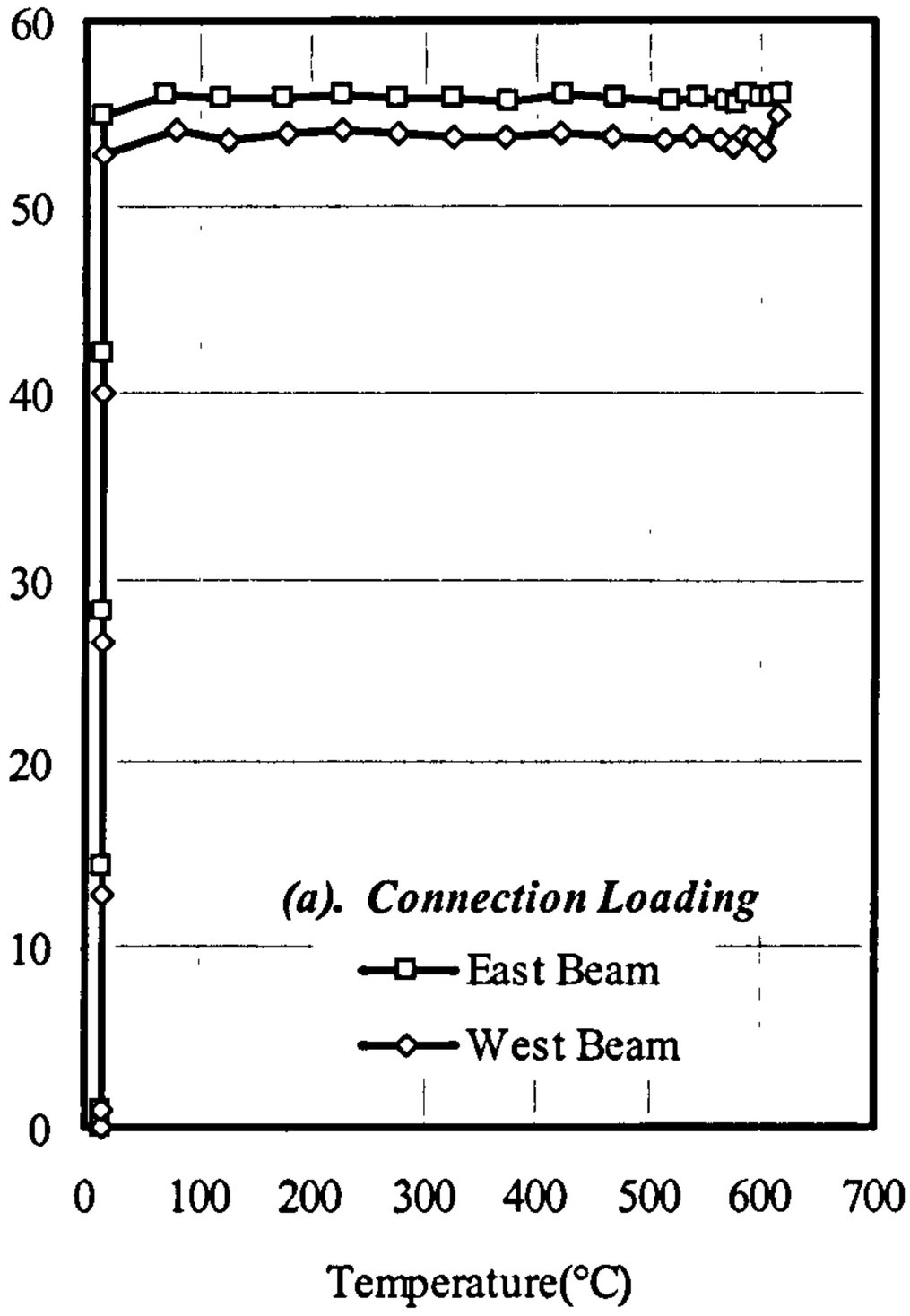

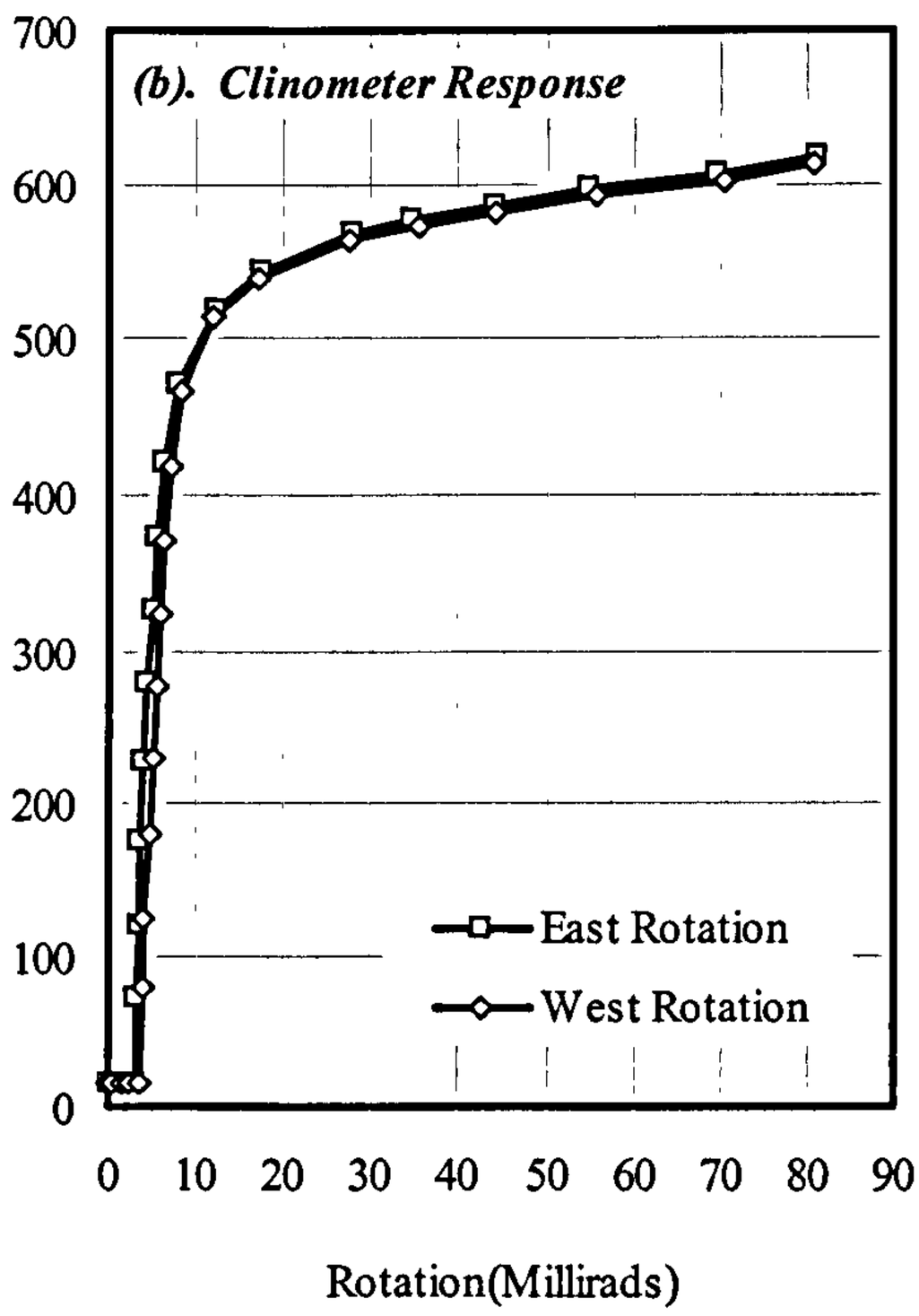

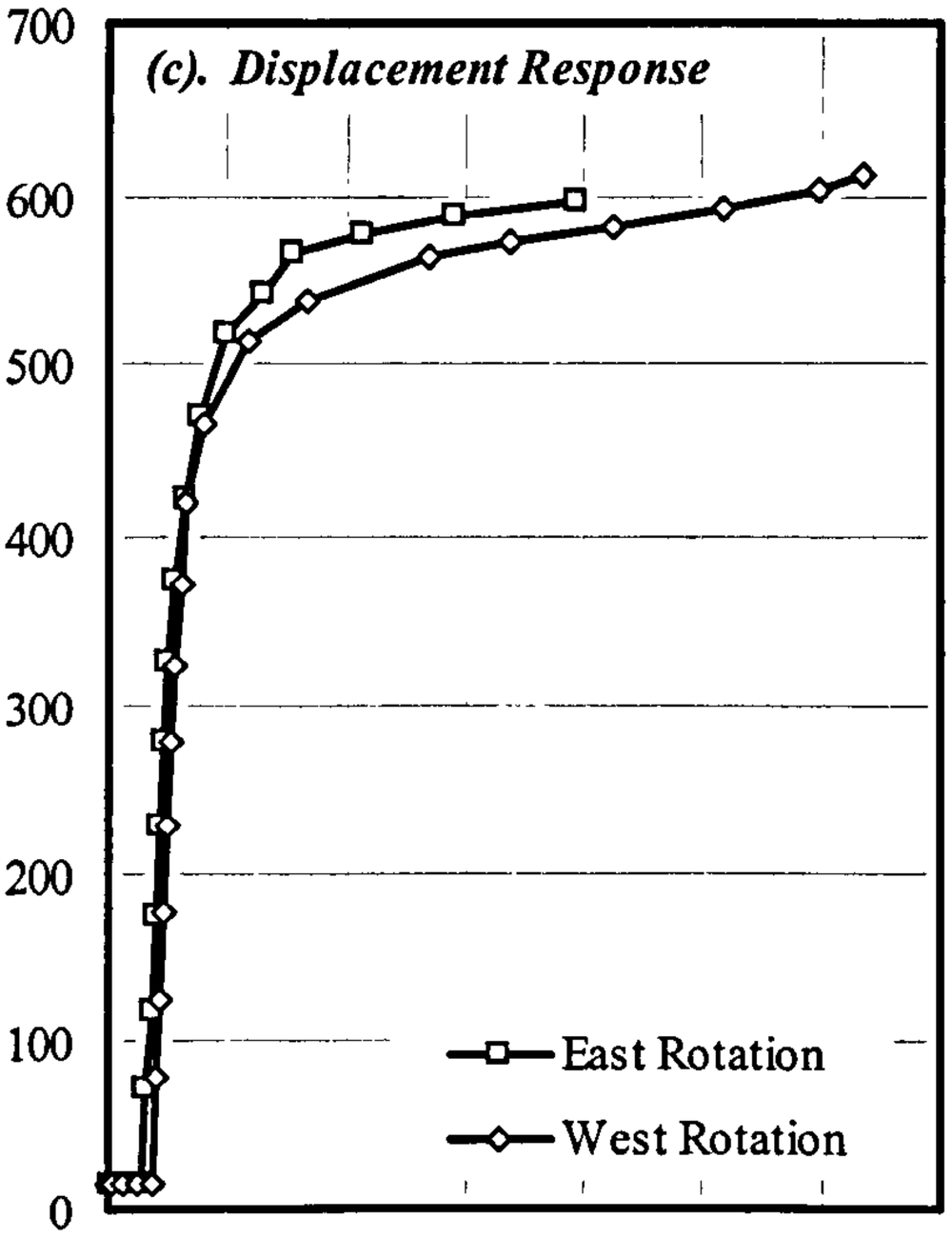

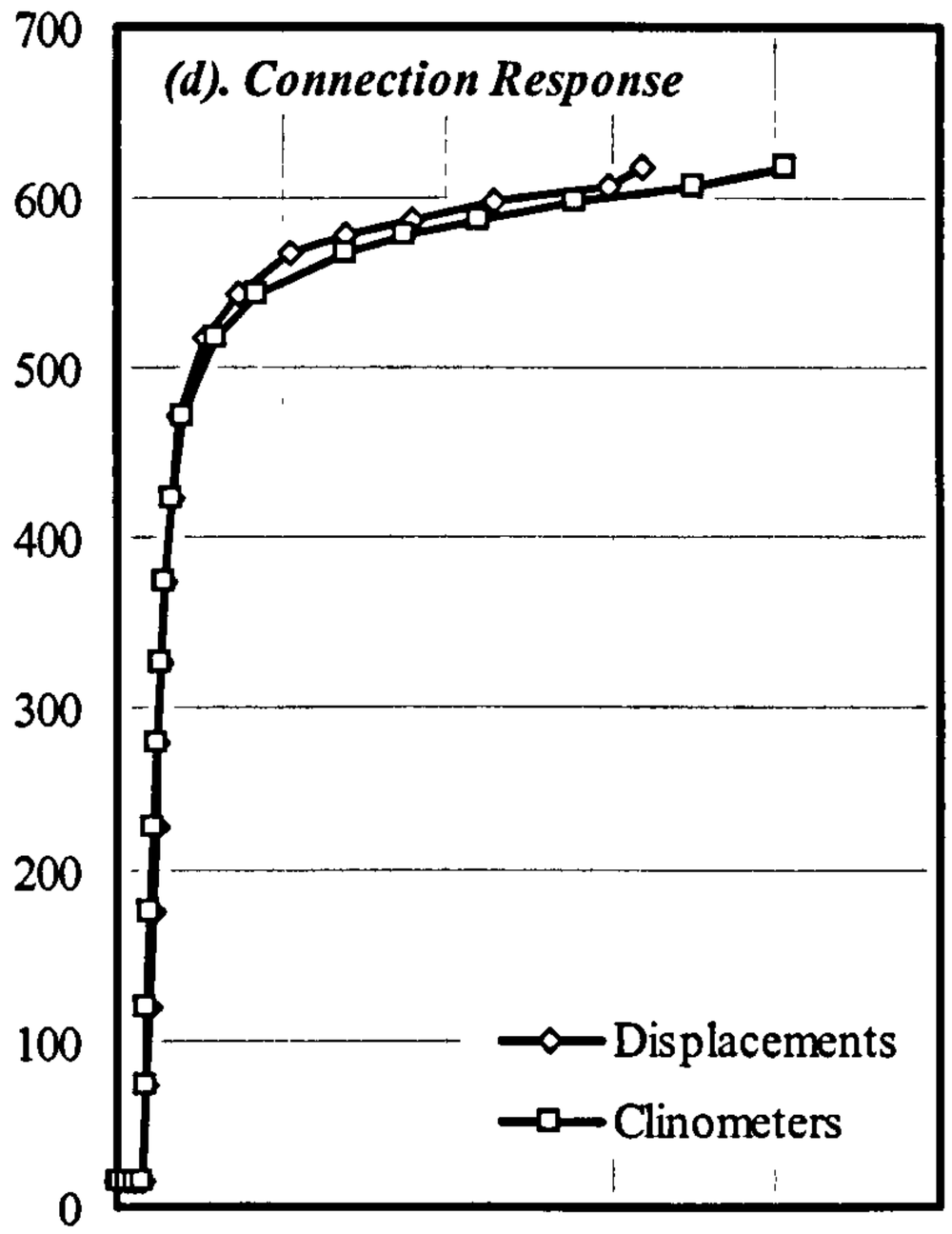

Figure 3.18: Summary of Results from Group 2: Fire Test 2 (FB22)

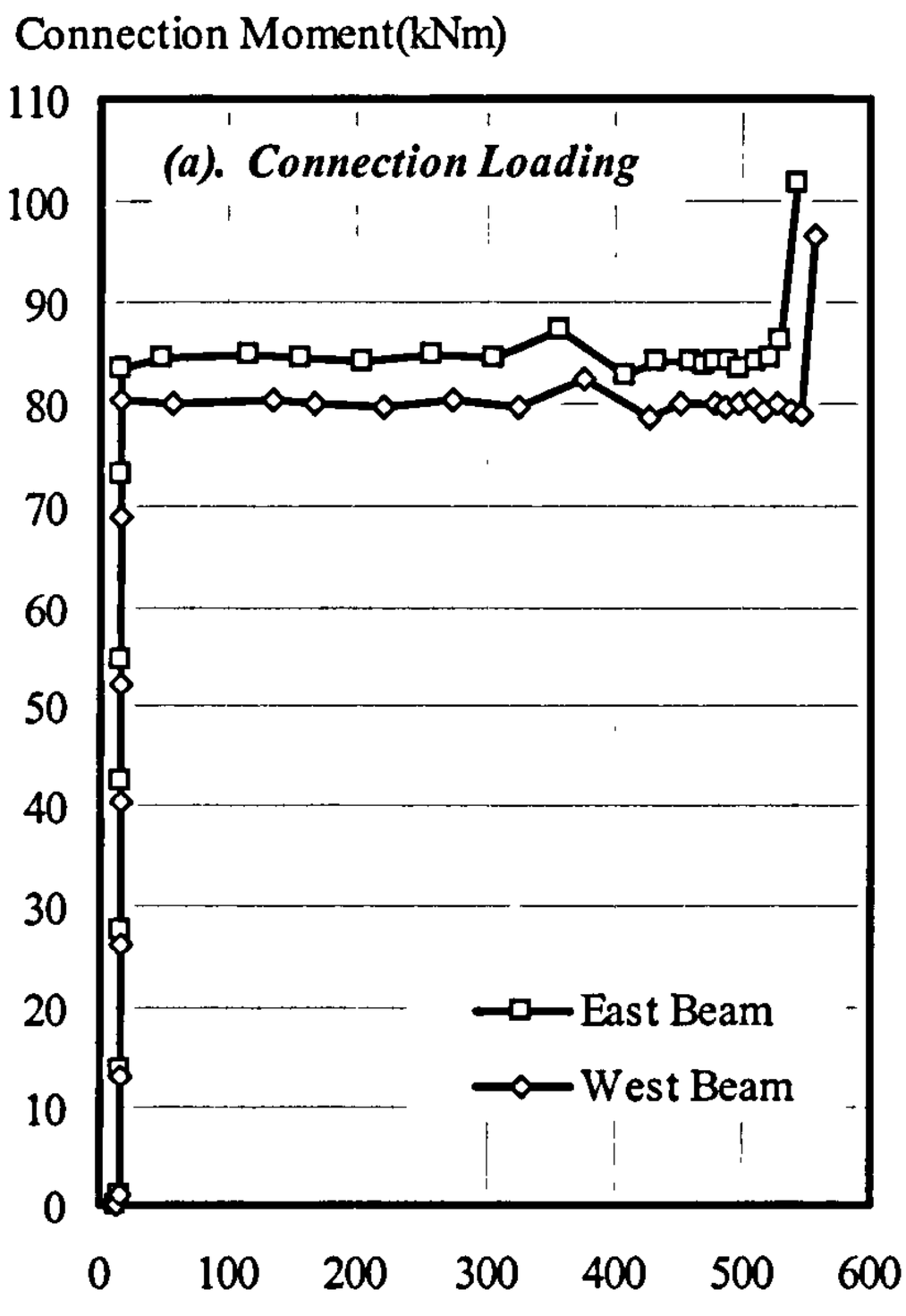

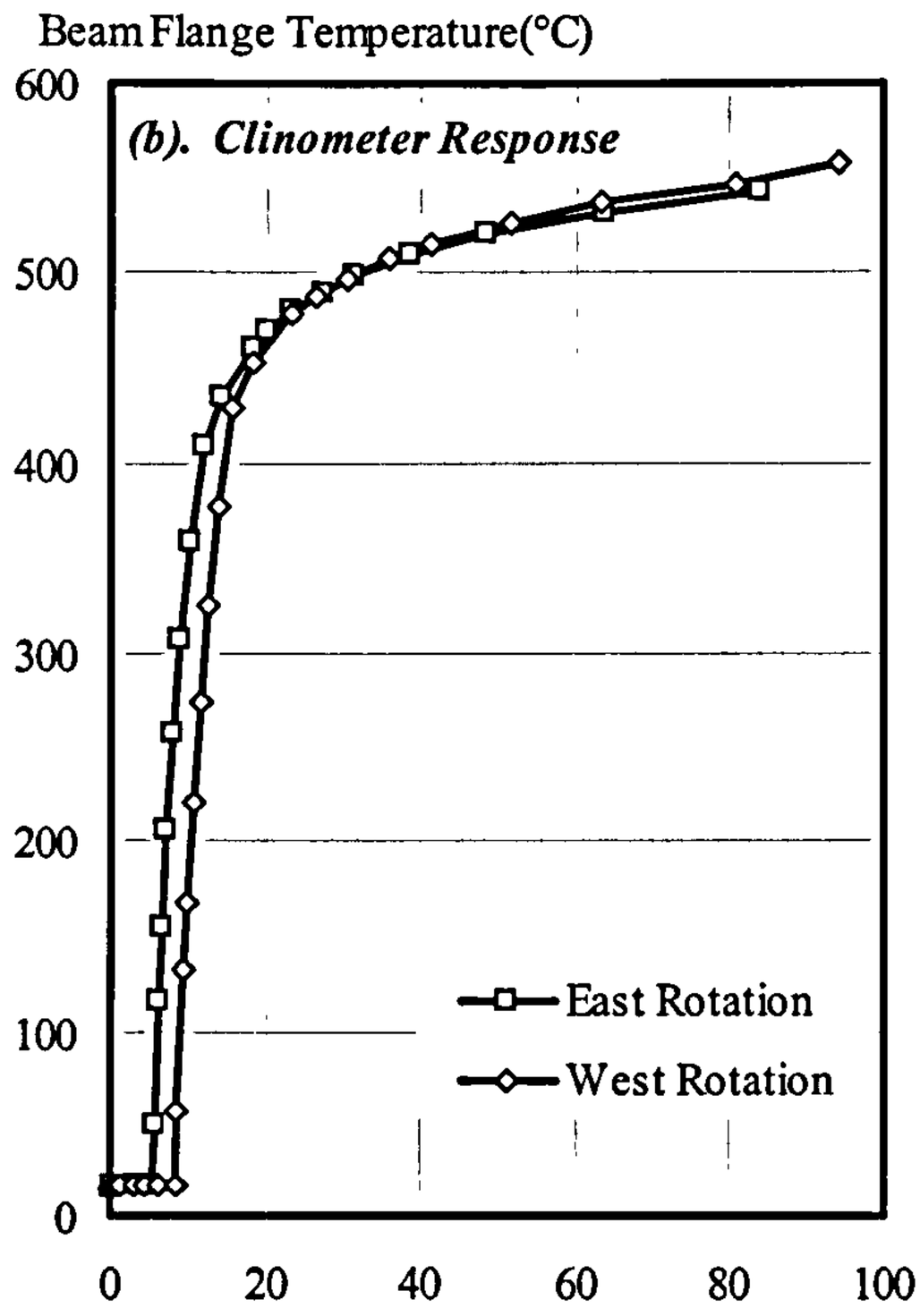

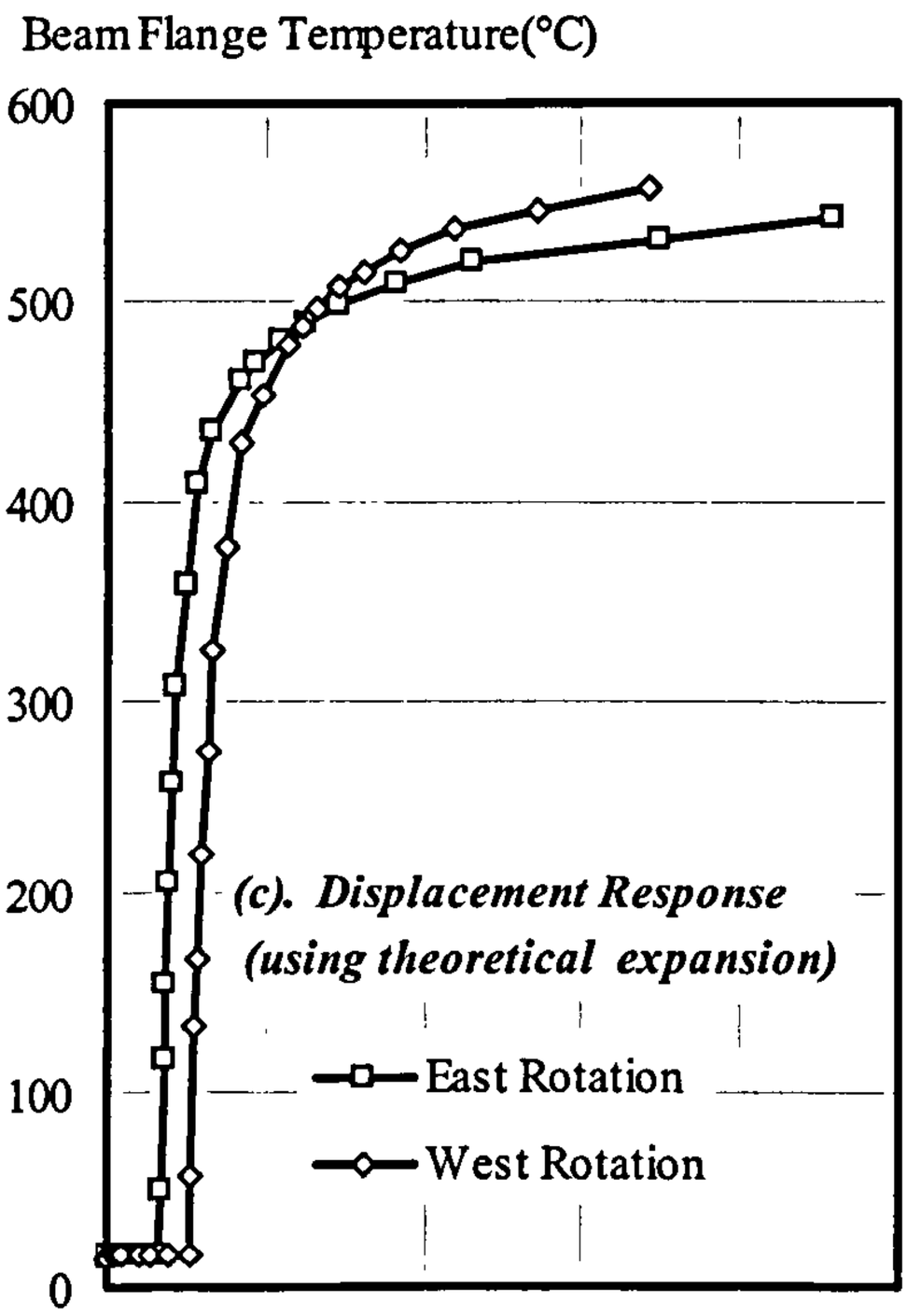

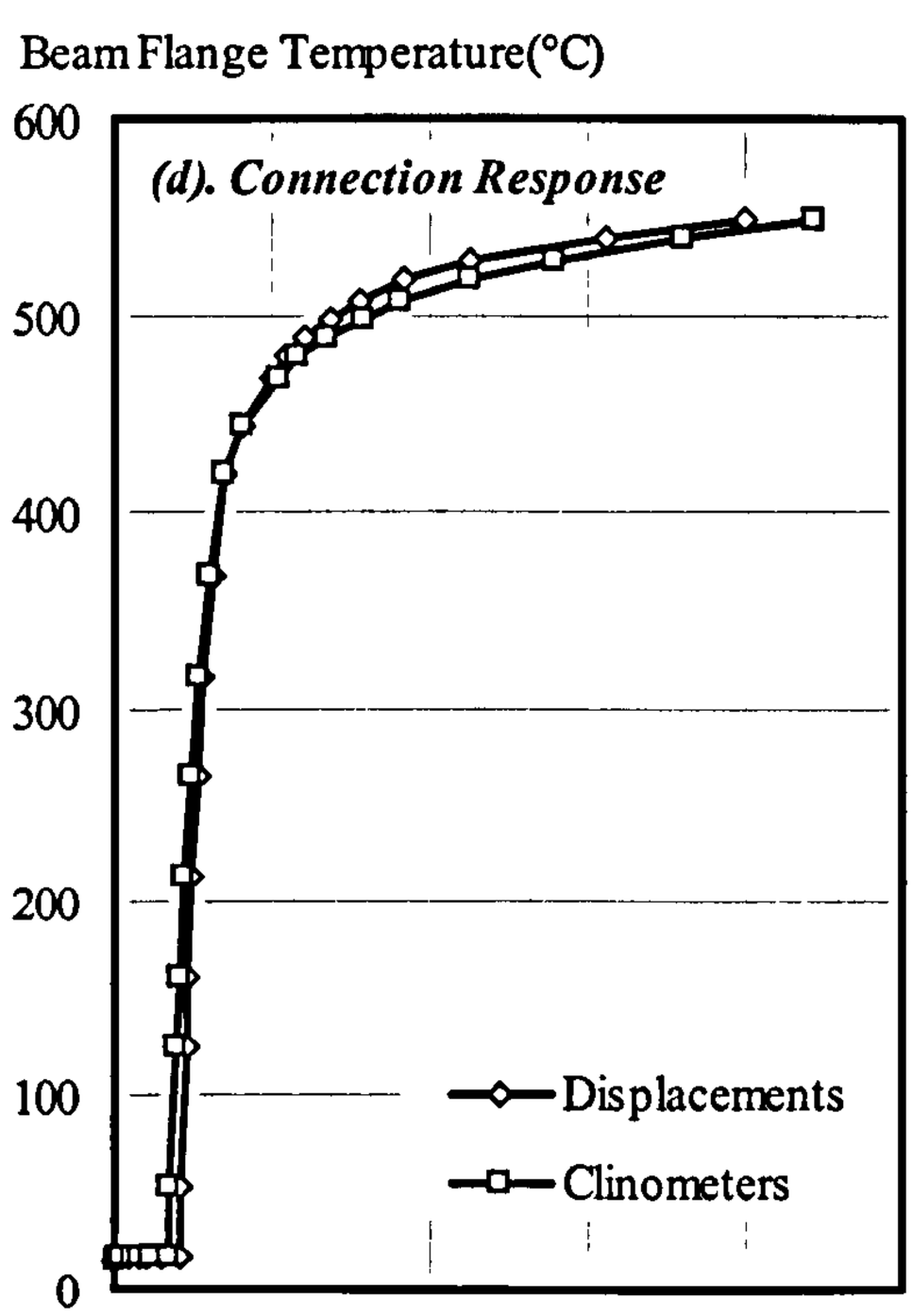

Figure 3.19: Summary of Results from Group 2: Fire Test 3 (FB23)

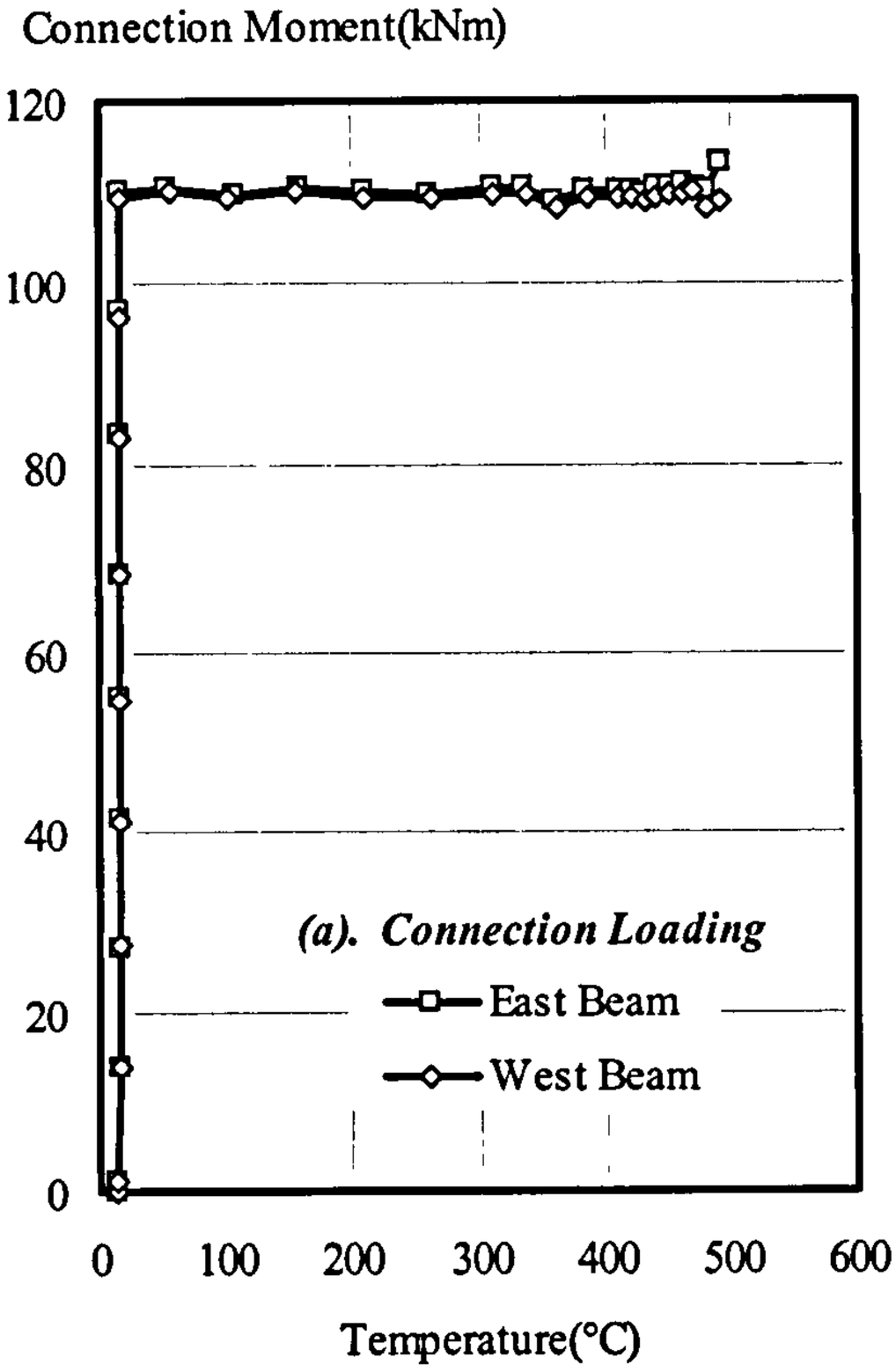

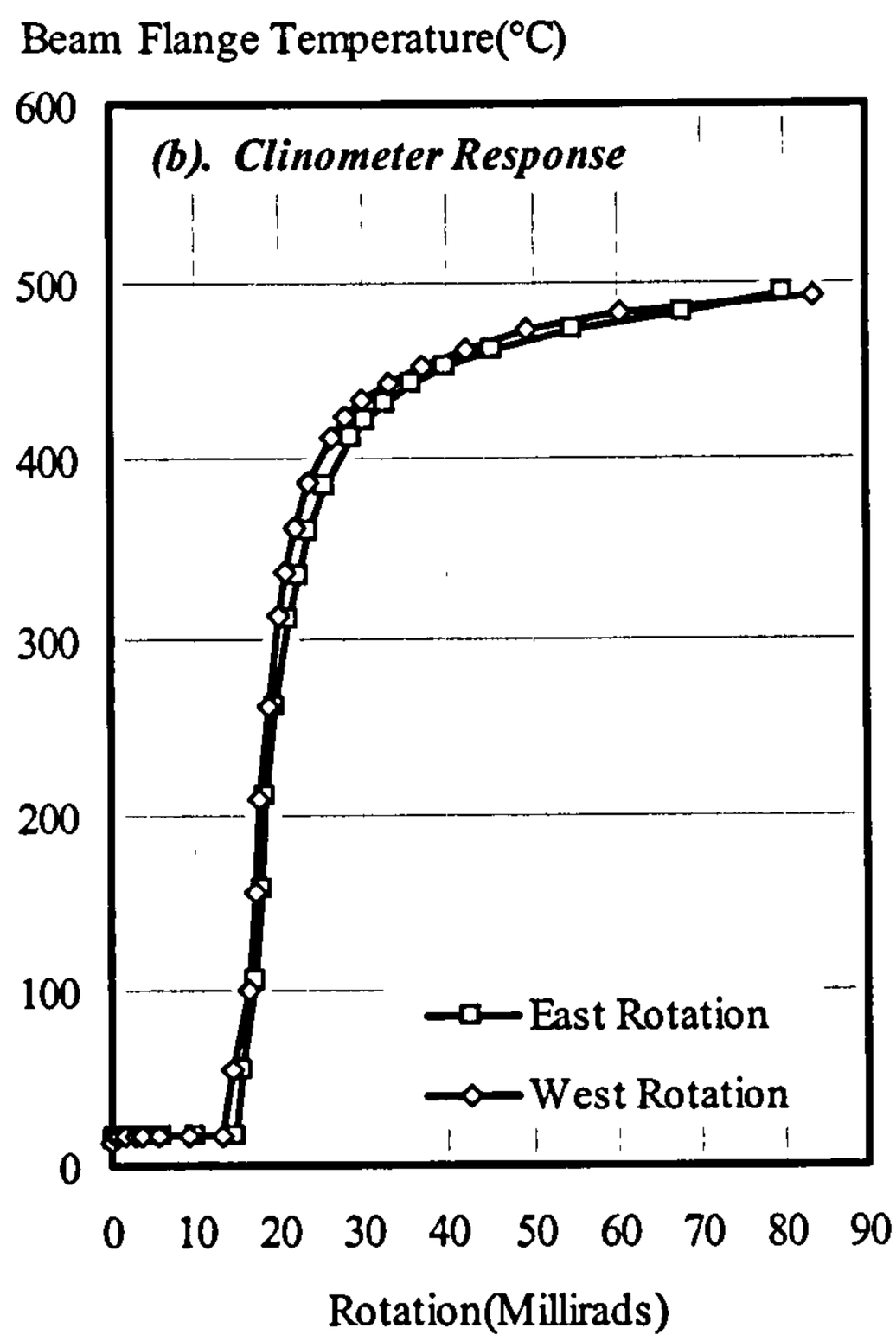

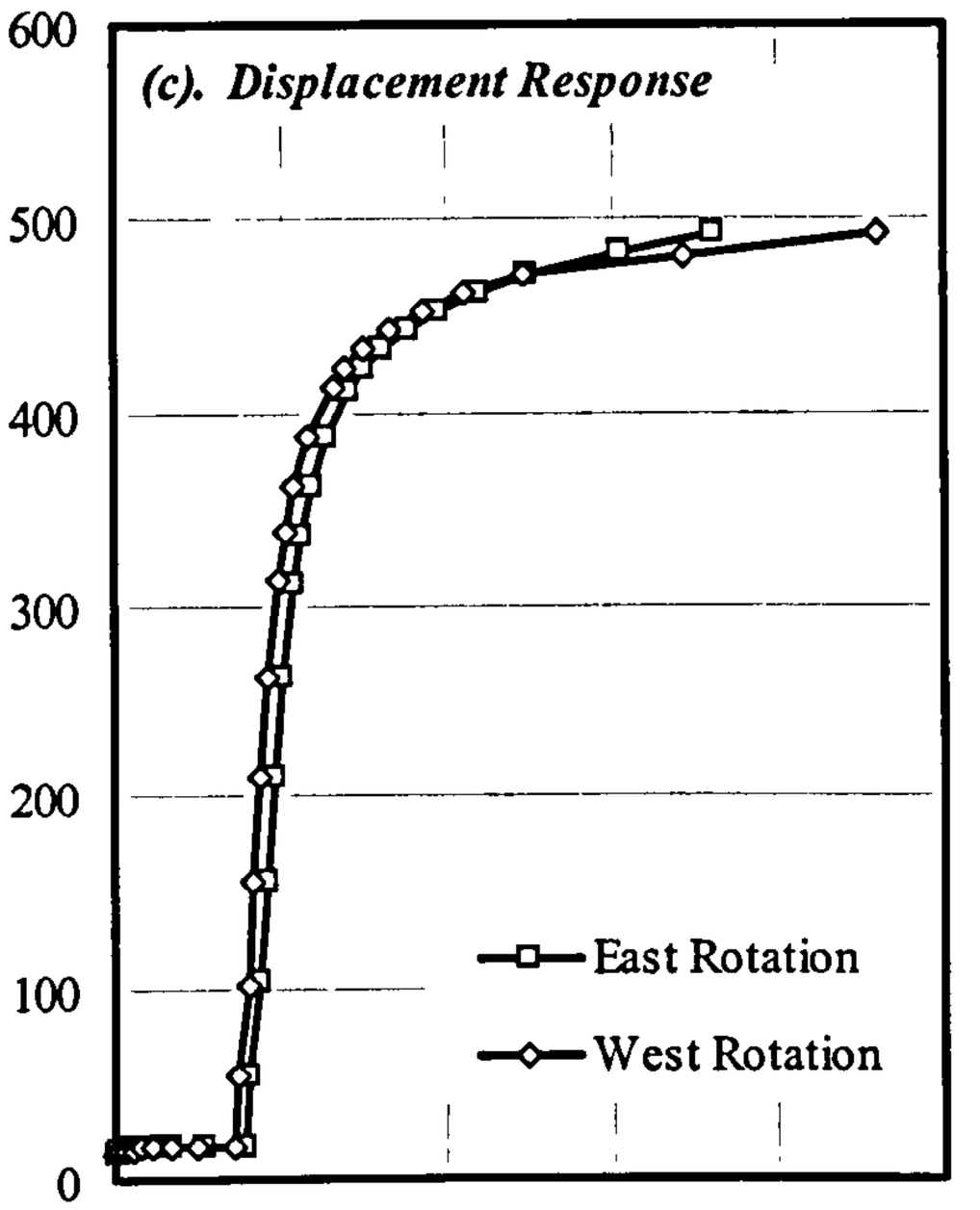

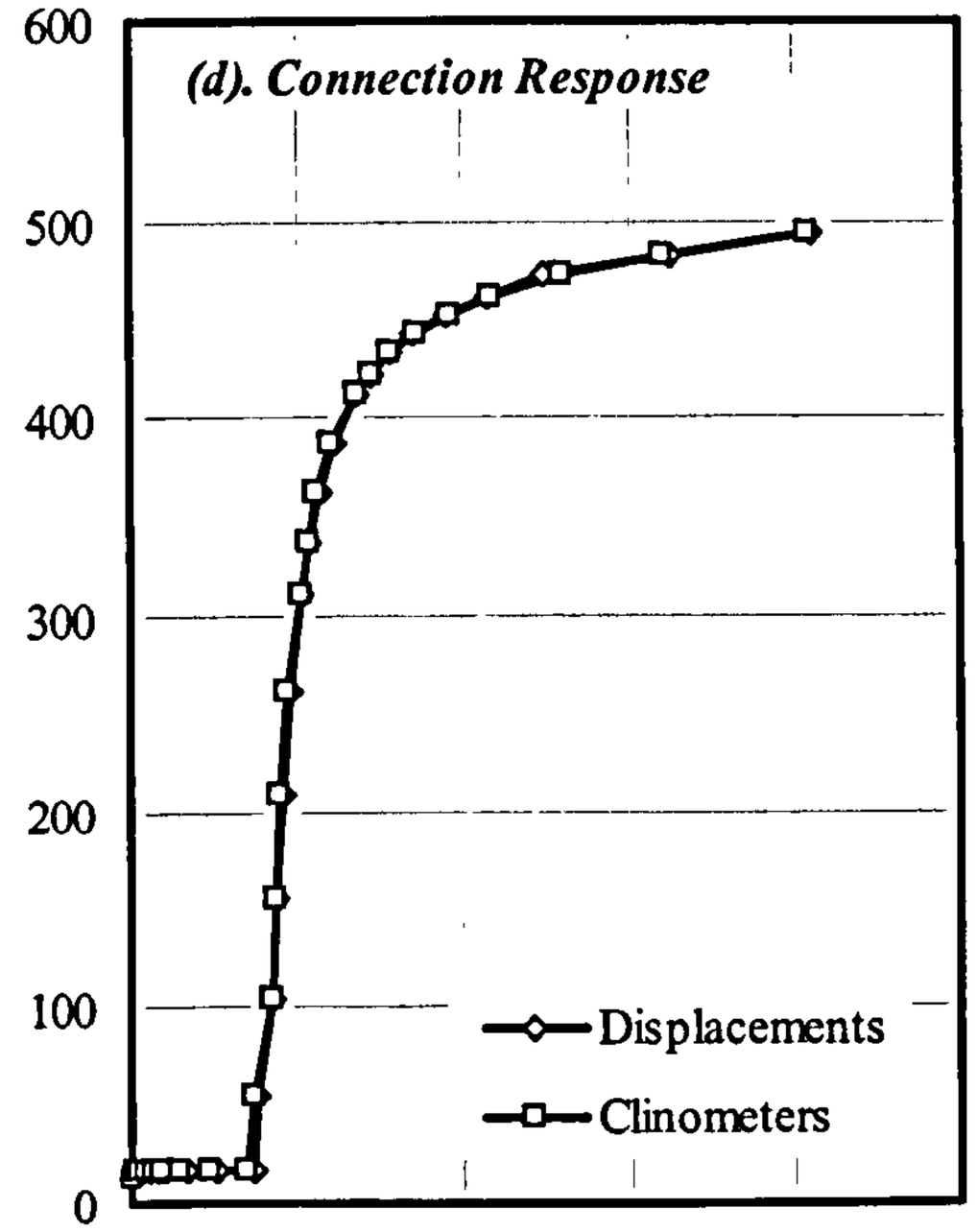

Figure 3.20: Summary of Results from Group 2: Test 4 (FB24)

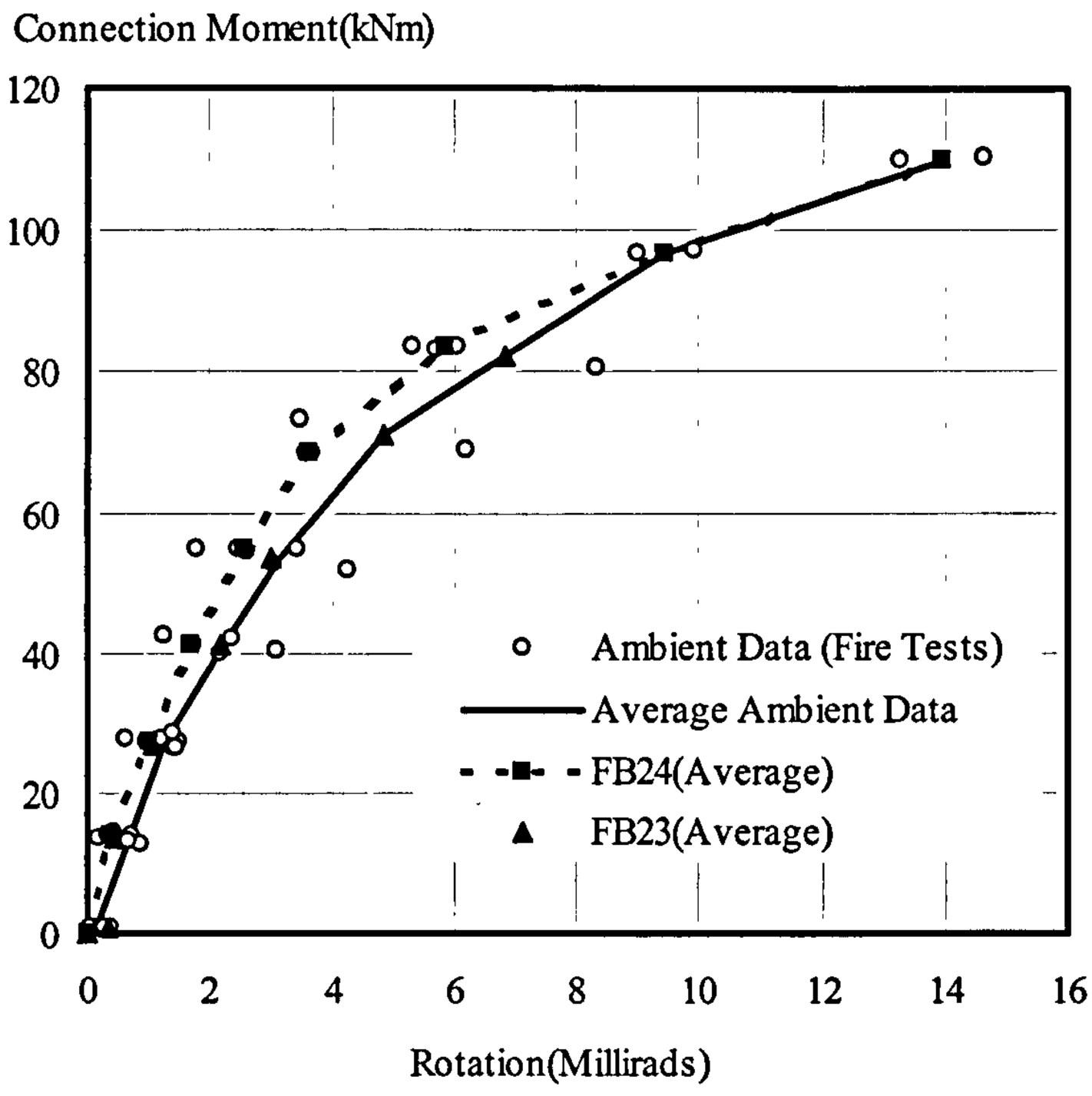

Figure 3.21: Ambient Temperature Response from Group 2 Fire Tests

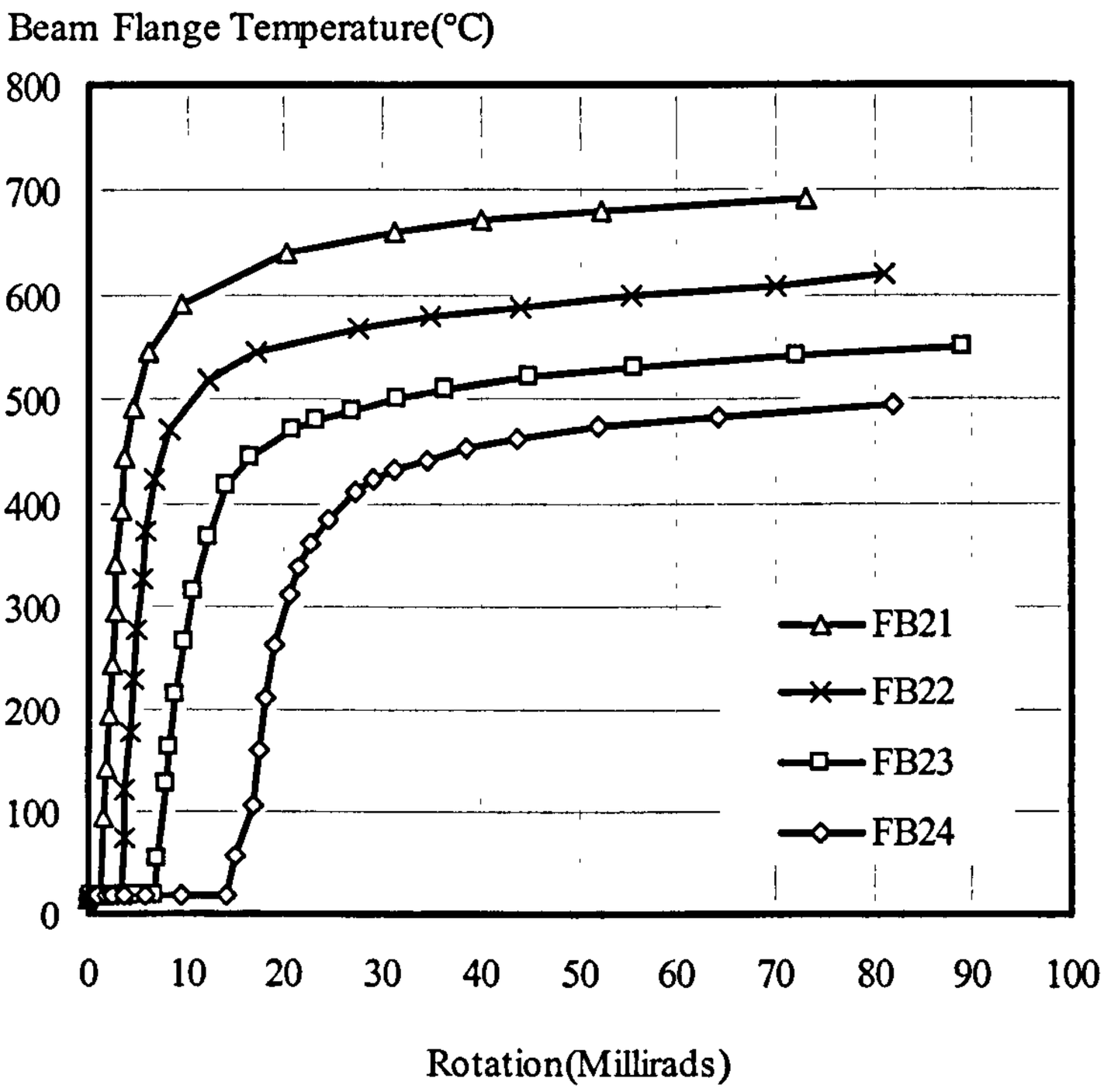

Figure 3.22: Elevated Temperature Connection Response of Group 2 Tests

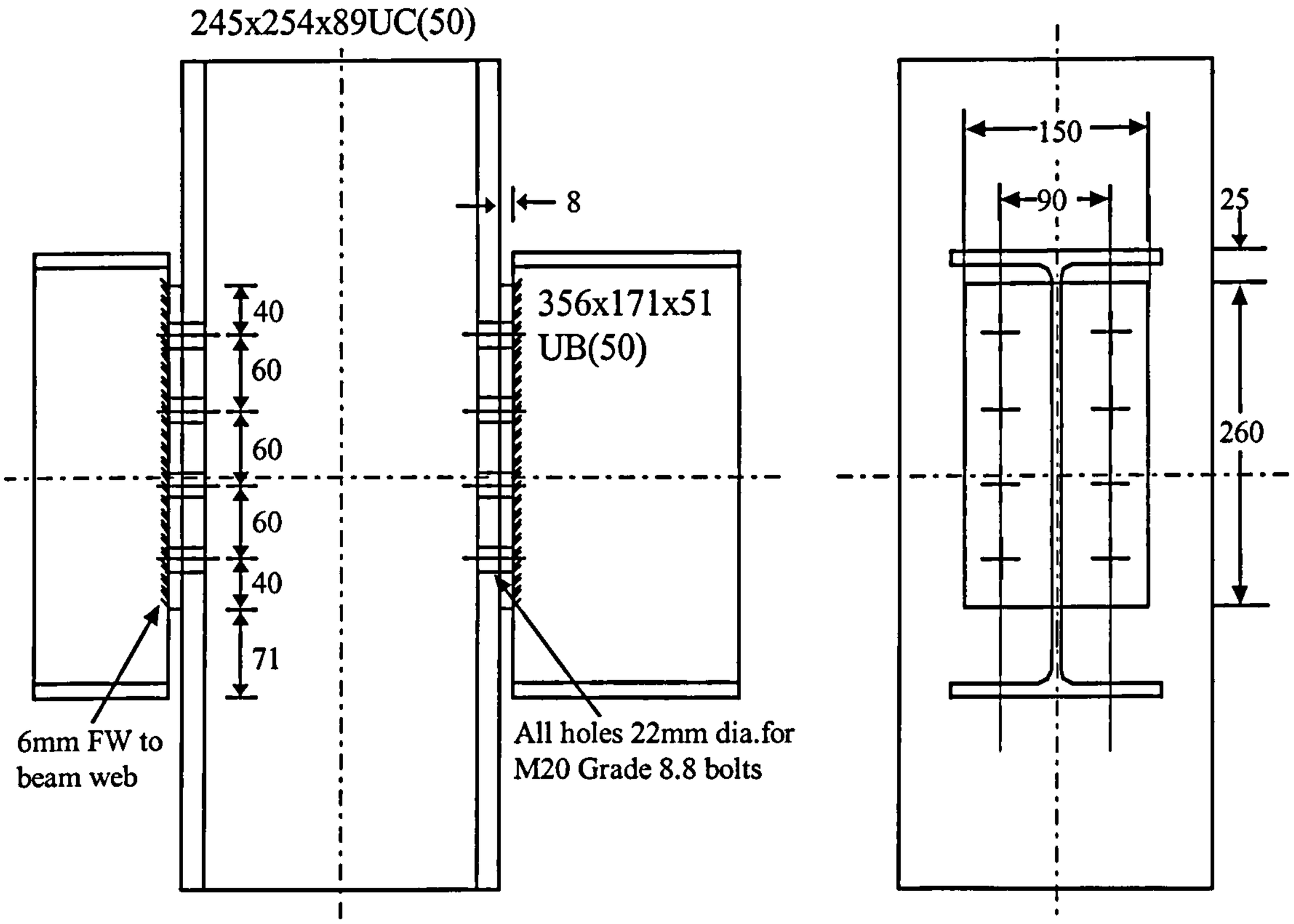

Figure 3.23: Bare-Steel Flexible End-Plate Connection Detail (Group 3)

One of the main characteristics of this type of connection is that it undergoes considerable rotation at relatively low moments due to the unhindered end-plate deformation until the lower flange of the beam comes into contact with the column flange. Beyond this, increased moments cause further rotations but at a much lower rate.

Unfortunately, the furnace doors could not accommodate the large associated beam deflections and if the elevated temperature tests were conducted as before, they would have had to be terminated prematurely before the actual failure of the connection. One of the solutions proposed, to enable testing the connection up to failure, was to support the furnace on moveable jacks and lower it as the bottom flange approaches the furnace door. This suggestion was discounted since it was felt that the movement of the furnace could disturb the test arrangement, instrumentation or gas supply. Eventually it was decided to conduct the test in a similar way to the previous tests. For tests involving low load levels, the test had to be terminated when the beam bottom flange contacted the furnace door, resulting in a conservative estimate of the connection failure temperature and rotation. To resolve this problem for higher load levels, the specimen was initially loaded to the desired load level at ambient temperature until the beams touched the furnace doors. The loads were then removed. The furnace was lowered until a gap is created between the furnace doors and the bottom flange of the beams allowing the connections to rotate further. The specimen was reloaded to the required level and the elevated temperature test started. This method allowed the specimen to be tested up to failure over the complete rotation and temperature ranges. Therefore the connection is assumed failed when either:

- both beams rest on the furnace doors, or
- the connection is unable to sustain the applied load level due to failure of one or more elements within the connection or increasing flexibility.

Three tests were carried out in this group. This is insufficient to generate representative data covering the entire connection response, so load levels were chosen to give a reasonable representation for the first stage. Load levels were based on the connection response observed by Boreman *et al.*[100]. The loads were applied to both connections at a distance of 1370 mm from the face of the column flange. Table 3.6 shows the testing programme for this group of tests, and a description of each individual test is presented below.

Table 3.6: Group 3: Bare-Steel Flexible End-Plate Experimental Programme

Test:	*Moment Level:*	*Applied Moment:*	*Temperature:*	*Comments:*
FLB31	$0.1M_{cc}$	8 kNm	10°C/minute	Group 3, Fire Test 1.
FLB32	$0.2M_{cc}$	16 kNm	10°C/minute	Group 3, Fire Test 2.
FLB33	$0.5M_{cc}$	40 kNm	10°C/minute	Group 3, Fire Test 3.

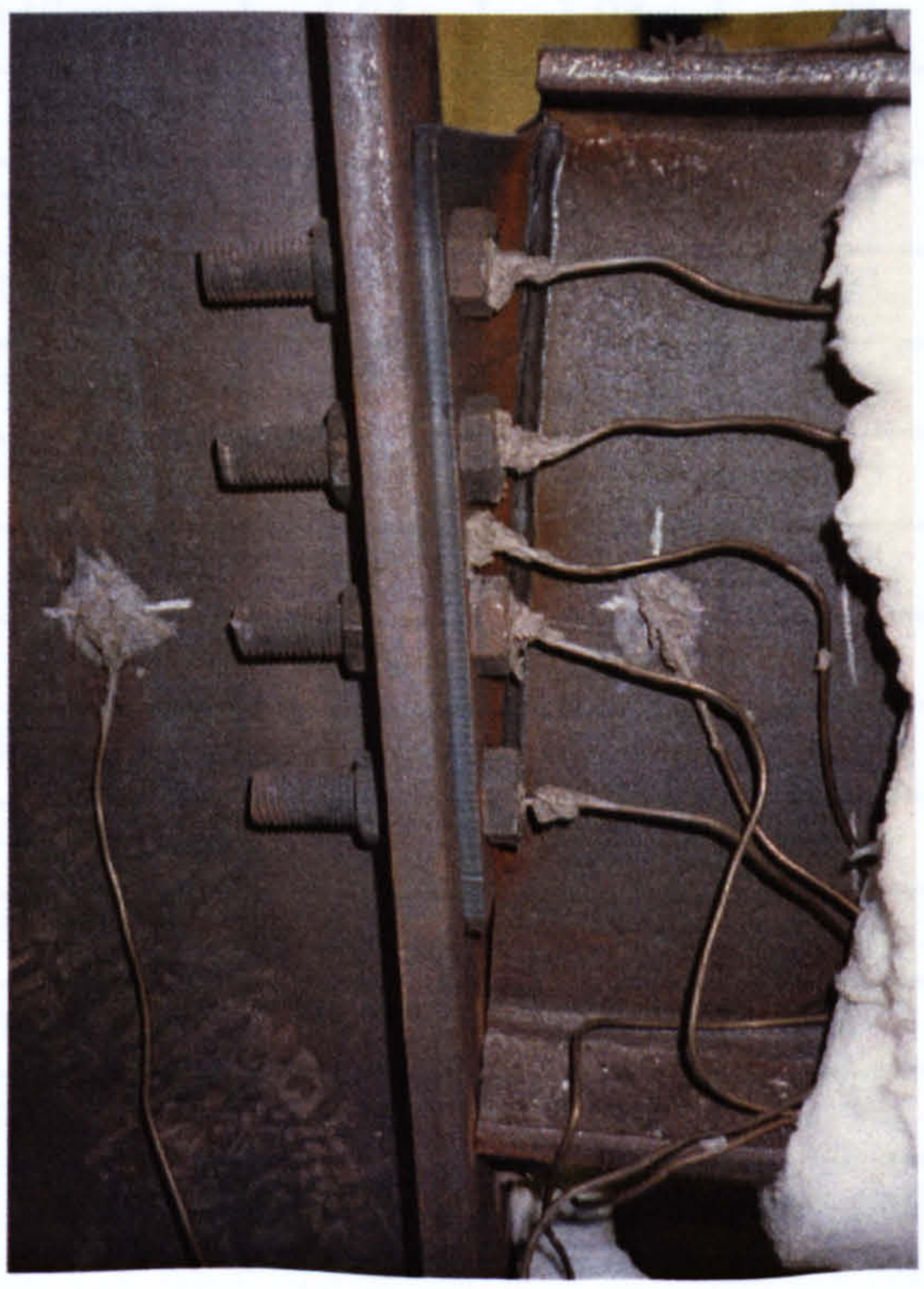

Figure 3.24: Elevated Temperature Connection Failure Mechanism for Group 3

3.8.1 General Observations from Group 3 Fire Tests

In all Group 3 tests, significant end-plate deformation was observed with the plate tending to pull away from the column flange at the top, and yielding ('plastic hinges') adjacent to the welds and bolts as shown in Fig. 3.24. A similar failure mode was

observed by Kenndey[101] and Owen and Moore[102] in experimental studies on flexible end-plate connections at ambient temperature. No distortion occurred in the beams or the column and there was negligible deformation of the bolts.

The temperature distribution across the connection depth is tabulated in Table 3.7 and is similar to those in Groups 1 and 2. There is a constant temperature gradient through the connection with little variation between the beam top and bottom flanges. Once more, the column web achieved the highest temperatures, being approximately 12% greater than the beam bottom flange. The relatively low temperature reached in the protection box proves again the efficiency of the cooling system devised to protect the clinometers. The average atmospheric temperature was 62% greater than the beam lower flange temperature. Also, there was little variation in temperatures between the East and West connections.

Table 3.7: Average Relative Temperature Profiles for Group 3 Tests

Element:	*FLB31:*	*FLB32:*	*FLB33:*	*Average:*
Beam Bottom Flange	1.00	1.00	1.00	1.00
Beam Web	1.10	1.03	1.04	1.06
Beam Top Flange	1.04	1.04	1.01	1.03
Beam Top Flange*	0.41	0.37	0.43	0.40
Beam Bottom Flange*	0.41	0.37	0.41	0.40
Top Bolt	1.02	0.93	0.93	0.96
2nd Row Bolts	1.03	0.93	0.96	0.97
3rd Row Bolts	1.01	0.92	0.95	0.96
Bottom Bolt	0.97	0.93	0.95	0.95
Column Web	1.20	1.08	1.08	1.12
Column Flange	1.01	0.94	0.93	0.96
Column Flange*	0.38	0.31	0.33	0.34
End-plate	1.02	0.91	0.94	0.96
Clinometer	0.11	0.13	0.10	0.11
Furnace Atmosphere	1.55	1.64	1.69	1.62

Note: * identifies insulated thermocouple locations

3.8.2 Group 3: Fire Test 1 (FLB31)

The first test was performed at a relatively low moment of 8 kNm. Results are summarised in Fig. 3.25. It may be seen that the East beam was subjected to a greater load level than the West beam but with little variation throughout testing. The average moment applied to the connection was observed to be nearly 8.2 kNm. The test was

terminated when both beams came into contact with the furnace doors resulting in a conservative representation of the connection response.

Rotations obtained from clinometers are plotted in Fig. 3.25*(b)*. It may be seen that readings for the East connection suggest more flexible response at temperatures in the range 200°C to 550°C, while for temperatures in excess of 550°C there is close correlation between the two connections. This suggests that the variation is probably due to the enhanced loading level applied to the East connection. Fig. 3.25*(d)* compares the average rotations recorded by clinometers and displacement transducers. Agreement is generally acceptable although the clinometer readings show a slightly more flexible behaviour at temperatures in the range 350°C to 600°C.

3.8.3 Group 3: Fire Test 2 (FLB32)

This test was conducted under a connection moment of approximately 16 kNm and the results are summarised in Fig. 3.26. It was terminated when both the beams rested on the furnace doors without the connection failing. Due to the variability of the loading levels, the average moment recorded for the connection was 16.5 kNm. Average connection rotations obtained from clinometers and displacement transducers compare well as shown in Fig. 3.26*(d)*.

3.8.4 Group 3: Fire Test 3 (FLB33)

The loading level in the final test provided a moment of approximately 40 kNm, applied in three equal increments. The test was carried out in two stages. In the first stage, the specified loading was applied to the specimen at ambient temperature. Then the load was gradually removed and the unloading response was carefully recorded. The furnace and the instrumentation were re-adjusted. The second stage involved re-loading the specimen to the desired level and starting the fire test. The resultant connection response was obtained by superimposing the responses of the two stages as shown in Fig. 3.27. By comparing the rotations recorded during the unloading and re-loading stages, it was found that the connection followed a similar path. There was negligible deviation in the rotation recorded for both connections during the removal and re-application of the loads.

A measured average moment of approximately 41.1 kNm was applied to the connection. Rotations measured for the East and West connections by clinometers and displacement transducers are presented in Figs. 3.27*(b)* and 3.27*(c)*. As for the other tests the connection response obtained from clinometers and displacement transducers compares well as shown in Fig. 3.27*(d)*.

3.8.5 Comparison of Results from Group 3 Elevated Temperature Connection Tests

Flexible end-plates are categorised as 'pinned' connections having the primary function of resisting shear forces. They have greater inherent flexibility than 'semi-rigid'

counterparts, and transfer of moments between the adjacent structural members is not accounted for.

The average connection response for Group 3 tests is presented in Fig. 3.28 based on the average clinometer readings for the East and West connections. Conducting three elevated temperature tests under constant load with increasing temperature seems to be insufficient to define accurately the flexible end-plate response since the behaviour is complicated by two stages of rotation. Therefore testing was concentrated towards establishing the elevated temperature characteristics of the first stage response.

The tests were performed in a satisfactory manner, except that in tests FLB31 and FLB32, the experiment was terminated prematurely due to the restrictions imposed by the furnace doors. In fact the specimens were capable of withstanding higher temperatures. Testing the third specimen FLB33 over the complete rotation range necessitated a two stage test as explained. There was close correlation between rotations recorded by clinometers and displacement transducer readings, confirming, once more, the reliability of both devices in describing the connection response.

3.9 CONCLUSIONS

Three series of tests were conducted in order to establish the moment-rotation-temperature response of bare-steel connections. Two connection types were considered; flush and flexible end-plates with small and medium member sizes. In general the elevated temperature tests produced failure modes similar to those at ambient temperature. In the flush end-plate connections this was generally a localised end-plate failure, although for tests in which the end-plate was oversized and the beam and column sections were small the column flange deformed and the column web buckled. For flexible end-plates, end-plate deformation was the dominant mode of failure. The specimen size seems to have had little effect on the failure temperatures. The bare-steel test series is consistent with those tests performed previously.

The temperature distribution across all bare-steel connection depths was consistently uniform temperature gradient and the connection element reaching the highest temperature was consistently the column web. A similar temperature profile was observed across the East and West connections for the same specimen.

The rotation-temperature curve of the connection is characterised by three regions. Initially there is an approximately linear response with increasing temperatures, until the onset of yielding in one or more of the connection components. There is then a curved knee, and finally as the connection failure becomes imminent, the rotation rate increases rapidly causing an almost flat plateau in the connection response. As the load level increases the connection failure temperature decreases.

Once the temperature-rotation response for the connection has been established at different load levels, it is possible to define the moment-rotation characteristics for the connection across a range of temperatures. It is recommended that a single test at ambient temperature is conducted in order to assess the actual response of the connection due to the variation between the design methods and the actual response.

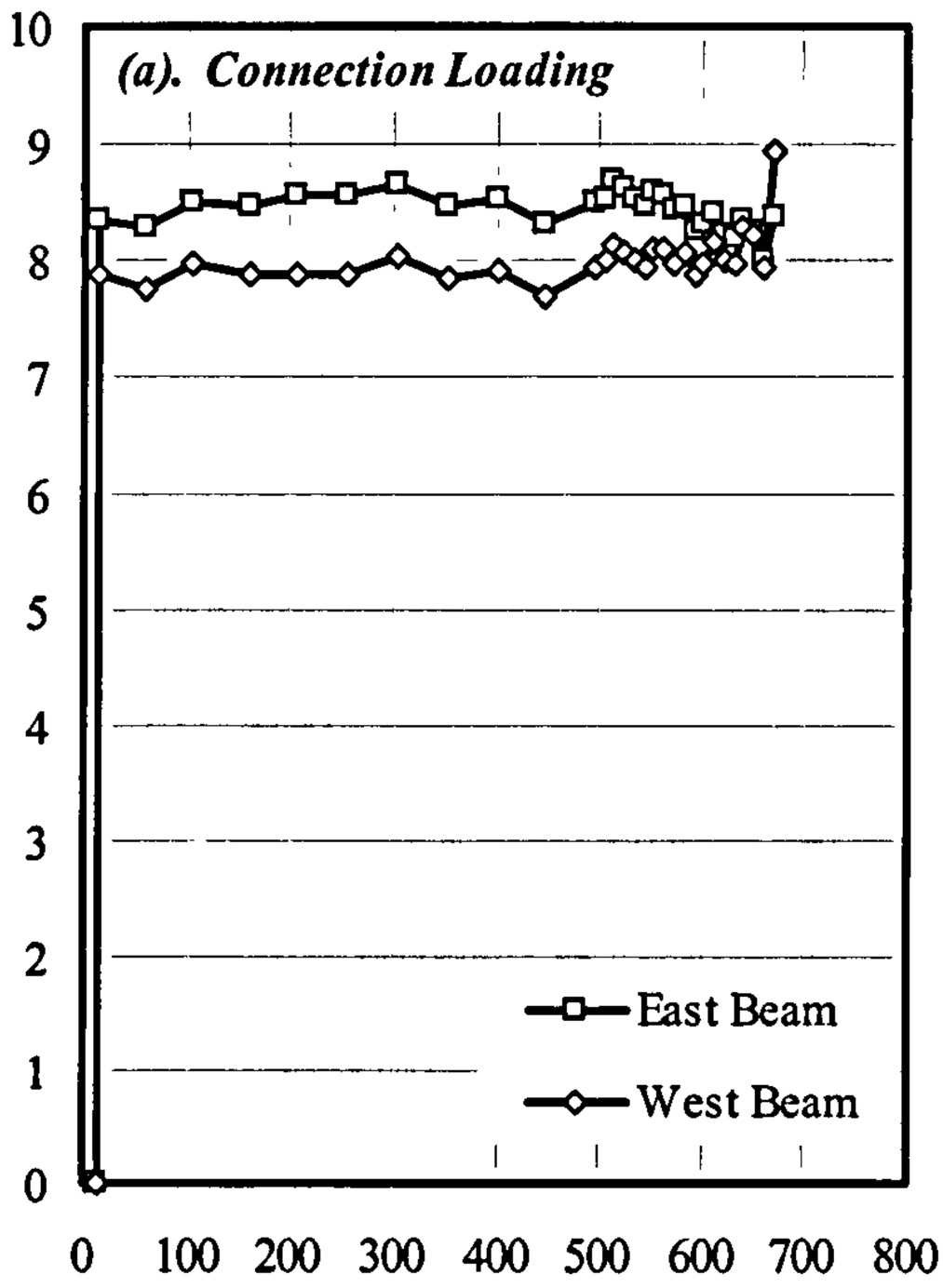

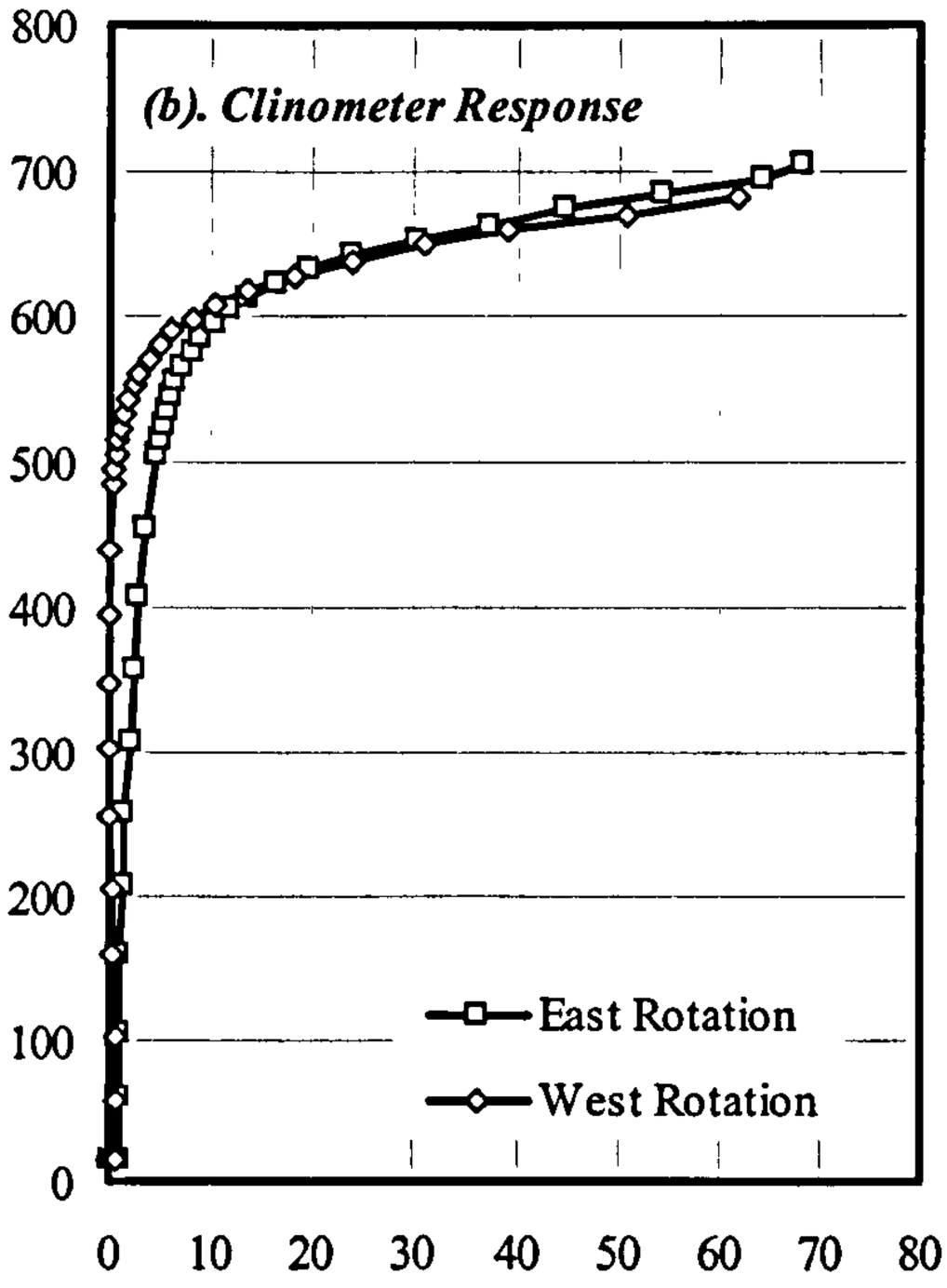

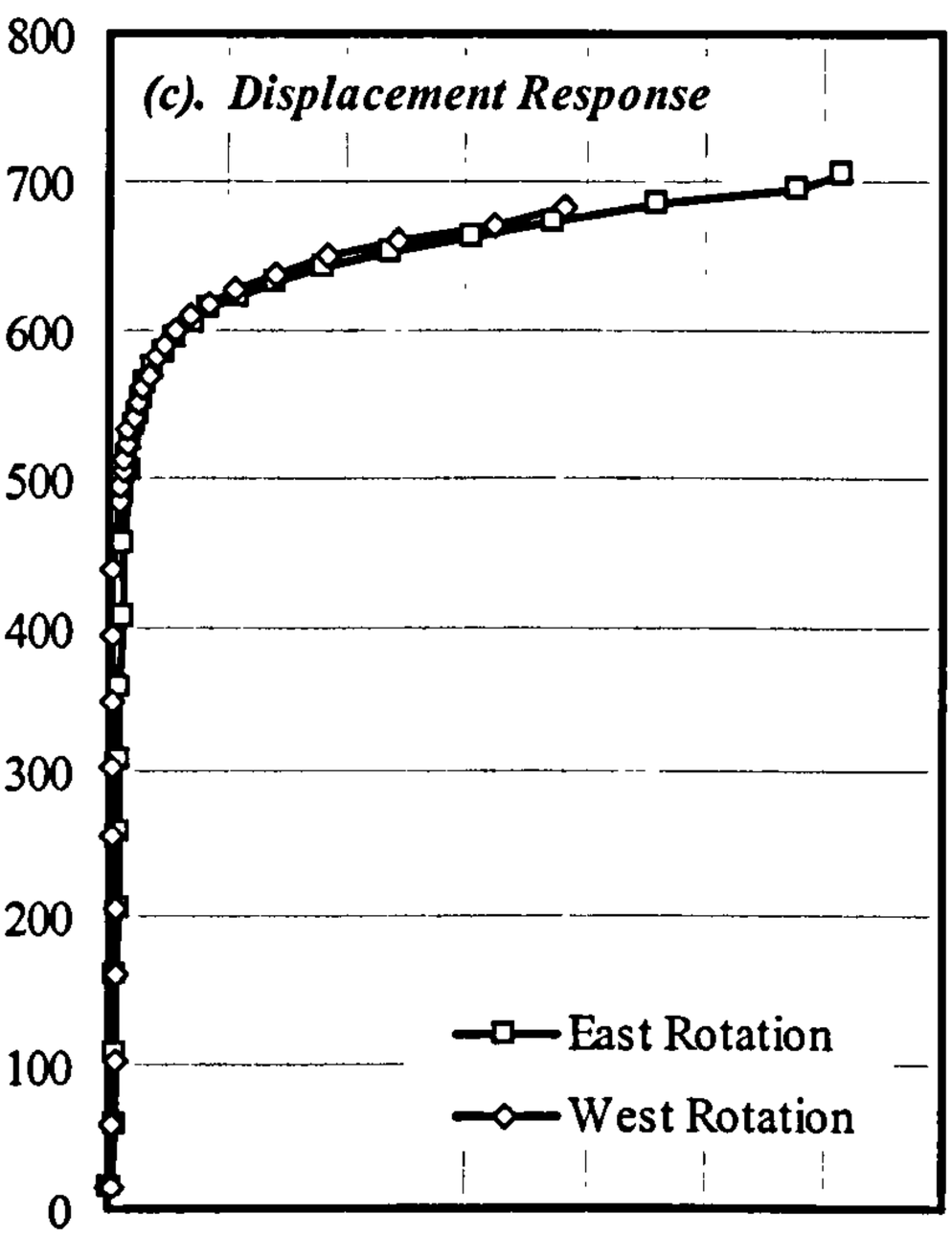

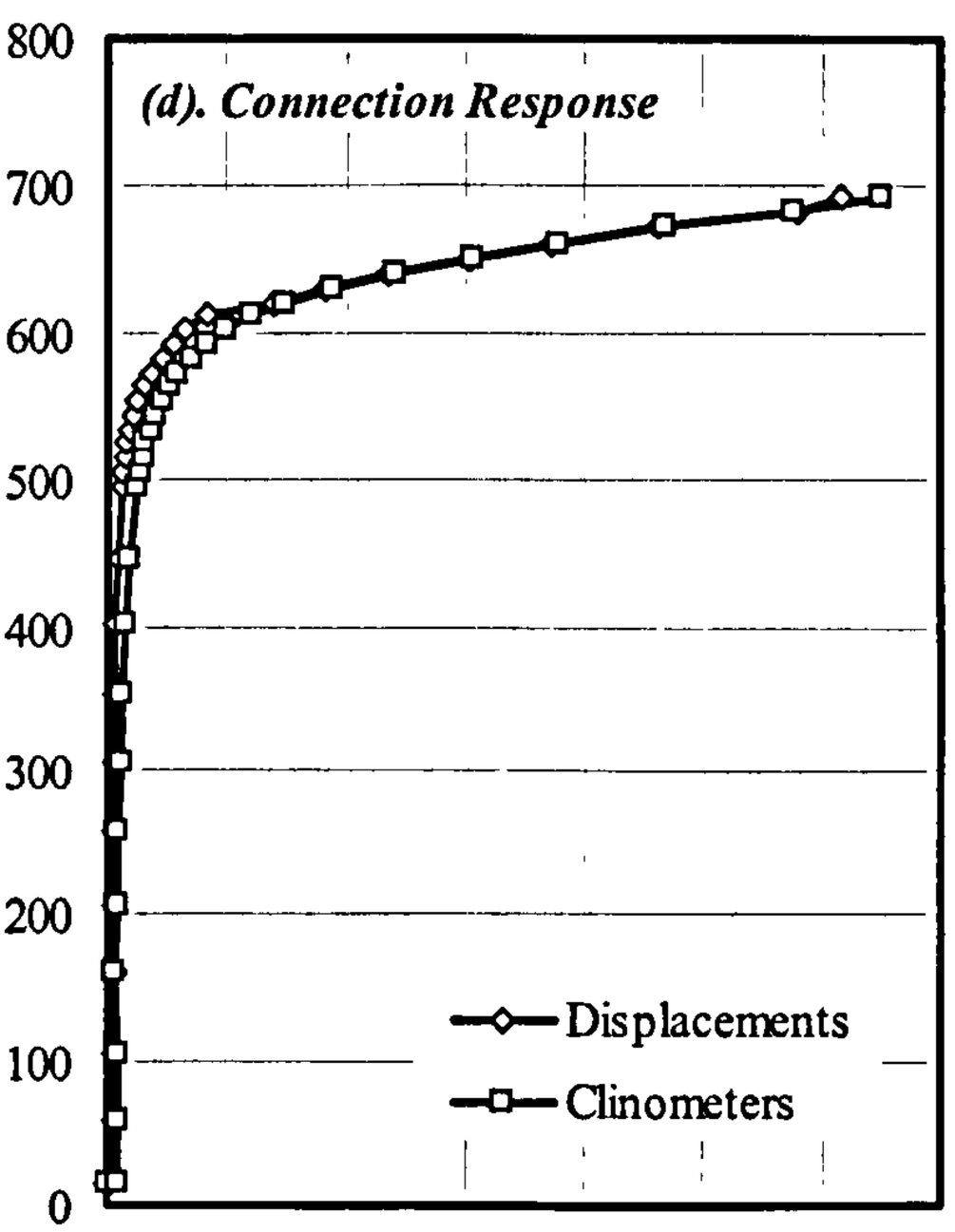

Figure 3.25: Summary of Results from Group 3: Fire Test 1 (FLB31)

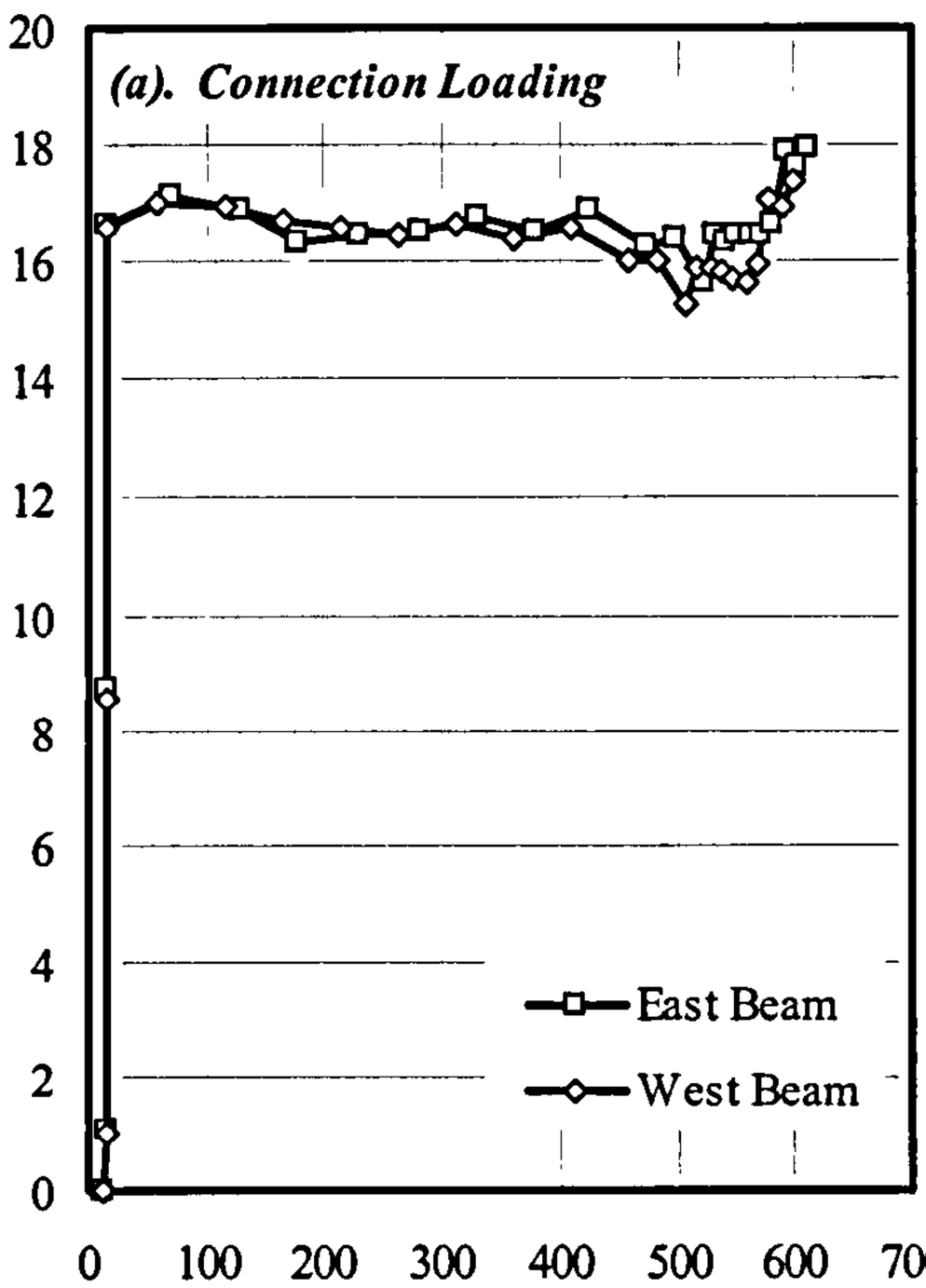

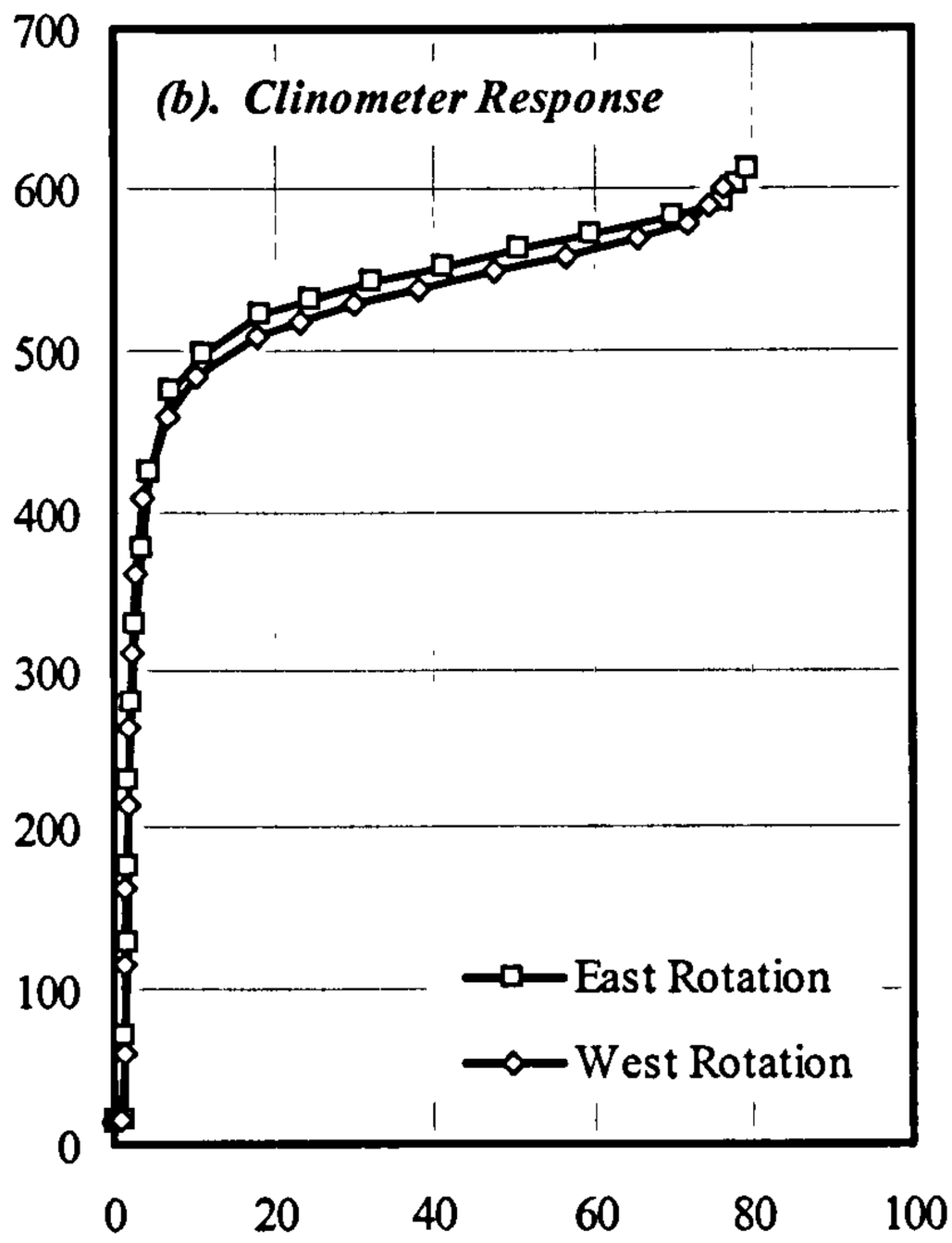

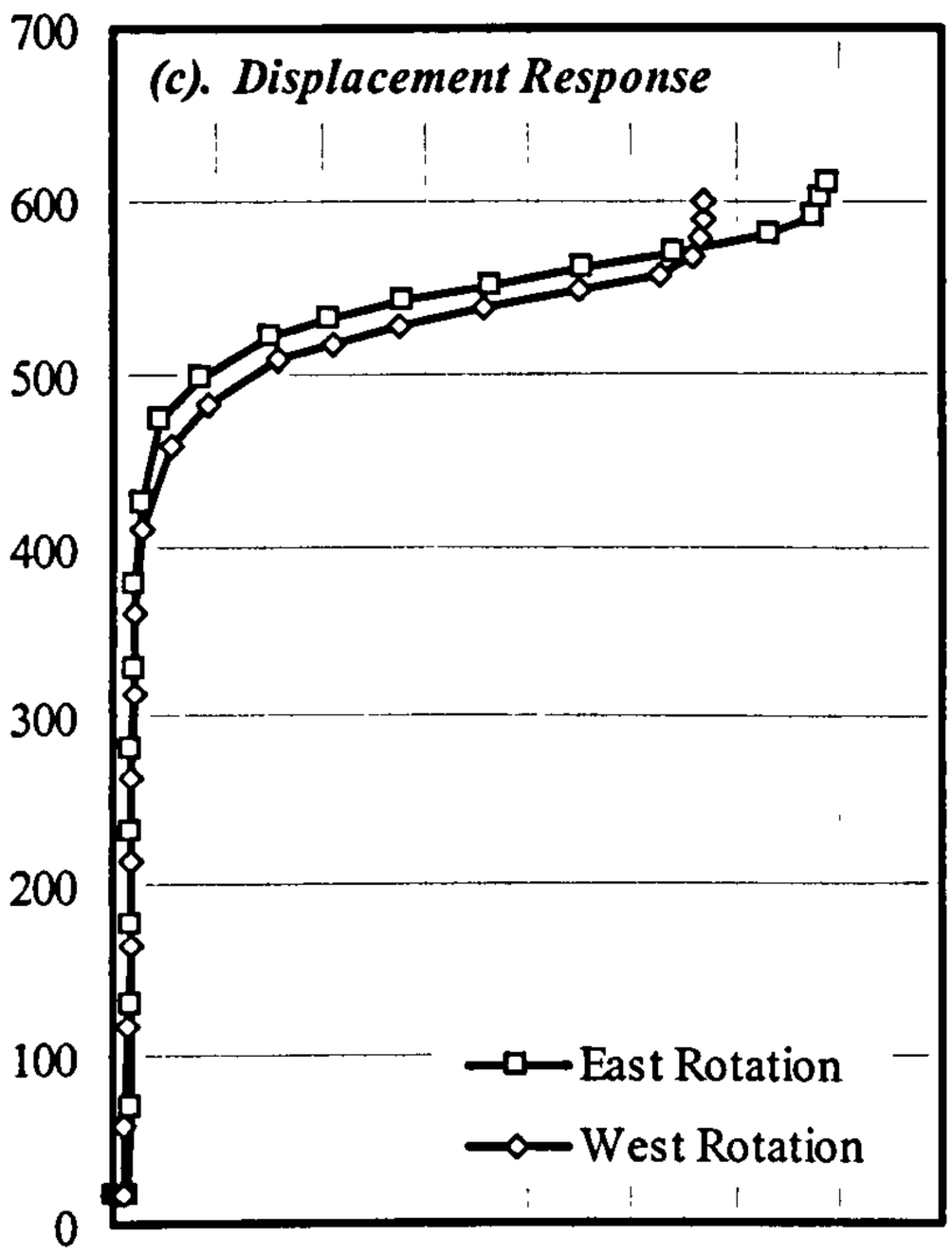

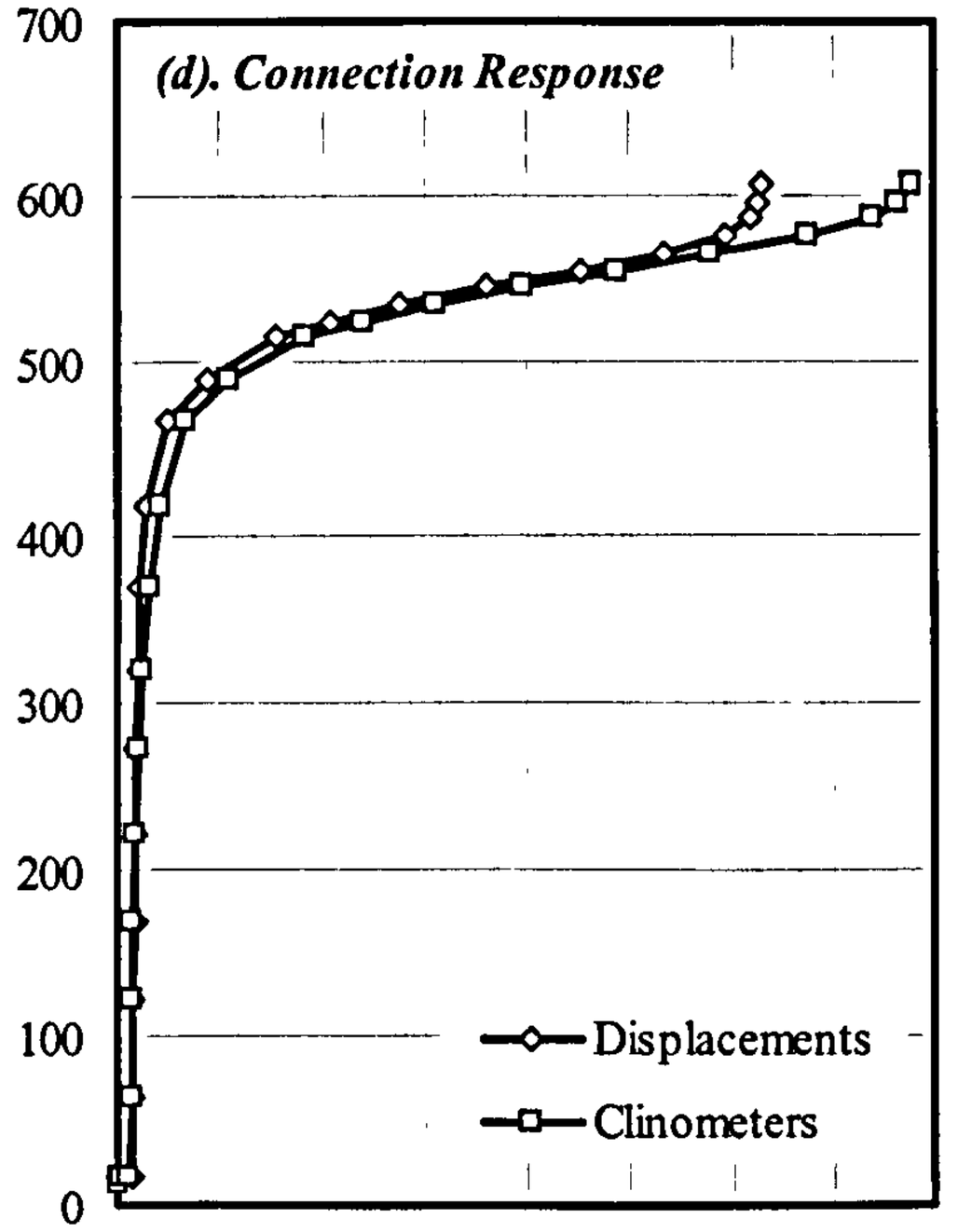

Figure 3.26: Summary of Results from Group 3: Fire Test 2 (FLB32)

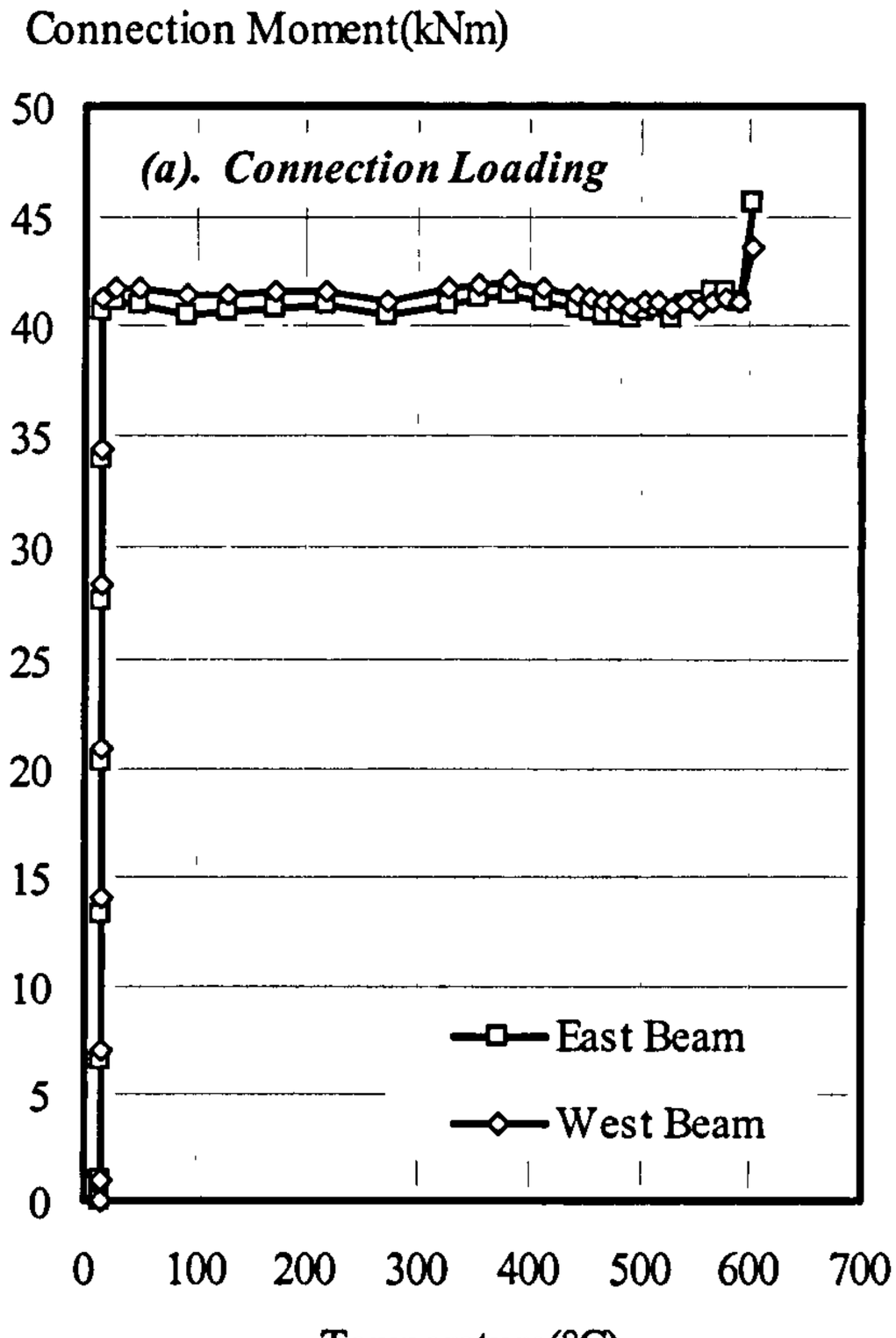

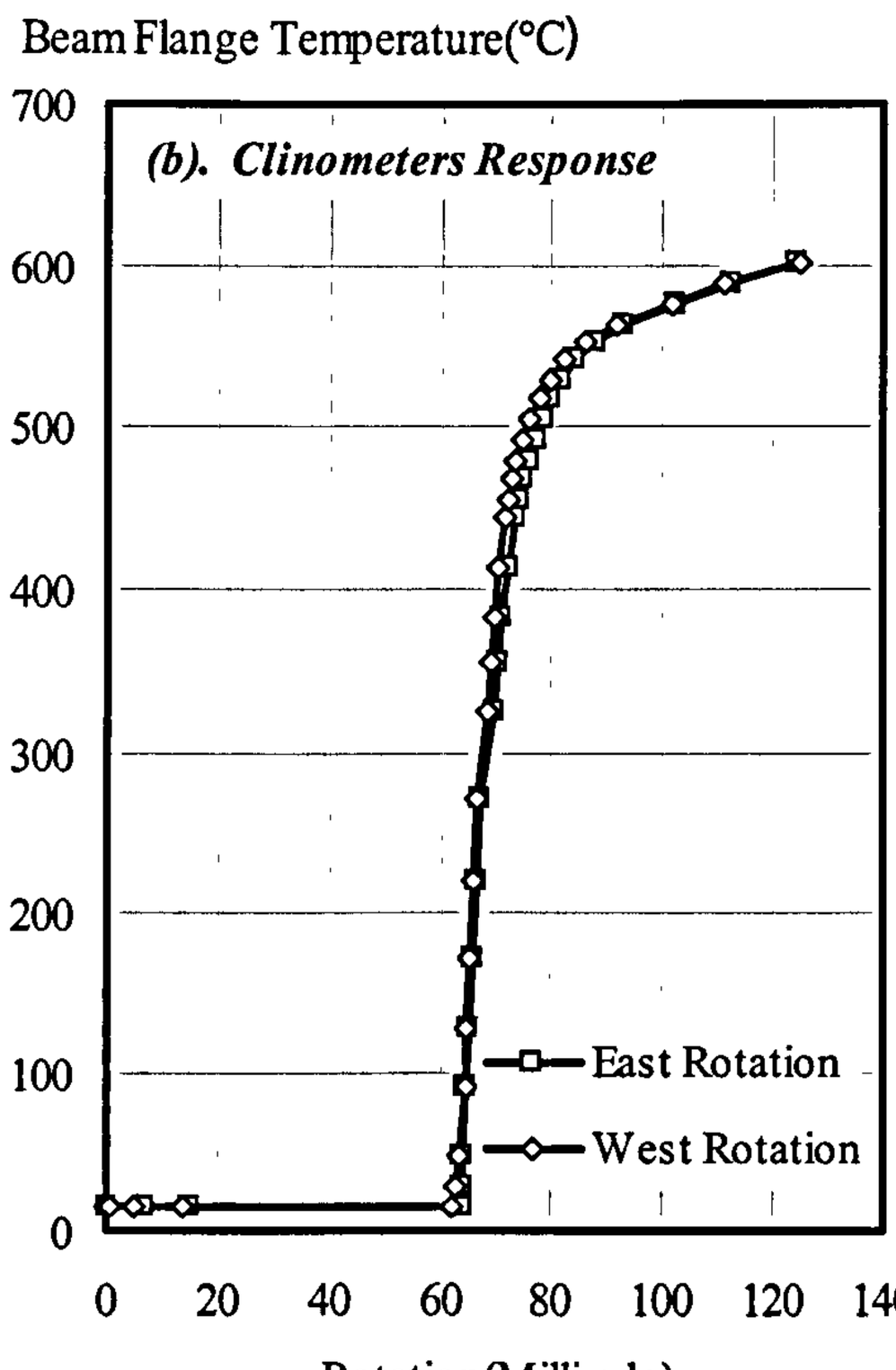

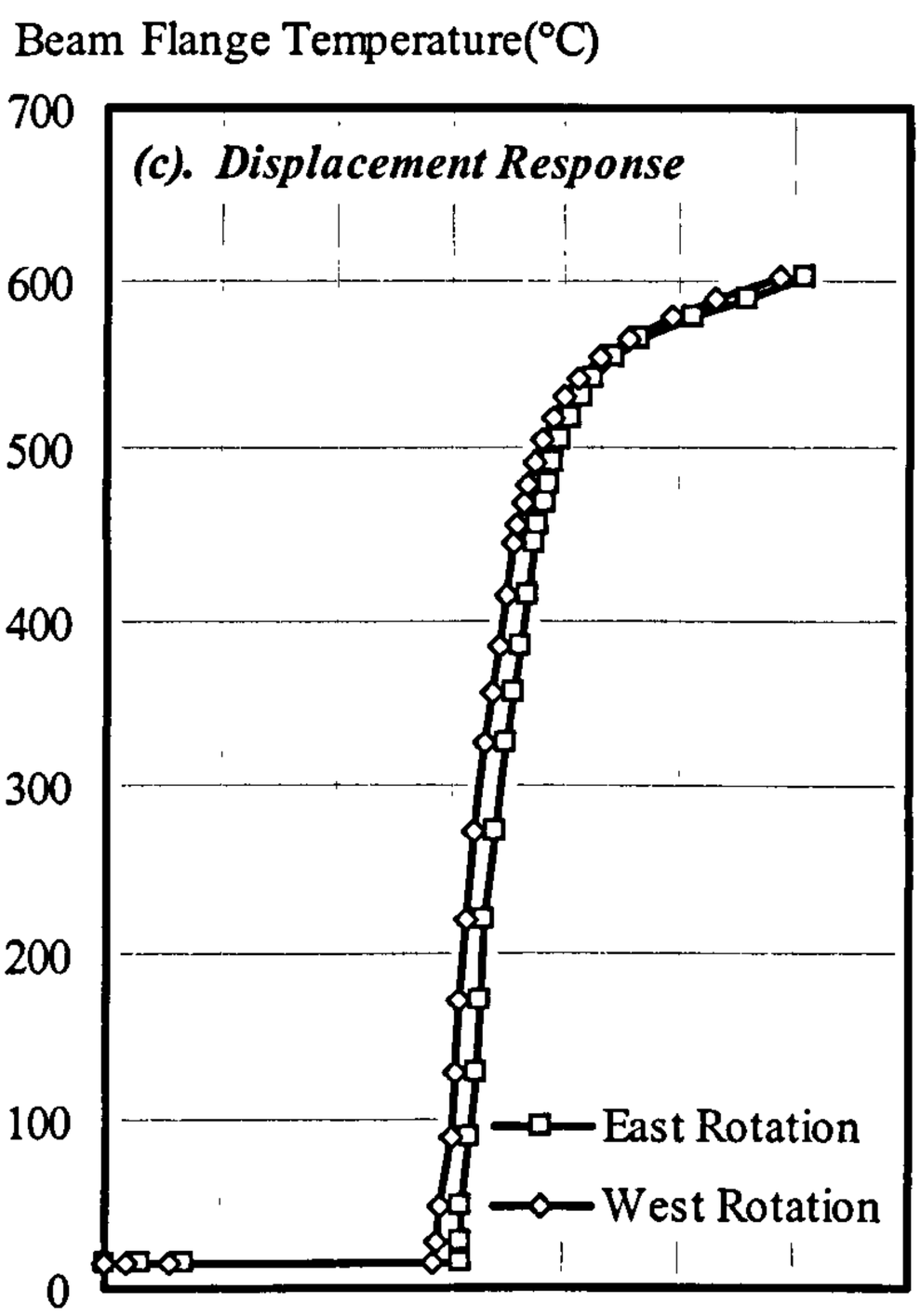

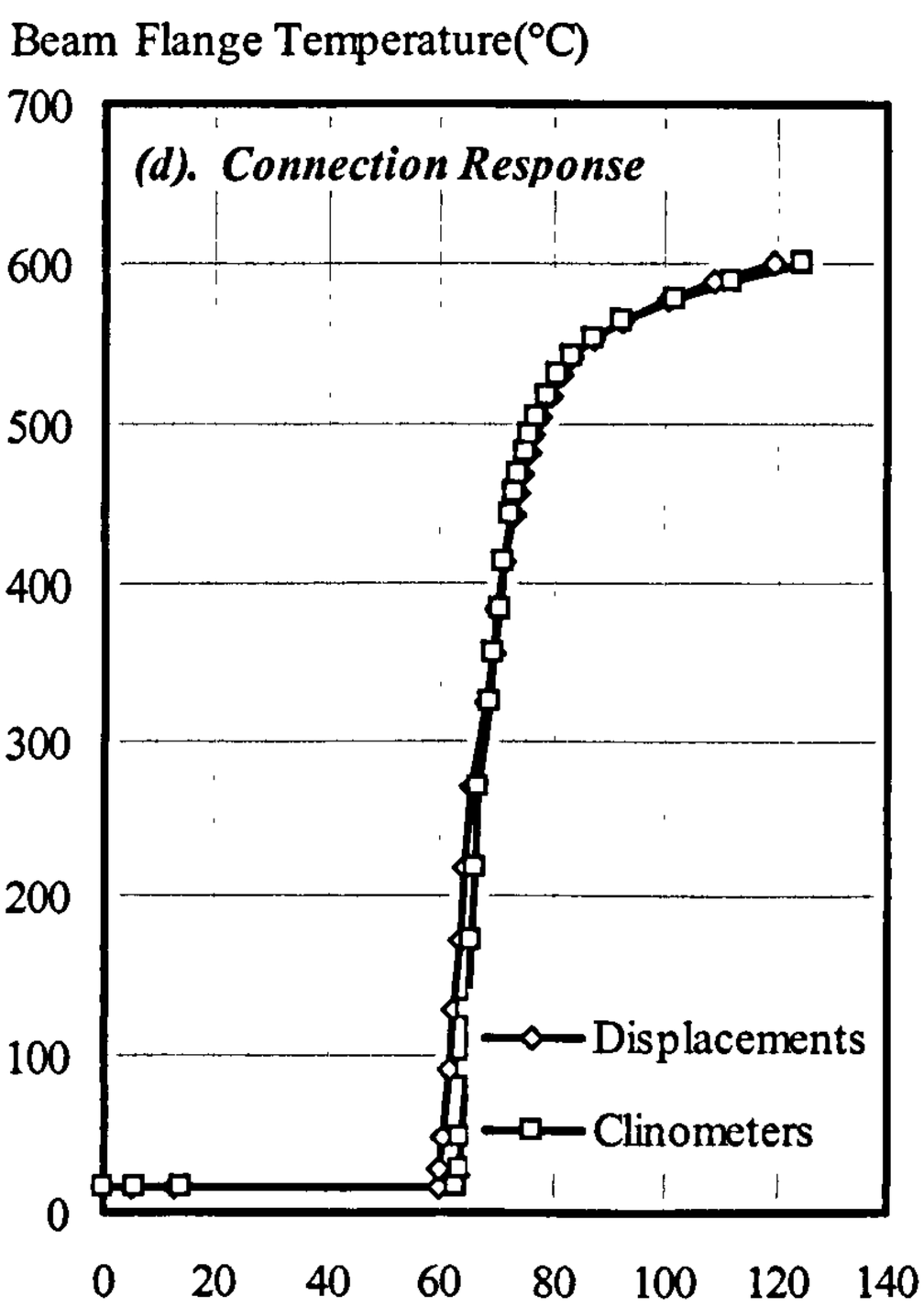

Figure 3.27: Summary of Results from Group 3: Fire Test 3 (FLB33)

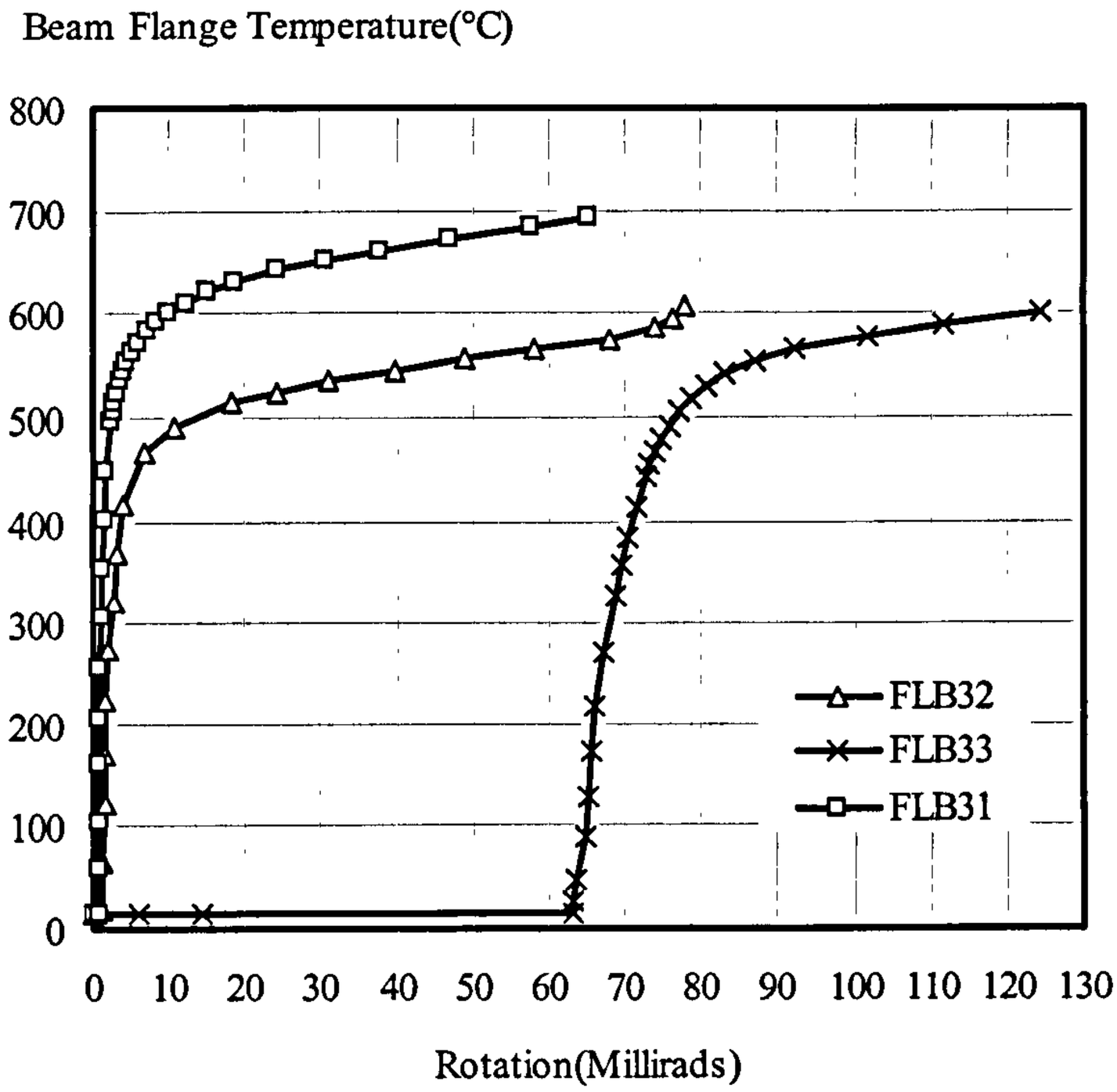

Figure 3.28: Elevated Temperature Connection Response of Group 3 Tests

4 ELEVATED TEMPERATURE MOMENT-ROTATION TESTS ON COMPOSITE CONNECTIONS

4.1 INTRODUCTION

Composite construction has become popular for multi-storey structures in the last two decades, due to its increased structural efficiency allowing the use of lighter sections leading to cost saving when compared with bare-steel construction. Similarly the behaviour of beam-to-column connections is significantly improved by incorporating a composite slab. The composite action is achieved by casting a concrete slab over the top flange of the beams. A nominal steel mesh is used to control the development of cracks as well as providing resistance to any applied tensile forces. Shear studs are used to ensure that the composite slab and the bare-steel section act compositely.

At elevated temperature the composite slab acts as insulation to the top part of the connection, reducing its temperature and thus potentially enhancing the inherent fire resistance of the structure. It has been found that the upper flange in a floor beam supporting a concrete slab is likely to reach significantly lower temperatures than the rest of the beam. The temperature difference may be as much as 40%[103]. The rate of degradation of the connection capacity should therefore be less than the bare-steel connection due to the beneficial effect of reduced temperatures. The behaviour in fire of unprotected composite beam-to-column connections has been investigated experimentally by Lawson[48] and more recently by Leston-Jones[50,51,52]. However, these provided information within a limited range of small section sizes only and a more representative investigation is required in order to achieve a better understating of the performance of composite connections in fire.

To study this, two series of tests were carried out using flexible connections. Flexible connections may be considered as simple connections, designed as nominally pinned, but possessing a degree of rotational rigidity. They are simple to fabricate and erect resulting in reduced construction costs. The connections were selected as being typical of those used in the Cardington full-scale test frame.

4.2 TEST ARRANGEMENT AND MATERIAL PROPERTIES

The cruciform test arrangement and furnace was as used in the bare-steel connection fire tests. The form of the composite slab was the same as that used for the Cardington test facility, namely PMF COMFLOR C70 decking with 130mm overall slab depth using lightweight concrete of Grade C35 with A142 mesh reinforcement. Slab dimensions were restricted due to the confinement of working within the furnace. The length of continuous slab across the connection was 1400mm and its width was 1200mm. The length of the slab was enough to allow two 100mm by 19mm shear studs at 300mm centres on each cantilever beam. Fig. 4.1 shows a typical composite connection. Insulation material was attached to the top of the concrete slab in order to prevent it from being heated on this surface, thereby simulating the condition in a real fire.

Figure 4.1: Typical Composite Specimen

Prior to concreting, a supporting structure was constructed for each specimen and secured to the floor. It was constructed in such way that prevented any movement of the test arrangement during casting that may result in separation of the steel sections and the concrete. Once the erection of the supporting structure was completed, the connection assembly was then lifted into the bay. The decking was orientated with the ribs parallel to the beams. A continuous 130mm trim was attached to the edges of the decking by a number of angle brackets using pop-rivets. The small gaps left between the column and the edge trim were filled with plasticine. Then the reinforcing mesh was cut to size and laid to rest on the top of the decking. A cut was made in the decking corresponding to the column section, in order to avoid any discontinuity in the decking in the vicinity of the column.

The characteristic strength of the concrete at 28 days was designed to be 35 N/mm^2 with a workability corresponding to a slump of 75mm. The maximum free water/cement ratio and the minimum cement content were not specified. Concreting work was conducted outside the testing laboratory. Casting of test cubes and cylinders was carried out at the same time. The cubes and cylinders were covered by polythene sheeting to minimise evaporation and left to cure near the specimens. They were tested after 28 days and on the day of the connection test, according to the BSI test standard. For the first test series, the concrete slab was allowed to cure for 28 days before starting the first test. However for the second series, the testing was started after 21 days from the day of casting due to time restrictions.

A summary of the mechanical properties for the reinforcement and concrete are detailed in Appendix A. The cross-sectional area of the reinforcing mesh was consistent with

the nominal value, with an area of approximately 28.82mm^2. However the yield strength of the reinforcement was found to be 6% greater than the nominal value. The average compressive concrete strength was 54.8N/mm^2 - considerably higher than specified.

4.3 INSTRUMENTATION

Instrumentation was similar to that used in the bare-steel connection tests. Thermocouples were attached to measure the temperature profile across the connection, with one more thermocouple positioned at the top of the slab beneath the ceramic blanket to monitor its surface temperature. Unfortunately it was not possible to measure the temperature distribution through the depth of the slab.

In order to measure connection rotations four displacement transducers were positioned at regular spacing along each cantilever beam. One additional transducer was placed in the column plane to monitor the column expansion during testing. Connection rotations were also recorded directly by clinometers that were attached along the centre line of the beam web at a distance of 250 mm from the face of the column flange. Loading was applied by means of hydraulic jacks and controlled by a manual pressure valve.

4.4 GROUP4: FLEXIBLE END-PLATE COMPOSITE CONNECTION TESTS (FLC4)

The connection type and the beam and column sizes were identical to those used in the Group 3 bare-steel tests. The specimen details are shown in Fig. 4.2. This type of connection was selected to provide a comparison between steel and composite connections at elevated temperatures.

Four tests were conducted at constant loads with increasing temperature while one additional test carried out at ambient temperature in order to establish the moment-rotation characteristics. The test programme is summarised in Table 4.1.

The calculated moment capacity of a composite connection usually accounts for the effect of reinforcement. Due to the lack of design guidance for flexible composite connections, the method adopted by SCI/BSCA[44] primarily for the design of composite moment connections was used. The centre of the connection rotation was assumed to be at the edge of the end-plate. The moment capacity of the connection was calculated as 104.5kNm based on the nominal material and geometrical properties. The test loads were applied at a distance of 1370mm from the face of the column flange, and monitored using compression load cells.

A description of each individual test is presented in the following sections.

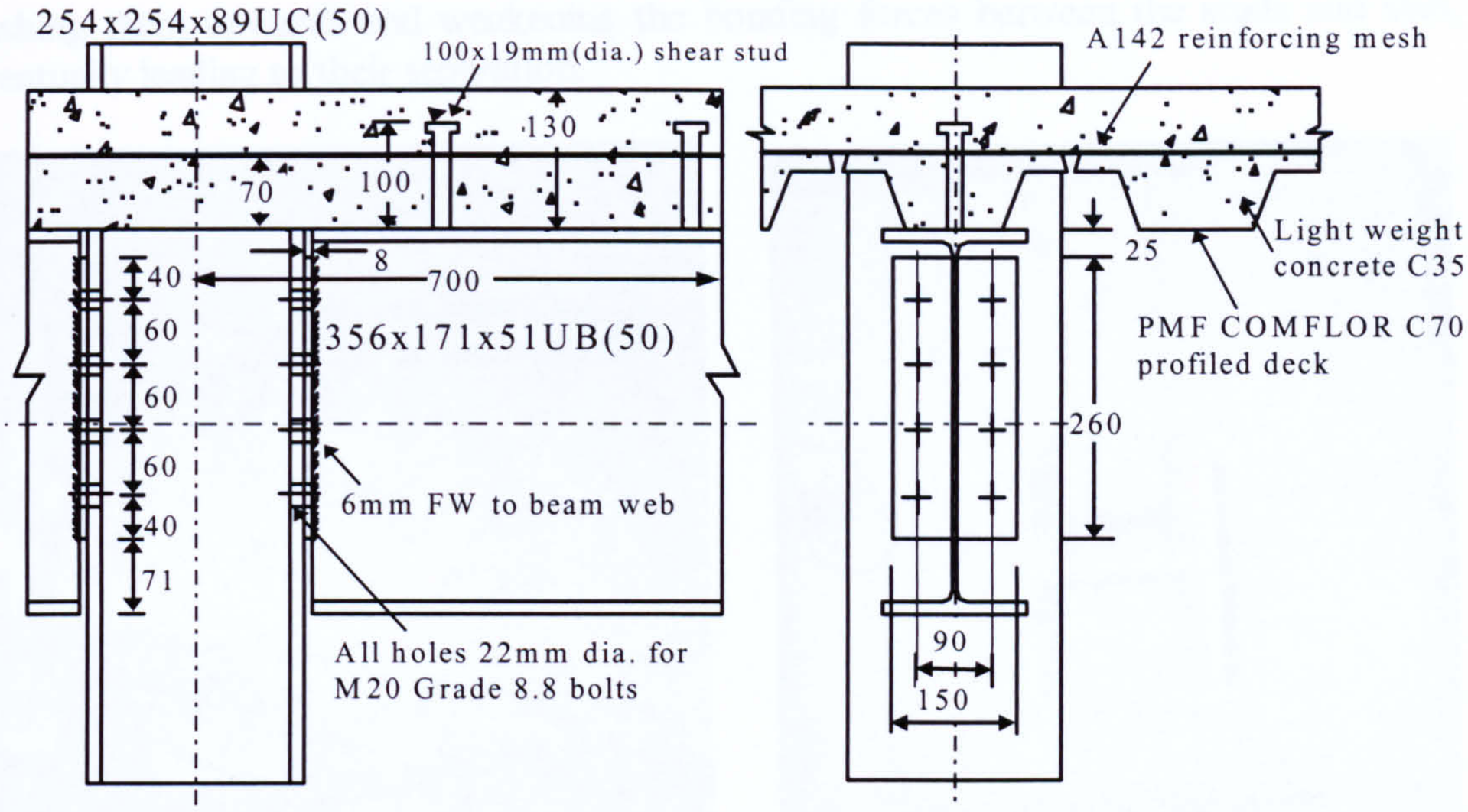

Figure 4.2: Flexible End-Plate Composite Connection Detail (Group 4)

Table 4.1: Group 4: Flexible End-Plate Composite Connection Experimental Test Programme

Test:	*Moment Level:*	*Applied Moment:*	*Temperature:*	*Comments:*
FLC4AMB	M_{cc}	Full Range	Ambient	Amb.-temp. M-ϕ
FLC41	$0.32M_{cc}$	34 kNm	10°C/minute	Group 4, Fire Test 1.
FLC42	$0.46M_{cc}$	46 kNm	10°C/minute	Group 4, Fire Test 2.
FLC43	$0.59M_{cc}$	62 kNm	10°C/minute	Group 4, Fire Test 3.
FLC44	$0.78M_{cc}$	82 kNm	10°C/minute	Group 4, Fire Test 4.

4.4.1 General Observations from Group 4 Connection Tests

Similar modes of failure were noticed in all Group 4 tests whether ambient or elevated temperature. Failure in the concrete slab firstly took place followed by failure of the flexible end-plate. In the concrete slab a large crack propagated from the face of the column flange parallel to the primary beam, resulting in fracture of some reinforcing bars and exposure of the shear studs as shown in Fig. 4.3*(a)*. This crack occurred due to a pulling through of the shear studs within the concrete slab. A major reason for this separation of the shear studs is that, due to the restricted space within the furnace, only one third of the beam span was constructed as composite allowing just two shear studs in each beam.

When the beam was loaded the end-plate rotated and the shear studs were exposed to a large tangential shear force. Moreover, with increasing temperatures there was an upward movement of the beam due to expansion. This exerted a force on the studs

pushing them upwards and weakening the bonding forces between the studs and slab, eventually leading to their separation.

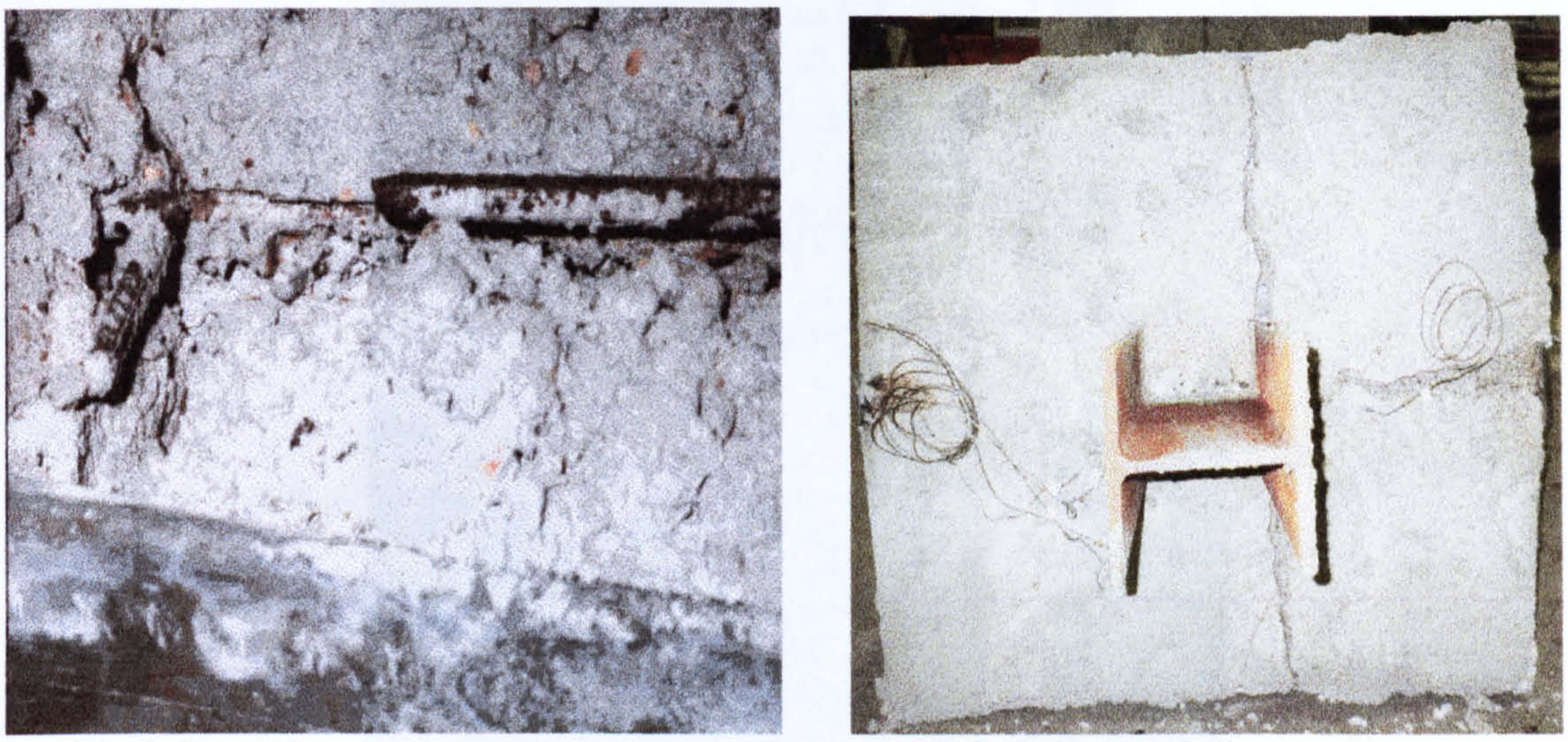

(a) Mesh Bars Fracture *(b) Slab Crack Patterns*

Figure 4.3: Concrete Slab Failure in Group 4 Tests

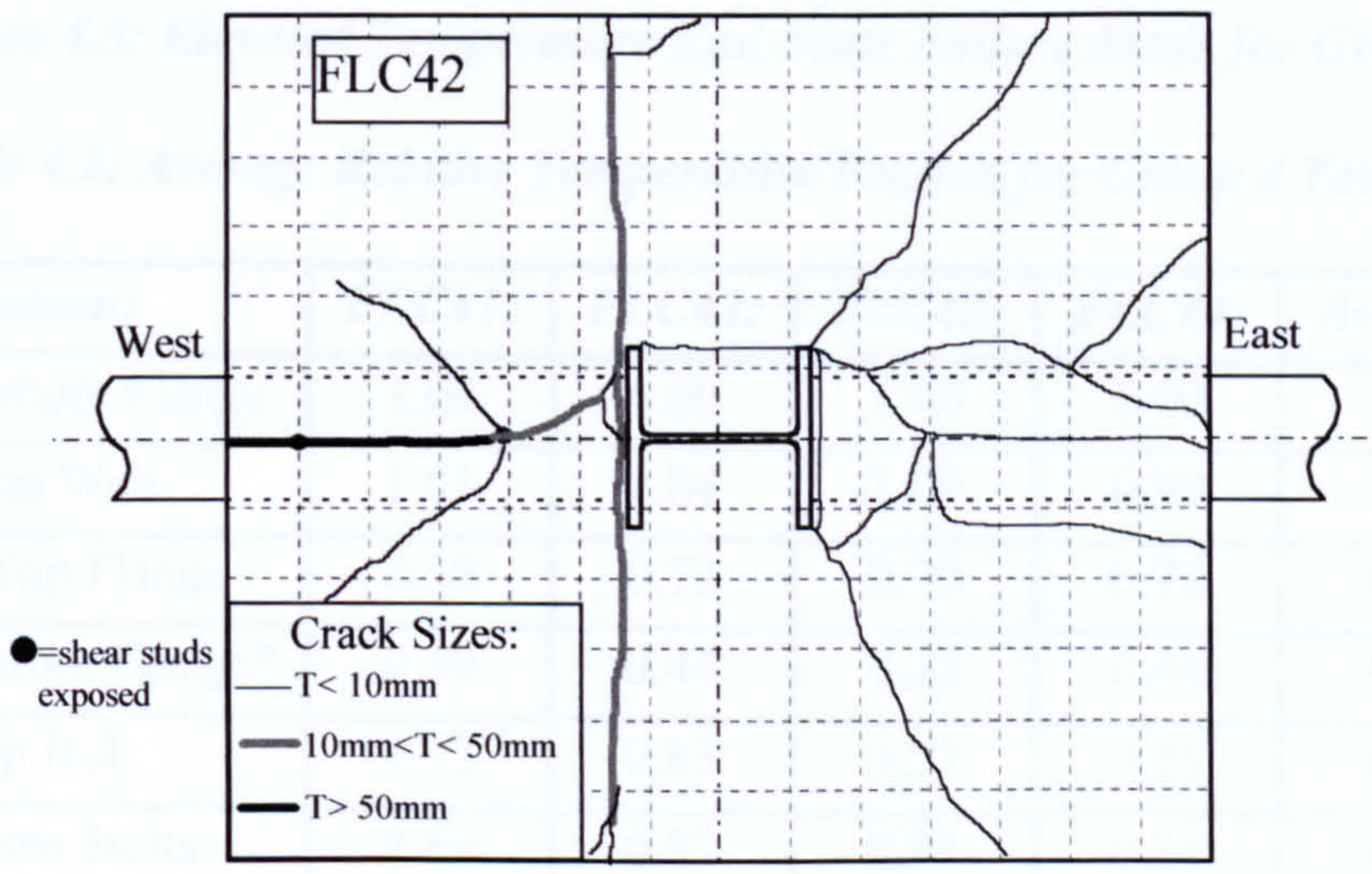

Figure 4.4: Typical Slab Crack Locations in Group 4 Tests

Two major secondary cracks were observed perpendicular to, and continuous across the connections on both sides of the slab. These cracks were narrower than the main crack and occurred due to the considerable end-plate deformation which imposed high tensile strain on the decking and slab as shown in Fig. 4.3*(b)*. There were also many tiny cracks in various areas in the slab.

Tests at the higher load levels resulted in more pronounced cracking. Despite similar cracking patterns in the ambient and elevated temperature tests, the crack width was also more pronounced at higher temperatures due to the evaporation of the moisture content causing the concrete to become dry and more brittle. Fig. 4.4 shows typical crack locations in the composite slab. There was no sign of distortion to the metal decking.

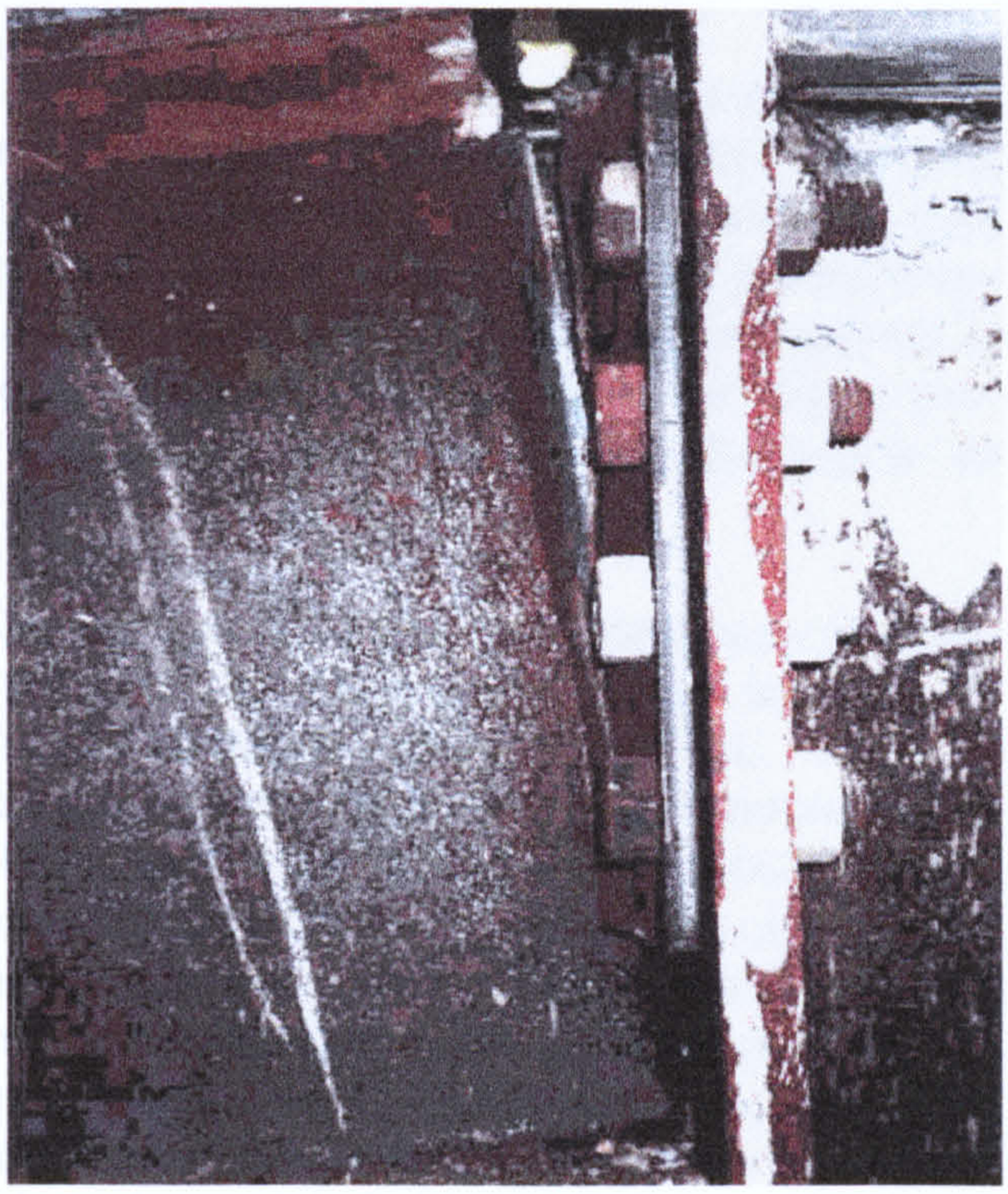

Figure 4.5: Elevated Temperature End-Plate Failure Mode for Group 4

Table 4.2: Average Relative Temperature Profiles for Group 4 Tests

Element:	*FLC41:*	*FLC42:*	*FLC43:*	*FLC44:*	*Average:*
Beam Bottom Flange	1.00	1.00	1.00	1.00	1.00
Beam Web	1.01	1.04	1.09	0.99	1.03
Beam Top Flange	0.58	0.72	0.70	0.72	0.68
Beam Bottom Flange*	0.39	0.44	0.33	0.44	0.40
Top Bolt	0.72	0.83	0.77	0.75	0.77
2nd Row Bolts	0.86	0.87	0.91	0.84	0.87
3rd Row Bolts	0.85	0.88	0.94	0.88	0.89
Bottom Bolt	0.92	0.92	0.92	0.91	0.92
Column Web	1.07	1.06	1.14	1.06	1.08
Column Flange	0.93	0.98	1.07	0.94	0.98
Column Flange*	0.33	0.35	0.40	0.37	0.36
End-plate	0.98	0.86	0.89	0.85	0.90
Concrete Surface	0.09	0.14	0.13	0.17	0.13
Clinometer Box	0.08	0.09	0.09	0.11	0.09
Furnace Atmosphere	1.35	1.35	1.59	1.58	1.47

Note: * identifies insulated thermocouple locations

After the concrete had cracked the stiffness of the connection gradually decreased, with the connection force transferred largely to the end-plate. In most tests the end-plate subsequently fractured along the toe of the weld connecting it to the beam web. This fracture started at the top of the end-plate, where the tension force is greatest, causing a large deformation. It should be noted that the end-plates did not completely fracture but in most cases extended over about two thirds of the depth, and on one side only, as illustrated in Fig. 4.5. There was no deformation observed to the beams, column and bolts.

Temperature profiles for Group 4 elevated temperature composite connection tests are detailed in Table 4.2, with the beam bottom flange temperature being chosen as the reference. This shows a consistent pattern for all tests. It may be seen that there was some degree of variation in temperature distribution across the depth of the connection, especially at the beam top flange due to the presence of the composite slab. The presence of the composite slab above the connection caused a reduction of 30% in the beam top flange temperature compared with the bottom flange temperature. This is due to the insulation and heat sink effect of the concrete slab and enhances the connection performance at elevated temperatures. Once again, the highest temperature - about 8% higher than the beam lower flange temperature - in the connection components was observed to be in the column web. The temperature maintained by the top surface of the concrete slab was approximately 13% of the beam lower flange temperature due to the protection of the fibre blanket. As in the previous tests the temperature in the housing box protecting the clinometer reached only 9% of the beam lower flange temperature.

4.4.2 Group 4: Ambient Temperature Test (FLC4AMB)

One reason for performing an ambient temperature test was to define appropriate load levels for the elevated temperature tests. An identical specimen to those used in the Group 4 elevated temperature tests was used. The load was initially applied in 10 kN steps, reducing to 2.5 kN as the connection approached failure. As the load applied to the connection increased, an almost linear response up to moments of approximately 50 kNm was observed with an enhanced stiffness compared with the corresponding bare-steel connection. At approximately 50 kNm, the composite slab started to crack. The crack width increased with increasing loads until moments of nearly 69 kNm were reached. At this point the concrete slab became unable to support any further loading within the connection due to tensile failure of the reinforcement and separation of the shear studs from the composite slab. As a consequence, the loads transferred to the end-plate, resulting in significant end-plate deformation. This is represented by a flat plateau in the moment-rotation curve.

Subsequent to the slab failure, the load applied to the connection slightly decreased due to the reduced stiffness of the connection. The connection regained equilibrium at a moment of approximately 64.5 kNm as the beam flange came into contact with the column at a rotation of about 65 millirads. This caused an increase in the connection stiffness with further rotation until a second plateau in the moment-rotation curve leading to the onset of connection failure. The test was terminated when there was an abrupt reduction in the loading mainly in the East connection due to fracture of the end-

plate. The average maximum moment recorded was approximately 101.6 kNm. The observed failure mechanism of the connection was similar to that for bare-steel and consistent with the elevated temperature composite connection tests.

Results from the ambient temperature test are summarised in Fig. 4.6. The connection rotations were measured using both clinometers and displacement transducers. Both clinometer and displacement transducer readings for the West connection produced erratic results for rotations greater than 30 millirads necessitating reliance on recorded East connection rotation. It may be seen from Figs. 4.6*(b)* and 4.6*(c)* that there was fairly close agreement between the rotation of the East and West connections with the West connection exhibiting a slightly stiffer response. Rotation readings for the East connection recorded by both clinometer and displacement transducers were in good agreement as shown in Fig. 4.6*(d)*.

4.4.3 Group 4: Fire Tests

The four fire tests were conducted in a similar manner to that adopted in the bare-steel connection tests. Again some of the tests had to be conducted in two stages, because of end-plate deformation which prevented testing the specimen up to failure. This is because the specimen beams came into contact with the furnace doors. However, the tests involving low levels of moment, had to be terminated prematurely when the beams came to bear against the furnace doors.

4.4.3.1 Group 4: Fire Test 1 (FLC41)

A small load level of approximately 34 kNm was applied to the connection, in three steps. The resulting connection response is summarised in Fig. 4.7. As in the bare-steel flexible end-plate tests conducted under low levels of loading, the test was terminated when both the beams touched the furnace doors. Fig. 4.7*(a)* shows that there was consistency in the applied load levels to the two connections throughout testing with the East beam experiencing a slightly higher loading than the West. This was probably caused by contact between the Macalloy bars and the laboratory floor. The average moment capacity of the connection recorded was approximately 34.3 kNm.

The connection response indicated by the clinometers and displacement transducers is shown in Figs. 4.7*(b)* and 4.7*(c)* showing close agreement between the rotation of both connections. The test was terminated at a temperature around 650°C, corresponding to the bearing of the beam flange against the column. At intermediate temperatures small reversals in rotation relative to the position at ambient temperature can be seen. This is possibly because of thermal bowing, due to the variation in expansion of the top and bottom beam flanges. Average rotations from clinometers compare closely with those obtained from displacement transducer readings as shown in Fig. 4.7*(d)*.

4.4.3.2 Group 4: Fire Test 2 (FLC42)

The second test was conducted under a nominal moment of 48 kNm, and the resulting behaviour is shown in Fig. 4.8. The average recorded moment applied to the

connection was approximately 47.5 kNm. Rotations recorded for the East and West connections were consistent as shown in Figs. 4.8*(b)* and 4.8*(c)* respectively. There was also good correlation between the response recorded by clinometers and displacement transducers as shown in Fig. 4.8*(d)*. The temperature profile and failure mechanism of the connection and the composite slab crack patterns were similar to the other tests performed in this group.

Fig. 4.8*(d)* shows a gradual increase in rotations for temperatures up to approximately 450°C, beyond which there is a knee in the temperature-rotation curve due to failure of the concrete slab. This is followed by a rapid increase in rotation as a result of end-plate deformation. At approximately 510°C and a rotation of 65 millirads, the connection enters the second phase of response. This is when the beam flange comes into contact with the column resulting in an enhanced connection response. After this contact, the connection was able to sustain a further temperature rise of 100°C without any sign of failure, and the test was terminated when both the beams came to bear against the furnace doors.

4.4.3.3 Group 4: Fire Test 3 (FLC43)

For this test the loading, equivalent to a connection moment of 62 kNm, was applied in five increments. The test was started following the normal procedures by increasing the loading up to the desired level and igniting the furnace. As the fire test started, a gradual increase in the connection rotation was observed, especially in the East connection. The deformation of both connections was carefully monitored visually and experimentally. At temperatures between 220°C and 250°C, the connection rotations increased rapidly and the East beam touched the furnace door. At this point there was no alternative but to abandon the test without any useful data.

With just one remaining specimen it would be difficult to generate the necessary representation of the connection response. Fortunately the specimen did not fail, although there was considerable end-plate deformation. Also, the steel should have retained most of its stiffness and capacity since it was only exposed to low temperatures. It was therefore decided to re-test the specimen up to failure, despite the fact that the connection may not behave exactly as it might if tested as normal.

The loads were removed and the resulting unloading rotation was monitored. The specimen was left to cool with the clinometers monitoring any changes in rotation. The next day, the specimen was carefully examined to check its integrity and that no connection component had suffered any form of failure or excess deformation which might affect the performance during repeat testing. After re-adjusting the furnace and the associated instrumentation, the specimen was loaded up to the same load level as in the initial test and the repeat test was started. The overall connection response obtained by superposition of the two stages is shown in Fig. 4.9

Fig. 4.9*(a)* shows that there is a reasonable consistency in the applied loading to the East and West Beams throughout the test, except at temperature 220°C, where the East beam is subject to a higher moment. This was probably due to the contact between the beam and the furnace door. The loading regime for the repeat test was observed to be

more stable than the first stage with a reduction in the loading as the connection failure became imminent. The average recorded moment was approximately 61.4 kNm.

After terminating the first phase of test it was found that the West connection clinometer and displacement transducers were not properly connected and thus generated unreliable results. Therefore, only results from the East connection were used for the first phase test. The overall connection response is shown in Figs. 4.9*(b)* and 4.9*(c)* for clinometer and displacement transducer readings respectively. Fig. 4.9*(d)* shows a comparison between the two. It can be seen that the magnitude of the rotation at which the East beam bears against the column is consistent with those rotations obtained from other tests.

4.4.3.4 Group 4: Fire Test 4 (FLC44)

A moment of approximately 82 kNm was applied to the connection. This load level was selected to provide information on the connection response after the beam comes into contact with the column. A similar test procedure was adopted to those tests with high load levels in that the test was carried out in two stages. In the first stage, the specimen was loaded up to 75 kNm in five steps at ambient temperature. The loads were then gradually removed with continuous monitoring of rotation as loading removed. The furnace and the associated instrumentation were re-adjusted to create a sufficiently deep slot between the beam bottom flanges and the furnace doors, allowing the beams to move down freely. The second stage started when the specimen was re-loaded up to the required load level (i.e. 82 kNm) and the elevated temperature testing commenced.

Results from the test are summarised in Fig. 4.10. It can be seen that the load levels for both the East and West beams were similar and consistent throughout testing with the average moment being approximately 82 kNm. There was a slight degree of variation in the ambient temperature rotations measured for the East and West connections by clinometers, probably as a result of rotation of the test arrangement as illustrated in Fig. 4.10*(b)*. However, the ambient temperature response for the East and West connections generated from displacement transducer readings are consistent, with the West connection demonstrating slightly stiffer behaviour as shown in Fig. 4.10*(c)*. The average rotations obtained from clinometers and displacement transducers are in close agreement as shown in Fig. 4.10*(d)*. Failure of the connection was similar to that observed previously but the slab cracks were more intense and the connection failure mode more pronounced.

4.4.4 Comparison of Results from Group 4 Flexible End-plate Composite Connection Tests

A comparison between the ambient temperature results obtained while loading the specimen in the initial stage of the elevated temperature tests, and the ambient temperature moment-rotation characteristics are shown in Fig. 4.11. It may be seen that there is close correlation between these. However the West connection in Test FLC44 is an exception to this behaviour demonstrating a greater stiffness than the ambient temperature test.

Ambient temperature moment-rotation characteristics for both the bare-steel and composite connection are compared in Fig. 4.12. The bare-steel connection characteristics are based on the results of an ambient temperature test conducted by Boreman *et al.*[100] to investigate characteristics of the connections utilised in the Cardington full-scale frame[18]. It may be seen that there is a significant enhancement due to composite action particularly at low levels of rotation. However the ultimate capacity for the bare-steel and composite are very close. This may be attributable to the limited extent of the composite slab and the small number of shear studs. This made it difficult to maintain the composite action between the steel section and the concrete slab throughout testing and failure of the slab occurred at low levels of rotation as discussed earlier. Subsequent to the concrete slab failure, the specimen would tend to behave as a bare-steel connection especially after contact between the beam and the column.

Temperature-rotation characteristics from all four elevated temperature composite connection tests are summarised in Fig. 4.13 based on clinometer readings. Tests FLC41 and FLC42 were performed satisfactorily with close correlation between the East and West connection responses as well as between the rotation measuring rotations. In the first the test was terminated prematurely when the beam flange came to bear against the column. However, as a result of conducting test FLC43 in two stages at elevated temperature, in which the first stage was terminated at a temperature around 250°C, the eventual failure temperature of the connection occurred at a lower temperature than that for test FLC44 although the latter involves application of higher load level. This was due to the effect of the first stage fire test in which the connection has lost some of its strength which consequently affected the actual connection response causing the connection to fail at low temperatures. Therefore, the temperature-rotation response of the connection was modified by increasing the failure temperature and rotation of the connection, since it was felt that this is what would be expected to represent the actual connection response if it was tested in one stage. Also, the temperature-rotation curve was smoothed to correspond to the responses experienced in the other three tests. In general the overall results from the series of tests show consistent elevated temperature degradation in the response of the connection with increasing temperatures and level of loading.

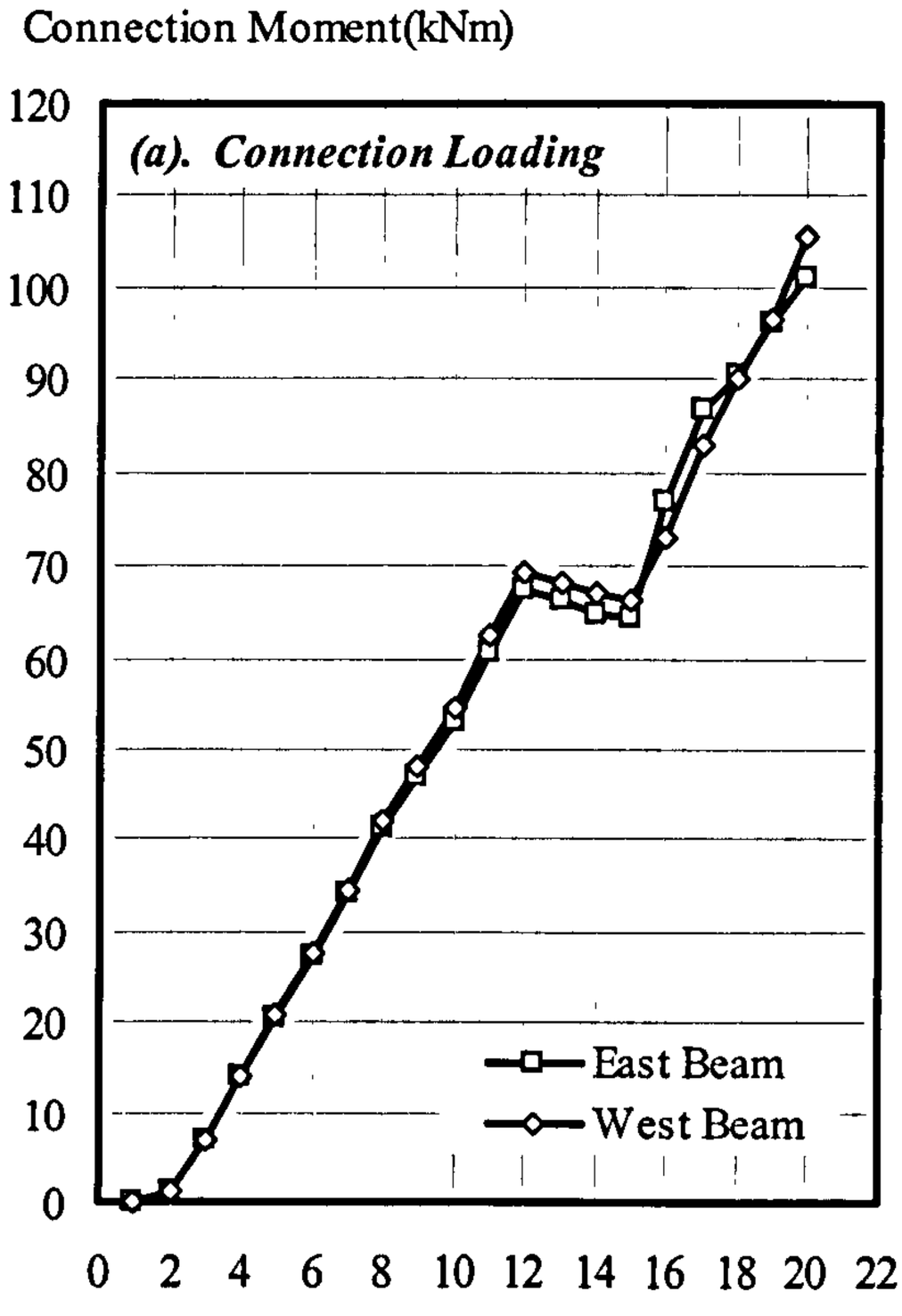

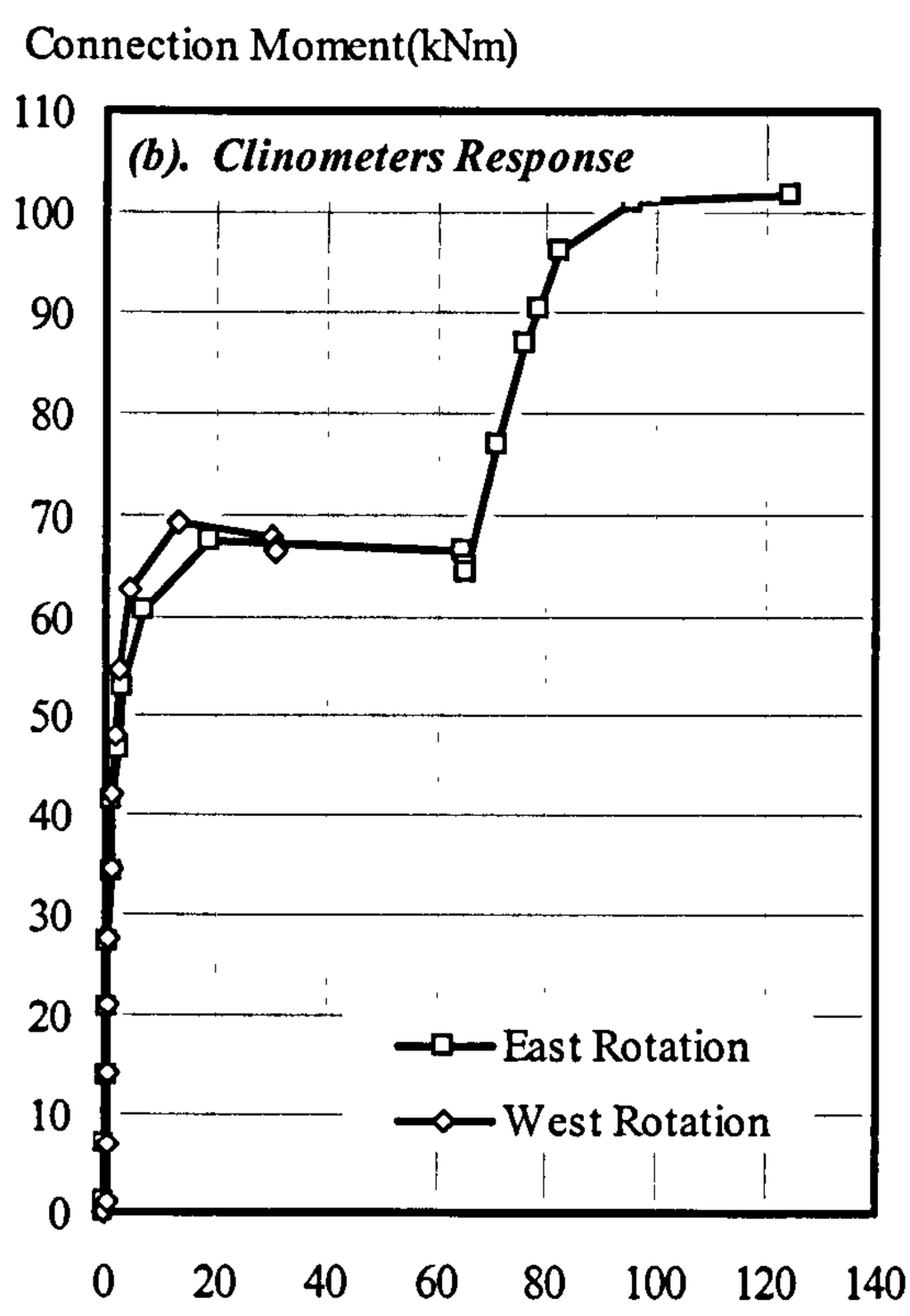

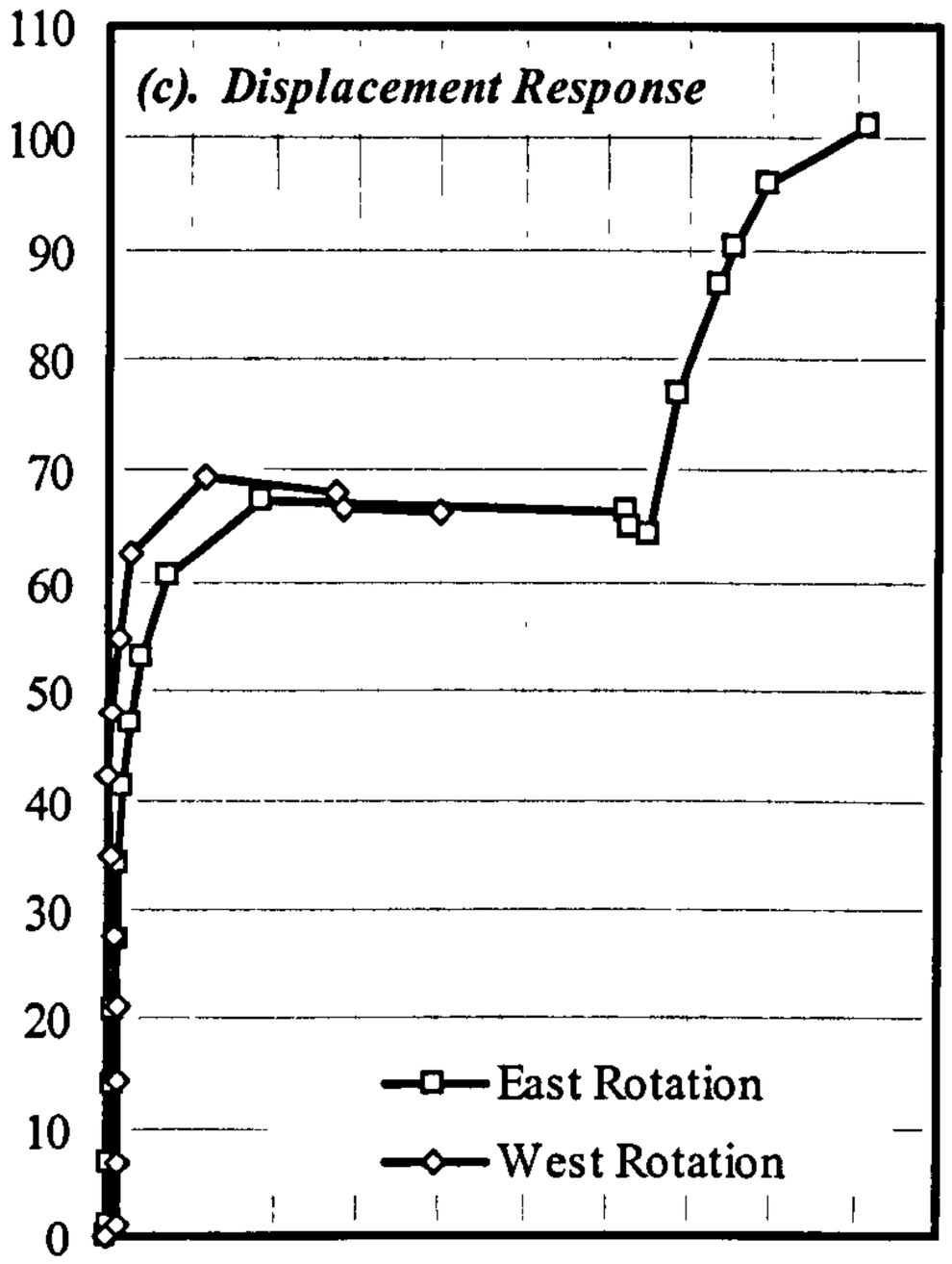

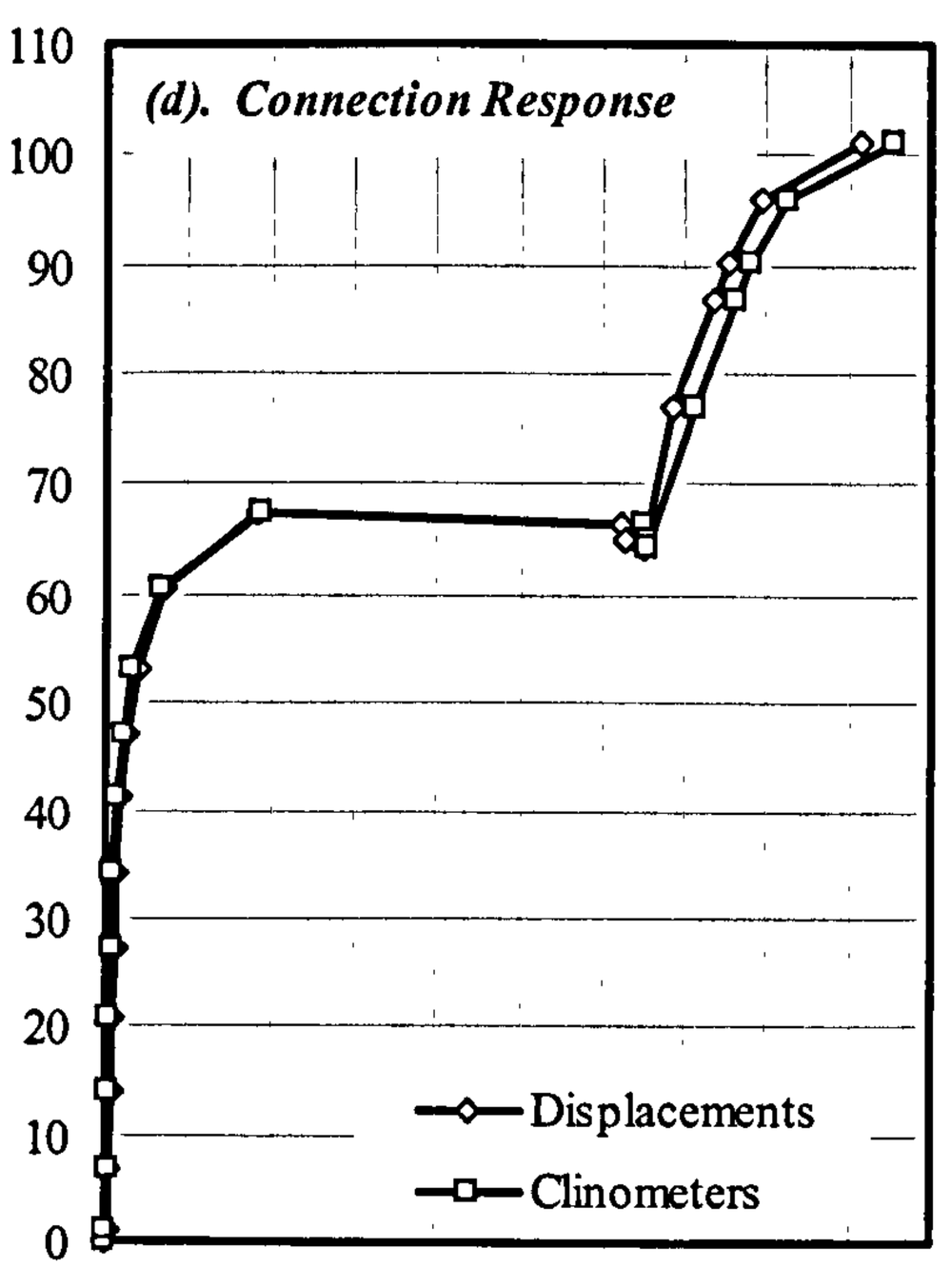

Figure 4.6: Summary of Results from Group 4: Ambient Temperature Test (FLC4AMB)

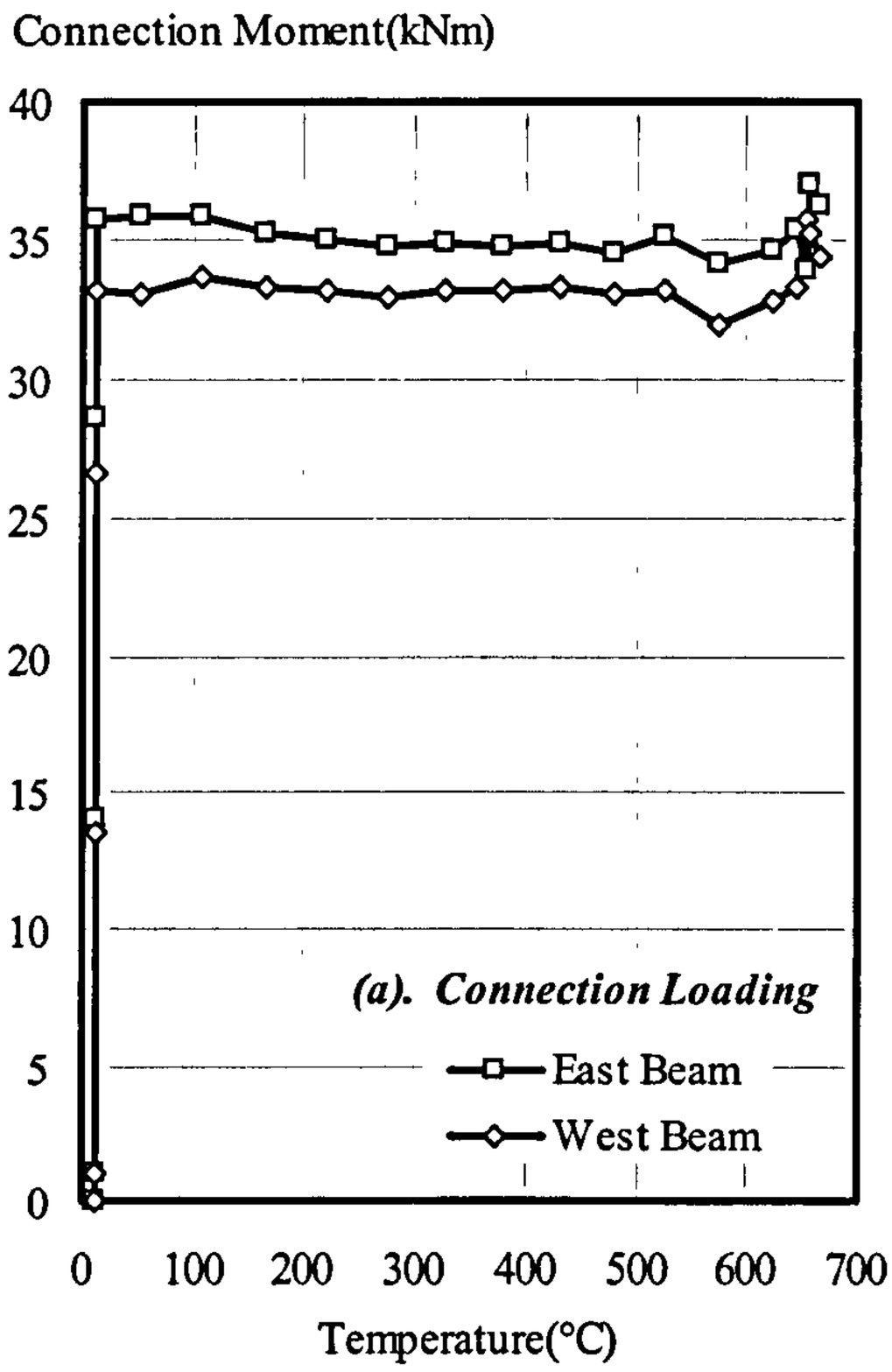

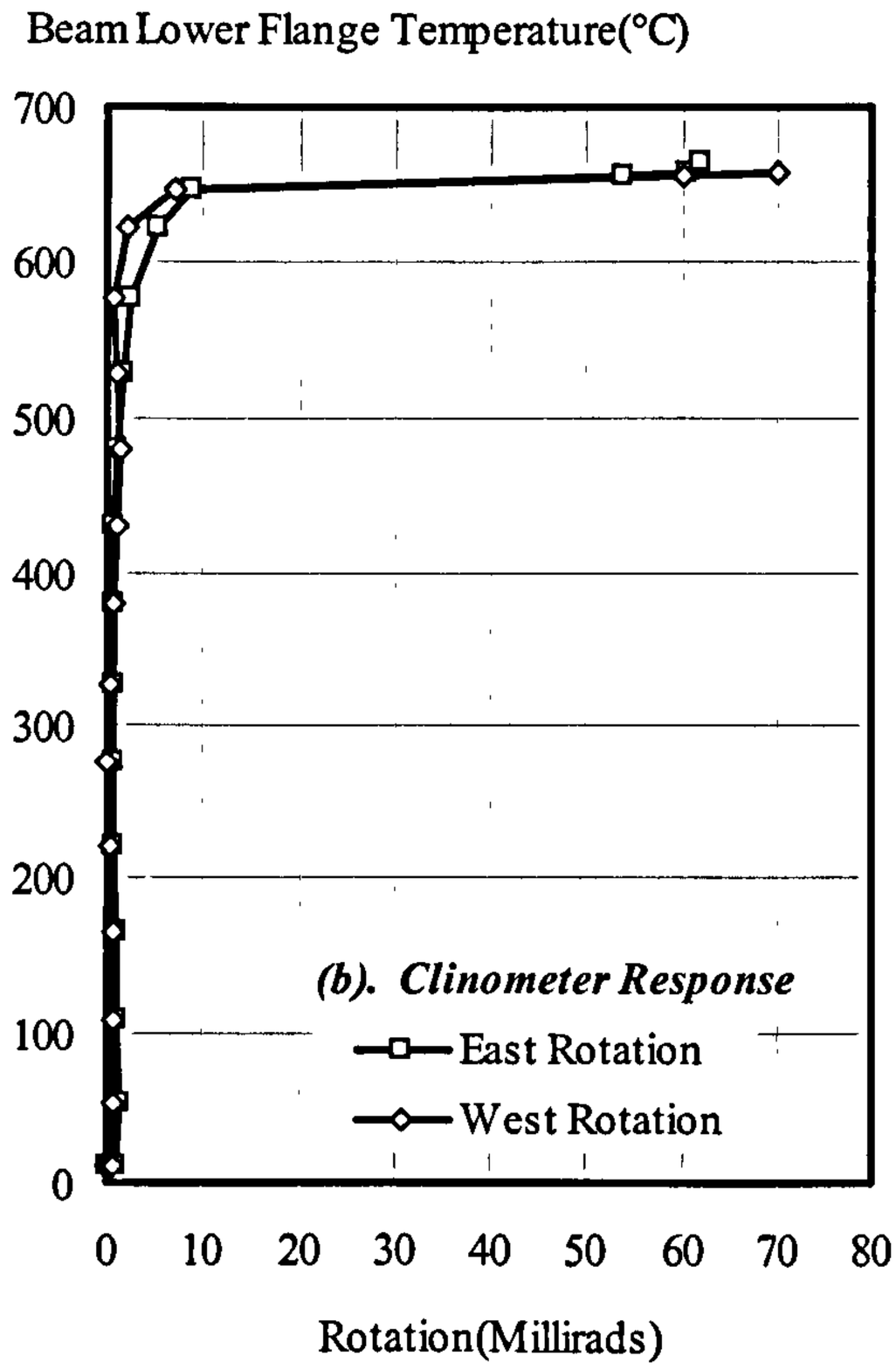

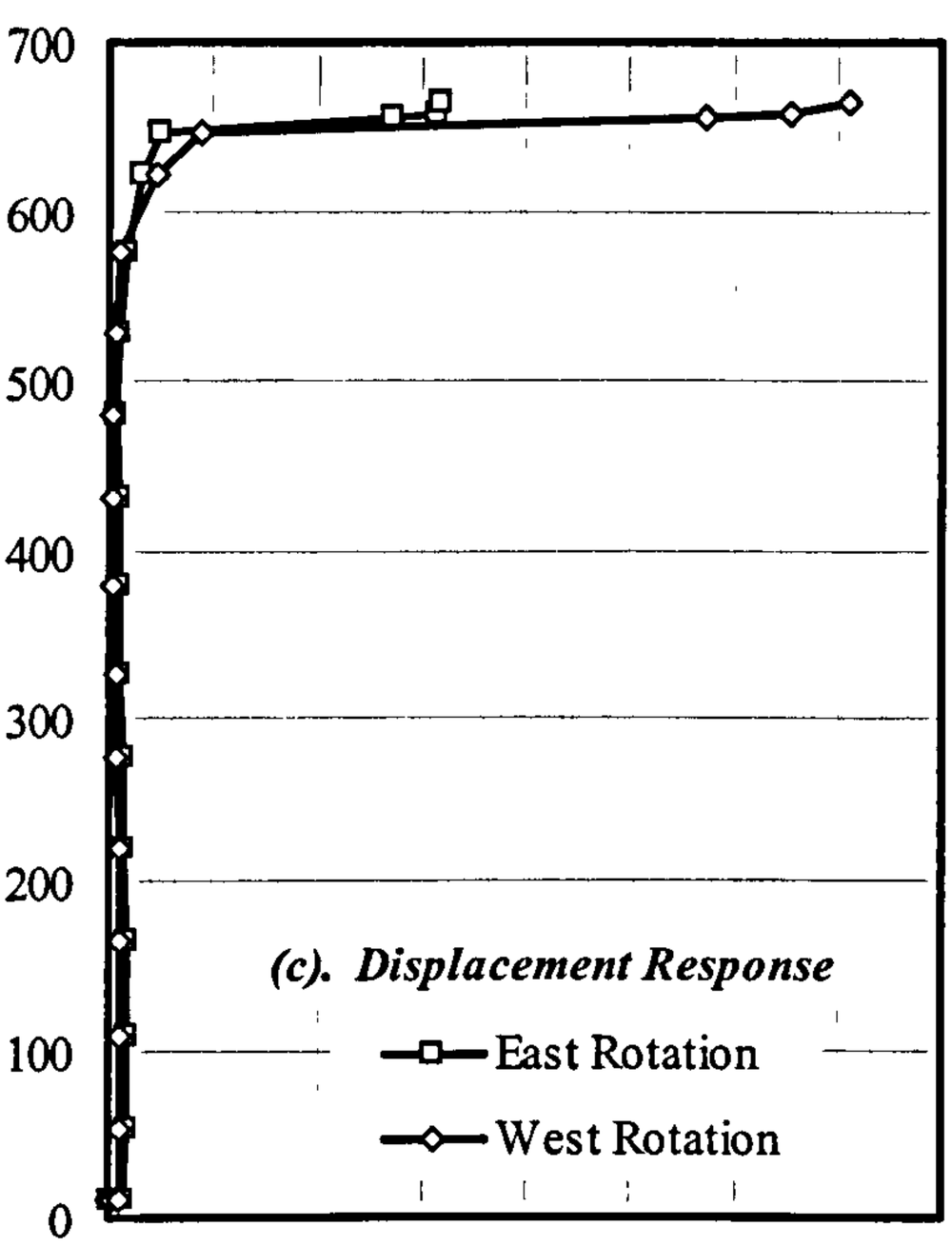

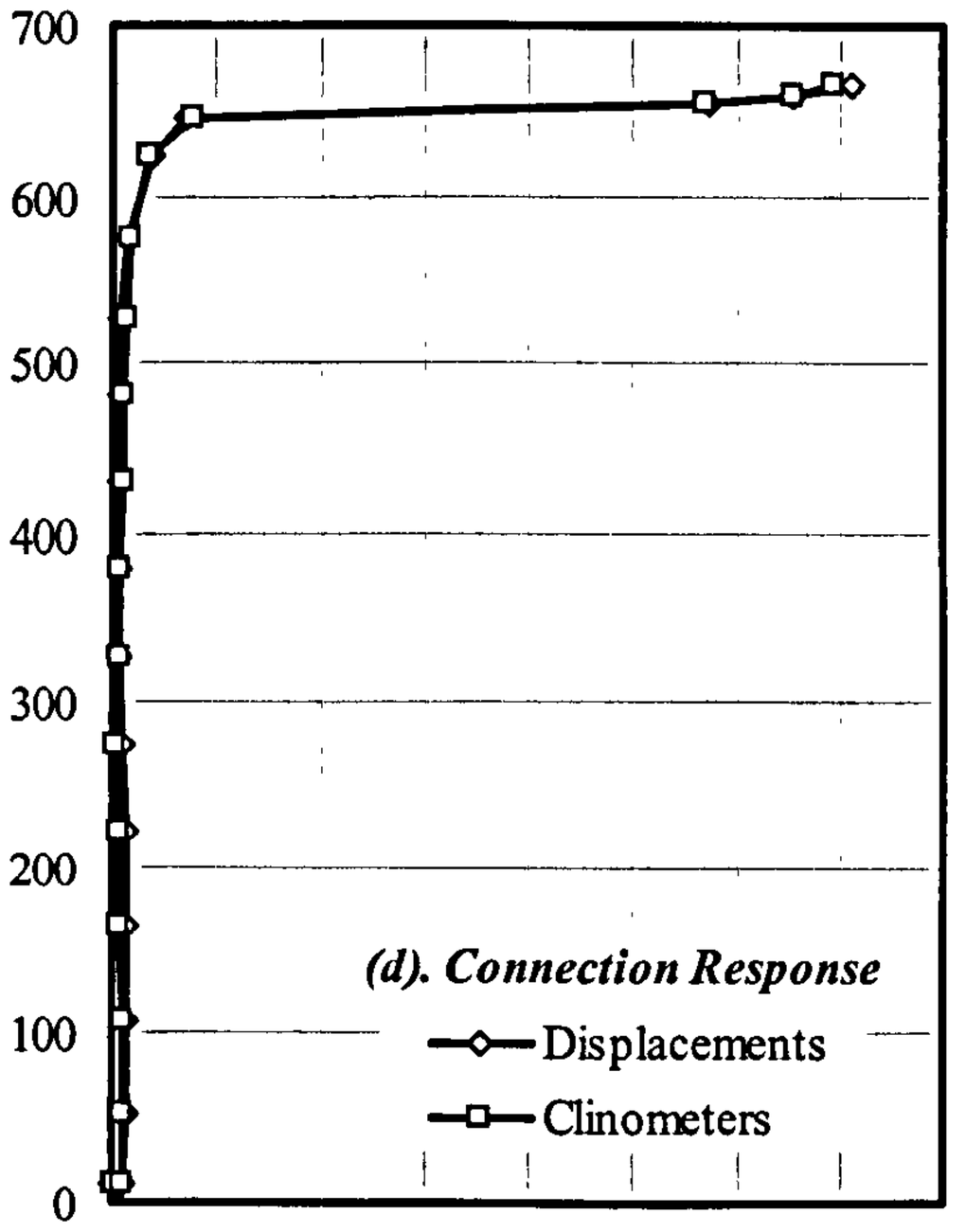

Figure 4.7: Summary of Results from Group 4: Fire Test 1 (FLC41)

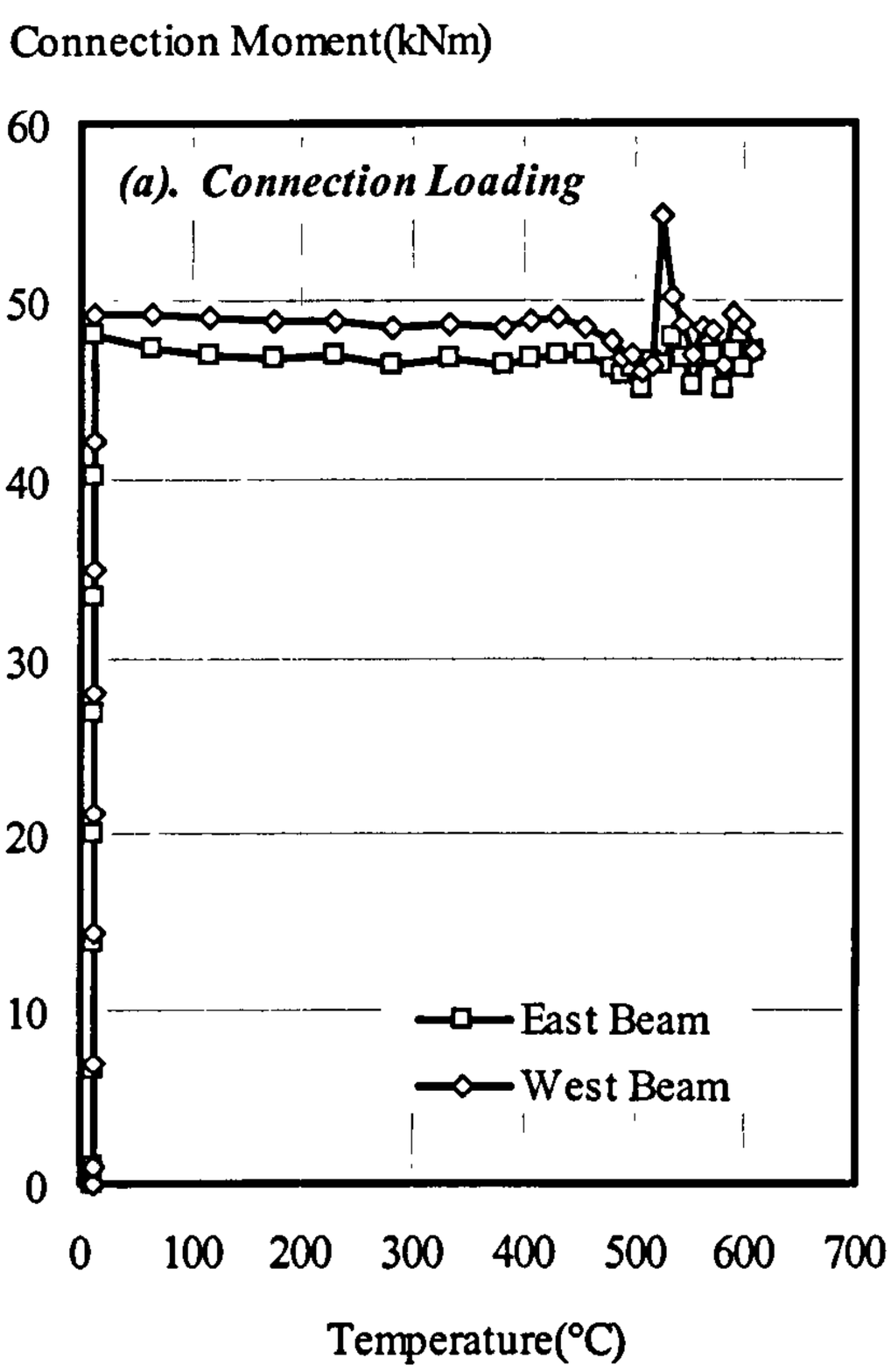

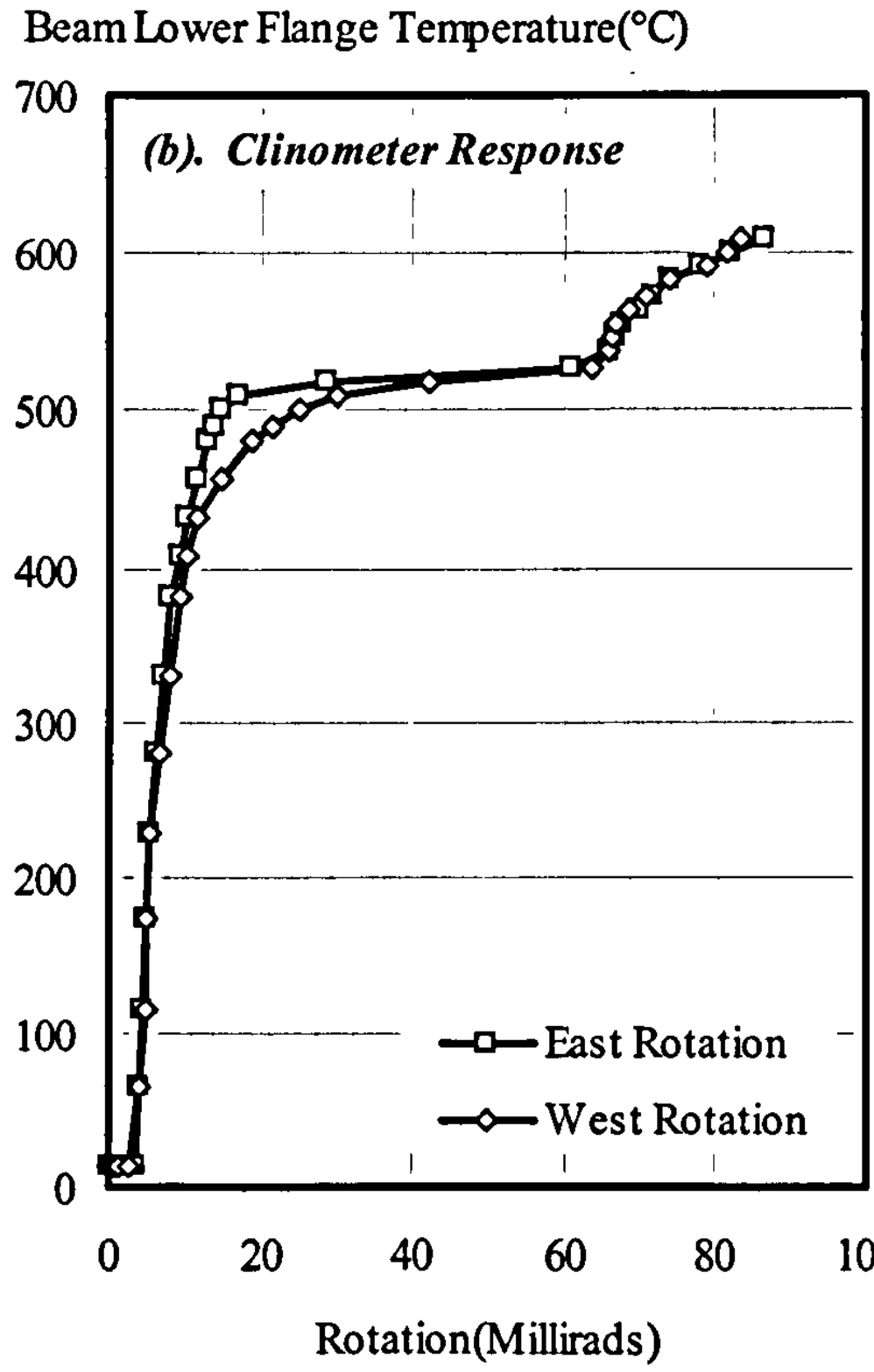

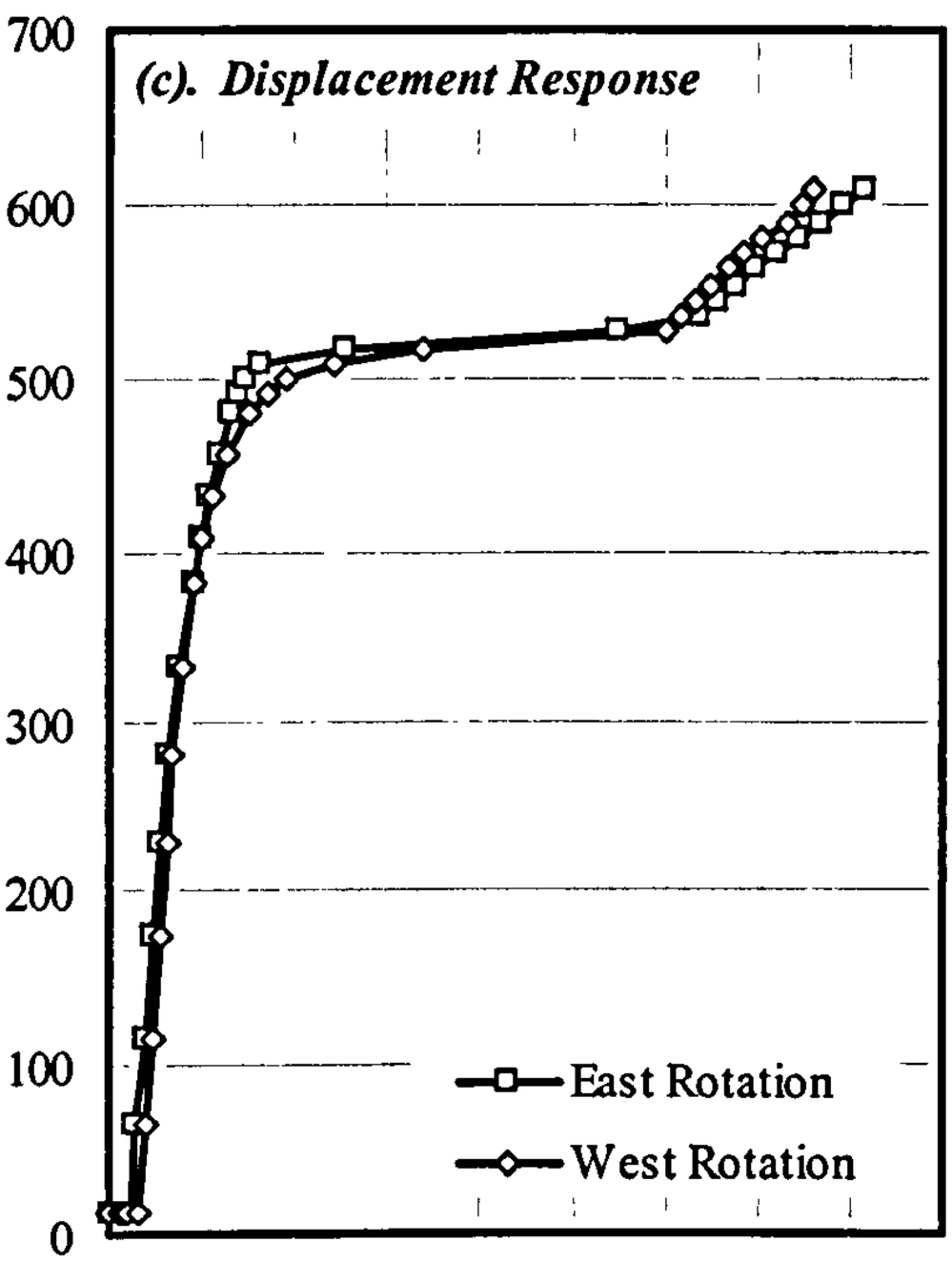

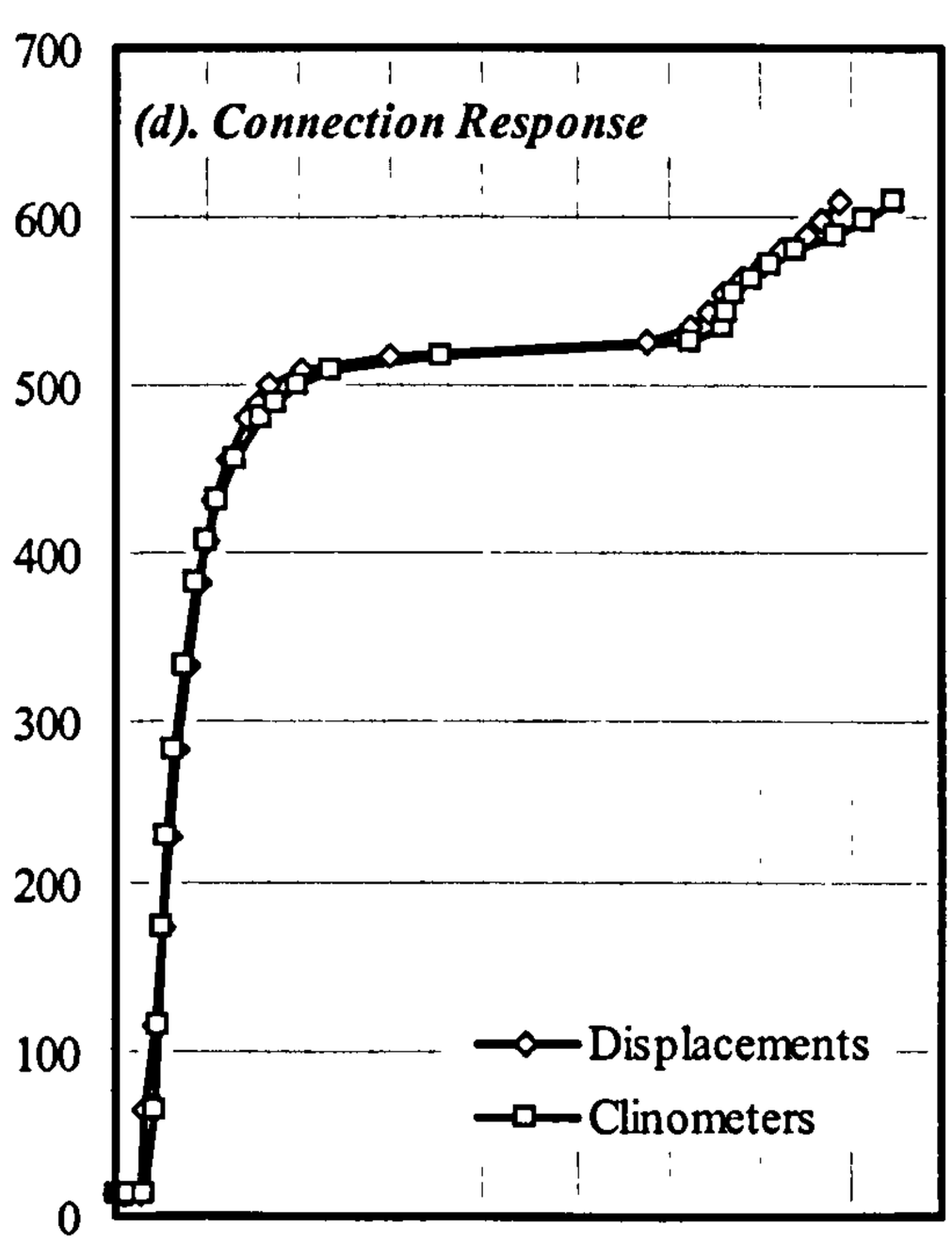

Figure 4.8: Summary of Results from Group 4: Fire Test 2 (FLC42)

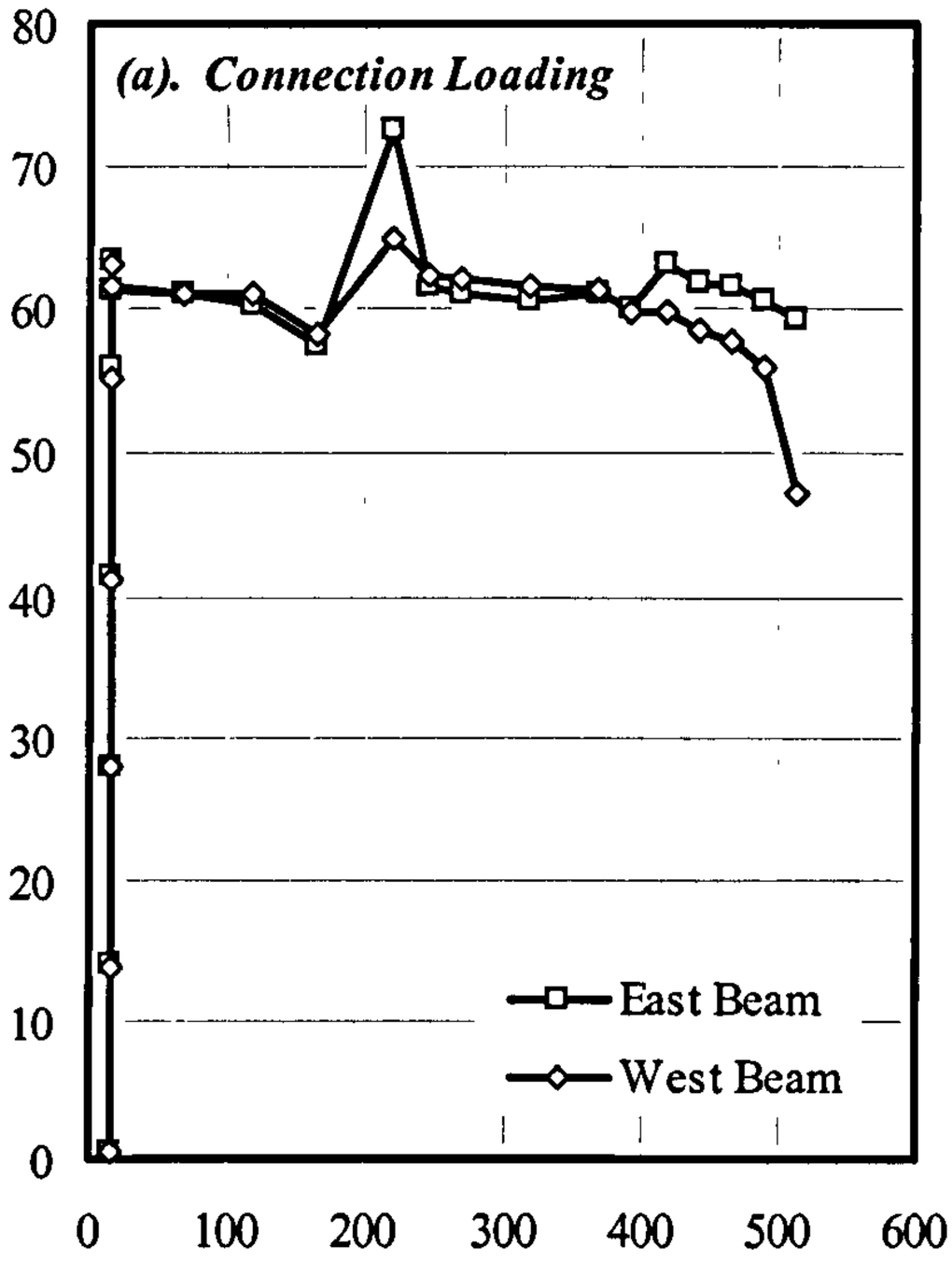

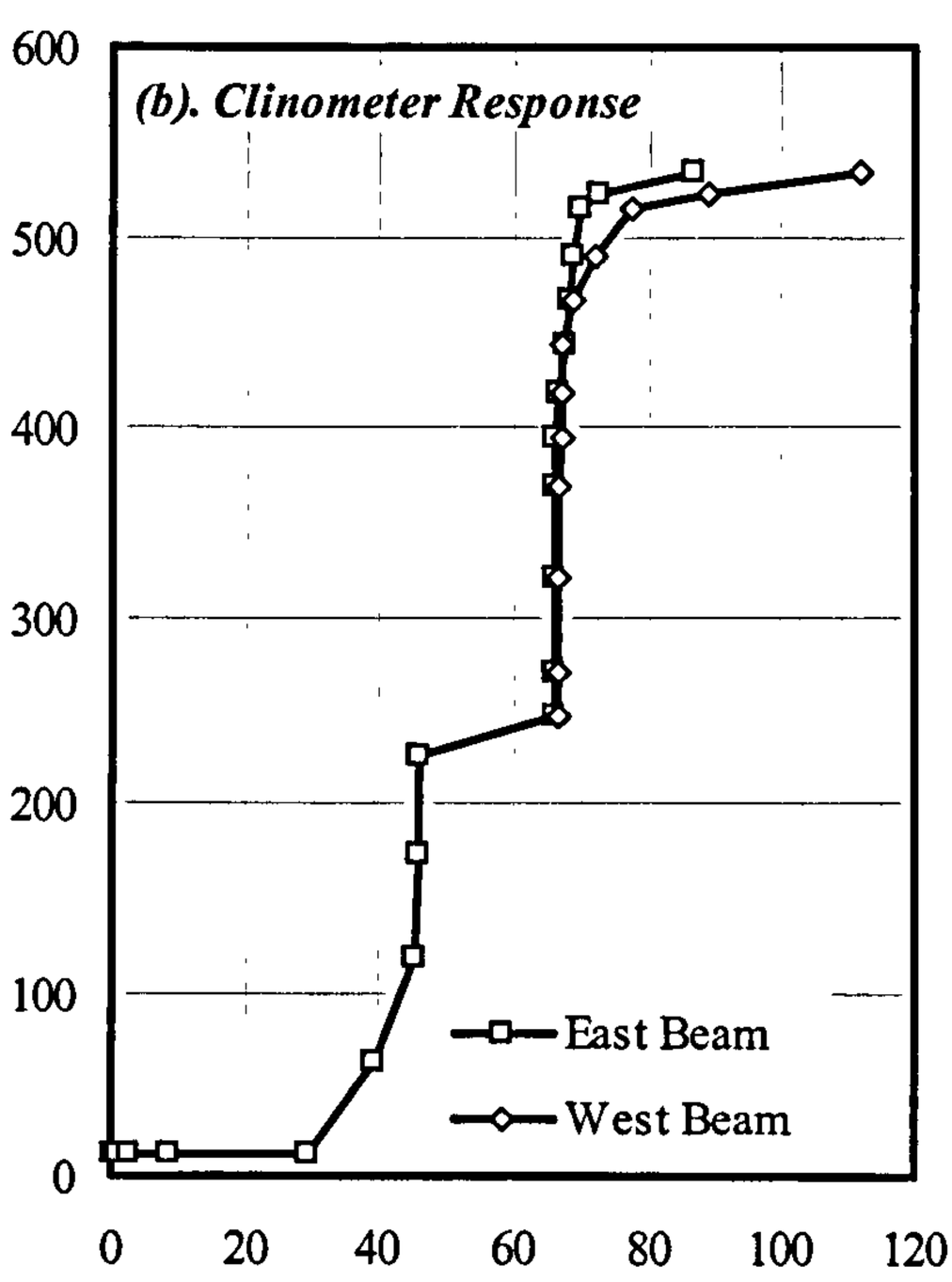

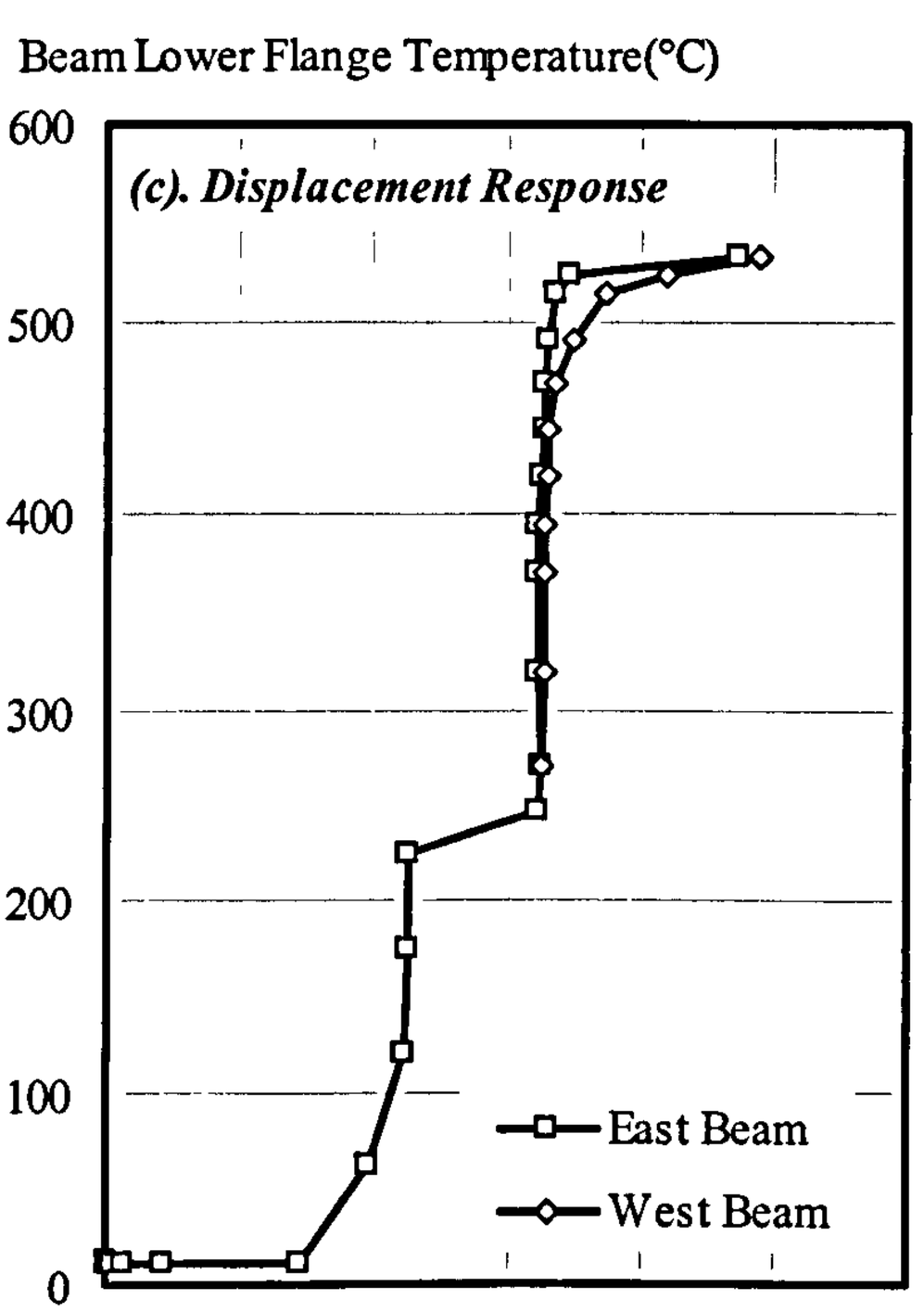

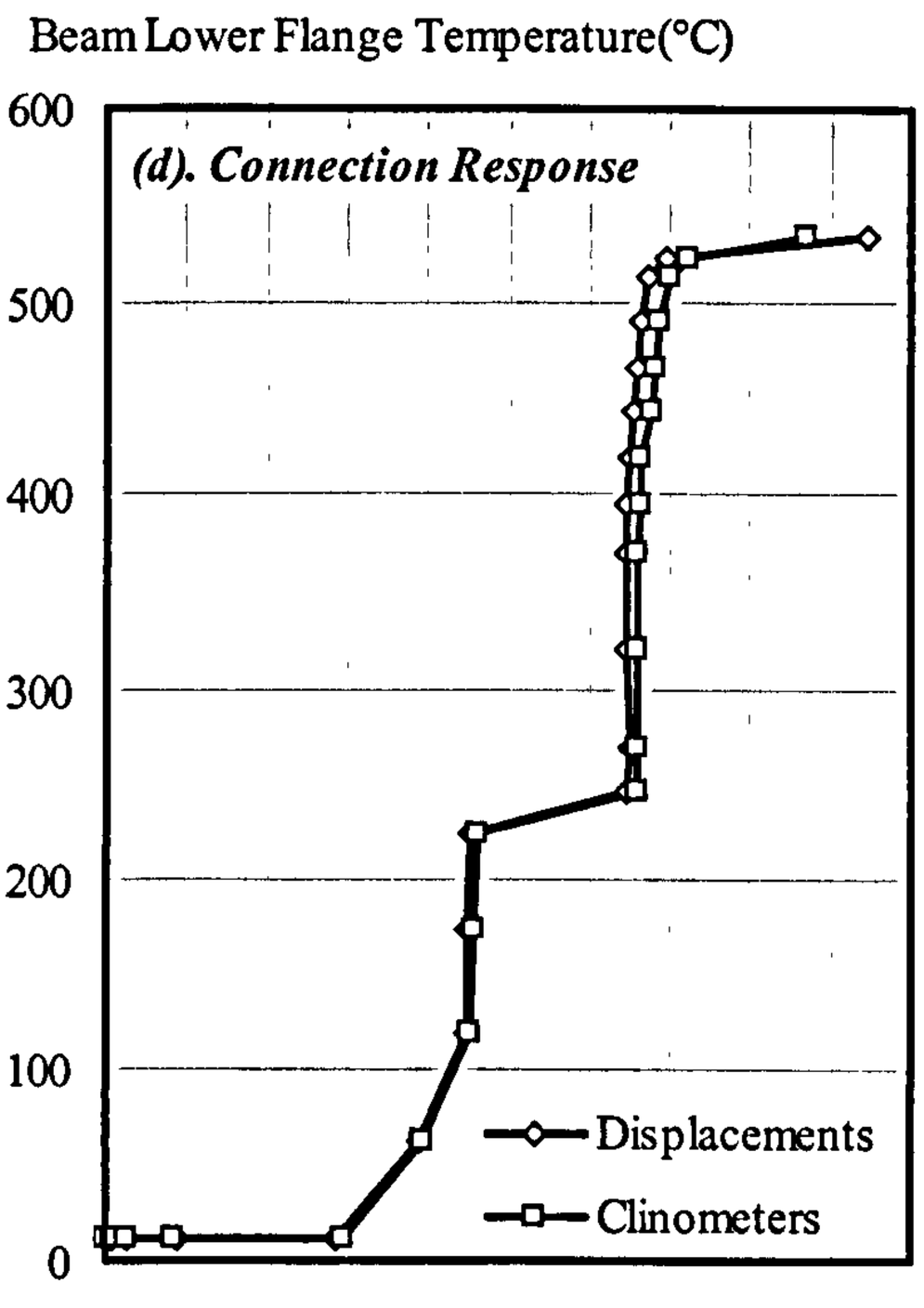

Figure 4.9: Summary of Overall Results from Group 4: Fire Test 3 (FLC43)

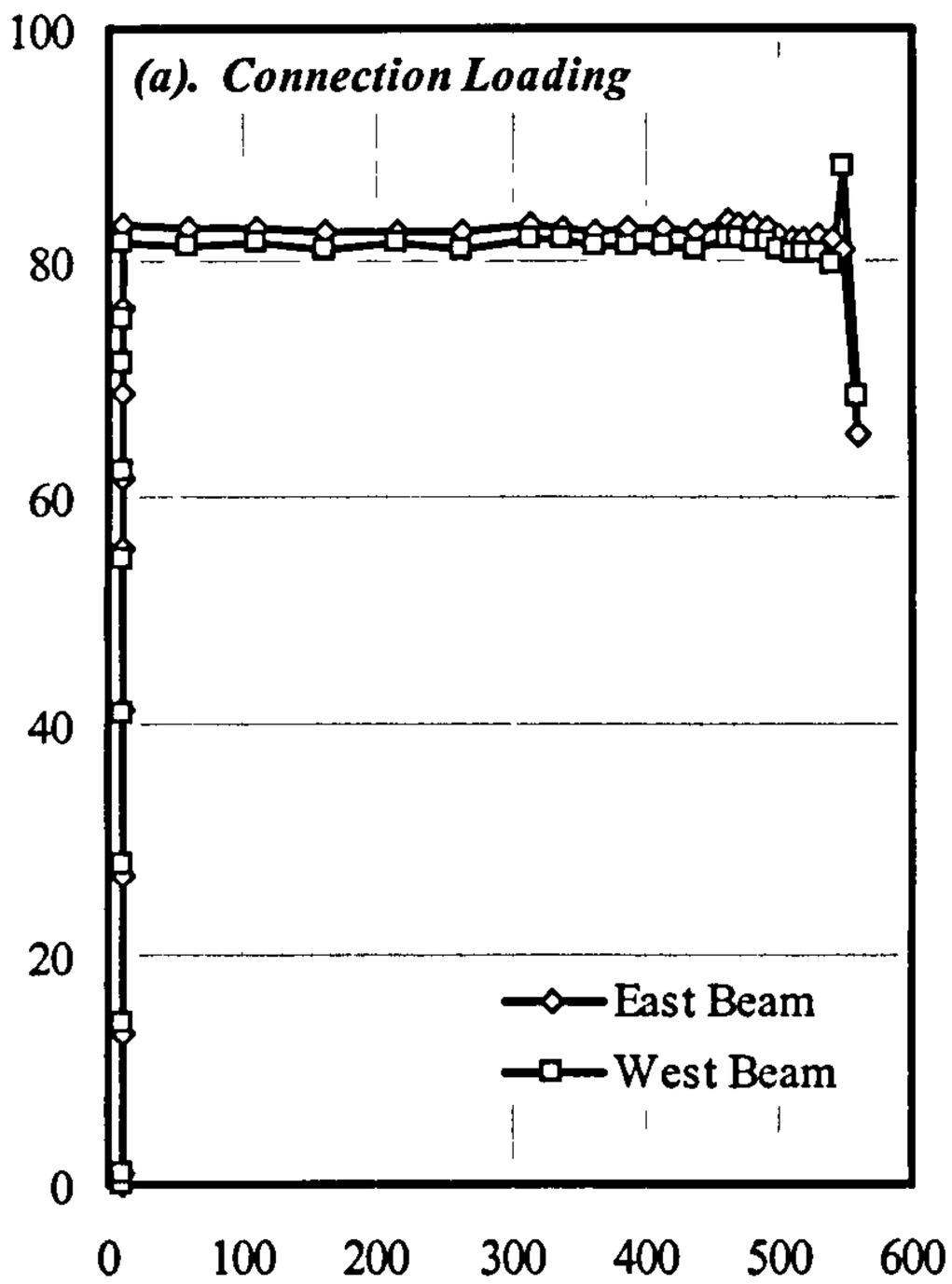

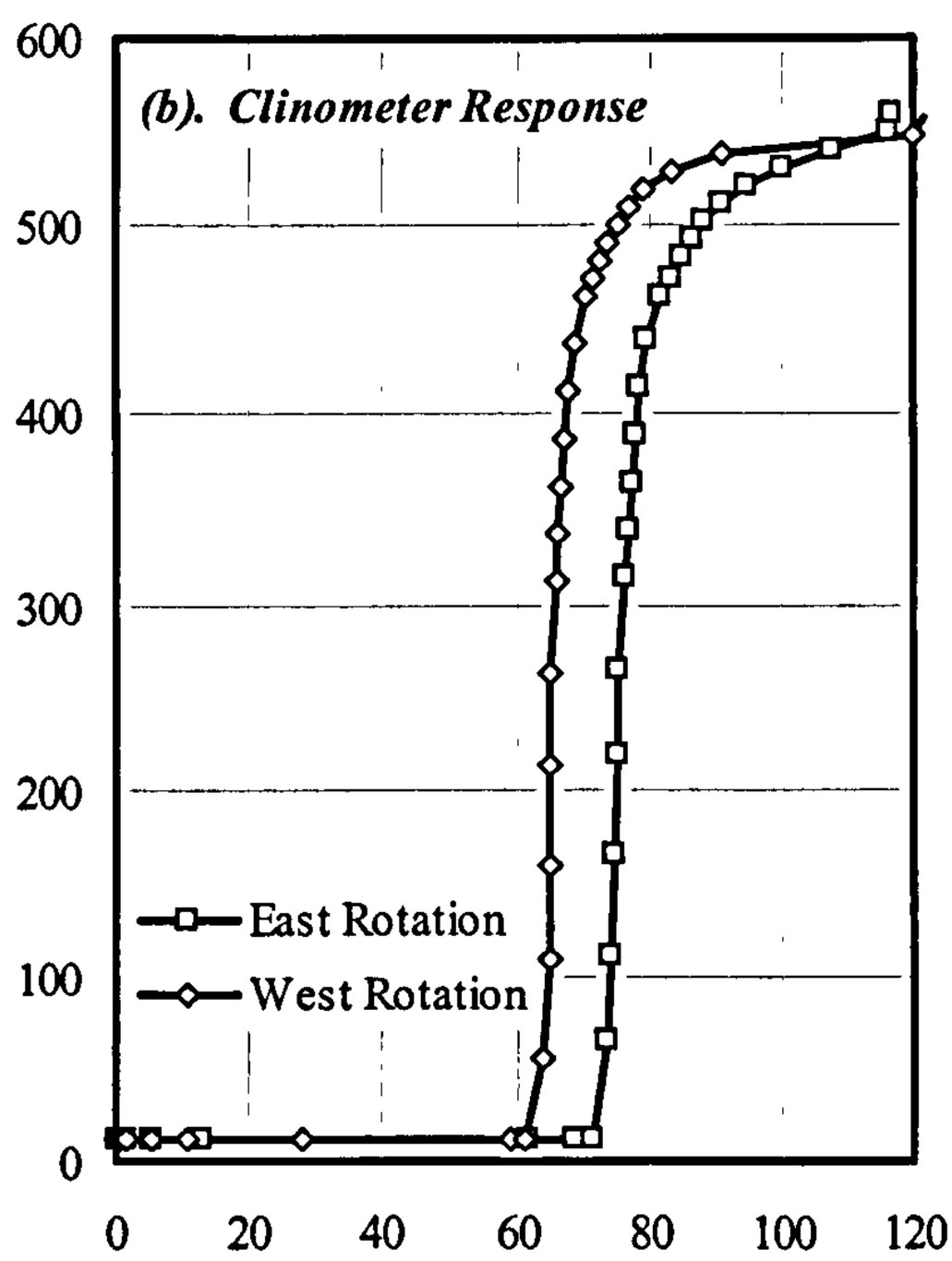

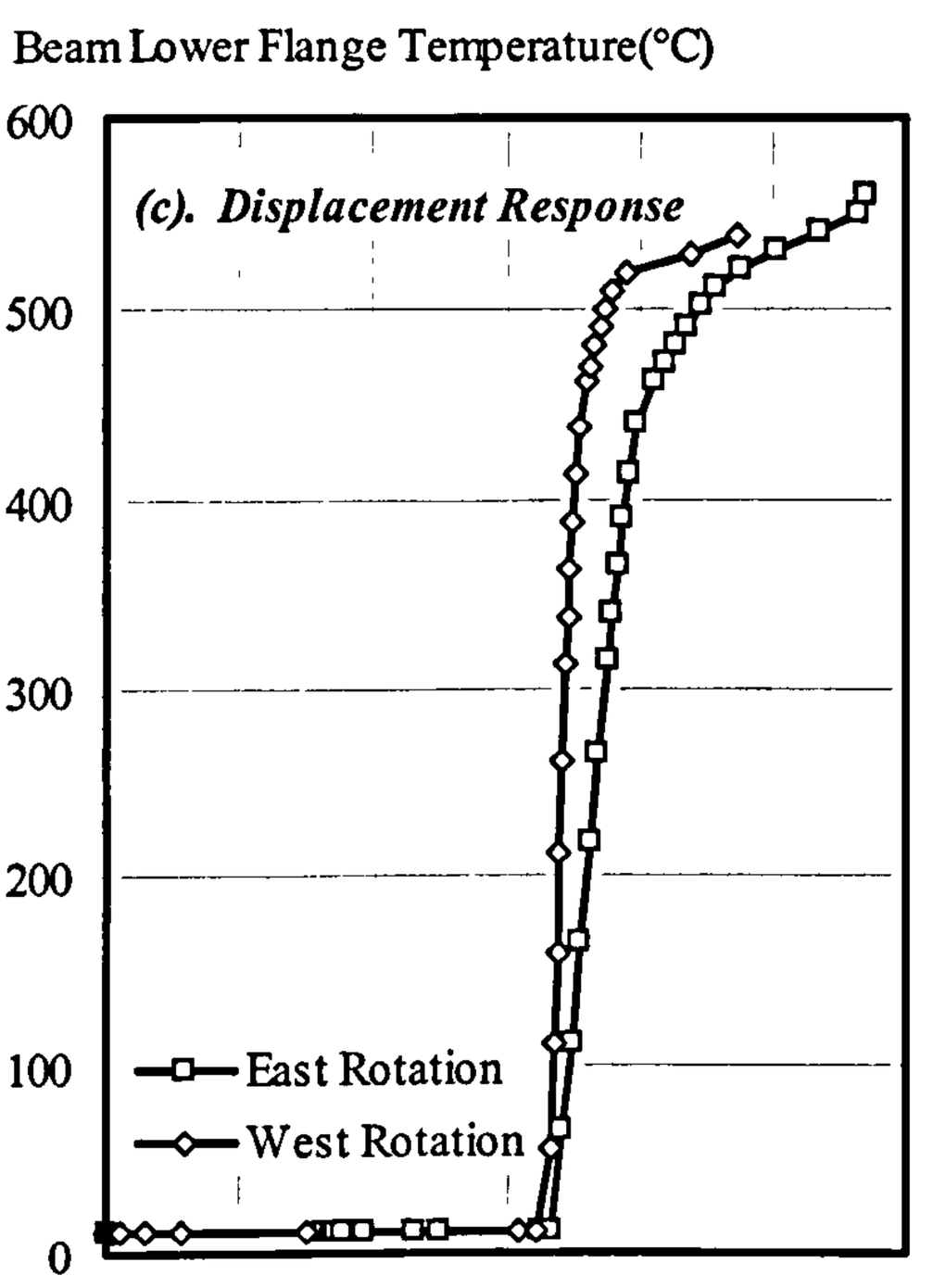

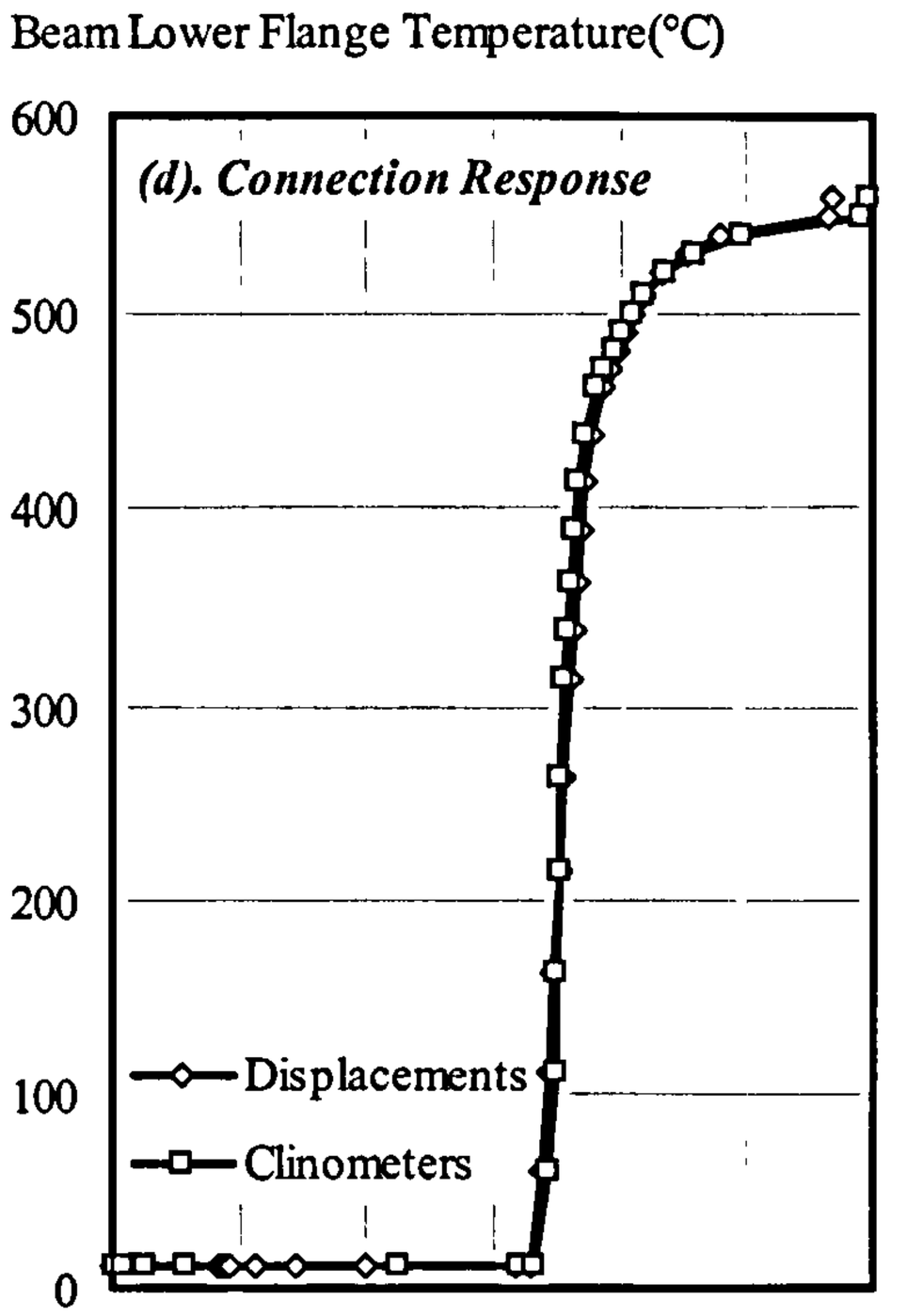

Figure 4.10: Summary of Results from Group 4: Fire Test 4 (FLC44)

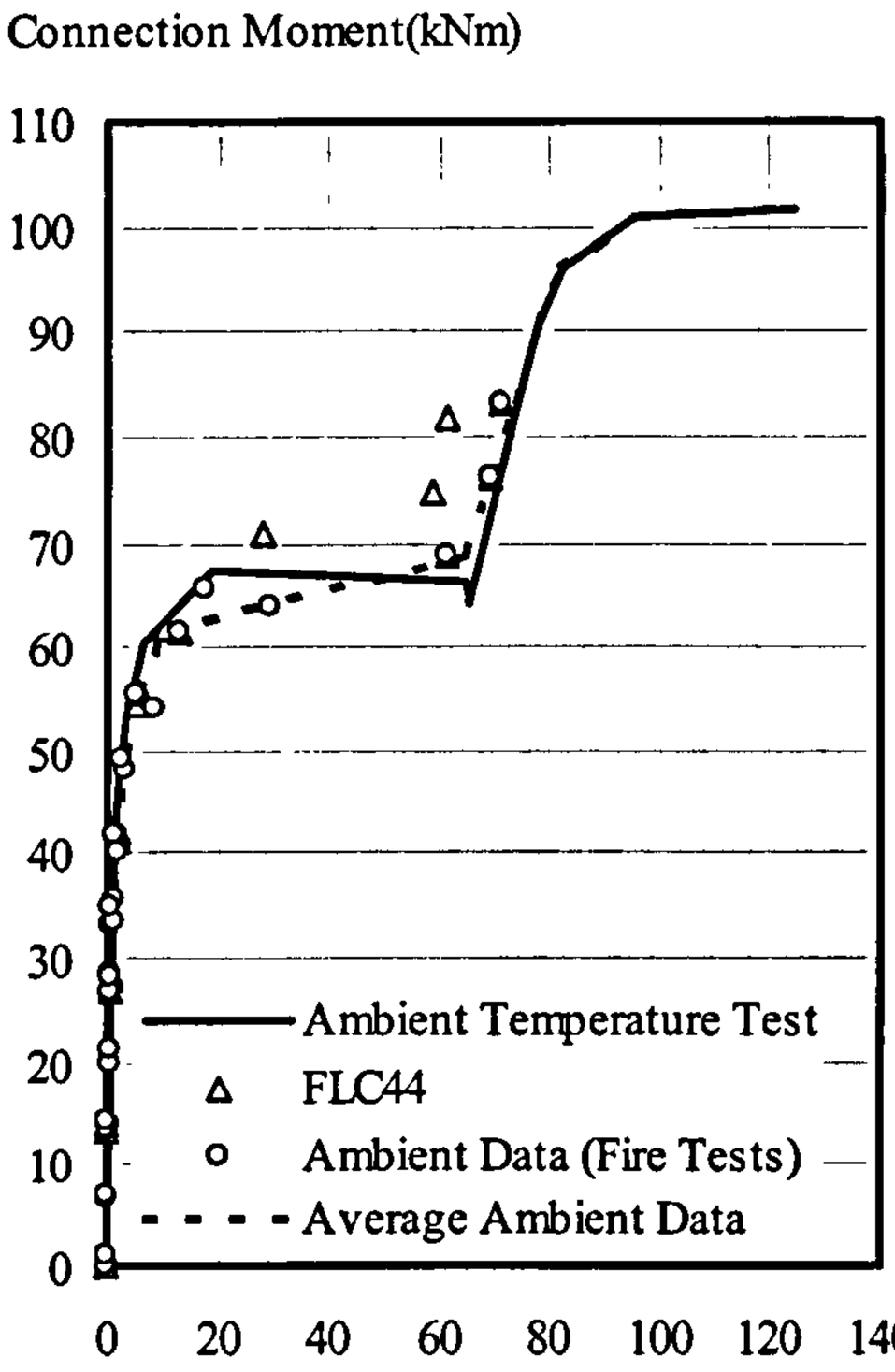

Figure 4.11: Ambient Temperature Response Compared with Ambient Temperature Data from Group 4Fire Tests

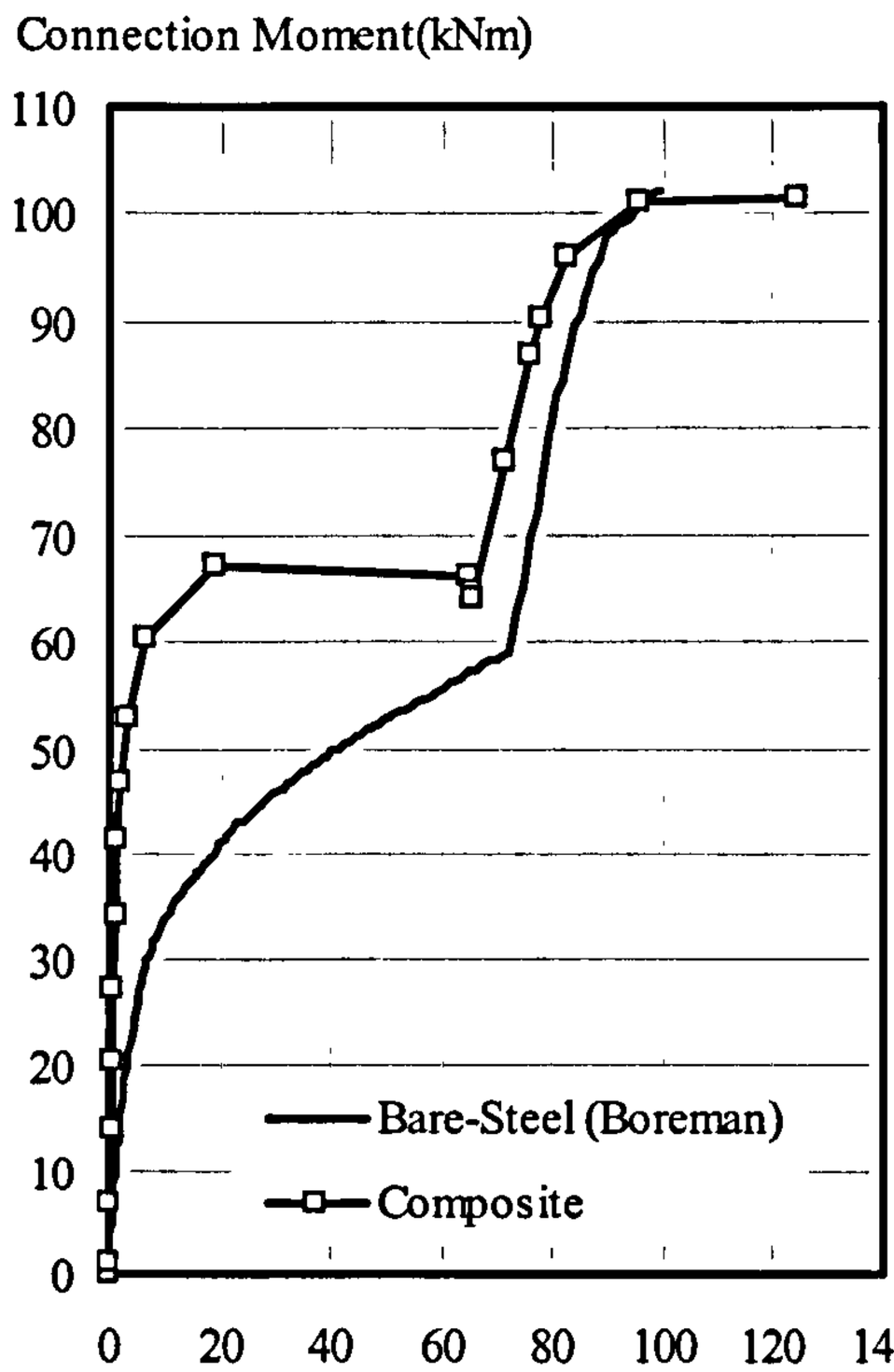

Figure 4.12: Comparison of Bare-Steel and Composite Connection Response for Group 4

Figure 4.13: Elevated Temperature Connection Response of Group 4 Tests

4.5 Group 5: Flexible End-plate Composite Connection Tests (FLC5)

The second flexible end-plate composite connection detail tested was typical of those used at Cardington and provides an indication of the influence of member size. It consisted of a pair of 610x229UB101 Grade 43 beams connected to a 305x305UC137 Grade 50 column by 10mm thick flexible end-plates with fourteen M20 Grade 8.8 bolts. The composite slab was identical to that used in Group 4 test series. The composite connection details for these Group 5 tests are shown in Fig. 4.14.

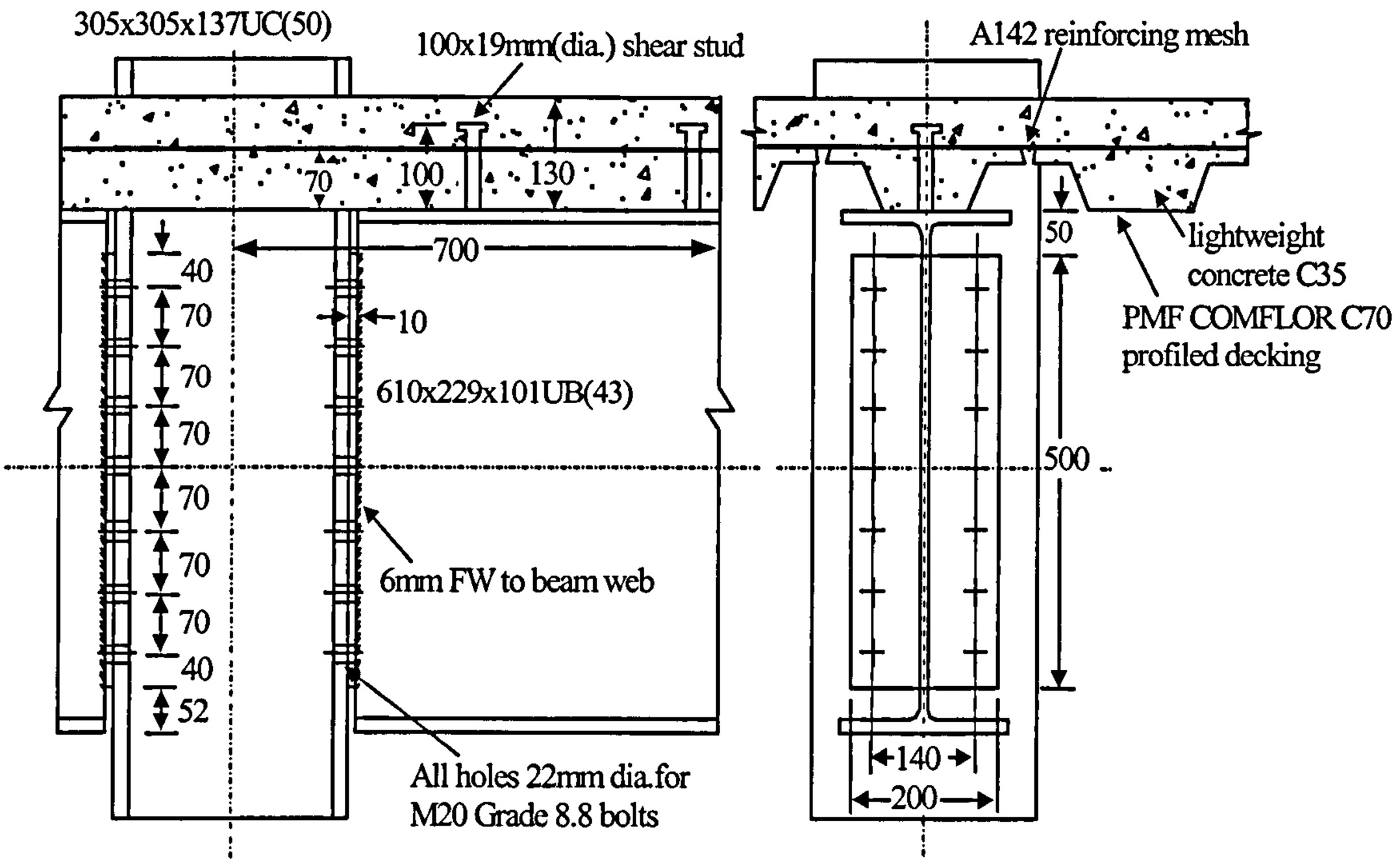

Figure 4.14: Flexible End-Plate Composite Connection Detail (Group 5)

Table 4.3: Group 5: Flexible End-Plate Composite Connection Experimental Test Programme

Test:	*Moment Level:*	*Applied Moment:*	*Temperature:*	*Comments:*
FLC5AMB	M_{cc}	Full Range	Ambient	Amb.-temp. M-ϕ
FLC51	$0.27M_{cc}$	47 kNm	10°C/minute	Group 5, Fire Test 1.
FLC52	$0.46M_{cc}$	80 kNm	10°C/minute	Group 5, Fire Test 2.
FLC53	$0.77M_{cc}$	134 kNm	10°C/minute	Group 5, Fire Test 3.

The furnace doors could not accommodate such a large beam depth, so the 610mm deep beam was spliced to a 356mm deep beam at the point where the composite slab ends. The beam-to-beam connection detail and the design calculations are presented elsewhere[98].

Before assembling the test specimens it was discovered that the bolt holes in the columns were wrongly spaced and did not match the bolt holes in the end-plates. Therefore new bolt holes were drilled in the columns at the BRE workshop under supervision of the author. To utilise the same columns it was necessary to turn them upside-down. As a result the specimen height from the mid-depth of the connection to the column base was reduced to 1240mm compared with 1390mm for the specimens in other test Groups.

Although it was proposed to perform four fire tests, only three tests were conducted at elevated temperature because one specimen failed at ambient temperature. This was due to an overestimation of the moment capacity of the connection. This was used as the ambient temperature test and the connection failure moment taken as the basis for determining the load levels in the subsequent elevated temperature tests. The experimental programme for Group 5 is presented in Table 4.3. The composite capacity of the flexible end-plate connection was determined to be 227 kNm based on the method proposed by SCI/BSCA for moment connections. The loads were applied at 1340mm from the face of the column flange. Due to time restrictions, testing commenced 21 days after casting the composite slab.

4.5.1 General Observations from Group 5 Connection Tests

There was some similarity in the behaviour of the two composite connections (i.e. Groups 4 and 5) despite the difference in detail and member size. Similar forms of failure were observed. Slab failure associated with cracking from the face of the column flange perpendicular to the beam resulted in separation of the shear stud from the concrete slab as shown in Fig. 4.15, causing tensile failure of some reinforcing bars. This was accompanied by two smaller continuous cracks over the connection as a result of excessive end-plate deformation with tiny cracks randomly distributed. Typical pattern locations observed in the composite slab are shown in Fig. 4.16. The second mode of failure was end-plate fracture along the weld particularly in the tension zone as illustrated in Fig. 4.17. The most unusual aspect was the end-plate fracture along the bolts in the ambient temperature test FLC5AMB following the failure of the end-plate on the other side of the same connection. This was probably due to the failure of the connection on one side causing lateral movement of the beam. This movement would be resisted by the bolts resulting in fracture of the end-plate along the bolt line on the other side of the connection. There was no sign of deformation to either the beams or the column due to their large size.

Table 4.4 shows the temperature distribution of various components through the depth of the connection for the three fire tests. The beam lower flange temperatures were once more selected as the reference temperature. The temperature distribution was consistent between the tests and was similar to that recorded for Group 4 tests. It was observed that the temperature of the top flange was approximately 19% lower than the bottom flange temperature due the protection provided by the composite slab. From Tables 4.2 and 4.4 it may be seen that there was about 11% difference in the top flange temperatures of Groups 4 and 5 connections with the top flange temperature of Group 4 connection being approximately 30% lower than the beam lower flange temperatures. This may be attributable to the greater surface area of the top flange exposed to temperature in Group 5 tests due to the larger size of the sections.

The column web once more achieved the highest temperature being approximately 26% higher than the beam lower flange temperature. The top surface of the slab maintained a temperature 15% of the lower flange which is consistent with the results of the Group 4 tests. The atmospheric temperature within the furnace was found to be 65% higher than the beam lower flange temperature.

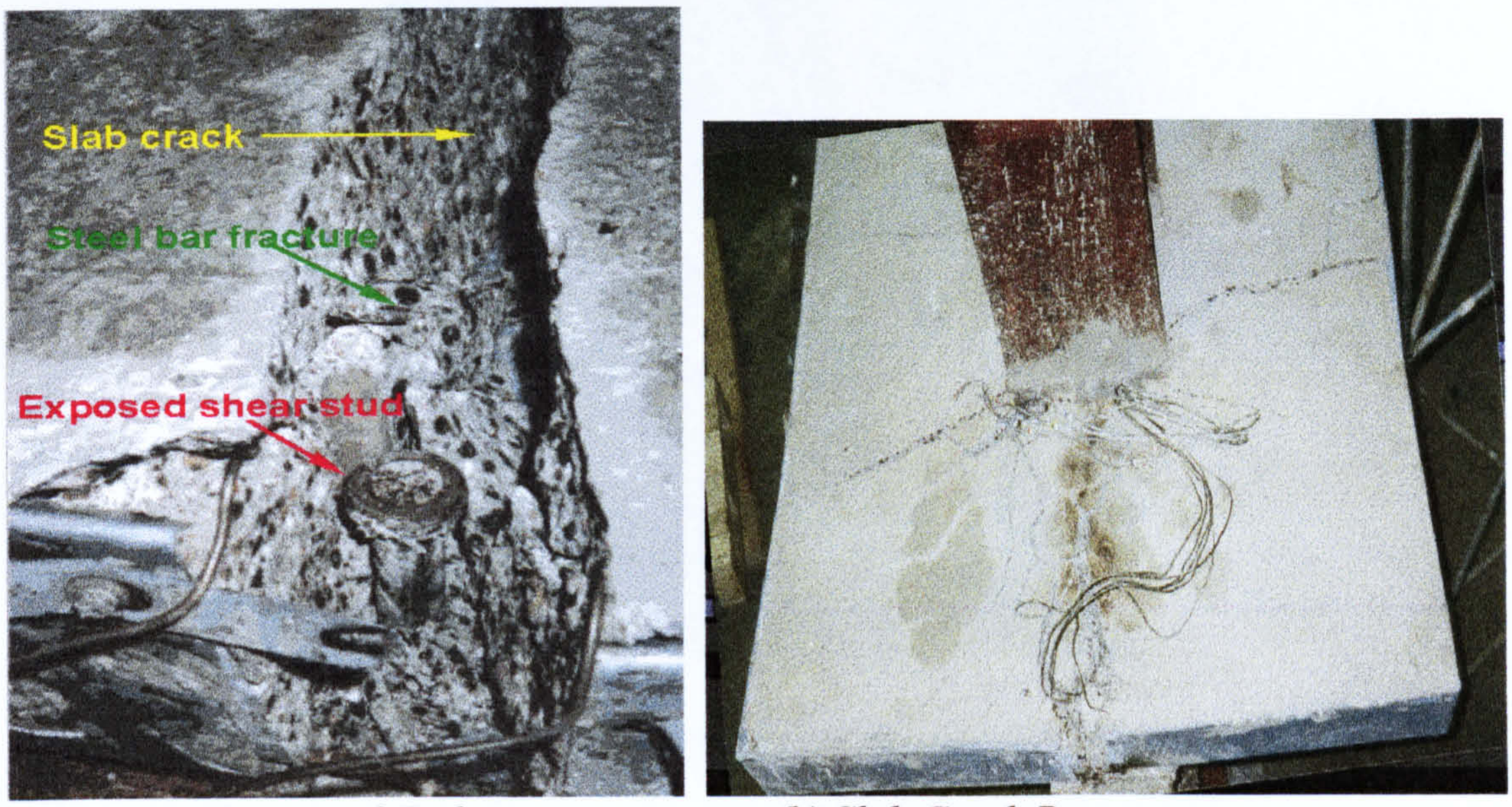

(a) Shear Stud Failure *(b) Slab Crack Pattern*

Figure 4.15: Composite Slab Failure in Group 5 Tests

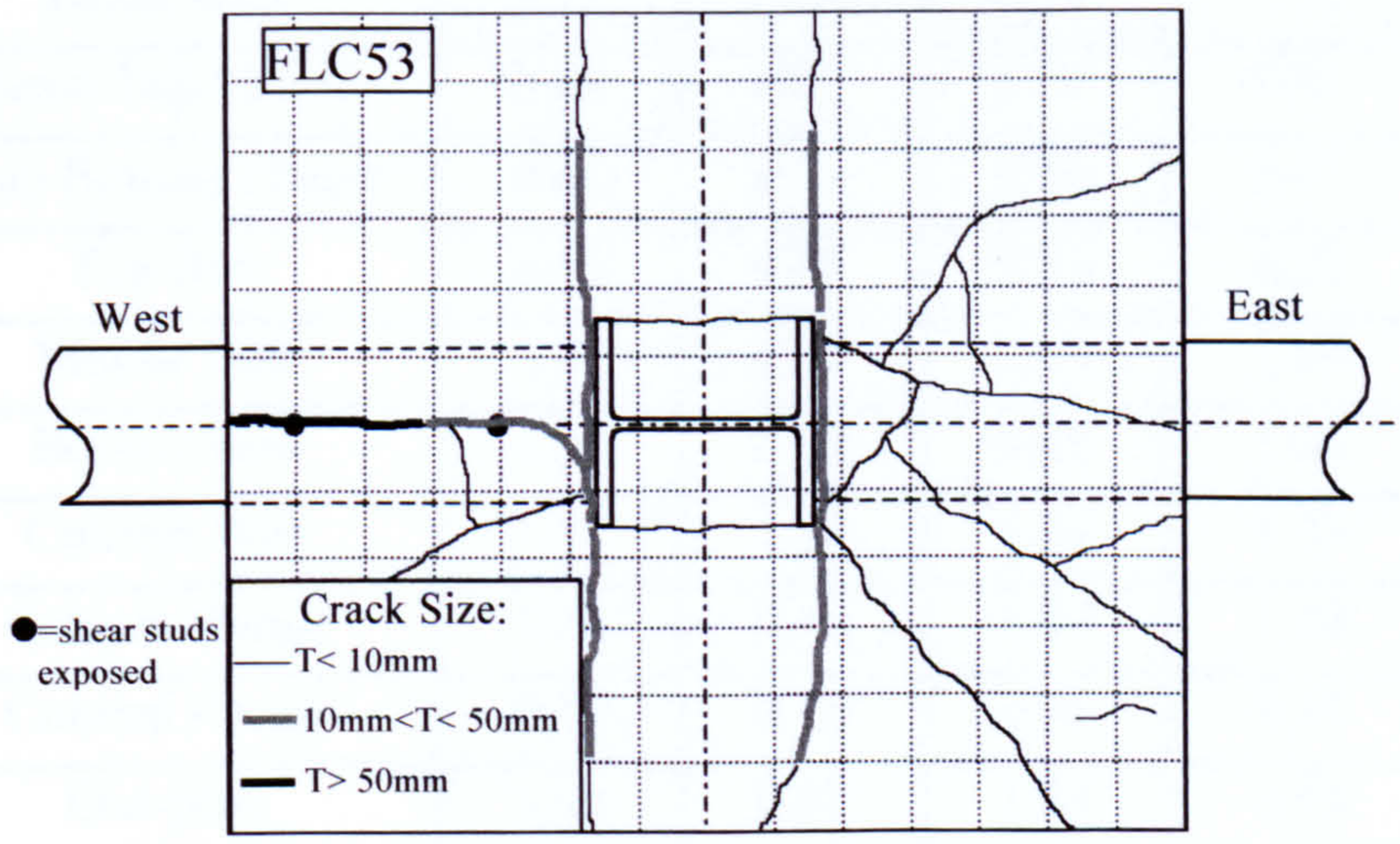

Figure 4.16: Typical Slab Crack Locations in Group 5 Tests

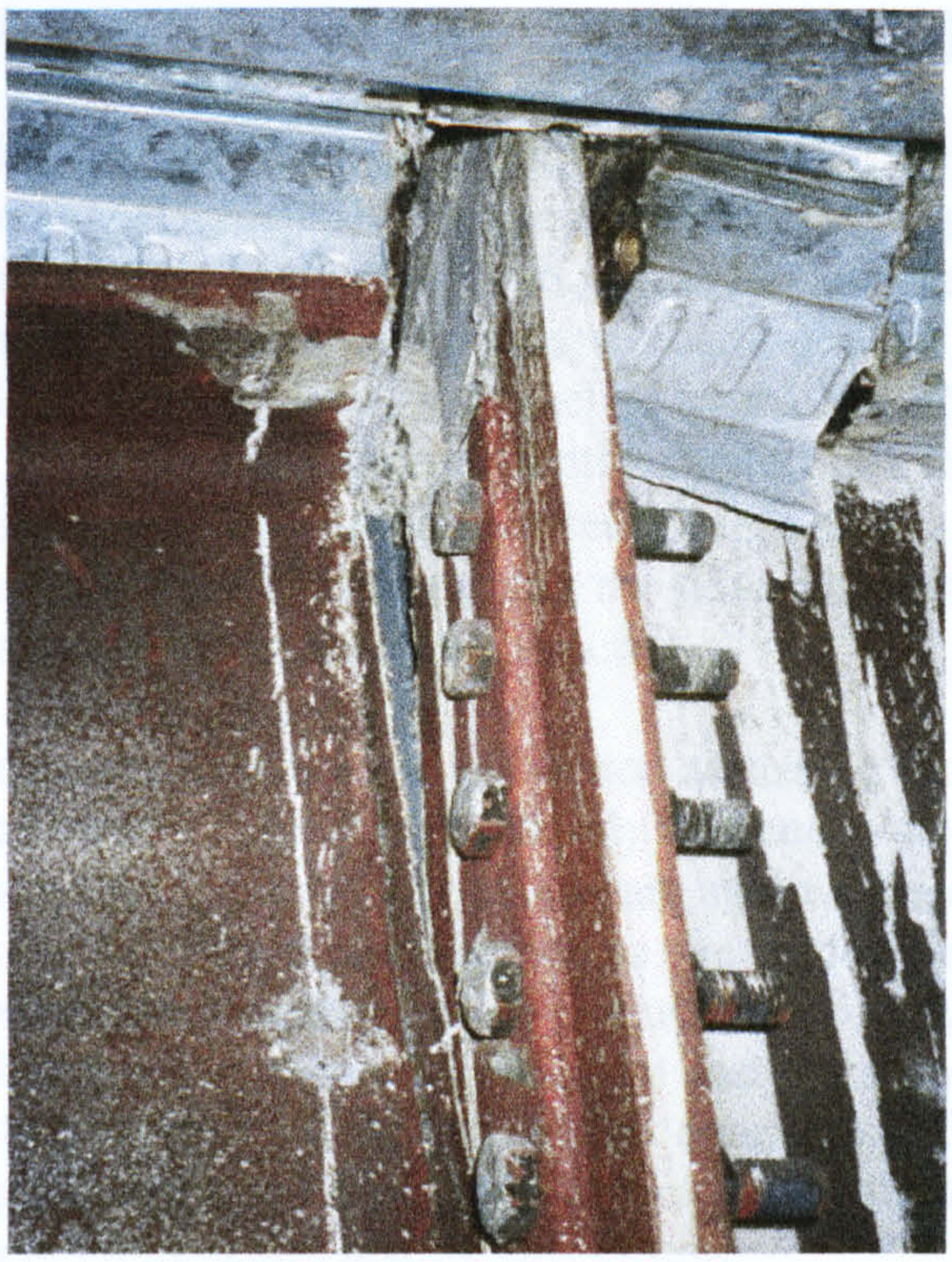

Figure 4.17: Elevated Temperature End-Plate Failure Mode for Group 5

Table 4.4: Average Relative Temperature Profiles for Group 5 Tests

Element:	*FLC51:*	*FLC52:*	*FLC53:*	*Average:*
Beam Bottom Flange	1.00	1.00	1.00	1.00
Beam Web	1.11	1.06	1.15	1.11
Beam Top Flange	0.84	0.82	0.77	0.81
Beam Bottom Flange*	0.62	0.78	0.44	0.61
Top Bolt	0.93	0.89	0.94	0.92
Middle Bolt	1.01	0.95	1.03	1.00
Bottom Bolt	1.00	0.99	1.01	1.00
Column Web	1.20	1.20	1.38	1.26
Column Flange	1.25	0.90	0.97	1.04
Column Flange	0.39	0.26	0.29	0.31
End-plate	1.00	0.95	1.03	0.99
Concrete Surface	0.18	0.13	0.13	0.15
Furnace Atmosphere	1.63	1.67	N/A	1.65

Note: * identifies insulated thermocouple locations

4.5.2 Group 5: Ambient Temperature Test (FLC5AMB)

This test was intended to be performed at elevated temperature under a load level of approximately 175 kNm. Unfortunately, even at ambient temperature, the specimen failed to support this applied load mainly in the West side and hence the test was terminated. The initial ambient temperature loading was increased at regular increments of 10 kN until the applied load reached about 130 kN when the connection failed. A thorough inspection was subsequently carried out in order to identify the exact cause of the failure, whether due to incorrect design or to a fault in fabrication. It was found that the method used in determining the moment capacity of the connection had led to overestimation of the connection capacity.

The capacity of the connection had been calculated assuming that it would behave in a similar manner to the Group 4 connections, namely that end-plate deformation would be followed by an enhanced response as the beam bears against the column. Consequently the bolts would make a significant contribution to the performance of the connection. In fact failure occurred at low rotations before contact between the beam and the mating column, indicating that the composite slab and the end-plate are the dominant factors defining the connection capacity. Design of the connection based on bolt strength therefore led to a significant overestimate of capacity. Fortunately this test could be regarded as the ambient temperature test for this Group.

A summary of the test results is shown in Fig. 4.18. As the connection experienced progressively higher deformations, its performance was carefully monitored and it was observed that there was a sudden reduction in the applied loading as a result of end-plate failure. The highest moment recorded was approximately 170 kNm and this value was taken to represent the moment capacity of the connection.

The connection rotations recorded by clinometers and displacement transducers for the West connection are shown in Figs. 4.18*(b)* and 4.18*(c)* respectively. The response of the East connection was disregarded since both devices gave erratic readings. Fig. 4.18*(d)* shows a comparison between responses obtained from clinometer and displacement transducer readings, from which it may be seen that they compare well.

4.5.3 Group 5: Fire Tests

Three elevated temperature tests were carried out under Group 5, following a similar testing procedure to that adopted previously. The level of loading was based originally on the calculated moment capacity. However these values were refined based on the ultimate moment capacity of the connection which had failed in the initial test at ambient temperature. A description of each test is given below.

4.5.3.1 Group 5: Fire Test 1(FLC51)

A relatively low moment of approximately 47 kNm was applied to the connection. Due to the low load level applied and the large size of the specimen it was expected that the connection would withstand very high temperatures possibly in excess of 800°C. The test was completed without achieving any significant rotation as the burner operating

system failed to deliver sufficient heat. The target time (90 min.) was reached without achieving the required temperature (900°C). This was mainly due to the high concentration of thermal mass within the furnace with relatively little oxygen available. The test was terminated at a control temperature of approximately 665°C after more than 90 minutes had elapsed. It was possible to modify the heating regime to achieve higher temperature for subsequent tests, but this was felt to be unnecessary as at high load levels the connection would fail at lower temperatures. Rotations in both connections were almost negligible and as a result the connection response at this load level could not be established.

4.5.3.2 Group 5: Fire Test 2 (FLC52)

In the second test the load level was increased to provide an applied moment of approximately 80 kNm to the connection in six equal increments and the results are summarised in Fig. 4.19. It may be seen that a consistent pattern of loading was maintained throughout testing, with the average moment applied being approximately 80.7 kNm. Rotations from clinometer devices were disregarded as they produced erratic results due to the destruction of the cabling and cooling pipes during the test, necessitating reliance on displacement readings. It can be seen from Fig. 4.19*(b)* that there is a fairly close agreement between results obtained for the East and West connections.

4.5.3.3 Group 5: Fire Test 3 (FLC53)

The final elevated temperature test in Group 5 was conducted under a moment of approximately 134 kNm. The results are summarised in Fig. 4.20. A consistent level of loading was maintained until the completion of the test, with an average recorded moment of approximately 133 kNm. The connection rotations were based on displacement transducer readings due to the failure of the clinometer devices during the test. It can be seen from Fig 4.20*(b)* there is a slight variation in the ambient temperature connection rotation calculated from displacement transducer readings. This may be as a result of movement of the testing arrangement during the initial loading.

4.5.4 Comparison of Results from Group 5 Flexible End-plate Composite Connection Tests

The ambient temperature bare-steel and composite moment-rotation behaviour of the Group 5 connection type is shown in Fig. 4.21. As before, bare-steel characteristics were obtained from ambient temperature tests carried out by Boreman *et al.*[100]. It can be seen that the composite connection initial stiffness is comparable with that for bare-steel. However, the capacity of the connection is higher than for the bare-steel connection. Fig. 4.22 shows a comparison between the ambient temperature moment-rotation response and ambient temperature results recorded whilst loading specimens prior to fire testing. It can be seen that there is fairly good agreement between these.

The high temperature connection response for the last two fire tests is shown in Fig. 4.23. For these tests it was necessary to base rotations on displacement readings, due to

the failure of the clinometer devices. The first fire test was completed without achieving any significant rotation and therefore it was not possible to obtain a temperature-rotation curve for that load level. Although only two fire tests were performed satisfactorily in Group 5, it seems that this was sufficient to provide a reasonable representation of connection response together with single ambient temperature test. It can be seen from Fig. 4.23 that the connection capacity decreases with increasing temperatures and load levels. Despite the similarity in the failure modes between the connections utilised in Groups 4 and 5, the response of the connections is quite different. For Group 4 flexible end-plate there was large end-plate deformation until the beam bears against the column resulting in an enhanced connection capacity with further rotation whereas for Group 5 connection failure occurs before the contact. Furthermore, the Group 5 connection is more rigid than Group 4 causing sudden failure at very low rotations.

4.6 CONCLUSIONS

Two series of tests have been carried out to investigate the influence of elevated temperatures on the response of flexible end-plate composite connections. Testing was limited to two connection types similar to those used in the Cardington full-scale frame due to the quantity of tests required to define accurately the behaviour of a single connection across a range of temperatures.

Failure of the composite connections was observed to be dominated by failure of the slab as well as failure of the end-plate. Fracture of the end-plate along the weld was the dominant mode of failure for flexible end-plate connections. In the composite slab the failure mode consisted of separation of the shear studs from the concrete slab together with tensile failure of some bars in the mesh. This is not necessarily representative of the behaviour in a composite frame, where a greater slab width and more shear studs spread along the beam span are available. Failure of the composite slab resulted in little enhancement in capacity compared with the bare steel detail. The failure modes observed at elevated temperature were similar to those at ambient temperature.

Some degree of variation in the temperature distribution across the connection was observed due to the presence of the composite slab. This is because the concrete slab acts as both a radiation shield and as a heat sink, keeping the upper flange cooler (by 19%-30% compared with beam lower flange) and thus increasing the failure temperature.

For some flexible end-plates, the response is complicated by two stages of rotation. Initially the connection experiences large end-plate deformation until the beam comes into contact with the column. Beyond this there is enhanced capacity with further small rotations. Some tests were conducted in two stages in order to obtain connection response over the entire rotation range. It appears that, for most connections, three elevated temperature tests and a single ambient temperature test are sufficient to obtain a reasonable representation of connection response. Despite the difficulty associated with conducting fire tests, the majority of elevated temperature tests were conducted satisfactorily.

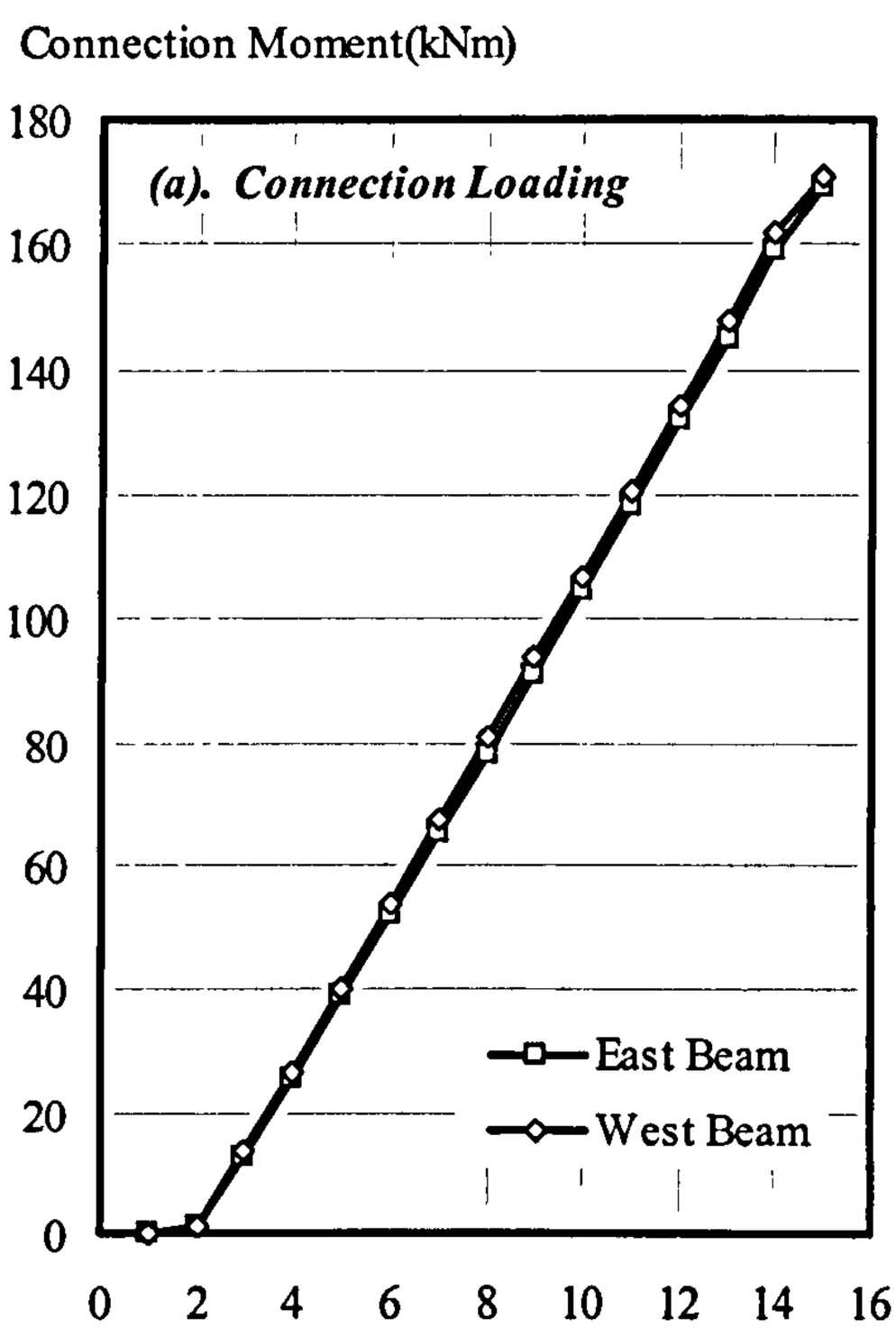

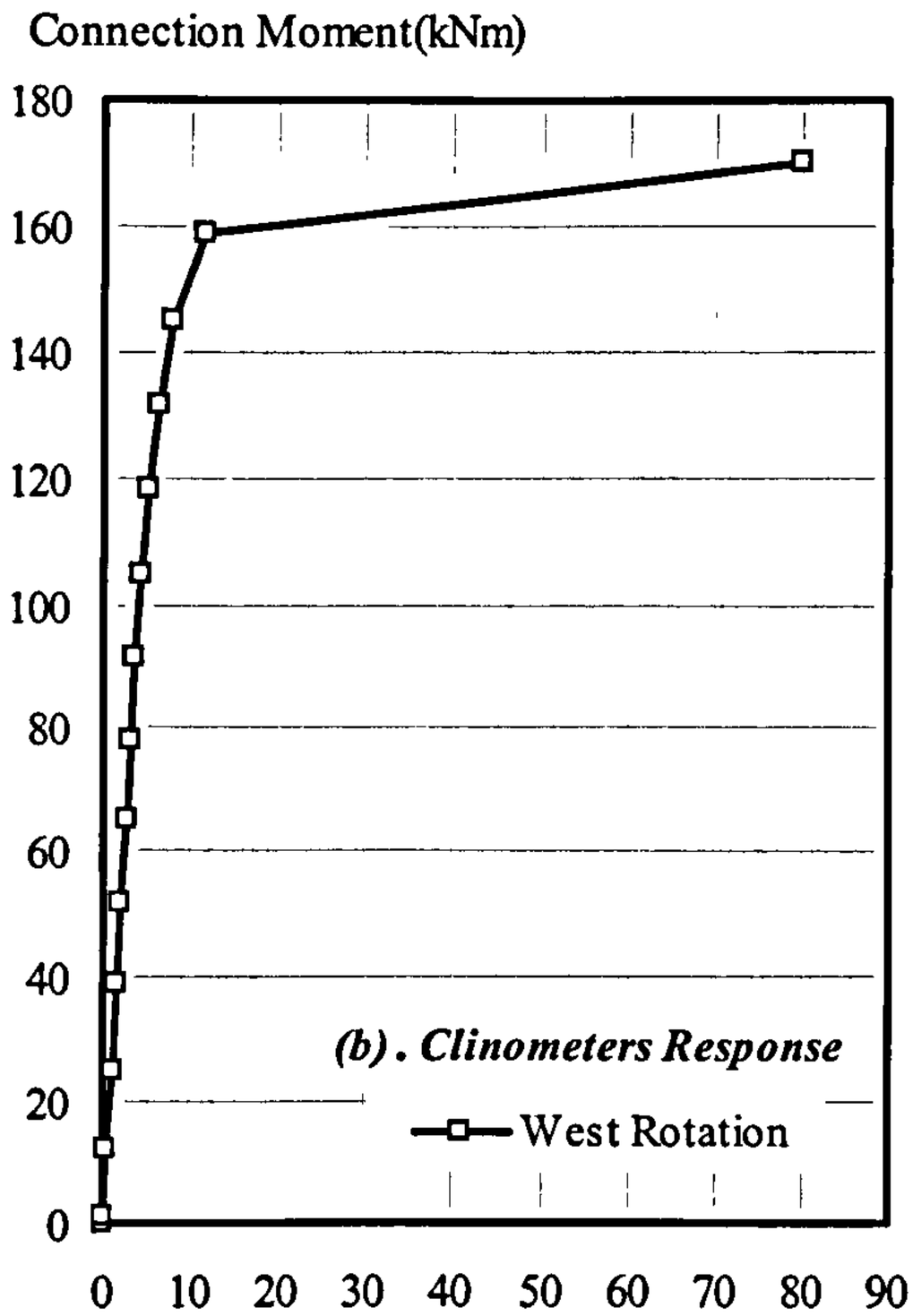

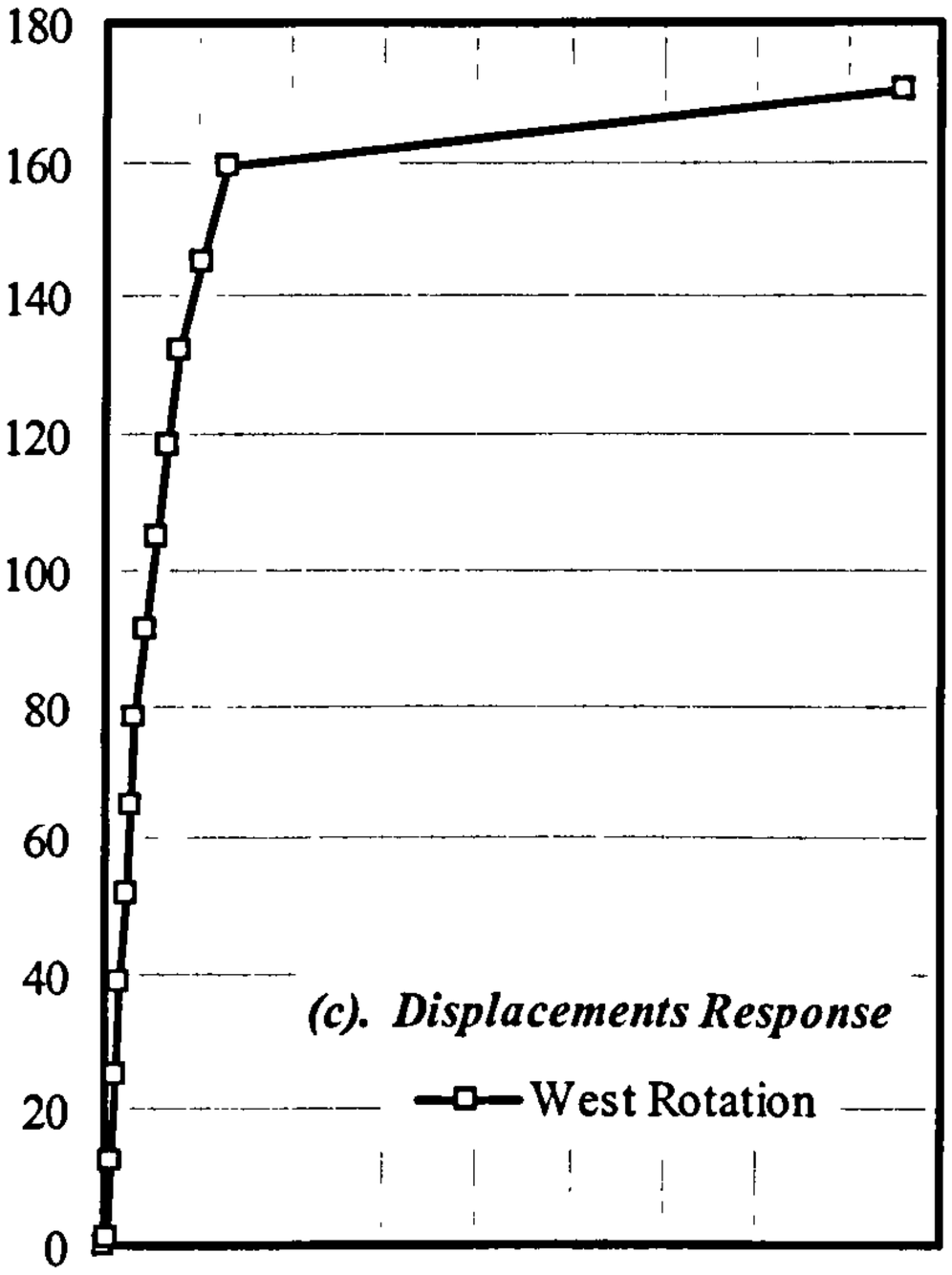

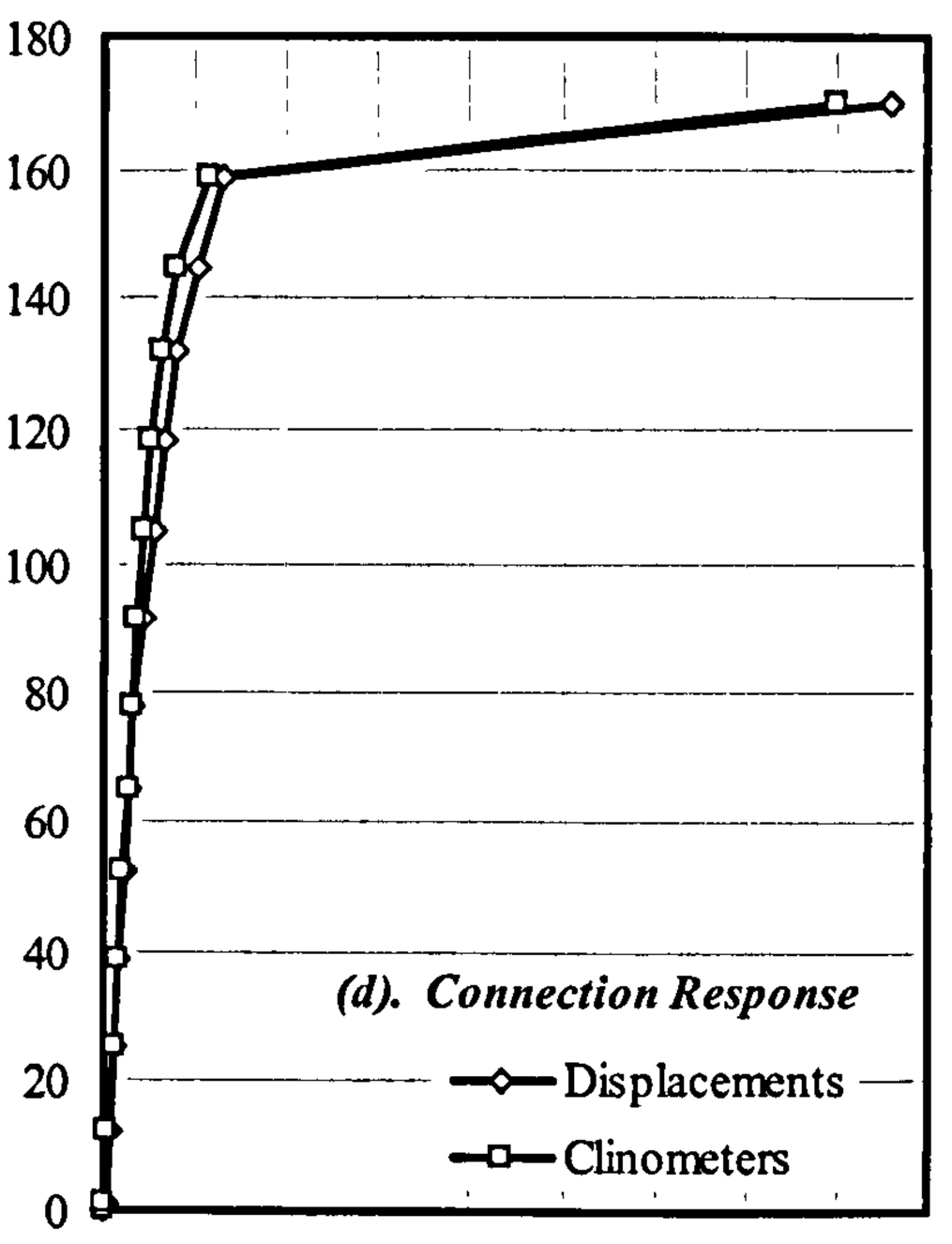

Figure 4.18: Summary of Results from Group 5 Ambient Temperature Test (FLC5AMB)

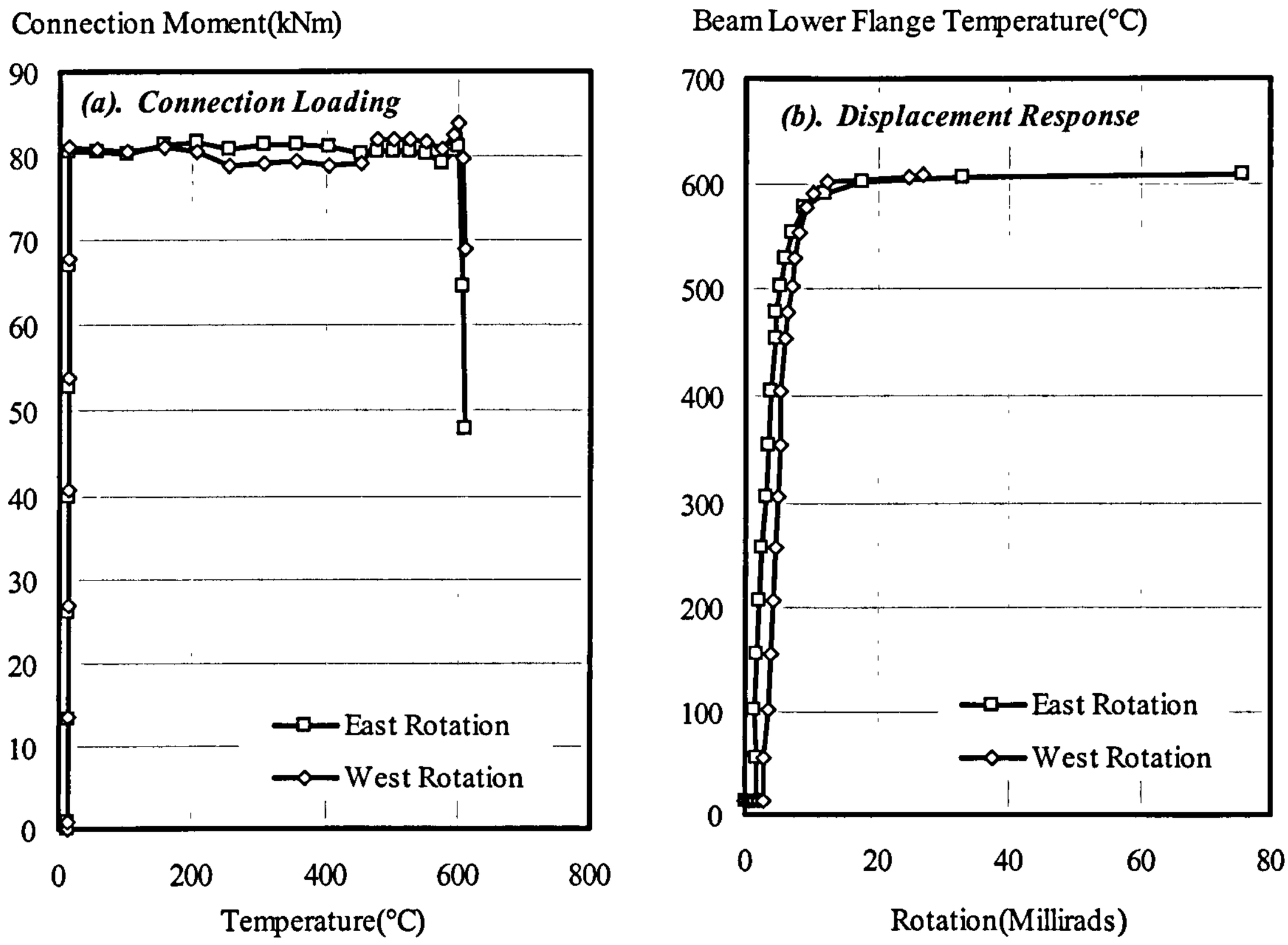

Figure 4.19: Summary of Results from Group 5: Fire Test 2 (FLC52)

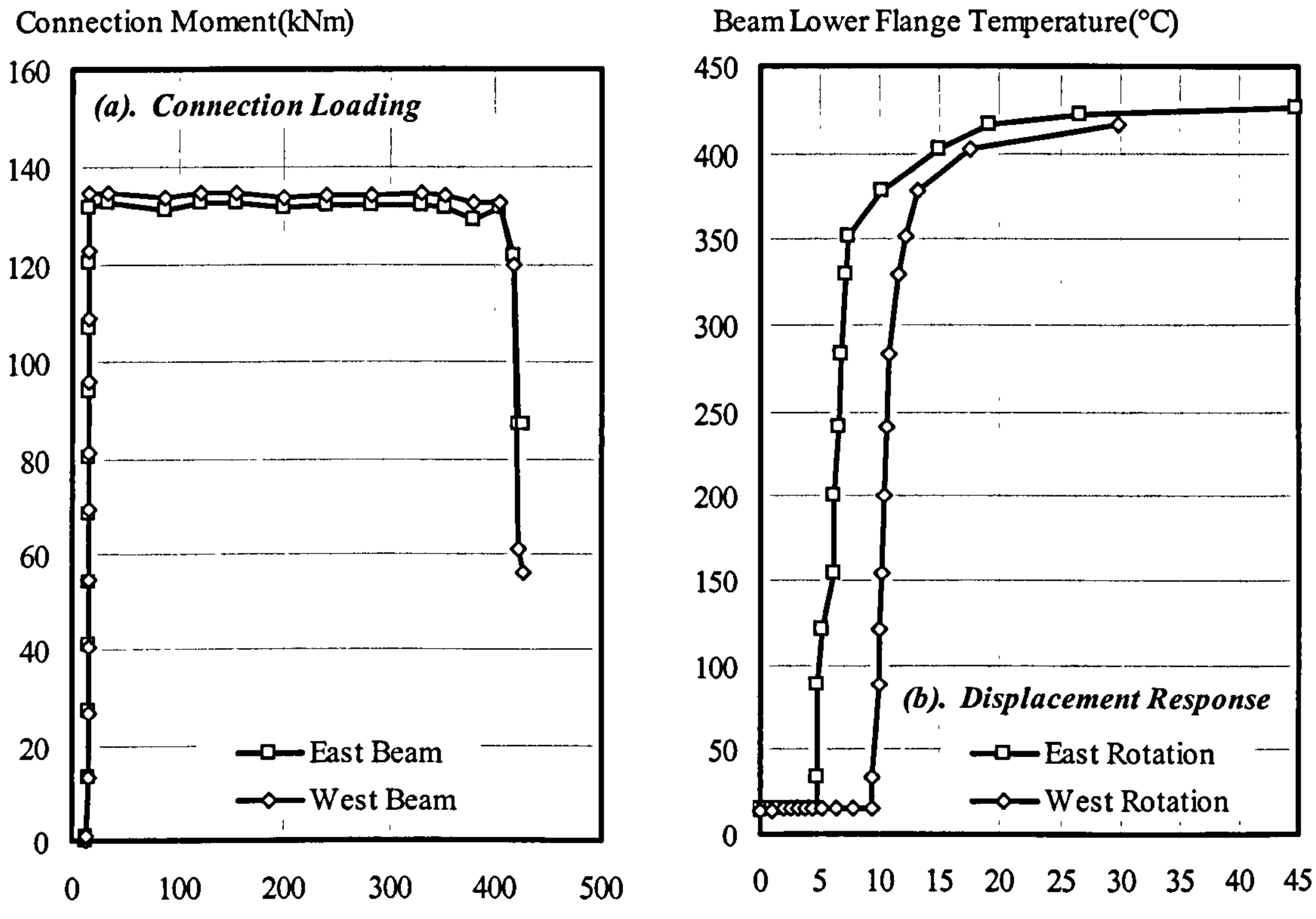

Figure 4.20: Summary of Results from Group 5: Fire Test 3 (FLC53)

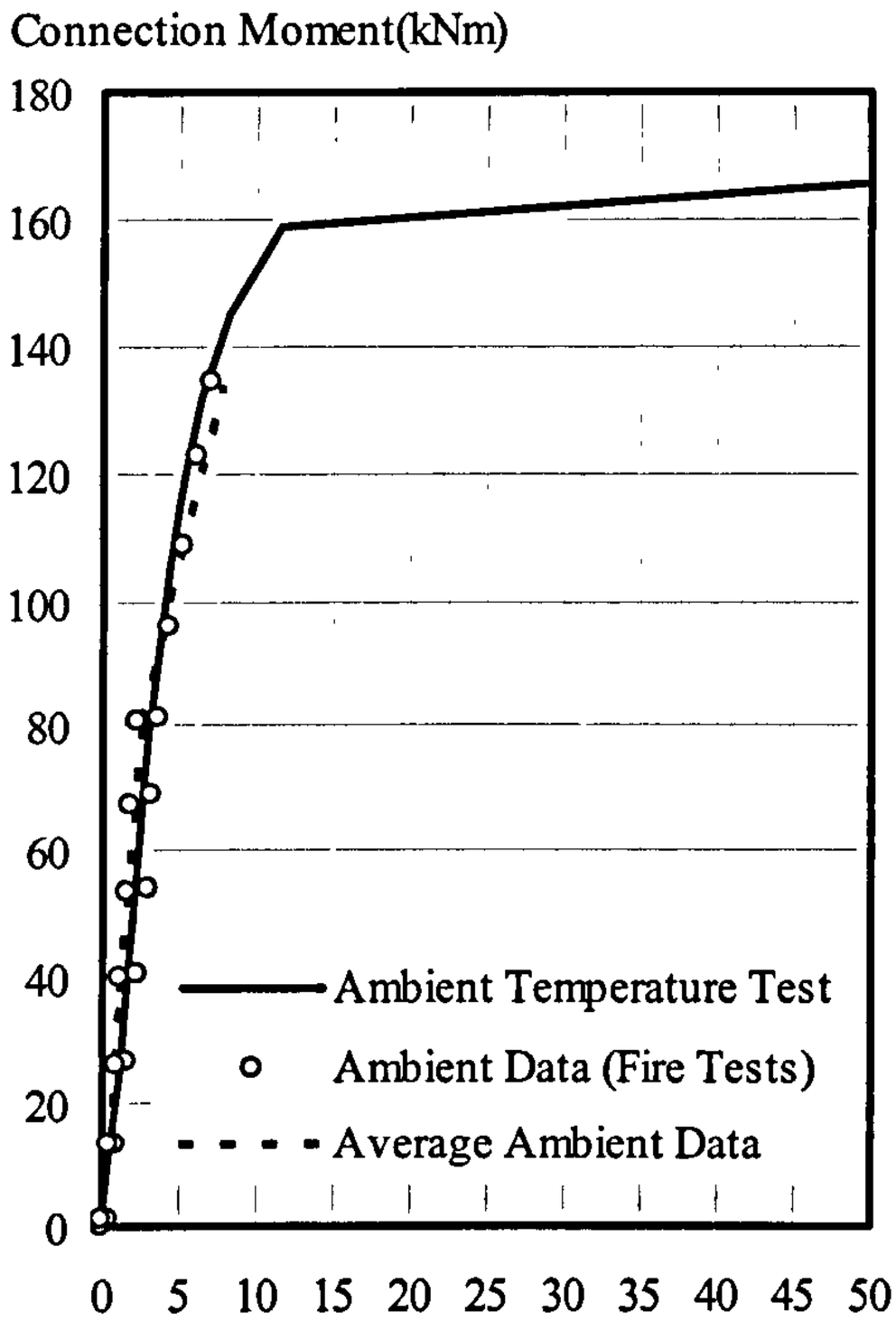

Figure 4.21: Ambient Temperature Response Compared with Ambient Temperature Data from Group 5 Fire Tests

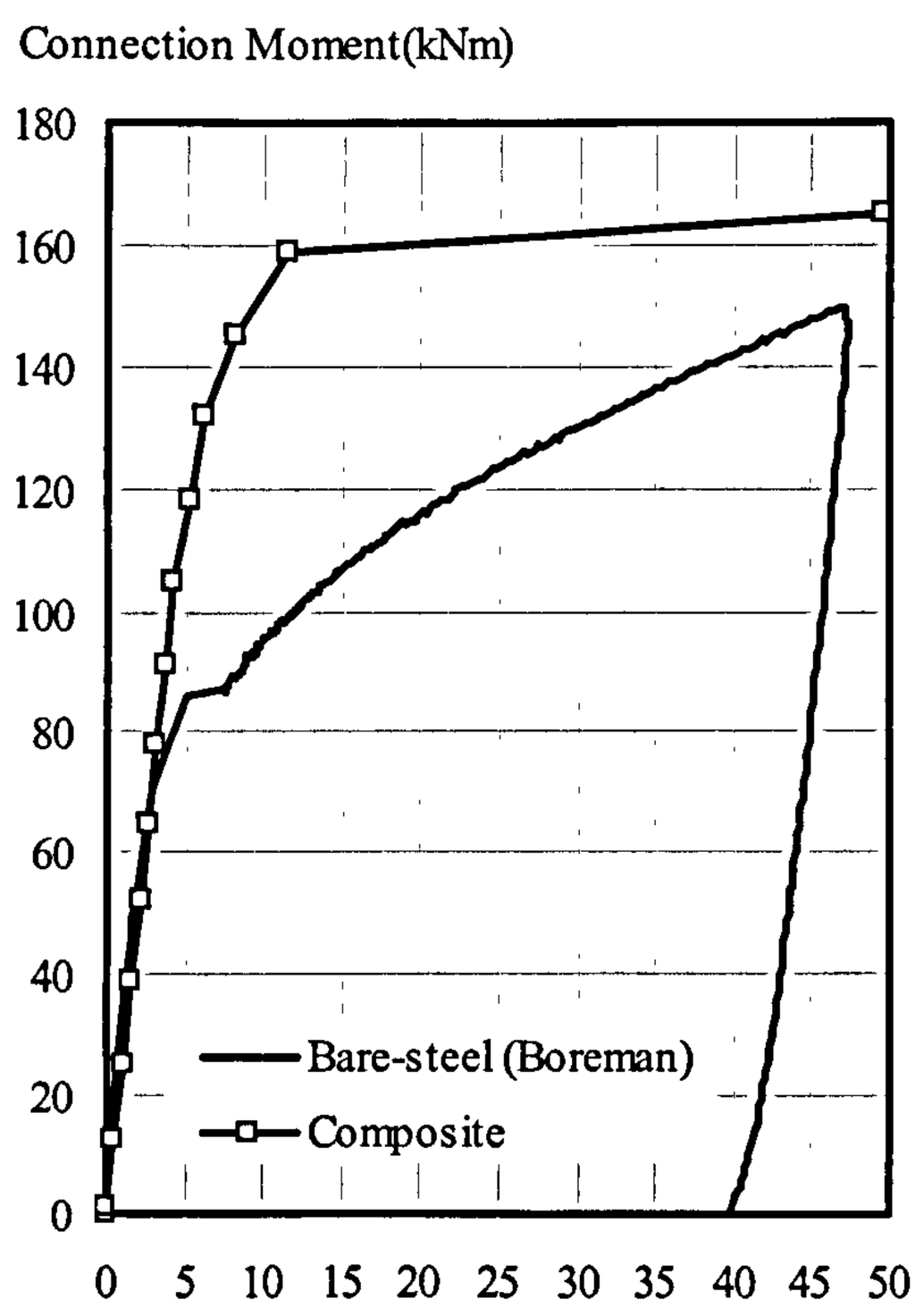

Figure 4.22: Comparison of Bare-Steel and Composite Connection Response for Group 5

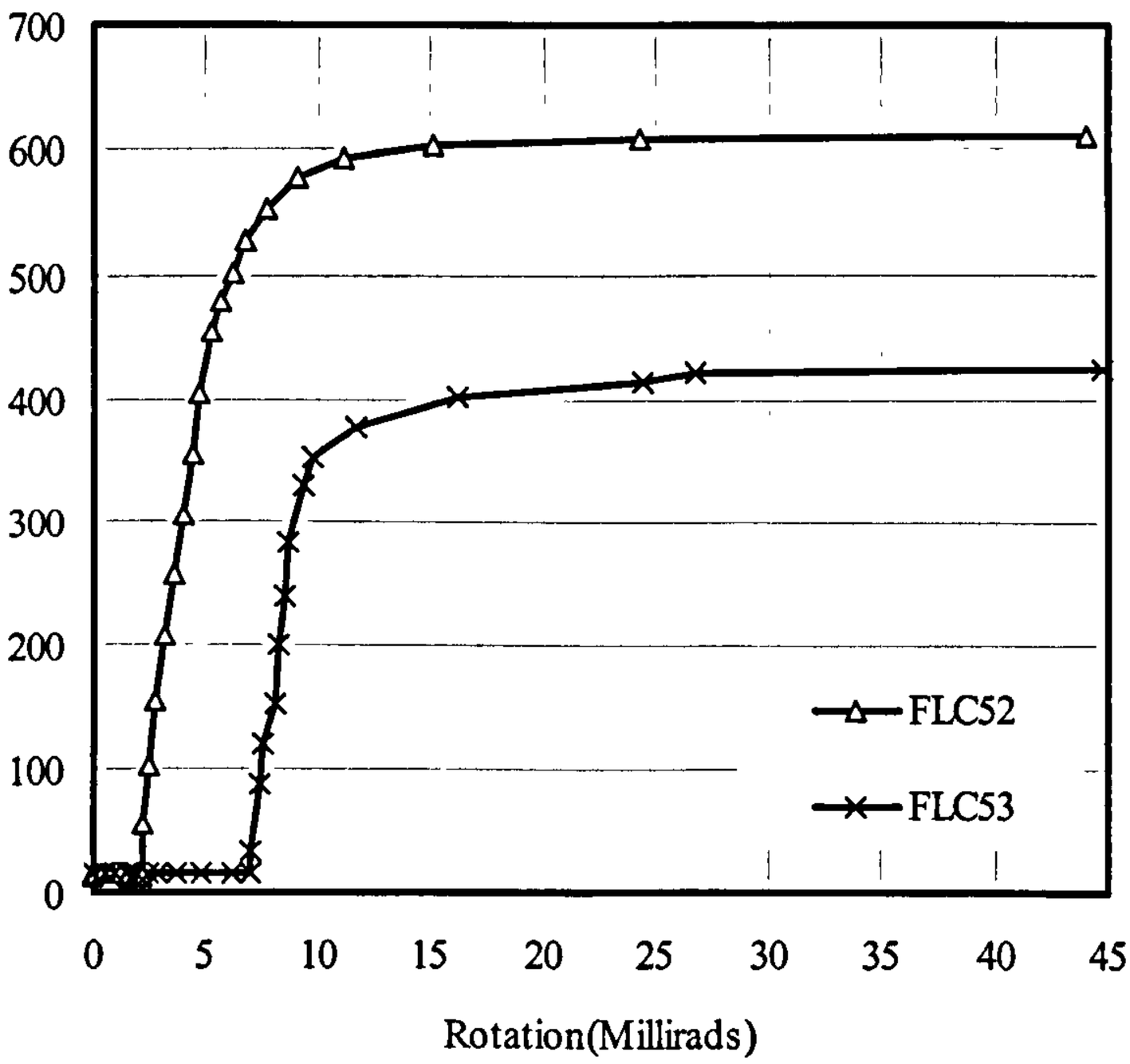

Figure 4.23: Elevated Temperature Connection Response of Group 5 Tests

5 CONNECTION DEGRADATION, REPRESENTATION AND FINITE ELEMENT MODELLING

5.1 INTRODUCTION

The expense of connection fire tests and the restrictions imposed by the furnace size as well as the wide variety of connection types utilised in practice, make it impractical to develop a comprehensive set of connection characteristics by tests alone. Even for ambient temperature there has been an identified need to seek alternative analytical methods, or direct extrapolation from the available databases[33] for determining connection characteristics. Accurate modelling of moment-rotation characteristics of the connection is necessary if the influence of connections is to be incorporated within the numerical analysis of the structure.

There is now a large volume of data[59] describing the elevated temperature properties of steel based on high-temperature tensile tests[71] on different steel types. This provides a sound basis for quantifying the rate of decay of connection characteristics by modification of the large quantity of ambient temperature data already available for a range of connections. Also, it provides valuable information for the development of simple models for predicting the response of connections at elevated temperatures.

In the most sophisticated analysis it may be necessary to include the complete moment-rotation characteristics. However, it may often be adequate to use simple connection models, representing key parameters such as stiffness, capacity and ductility. Various forms of analysis and modelling methods have been suggested including simple curve fitting techniques, simplified analytical methods and sophisticated finite element models for both bare-steel and composite connections.

In this chapter, the degradation of the connection stiffness and capacity at elevated temperatures for both bare-steel and composite connections are compared with the rates of degradation of structural steel as adopted in EC3: Part 1.2[59]. The method adopted for representing the connection characteristics at elevated temperature is described. The different finite-element models developed to model the connection behaviour at ambient and elevated temperature are reviewed.

5.2 DEGRADATION OF CONNECTION CHARACTERISTICS

Test data for the degradation of the connection characteristics at elevated temperatures provides a useful basis for establishing a method of modifying ambient temperature data. This is considered by examining the degradation of the connection characteristics in relation to that of structural steel.

The initial stiffness of the connection is of major importance in the elastic range, and it might be expected that there is a direct relation between connection stiffness and the elastic modulus of the material. Because of the absence of a distinct yield point at high temperatures design codes often define material degradation at specific strain limits and the determination of the connection strength and stiffness will depends on the strain

limit chosen. In EC3: Part 1.2[59] strain levels up to 2.0% are allowed to define the ultimate capacity whilst for design purposes a proof stress corresponding to 0.2% strain limit is normally used to determine when the steel becomes plastic[77]. These are related to stiffness and strength retention factors which define the properties of steel at a given temperature and strain level relative to its room temperature characteristics. EC3: Part 1.2 uses a "bilinear-elliptical" stress-strain material model in which a linear-elastic part is connected to a yield plateau by an elliptical curve. Consequently, the material stiffness depends on the strain level. The modulus of elasticity is generally based on the strain at the limit of proportionality.

5.2.1 Degradation of Bare-Steel Connection Characteristics

The degradation of connection stiffness with increasing temperatures is normalised in relation to ambient temperature stiffness. The experimental rate of connection degradation was based on the two tests involving the lowest load levels. The experimental connection stiffness is compared with the recommendations adopted in EC3 for the level of strain contained within the proportional limit and levels of strain 0.2%, and 0.5%, as shown in Fig. 5.1*(a)* for the bare-steel connections.

It may be seen that the rate of decay of Group 1 connections follows closely that represented by the proportional limit for temperatures up to approximately 400°C, beyond which the theoretical rates of degradation slightly underestimate those actually observed. However, despite the large section sizes and connection detail adopted in Group 2 connections, the connection stiffness seems to degrade at a higher rate than that of Group 1 connections for temperature up to 350°C. This is probably due to the enhanced capacity of the connection that causes increased forces in the compression zone. Also the observed rate of degradation is a little greater than theoretical rates. Fig. 5.1*(a)* indicates that the rate of degradation for flexible end-plate stiffness is somewhat lower than that for both flush end-plate connections for temperatures up to 350°C, beyond which the rate of decay is comparable. This may be attributed to the low force levels applied to the compression zone since the connection undergoes unhindered end-plate deformation until the beam bears against the column. The degradation of flexible end-plate stiffness compared closely with the strain level corresponding to proportional limit and in general, it seems this the level of strain may be adopted to represent reasonably the rate of degradation of stiffness of the bare-steel connections.

The observed degradation of the connection strength for the bare-steel connections is compared with theoretical degradation adopted in EC3 based on levels of strain at 0.5%, 1.0%, and 2.0% in Fig. 5.1*(b)*. The rate of degradation of Groups 1 and 2 connections was based on a rotation of 60 and 70 millirads, corresponding to the maximum levels of rotation in tests FB11 and FB21 respectively. However, in order to obtain a reasonable rate of degradation for Group 3 connections, the degradation was based on a rotation of 80 millirads which was approximately the maximum level of rotation in test FLB32.

It may be seen that the levels of strain of 0.5% and 1.0% more accurately model the actual degradation of the connection capacity than the strain level of 2.0% which underestimates the degradation of connection capacity. It seems that a reasonable representation of the degradation of the capacity of the connection may be obtained if it is assessed based on a level of strain of 1.0%. Generally the degradation of the

connection capacity is similar among the bare-steel connections irrespective of the connection type and specimen size.

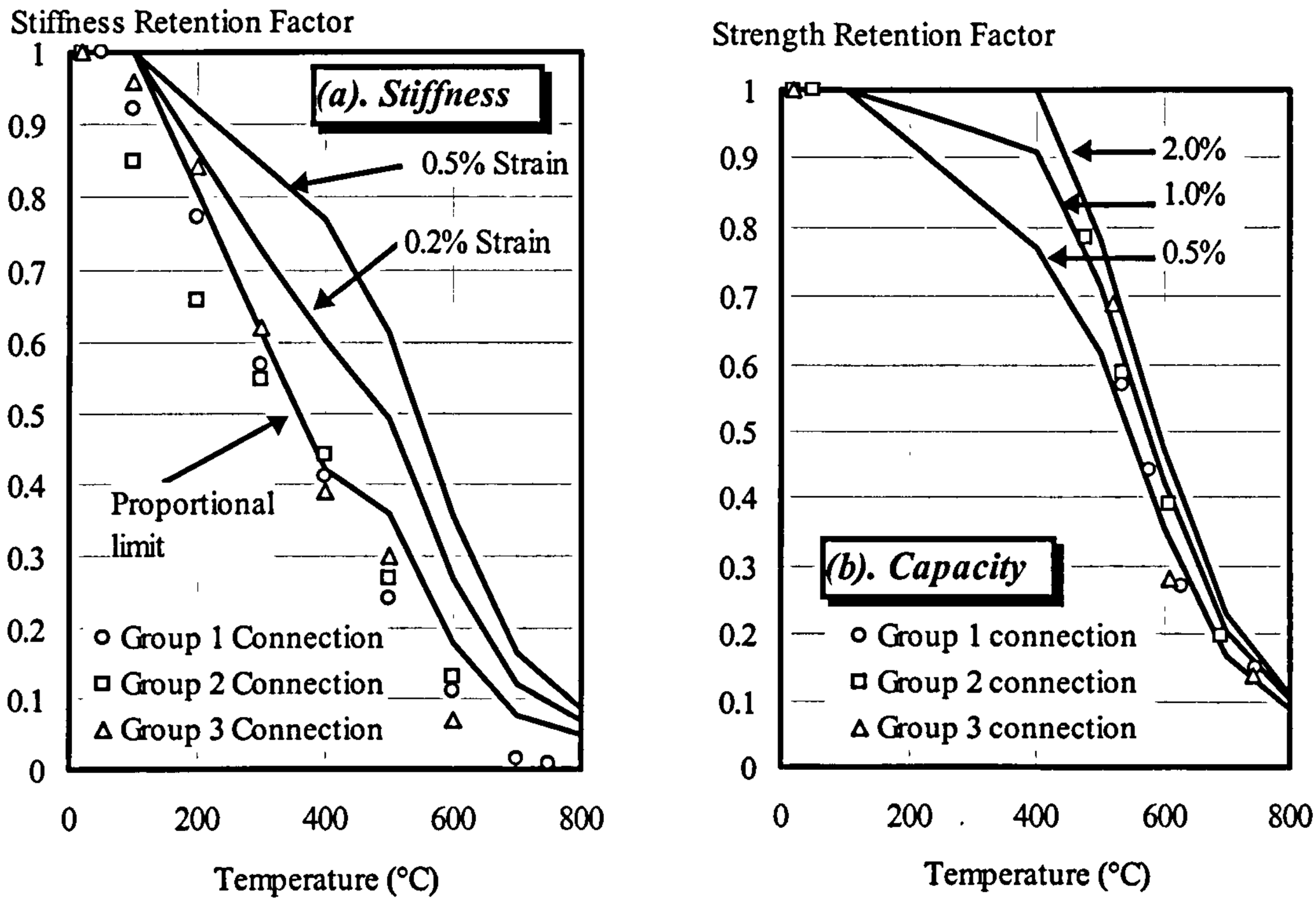

Figure 5.1: Degradation of Bare-Steel Connections with Temperature

5.2.2 Degradation of Composite Connection Characteristics

Casting a composite slab over the connection is known to significantly enhance the connection characteristics at ambient temperature. In fire conditions the composite slab retains most of its strength causing the connection to degrade at lower rates than the bare-steel connections due to the influence of reinforcement which remains at a relatively lower temperature than the bare steel.

The observed degradation of stiffness for composite connections is compared with that presented in EC3 in Fig. 5.2*(a)* assuming levels of strain 0.2%, 0.1% and that corresponding to the limit of proportionality. It may be seen that the rate of stiffness degradation is considerably lower than that for bare-steel connections. The observed degradation of Group 4 connection compares closely with the degradation of the steel at a strain level of 0.5%, whereas the strain at the proportional limit provides a conservative representation for flexible connections. The stiffness for Group 5 connections was observed to degrade in a similar manner and comparable to that of Group 4.

Recent design guides[44] recommend that the influence of the reinforcement should be taken into account when calculating the overall capacity of the composite connection. Therefore the overall capacity of the connection may be determined by adding the forces generating from the resistance of the reinforcement in the slab to the moment capacity of the bare-steel connection. Due to the presence of the composite slab it may

be anticipated the rate of degradation of the bare-steel section would be greater than that of the reinforcement.

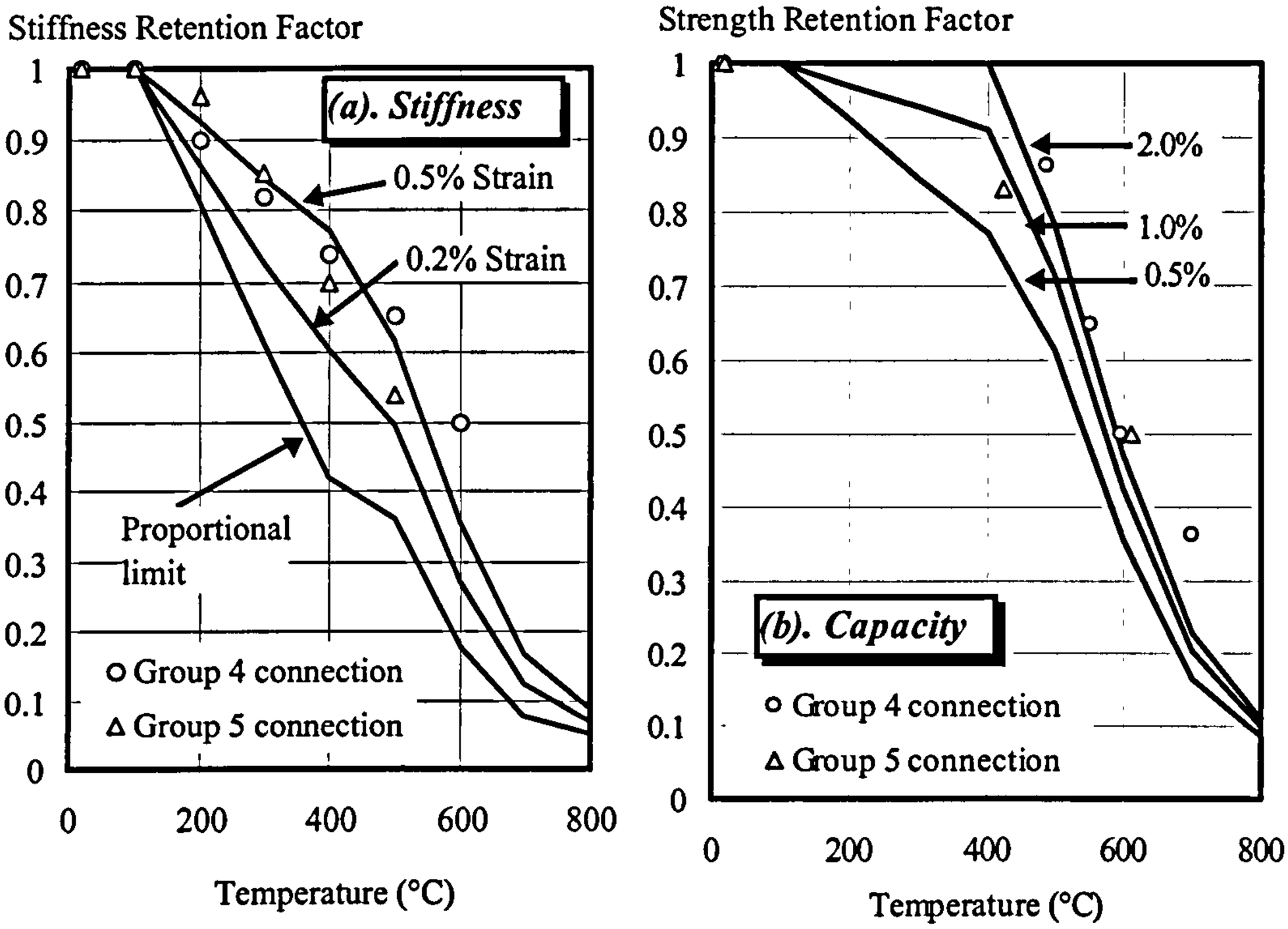

Figure 5.2: Degradation of Composite Connections with Temperature

Once more the degradation of the connection capacity is compared with the theoretical degradation of bare-steel according to EC3 recommendations at levels of strain 0.5%, 1.0% and 2.0% as shown in Fig. 5.2*(b)*. It may be seen that the general form of capacity degradation follows closely the theoretical degradation rate at 2.0% strain for Group 4 and 5 connections. Nevertheless, with only two points it was not possible to assess the degradation rate for Group 5 connections effectively. Despite the enhancement in the connection response provided by the incorporation of the composite slab, it seems that the observed rate of degradation of the connection capacity presented above underestimates the actual rate of degradation that is likely to occur in a typical composite connection[52]. This is mainly due to the failure of the test specimen to maintain its 'composite' integrity during the fire tests. Since only one third of the beam span was cast with the composite slab only two shear studs were included in each beam. Failure was associated with separation of the shear studs from the slab at an early stage in the test. The connection subsequently behaved as bare-steel, resulting in an increase in the rate of degradation. Unfortunately the degradation of composite connections cannot be assessed for temperatures below 400°C due to the levels of moment adopted during the tests. In general the rate of degradation of steel at 2.0% strain provides a close representation to the degradation of capacity of flexible end-plate composite connections.

5.3 REPRESENTATION OF THE CONNECTION CHARACTERITICS

Mathematical expressions are used to fit test data for the connection type considered facilitating the incorporation of such data within analytical models. The curve-fitting expressions should be capable of representing the connection response over the entire range. Moreover, in the case of flexible end-plate connections the form of expression should have the ability to represent the enhancement in the connection stiffness following the contact between the beam lower flange and the column flange. It is also desirable that the slope of the function, which corresponds to the rotational stiffness of the connection, is always positive.

Early modelling of connections was largely based on the assumption that the behaviour is linear elastic over the entire moment-rotation response, thus making the overall structural response elastic. However due to the complicated nature of connections, the real moment-rotation relationships are generally non-linear. Such behaviour can be represented in a number of different ways with various levels of complexity. For ambient temperature analyses, it was found that[104] connection rotations in excess of 50 millirads have negligible practical influence on the response of isolated restrained members and steel-framed structures. In fire conditions however structural members are allowed much larger levels of deflection and therefore considerable levels of rotation are generated requiring more extensive data to describe the behaviour.

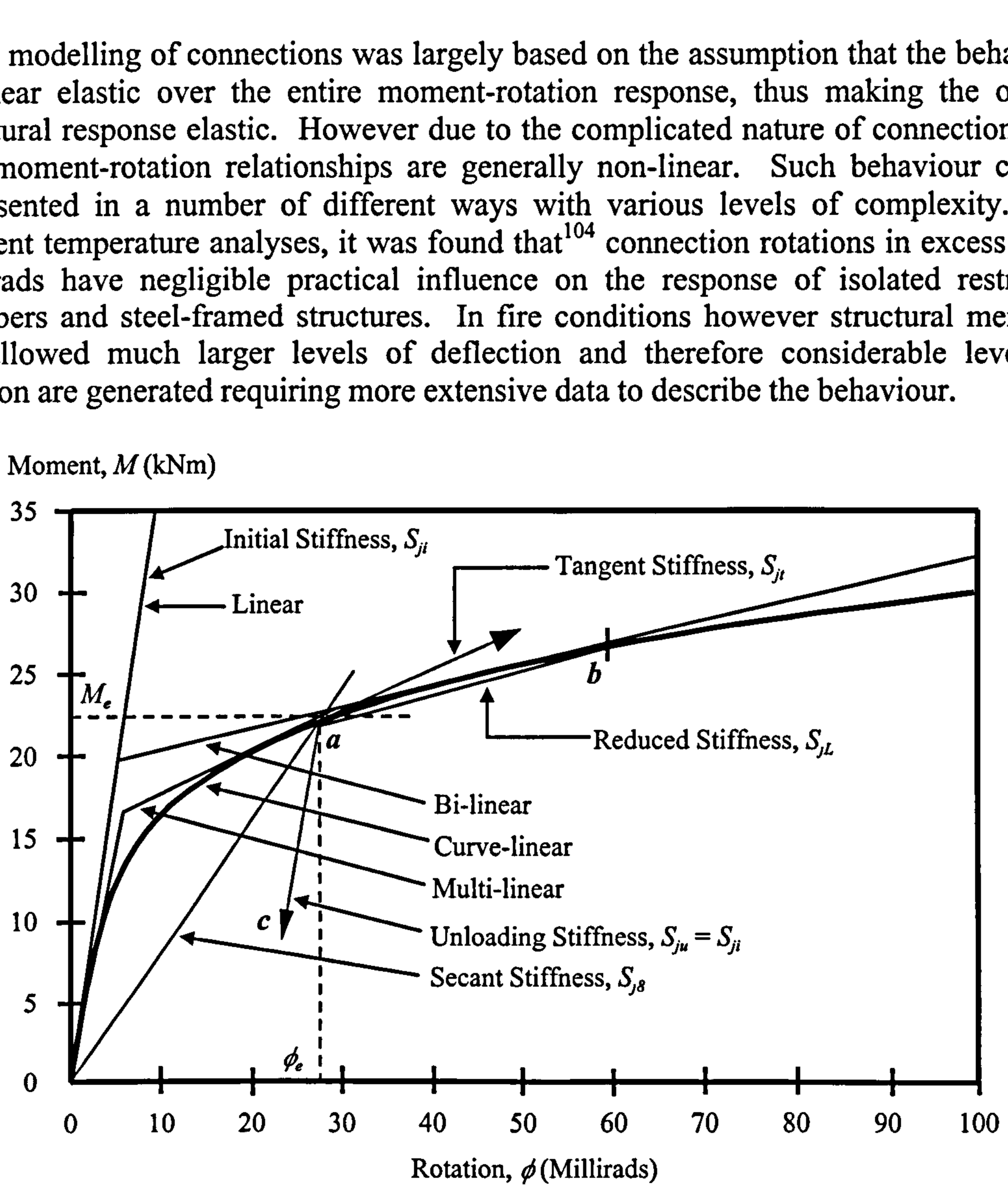

Figure 5.3: Forms of Curve-Fit and Stiffnesses for a Typical Semi-Rigid Connection

The earliest attempts to fit a mathematical function to experimental moment-rotation relationships date back to the work of Baker[105] in 1934 and Rathburn[106] in 1936 who fitted a single straight line tangent to the initial slope of the connection[107]. A semi-rigid

connection factor Z was introduced which was expressed in terms of the angle per unit moment:

$$Z = \phi/M \qquad 5.1$$

Such factors were incorporated into the early computer-based structural analysis methods such as slope-deflection and moment distribution[108] to study the significance of semi-rigid end restraint. The expression is simple to use but it is very limited since it represents the elastic response of the connection which in most cases is conservative as shown in Fig 5.3. Such an approximation may be suitable for highly rigid cases at ambient temperature. However, at elevated temperatures far greater levels of rotation are often associated with non-linear response at relatively low levels of moment and linear approximations are of limited applicability in the analysis of elevated temperature frame response with nominally semi-rigid connections.

In the 1970's the use of computers encouraged the development of more refined representations of connection characteristics. Lionberger and Weever[109] and Romstad and Subramanian[110] developed a bi-linear approximation for double angle connections up to high deformation levels. When dealing with bi-linear approximations it is difficult to determine accurately the elastic portion of the response and the exact point corresponding to the onset of plasticity. A number of authors[52] have therefore suggested the use of the secant-stiffness. This approach has been adopted in EC3: Annex J[40], with the secant stiffness assumed to intersect the experimental moment-rotation curve at a moment equivalent to two-thirds of the connection capacity. Beyond this a reduced stiffness of typically half of the secant stiffness is assumed.

The bi-linear expressions are simple to use, but do not provide a very precise model for actual behaviour, especially at high levels of rotation. Tri-linear and multi-linear forms of curve-fit have been proposed by Moncarz and Gerstle[111] and Poggi and Zandonini[112] respectively. Sommer[113] introduced a polynomial form based on a least-square curve fitting procedure and standardised moment-rotation functions have been derived for a series of flexible end-plate connections. The general form of the expression is described below:

$$\phi = \sum_{i=1,3,5} C_i (KM)^i \qquad 5.2$$

where,

K = standardisation parameter depends on the connection type and geometrical properties;

C_i, i = curve-fitting constants and odd powers respectively.

Fry and Morris[114] later applied the same principles to develop non-dimensional expressions for seven connection types and incorporated these in numerical software to study the influence of connections on the behaviour of planar frames. However, although polynomial functions can accurately represent the non-linear behaviour of connections, they do suffer from an inherent oscillatory nature[115] which may produce negative connection stiffness.

An improved form of expression was developed by Richard and Abbott[116] based on the least-squares curve-fitting procedure in which only four parameters are required to establish the moment-rotation characteristics of a particular connection. Ang and Morris[117] proposed an alternative expression following the same procedure while utilising a Ramberg-Osgood[118] function which was originally developed to define the non-linear response of stress-strain characteristics. This has the advantage of always yielding positive connection stiffness but it cannot be derived for the moment in terms of rotation.

Jones *et al.*[22,119] suggested a cubic-B-spline technique from which the connection rotation is divided into a finite number of smaller ranges. A cubic function is fitted within each range, with first and second derivative continuity maintained between ranges. This method represents the experimental moment-rotation response very closely and avoids negative slopes. Nevertheless, in order to obtain the desired results from the curve-fitting process, a large body of experimental data is required. Chen and Liu[120,121] proposed an exponential model which provides a comparable representation. However, the model requires four or more constants to describe effectively the moment-rotation characteristics. Also, it remains untried outside the range of calibrated data[107] and requires iterative solution, as the response is non-linear. The Chen-Liu exponential model was further refined by Kishi and Chen[31] to accommodate linear components and deal with both loading and unloading for the full range of rotation.

Some of the models described above have been modified to suit a particular connection type[122,123,124]. When deciding between different curve-fitting models, it is essential to take into consideration the purpose for which the representation is required whether it is for sophisticated numerical representation or a simplified behavioural analysis. For example, the secant stiffness approach in EC3[40] is sufficient for simple design, but it may not be appropriate for an advanced frame analysis that requires a complete moment-rotation relationship.

5.4 REPRESENTATION OF THE CONNECTION FIRE TESTS RESULTS

Under fire conditions the structural members undergo a considerable deformation far in excess of that normally occurring at ambient temperature and thus the adjacent connections experience high levels of rotation. When modelling the connection characteristics for fire conditions, it is very important to select the form of curve-fit that represents accurately the actual connection response throughout the entire range of rotation and temperature.

El-Rimawi[4] modified the Ramberg-Osgood function[118] to represent the moment-rotation response of the connection at elevated temperatures. This has been incorporated into a number of structural analysis models[4,54]. Recently Leston-Jones[52] used the suggested curve-fitting expressions to conduct studies into the effect of actual bare-steel and composite flush end-plate connections on frame behaviour at elevated temperature. Due to the applicability of the Ramberg-Osgood function to describe the connection response, it was selected to represent the elevated temperature connection tests presented in Chapters 3 and 4. The modelled moment-rotation characteristics are used to carry out further parametric studies on the influence of different connections on the

behaviour of steel and composite frames as described in Chapter 6. The modified Ramberg-Osgood moment-rotation function may be expressed in the following form:

$$\phi = \frac{M}{A} + 0.01\left(\frac{M}{B}\right)^{n} \qquad 5.3$$

where,

ϕ, M = connection rotation and the corresponding level of moment respectively;
A, B and n = temperature dependent parameters.

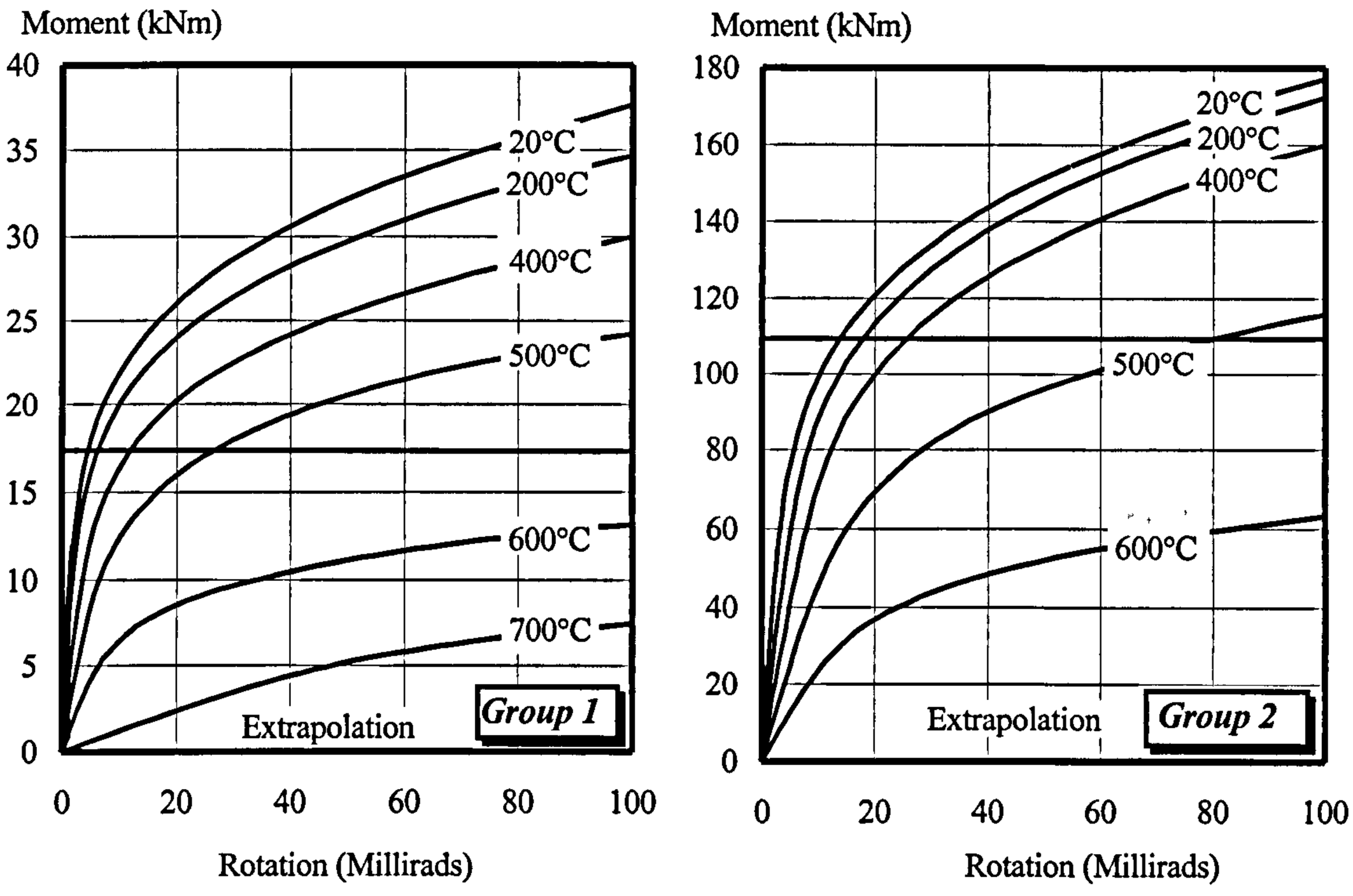

Figure 5.4: Ramberg-Osgood Curve-fit for Flush End-Plate Bare-Steel Connections Tested

In order to represent the elevated temperature connection test data in a form suitable for incorporation in numerical modelling, the moment-rotation-temperature data derived from the connection tests were fitted using the described Ramberg-Osgood expression. This was firstly based on the derivation of the experimental moment-rotation response for the connections tested. The experimental response of the connections was based on the experimental temperature-rotation curves at various load levels as presented in Figs. 3.14, 3.22, 3.28, 4.13 and 4.23 for Groups 1, 2, 3, 4, and 5 respectively and the ambient-temperature response (where available). Each temperature-rotation curve represents one point in the moment-rotation response for any temperature. The representation procedure may be summarised as follows:

- the tests were conducted at constant load with increasing temperatures, therefore – for each group – a set of temperature-rotation curves are available at different levels of moment,
- at each level of moment, the connection rotation was interpolated linearly corresponding to the required temperature,

- a set of experimental moment-rotation curves is derived with increasing temperatures;
- the Ramberg-Osgood equation was used to fit the derived moment-rotation curves by assigning different values for the parameters *A* and *B* which represent the connection stiffness and capacity respectively so that the generated curves were passing through the experimentally derived tests data.
- the modelled moment-rotation-temperature curves based on the experimental test data are shown in Figs. 5.4, 5.5 and 5.6 for both the bare-steel and composite connections with increasing temperatures. The associated temperature dependent parameters are presented in Appendix B.

It should be noted that the moment-rotation-temperature response beyond the level of loading is extrapolated (as shown shaded in Figs. 5.4, 5.5 and 5.6) based on the resulting shape of the modelled response and the ambient temperature moment-rotation response of the connection.

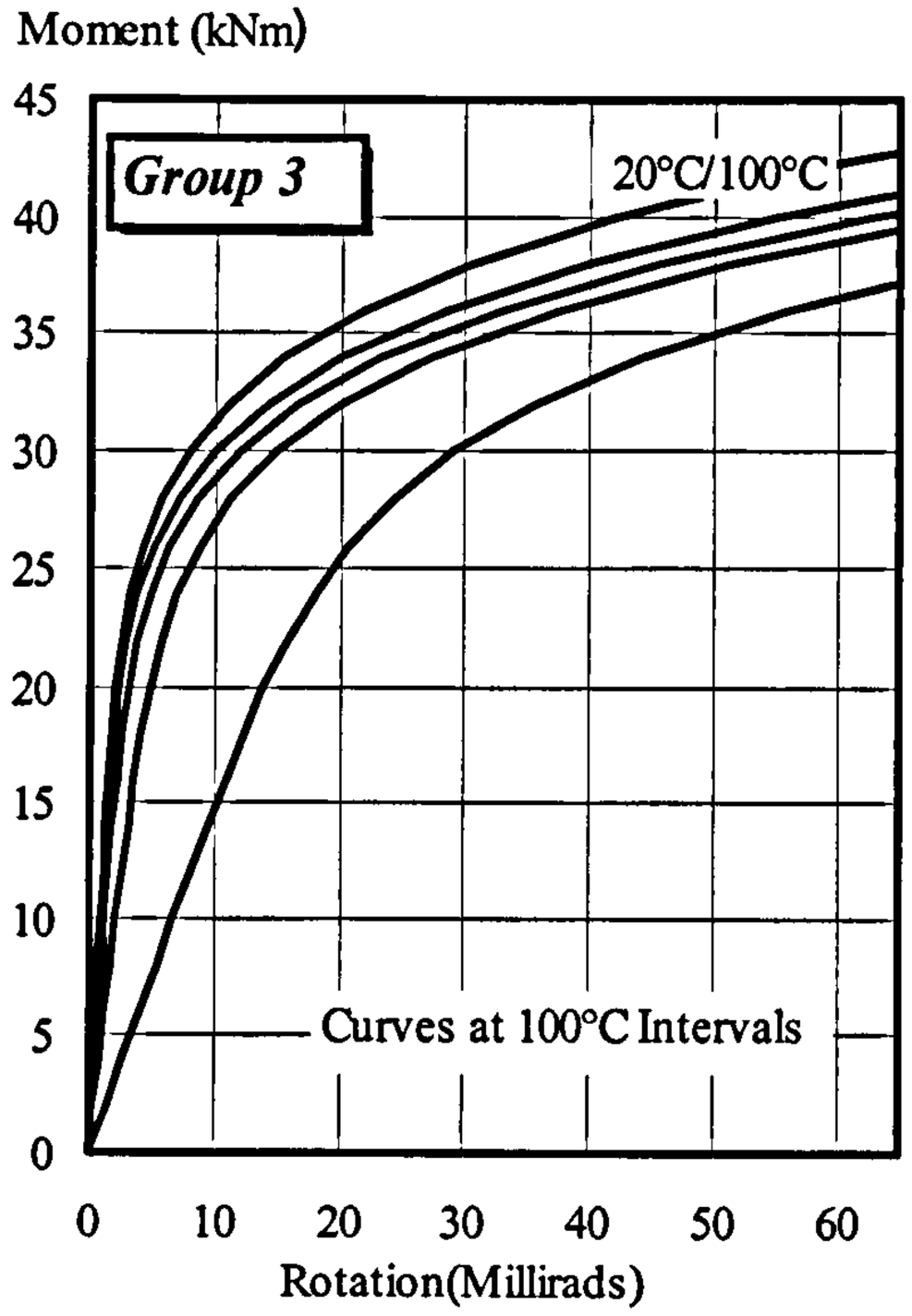

Figure 5.5: Ramberg-Osgood Curve-fit for Flexible End-Plate Bare-Steel Connection Tested

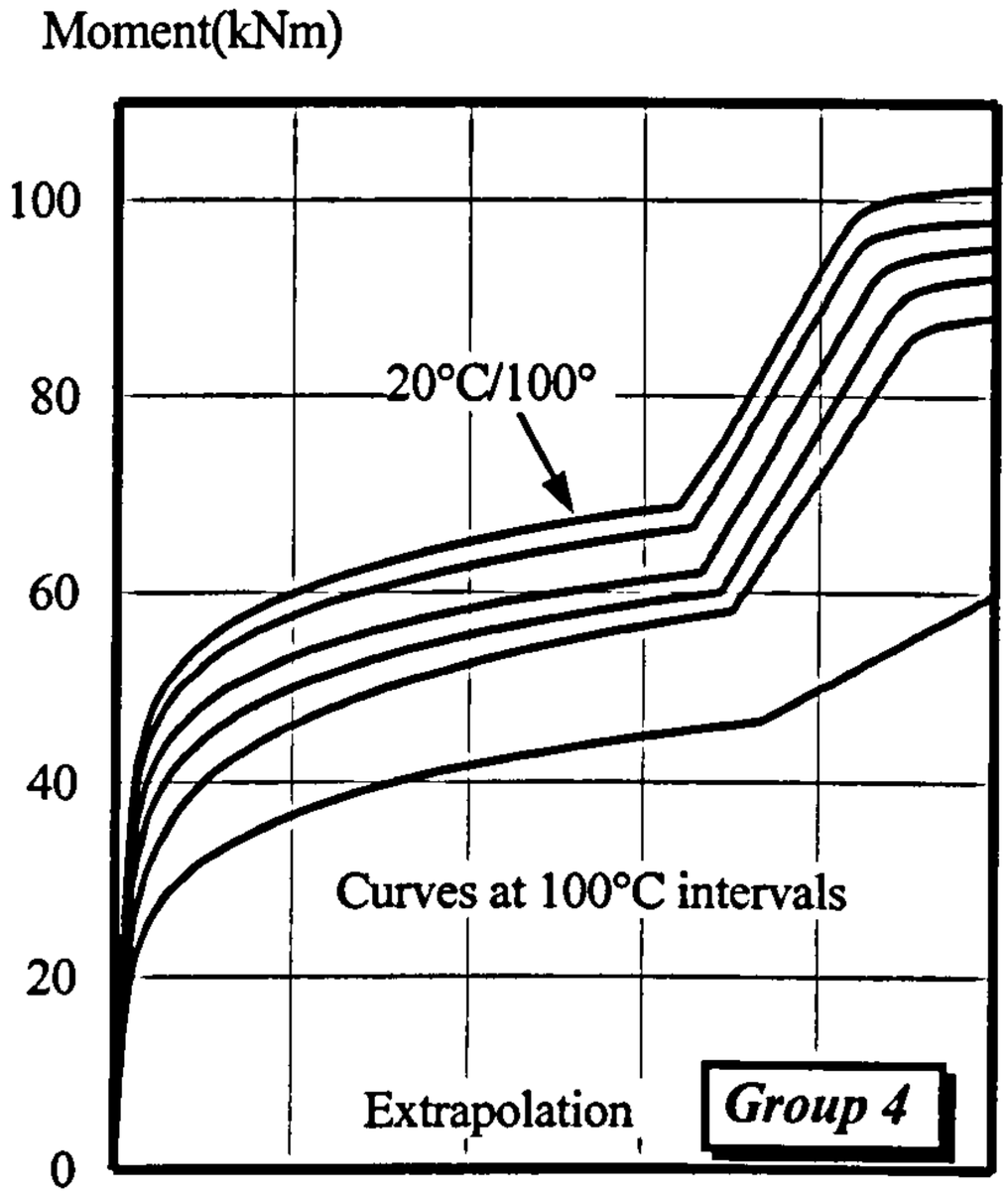

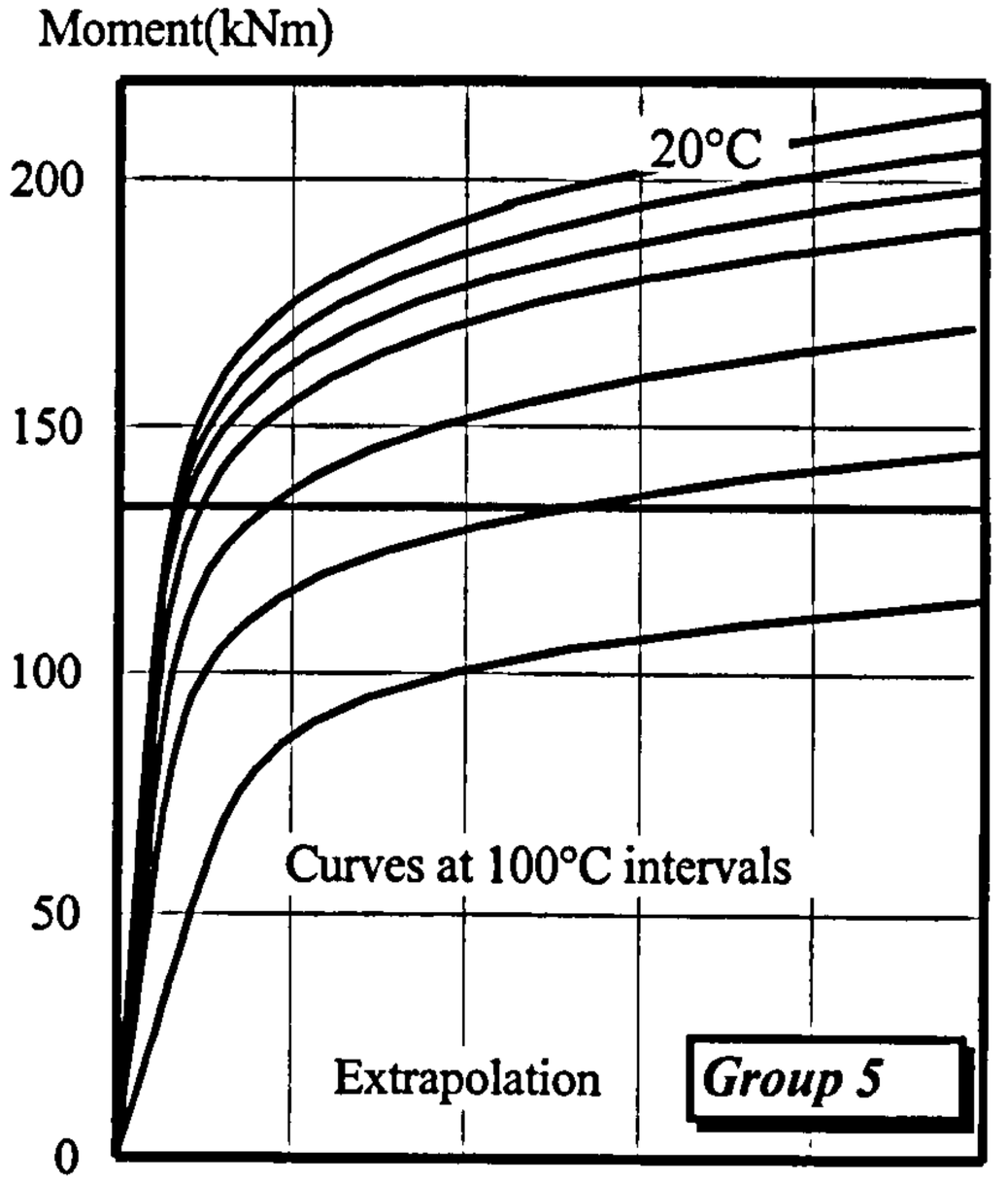

Figure 5.6: Ramberg-Osgood Curve-fit for Flexible End-Plate Composite Connections Tested

More accurate fit was obtained through an iterative procedure of visual refinement and inspection. In most of the connections modelled it was observed that the shape function remained constant with increasing temperatures. Therefore better representation of the connection response may be achieved by utilising a constant value of n, with the parameters representing the connection stiffness, A and capacity, B reducing with increasing temperatures. It should be remembered that incorporating varying values of n would not adversely the influence the overall response although in some cases it may result in values of tangent stiffness which do not degrade with increasing temperature. In the case of flexible end-plate bare-steel connections (i.e. Group 3), it was possible to fit the moment-rotation relationships up to a rotation of approximately 70 millirads corresponding to the rotation at which the beam comes into contact with the column as shown in Fig. 5.5. Beyond that it was not possible to fit the curve due to the lack of test data.

5.5 POSTULATION OF ELEVATED TEMPERATURE CONNECTION RESPONSE FROM AMBIENT TEMPERATURE DATA

Results from connection fire tests and previous experimental studies[52] demonstrate the possibility of representing the elevated temperature characteristics of a connection based on ambient temperature behaviour and knowledge about the rate of degradation of connection characteristics at elevated temperature. For bare-steel connections it was found that an acceptable representation of the rate of degradation may be achieved based on the high temperature properties of structural steel presented in EC3: 1.2[59]. Levels of strain at the proportional limit and 0.5% can be used to represent the rate of degradation of connection stiffness and strength respectively.

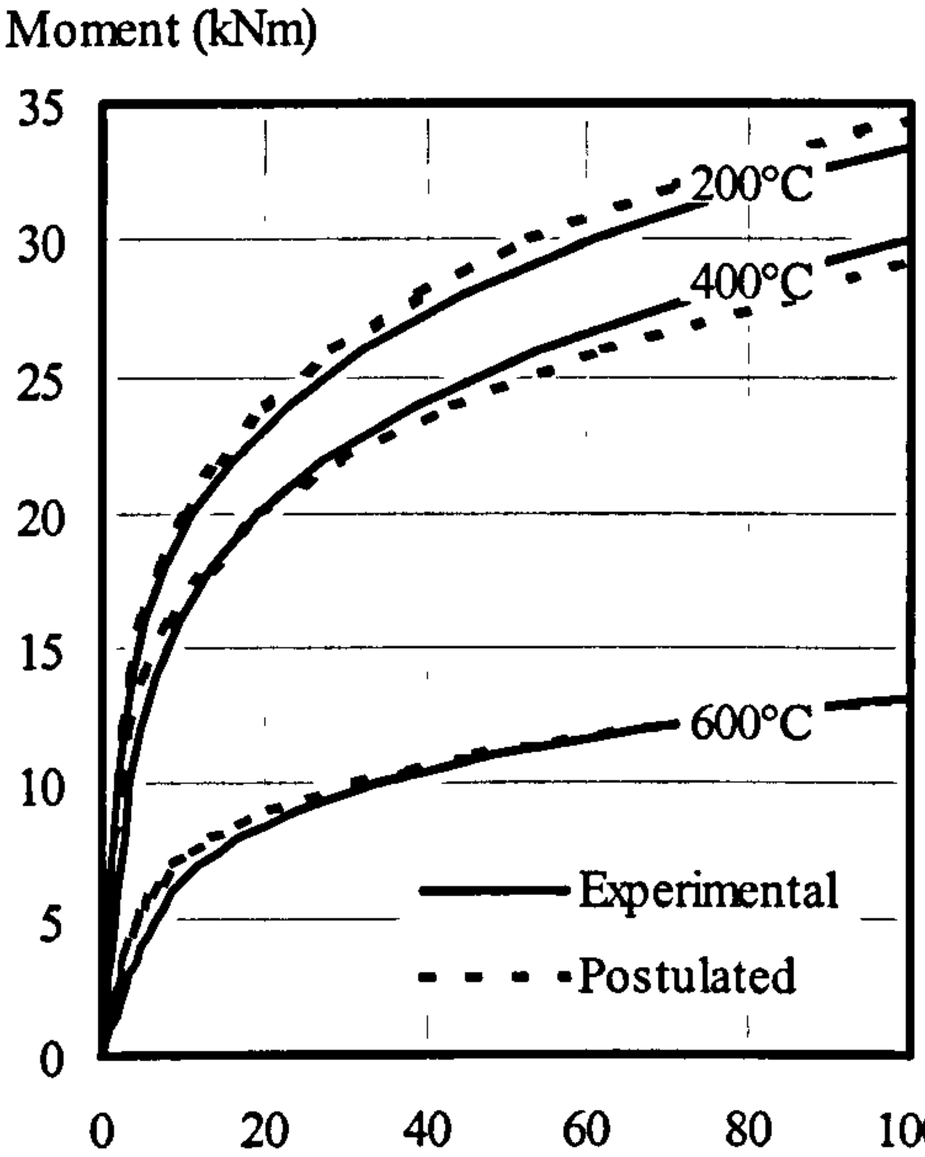

Figure 5.7: Comparison between Experimental and Postulated Elevated Temperature Response for Group 1

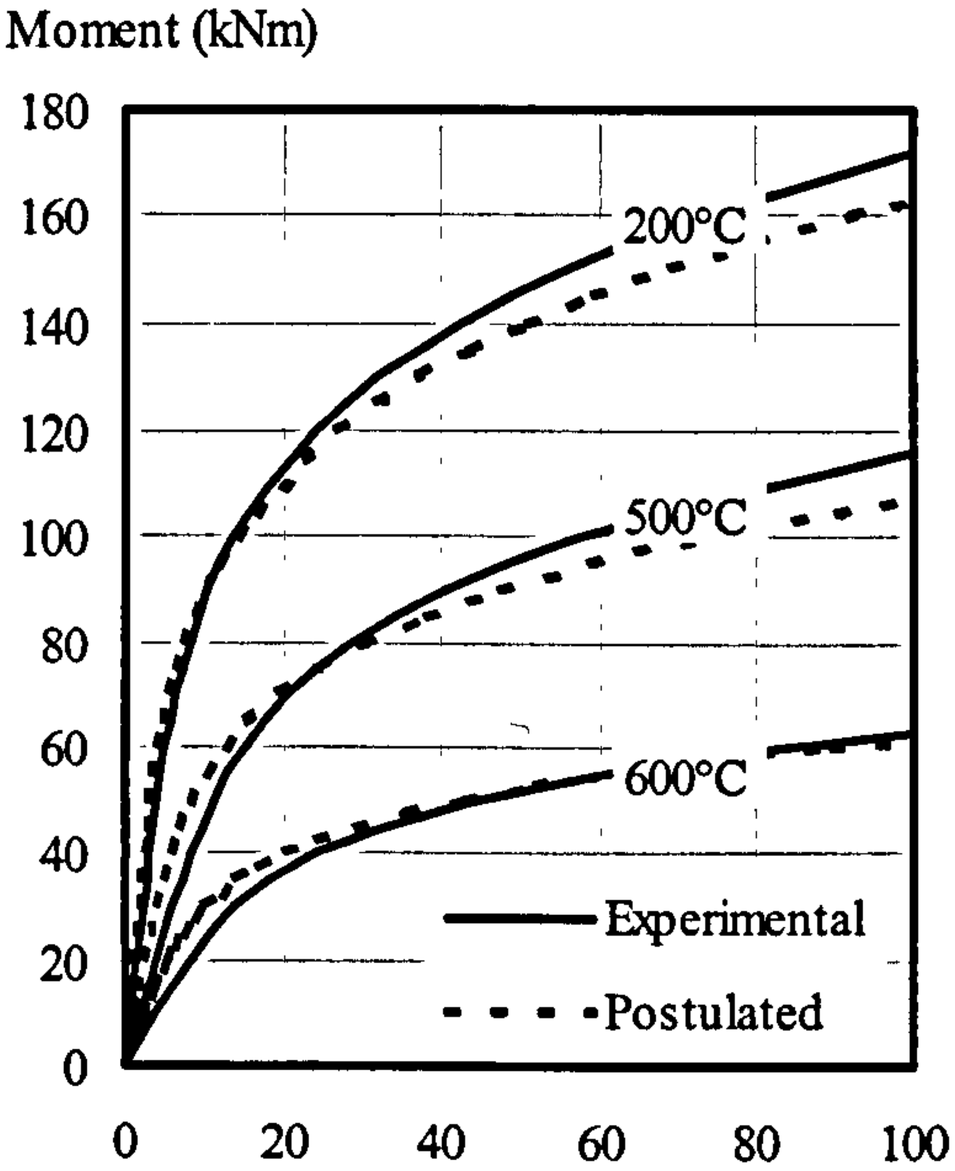

Figure 5.8: Comparison between Experimental and Postulated Elevated Temperature Response for Group 2

In order to do this, the Ramberg-Osgood expression was first applied to the ambient temperature connection characteristics. Then the parameters: *A* and *B*, representing the stiffness and capacity of the connection were degraded with increasing temperatures based on the levels of strain recommended. The postulated moment-rotation characteristics were compared with experimental results for flush end-plate connections in Groups 1 and 2 as shown in Figs. 5.7 and 5.8 respectively. It can be seen that there is close correlation between the experimental and postulated responses. Based on these results, this approach has recently been adopted by Allam *et al.*[125] in order to study the effects of restraint on the behaviour of steel frames in fire.

In order to postulate the elevated temperature characteristics for composite connections, the ambient temperature characteristics were degraded in accordance with the findings presented in section 5.2.2. The degradation procedure is similar to the one used for bare-steel connections data. The postulated moment-rotation characteristics are shown in Figs. 5.9 and 5.10 for Groups 4 and 5 connections, together with experimental results for comparison. It can be seen that the initial stiffness is well predicted, whereas the analytical method overestimates the capacity of the connection a little, especially at intermediate temperatures. This may be attributable to the failure of the composite slab before the actual failure of the connection causing the capacity to degrade at faster rates.

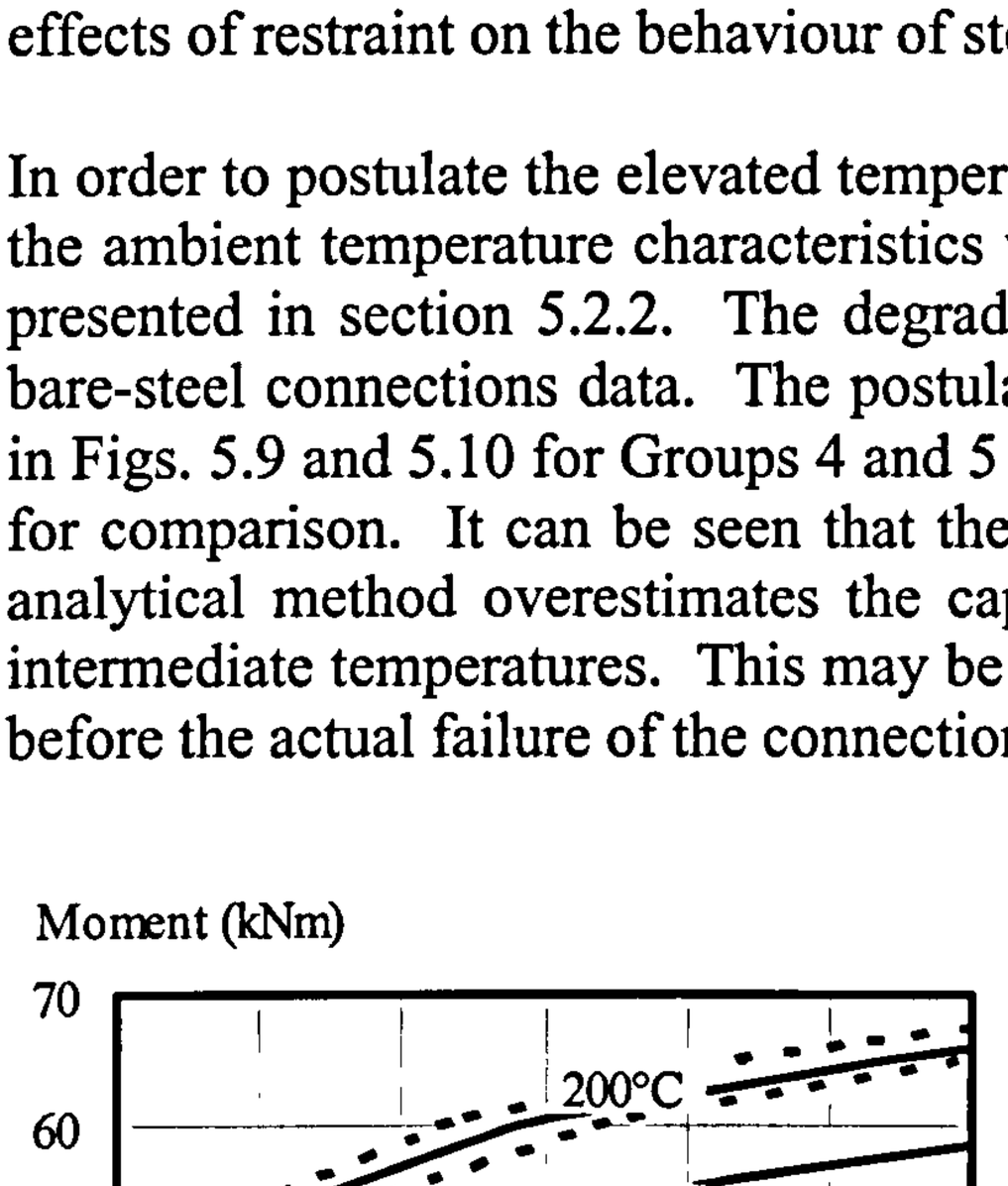

Figure 5.9: Comparison between Experimental and Postulated Elevated Temperature Response for Group 4 (Stage 1)

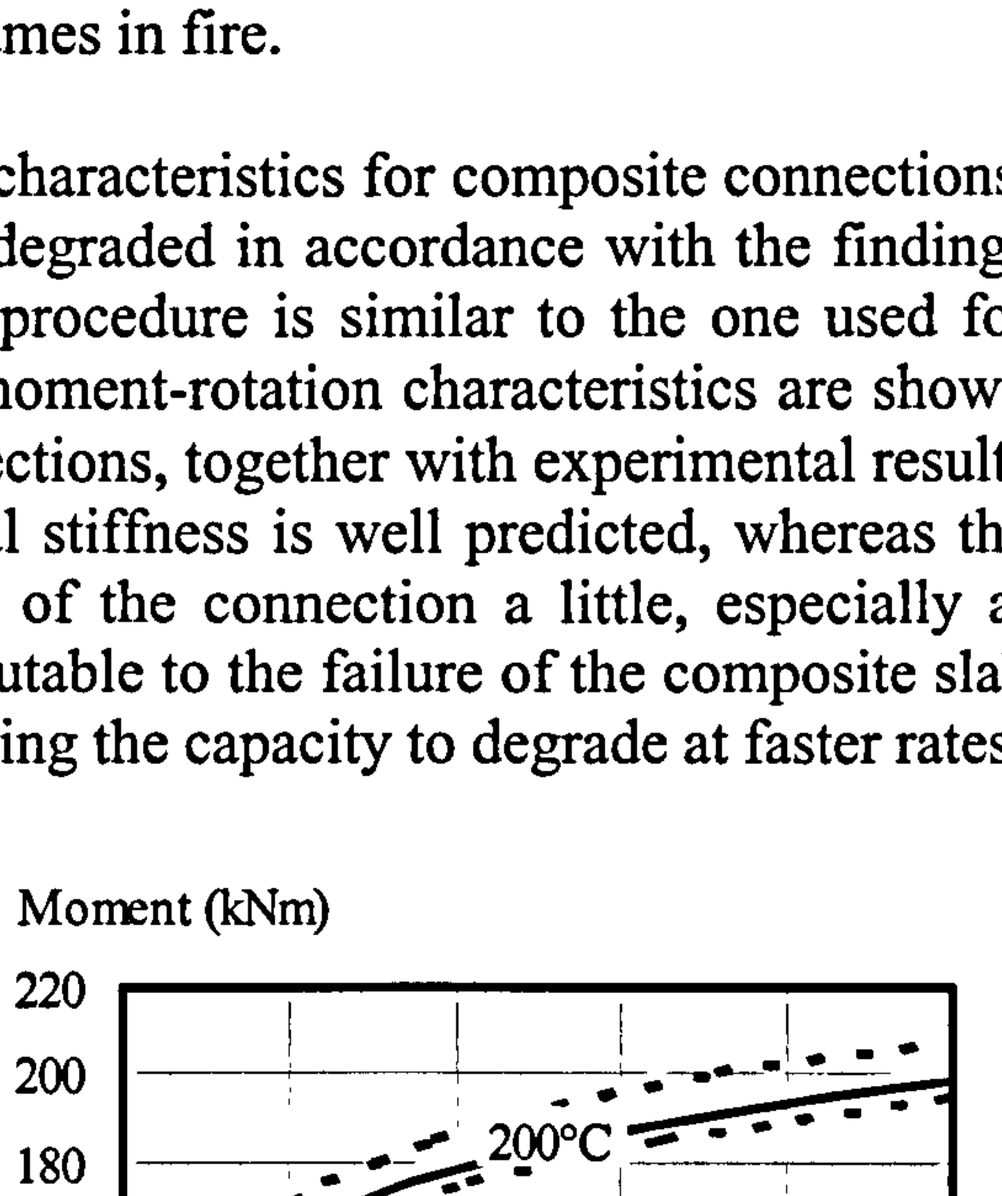

Figure 5.10: Comparison between Experimental and Postulated Elevated Temperature Response for Group 5

It is well accepted that, in fire conditions, the structure is allowed to undergo levels of deformation significantly higher than those normally occurring at ambient temperatures. Previous studies[52] have demonstrated that the overall frame response is not highly sensitive to the rate of degradation of connection characteristics. The proposed approach seems to represent to an acceptable degree of accuracy the elevated

temperature characteristics of the connection based on ambient temperature data. This will have a beneficial value in using the existing ambient temperature connection data for elevated temperature analyses and will facilitate the development of simple numerical models dealing with connection behaviour in fire.

5.6 FINITE ELEMENT MODELLING OF THE CONNECTION RESPONSE

A number of analytical models have been developed to predict the connection response in both normal conditions or in fire. The use of such models depends on the ability to approximate and model the actual response of the main components of the connection that have significant influence on the response. Depending on their applicability and ability to establish accurately the connection response, various forms of connection modelling have been developed ranging from simplified analytical models to more sophisticated finite element analysis. The finite element technique represents, in principle, a powerful tool capable of accurately predicting connection response. The use of finite element modelling for studying the connection behaviour started in the early 1970's, as the application of computers in solving structural problems became evident.

Bose *et. al.*[126] made the first attempt to investigate the connection response making use of finite element analysis in studying the behaviour of welded beam-to-column connections. Three factors affecting the connection response: strain hardening, buckling and material plasticity were considered in the analysis. The results compared closely with the available experimental data. Patel and Chen[127] also studied welded connections where the beam was either fully welded to the column or partially welded at the flange. The connection was treated as a two-dimensional problem. The whole connection was analysed using the general purpose program NONSAP developed by Bathe *et al.*[128] using plane stress isoparametric elements. A satisfactory correlation was observed with experimental results. Three-dimensional finite element analyses were conducted by Atamiaz and Frey[129] on unstiffened welded connections using shell elements. The good agreement between the experimental data and numerical results indicated the efficiency of the finite element techniques in predicting accurately the behaviour of welded beam-to-column connections.

In order to study the behaviour of bolted end-plate connections Krishnamurthy[130,131,132] developed a finite element methodology for the analysis of splice-plate connections. A moment-rotation relationship was proposed based on analyses of a large number geometric configurations of connections. Lipson and Hague[133] developed a finite element model with the primary aim of improving the understanding of single angle connections welded to the column flange and bolted to the beam web. Richard *et al.*[134] conducted finite element analyses on single web plate connections with the capability of the model to simulate the full connection arrangement as well as part of the beam. An inelastic finite element was developed to account for the bolt response based on a statistical evaluation of tests on single bolts. Also, Richard *et al.*[135] developed a finite element model to predict the response of double web cleat connections. A good agreement was observed with experimental data. Krishnamurthy[136] developed a sophisticated finite element model that takes into account the bolt pre-loading and considers the support of the end-plate as rigid. The close correlation between the numerical results and experimental data demonstrated the importance of including the

bolt heads and welds in the numerical models in order to define accurately the connection response. Based on the work conducted by Krishnamurthy *et al.*[132], Murray and Kukreti[137] studied the behaviour of flush end-plate connection and eight types of extended end-plate arrangement.

General purpose finite element models have recently been developed by various software companies that have the capability to model the behaviour of connections. LAGAMINE and ABAQUS finite element codes were used by Bursi and Leonelli[138] to model bolted end-plate connections with three-dimensional elements. A simplified tee-stub connection was introduced to study the influence of bolts on the overall connection response. Sherbourne and Bahaari[139] developed a finite element methodology to investigate the behaviour of bolted connections using ANSYS code for equivalent three-dimensional analysis. The model generated a satisfactory prediction. The ADINA code was used thoroughly by Choi and Chung[140] to model extended end-plate connections with and without stiffened compression zone. The effect of bolts pre-tensioning and the shapes of the bolt shank, head and nut were taken into consideration in the modelling. The comparison of moment-rotation relationships obtained from the model with the experimental results revealed that the proposed model can properly simulate the actual behaviour of the end-plate connection. Recently, Troup *et al.*[141] used the finite element program ANSYS to create a numerical model of a tee-stub and an extended end-plate connection. Simplified bi-linear stress-strain curves for the steel sections and bolt shank were adopted. Material non-linearity has been considered for steel members and connecting components, together with geometric non-linearity due to the changing area of contact between the faces of the end-plate or tee-stubs. An encouraging correlation between the model and test was observed, with a good comparison of the stiffness in both thick and thin plate conditions.

Despite the complexities associated with modelling composite connections a similar approach may be adopted as for bare-steel connections. Early attempts to use the finite element models in studying the behaviour of composite connections were undertaken by Leon and Lin[142] and Leon *et al.*[143] on composite flange and web cleats using ADINA. In order to simplify the modelling procedure, the cleat angles used for the web and flange were analysed separately to provide load deformation characteristics. The interface between the beam and the slab as well as the influence of shear stud deformation were not considered in the model. Comparison with experimental data suggested that the model needs refinement. Puhali *et al.*[144] used the non-linear finite element package ABAQUS to present a finite element model for composite connections. The steel beam and the composite slab were simulated using beam type element whereas the shear connector flexibility was modelled using non-linear spring elements. The column was not included in the modelling, but restraint conditions were introduced to the composite beam to represent the deformation of column flange. The good agreement between the numerical results and experimental data demonstrated the ability of the model to model accurately the connection response.

Davison *et al.*[27] performed a detailed analysis on composite connections using a finite element program SERVAR which has the ability to model the non-linear connection characteristics. The results obtained from the modelling compared closely with the experimental results, with consistent failure loads being observed, despite the variation in the corresponding levels of rotation. A numerical model using ABAQUS has been developed by Ahmed and Nethercot[145] to simulate the response of flush end-plate

composite connections. The model was capable of considering both geometric and material non-linearities. Shell elements were used to model the steel beam, column and the end-plate, while a combination of shell and spring elements was selected to represent each bolt. To simplify the analysis, the concrete was ignored in the model and instead multi-point constraints were used in the stud sections. From the comparison of the rotations, strains and forces, it was found that the model can accurately predict the semi-rigid composite connection response.

Very little work has been conducted so far into modelling the behaviour of the different types of connection in fire. This is probably related to the large number of parameters which need to be considered as well as the limited number fire tests available to provide essential information on the response of connections

Recently, Liu[146,147] has developed a sophisticated three-dimensional finite element model following a similar procedure to a previously developed ambient temperature end-plate model[148] to simulate the response of various types of connection in the event of fire. The beam, column, end-plate and stiffeners were modelled using eight-noded shell elements including the consideration of the material plasticity and degradation with temperature, non-uniform thermal expansion across a section and large deflections at very high temperatures. The response of bolts and the contact 'link' between the column flange and end-plate was simulated using a beam element with special characteristics to take into account the behaviour of bolts during the course of expansion at elevated temperature. The stress-strain-temperature characteristics were adopted based on recommended values from experimental tests. "Failure" of a connection in a fire was defined when its rotation exceeds 100 milliards. The model called "FEAST" was further developed to take into consideration the analysis of composite connections[149,150]. The concrete slab was modelled using brick elements with 8 corner nodes. Concrete in compression and tension was modelled as an elastic-plastic strain hardening and softening material. The reinforcement mesh was modelled as a smeared layer with equivalent material properties, whilst one-dimensional line beam elements were adopted to simulate the response of shear studs. A close comparison was observed with experimental work. The discrepancies between the results were suggested to be partly due to limited data of temperature distribution and actual stress-strain relationships as well as the difference in the adopted material properties and those which truly existed.

Using FEAST, finite element analyses have been conducted by Liu[151] to predict the response for the bare-steel and composite connections tested by the author as described in Chapters 3 and 4. The finite element mesh was constructed in a form representing the actual shape of the connection arrangements. The connection is divided into more than 600 elements, the majority of which are concentrated at the connection zone. The modelling of the five series of tests were performed utilising the experimentally derived material properties and temperature distribution of the connection elements. The finite element analyses were subjected to a similar temperature regime to that used in the fire tests. The scenarios used in the numerical modelling were identical within the same group of tests.

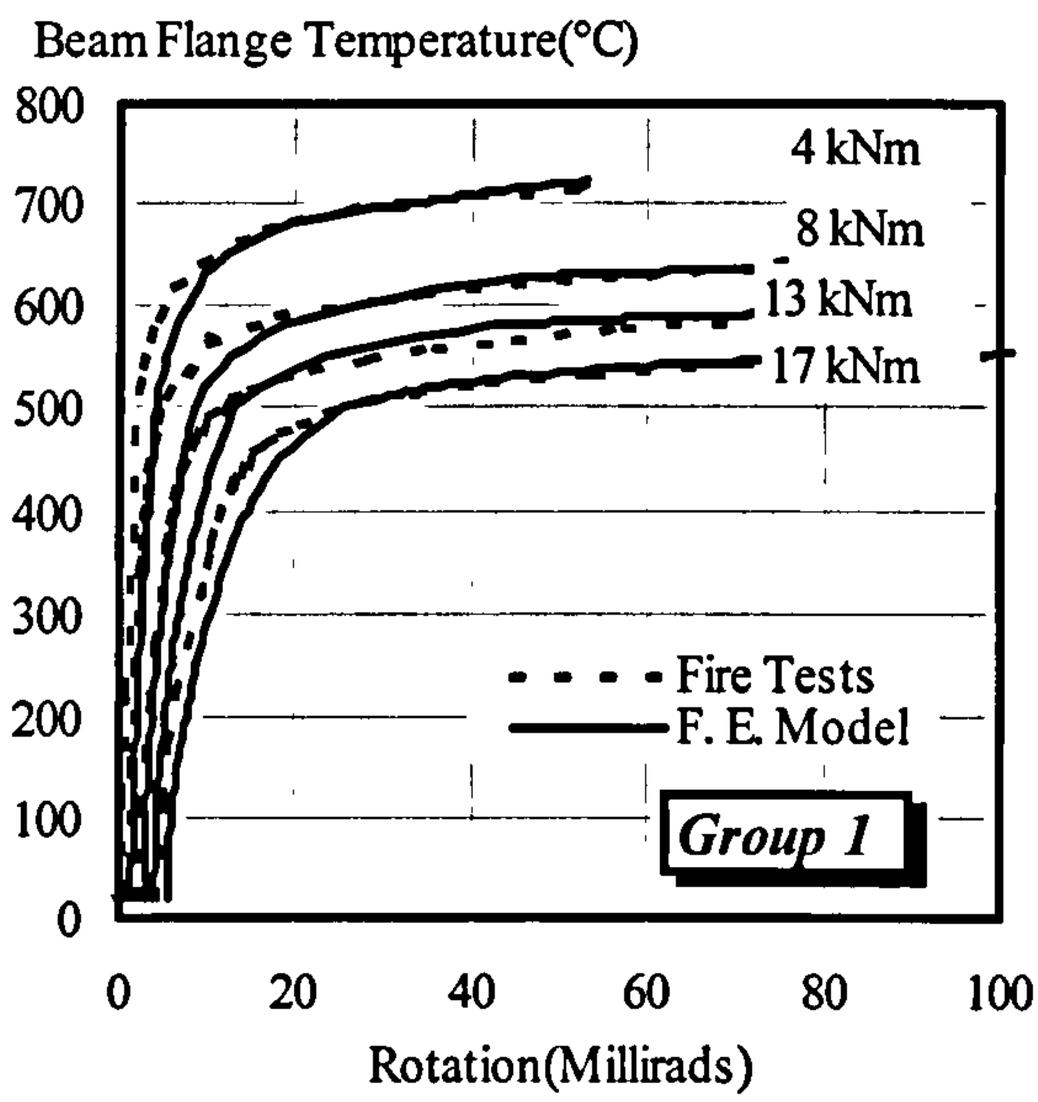

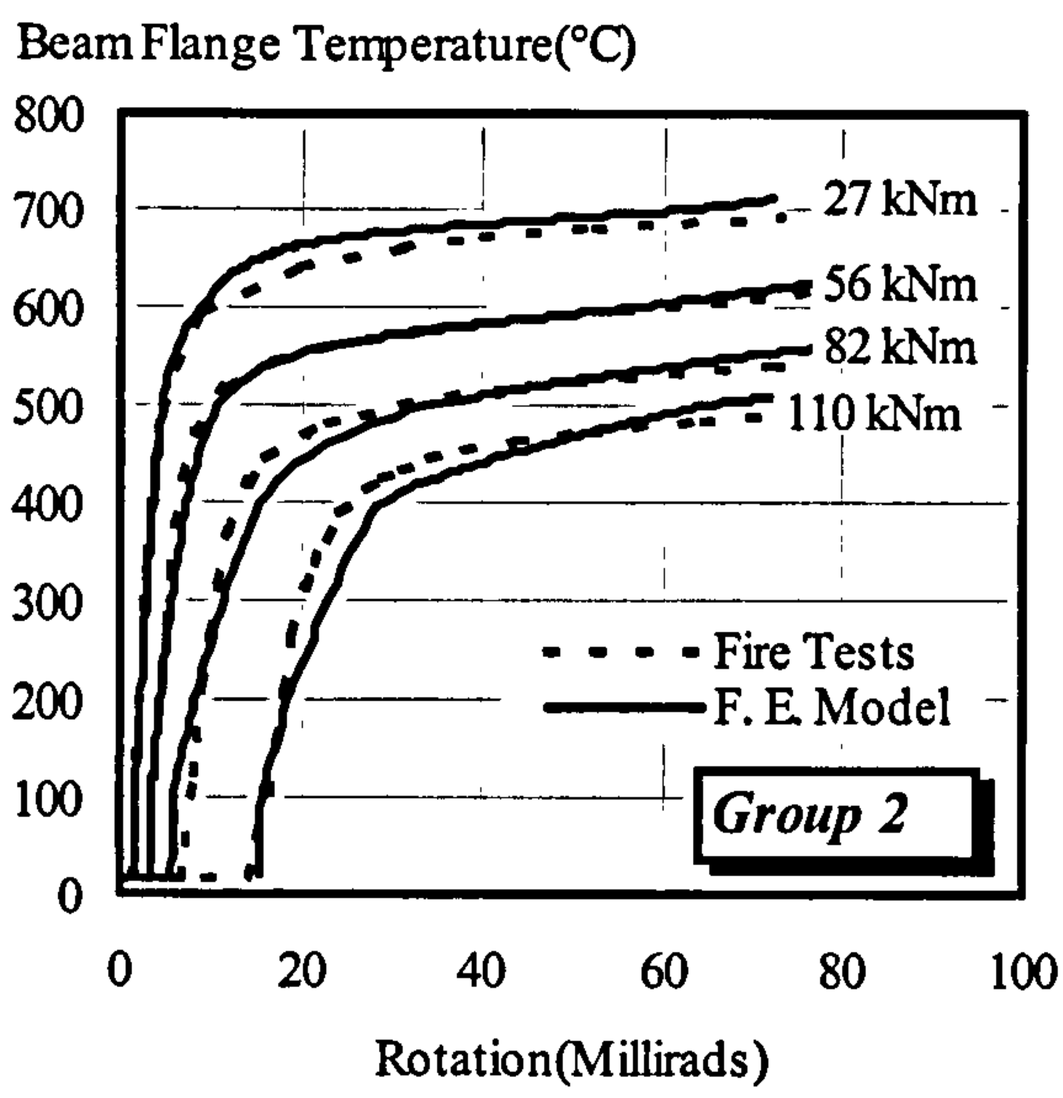

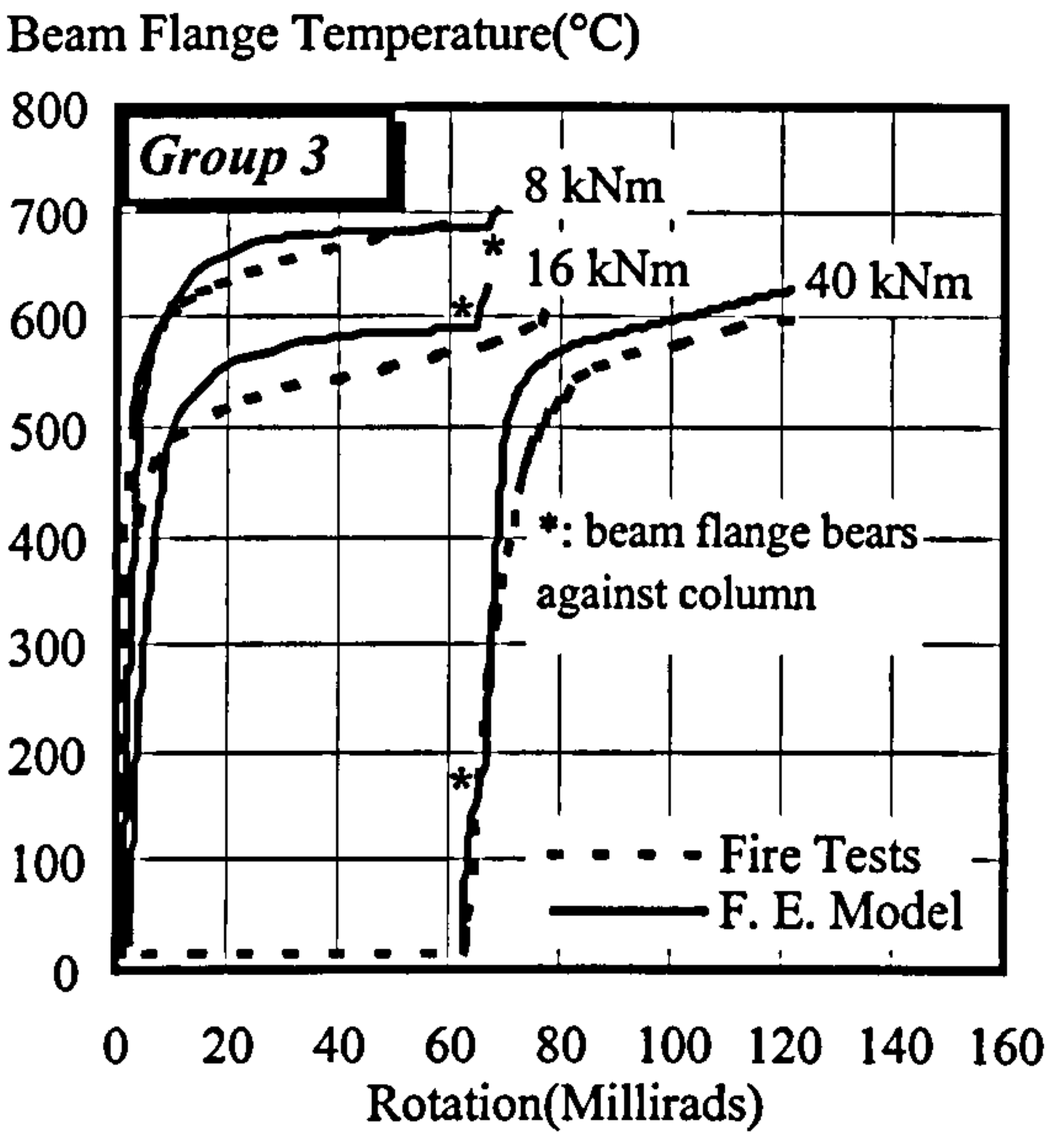

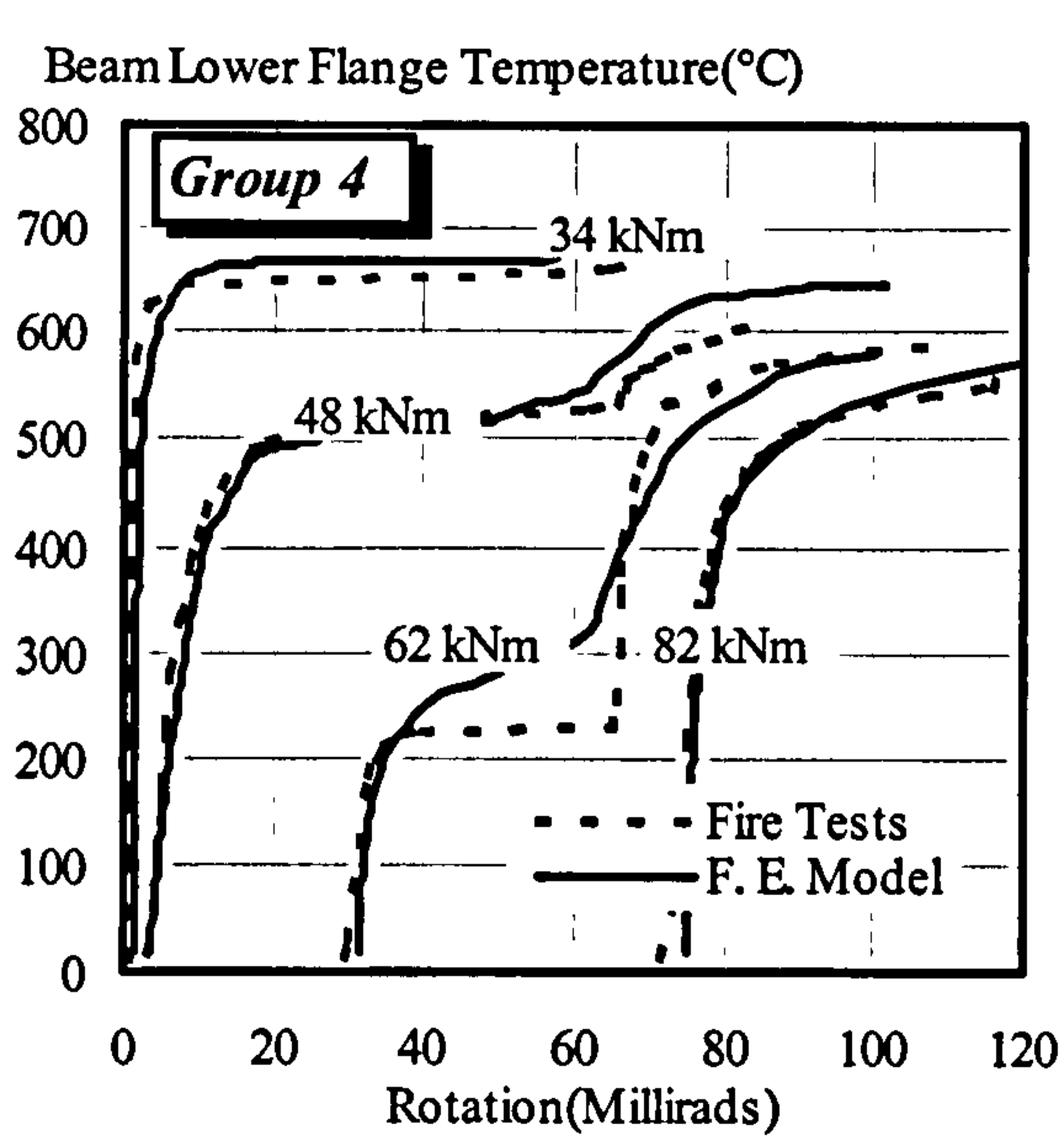

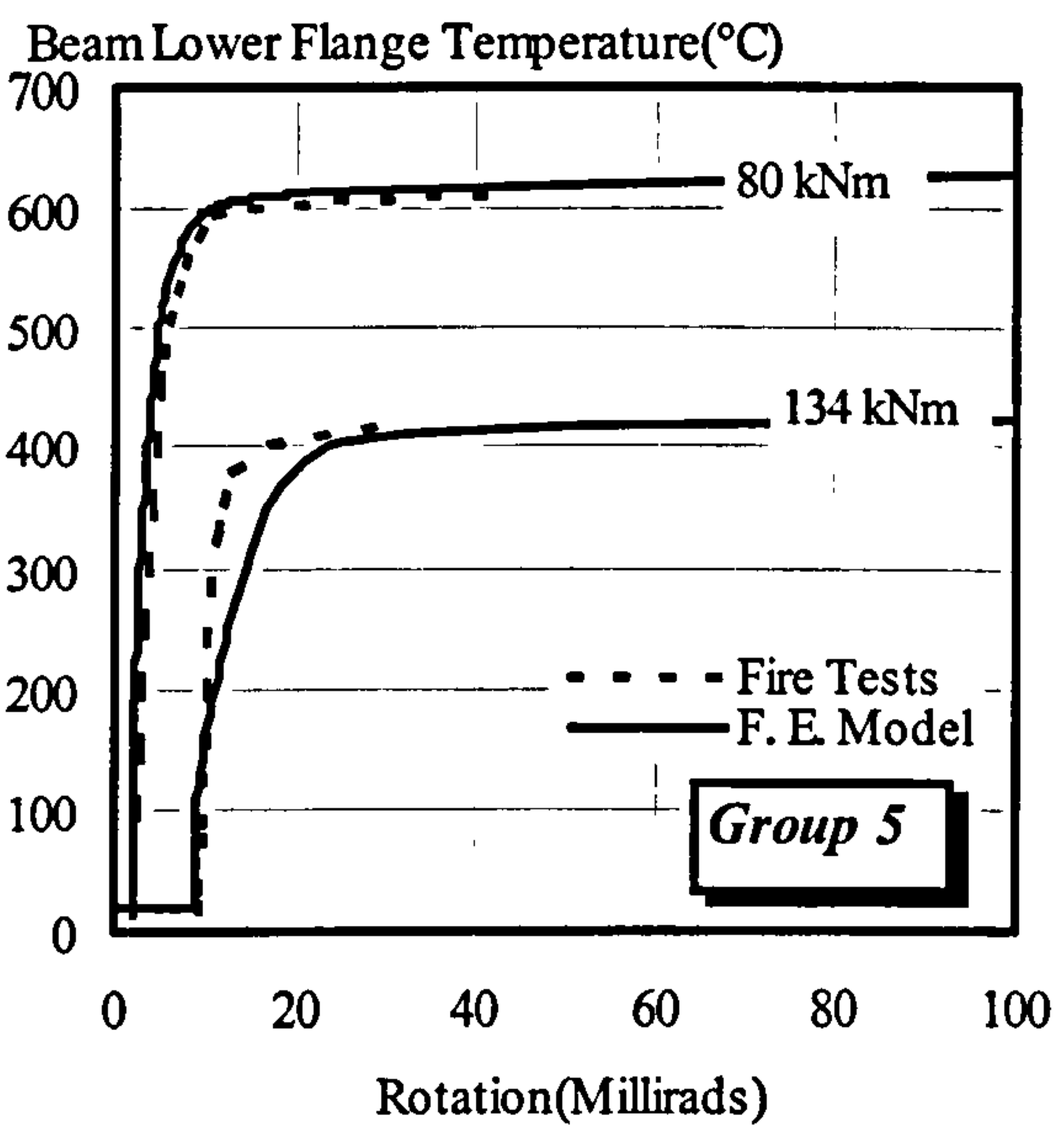

Fig. 5.11: Comparison of Finite Element Modelling of Connection Response with Experimental Results

The predicted connection response at various levels of moment within each group is compared with test results in Fig. 5.11. It may be seen that, in general, predicted response by the model compares closely with that observed from fire tests, although at very low levels of load and rotation the fire test curves showed stiffer behaviour especially in Groups 1 and 3. Also, in almost all of the tests, there was a very good agreement between the actual and predicted initial rotations at ambient temperature suggesting that the finite element model is capable of accurately simulating the ambient temperature connection response. The variations in the flange failure temperatures between the numerical modelling and the experimental results were at most 5%. In Group 3, both the experimental and numerical results revealed that the rotations at which the beam bottom flange came into contact with the column flange were about 70 millirads. The model did not account for large deformations and any fracture of the steel components, which were found to be the dominant failure modes in the fire tests. This was probably the primary cause of the discrepancy between the experimental and theoretical results at high levels of rotation in both bare-steel and composite flexible end-plate connections.

In the model it was assumed that there is a uniform temperature distribution across the slab depth and all temperatures within the concrete slab increased at a constant rate since temperature measurements inside the composite slab were not available. Despite this uncertainty, the theoretical results for Groups 4 and 5 showed a reasonably good correlation with the experimental response. The limiting temperatures were accurately predicted despite the less accurate prediction of centre of rotation. The model was not capable of accurately predicting the response for the connections with the high level of moments in Groups 4 and 5. This is due to the fact that the numerical model found it difficult to simulate the separation of the composite slab from the supporting beams as such a phenomenon is not accounted for in the model. Generally, there was a close agreement between the fire tests and numerical modelling. The slight discrepancies may be attributable to differences in the adopted and actual temperature-dependent material properties and unavailability of some of the important temperature distributions.

Recently, a three-dimensional finite element model has been developed by El-Houssieny *et al.*[152] to simulate the response of extended end-plates at both ambient and elevated temperatures. Close agreement was obtained with experimental work and subsequent parametric studies were conducted to investigate the influence of connection behaviour at normal and elevated temperatures.

5.7 CONCLUSIONS

The degradation of both connection stiffness and capacity with increasing temperatures has been investigated for both the bare-steel and composite connections tested. The connection stiffness and capacity were observed to reduce for both bare-steel and composite connections as temperature increases. For bare-steel connections, approximately similar rates of degradation of both stiffness and capacity were observed regardless of the connection type and size. It was found that the rate of degradation of stiffness follows closely the level of strain at the limit of proportionality and therefore it may be adopted to represent the degradation of stiffness with increasing temperatures.

Reasonable representations of rate of degradation of capacity were possible based on levels of strain between 0.5% and 1.0%.

Initial assessment of the degradation of the composite connection characteristics is greatly influenced by the composite slab which keeps the upper portion of the connection at lower temperatures, enhancing the moment capacity of the connection. The degradation rate is also complicated by the influence of the reinforcement which remains at relatively low temperatures compared with bare-steel section. It was found that the characteristics of the composite connection degrade at lower rates than the bare-steel. The degradation of stiffness of composite connections was found to be reasonably represented based on a level of strain of 0.5% whereas reasonable approximations of the degradation of capacity were possible on the basis of a strain level of 2.0%.

The most appropriate way to represent the connection response is to consider the form of curve-fitting expression that can represent the entire non-linear response. The Ramberg-Osgood expression has been selected to model the connection response at elevated temperature. This is defined by single equation and only three parameters are required to define satisfactorily the connection response. Furthermore, the tangent-stiffness of the connection represented by this equation is always positive and the connection characteristics are simple to degrade with increasing temperatures. The moment-rotation-temperature response for both bare-steel and composite connections tested as described in Chapters 3 and 4 have been represented using Ramberg-Osgood expressions in a form suitable for incorporation within numerical frame analysis.

The most accurate prediction of the connection behaviour can be achieved through the use of finite element forms of model which provides a powerful tool capable of considering the influence of various components such as bolt forces, contact zone, composite slab and reinforcement. As a result of the progressive developments in the information technology, a large number of finite element models currently exist, which provide an accurate prediction of the entire range of response for both bare-steel and composite connections. The results from experimental fire tests described in Chapters 3 and 4 have been compared with the predicted results obtained from the finite element model developed by Liu. The model is suitable for different types of connection and arrangement as well as being capable of representing the connection response at ambient temperature. It was found that there was an excellent agreement between the actual and predicted connection responses demonstrating the ability of the model to predict the connection behaviour at elevated temperatures. Since the finite element modelling can accurately represent the response of the connections, it offers a reliable and cost-effective alternative solution to experimental testing.

6 INFLUENCE OF CONNECTION CHARACTERISTICS ON FRAME BEHAVIOUR IN FIRE

6.1 INTRODUCTION

The primary aim of connection tests is to use the resulting connection characteristics to study their influence on frame behaviour. It is well known that, at ambient temperature but even more at elevated temperatures, a complete structure behaves better than its individual members in isolation. This is due to the considerable influence of structural continuity. Parametric studies investigating the influence of various parameters on the elevated temperature response of the beam within a sub-frame structure are reported. Analyses were performed using a finite element program developed at University of Sheffield.

The construction of the Cardington Frame Test Facility[153,154] has provided a unique opportunity for researchers to study experimentally the behaviour of a complete building structure in fire conditions. Moreover, such tests form an important source of data for validating numerical models, and will help in refining design guidelines which are largely based on isolated member tests. In view of this, one of the Cardington tests is used here as the basis for a study of the influence of connections on frame behaviour, using a three-dimensional analysis.

Despite their limitations, isolated connection tests have the advantage of simplicity and efficiency. The behaviour of connections in the Cardington frame and observations from isolated connection tests under fire conditions are compared. The similarities and differences in behaviour between the two are briefly explained.

6.2 DESCRIPTION OF THE FINITE ELEMENT PROGRAM

The basic concept of the finite element analysis is that the structural member is divided into a number of elements of finite length connected at nodal points. The displacements of the nodal points are the basic unknown parameters of the problem. Within each element a displacement function is selected which maps the nodal degree-of-freedom values to all points within the elements and could take the form of linear, quadratic or cubic polynomial function. The shape function is then used to form an element stiffness matrix. A global stiffness matrix is formed by assembling the local stiffness matrices of the elements and the boundary conditions are imposed. The displacements at each node and the stresses within each element are then determined by means of solving simultaneous equations.

Despite the availability of general purpose finite element programs that can simulate the effect of connections within structural frames at elevated temperatures, research oriented models are often preferable due to their reduced computing requirements. The parametric studies described in this chapter have been conducted using a finite element program developed by Bailey[54] at Sheffield University to model two- and three-dimensional structural frames under fire conditions. The program was based on an existing two-dimensional program INSTAF developed by El-Zanaty and Murray[155] to

investigate the response of steel frames at ambient temperature taking into account yield spreading and geometrical non-linearity. This was developed by Saab[156] to account for elevated temperature material properties. Najjar[157] extended the program to include three-dimensional behaviour of bare-steel frames in fire.

Further significant improvements in the model were made by Bailey[54,158] who introduced spring elements to model temperature-dependent connection characteristics, including unloading. He also incorporated lateral torsional buckling, continuous concrete flooring and the effects of cooling by allowing extensive strain reversal within the material's constitutive relationship[159]. More recently Haung[160] has made significant improvements to the slab model, incorporating material non-linearity within laminated flat shell elements. The model has been verified against experimental data at each development stage. The present analyses were conducted using the version of the program developed by Bailey[54] as the recent developments were not complete when these studies were conducted.

In order to represent the connection characteristics within the model, a two-noded spring element with zero length and eight degrees-of-freedom in local co-ordinates is adopted as shown in Fig. 6.1. Similar to the beam and column elements, the spring element possesses eleven degrees-of-freedom in global co-ordinates after transformation. The independent modelling of the eight degrees-of-freedom allows each to be modelled by a separately specified moment-rotation or force-displacement relationship. The spring element is very versatile and can be placed at any position within the frame since in-plane, out-of-plane, torsion, warping and translational displacements are represented.

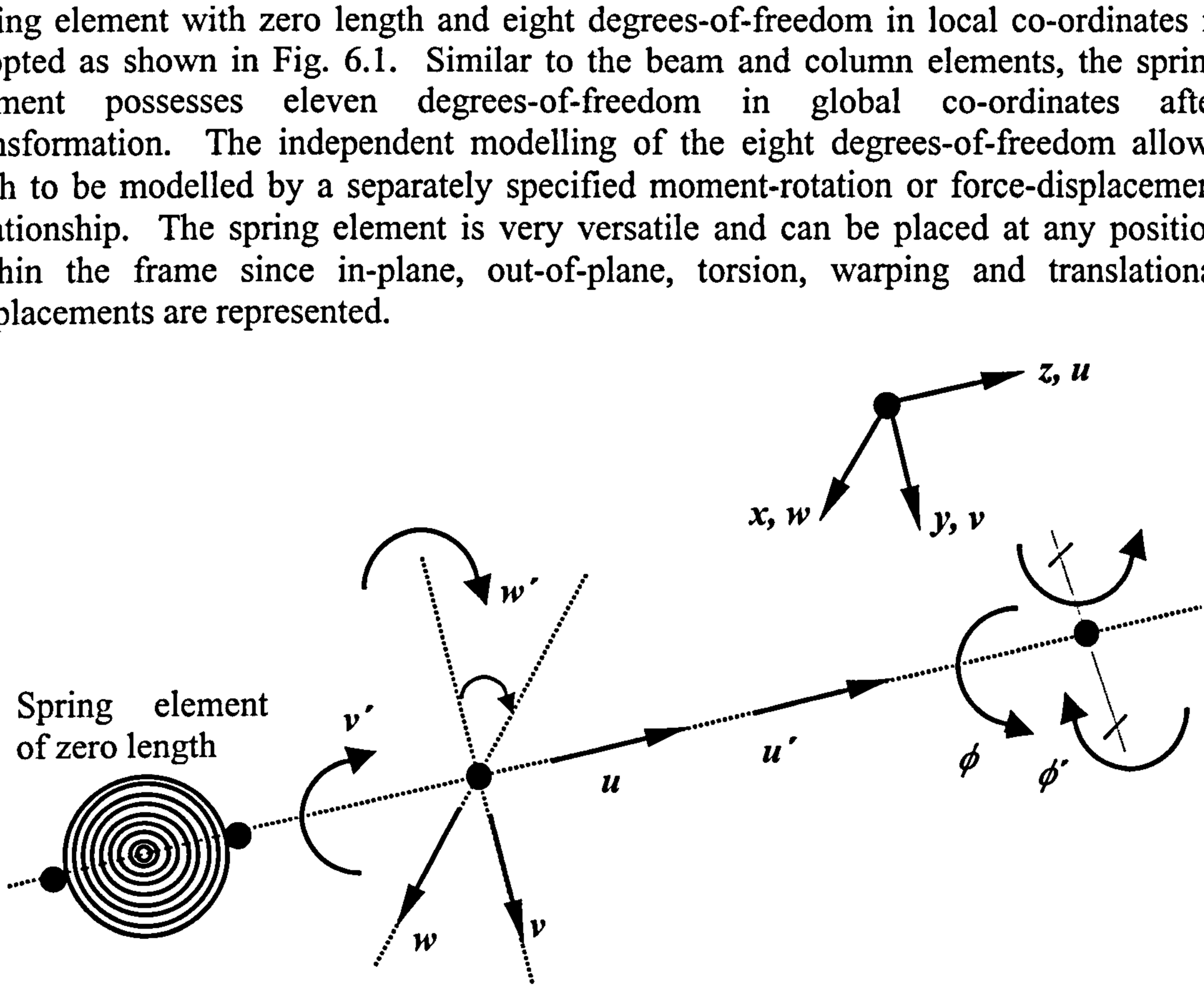

Figure 6.1: Representation of Spring Element and Degrees-of-Freedom in Local Co-ordinates

6.3 PARAMETRIC STUDIES ON SUB-FRAME ARRANGEMENT

To study the effect of connections on the behaviour of the connected structural members, it is necessary to conduct systematic parametric studies. This is only

practically possible using numerical modelling, and the finite element program described above has been used for this. Various parameters affecting the beam behaviour at elevated temperature are considered.

6.3.1 Sub-frame Layout and General Sub-frame Response

When conducting parametric studies it is very helpful to consider the analysis of a 'representative' sub-frame rather than a complete structure. Despite the fact that fairly limited sub-frames provide good predictions of structural behaviour when compared with whole-frame modelling, BS5950[39] adopted a number of sub-frame arrangements, which were suggested to be suitable for representing beam behaviour in rigidly connected frames as shown in Fig. 6.2. Analytical studies have been conducted by El-Rimawi[161] to compare the responses obtained from the aforementioned sub-frames with those obtained from the whole-frame. It was concluded that these sub-frames are capable of producing results that are reasonably comparable with those from the full-frame under fire conditions using a fraction of the computing effort required. Further extensive parametric studies have been conducted[52,54] using similar sub-frame arrangements to investigate the influence of connection characteristics on beam performance at elevated temperatures using either experimental or postulated moment-rotation characteristics.

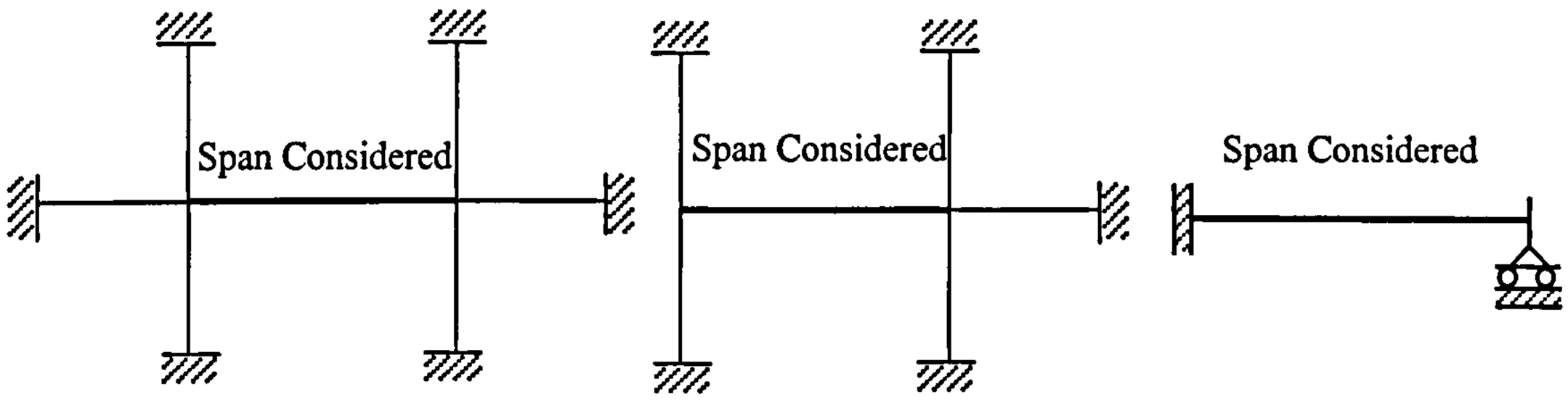

Sub-frame 1(middle beam) *Sub-frame 2(outer beam)* *Isolated beam*

Figure 6.2: Sub-Frame Details Considered in BS 5950 and Isolated Beam Arrangement

The same sub-frame layout has been adopted in the present studies in order to investigate the influence of various parameters on the behaviour of the frame with increasing temperatures. A similar arrangement was used corresponding with the member sizes utilised in the connection fire tests as detailed in Chapters 3 and 4. The Ramberg-Osgood curve-fitting equation described in Chapter 5 was incorporated to represent the moment-rotation characteristics of the bare-steel and composite beam-to-column connections at elevated temperatures, although different forms of curve-fitting expressions are possible. The general sub-frame arrangement and temperature distribution adopted are illustrated in Fig. 6.3.

The sub-frame with a middle beam was selected to study the influence of the connection characteristics on frame response, along with the isolated member arrangement for comparison. Analysis was performed using the recorded material properties of the

members obtained from connection tests as detailed in Appendix A. Restraint conditions at the end beams were modified to allow lateral movement, while columns were allowed to expand vertically. The beams were uniformly loaded with a load ratio of 0.6. An axial load was applied to the column which together with the reactions from the beam generated a load ratio of 0.4 (load ratio is as defined in BS5950: Part 1[39]). The lengths of the primary and secondary beams were 4.5m and 2.25m respectively, whilst the column length was 6.0m.

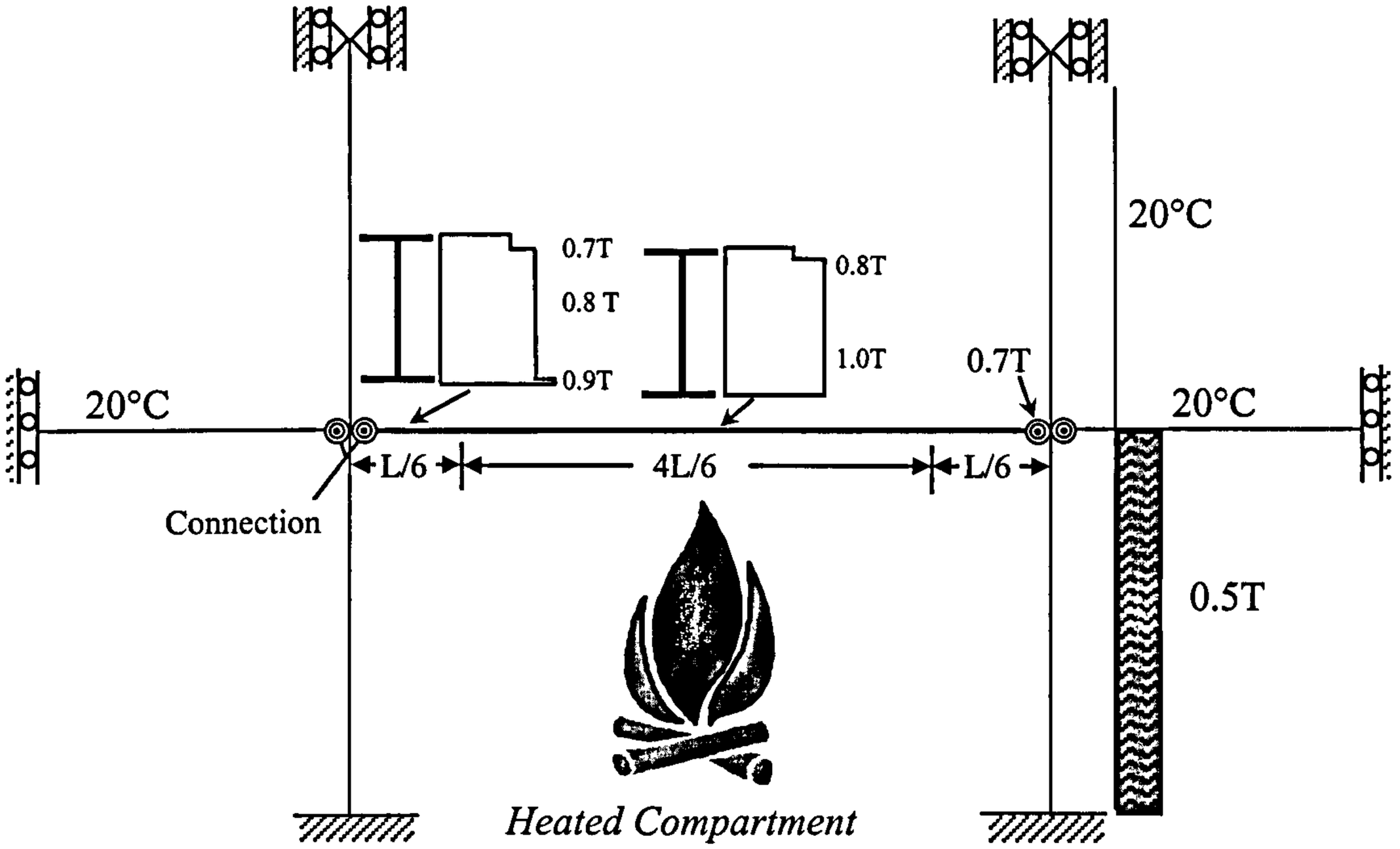

Figure 6.3: Sub-Frame Arrangement and Temperature profile used in the Fire Zone

Heating regimes adopted in the analysis are illustrated in Fig. 6.3. The connected beams and their connections outside the fire zone were assumed to remain at 20°C, along with the upper columns. To resemble an actual situation where the supporting columns are usually fire protected, they were assumed to be exposed to a reduced rate of heating corresponding to 50% of the beam bottom flange temperature, *T*. The temperature of the connections in the heated compartment was assumed to be 70% of the beam bottom flange temperature as suggested by Lawson[48]. This contrasts with the more uniform temperature distribution observed from fire tests on isolated connections as described in Chapter 3 and observed by Leston-Jones[52]. The influence of connection temperature is dealt with in more detail later in this Chapter. Based on experimental observations[52], the beam was exposed to a temperature profile similar to that illustrated in Fig. 6.3.

The influence of the composite slab on beam behaviour is investigated by considering a 130mm deep profiled slab consistent with the test arrangement. Only the top 70mm of the slab was considered in the analysis representing the continuous thickness of concrete above the steel deck. In the frame analysis the slab elements above beam-to-column connections are reduced to 6mm thick which corresponds to the thickness of the mesh in the slab. The effective width of the composite slab adopted in the two-dimensional analyses was one sixth of the span. The material properties of the concrete,

and reinforcement used in the analysis are those obtained from tensile and compressive material tests as shown in Appendix A. A thermal expansion coefficient of 14.0×10^{-6} /°C and Poisson's ratio of 0.2 is used for concrete. The temperature of the composite slab is assumed to be 20% of the hottest part of the steel. If the slab is in hogging the maximum tensile stress is defined as 10% of the maximum compressive strength. If this is exceeded then all concrete in tension is ignored.

The term 'failure temperature' used in the subsequent parametric studies is assumed to be the temperature at which the central deflection of the beam reaches a limiting deflection of span/20 as recommended by BS 476: Part 21[65]. It should be noted that a limiting temperature of 950°C is imposed by the program due to the lack of material data beyond this. It should be recognised that the concept of 'failure temperature' adopted as a basis for comparing performance. However, in actual fire conditions this is not necessarily compared to true failure.

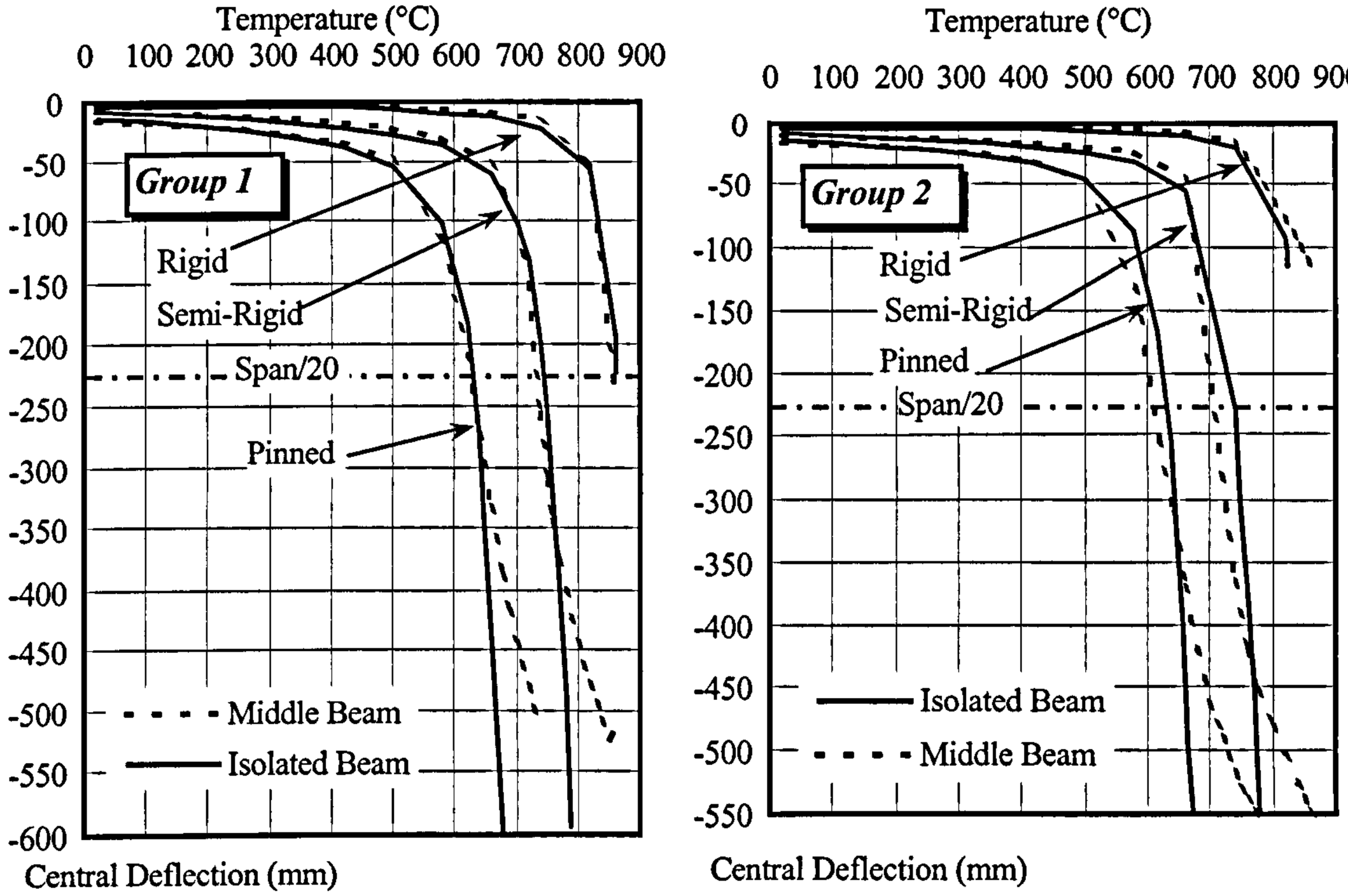

Figure 6.4: Sub-Frame Response Resulted from Incorporating Bare-Steel Flush End-Plate Connections Characteristics

The sub-frame response is shown in Figs. 6.4 and 6.5 for flush and flexible bare-steel connections respectively, along with the idealisation of the connection characteristics as 'fully' rigid and 'perfectly' pinned. The sub-frame response is also compared with that obtained for an isolated beam with no axial restraint. The connection characteristics obtained from the elevated temperature composite connection tests as detailed in Chapter 4 were also incorporated in the model in order to investigate the performance of composite frame in fire. The study described above was repeated for nominally identical arrangements but with the incorporation of a composite slab. Results for an isolated beam and the middle beam within the sub-frame are shown in Fig. 6.6, using

the connection characteristics obtained from Group 4 and 5 tests. The results for rigid and pinned connections are also shown for comparison.

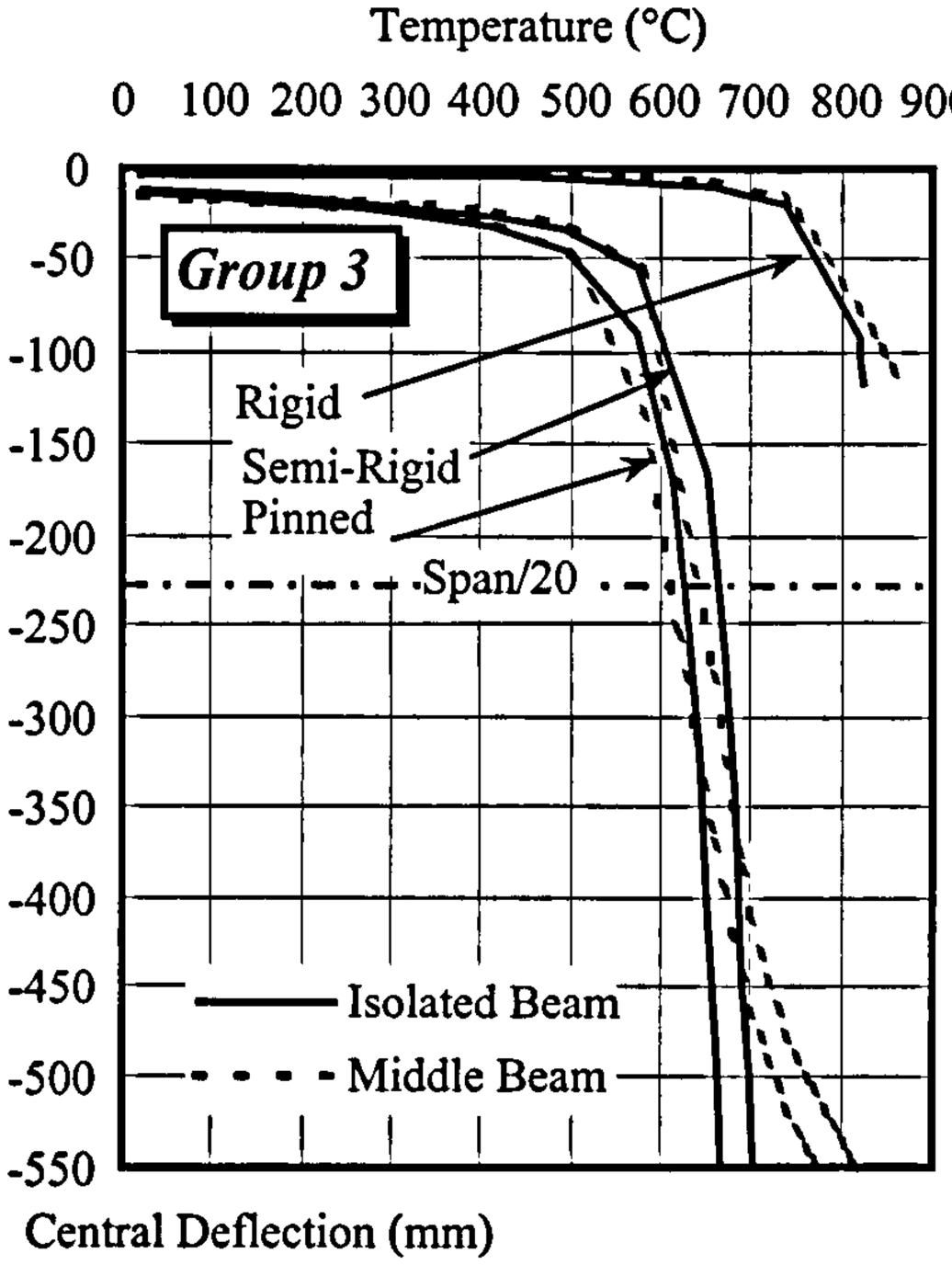

Figure 6.5: Sub-Frame Response Resulted from Incorporating Bare-Steel Flexible End-Plate Connection Characteristics

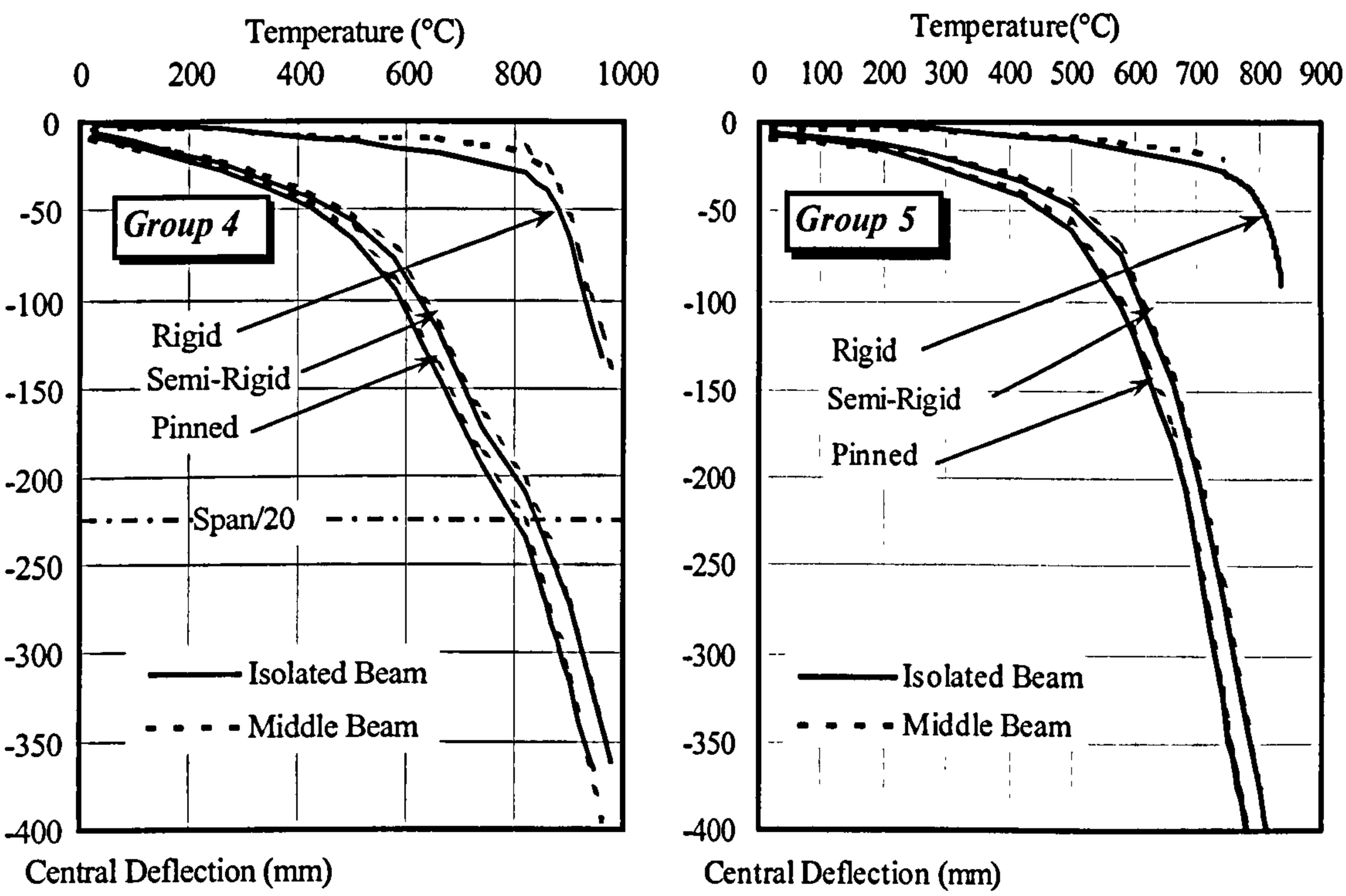

Figure 6.6: Sub-Frame Response Resulted from Incorporating Flexible End-Plate Composite Connection Characteristics

It can be seen that the central deflections for the sub-frame in most cases are consistently less than for the isolated beam due to the structural continuity which provides some degree of restraint. This difference is small for temperatures up to 650°C and 750°C for pinned and semi-rigid connections respectively. At higher temperatures the isolated beam continues to deflect rapidly, whereas the rate of deflection of the beam within the sub-frame arrangement eases a little. The influence of various parameters on the performance of the beam at elevated temperature is described in the following sections.

6.3.2 Influence of Connection Type

Several types of connection are used in multi-storey steel-framed structures. The considerations when selecting connection type are economy, ease of fabrication and speed of erection. Bolted end-plate connections: extended, flush and flexible are very common. Extended end-plates, which are usually classified as "rigid", are often used in portal frames. Flush and flexible end-plates are widely utilised in single and multi-storey buildings where connection simplicity leads to economy.

In order to study the influence of connection type, the beam response with both flush and flexible connections as shown in Figs. 6.4 (Group 2) and 6.5 (Group 3) respectively is compared, together with the 'failure temperature' of the beam corresponding to the type of connection used. This comparison is illustrated in Fig. 6.7.

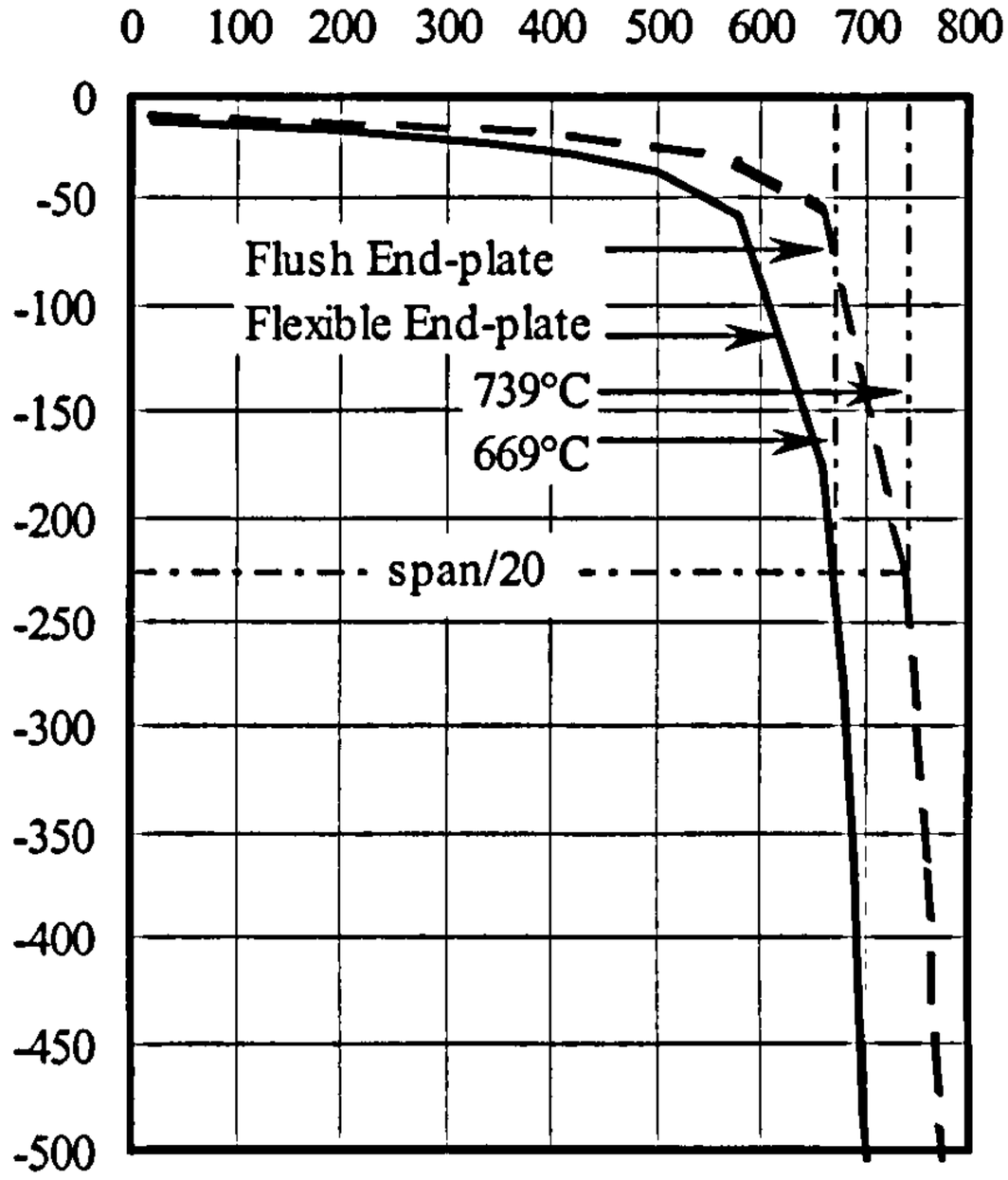

Figure 6.7: Influence of Connection Type on Beam Response with Increasing Temperatures

It may be seen from Figs. 6.4 and 6.5 that the central deflections of the beam gradually increase up to temperatures of approximately 720°C and 450°C for both rigid and pinned connections respectively. Further increase in temperature causes a progressive increase in the deflection rate until the onset of failure at temperatures of 850°C and 650°C respectively. The failure temperature of the beam with rigid connections is nearly 200°C higher than that for the pin-ended beam. The incorporation of semi-rigid connection characteristics representing a flush end-plate, results in an intermediate response between these extremes with a significant reduction in the beam deflections compared with pinned ends. However, the incorporation of flexible end-plate characteristic results in frame response comparable with that for a 'pinned' connection. Also it may be seen from Fig. 6.7 that as expected the central deflection of the beam with flexible end-plates is consistently higher than for the beam with flush end-plates. This is because flexible end-plates are possessing negligible degree of end-restraint

allowing little redistribution of forces at high temperatures, with the capacity being 10-20% of that for the beam. In contrast flush end-plates provide a high degree of restraint, with the capacity up to 75% of that for the beam. This considerably reduces the central deflection and hence enhances the performance of the beam in fire. As can be seen from Fig. 6.7 that there is an increase in the beam failure temperature of about 70°C when using flush end-plate. It is apparent that as the rigidity of the connection increases, the survival time of the structure increases and the beam mid-span deflections decrease.

6.3.3 Influence of Composite Slab

Results of the elevated temperature composite beam response are shown in Fig. 6.6, using the connection characteristics obtained from Group 4 and 5 tests. It may be seen that deflections remain small for rigid connections up to temperatures of approximately 900°C and 800°C for Group 4 and 5 test arrangements respectively. This is followed by a rapid increase in the central deflections. When compared with bare-steel connections, the presence of the composite slab causes a reduction in beam deflection and increases the failure temperatures. When the experimental connection characteristics are used in the sub-frame analysis the failure temperature corresponding to a deflection of span/20 are approximately 720°C and 845°C for Groups 5 and 4 respectively. This difference in the failure temperatures despite the same load ratio (i.e. 0.6) is perhaps due to the greater ductility of the Group 4 connection. Also, it can be seen that the composite beam response with flexible end-plate connections is only slightly better than the 'pinned'.

In order to study the influence of the composite slab on the beam performance at elevated temperature, the beam response with composite arrangement shown in Fig. 6.6 (Group 4) is compared with that with bare-steel arrangement as presented in Fig. 6.5. For temperatures up to 600°C there is a small difference between the deflection of the two beams. However for temperatures above 600°C the deflection rate for the bare-steel beam accelerates. The failure temperature corresponding to a deflection of 225mm is approximately 640°C and 845°C for the bare-steel and composite cases respectively. This represents a considerable improvement for the composite beam, demonstrating the significance of the composite slab in enhancing the performance of the beam at elevated temperatures.

6.3.4 Influence of End-Plate Thickness

To study the effect of end-plate thickness on the beam behaviour, two analyses were conducted with end-plate thickness of 8mm and 12mm. The sub-frame arrangement used was similar to the one adopted in Group 1 fire testing (i.e. 254x122UB22 and 152x152UC23). For the connection with 12mm end-plate thickness, the moment-rotation-temperature relationship derived by Leston-Jones[52] was used. The resulting response is shown in Fig. 6.8. Despite the variation in the end-plate thickness, there was negligible variation in the central deflection of the beam for temperatures up to 730°C, beyond which the deflection of the beam connected with 8mm end-plate thickness is slightly greater. This is consistent with end-plate thickness was observed to have little effect in the rate of degradation of stiffness and capacity with increasing

temperatures.

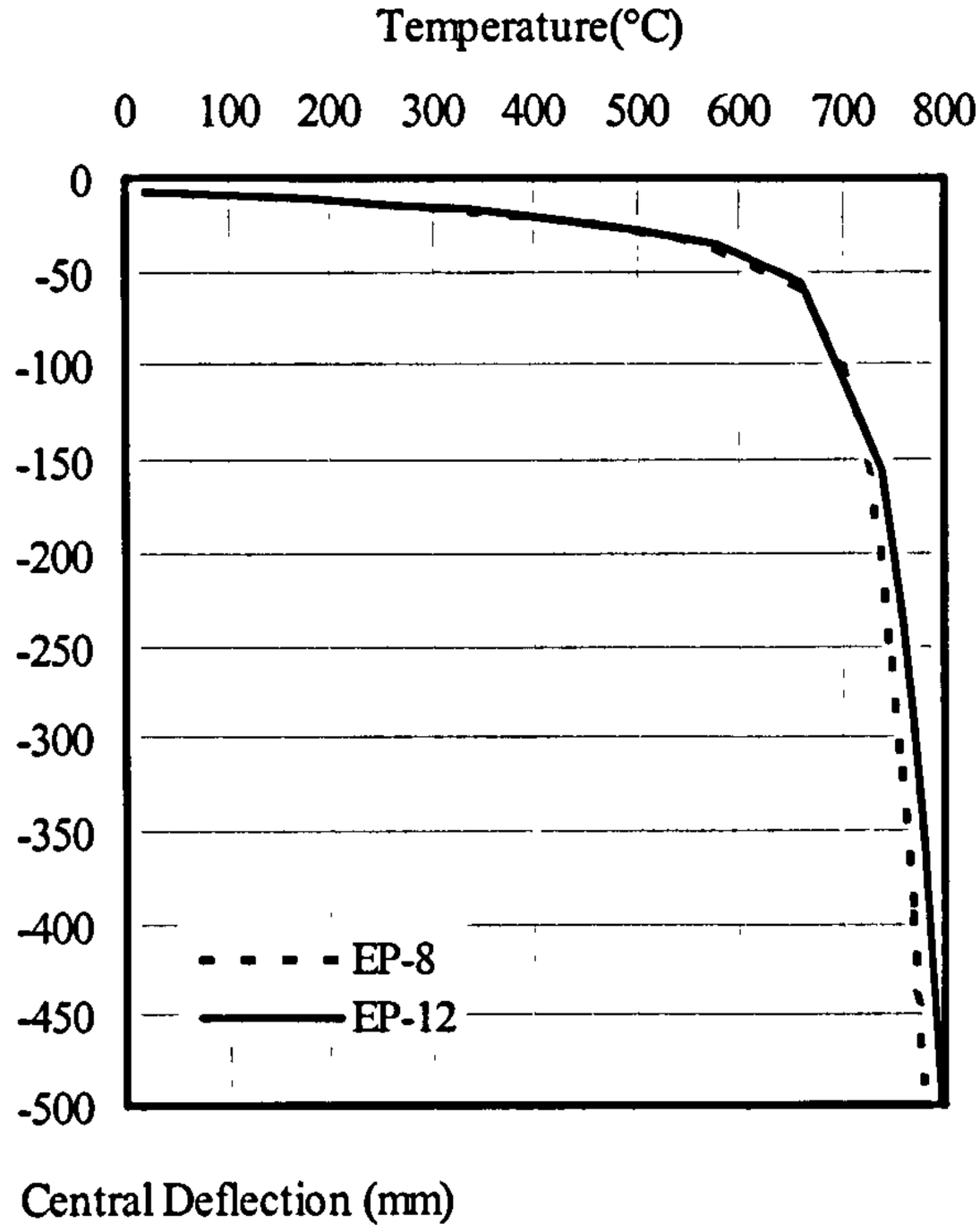

Figure 6.8: Influence of Connection Thickness on Beam Response with Increasing Temperatures

6.3.5 Influence of Concrete Strength

In composite construction, concrete strength is usually less than 50 N/mm^2. However, due to the natural variability of the constituent materials, significantly higher strengths are often achieved[162]. Therefore, analyses were conducted to study the effect of concrete compressive strength on the beam behaviour. The sub-frame members was selected to be typical those used in group 2 connection testing assuming semi-rigid connection characteristics.

The concrete strengths considered ranged between very low (5N/mm^2) to high (105N/mm^2), and the corresponding beam deflections with increasing temperatures are shown in Fig. 6.9. For (steel) temperatures up to 800°C, concrete strength has little effect. At this point the concrete is assumed to have reached a temperature of approximately 160°C and is still retaining most of its strength and stiffness. For temperatures in excess of 800°C, there is an abrupt increase in the beam deflections with increasing temperatures. This is probably attributable to cracking of the concrete resulting in a sudden reduction in capacity of the section and thus increasing the beam deflection. The central deflection of the beam with low concrete strengths is greater than for higher strength concrete although the difference is small.

Table 6.1 shows the failure temperature of the beam (based on a limiting deflection of span/20) for various concrete strengths. As the concrete strength increases, the failure

temperature of the beam also increases. However the difference is only about 62°C for concrete strengths of 5N/mm^2 and 95N/mm^2. It is apparent that concrete strength has some influence on the performance of composite beams at elevated temperature, although for practical purposes this is negligible.

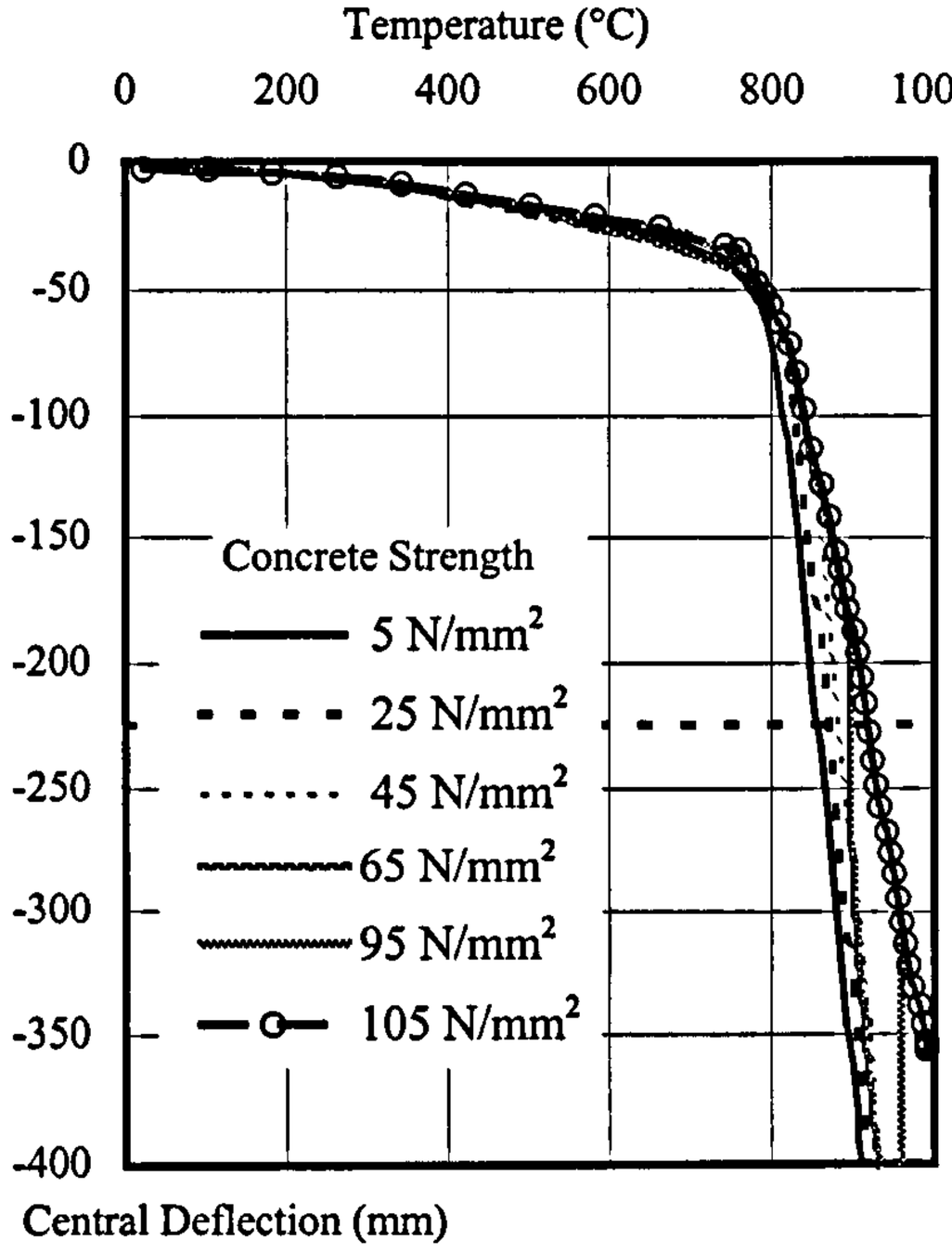

Figure 6.9: Influence of Concrete Strength on Beam Response with Increasing Temperatures

Table 6.1: Failure Temperature of the Beam with Increasing Concrete Strength

Strength (N/mm^2):	5	15	25	35	45	65	95	105
Failure Temperature (°C):	857	868	870	879	881	898	919	919

6.3.6 Influence of Connection Temperature

The parametric studies above assumed a connection temperature 70% of the beam bottom flange temperature as recommended by Lawson[48]. However the temperature variation observed in the present connection tests (Chapters 3 and 4) and those conducted by Leston-Jones[52] was almost uniform. This contradiction is probably due to factors such as the rate of heating, the degree of shielding and material size and thickness.

The effect of the relative temperatures of the beam and connection is shown in Fig. 6.10 for various bare-steel and composite connection details. It may be seen that for the arrangement with flush end-plates, there is negligible variation in the beam response for a connection temperature-ratio up to 0.5, beyond which there is a gradual decrease in the failure temperature with increasing temperature-ratio. Thus the temperature of the

connection has a significant effect on the beam response for flush end-plate connections. Therefore in order to improve the performance of the beam in fire it is necessary to keep the connection temperature relatively low (i.e. not exceeding half of the connected beam). This may be achieved by extending the protection provided to the column to include the connection.

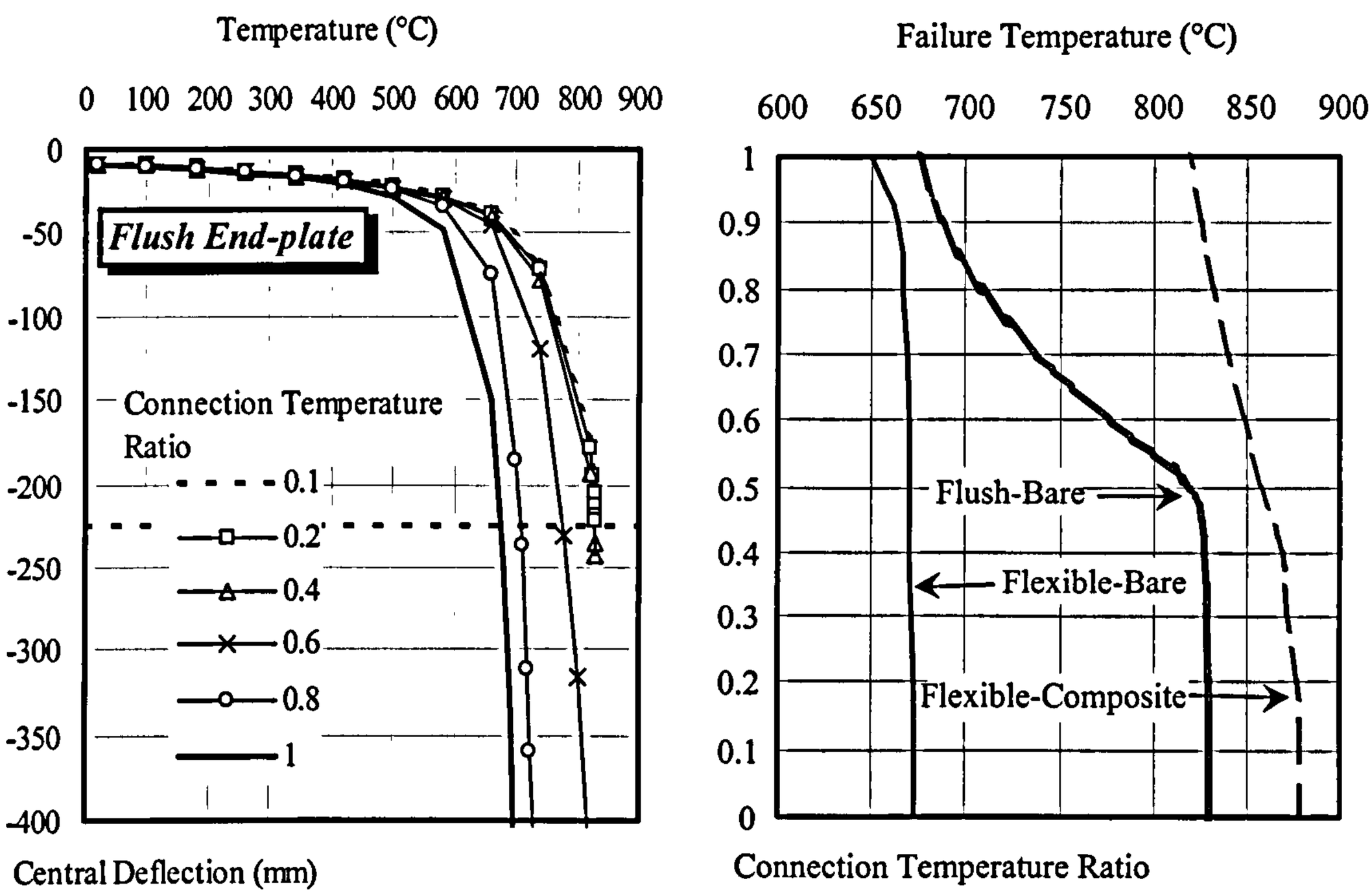

Figure 6.10: Influence of Connection Temperature on Beam Response with Different Connection Characteristics

It seems that for both bare-steel and flexible end-plate composite connections the relative temperature of the connection has little influence on the failure temperature. This is probably due the inherent nature of flexible end-plates, with relatively large rotations and low moment capacity.

6.3.7 Influence of The Applied Load-Ratio

BS5950: Part 8[19] uses the concept of load ratio defined as the applied load or moment at the time of a fire divided by the load or moment resistance at 20°C. For the parametric studies described above, a load ratio of 0.6 was generally used representing typical full service loading. In practice load levels may vary, and the following study investigates the effect of this on structural performance in fire.

Fig. 6.11 shows failure temperatures for load ratios up to 0.8, for bare-steel and composite sections with flexible connection characteristics. There is a significant decrease in the failure temperature as the load ratio increases for both bare-steel and composite cases. At a very low load ratio of 0.1, failure temperatures exceed 950°C. For the composite arrangement there is no change in the failure temperature up to a load ratio approaching 0.25, beyond which it progressively reduces. For the bare-steel

section, the applied load-ratio has almost a linear effect on the overall failure-temperature. This decrease in failure temperature with increasing load ratio is due to the fact that the connections undergo considerable rotations resulting in a significant increase in deformation of the beam and consequently reducing the failure temperature.

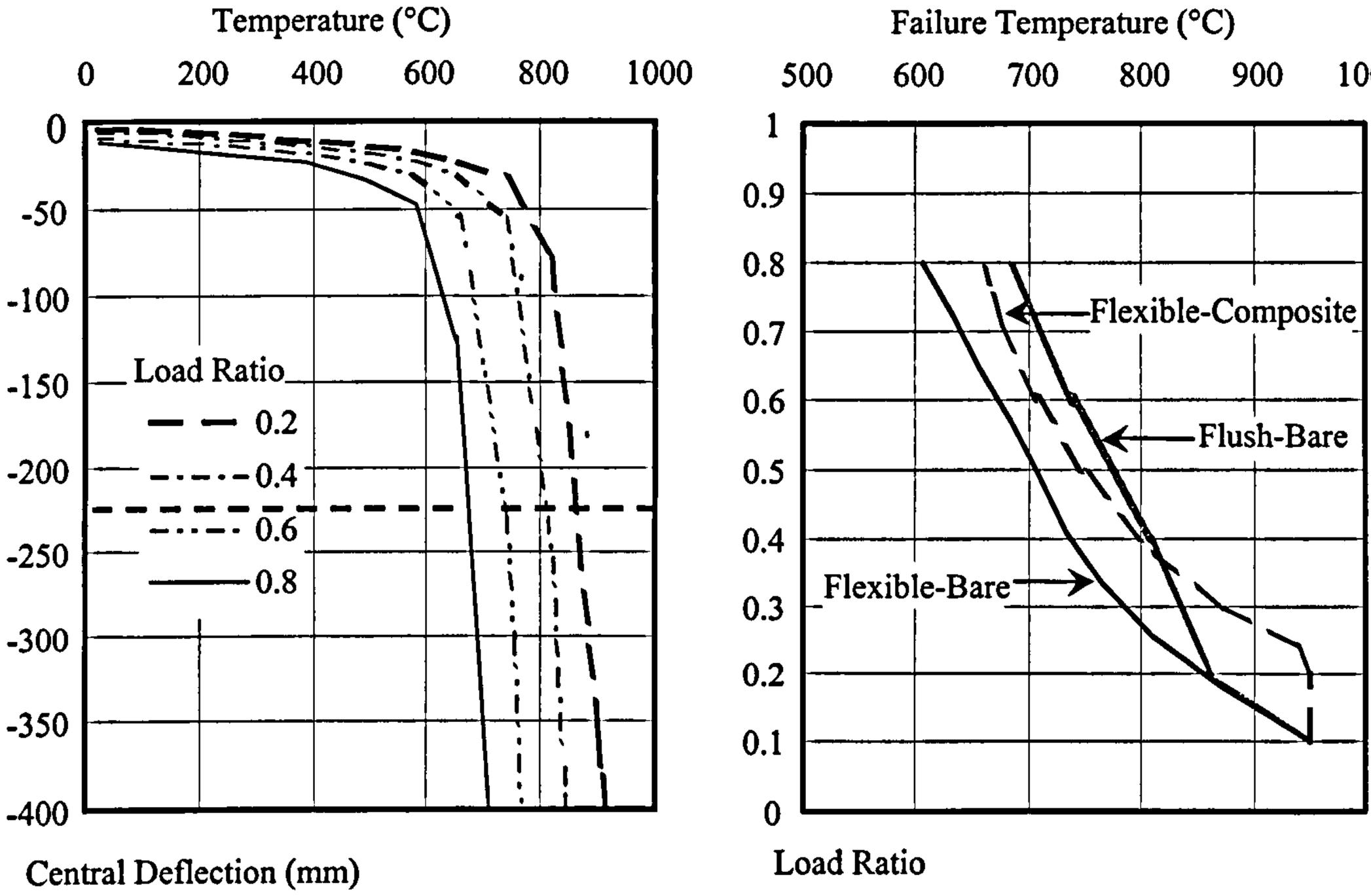

Figure 6.11: Influence of Applied Load-Ratio on Beam Response with Different Connection Characteristics

It is apparent from Fig. 6.11 that the load ratio can have a significant influence on the performance of the member in fire irrespective of connection type adopted. It should be remembered that adopting a load ratio of 0.6 forms a realistic maximum bound normally used in fire design, since it corresponds to the full design condition (at ambient temperatures). Therefore it is not practical to use a higher load ratio for fire conditions. In fact EC3[59] suggests reduced loads for fire design, and the corresponding load ratio would be about 0.5.

6.3.8 Influence of Connection Response Phase

As discussed in Chapter 4, some flexible end-plate connections have two phases of response:

1. the unobstructed rotation of the end-plate, until;
2. the beam bottom flange comes into contact with the column, resulting in significant increase in stiffness with further rotation.

This form of behaviour may be clearly observed from the results of the Group 4 tests (Fig. 5.6). Despite the fact that large levels of rotation are generated, Nethercot *et al.*[104] reported that connection behaviour at rotations beyond 50 millrads had little practical significance. Therefore it was suggested that in those connections where the lower

flange of the beam eventually bears directly against the column face due to beam rotation, only that part of the moment-rotation curve at lower rotations is of real interest. This effect may be limited by positioning the end-plate as close to the beam lower flange as possible [163] which would result in considerable enhancement in the stiffness and capacity of the connection compared with positioning the end-plate close to the beam upper flange.

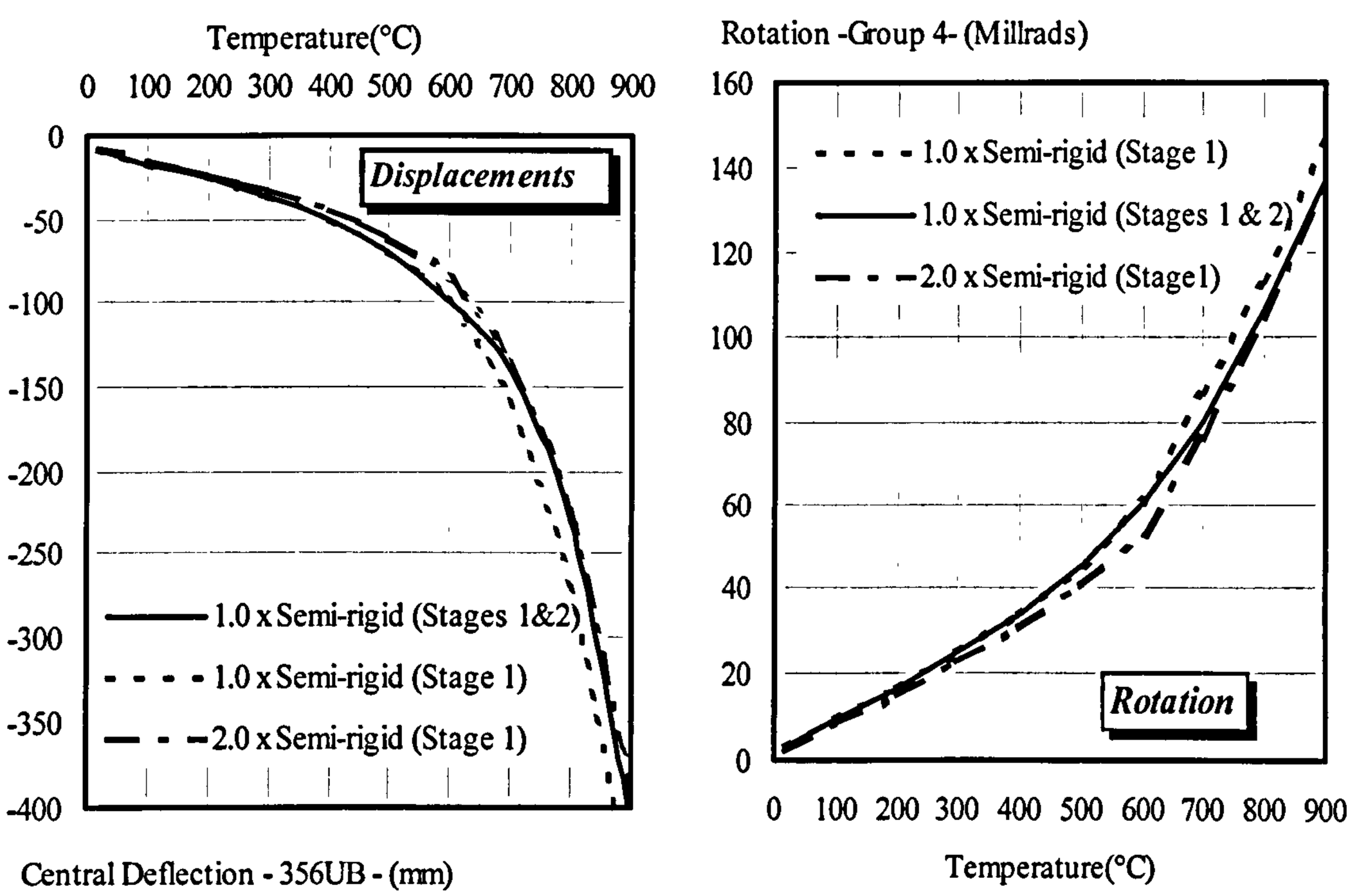

Figure 6.12: Deflections and Corresponding Rotations for 356UB Incorporating Flexible End-Plate Composite Connection Characteristics

In fire conditions the structure experiences deflections significantly greater than normal and the entire rotation range may therefore be relevant. In order to study this the composite sub-frame was analysed incorporating the moment-rotation-temperature characteristics for the flexible end-plate assuming the entire connection response. Fig. 6.12 shows the central deflection of the beam and the corresponding rotation of the connection assuming the entire response, along with those obtained ignoring the influence of stage 2.

For temperatures up to approximately 625°C beam deflections resulted from incorporating the entire connection response remained unchanged whereas the corresponding rotation at this temperature is approximately 65 millirads. This suggests that stage 1 rotation is still governing the connection response. With increasing temperatures beyond 625°C it may be seen that the connection gradually enters stage 2 of the response causing a small decrease in both the deflection of the beam and the rotation of the connection. This occurred as a result of enhancement in the connection response due to the contact between the beam lower flange and the face of the column. This corresponds to a beam deflection of about 145mm which is obviously less than the specified 'limiting deflection' (i.e. 225mm) corresponding to the nominal failure

temperature of the beam. Despite the fact that the use of the entire connection response has resulted in a reduction in the beam deflection, this enhancement in the beam behaviour is not significant. Therefore it seems the use of the first phase of response is adequate for studying the influence of flexible end-plates on the performance of the beam in fire.

6.4 CARDINGTON FULL-SCALE TEST FRAME STUDIES

The existing models for the analysis of structures in fire adopt empirical relationships to account for the degradation of the connections, derived either from ambient temperature tests or small amounts of elevated temperature data. Clearly this may yield results which are not representative of real conditions. The Building Research Establishment and British Steel conducted a series of fire tests on a full-scale building structure at Cardington[153,164] which was designed to be representative of current practice. Most of the analytical studies conducted[54,160,165] so far to simulate the Cardington fire tests have assumed the connections to behave as 'pinned' with no consideration given to the moment-rotation-temperature characteristics of the connections within the frame. This is primarily due to the lack of experimental data for the connection characteristics in fire. A three-dimensional analysis was carried out on one of the Cardington tests to investigate the influence of the connection characteristics on the frame response. The analysis procedure and the resulting behaviour are discussed in the following sections.

6.4.1 The Cardington Frame Arrangement and The Associated Tests

The Cardington full-scale eight-storey steel framed test building was constructed by the Building Research Establishment in 1994-95 in its Large Building Test Facility (LBTF), which enables this scale of experiment to be conducted indoors. The structure was designed to be a composite building typical of contemporary medium-rise commercial buildings in the United Kingdom, with roof-mounted services. The plan dimensions are 45 x 21m which provides a footprint area of 945 m^2. The form of frame was selected as a braced frame with composite simply supported beams. For all floors the design loads selected was 2.5 + 1.0 kN/m^2 whereas at roof level the load applied was 7.5kN/m^2. A number of flexible end-plate for beam-to-column connections and fin-plate connections for beam-to-beam connections were adopted. The general beam framing arrangement of the Cardington test frame shown in Fig. 6.13.

In total six fire tests were conducted during 1995-96 by the Building Research Establishment and British Steel on the composite frame[153,154,164,165]. Fig. 6.14 shows a plan of the locations of the fire tests within the building. A brief description of each test is given below:

1. *A Restrained Beam Test:* comprising a heated area 8m by 3m on the seventh floor. A gas furnace was used to heat the unprotected 9m 305x165UB40 secondary test beam over the central 8m of its length.

2. *A Plane Frame Test*: Conducted using a gas-fired furnace to heat an area of 21m x 2.5 m located on the fourth floor, and including the three connected spans of primary beams.

3. *The First Corner Test:* Carried out in an area 10m by 7m on the second floor. The fire was generated by firing wooden cribs with a density of 45 kg/m^2 of wood. The internal beams were left unprotected while the columns and edge beams were protected. Lightweight concrete block walls were used in the construction of compartment.

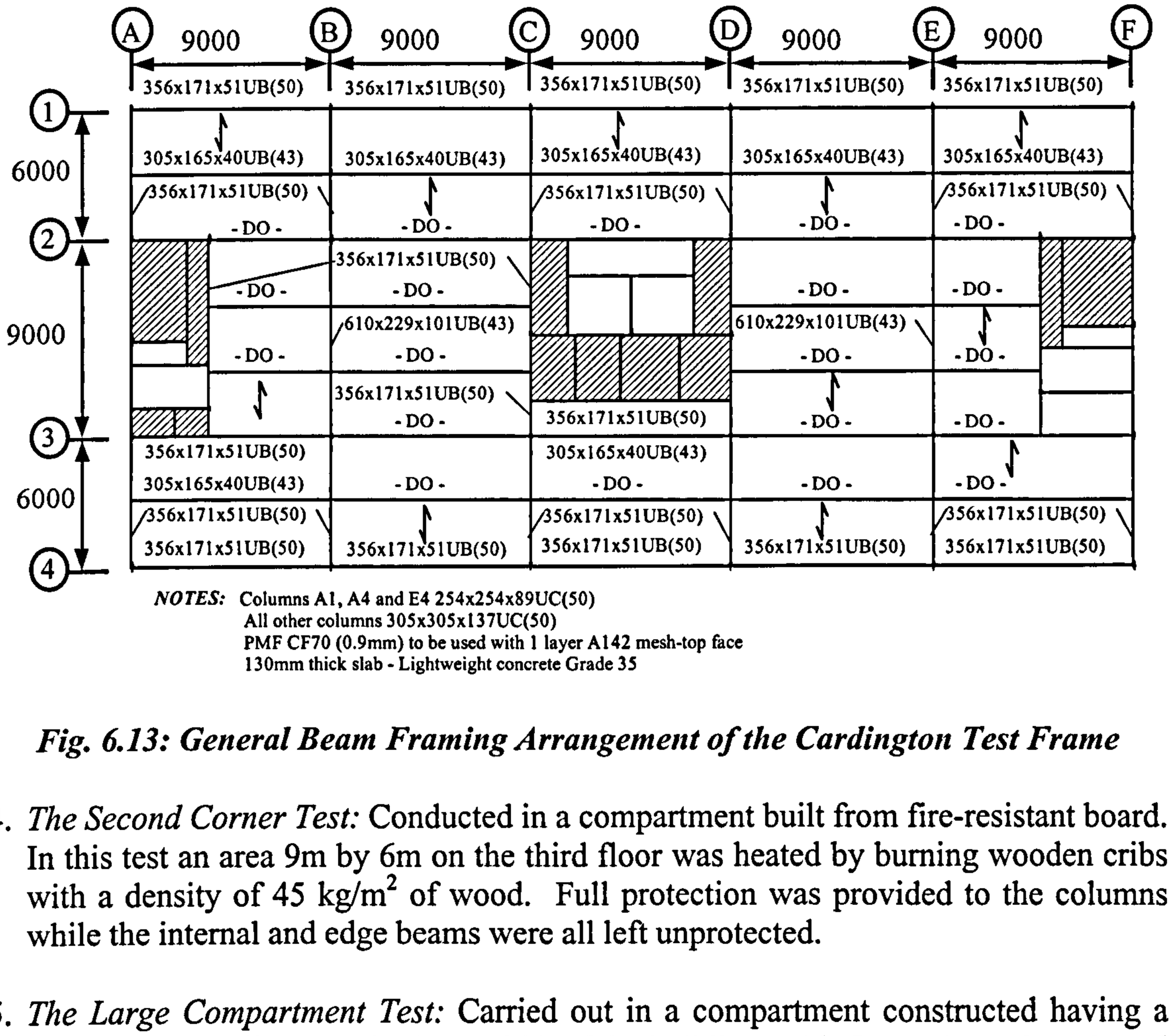

Fig. 6.13: General Beam Framing Arrangement of the Cardington Test Frame

4. *The Second Corner Test:* Conducted in a compartment built from fire-resistant board. In this test an area 9m by 6m on the third floor was heated by burning wooden cribs with a density of 45 kg/m^2 of wood. Full protection was provided to the columns while the internal and edge beams were all left unprotected.

5. *The Large Compartment Test:* Carried out in a compartment constructed having a fire resistant-wall across the 21m width of the building, with fire-resistant board used to block off the entrance to the passenger hoist. As in the two previous tests the fire in the compartment was generated by burning wooden cribs of 40 kg/m^2 of wood in an area 21m by 18m on the third floor.

6. *A Demonstration Office Fire Test:* Carried out on a compartment constructed using concrete blockwork. The fire load was provided by actual office furniture and documents equivalent to 45 kg/m^2 of wood. The test area was 18m wide by up to 10m deep. Protection was provided to the columns and beam-to-column connections whilst the primary and secondary beams were left unprotected.

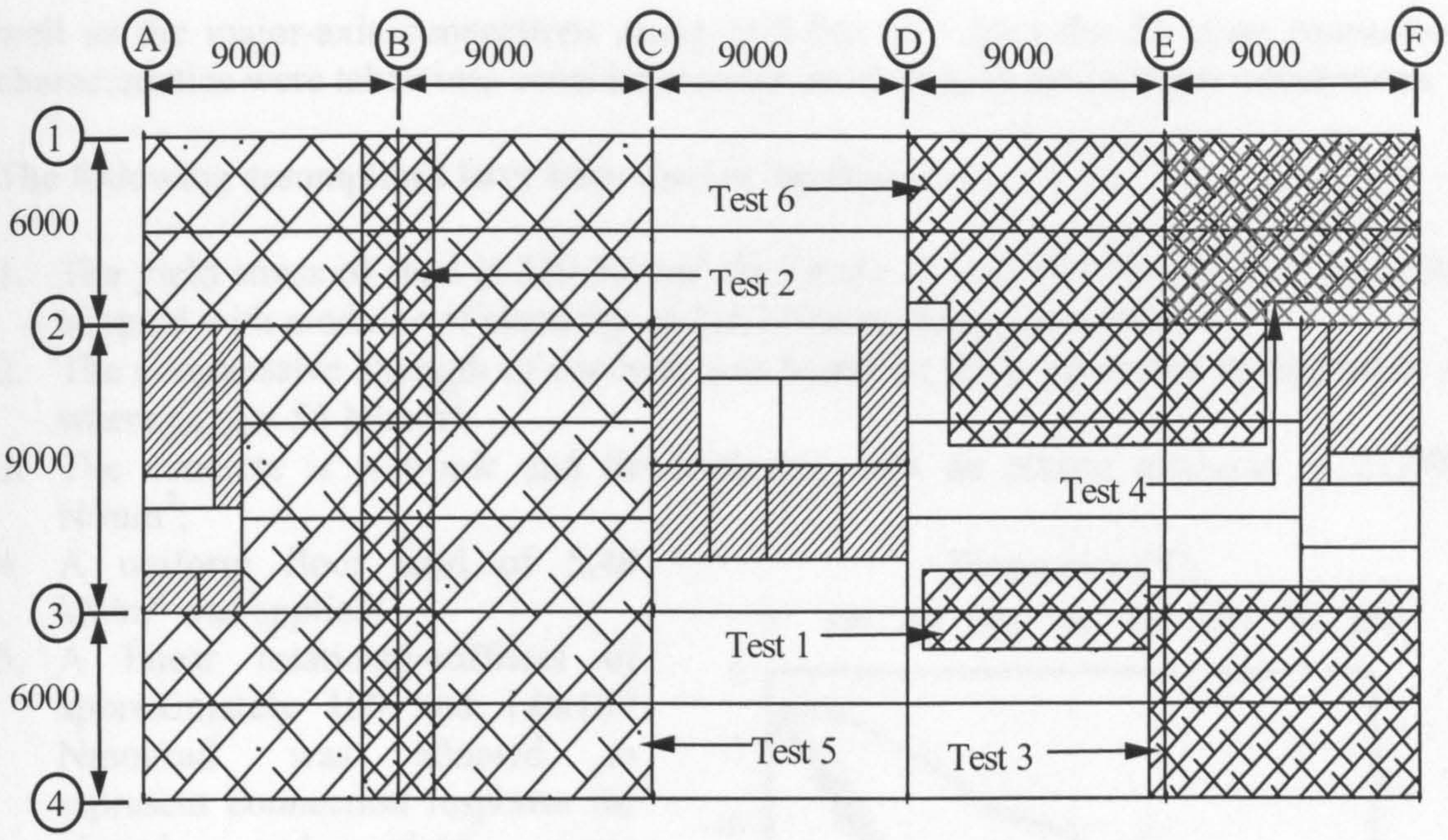

Fig. 6.14: Floor Plan of Cardington Test Frame Showing Location Fire Tests

6.4.2 The Effect of Connection Characteristics on the Performance of Cardington Frame in Fire

To study the influence of connections on the performance of a complete steel-framed structure in fire, the Cardington large compartment test (Test 5) was modelled incorporating connection characteristics in the analysis, using the three-dimensional finite element program developed by Bailey[54]. The extent of the structure modelled and the location of the plotted deflections are shown in Fig. 6.15.

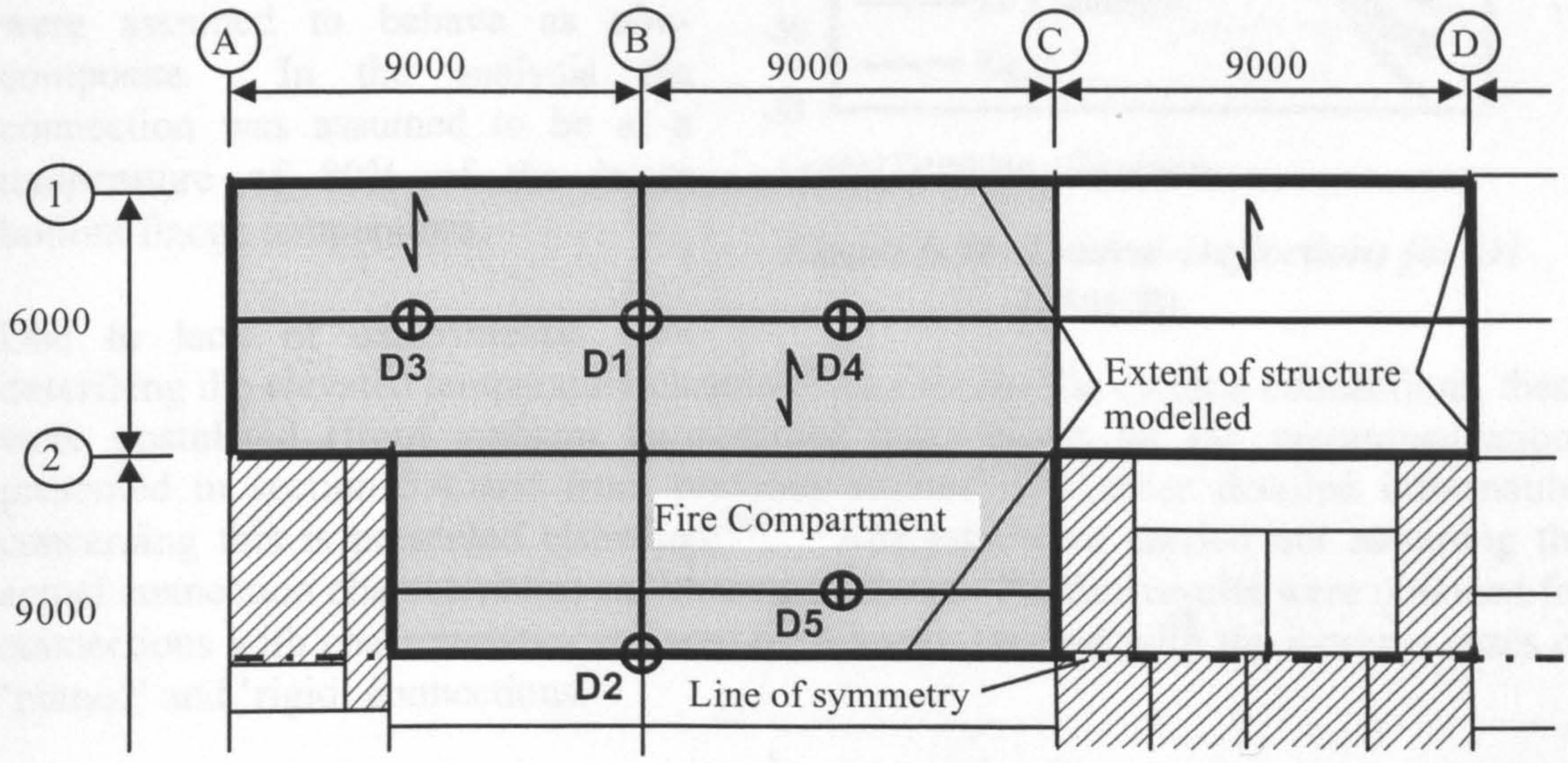

Figure 6.15: Large Compartment Test Sub-Frame Layout and Location of Plotted Deflections

To reduce the computation time structural symmetry was taken into account along the assumed grid-line 2.5. The modelled sub-frame included minor-axis connections as

well as the major-axis connections along grid-line B. Also the fin-plate connection characteristics were taken into consideration for modelling beam-to-beam connections.

The following assumptions have been used in the analysis:

1. The yield stress of steel is 320 N/mm^2 for Grade 43 and 420 N/mm^2 for Grade 50, adopted with modulus of elasticity of 210 kN/mm^2 being assumed;
2. The compressive strength of concrete was based on those presented in Appendix A where $f_{cu,\,28} = 55$ N/mm^2;
3. The concrete is isotropic and linear-elastic, with an elastic modulus of 21,000 N/mm^2;
4. A uniform floor load of 5.48 kN/m^2 was applied;
5. A linear rotational-stiffness of approximately 100 and 1.0x10^{20} Nmm/rad. was adopted to represent connection response for pinned and rigid cases respectively.

To simulate the actual fire scenario, beams were left exposed, while columns were protected for the full storey length resulting in the connections remaining at a considerably reduced temperature. Due to lack of continuity of reinforcing mesh, connections located at the edges of the modelled structure were assumed to behave as non-composite. In the analysis the connection was assumed to be at a temperature of 80% of the beam bottom flange temperature.

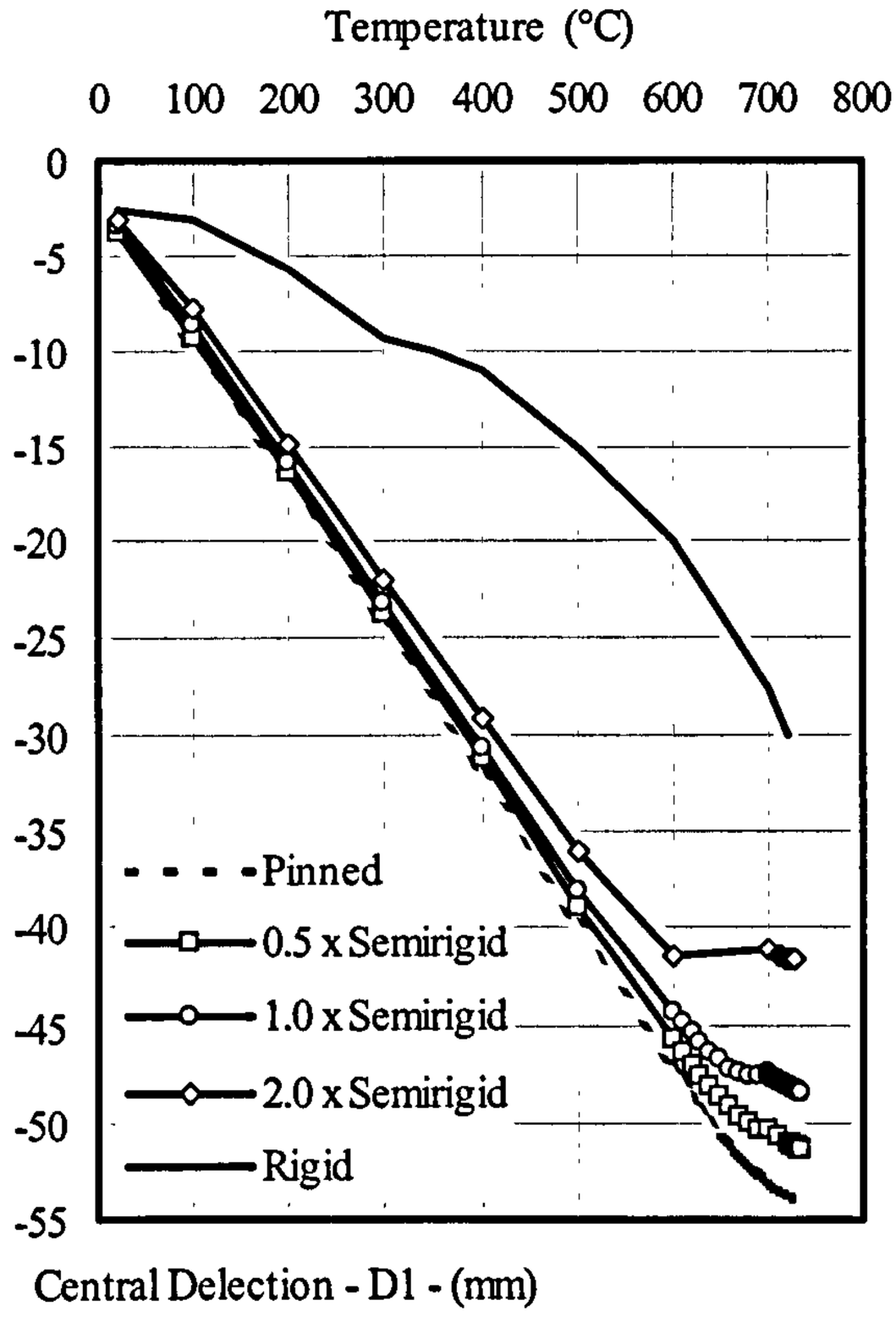

Figure 6.16: Central-Deflections for D1 (356UB)

Due to lack of experimental data describing the elevated temperature characteristics for the Cardington connections, these were postulated (from ambient temperature data) based on the recommendations presented in section 5.4 and from previous studies[52]. Further detailed information concerning this is presented elsewhere[166]. Analyses were carried out assuming the actual connection characteristics and those postulated. Further results were obtained for connections with characteristics factored by 0.5 and 2.0, and with the extreme cases of 'pinned' and 'rigid' connections.

Figs. 6.16 to 6.20 show mid-span deflections for primary beams at locations D1 and D2 and secondary beams (D3 to D5). In all cases the incorporation of 'actual' connection characteristics in the analysis results in only little enhancement in fire resistance for the beams when compared with the assumption of pinned connections. This may have been expected since these types of connection possess relatively low inherent moment capacity relative to that of the connected beam, being approximately in the range 10%-

20% of the beam plastic moment capacity. The implication is that the beams are behaving effectively as simply supported. This behaviour conforms with observations of the damaged structure after completing of the test[167] (as described in section 6.3.5). Also, it may be seen that the enhancement in the response is greater for the primary beams (356UB and 610UB) connected to the major-axis connections. This is due to the enhanced stiffness and capacity of the major-axis connection compared with minor-axis counterpart. Moreover, the deflections experienced, when adopting three-dimensional analysis, were considerably lower than for the two-dimensional analysis conducted on a similar composite frame[52].

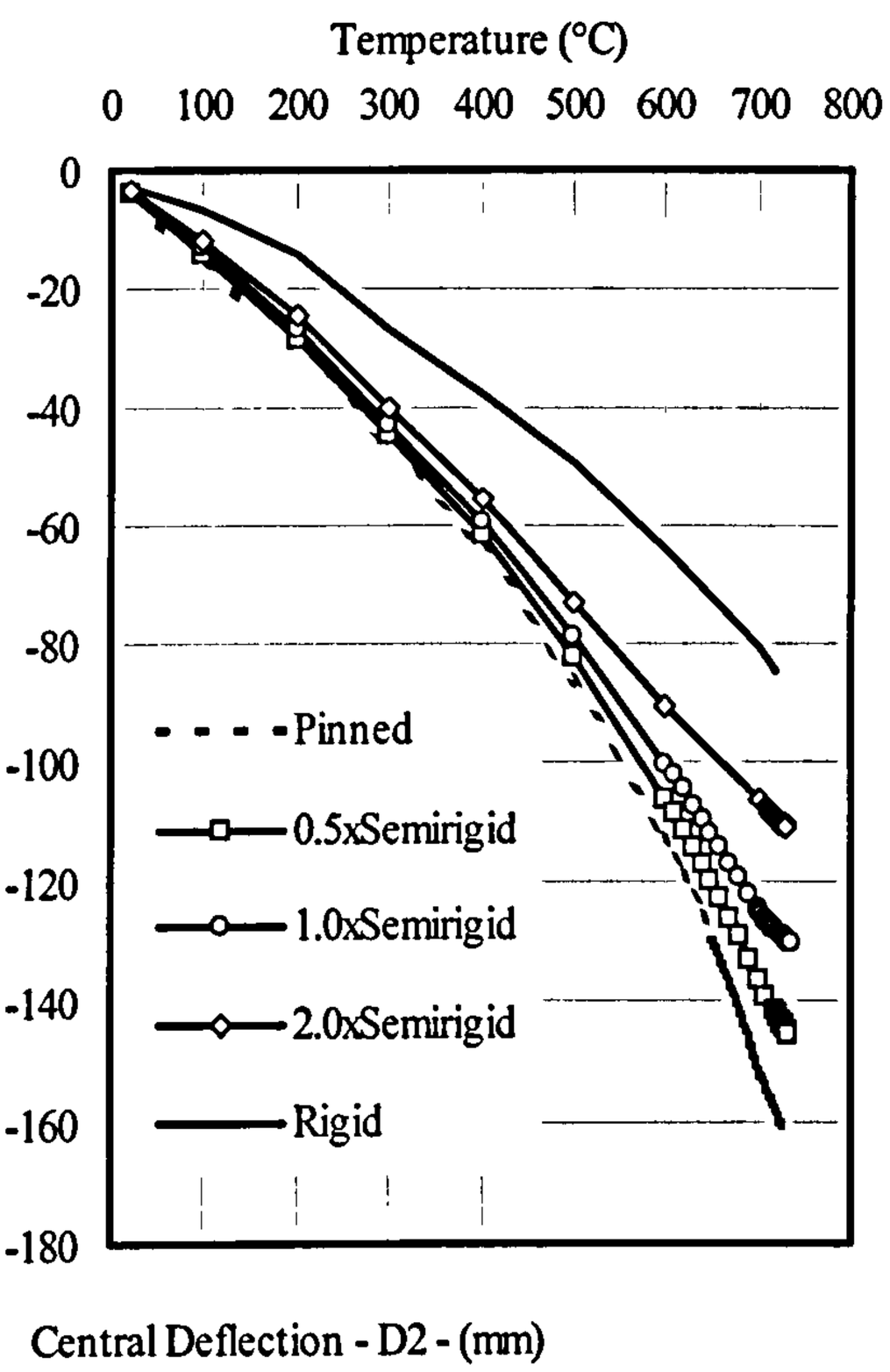

Figure 6.17: Central-Deflections for D2 (610UB)

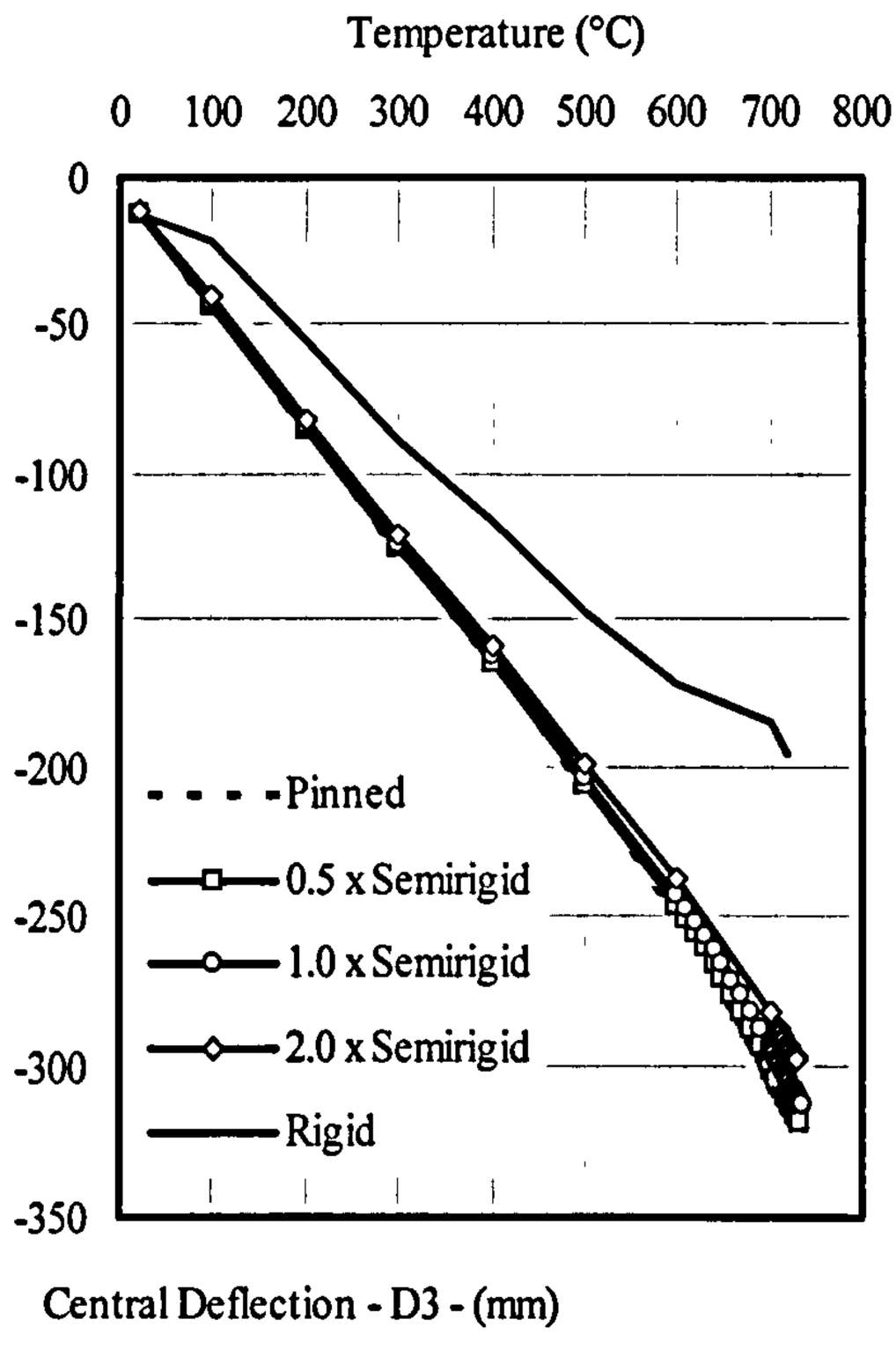

Figure 6.18: Central-Deflections for D3 (305UB)

The analyses stopped at temperatures of about 720°C because of convergence failure. Similar numerical instability within the program was observed previously by Bailey[54] and then Leston-Jones[52], and is due mainly to cracking of the concrete in the tension region.

Despite the fact that results from the present analysis suggesting that flexible end-plates are behaving as "pinned" connections in the event of a fire, observations from Cardington tests revealed that their integrity is maintained during fire without causing any form of collapse to the connected beams[167]. This demonstrate that when considering the connection to act in a composite manner even flexible end-plate connections can have some influence on the performance of beams in composite framed structure in fire conditions.

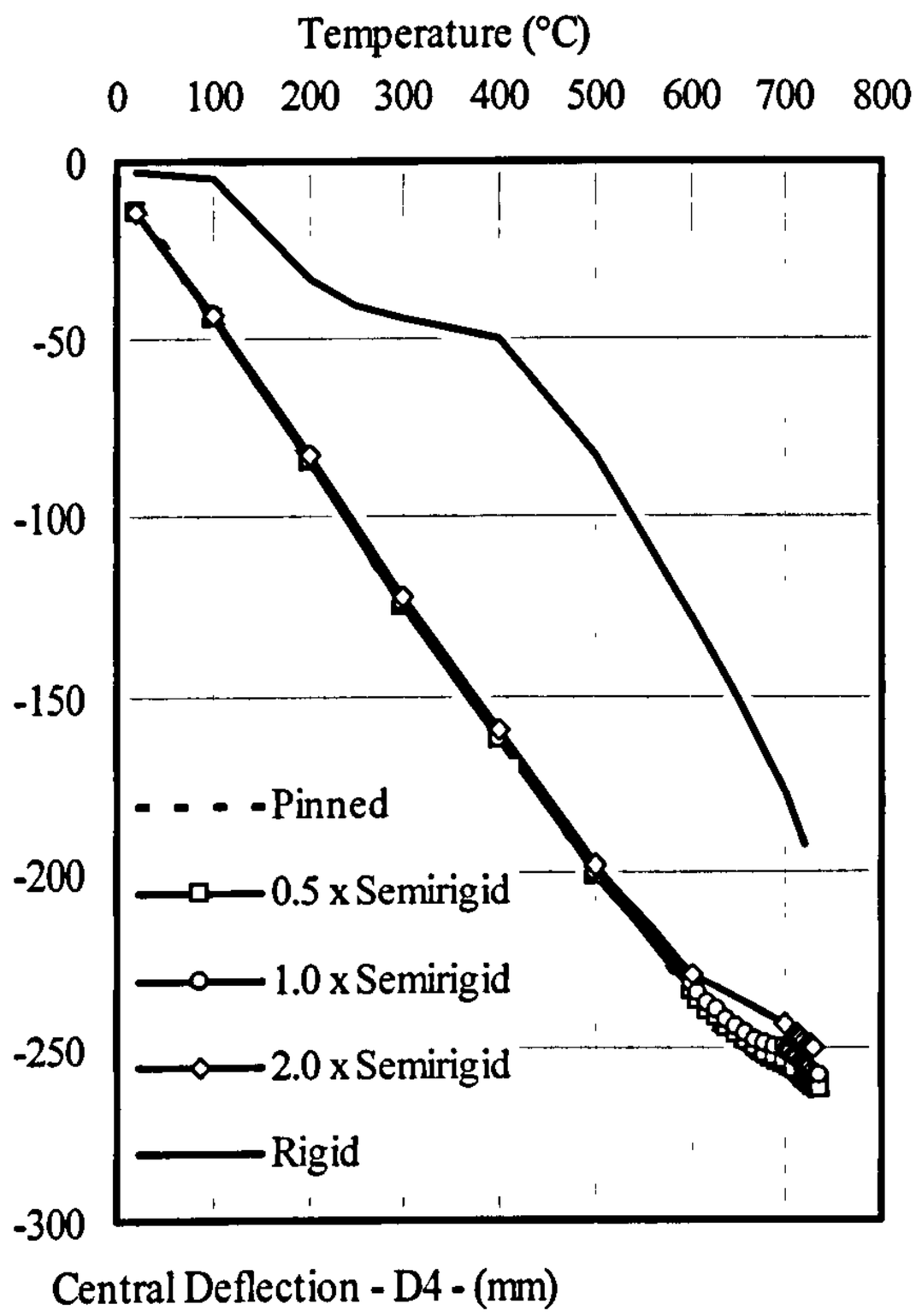

Figure 6.19: Central-Deflections for D4 (305UB)

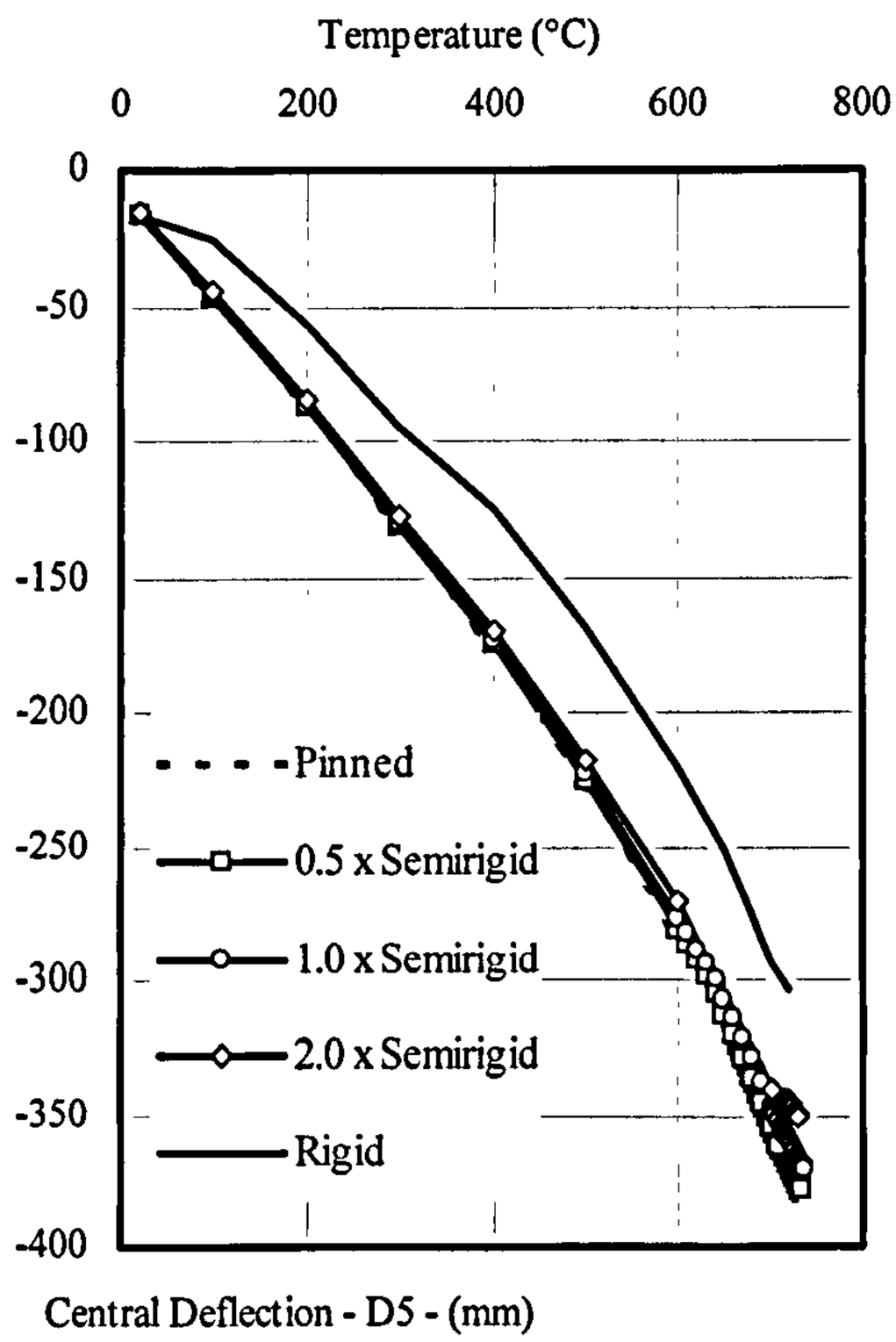

Figure 6.20: Central-Deflections for D5 (305UB)

6.5 COMPARISON BETWEEN CONNECTION RESPONSE IN THE CARDINGTON FRAME AND ISOLATED TESTS

Despite the beneficial value of isolated connection tests in providing raw data for modelling and verification of numerical techniques, as well as providing guidelines in developing design methods for engineers, they do not truly reflect the behaviour of complete buildings under fire conditions. Many aspects of structural behaviour occur when steel members are connected together which cannot be predicted or explained by isolated member tests. Global and local failure of buildings, the restraint to thermal expansion in fire caused by the adjacent cold structure and force redistribution capability of highly redundant structural systems[168] are some of the features occurring when steel members interact with each other which cannot be explained or predicted by isolated element testing. An improved understanding of the real behaviour of complete building structures, rather than structural members considered in isolation, should lead to more rationality in future design guides.

The behaviour of the connections in the Cardington frame and observations from isolated connection tests under fire conditions are compared. Many different local failure modes were observed in the Cardington tests, of which some have and some have not occurred in the isolated connection tests.

6.5.1 End-plate Failure

In the Cardington frame tests, partial end-plate fracture occurred in the restrained beam test, the plane frame test, the large compartment test and the demonstration test. In these tests there was a complete fracture of the end-plate along its full depth at weld which connects the end-plate to the beam flange as shown in Fig. 6.21, and in some cases this was also accompanied by shear failure of some bolts. This failure mode almost certainly occurred as a result of the high tensile forces developed during the cooling phase. During cooling steel contracts, causing a reduction in the vertical deflection of the beams whilst a significant tensile force is applied to the weld connecting the partial-depth end-plate to the beam flange. This force is relieved by fracture of the end-plate. A similar mode of failure was found in the Broadgate Phase 8 structure after it was extensively damaged by fire[9].

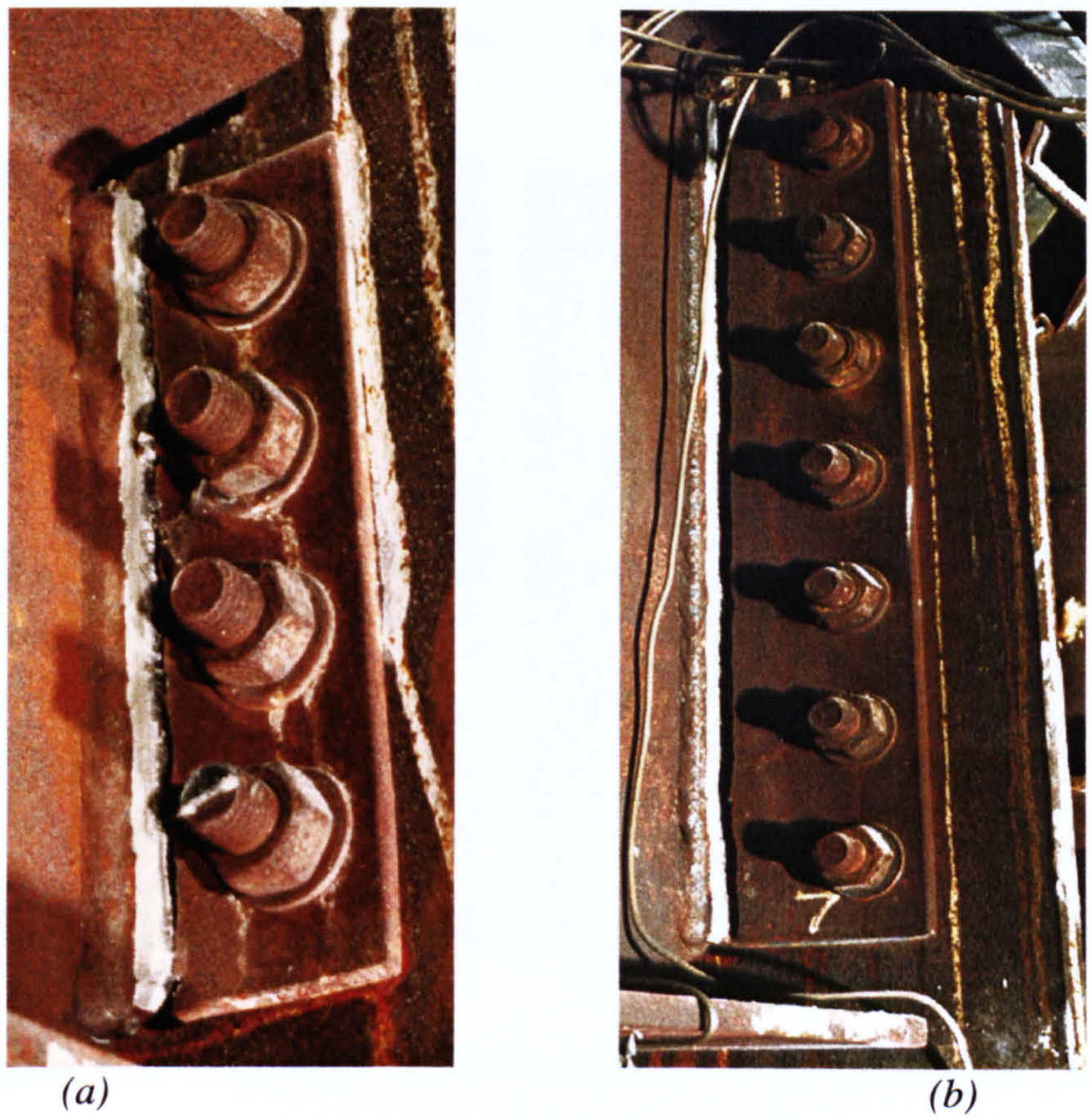

(a) *(b)*

Figure 6.21: Typical Flexible End-Plate Failures in the Cardington Tests

However, in the isolated member connection tests, although the dominant observed failure mechanism for the bare and composite flexible connections was the fracture of the end-plate along the welds, this failure was because of the large rotation associated with flexible end-plate connections (see Figs. 4.5 and 4.17). In both the Cardington frame and the connection tests the fracture occurred along only one side of the connection, while the other side remained intact. This is probably because after one side of the flexible end-plate has fractured, the flexibility of the end-plate is considerably increased allowing larger deformations without further fracture. This causes a redistribution of the forces so that the vertical shear is carried by the intact part of the connection and the tension reinforcement in the composite slab. Thus it should

be ensured when designing connections at fire limit state that the capacity of the weld is at least twice that needed to carry the resultant vertical shear forces at ambient temperature to prevent failure.

6.5.2 Mesh Continuity Failure and Composite Slab Cracks

There is some similarity in this failure mode between the Cardington frame and the isolated connection tests. In the Cardington frame, there was a distortion of the metal decking in almost all the tests, and some bars of the reinforcing mesh appeared to be fractured as shown in Fig. 6.22*(a)*. In some cases, the metal decking lost its connection with the concrete, with some accompanying spalling. In one of the Cardington tests, an abrupt shear deformation of slabs was observed along some perimeter beams. At present, it is unclear whether this was due to a failure of the reinforcing mesh or to a lack of continuity of the mesh across these beams because of poor site control during contraction. Fig. 6.22*(b)* shows typical crack patterns near the connection.

(a) Slab Cracking and Fracture of Bars *(b) Cracking Patterns around Column*

Figure 6.22: Composite Slab Failure Modes in the Cardington Tests

In the isolated connection tests the composite slab failure mode was similar to some extent to that observed in the Cardington frame tests. In the concrete slab, there was a large crack running parallel to the primary beam, resulting in fracture of some bars in the steel mesh. Two major secondary cracks were observed perpendicular to and continuous over the connections on both sides of the slab. There was no sign of the distortion to the metal decking which was clearly observed in the Cardington frame tests.

6.5.3 Local Buckling

One of the main failure mechanisms which is very likely to occur in full-scale tests but is less likely to happen in isolated tests, is local buckling of the beams and other members. Local buckling of structural members was very clearly observed in most of the Cardington frame tests due to their structural continuity and the restraint to thermal expansion provided by the adjacent cool structure. Local buckling was observed in the lower beam flange and web, usually adjacent to the connection as shown in Fig. 6.23. This suggests that the flexible end-plates act as 'pinned' connection incapable of transmitting the generated high forces in the beams to the adjacent columns causing local buckling of the beam flange and sometimes web in the vicinity of the connection. It is possible that in such cases the beam could be assumed 'simply supported', allowing much larger mid-span deflection to be developed than when beams are semi-rigidly connected. This contrasts with what was suggested previously regarding the behaviour of connections in fire. In view of observations from Cardington fire tests, it was recommended that all connections at fire limit-state should be conservatively considered as pinned[168]. This has raised doubt about the current design guides[48] which take into account the rotational restraint provided by the connection as these guides were primarily developed based on isolated connection tests.

Figure 6.23: Local Buckling of Beam Flange and Exposed Column Zone in Cardington Tests

Local buckling has also been observed in large-scale frame tests at ambient temperature[169] in which the cause was a high hogging moment in the composite beams caused by unbalanced loading in a frame test. This behaviour has been absent in some isolated ambient temperature connection tests[170] whilst it has been more pronounced in others[171]. This variation in the behaviour is probably due to the types of the end-plate used and the test arrangements. However in the case of current isolated elevated temperature connection tests, there was local distortion. This distortion affected the column flange together with web for small-sized flush end-plate connections only in

Group 1 tests which were characterised by small member sizes and relatively stiff connection details. There was no local buckling observed of either the beams or columns in the other test groups because of their larger member sizes and better balanced connection details. The absence of any superimposed axial thrust in these tests is probably the key difference from the full-scale frame tests.

6.5.4 Other Observed Mechanisms

Other failure modes were observed in the Cardington frame tests which did not happen in the isolated connection tests. These are listed below:

- Lateral-torsional buckling of some beams due to a lack of lateral restraint which was observed mainly in the second corner test and the demonstration office fire test.
- Shear fracture of bolts in some connections (especially beam-to-beam fin-plates). In the isolated connection tests, there was no evidence of fracture of bolts.
- In the isolated connection tests significant rotation angles were achieved by the end-plates, which are unlikely to occur in full-scale frames due to boundary restraint and continuity.

6.6 CONCLUSIONS

Parametric studies have been conducted to investigate the effect of connection characteristics on frame response in fire. Analyses were carried out using a finite-element program developed by Bailey[54] and incoporating moment-rotation characteristics for both bare-steel and composite flush and flexible connection characteritics. This program was selected due to its capability of modelling connection characteristics within a three-dimensional frame analysis in fire. In order to reduce the analysis time, a suitable two-dimensional sub-frame arrangement was selected which was reported[161] to generate results comparable with those obtained from large-scale frames.

Load ratios of 0.6 and 0.4 were adopted for beams and columns respectively in order to represent the level of loading which may realistically exist under fire conditions. The Ramberg-Osgood curve-fitting expression was adopted to represent the connection characteristics since it has the ability to define the connection response over the entire range. The influence of connection characteristics on frame response is considered by incorporating the moment-rotation characteristics for flush and flexible end-plate connections within both bare-steel and composite sub-frame analyses, along with the assumptions of pinned and rigid connection response.

The results obtained for the bare-steel sub-frame demonstrated that the failure temperature for the beam with flush end-plate connection was almost 70°C higher than for the beam with flexible end-plates and the response was approximately mid-way between that for rigid and pinned characteristics. This suggests that the connection type has considerable influence on the performance of the structural member in fire. However, there was only a slight enhancement in the beam response with flexible end-plate for both bare-steel and composite arrangements compared with pinned condition, irrespective of connection size. This demonstrate that flexible end-plates behave as

'pinned', and the connected beams may be treated as simply supported. Moreover, analysing a typical sub-frame with flush end-plates having different thicknesses revealed that thickness of the end-plate has little influence on the beam behaviour.

The analysis was repeated on a composite sub-frame to study the influence of the composite slab on the frame response from which it was found that the performance of the beam is greatly enhanced. The resultant increase in failure-temperature of the beam was observed to be of the order 200°C. Analyses were carried out to investigate the influence of concrete strength on the beam response considering both low strength (< 10 N/mm^2) and high strength (> 70 N/mm^2) concrete. Results showed that concrete strength has some effect on the structural response at elevated temperature, although this enhancement is not considerable.

To study the sensitivity of the connection temperature to the frame response a range of ratios between the connection temperature and that of the beam bottom flange were considered. For bare-steel flush end-plates it was concluded that failure temperature is sensitive to the connection temperature adopted for ratios higher than 0.5. However, for both bare-steel and composite flexible end-plates it was found that the connection temperature has negligible influence on the failure temperature of the beam. A number of applied load ratios was considered in order to study the effect of load ratio on frame response from which it was found that increasing load ratio has a considerable effect in reducing the failure temperature of the beam irrespective of the connection type and arrangements. Also in the case flexible end-plates it was found that the enhanced response resulting from the contact between the beam and the column had only a small influence.

The scope of the analysis was extended to consider the influence of connections on the response of a realistic structure. The large compartment test at Cardington was selected as a case study representative of current practice. Analysis was conducted using the three-dimensional program developed by Bailey[54] incorporating both the actual and postulated connection characteristics in order to determine the frame response in fire. Incorporation of connection characteristics and composite action resulted in a slight enhancement in the beam response compared with pinned connections. This response was observed in all beams regardless of connection types and orientations, suggesting that the connections within the Cardington frame are tending to behave as though 'pinned'.

Comparisons have been made between the behaviour observed in the Cardington frame fire tests and the observations from isolated furnace tests. Fracture of the end-plate was observed in both the Cardington frame tests and isolated connection tests. In the former case this occurred due to high tensile forces induced during the cooling phase, whilst in the latter was as a result of the large rotations associated with flexible end-plates. Local buckling of the beam lower flange and web in the proximity of the connection was observed in most of the tests suggesting that the connections are effectively behaving as pinned.

7 A COMPONENT-BASED MODEL FOR FLEXIBLE END-PLATE CONNECTIONS AT ELEVATED TEMPERATURE

7.1 INTRODUCTION

A series of tests was conducted for flush and flexible end-plate connections, both as bare-steel and composite with a slab, to study the performance of these connections at elevated temperature as presented in Chapters 3 and 4. As a direct outcome of these tests moment-rotation characteristics describing the connection response have been derived with increasing temperatures. Also results have been presented concerning the elevated temperature failure mode of the connections and the temperature profiles. Results from such tests will be of great value in providing basic data for developing numerical techniques to predict connection response at elevated temperature.

To reduce the cost and time associated with experimental studies, a number of numerical techniques have been proposed for modelling ambient temperature connection behaviour. These have been summarised by Nethercot and Zandonini[107] and may be categorised as simplified analytical models, component-based (or mechanical) models and finite-element models. Component-based models are attractive because of their relative ease of application and their capability to provide a reasonable representation of the full range of connection response.

Models for predicting elevated temperature connection response have only recently begun to be developed. Even studies based on complicated finite element models such as that proposed by Liu[150] are rare. This is partly because a reasonable body of experimental data had not previously been available. In this chapter a simplified component-based model is developed to predict the behaviour of both bare-steel and composite flexible end-plate connections at elevated temperature. The response of flush end-plate bare-steel connections is also modelled based on a previously developed component model[52].

7.2 DEVELOPMENTS IN THE COMPONENT-BASED MODELS

This category of model can predict the connection characteristics across the full connection response by superposition of the contribution of connection components. The response of constituent components may be based on experimental results or analytical models. The number of components incorporated has an important influence on the accuracy and this type of model has therefore been restricted principally to connections where the number of key parameters is limited.

An early attempt to use component models was made by Wales and Rossow[172] who developed a component-based model for double web-cleat connections, in which the connection was modelled as two rigid bars linked by independent non-linear springs. These springs simulate segments of the double-web angle. The parameters defining the deformation characteristics of the springs were obtained from analysis of the double web-cleat, in simple tension and compression. The model included the coupling effects between bending moment and axial force applied to the connection and generated satisfactory results when compared with results from a single test.

A similar approach was used by Kennedy and Hafez[173] who developed a simple T-stub model to represent the behaviour of a flexible end-plate in both the tension and compression regions. In order to determine the moment-rotation response, a trial and error procedure was used to define the position of the centre of rotation. The model was validated against test data from which it was shown that there was close agreement in terms of ultimate capacity, although there was some discrepancy in the corresponding level of rotation.

Richard *et. al*[174] adopted the form of model proposed by Wales and Rossow to predict the response of all types of cleated joints subject to shear and bending. The force-deformation characteristics of the double-angle segments were calibrated by curve-fitting against experimental data. The validity of the model was verified against an extensive range of test results, producing satisfactory results especially in cases where deformation of column components and slip of bolts were negligible.

One extensive investigation into the response of fully welded connections has been carried out by Tschemmernegg[175] in order to develop a suitable design method. A broad range of beam and column sections was investigated in order to allow the calibration of spring elements describing connection response. The model comprises an arrangement of springs describing the response of the beam and column, and the shear deformation of the column web. The connection response is obtained by superposition of the response of the two sets of springs.

A series of component-based models has been proposed by Madas[176] for various forms of both bare-steel and composite connection types. Flexible end-plate, double web-angle, top- and seat-angle connections were considered. A number of components, such as column and bolt deformation, remain transferable between different connection types. In order to account for non-uniform deformations through the thickness of the slab, the concrete was sub-divided into a finite number of layers with an effective width. The influence of both shear connectors and reinforcement was included. Comparison with test data demonstrated close agreement in terms of both the observed failure mechanisms and the overall form of response.

Tschemmernegg[177] also developed a revised model applicable to composite connections. An additional spring in the tension zone was incorporated to represent the reinforcement and a load induction spring to model the change in loading in the compression zone. The effects of shear connectors and shear lag in the composite beam were not accounted for which may considerably influence the connection response.

EC3: Part 1.1 Annex J[40] permits the use of a component model in order to determine the key parameters that define the connection response such as initial stiffness and moment and rotational capacity. However, due to the lack of experimental data describing the connection response at elevated temperature, elevated temperature component-based models are limited and restricted to single connection types. Based upon the EC3 component approach, Leston-Jones[52] proposed a component model for bare-steel and composite flush end-plate connections at elevated temperature. The bare-steel model compared well with test data for both a major and minor axis flush end-plate connections. However, the composite model showed a significant difference in the rate of degradation compared with experimental results for elevated temperatures. It was

suggested that this was due to neglecting the movement of the axis of rotation in the composite model in the context of the increased load applied to the column web.

7.3 MODELLING OF BARE-STEEL FLUSH END-PLATE CONNECTIONS AT ELEVATED TEMPERATURE

The model developed by Leston-Jones[52] was used to model the bare-steel flush end-plate connections tested at elevated temperature in Groups 1 and 2. It was also utilised as the basis for developing a component model for predicting the behaviour of flexible end-plate connections both as bare-steel and composite. It was originally developed to model connections with only two bolt rows in tension and has been modified to account for more bolt rows and larger connection details. The experimentally observed temperature profiles are used to simulate the temperature distributions across the connection depth, whilst the actual material properties are used as detailed in Appendix A.

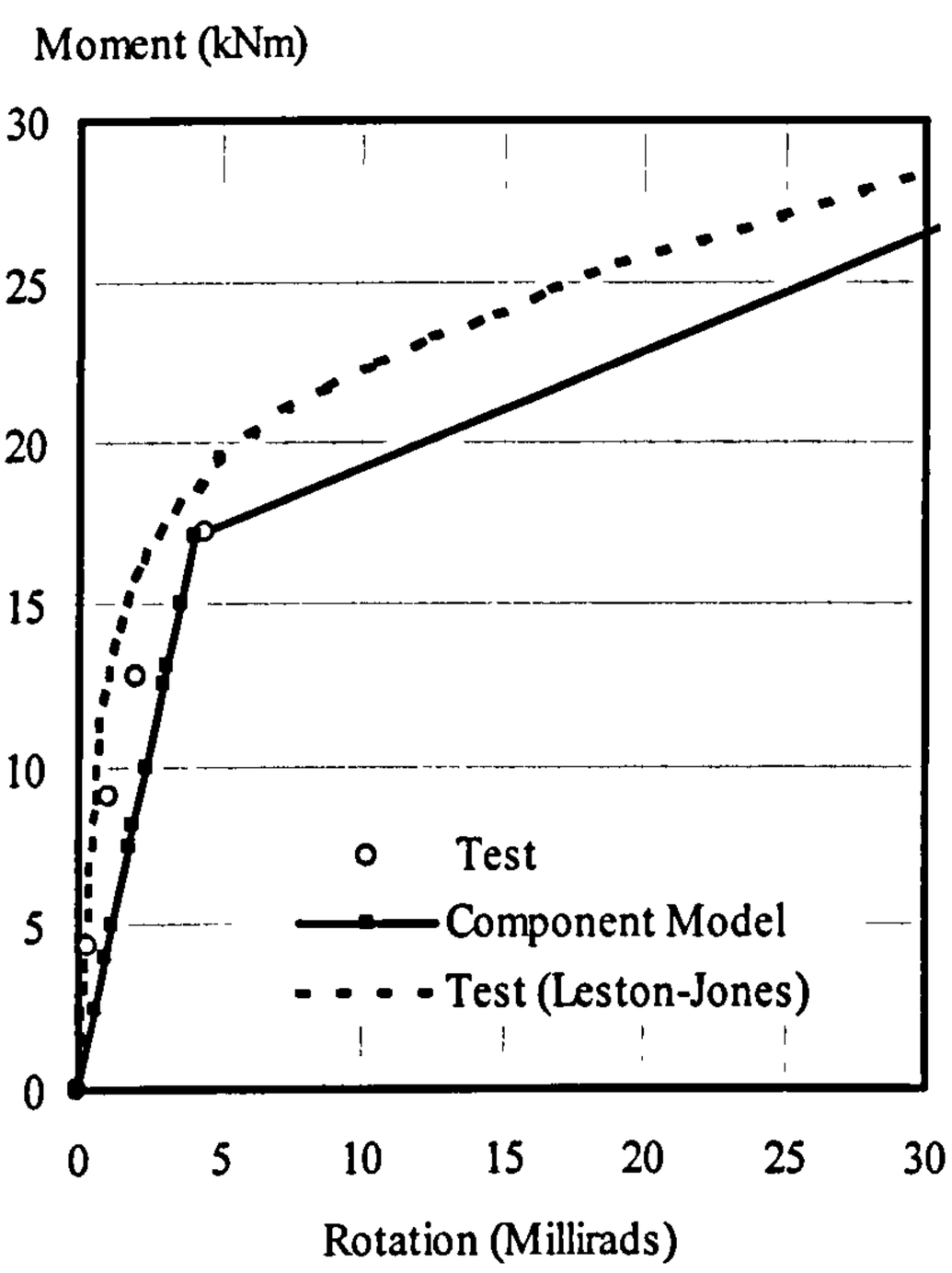

Figure 7.1: Comparison of Predicted Ambient Temperature Response with Group 1 Tests Results

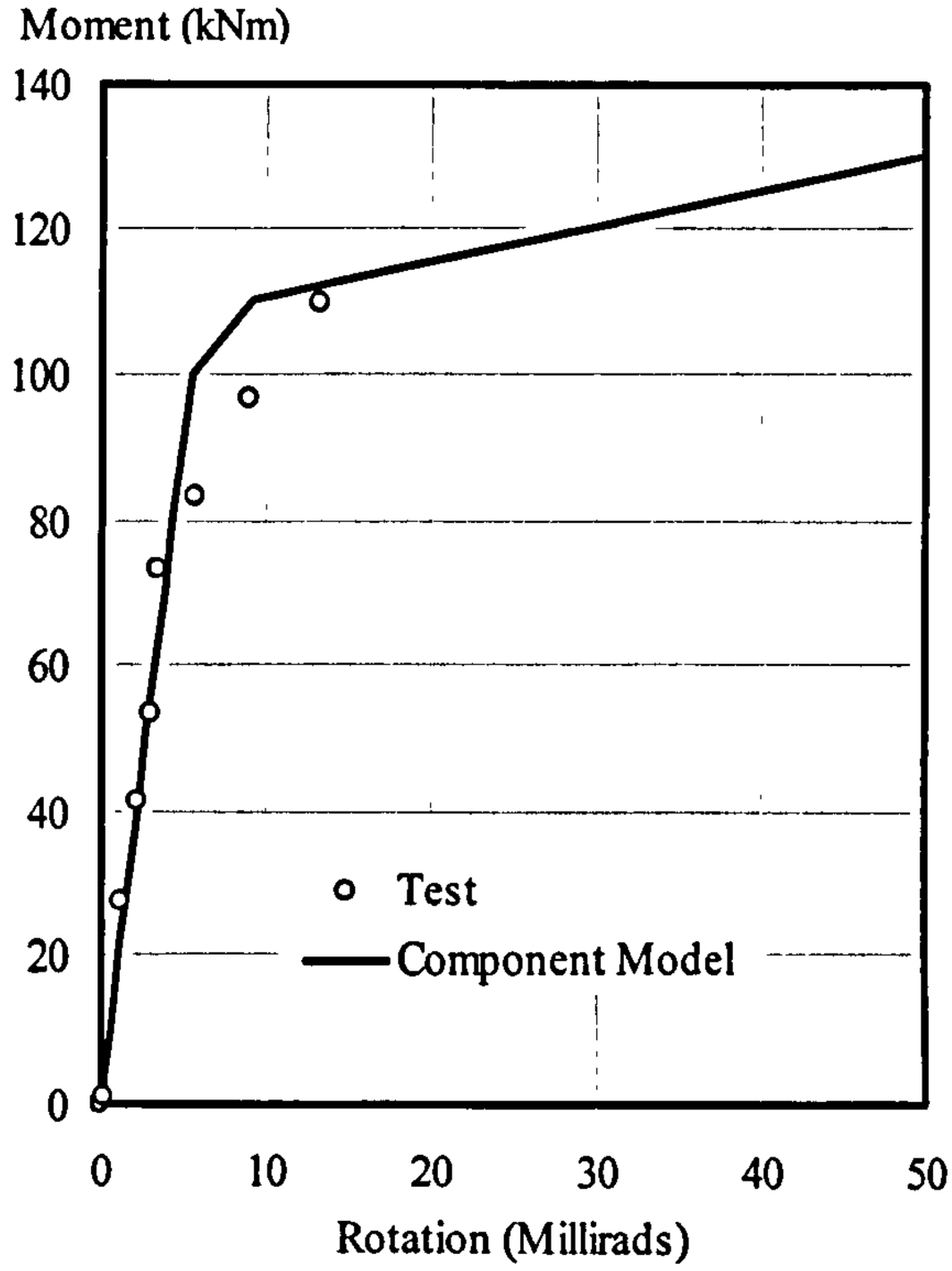

Figure 7.2: Comparison of Predicted Ambient Temperature Response with Group 2 Tests Results

Comparisons of predicted and experimental ambient temperature response for Group 1 and Group 2 tests are shown in Figs. 7.1 and 7.2 respectively. It may be seen from Fig. 7.1 that there is a close agreement between the predicted ambient temperature response of Group 1 connection and the experimental one. In order to assess the model's ability to predict the connection response over the entire moment-rotation relationship, the experimental connection response obtained by Leston-Jones[52] for a similar connection with thicker end-plate (i.e. 12mm) is compared with the predicted response. As can be seen the model can predict the entire connection response although the plastic response

of the connection is underestimated due to the use of a thin end-plate (i.e. 8mm) in the modelling. The model predicted connection deformation controlled by end-plate and column flange deformation in the tension zone, and column web crushing in the compression zone, corresponding with the experimental observations. Similarly, it may be seen from Fig. 7.2 that the component model provides close prediction of the initial stiffness of the connection at ambient temperature. The model somewhat overestimates the yield capacity of the connection, but the observed discrepancy is relatively small and may be attributable to variations in material properties. Unfortunately test data describing the strain hardening and ultimate connection response is not available, due to the levels of loading adopted in the elevated temperature tests. The failure mode of the connection was predicted as being governed by end-plate deformation in the tension zone corresponding with experimental observations, with the actual failure of the connection occurring as a result of end-plate deformation.

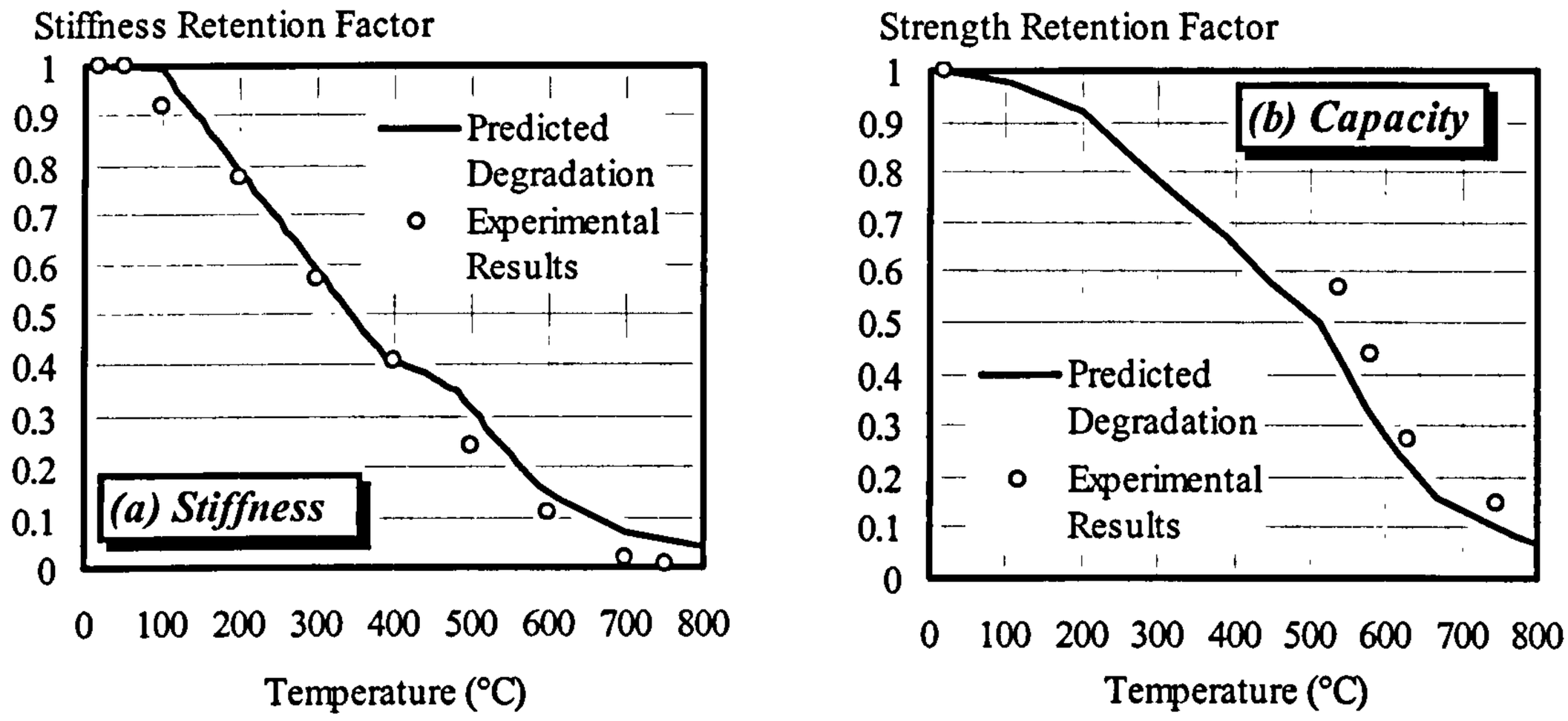

Figure 7.3: Predicted Degradation of Connection Characteristics Due to the Influence of Temperature for Group 1 Connection

The experimental degradation of the connection characteristics is compared with those predicted for Groups 1 and 2 connections in the form of stiffness/capacity retention factors plots in Figs. 7.3 and 7.4 respectively. It may be seen that for both connections the predicted degradation of stiffness with temperature compared closely with that recorded. Predicted degradation of Group 1 connection capacity compared well with experimental results, although the model slightly underestimates the actual rate of degradation. However, for Group 2 connection, the model underestimates the recorded degradation of the connection capacity especially for temperatures between 450°C and 600°C. For both connections the model prediction of the degradation of the connection capacity was conservative. Unfortunately experimental data was not available for temperatures below 500°C and 450°C for Groups 1 and 2 connections respectively, due to the levels of loading adopted in testing.

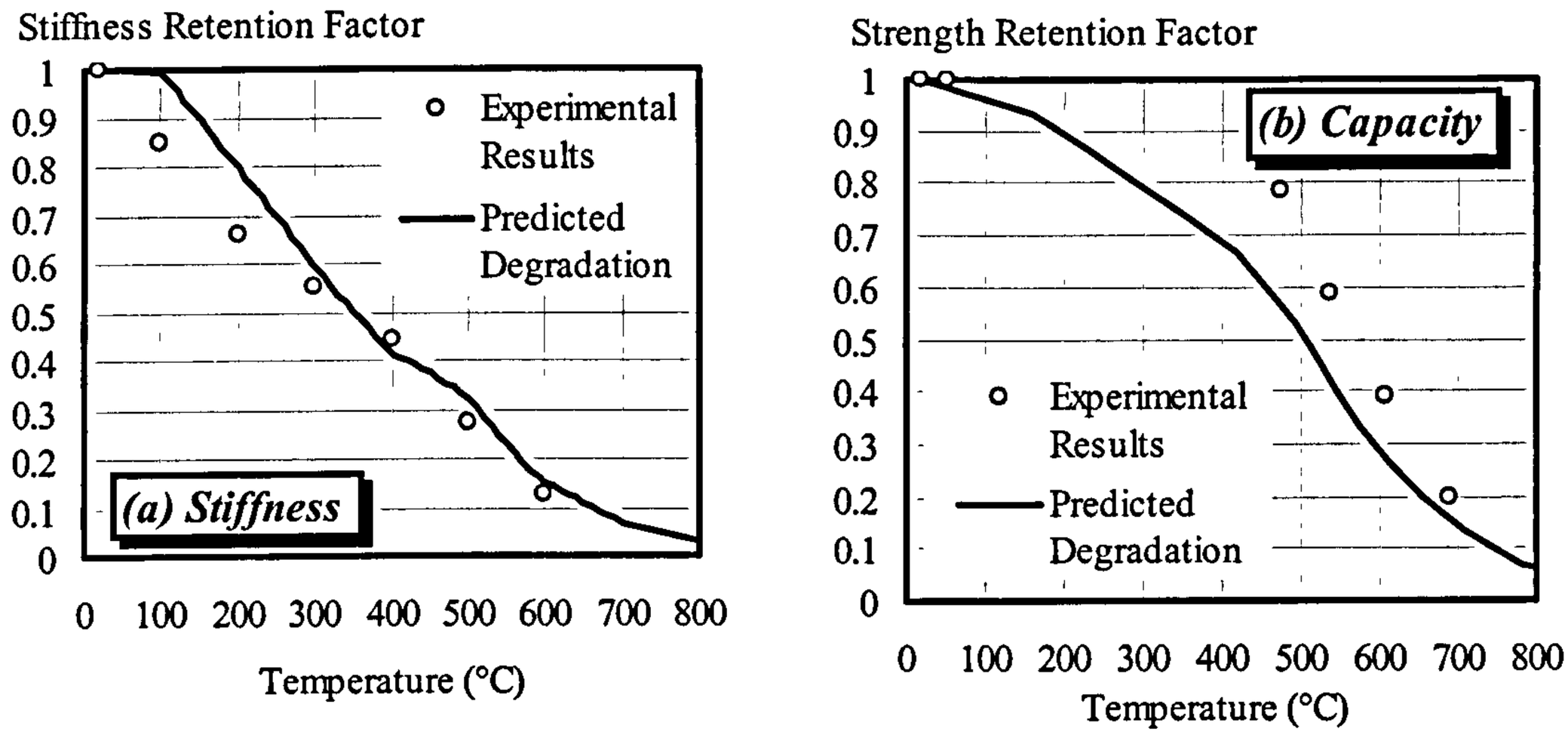

Figure 7.4: Predicted Degradation of Connection Characteristics Due to the Influence of Temperature for Group 2 Connection

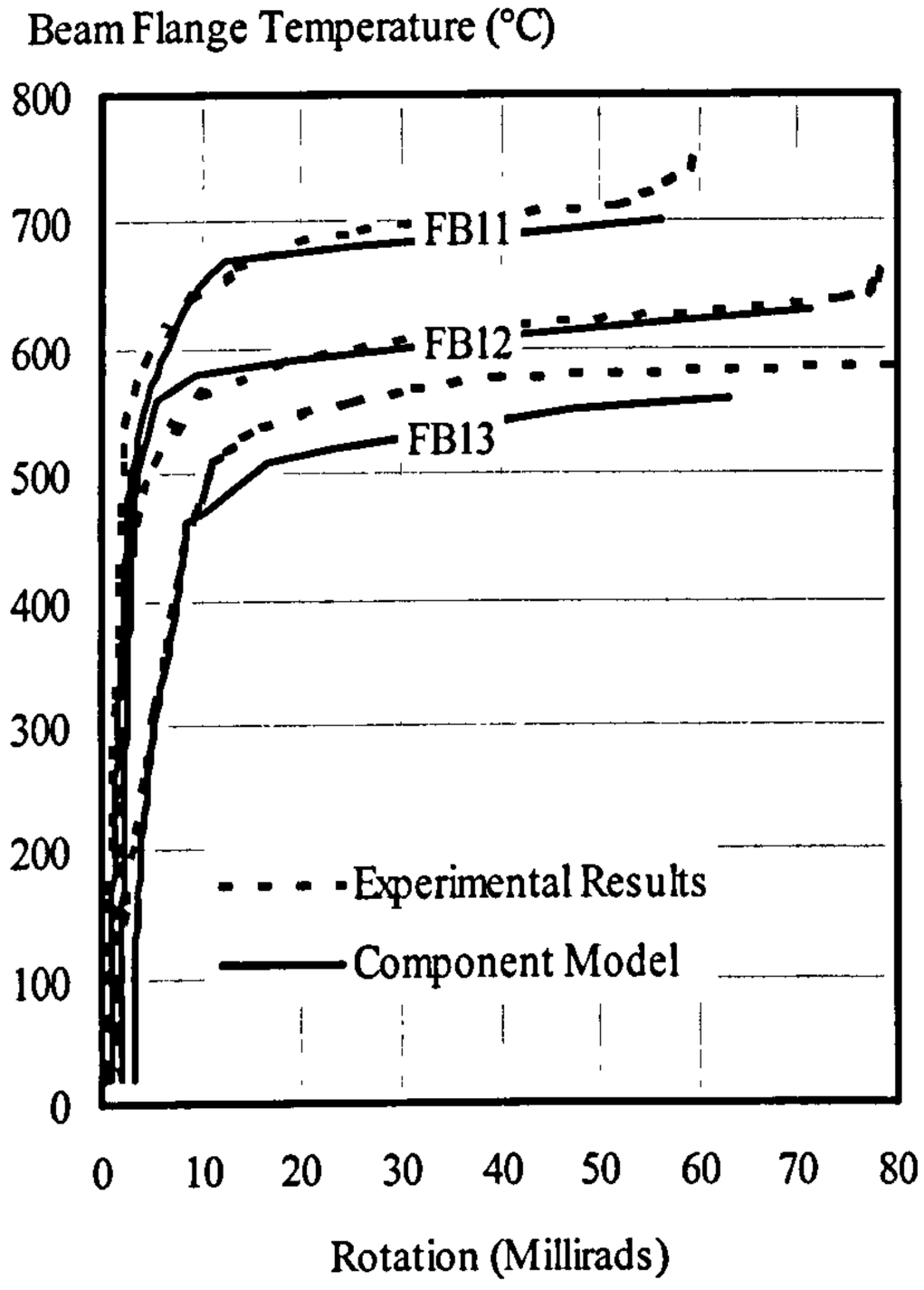

Figure 7.5: Comparison of Predicted Elevated Temperature Response with Group 1 Tests

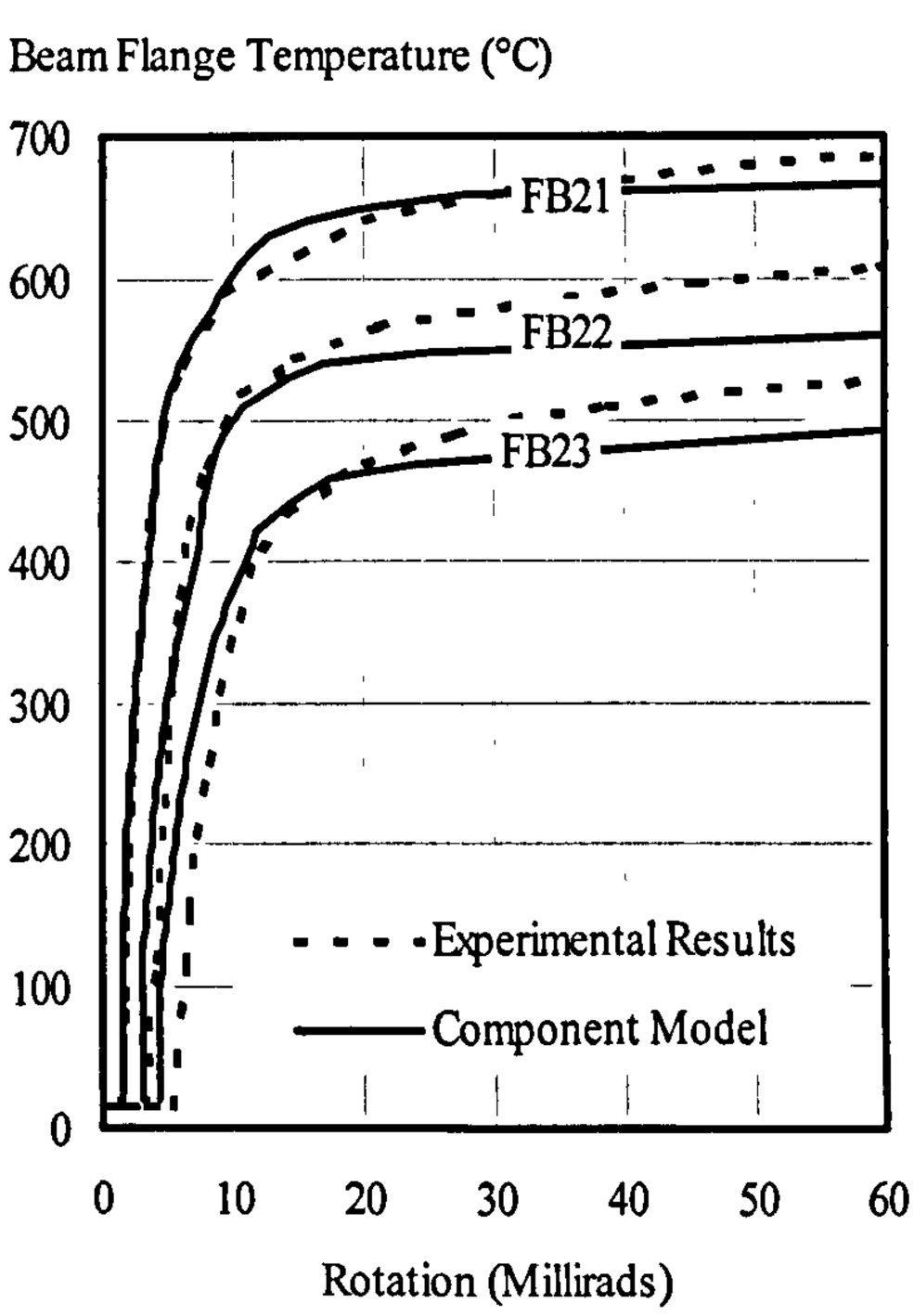

Figure 7.6: Comparison of Predicted Elevated Temperature Response with Group 2 Tests

Three tests in each group were modelled by incorporating a constant moment and generating the temperature-rotation characteristics of the connection. The predicted elevated temperature response of the connections is compared with experimental results as shown in Fig. 7.5 for Group 1 tests and Fig. 7.6 for Group 2 tests. It may be seen that there is reasonable agreement between the predicted and the experimental response. The initial and yielding responses of the connection are well predicted by the model

whereas the model seems to underestimate the connection response in the strain hardening zone. This may be due to a lack of information concerning the strain hardening response of the connection components. In the model the strain-hardening stiffness of the connection components was assigned a reduced value based on the connection initial stiffness. Nevertheless, it is apparent that the component model proposed by Leston-Jones[52] can predict the connection response at both ambient and elevated temperatures to a reasonable accuracy especially in the elastic zone.

7.4 THE COMPONENT MODEL FOR FLEXIBLE END-PLATE CONNECTIONS

Following a similar approach to the one suggested by Leston-Jones[52] a component model was developed for modelling the elevated temperature response for bare-steel and composite flexible end-plate connections. This type of connection is currently very popular because of its ease of fabrication[178]. It was also adopted for the Cardington test frame[179] and the elevated temperature tests described in Chapters 3 and 4 were conducted on such connections.

The proposed model is based on the component-based approach representing the connection as a set of rigid and flexible elements. The connection components assumed when developing this model are the bolts, the column flange and the end-plate which are all assumed to act in the tension zone, and the column web panel in the compression zone. By assembling the stiffnesses of these components in both the tension and compression zones, the entire connection response may be obtained. In such models the accuracy and applicability depend upon the number of components accounted for. As the number of components increases, the accuracy of the model generally improves.

EC3: annex J[40] and similar ambient temperature connection models focus on the elastic response and the capacity of the connection is defined by a plastic plateau. At elevated temperature the entire connection response needs to be considered since large deformations and consequently rotations are possible. Strain hardening of the steel in the plastic zone therefore has a significant influence. To model the full connection response yet avoids complexities arising from full non-linear modelling, a tri-linear representation is proposed. It is assumed that the connection would experience an elastic response (represented by an elastic stiffness) until the onset of plastification as a result of yielding of one or more of the connected components. Then a reduced stiffness representing a strain hardening stiffness may be adopted based upon revised elemental stiffnesses. This procedure is repeated as more elements enter the strain hardening region.

Only those parameters such as elastic modulus, yield and ultimate tensile strength which represent the stiffness and strength of the connection are assumed to degrade with increasing temperatures. The model is capable of allocating individual temperatures to each element at a given bolt row, allowing the modelling of the any form of temperature distribution based on test data or simulations of the temperature profile across the depth of the connection.

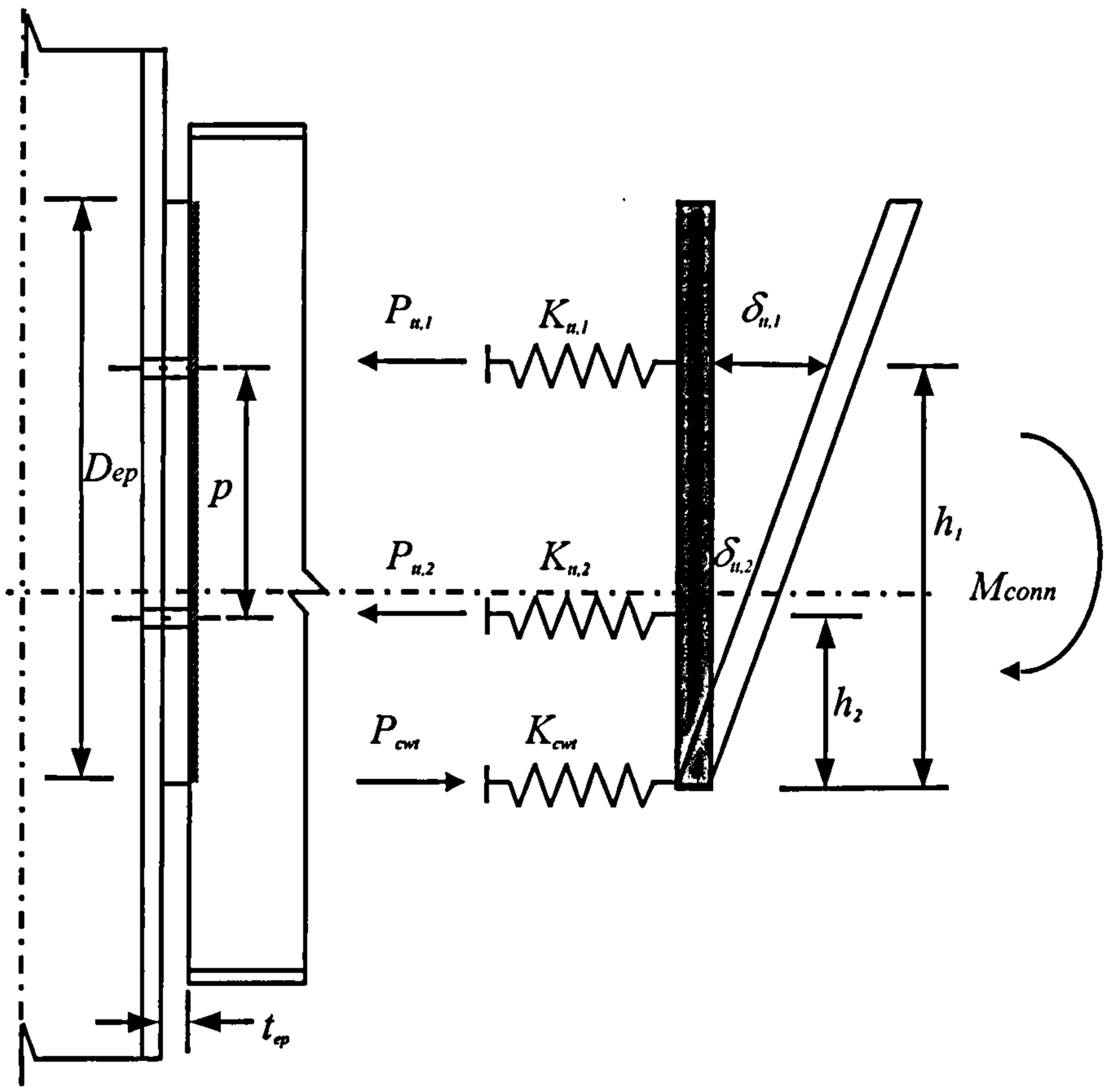

Figure 7.7: General Representation of Bare-steel Component Model

The component model proposed is only applicable to balanced cruciform connection arrangements, in which there is no shear deformation arising from out-of-balance moments. Moreover, the model does not account for the effect of time-dependent factors such as creep.

7.5 BARE-STEEL COMPONENT MODEL

It is believed that by developing a high temperature component connection model similar to that normally proposed at ambient temperature an acceptable representation of connection behaviour may be obtained. Connection elements are simulated by individual springs at each bolt row representing the stiffnesses of the components which are assumed to follow a pre-defined force-displacement relationship. For simplicity, an equivalent single spring stiffness is used to represent the stiffness of all components in the tension zone in accordance with EC3: Annex J[40] whilst the compression zone is defined by a separate spring. A general representation of the bare-steel flexible end-plate model is shown in Fig. 7.7.

One of the main characteristics of a flexible end-plate is that the response has two stages:

1. the unobstructed rotation of the connection, until;
2. the beam lower flange bears against the column.

Prior to contact, the connection is assumed to rotate about the lower edge of the end-plate, whilst after bearing the rotation is assumed to take place at the centre-line of the bottom flange as shown in Fig. 7.8, resulting in an enhanced stiffness and capacity. Due to lack of elevated temperature experimental data for the second stage, only the first stage is accounted for in the model. However, an easy modification of the model is possible to accommodate this response once test data becomes available.

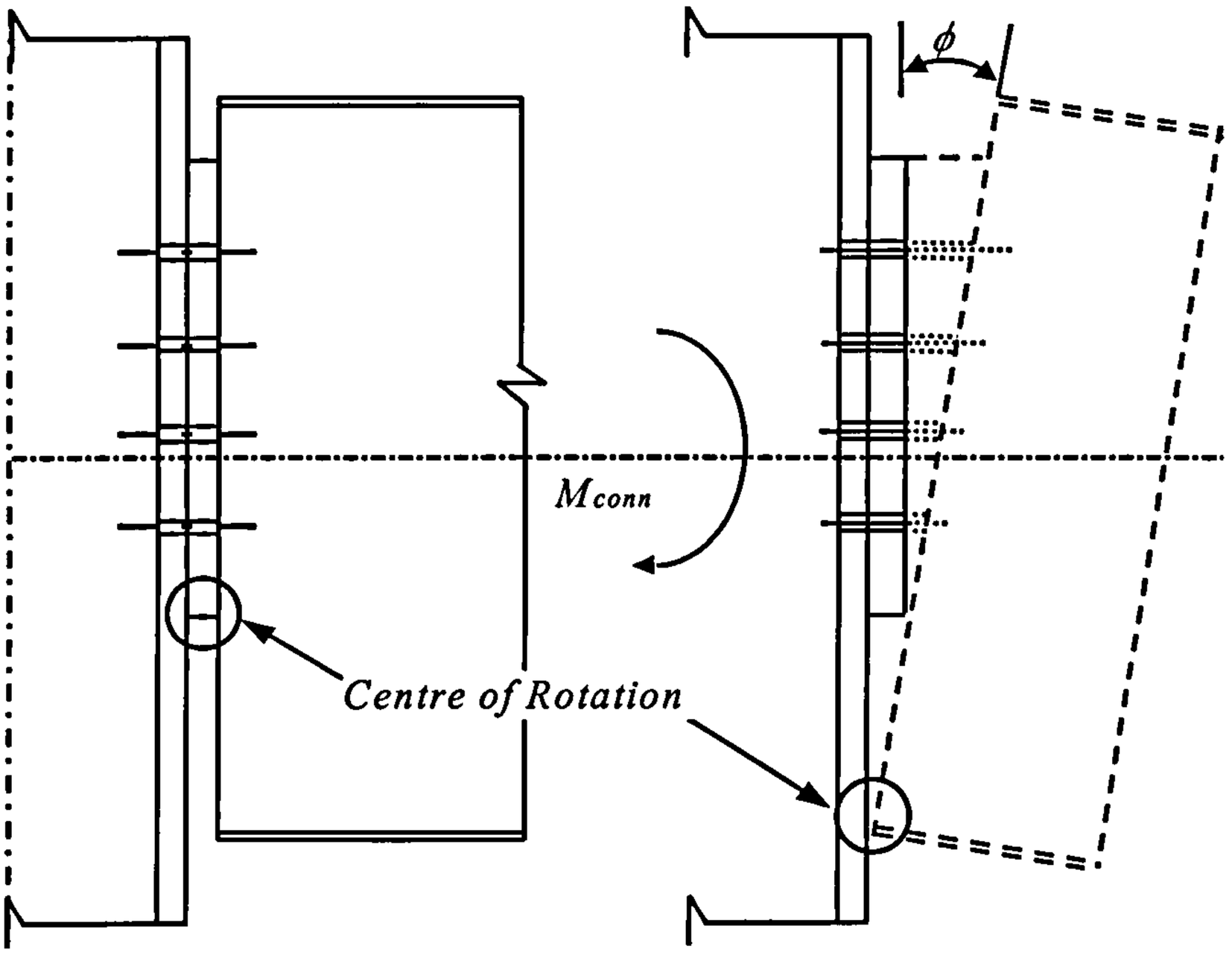

a) Before contact *b) After contact*

Figure 7.8: Behaviour of Flexible End-plate Connection

The following assumptions are adopted in the model:

1. Geometrical properties are nominal values;
2. Material properties for the beam and column sections are based on those presented in Table 2.1, whilst nominal values are adopted for bolts and end-plate;
3. The temperature profile across the connection depth is based on experimental observations;
4. The degradation of structural steel is based on EC3: Part 1.2 recommendations, with a strain level of 0.5% for strength. The degradation of bolt stiffness and capacity is based on recommendations presented by Kirby[71] as discussed in Chapter 2.

The global rotational stiffness, S_{Ct} of the connection can be determined for any given temperature and moment based on the assembled stiffness, K_{eqt}, of the components acting in the tension zone, and the compression zone (i.e. the column web stiffness). The general representation of the bare-steel component-based model is shown in Fig. 7.7. Therefore the overall connection stiffness of the connection may be expressed as:

$$\frac{1}{S_{Ct}} = \frac{1}{S_{tt}} + \frac{1}{S_{ct}} \qquad 7.1$$

$$\frac{1}{S_{Ct}} = \frac{1}{\left(K_{eqt}.z^2\right)} + \frac{1}{\left(K_{cwt}.z^2\right)} \qquad 7.2$$

where,

S_{Ct} = the global connection rotational stiffness of the bare-steel connection for a given temperature;
S_{tt} = the connection rotational stiffness in the tension zone;
S_{cc} = the connection rotational stiffness in the compression zone;
K_{eqt} = the stiffness of the equivalent tension spring;
K_{cwt} = the stiffness of the column web for a given temperature;
z = the distance from the centre of rotation to location of equivalent tension spring (the centre of the tension zone).

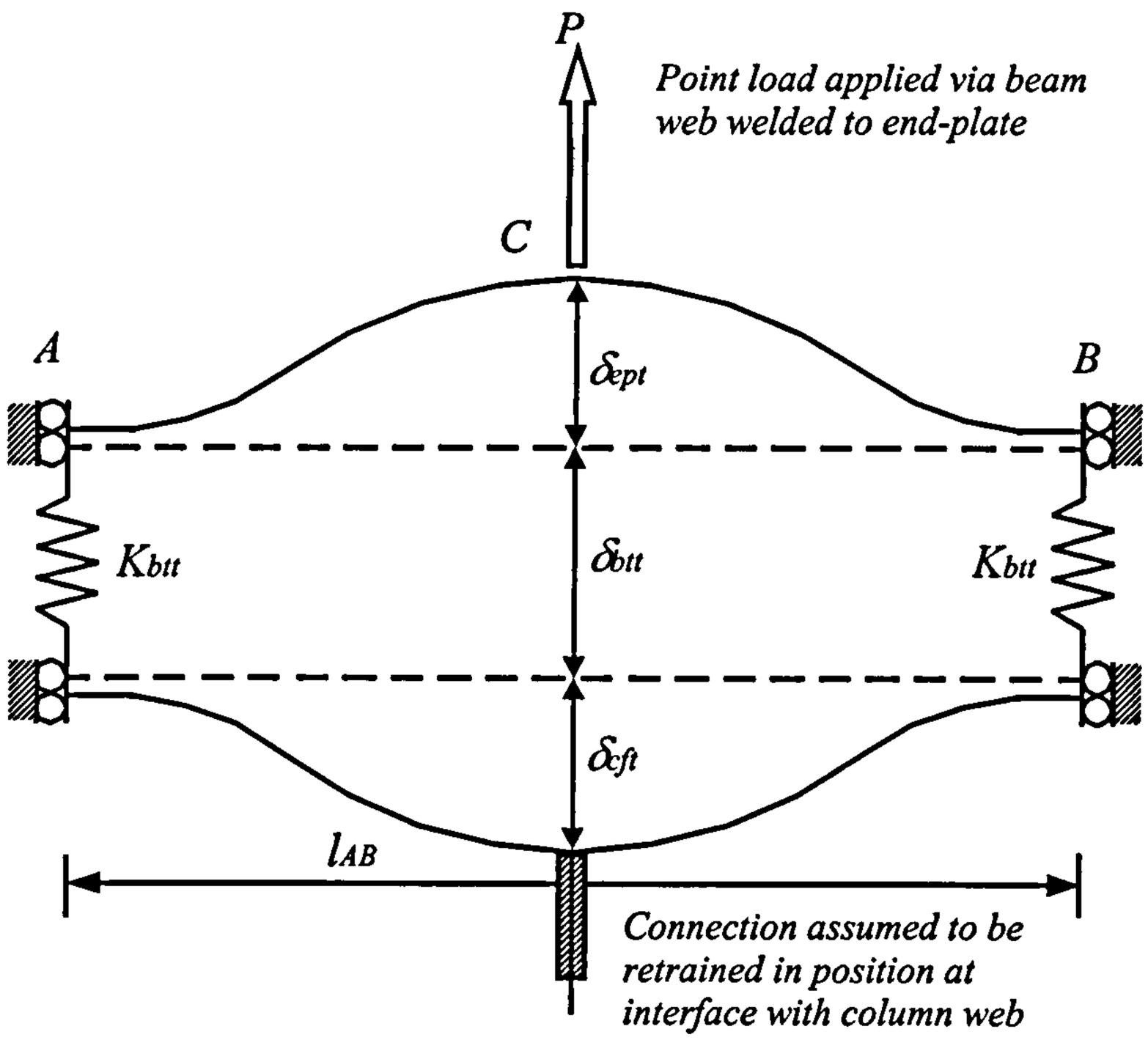

Figure 7.9: Idealised Connection Deformation in the Tension Zone

Fig. 7.9 shows the deformation of components for a typical bolt row acting in tension. The overall stiffness for a bolt row at a given temperature may be written as:

$$\frac{1}{K_{tt,n}} = \frac{1}{K_{ept}} + \frac{1}{2K_{cft}} + \frac{1}{N_{bt}.K_{btt}} \qquad 7.3$$

where

$K_{tt,n}$ = the spring stiffness in the tension zone at a given temperature, for the bolt row under consideration;
K_{ept} = the stiffness of the end-plate;
K_{cft} = the out-of-plane stiffness of the column flange;
K_{btt} = the stiffness of the bolt;
N_{bt} = the number of bolts in tension at a given bolt row.

EC3: Annex J[40] permits the use of a single spring of equivalent stiffness to represent the stiffnesses of the springs in the tension zone where there is more than one bolt row in tension. This can be determined from the following expression:

$$K_{eqt} = \frac{\sum_{n}\left(K_{tt,n}.h_n\right)}{z} \qquad 7.4$$

where

h_n = the distance between bolt row n and the centre of rotation.

When considering the stiffness of the equivalent spring in the tension zone K_{eqt}, it is necessary to determine the distance from the centre of rotation to the location of the equivalent tension spring. This is the lever arm, z. For bolted connections with only a single bolt row in tension, the lever arm, z, is taken as the distance from the centre of rotation to the centre-line of the bolt row in tension as illustrated in Fig. 7.10*(a)*. However, for connections with more than one bolt row acting in tension (Fig. 7.10*(b)*), the lever arm, z, may be calculated by the following expression:

$$z = \frac{\sum_{n}\left(K_{tt,n}h_n^2\right)}{\sum_{n}\left(K_{tt,n}h_n\right)} \qquad 7.5$$

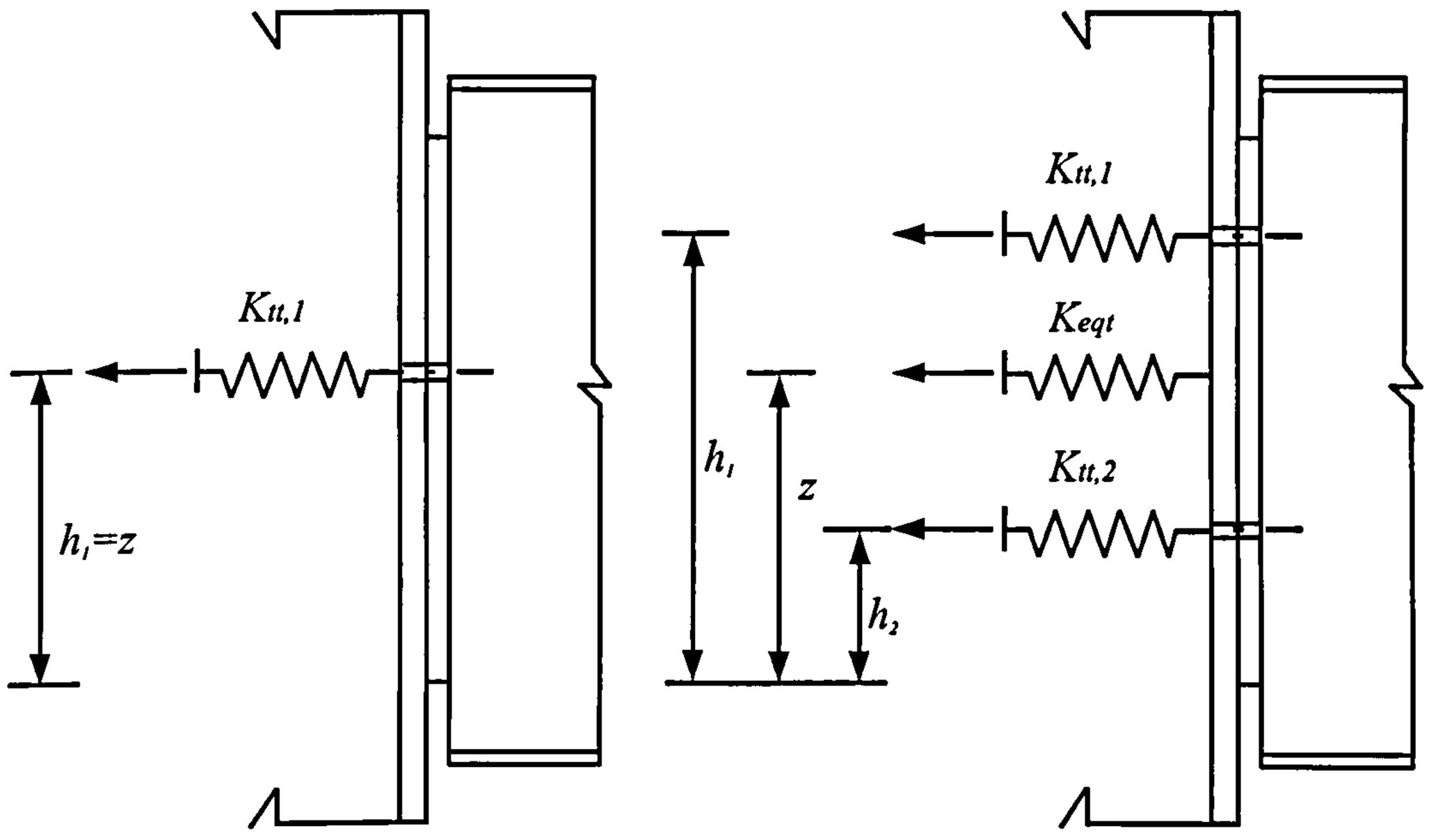

(a) single bolt row in tension *(b) more than one bolt row in tension*

Figure 7.10: Determination of Lever Arm z

A number of force distribution models have been suggested[180] for estimating the capacity of the connection. This requires the capacities of individual elements in the model to be determined. The distribution of internal forces within the connection may be assumed to follow the pattern presented in Fig. 7.11. At low load levels, the force

distribution pattern shown in *(a)* is usually accepted. As the loading increases, the distribution of internal forces tends to the one presented in *(b)*. Based upon experimental observations, it was suggested that such a pattern provides a reasonable representation of the internal force distribution in the elastic region. To model force distribution in the plastic region and up to failure, a plastic distribution is used in the model as shown in *(c)*. Each bolt row is allowed to attain its full design strength. If this condition is not satisfied then the force in the lower bolt is restricted to a value derived from the linear distribution pattern *(a)*. By knowing the connection rotation and bolt row stiffness, the internal force at a given bolt row, F_n may be calculated as:

$$F_n = \phi . K_{tt,n} . h_n \qquad 7.6$$

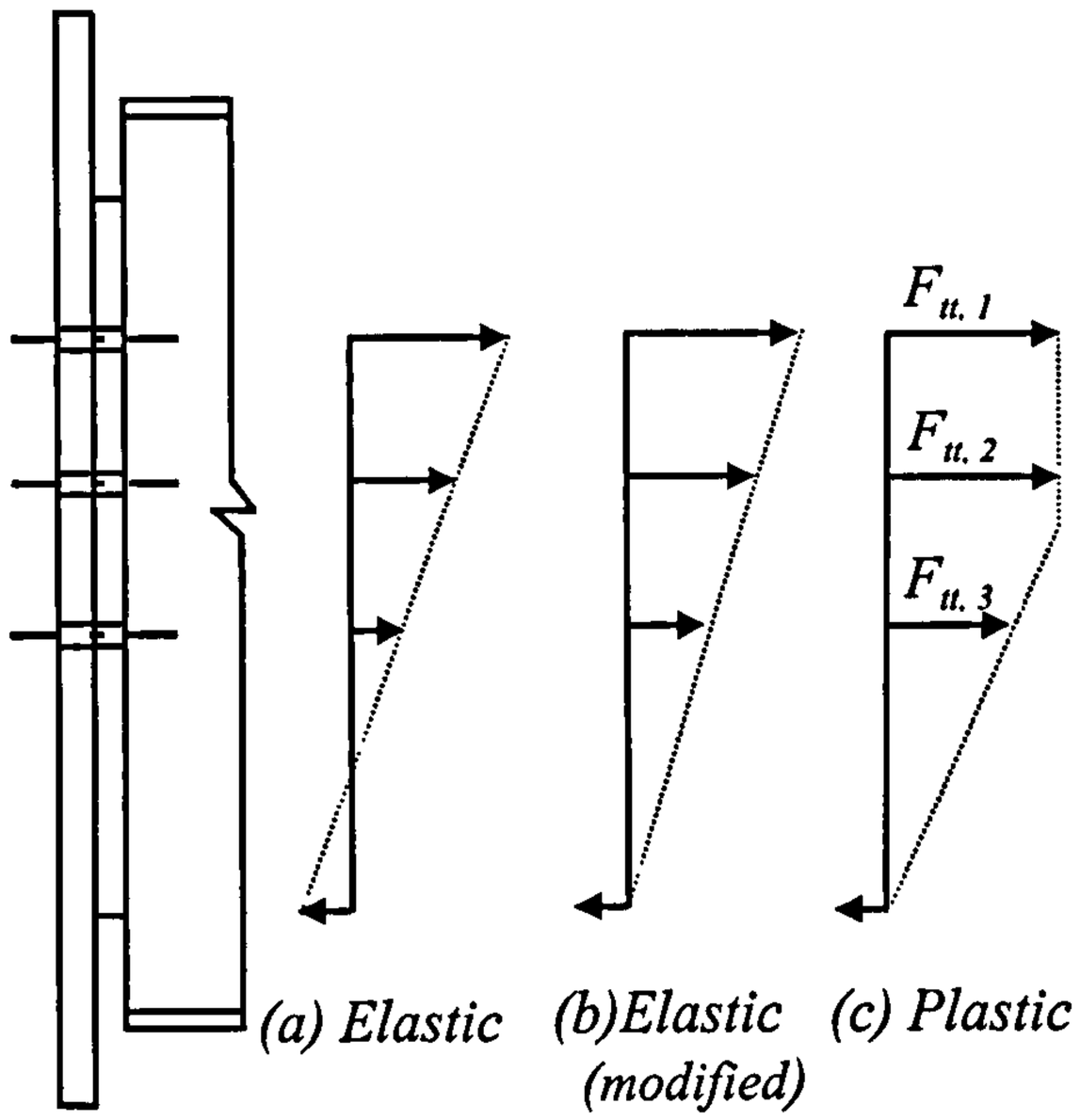

Figure 7.11: Force Distribution Patterns

In order to determine the overall stiffness and capacity of the connection, the response of individual connection elements must be evaluated. The sections below describe the models used to describe these.

7.5.1 Column Flange Behaviour

In order to simulate the column flange in the tension zone, the model proposed by Jaramillo[181] is adopted. Jaramillo idealised the column flange as an infinitely long cantilever plate of breadth, a, and thickness t_{cf}, subject to a transverse random point load P, acting at a distance s from the support as shown in Fig. 7.12. Hence, the out-of-plane stiffness of the column K_{cft} in the tension zone may be given as follows:

$$K_{cft} = \frac{\pi D}{\beta a^2} \qquad 7.7$$

where,

D = The flexural rigidity of the plate;

β = dimensionless coefficient;
a = half the column flange width = ($B_{cf}/2$)

The term 'D' may be evaluated using the following expression:

$$D=\frac{E_{st}\, t_{cf}^{3}}{12(1-\upsilon^{2})} \qquad 7.8$$

where,

E_{st} = Modulus of elasticity for steel at a given temperature;
t_{cf} = The column flange thickness;
ν = The Poisson's ratio for steel (≈ 0.3).

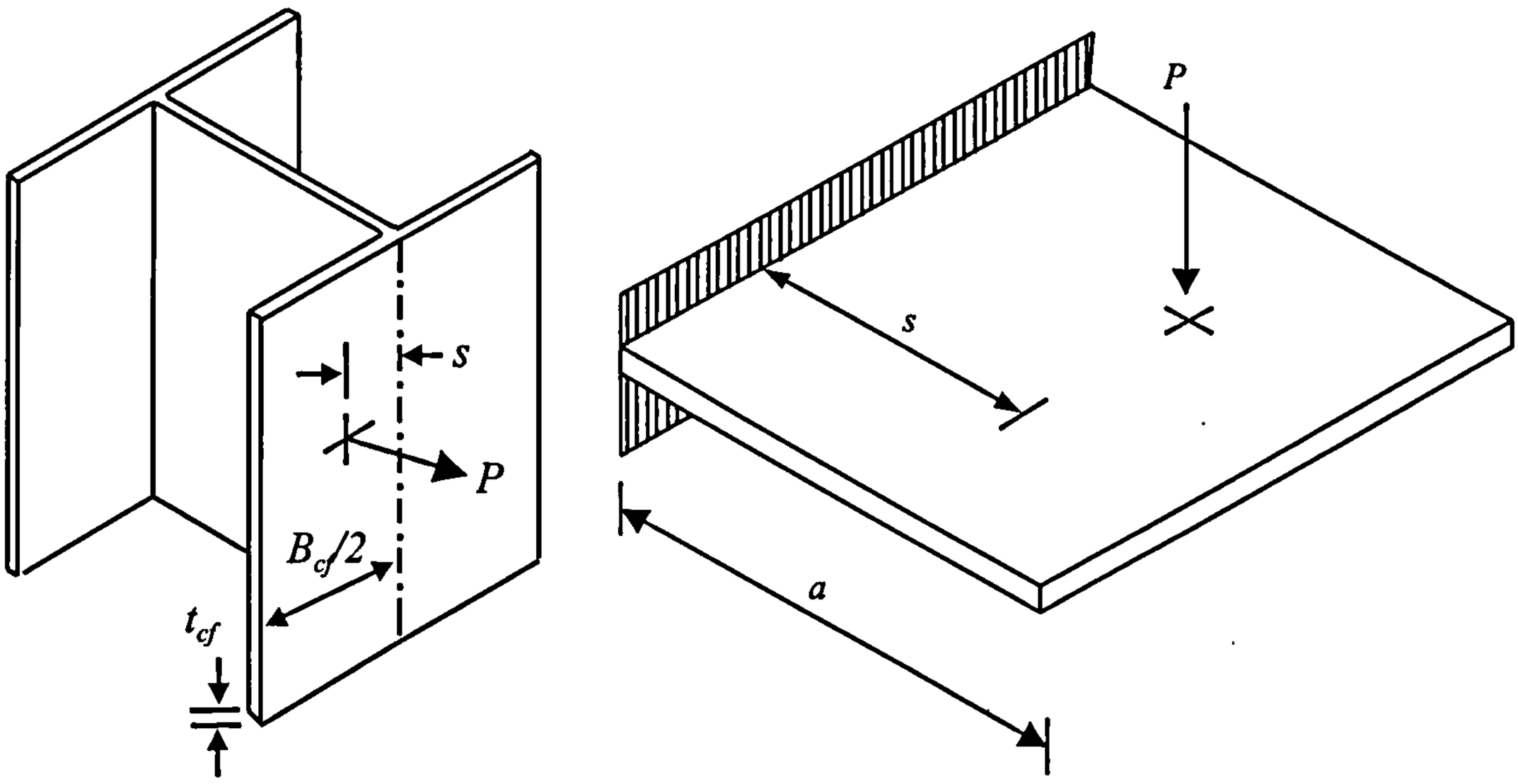

(a) Column flange subject to point load *(b) Infinitely long cantilever plate*

Figure 7.12: Idealisation of Column Flange Response in the Tension Zone

The dimensionless coefficient β is a function of the distance s which is the distance from the centre-line of the column web to the centre of the bolt hole, s *(= gauge length/2)*, and half flange breadth, a. Representative values of β for different values of *(s/a)* are given in Table 7.1 below:

Table 7.1: Values of Coefficient β

s/a	0.25	0.50	0.75	1.00
β	0.0168	0.0794	0.220	0.525

In order to represent values of β, a third order polynomial has been fitted to the values in Table 7.1, as shown in Fig. 7.13 and expressed as follows:

$$\beta = -0.0542 + 0.416\left(\frac{s}{a}\right) - 0.7584\left(\frac{s}{a}\right)^2 + 0.9216\left(\frac{s}{a}\right)^3 \qquad 7.9$$

The force F_{cfpt} that causes plastification within the column flange, at a given temperature, may be defined as:

$$F_{cfpt} = \frac{f_{ycft} t_{cf}^2 l_{eff\_cf}}{m} \qquad 7.10$$

where

f_{ycft} = the yield strength of the column flange at a given temperature;
l_{eff_cf} = the effective length assuming the column flange to act as an equivalent T-stub;
m = the distance from bolt centre to 20% into the column root radius.

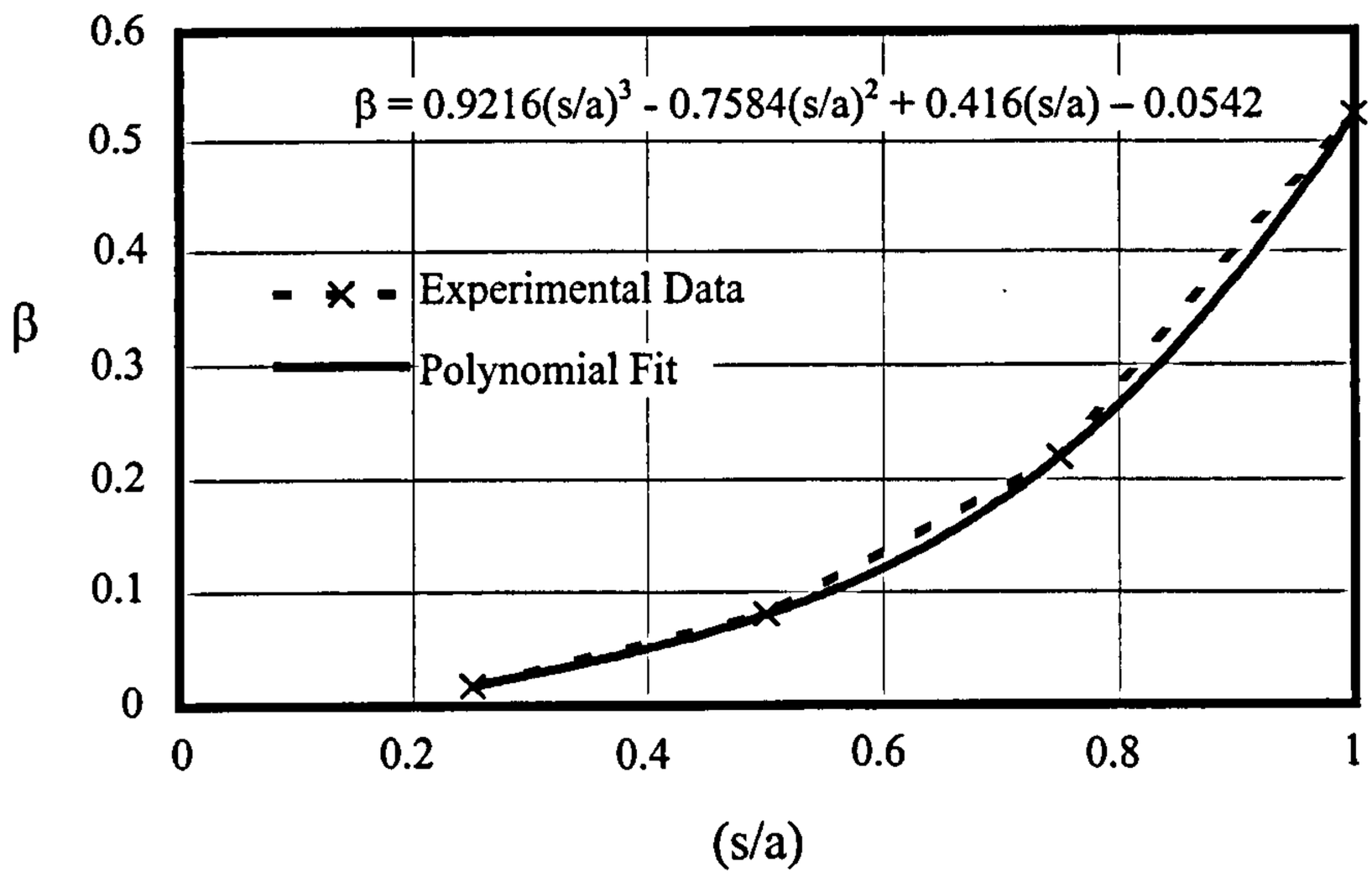

Figure 7.13: Polynomial Fitting for Values of β

The determination of the effective length for the column flange is based on the yield line method recommended in EC3: Annex J[40] for an equivalent T-stub as presented in Appendix C.

Following the onset of plasticity, a strain-hardening stiffness is adopted and may be expressed as:

$$K_{cfpt} = \mu_s K_{cft} \qquad 7.11$$

where,

K_{cfpt} = the strain hardening spring stiffness of column flange at a given temperature;
μ_s = the strain hardening coefficient for structural steel.

The strain hardening coefficient is defined as the ratio of the strain hardening stiffness to the elastic stiffness and is usually based on existing data. Due to the lack of available test data, Atamaz Sibai and Frey[129] recommended a value in the range 0.019-0.024 for mild steel at ambient temperature. Recently, Ren and Crisinel[182] adopted a value of 0.06 for modelling of double web cleat connections at ambient temperature. In the current model a strain hardening coefficient of 0.05 is adopted. Due to lack of experimental data describing the strain hardening at elevated temperature, the same coefficient is used as at ambient temperature.

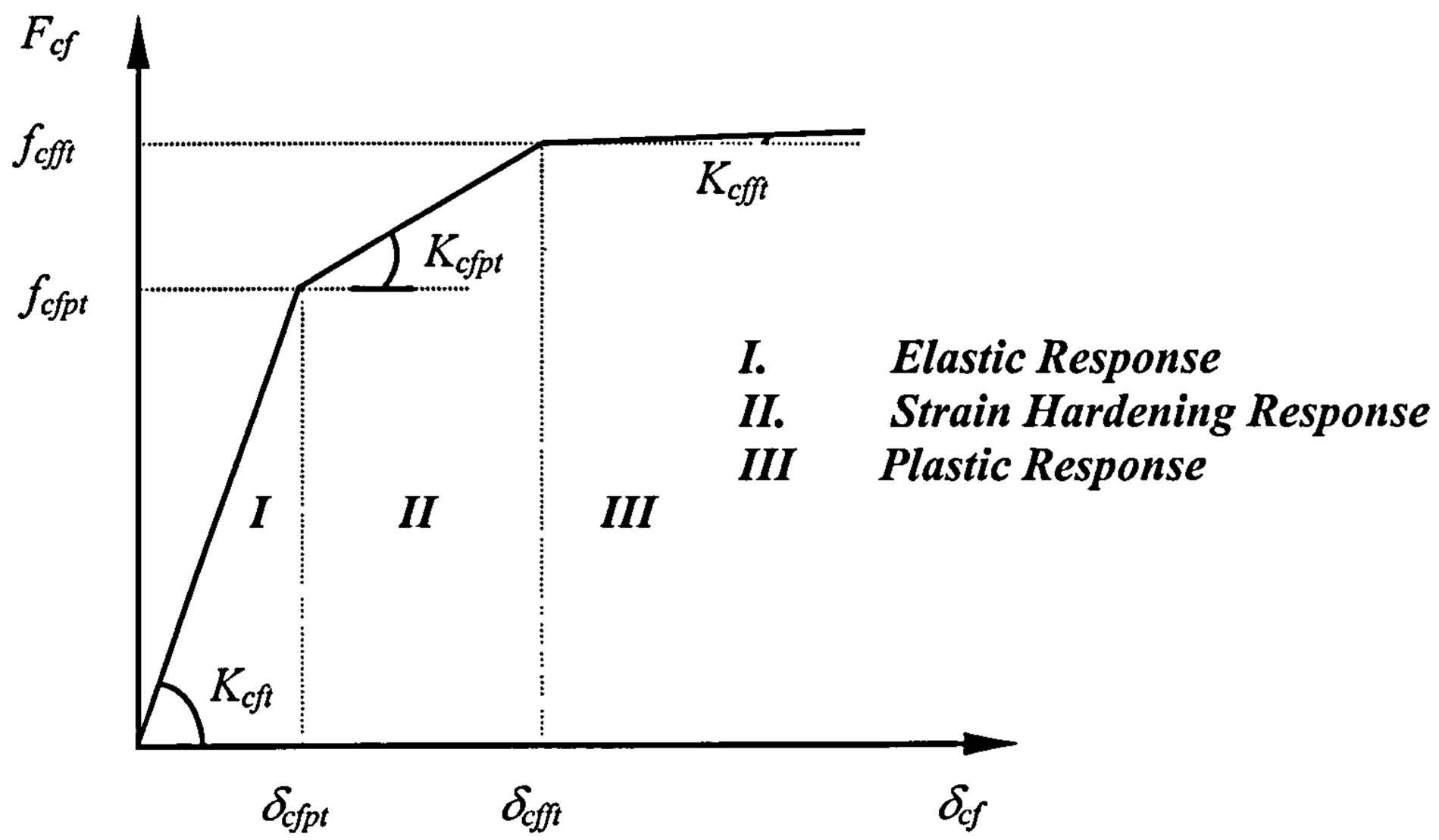

Figure 7.14: Assumed Load-Displacement Relationship

The ultimate capacity of the column flange may be assessed in a similar manner to the plastic capacity as expressed in Eq. 7.10, replacing the yield strength of the column flange with the ultimate strength f_{ucft}. Following the onset of failure, the stiffness of the column flange approaches zero. The final stiffness K_{cfft} may be calculated using a reduced stiffness coefficient of 0.01 and expressed as:

$$K_{cfft} = 0.01K_{cft} \qquad 7.12$$

Despite the fact that EC3[183] suggests a final coefficient of approximately 0.0001 at ambient temperature, the value adopted in the model was found to generate a closer prediction of the connection response. This is probably due to the much higher levels of rotation experienced at elevated temperature. The resulting form of force-displacement response adopted is shown in Fig. 7.14. The other connection components are assumed to behave in a similar manner to the column flange as described below. The degradation of the column flange stiffness and capacity may be based on recommendation presented in Chapter 2.

7.5.2 Bolt Behaviour

When studying the bolt behaviour, two phenomena should be considered which can have considerable influence. These are the pre-stress forces in the bolts and the

existence of prying forces. The former can have beneficial effects on the behaviour of the bolts as little deformation would occur until the external force exceeds the pre-stress forces, while the latter can have a detrimental effect, increasing the loading applied to the bolts and thus deformation. Prying forces are contact forces developed between the end-plate and the column flange caused by bending curvature of the end-plate.

The influence of prying forces could be significant in the case of flexible end-plates, with flexural deformations within the plate inducing additional prying forces in the bolts, possibly resulting in a reduction in overall connection stiffness and capacity.

The bolts are considered to be subjected to direct tensile force in isolation. By applying the principles of Hooke's law, the elastic stiffness of the bolt K_{btt} may be expressed as:

$$K_{btt} = \frac{A_s . E_{btt}}{l_{btt}} \qquad 7.13$$

where,

A_s = the bolt shaft area;
E_{btt} = modulus of elasticity of the bolts at a given temperature;
l_{btt} = the bolt elongation length

In determining the bolt elongation, Agerskov[184] reported that the influence of nut and washer had not been taken into account in previous analytical models. He suggested that the effect of these should be considered and proposed the length of the bolt may be adopted as equivalent to the total thickness of the end-plate, column flange and washers (grip length) in addition to half the height of the bolt head and nut. Yee and Melchers[185] subsequently included the influence of washer and nut on the bolt behaviour. Leston-Jones[52] also considered this when studying the behaviour of flush end-plates at elevated temperature. The bolt elongation may be obtained from the following relationship based on Agerskov[184] recommendations:

$$l_{btt} = t_{ep} + t_{cf} + 2.t_w + \left(\frac{t_{bh} + t_{bn}}{2} \right) \qquad 7.14$$

where,

t_{ep} = the thickness of the end-plate;
t_w = the thickness of the washer;
t_{bh} = the thickness of the bolt head;
t_{bn} = the thickness of the bolt nut

The force, F_{btpt} that causes yielding within the bolts, at any given temperature, may be defined as:

$$F_{btpt} = f_{ybtt} . N_{bt} . A_s \qquad 7.15$$

where,

f_{ybtt} = the yield strength of bolts for a given temperature (yield strength reduced to allow for prying forces).

It is worth mentioning that in Table 32 of BS5950[39] the bolt strength values are reduced to take into consideration the effect of prying forces. Subsequent to the onset of plasticity, a reduced stiffness may be assumed as for the column flange in order to avoid computational difficulties. The degradation of the connection stiffness and capacity may be based on the recommendations presented in Chapter 2.

7.5.3 End-Plate Behaviour

When load is applied to the connection and the end-plate is pulled away from the column face, it is assumed that the element is subject to pure bending. A number of authors[102,173,176] have considered a flexible end-plate to act simply as a rigidly fixed beam subject to a point load. The end-plate component is considered to act as a T-section, where the flange of the T represents the end-plate, and the stem simulates the beam web. The end-plate is restrained against rotation by the weld which connects the beam web, and at bolt locations. Due to the non-uniform deformation the end-plate experienced in the vertical direction, it must be subdivided into a finite number of segments with an effective width d_y. Fig. 7.15 shows the idealisation of the end-plate in the tension zone. From simple beam-deflection theory, it may be shown that the elastic end-plate stiffness, K_{ept} may be expressed as:

$$K_{ept} = \frac{16 E_{st} d_y t_{ep}^3}{l_{AB}^3} \qquad 7.16$$

Where,

d_y = the assumed effective width for the end-plate segment =(D_{ep}/n);
l_{AB} = the assumed length of the end-plate element = (gauge length less diameter of bolt hole);
D_{ep} = the depth of the end-plate;
n = the number of tension springs considered in the model.

Based on a series of ambient temperature tests, this approach has been validated by Kennedy and Hafez[173], taking into account a practical range of end-plate thicknesses, connection depths and gauge lengths.

The stiffness of the end-plate is assumed to be elastic until the formation of plastic hinges. The force F_{eppt} which causes yielding of the element at a given temperature may be expressed as:

$$F_{eppt} = \frac{2.f_{yept}.t_{ep}^2.d_y}{l_{AB}} \qquad 7.17$$

where,

F_{eppt} = the yield strength of the end-plate at a given temperature,

Strain hardening and final stiffnesses of the end-plate may be estimated based on the principles presented for the end-plate.

It is worth remembering that the model is only applicable for the first stage of response (i.e. before the beam bears against the column), due to lack of elevated temperature data

describing the second stage of response. However, a detailed description of the second stage response of the end-plate has been presented by Madas[176] for ambient temperature conditions.

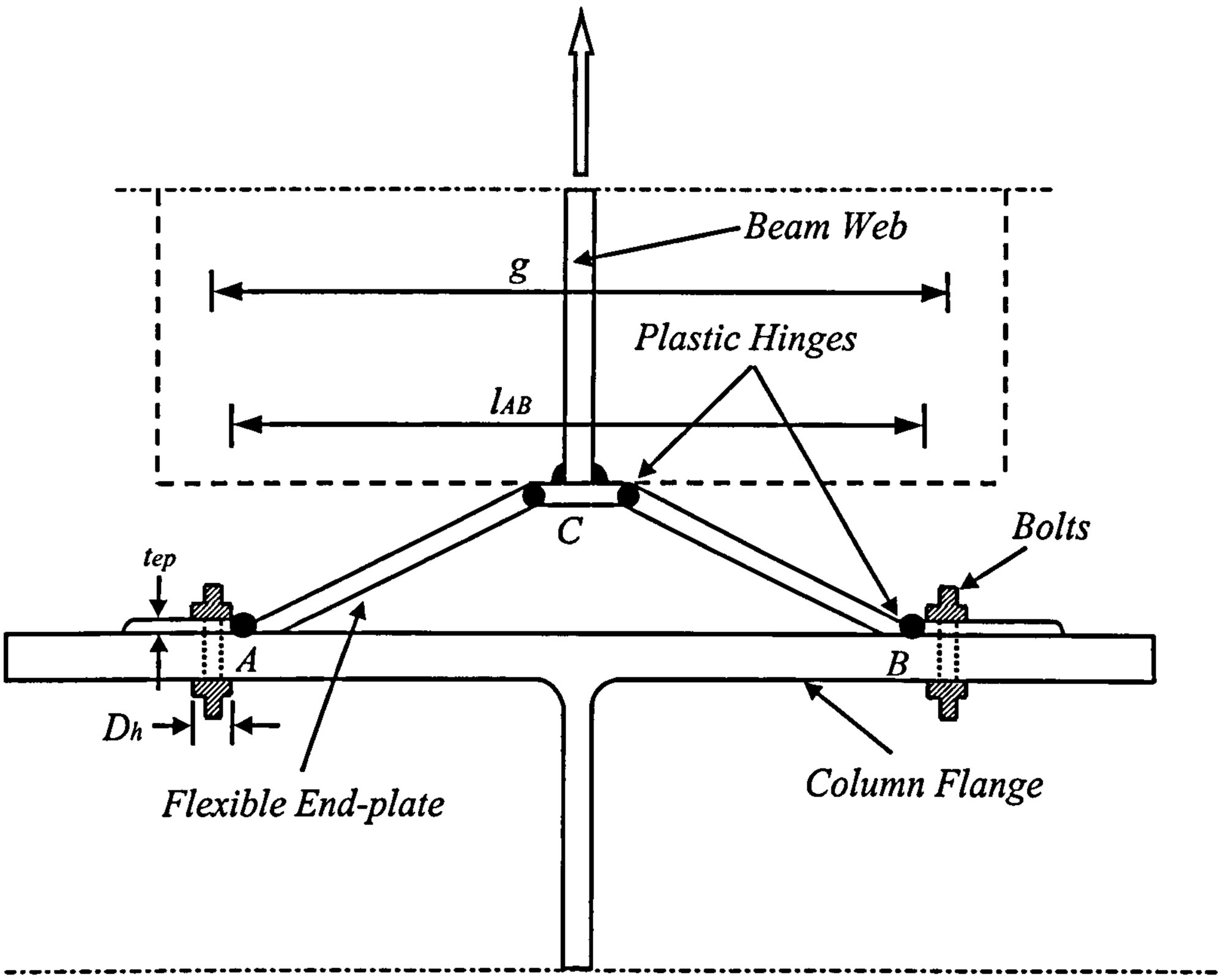

Figure 7.15: Deformed Flexible End-plate

7.5.4 Column Web Behaviour

The column web in the compression zone can have a significant influence on the overall connection response especially in the case of unstiffened connections which are popular for economic reasons. In the case of stiffened connections, however, the influence of the column web deformation becomes negligible and it may be assumed to be infinitely stiff.

The stiffness of the column web K_{cwt} in the compression zone may be estimated by idealising it as a plate of dimensions d_c x b_{eff} subject to a uniform compressive force from the beam over the whole depth of the end-plate. Also, the plate is assumed to be fully restrained in the vertical direction as shown in Fig. 7.16. By assuming that the plate obeys Hooke's law, the elastic stiffness of the column web may be expressed as:

$$K_{cwt} = \frac{E_{st}\, t_{cw}\, b_{eff}}{d_c} \qquad 7.18$$

Where,

t_{cw} = the thickness of the column web;
b_{eff} = the assumed effective width of the column web;

d_c = the depth of the column flange between fillets.

Previous studies[186,187] on simple connections - mainly web cleats and fin-plates - have revealed that the depth of the compression zone in the column web can be as great as the depth of the end-plate as shown in Fig. 7.16. Therefore, the effective column web area resisting the compression force is substantial and overstressing of the column web is unlikely. However, for flexible end-plate connections, this is may be true up to the point when the beam flange comes into contact with the column, but after this overstressing may occur in some cases. For simplicity overstressing forces may be neglected and it seems reasonable to assume the effective compression area covers the whole end-plate depth and is large enough to resist any compression force applied. Therefore the effective width of the column flange in the compression zone may be determined from the following expression:

$$b_{eff} = D_{ep} + 5k \qquad 7.19$$

where,

k = the distance from the outer face of the flange to the web toe fillet;
$k = t_{cf} + r_c$;
r_c = the column root radius.

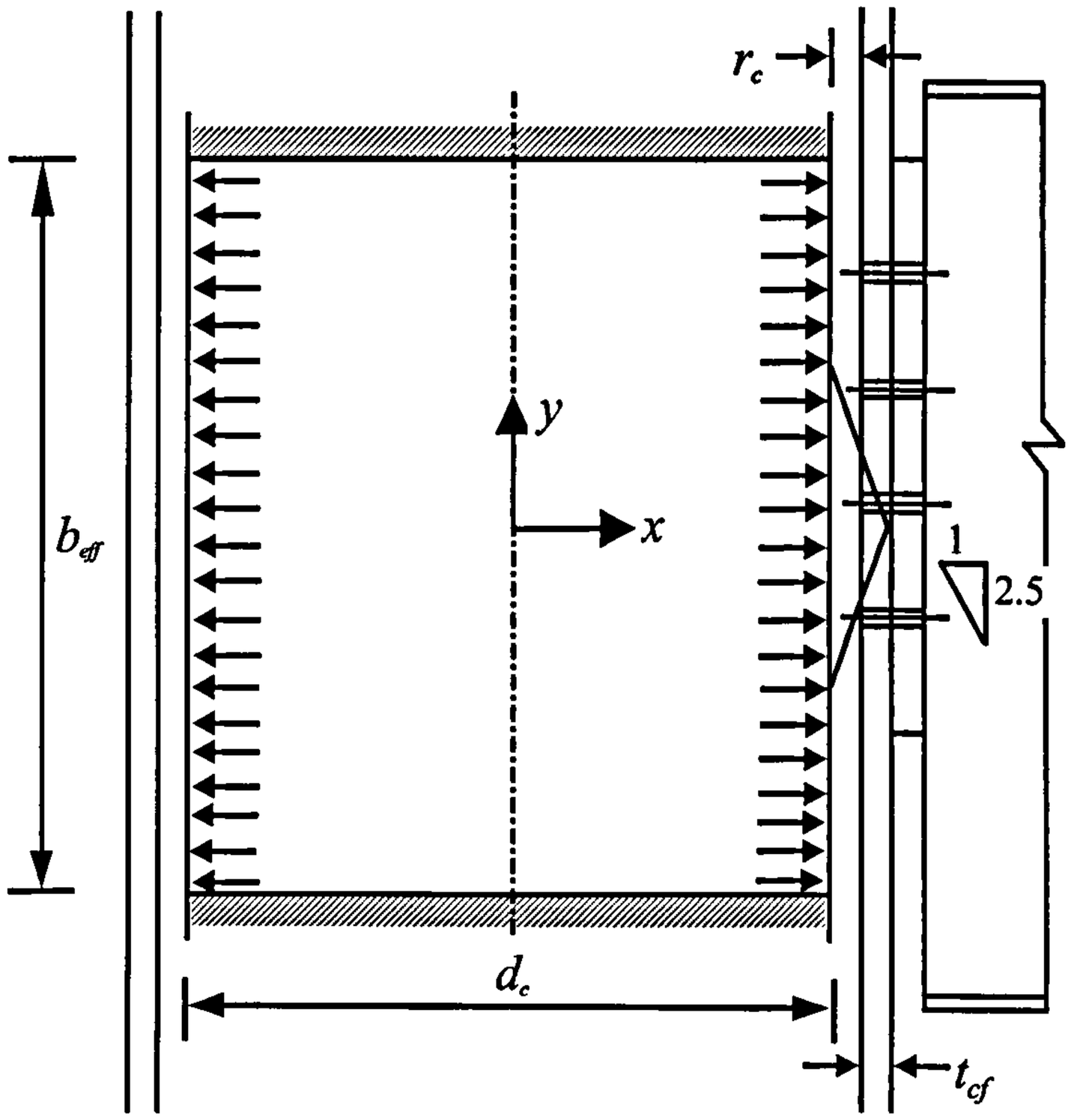

Figure 7.16: Idealised Column Web Behaviour in Compression Zone

When the column web is subject to a compression force, the stiffness of the column web is assumed to remain constant until one of two modes of failure occurs within the depth of the column web. These are compression (i.e. crushing) of the web close to the flange or buckling of the web over part or most of the depth of the member. The former is

likely to take place in ordinary rolled I or H beams, whilst the latter is dominant in welded built-up members, members with slender webs and members of high strength steel grades. The critical force F_{cwpt} for the column web may be determined as the lesser of the buckling and compression forces as described below:

7.5.4.1 Compression Resistance

The compression resistance is based on the assumption that the compression force applied is distributed across the depth of the end-plate and the column flange is assumed to act as a bearing plate. Therefore the force that causes crushing F_{ccwt}, at a given temperature may be given by the following expression:

$$F_{ccwt} = b_{eff}\, t_{cw}\, f_{ywt} \qquad 7.20$$

where,

f_{ywt} = the column web yield strength at a given temperature;

7.5.4.2 Buckling Resistance

When considering buckling of the column web, the effective buckling width of the column needs to be defined. The buckling force F_{bcwt} of the column web at a given temperature based on the empirical relationship suggested by Ahmed *et al.*[187] may be written:

$$F_{bcwt} = 8.4 b_{eff-b}^{0.017} . D_c^{0.60} . t_{cw}^{1.43} . f_{ywt}^{0.76} \qquad 7.21$$

where,

$b_{eff\text{-}b}$ = the effective buckling width of the column web;

$b_{eff\text{-}b} = \sqrt{\left(D_c^2 + D_{ep}^2\right)}$;

D_c = depth of the column.

Therefore, the critical force of the column web may be determined as:

$$F_{cwpt} = Min.\ of \begin{bmatrix} Eq.\ 7.20 \\ Eq.\ 7.21 \end{bmatrix} \qquad 7.22$$

Subsequent to the onset of plasticity, a reduced stiffness must be adopted. In order to estimate the post buckling stiffness of the column web, the technique proposed by Walker[188] has been used. By using a McLaurin series of expansion, Walker assessed the post buckling stiffness of flat plates in order to analyse shells in the post buckling range. The column web in the compression zone was simulated as a simply supported plate subjected to a uniform compression force. Hence, the post buckled stiffness for the column web in the compression zone K_{cwpt} may be expressed as:

$$K_{cwpt} = \frac{K_{cwt}}{2.45} \qquad 7.23$$

The above expression has previously been used by Yee and Melcher[185] in order to describe the post-buckled behaviour of the column web in the compression zone for both bare-steel and composite connections. It is worth mentioning that the plastic stiffness may be based on the above recommendations irrespective of whether compression or buckling dominates.

7.5.5 Verification of the Proposed Model

Before verifying the model against elevated temperature tests, initial verification was carried out at ambient temperature as shown in Fig. 7.17. This was based on relevant data from the current Group 3 tests as well as existing test data reported by Boreman *et. al.*[100]. The proposed model predicts closely the initial stiffness of the connection but underestimates the response in the plastic zone. This may be attributable to the lack of experimental data in the strain hardening zone which represents a large proportion of the moment-rotation response. Also, the ultimate capacity of the connection is underestimated with a maximum difference of about 10 kNm. Further investigation is therefore required in the plastic zone.

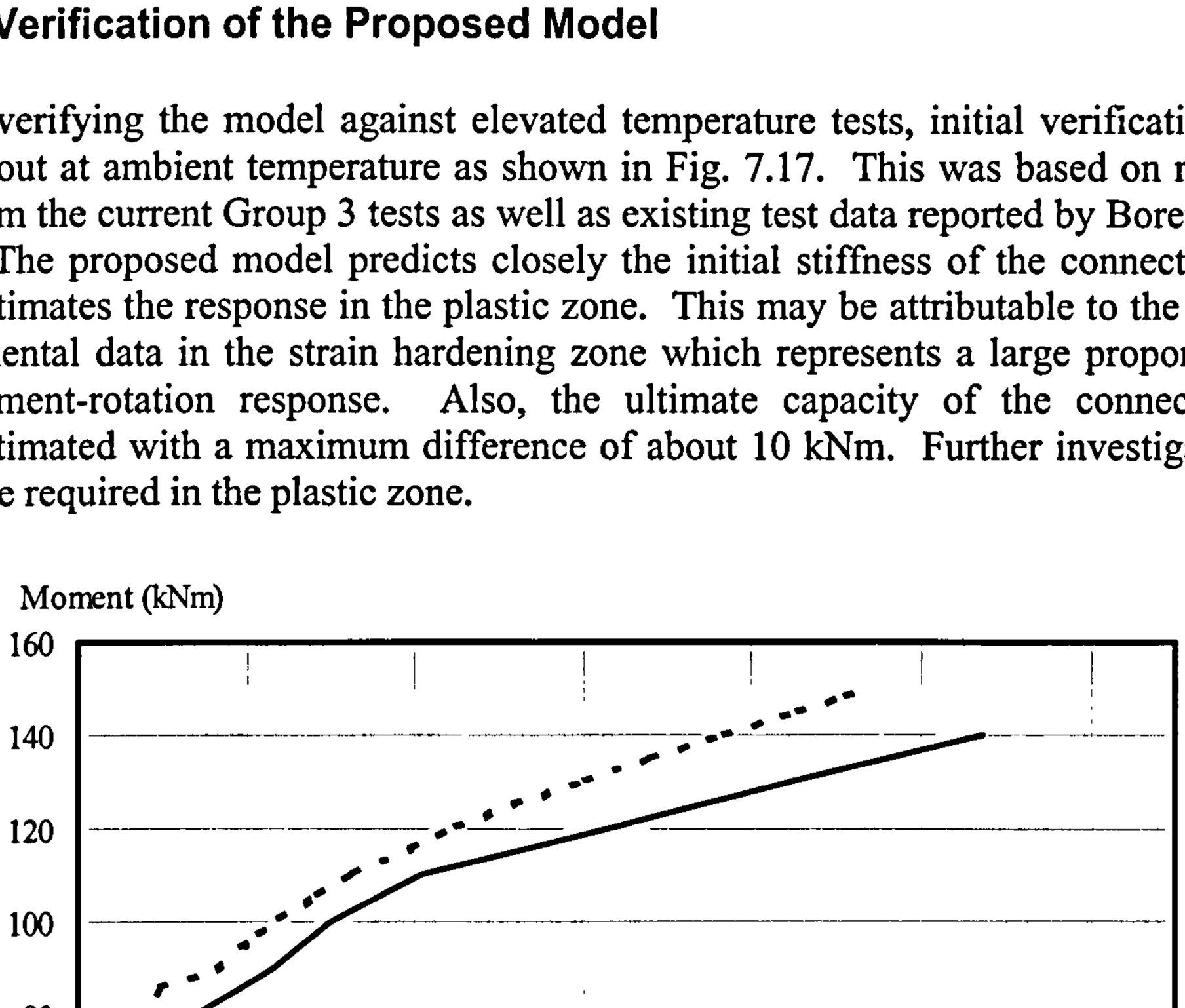

Figure 7.17: Comparison of Predicted Ambient Temperature Response with Tests Results

Fig. 7.17 also shows a comparison between the model and the experimental ambient temperature response of Group 3 connections, using measured material properties. The initial stiffness and strain hardening stiffness of the connection is closely represented, but it was not possible to compare the ultimate capacity because only the first stage of response (i.e. before the beam bears against the column) is accounted for in the model. The predicted mode of failure of the connection was end-plate deformation similar to

that observed experimentally. The predicted failure mode was associated with the behaviour of the end-plate. This agrees with experimental observations of excessive end-plate deformation.

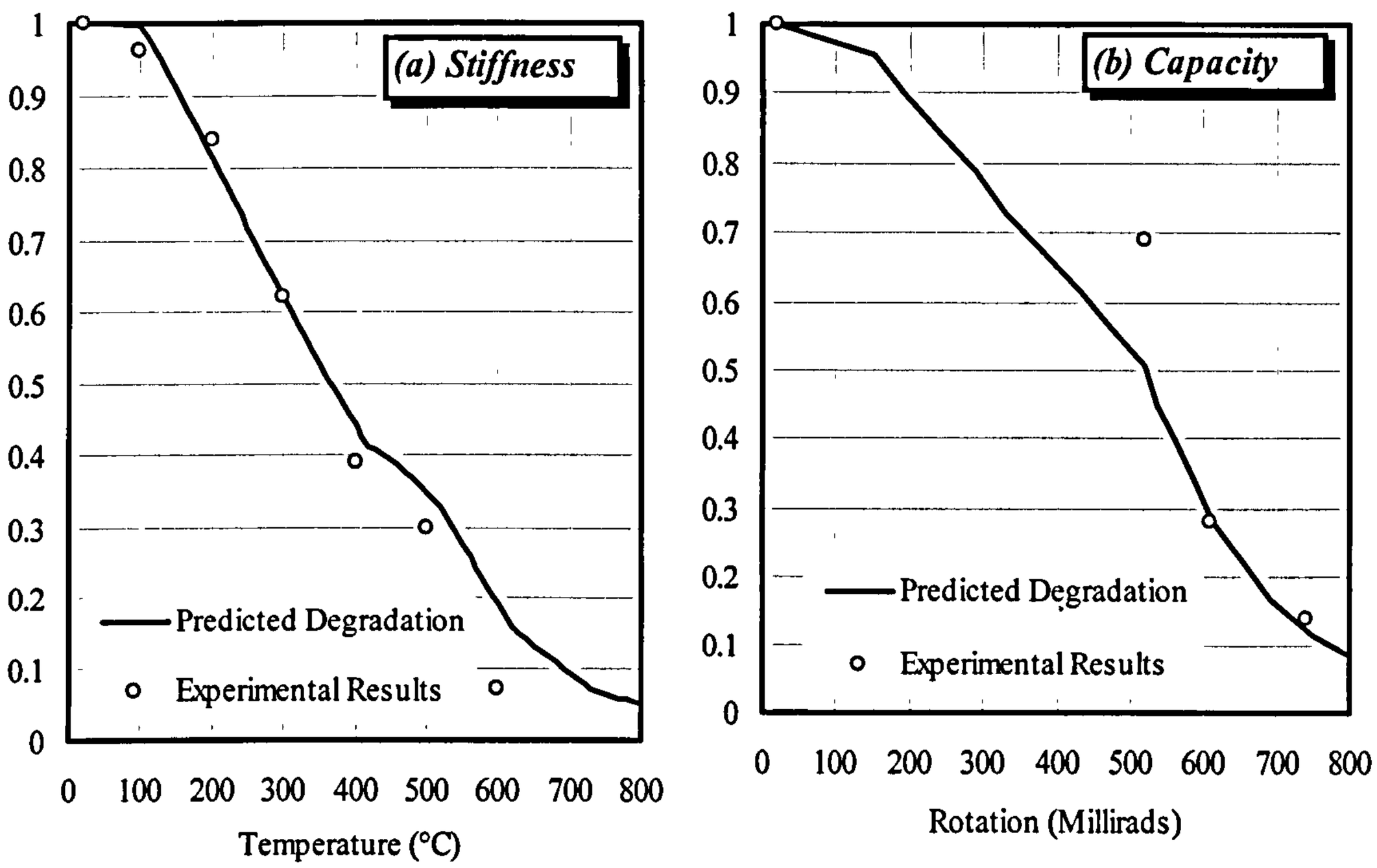

Figure 7.18: Predicted Degradation of Connection Characteristics Due to the Influence of Temperature for Group3 Connection

Verification of the model at elevated temperature was based on the three tests on bare-steel flexible end-plate connections (i.e. Group 3 tests) as described in Chapter 3. The temperature distribution and material properties used were those obtained experimentally. Fig. 7.18 compares the experimental degradation of stiffness and strength of the connection with those generated from the model in the form of stiffness/capacity retention factors. It can be seen from Fig. 7.18*(a)* that the predicted stiffness compares well with that obtained experimentally for temperatures up to 400°C, beyond which the model gives a slight overestimate. The predicted and recorded degradation of connection strength are compared in Fig. 7.18*(b)*. For temperatures between 500°C and 600°C the model underestimates the strength, whereas for higher temperatures there is close agreement between the experimental and predicted results. Unfortunately test data was not available for temperatures below 500°C, due to the levels of loading during testing. Therefore, at this stage it is difficult to draw definite conclusions concerning the degradation of connection capacity since only three test points were available, all at temperatures greater than 500°C. It is worth remembering that the degradation of connection capacity was based on the first stage of behaviour.

The elevated temperature connection model was compared with two Group 3 tests in Chapter 3 for moments of approximately 8 and 16 kNm. These tests had to be terminated prematurely immediately after the test entered the second stage. Verification of the model is therefore based upon the first stage. The test results showed good

agreement between the two connections and the two methods used to measure the experimental connection rotation, providing an indication of the reliability of the results.

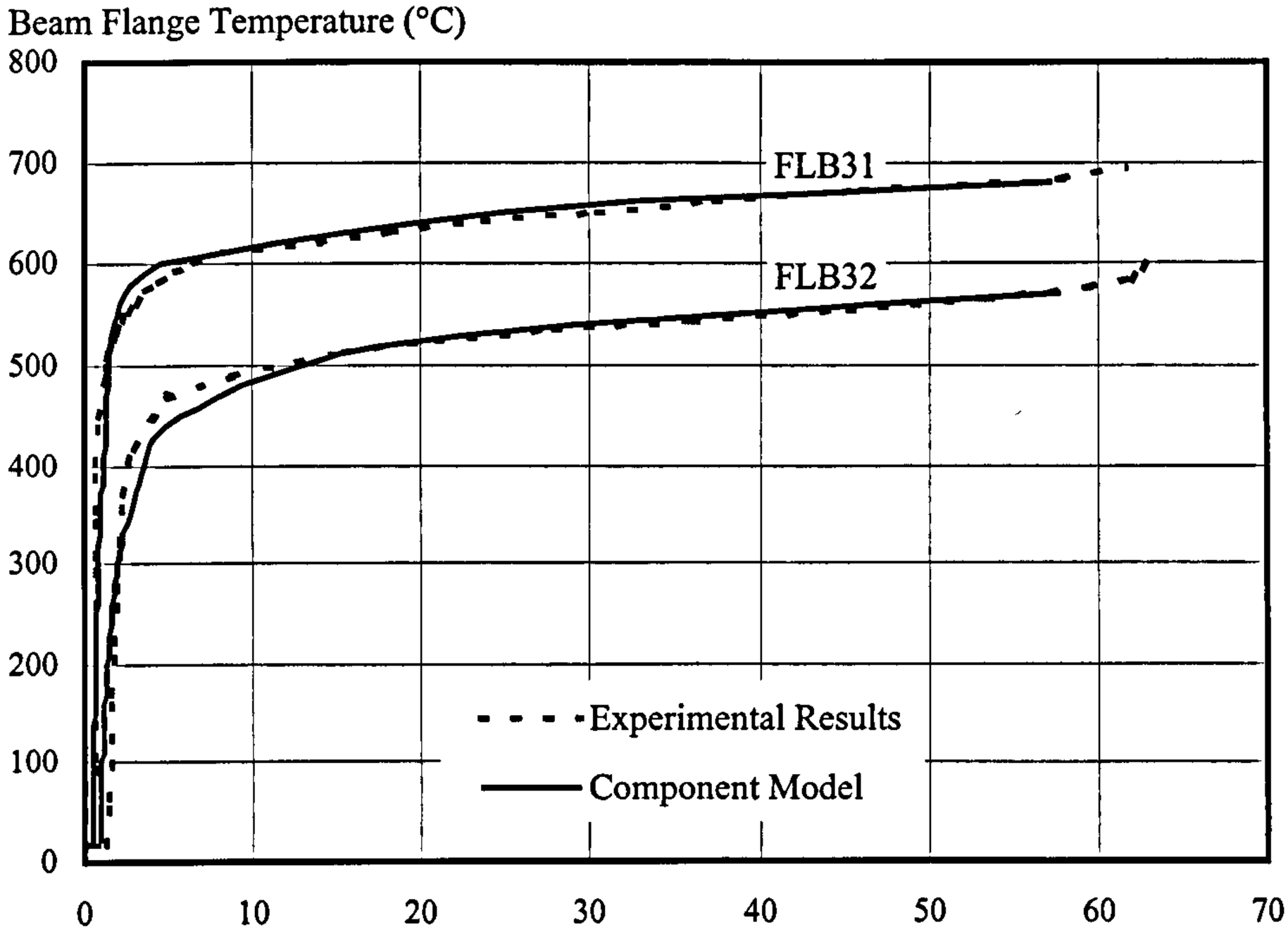

Figure 7.19: Comparison of Predicted Elevated Temperature Response with Group 3 Tests

Fig. 7.19 compares the experimental results for Tests FLB31 and FLB32 with those predicted by the described component model. These compare very closely for both tests. In both cases little rotation was measured for temperatures up to approximately 510°C, beyond which the connection gradually plastifies until failure due to excessive end-plate deformation. The proposed model predicts a similar response. The temperatures at which both test specimens failed, and the corresponding mode are well predicted by the model.

7.6 FLEXIBLE END-PLATE COMPOSITE MODEL

The role of the composite slab is well recognised in greatly enhancing the performance of connections at both ambient and elevated temperatures. At ambient temperature studies have shown that there is a considerable enhancement in the connection characteristics (i.e. strength and capacity) as a result of the continuity of mesh or reinforcing bars in the tension region as well as the presence of shear studs. It has been suggested that their influence will be even greater in fire, partly because of the relatively low temperature of the reinforcement.

The connection characteristics of the composite connection may be assessed by taking into consideration the bare-steel section, reinforcement and shear studs. Therefore, the rotation, ϕ, of the composite connection at any given moment, M may be expressed as:

$$\phi = \frac{M}{S_{CC}} \qquad 7.24$$

where,

ϕ = the rotation of the composite connection;
M = the bending moment;
S_{CC} = the initial stiffness of the composite connection.

A number of authors have proposed a simple form of equations in order to predict initial stiffness of the connection. Aribert and Lachal[189] developed a simple equation for calculating the initial stiffness suitable for flush end-plate composite connections based on eight tests. This may be defined as:

$$S_{CC} = S_C + \frac{D_b}{\frac{D_c}{2E_r A_r h_r} + \frac{\alpha}{Nkh_b}} \qquad 7.25$$

where,

S_C = the stiffness of the corresponding bare-steel connection;
E_r = the elastic modulus of reinforcement;
A_r = the cross-sectional area of the reinforcing bar;
h_r = the distance from the reinforcement to the centre of rotation;
N = the number of active shear studs;
D_b = the depth of the steel beam;
k = the secant stiffness of one shear stud;
α = the increase factor ($\cong 2$).

This simple approach does not account for the actual distribution of internal forces.

Anderson and Najafi[190] proposed a model relating rotation and moment and given by the following expression:

$$\phi = \frac{M}{\left[\frac{K_r.K_s.h_r.h}{K_r + K_s} + K_b.h_b^2\right]} \qquad 7.26$$

where,

h_r = the distance between the centroid of reinforcement and centre of rotation;
h = the distance from the beam slab interface to the centre of rotation;
h_b = the distance between centroid of top row of bolts and centre of rotation;
K_r, K_s *and* K_b = the axial spring stiffness of the reinforcement, shear stud and bolt respectively.

It considered the slip caused by shear studs at the beam-column interface.

Ren and Crisinel[182] developed a relation between the moment and rotation for composite flush end-plate connections which can be used to predict the initial stiffness of the connection. The derivation of the model assumed that the moment capacity of a

connection is the sum of the reinforcement and the bare-steel capacity. The method considers the deformation of the column web due to the compression at the level of the beam bottom flange. The model may be expressed as:

$$\phi = \frac{M}{\frac{h_r}{\frac{1}{K_r} + \frac{1}{K_s} + \frac{1}{K_c}}} \qquad 7.27$$

where,

K_c = the stiffness of the steel section.

A more generalised stiffness model has recently been proposed by Ahmed and Nethercot[191] to predict the initial stiffness for flush end-plate composite connections. The initial stiffness of the connection may be expressed as:

$$S_{CC} = \frac{h.h_r\left(\frac{1}{K_b} + \frac{1}{K_{cw}}\right) + h_b^2.\left(\frac{1}{K_r} + \frac{1}{K_s} + \frac{1}{K_{cw}}\right) - h_b.(h + h_r).\frac{1}{K_{cw}}}{\left(\frac{1}{K_r} + \frac{1}{K_s} + \frac{1}{K_{cw}}\right).\left(\frac{1}{K_b} + \frac{1}{K_{cw}}\right) - \frac{1}{K_{cw}^2}} \qquad 7.28$$

where,

K_{cw} = the stiffness of the column web.

The form of model proposed by Anderson and Najafi[190] has been adopted in the present work for elevated temperature flexible connection model. The model has been modified to consider the effect of elevated temperatures and to maintain consistency with the bare-steel component model. Fig. 7.20 shows the general representation of the proposed composite model. The stiffness of the composite connection may be obtained by adding the stiffness of the bare-steel connection to that of the reinforcement and shear connectors. Therefore, the stiffness of the composite connection may be expressed as follows:

$$S_{CCt}^{-1} = \left[\left(K_{eqt} + K_{cwt}\right)z^2 + \frac{K_{rt}.K_{st}.h_r.h}{K_{rt} + K_{st}}\right]^{-1} \qquad 7.29$$

where,

S_{CCt} = the rotational stiffness of the composite connection for a given temperature;

K_{rt} = the stiffness of the spring representing the reinforcement for a given temperature;

K_{st} = the stiffness of the spring representing shear connection for a given temperature.

By introducing temperature-dependent parameters that have the capability of predicting the response of additional components required for composite action, it is possible to follow the entire moment-rotation characteristics in a tri-linear form. It should be noted that, as with the bare-steel connection model, only the first stage of response is

considered when developing the model. The model also requires suitable representations of the composite slab elements such as reinforcement and shear studs. The response of reinforcement and shear studs is described below.

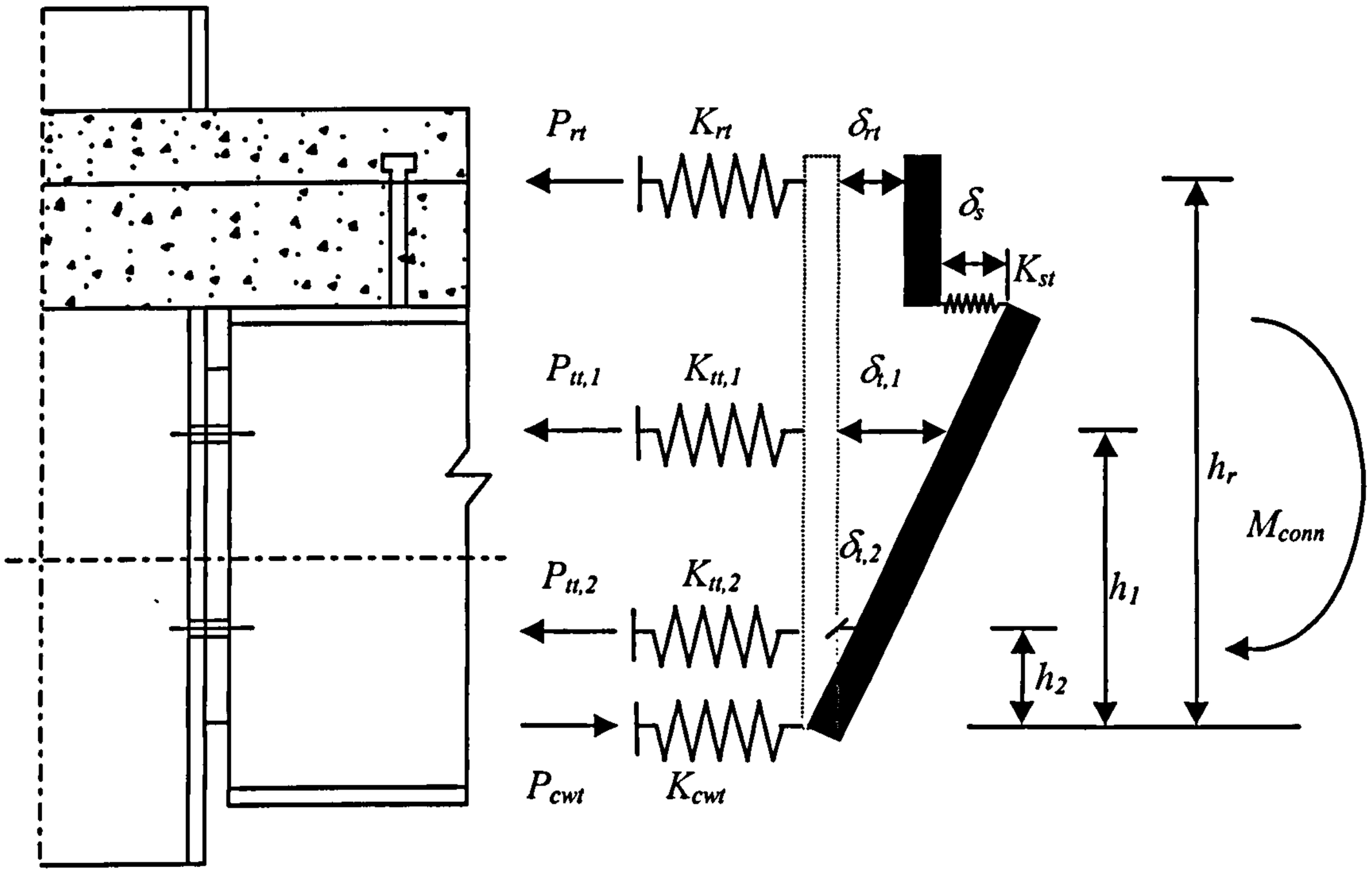

Figure 7.20: Elevated Temperature Composite Connection Model

7.6.1 Reinforcement Response

In the model proposed it is assumed that the concrete has negligible tensile strength, and that the reinforcement resists the internal tensile forces generated in the connection under load. A number of authors[182,189,190,191] have suggested that the reinforcement obeys Hooke's law. Hence, the stiffness of the reinforcement, K_{rt}, at a given temperature may be given by:

$$K_{rt} = \frac{E_{rt}.A_r}{l_r} \qquad 7.30$$

where,

E_{rt} = modulus of elasticity of the reinforcement (mesh and reinforcement bars), at a given temperature;

l_r = the assumed length of reinforcement (≈ 23.8mm).

It is anticipated that the reinforcement will behave elastically until the onset of plasticity. Thus, the force, F_{rpt} that causes yielding in the reinforcement, at a given temperature, may be expressed as:

$$F_{rpt} = f_{yrt}.A_r \qquad 7.31$$

Where,

f_{yrt} = the yield strength of the reinforcement at a given temperature;

As for the bare-steel component model, a reduced stiffness is assumed in the strain hardening zone following the onset of yielding, which may expressed as:

$$K_{rpt} = \mu_r . K_{rt} \qquad 7.32$$

where,

K_{rpt} = the strain hardening stiffness of the reinforcement at a given temperature,

μ_r = the strain hardening coefficient for the reinforcement.

The strain hardening coefficient for the reinforcement adopted is similar to the one used for structural steel.

The force in the reinforcement for a give rotation may be expressed as:

$$F_{rt} = \left(\frac{K_{rt} . K_{st} . h}{K_{rt} + K_{st}} \right) . \phi \qquad 7.33$$

The rate of degradation of reinforcement stiffness and capacity is based on the recommendations presented in Chapter 2.

7.6.2 Stiffness of the Shear Studs

All studs in the hogging moment region should be considered when calculating the stiffness of the shear studs. If the connection has more studs than are required for full interaction the actual number of studs required for full interaction should be utilised. Results from push out tests[192,193,194] show that the elastic stiffness of shear studs is in the range 200 - 350kN/mm. Also, the load slip curve adopted for numerical analysis of composite beams by Mistakidis *et al.*[195] obtained from experimental data of other researchers gives a stiffness of 110 kN/mm. Hence it is apparent that the stiffness of the shear studs is likely to be in the range 110 - 350 kN/mm. Based on these findings it is proposed that an approximate value of 200 kN/mm is adopted to represent the stiffness of the shear studs in the current model. Due to the great variation in the structural form it is not feasible to propose generalised guidelines for the shear stud response and at present it is more appropriate to use an estimated value based on test results. The degradation characteristics of shear studs at elevated temperatures may be based on the recommendations presented in Chapter 2.

7.6.3 Verification of the Composite Model

There is no doubt that the stiffness of the connection is significantly enhanced by the incorporation of the composite slab. On the other hand the ultimate capacity depends on the size of the slab, number of shear studs and the eventual failure of reinforcement. Results obtained from the model described above after accounting for the influence of

the composite slab are compared with Group 4 connection test results conducted at both ambient and elevated temperatures as described in Chapter 4.

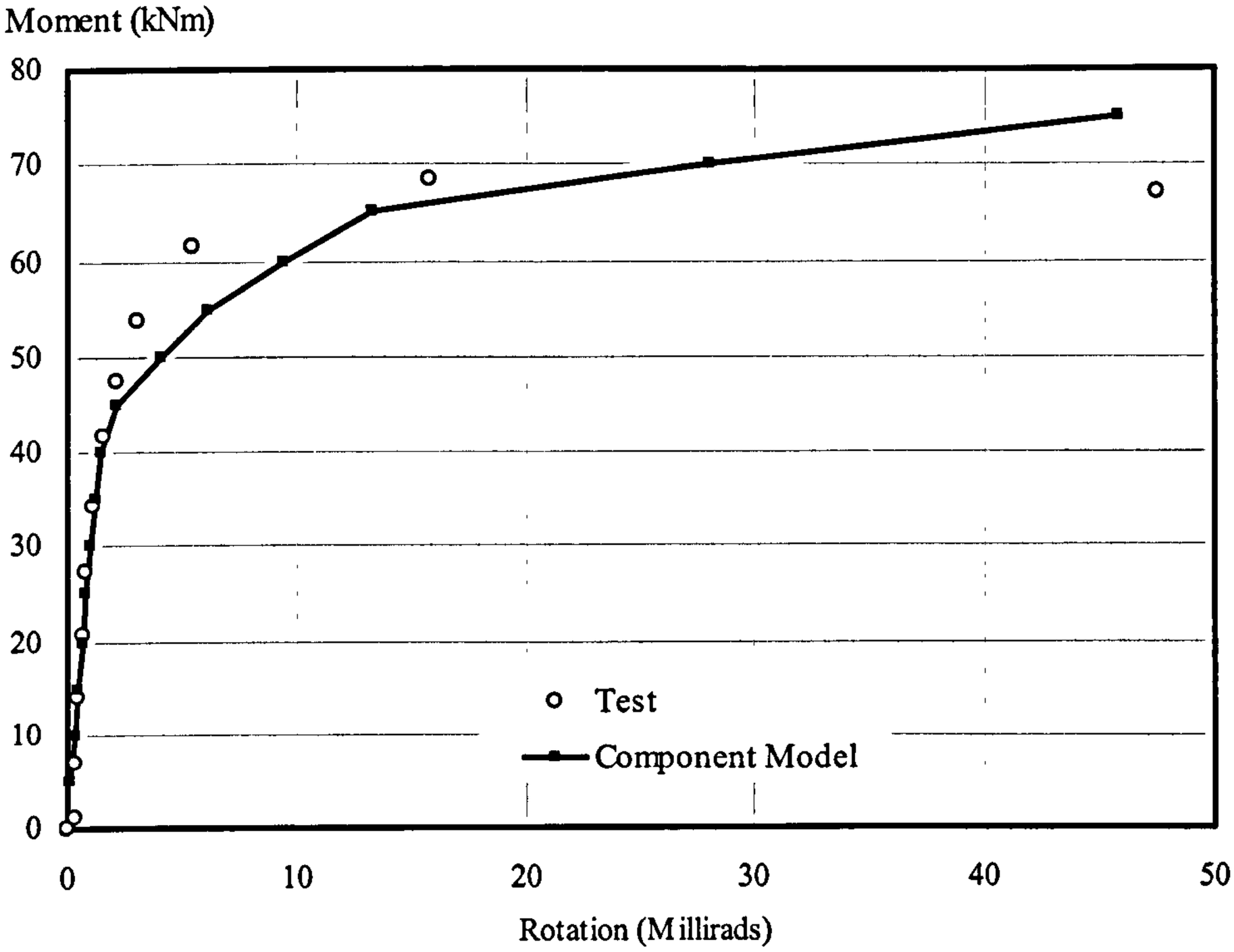

Figure 7.21: Comparison of Predicted Ambient Temperature Response with Group 4 Tests Results

Five tests have been carried out, four at elevated temperature and one at ambient temperature. Two elevated temperature tests were conducted within the first stage of the connection response and used in the validation of the model. Results from the ambient temperature test are compared with the predicted response from the model as shown in Fig. 7.21. The stiffness of the connections remain constant up to a moment of approximately 45 kNm, after which curved knee appears in the moment-rotation response due to the yielding of the reinforcement and failure of the composite slab. This is followed by response is represented by flat plateau due to the significant end-plate deformation until the beam bears against the column at a rotation of approximately 65 millirads.

As can be seen from the plotted results that the predicted elastic response of the connection compares closely with the experimental results suggesting that the proposed model is capable of predicting the initial stiffness of the connection accurately. However, the model predicts a more flexible response in the plastification zone up to approximately 15 millirads, beyond which the predicted response becomes stiffer. This difference in the strain hardening zone is probably due to the actual variation in the material properties as well as lack of data defining the connection components responses in the plastification zone. Despite the slight variation in the response, the model can predict the connection response to a reasonable accuracy. The failure mechanism of the connection was correctly predicted being governed by failure of the reinforcement in the composite slab and excessive deformation of the end-plate.

It may be anticipated that the reinforcement and shear studs would remain at a relatively low temperature due to the protection provided by the concrete. It is therefore assumed that this temperature is 20% of the beam bottom flange temperature. The analysis was repeated using the experimental temperature profiles to investigate the ability of the model to predict the performance of the composite connection at elevated temperature. The degradation of both stiffness and capacity is compared with those recorded as shown in Fig. 7.22.

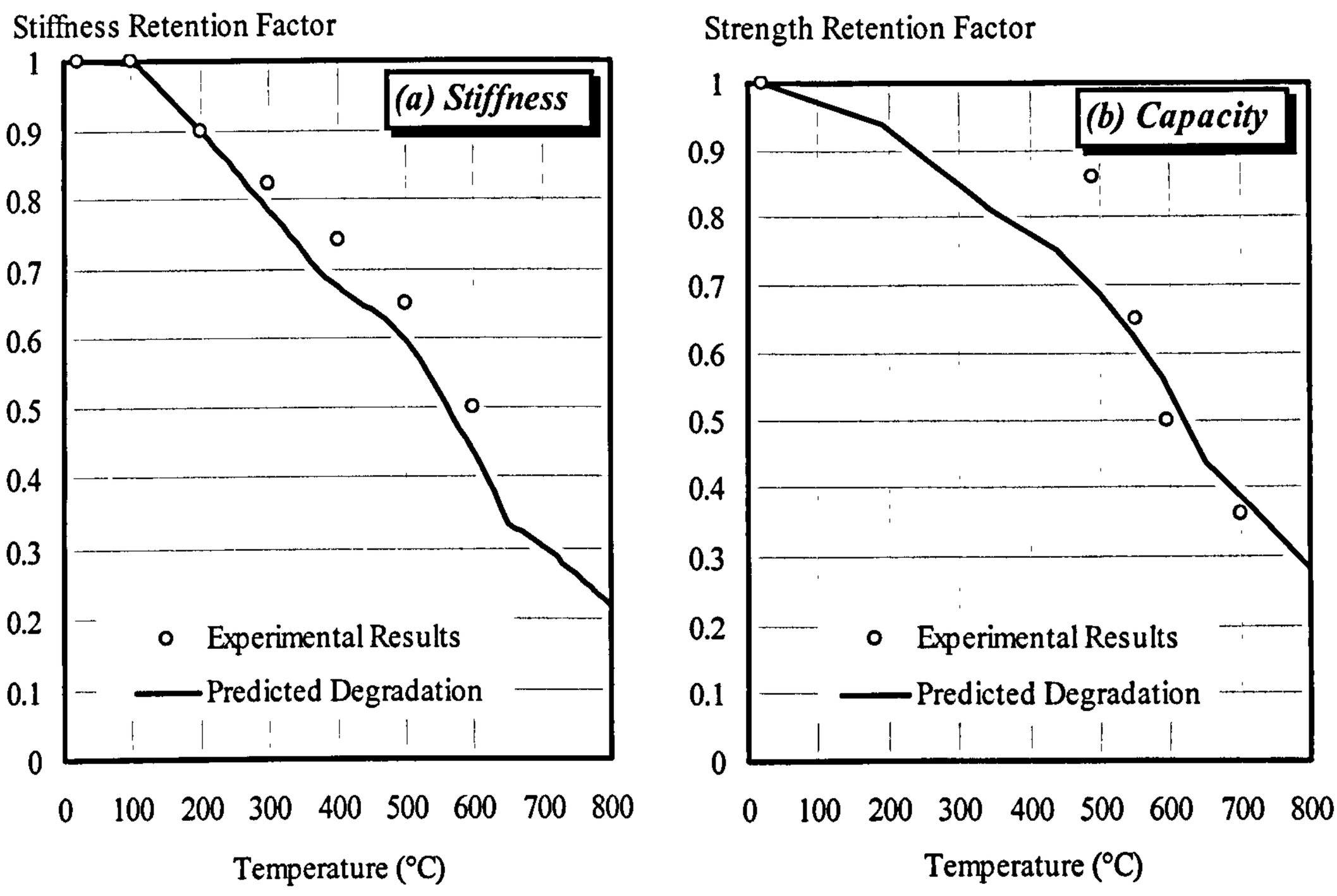

Figure 7.22: Predicted Degradation of Connection Characteristics Due to the Influence of Temperature for Group 4 Connection

It may be seen from Fig. 7.22*(a)* that there is close agreement between the predicted rate of degradation of stiffness and that observed experimentally. This demonstrates that the degradation of connection stiffness is primarily controlled by the degradation of the reinforcement in the tension zone since in the first stage of response the exposed column web in the compression zone has little influence on stiffness degradation. Considering connection capacity, it may be seen from Fig. 7.22*(b)* that there is a reasonable correlation between the predicted and experimental data, with the proposed model predicting a greater degradation rate than the recorded at intermediate temperatures. This difference is more pronounced at low failure temperatures where the connection is exposed to high levels of loading. This is probably due to the fact that the degradation of capacity adopted in the model was based on a strain level of 0.5% which underestimates the actual rate of degradation of connection capacity. Unfortunately experimental data was not available for temperatures below 480°C, as a result of the levels of moment utilised in testing.

The applicability of the model to predict the connection response at elevated temperature is investigated against two elevated temperature tests conducted within the first stage of response i.e. tests FLC41 and FLC42. These tests were conducted at moments of approximately 34 and 46 kNm respectively. Experimental results are compared with those obtained from the proposed component model in Fig. 7.23 based on experimental material properties and temperature profiles. The experimental connection response is based on the average rotation obtained from East and West connections. It may be seen that the proposed component model provides a reasonable prediction of the initial stiffness and capacity of the connection for both tests. However, for the first elevated temperature test (FLC41), the model slightly underestimates the yield capacity of the connection at high temperatures, whilst it provides a close prediction of initial stiffness. However, this variation may be attributable to a reversal in the connection rotation in the first test (FLC41) at temperatures between 300°C and 500°C due to thermal bowing. The current model does not account for this.

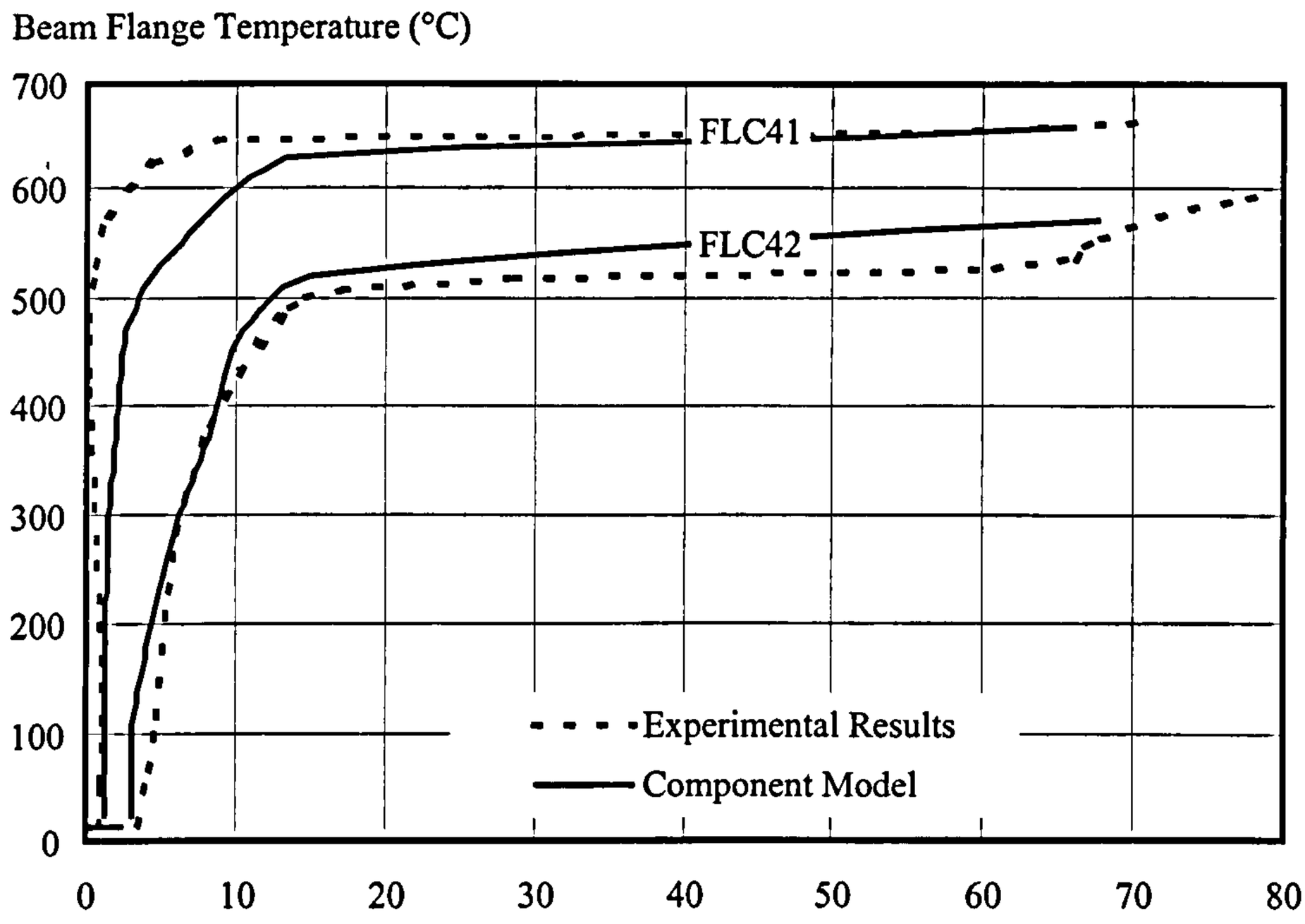

Figure 7.23: Comparison of Predicted Elevated Temperature Response with Group 4 Tests

It is worth remembering the following points when using the proposed model for subsequent studies:

- The model is only suitable for modelling the first stage of flexible end-plate behaviour - that is before the beam flange comes into contact with the column. However, the second phase of response subsequent to the contact can be incorporated within the model when data is available. The model is suitable for modelling isolated connections. If the influence of structural continuity needs to be investigated, then the axial restraint to thermal expansion must be taken into consideration;

- The influence of shear deformation of the column web is not accounted for, since the model is primarily developed to suit connections with double sided and symmetrical loading;
- For flexible end-plate connections it was observed that the column web in the compression zone is capable of resisting the applied compression force and overstressing is unlikely to occur especially in the first phase of response. Therefore it is anticipated that the incorporation of the movement of the axis of rotation would have little influence on the predicted response. It would also add significant complexities in the formulation of the model and one of the main goals is to develop a simple model suitable for manual calculation.

7.7 CONCLUSIONS

Due to the large number of connection types and arrangements used in building construction it is unrealistic to develop characteristics for each by testing. The simplified component models offer an alternative solution to minimise the reliance on experimentation to investigate the connection response and thus reduce expense and time as well as easing the numerical complexities associated with modelling. Simple component models have been developed for both bare-steel and composite flexible end-plate connections. This approach was adopted for ease of application and modification for alternative arrangements.

A simplified component model has been presented for modelling the elevated temperature response of flexible end-plate connections as both bare-steel and composite. Connections were modelled by assembling the contributions of individual components. Tri-linear modelling was adopted, with the separation of the connection into its main components allowing the use of any chosen temperature profile. The main parameters describing stiffness and capacity of the elements were degraded with increasing temperatures.

Comparison of the bare-steel model with existing test data generated good results, and accurately predicted failure modes in all cases. However for large sections the model underestimates the connection response probably as a result of inadequate modelling in the plastic zone. The predicted rate of degradation of the connection stiffness and capacity compares well with experimental results. For composite connections the predicted and measured responses compared well for ambient temperature. Results were also encouraging for elevated temperatures, but in some respects more experimental data is required to draw positive conclusions.

The use of component-based models proved desirable due to their simplicity and efficiency and the advantage of this form of model to be easily modified to account for alternative arrangements.

8 CONCLUSIONS AND FURTHER RECOMMENDATIONS

8.1 INTRODUCTION

Until recently most steel and composite steel framed structures have been protected from the effects of fire by applying some form of insulating material. This has the main goal of limiting the temperature of the steel so that sufficient strength is maintained throughout the duration of a fire. The application of such materials is costly, increasing the overall cost of the structure up to 30%[4]. From an engineering perspective it is more logical to design the structure against fire rather than designing it for normal conditions and then applying fire protection. It is now well established that real frames, both bare-steel and composite, survive better than indicated by the response of isolated members. This is partly because structural members such as beams, columns and floor slabs interact with each other enhancing the frame fire resistance. This has led to much interest being focused on studying the fire resistance of steel structures in order to minimise the high cost of fire protection.

Traditionally the behaviour of bare-steel and composite beam-to-column connections at the fire limit state is assumed to be the same as used in the design at ambient temperature. That is a connection which is assumed to be pinned at ambient temperature is also assumed to be pinned at elevated temperature. However, observations from damaged structure[9] and recent fire tests at the Cardington LBTF[18,153,154] have demonstrated that even pinned connections can provide considerable levels of both stiffness and strength at elevated temperature and hence have beneficial influence on the fire resistance of steel structures. The assessment of the influence of connection response on frame behaviour has not yet been fully established due to the lack of experimental studies. This has limited the effective use of the inherent connection characteristics at elevated temperatures in the design of framed structures. Recent experimental tests on small-scale specimens have shown that it is possible to derive accurately the moment-rotation relationships at elevated temperature and have established the principles by which this could be achieved. Therefore it was felt that further studies should be conducted in order to achieve better understanding of the connection response in fire conditions

8.2 EXPERIMENTAL STUDIES ON BARE-STEEL CONNECTIONS

Unlike ambient temperature connection tests where a single test is sufficient to describe the entire connection response, a series of tests are required in order to establish the entire response at elevated temperature. For this purpose, three series of tests were conducted for different bare-steel connections. Two connection types were considered: flush and flexible end-plates, with the member sizes considered being in the lower and medium-sized sections.

In total eleven tests were carried out, divided into three groups of different member sizes and connection types. Group 1 consists of two 254x102UB22 beams connected to a 152x152UC23 column by 8mm thick flush end-plates. This group of tests was chosen for comparison with previous experimental data[52], the only difference being the adoption of a more realistic end-plate thickness. Group 2 comprises a pair of

356x171UB51 beams connected to a 254x254UC89 by 10mm flush end-plates. This detail was selected to provide an indication of the influence of member size on the performance of steel connections at elevated temperature. The section sizes of Group 3 connections are identical to group 2 but with an 8mm thick flexible end-plate, typical of connections used in the Cardington full-scale test frame.

A cruciform test arrangement was used with the specimen being tested under a constant load and increasing temperature in a portable furnace specially designed to test two- and three-dimensional assemblages. Instrumentation included thermocouples, clinometers, displacement transducers and load cells. A number of thermocouples were attached to the specimen in order to measure the temperature distribution across the depth of the connection. One clinometer was attached to each beam in order to measure the beam rotations as the connections deformed. The limiting temperature for the clinometers was approximately 80°C (compared to maximum furnace temperature approaching 800°C), with working temperatures being limited by situating the devices within protective housings cooled by compressed air. In order to provide a direct check on connection rotation, a number of displacement transducers were attached along the length of each beam. Calibrated compression load cells were used to measure and monitor the loads applied to the beams throughout the tests.

Four elevated temperature tests were conducted under Groups 1 and 2, whilst only three tests were carried out under Group 3, at different levels of moment, with increasing temperatures. Each test contributes one point on the moment-rotation response at any given temperature. In all tests conducted in Group 1, the modes of failure were similar in that a localised deformation at the top of the end-plate occurred, particularly around the top bolt, accompanied by deformation of the column flange and buckling of the column web. This mode of failure was not surprising given the relative dimensions of the end-plate and the unstiffened column flange. The failure mechanism for Group 2 tests was a localised end-plate deformation at the top of the end-plate without any damage to the beams and the column. The member sizes in this group are much larger than those in Group 1, whereas the end-plates are only slightly thicker. The most unusual aspect was the slipping of the top bolts in the tension zone, probably due to the softening of the bolts at high temperature, particularly the top bolts which experienced the largest tensile force in comparison to others. At high levels of loading, cracks in the end-plate were observed along the welds in both the beam web and flange.

Unlike flush end-plate connections, some flexible end-plates undergo two stages of response, that is a free end-plate deformation until the beam flange bears against the column beyond which there is an enhanced response with further rotation. Hence, during the flexible end-plate tests (i.e. Group 3) there was a problem of large rotation at low moments. This was due to end-plate deformation which prevented testing the specimen up to failure because the beams came into contact with the furnace doors. For low load levels it was not possible to test the specimen to failure, and the tests were terminated when both the beams rested on the furnace doors. To resolve this problem for high load levels the specimen was initially loaded to the desired level at ambient temperature. The loads were removed, and the furnace and instrumentation were re-adjusted. The specimen was re-loaded to the required level and the elevated temperature test started. This method allowed the specimen to be tested up to failure over the entire rotation range. Because of the limited number of specimens tested it was only possible to consider the first stage of response for the Group 3 specimens. Similar

modes of failure were observed in all Group 3 tests, with significant end-plate deformation but no damage to the beams, column or bolts.

In all the elevated temperature tests failure modes were similar to those observed for the same connection at ambient temperature.

In the bare-steel connection tests both top and bottom flanges were kept unprotected near the connections. There was little variation in temperature across the depth of the connections and hence, the temperatures can be represented by the average value of the beam top and bottom flange temperatures. Also it seems that specimen size has little influence on the failure temperature of the bare-steel connections for small and medium size sections since most of these failed at similar temperatures. Both stiffness and capacity of the connection were seen to decrease with increasing temperatures, with a significant reduction in the range 400°C to 600°C.

8.3 EXPERIMENTAL STUDIES ON COMPOSITE CONNECTIONS

Two series of tests were conducted on flexible end-plate composite connections in order to investigate their degradation at elevated temperatures. The member sizes, connection details and composite slab layout were similar to those used in the Cardington full-scale frame. The connection type, and the beam and column sizes adopted in the first series of composite connection tests were identical to those used in the Group 3 tests, the only difference being the casting of the composite slab on the specimen. This arrangement was selected to provide an indication of the difference in stiffness and strength between steel and composite connections at elevated temperature. The second composite group used 610x229UB101 beams connected to a 305x305UC137 column by 10mm thick end-plates.

The form of the composite slab was the same as that used in the Cardington test facility, namely COMFLOR C70 decking with 130mm overall slab depth using lightweight concrete of Grade C35. The slab was nominally reinforced with A142 mesh reinforcement. The length of continuous slab across the connection was 1400mm and its width was 1200mm. The length of the slab was enough to allow the use of two shear studs on each cantilever beam. Similar failure mechanisms were observed for both groups of composite connections. Failure in the concrete slab was initiated with a large crack propagating from the face of the column flange parallel to the beam resulting in fracture of some bars in the steel mesh. Two large cracks occurred perpendicular to, and continuous across, the connection on both sides of the slab. Consequent to failure of the composite slab, the load applied was transferred to the connection and thus an end-plate failure was observed; in most tests the end-plate was broken along the weld which connects it to the beam web. As with the bare-steel tests the failure modes occurring at elevated temperatures are similar to those at ambient temperature.

The presence of the concrete slab over the connections caused a 20%-30% reduction in the beam top flange temperatures compared with the beam lower flange in both test groups causing a variation in the temperature profile across the connection. This is because the concrete slab is acting as insulation and as a heat sink to the top of the beam which enhances connection performance at elevated temperature. Therefore, the beam bottom flange temperature was adopted as the representative connection temperature.

The test results indicated a considerable reduction in strength for temperatures in the range of 500°C to 600°C. Also it was observed that the stiffness of the composite connections degraded at a significantly lower rate than the bare-steel counterpart. However, the capacity is less affected probably due to the size of the composite slab adopted in the elevated temperature tests.

8.4 DEGRADATION OF CONNECTION CHARACTERISTICS

The degradation of both stiffness and capacity of the connections was quantified against the degradation of structural steel properties based on EC3: Part 1.2[59] recommendations. It was observed that the level of strain at the proportional limit provided a good representation of the degradation of the stiffness for all bare-steel connections irrespective of their type and size. Degradation of the strength of the bare-steel connections was seen to be approximated with a sufficient degree of accuracy adopting the material degradation specified in EC3: 1.3[59], for a level of strain of 0.5%.

With increasing temperatures it would be expected that both the stiffness and capacity of composite connections would degrade at a lower rate than their bare-steel counterpart. The observed degradation of the stiffness of composite connections compared closely with the degradation of steel at a level of strain of 0.5%, whereas the strain level at the proportional limit provided a conservative approximation for the rate of degradation of stiffness of flexible end-plate composite connections. From experimental results it was found that degradation of the composite connection capacity closely followed the degradation of steel, for a level of strain of 2.0% (plastic range). However, due to the composite slab arrangement adopted in the elevated temperature tests it seems that the observed degradation of capacity underestimates to some extent the actual rate.

8.5 REPRESENTATION OF CONNECTION CHARACTERISTICS

Defining a suitable mathematical expression to represent the experimental connection characteristics at elevated temperature is important for incorporation within analytical analysis. The form of expression should represent the connection response in terms of the main parameters such as initial stiffness and moment capacity and should have the capability of representing the entire non-linear moment-rotation response.

The Ramberg-Osgood function[118] was selected to represent the moment-rotation relationships with increasing temperatures for the tested connections. The moment-rotation response at a given temperature is defined by a single expression and always yields a positive slope corresponding to the tangent-stiffness of the connection. When using the Ramberg-Osgood expression to fit elevated temperature test data, the degradation of the connection may easily be incorporated by modifying the coefficients representing the stiffness and strength. This allows a consistent moment-rotation-temperature relationship for a range of temperatures.

8.6 INFLUENCE OF CONNECTION RESPONSE ON FRAME BEHAVIOUR

A finite element program developed by Bailey[54] was used to conduct parametric studies on the influence of connection characteristics on frame response. Elevated temperature moment-rotation characteristics for the bare-steel and composite connections were incorporated in the program after fitting the test data using the Ramberg-Ogood expression. In order to reduce the computational efforts a typical sub-frame was used, having demonstrated that this gave results comparable to those obtained from full-frame analysis.

It was observed that incorporating experimentally generated characteristics for flush end-plate bare-steel connections resulted in frame response intermediate between rigid and pinned. This caused a significant reduction in deflections compared with the common assumption of pinned behaviour. However, the frame response resulting from the incorporation of flexible end-plate characteristics for both bare-steel and composite connections was comparable to the assumption of pinned connections. There was a considerable reduction in the central deflection of the beam for flush end-plates compared with flexible end-plates with the resultant failure temperature increasing by over 70°C, corresponding to "limiting deflection" of span/20. This suggests that the connection type have considerable influence on frame behaviour.

To investigate the effect of end-plate thickness on beam behaviour, two analyses were conducted with end-plate thickness of 8mm and 12mm. The sub-frame arrangement used was similar to that adopted in Group 1 fire tests, with the same load ratio being applied. The results have demonstrated that end-plate thickness has negligible influence on the beam response at elevated temperature.

Inclusion of composite connection characteristics within the analysis also resulted in an increase in the failure temperature for the arrangement tested. For a central deflection of 225mm (span/20) there was an increase in the 'failure' temperature of approximately 200°C for composite connection characteristics compared with the equivalent bare-steel condition. This is mainly due to the fact that whilst the capacity of composite connections generally degrades at a lower rate than for bare-steel connections, the beam capacity also reduces at a lower rate. The analysis was repeated on composite arrangements with varying concrete strength, since previous observations have suggested that normal strength concretes could possess considerably greater strength than specified. Various concrete strengths were considered and although the performance of the beam response was affected, this was not very significant. The difference in the failure temperatures when using concrete strengths of 5 and 95 N/mm^2 was approximately 60°C.

The influence of connection temperature was considered for different sub-frame arrangements including flush and flexible end-plate connections. A range of connection temperatures relative to the beam bottom flange were considered. For bare-steel flush end-plates it was observed that the failure temperature was not affected by the increase of the connection temperature up to a ratio of 0.5, beyond which the failure temperature increases with increasing connection temperature. This suggests that failure temperature of the beam is sensitive to the temperature of the connection and it should be ensured that the connection temperature remains less than half of the temperature achieved by the beam bottom flange temperature. Therefore in order to maintain the

enhancement in the response due to semi-rigid connections, the fire protection applied to the columns should be extended to include the connections. On the other hand, the connection temperature has little influence on the failure temperatures of beams with flexible end-plates for both bare-steel and composite conditions. This may be attributable to the inherent characteristics of flexible end-plates which provide little or no end restraint. This suggests that providing protection to flexible end-plate connections would have minimal effect in increasing the fire resistance of the frame at elevated temperature.

Studies have been presented considering the influence of varying load ratio on failure temperature. It was observed that the beam failure temperature is sensitive to the load ratio applied - that is increasing the load ratio reduces the failure temperature irrespective of the type of connection or arrangement adopted. Therefore care should be taken when selecting the load ratio to be used in the design.

At ambient temperature, experimental studies[104] on both individually restrained members and frames have shown that behaviour beyond 50 millirads has little practical significance and therefore in the case of flexible end-plates the first phase of response is most important. However, rotations in excess of 100 millirads are common at high temperatures. Therefore, the second phase of response in flexible end-plates may be significant. In order to study this, two analyses were conducted on flexible connections, one involving only the first stage, the second incorporating the entire connection response. It was found that the central beam deflection is slightly reduced when using the entire response. The temperature at which the connection enters the second stage of the response was found to be within the temperature range experienced in real fires. The second phase had marginal influence on the composite beam behaviour.

8.7 CARDINGTON FRAME STUDIES

Further analysis has been presented to consider the influence of the connection characteristics on the response of a real structure. The large compartment test in the Cardington test programme was selected for this. The postulated and actual elevated temperature characteristics of the Cardington frame connections were used in the analysis.

Once again the analysis was carried out utilising the three-dimensional finite element program developed by Bailey[54]. Results showed that there was only a slight enhancement in the frame response due to the connection characteristics compared to the assumption of pinned connections. Similar behaviour was observed in all beams irrespective of connection type and orientation. This suggests that the connections within the Cardington frame are tending to behave as 'pinned'.

The role of isolated connection tests is well recognised in facilitating verification of numerical models and assisting in developing new design methods. However, they do not accurately reflect the behaviour of a complete building, due to their small size and the absence of the interaction provided by the connected members. In order to distinguish between the behaviour when the connections are tested in isolation and their behaviour as a part of a complete structure, comparisons have been made between the response observed in the Cardington frame fire tests and the observations from isolated

furnace tests. Fracture of the end-plate was observed in both isolated connections tests and Cardington frame tests. In the former case this was due to large rotations whilst the in the latter was due to induced tensile forces during cooling phase. In both cases the fracture was observed to occur along one side of the connection, the other side remaining intact. However, local buckling was observed in the lower flange and web in the proximity of the connection in most of the Cardington tests whereas this behaviour was not seen in isolated tests. This takes place due to the presence of axial restraint provided by the adjacent members.

It is hoped that results from both isolated connections and Cardington frame tests would be of great value in developing a new design approach based upon the consideration of the complete building which will supersede the current design guides. The new design approach will be developed from extensive computer modelling followed by verification against test results.

8.8 MODELLING OF CONNECTION RESPONSE

Experimental tests still provide the most reliable method for establishing connection characteristics at elevated temperature. However, numerical modelling offers an alternative source avoiding complexities associated with testing procedures as well as minimising expense and time. Various numerical models have been developed ranging from simple analytical methods to sophisticated finite element models. Two types of numerical method have been used to model the response of the present elevated temperature connection tests. These were finite element and component models.

A component-based model has been developed for predicting the elevated temperature bare-steel and composite flexible end-plate connection response. The model can follow the entire response of the connection based on its constituent parts. The model uses a tri-linear representation and was formulated to incorporate any selected temperature profile across the depth of the connection. The first phase of flexible end-plate response was considered, with the centre of rotation assumed to be about the lower edge of the end-plate.

Deformation of end-plate, bolts and column flange in the tension zone and column web in the compression zone was assumed to represent the flexible end-plate bare-steel connection response. The response of the connection elements was defined by simplified mechanical models developed for modelling connection response at ambient temperature. The influence of elevated temperature was taken into account by degrading the material properties of the components with increasing temperatures in accordance with EC3: Part 1.2[59] recommendations. Comparison of the bare-steel model with existing test results showed that the model can accurately predict the connection response and failure mode at both ambient and elevated temperatures. With increasing temperatures the degradation of connection stiffness was seen to compare well with that observed for flexible end-plate bare-steel connection tests over the entire temperature range.

The bare-steel model was further developed to take into account composite action by incorporating two springs representing the reinforcement and shear studs. The reinforcement was assumed to remain at a temperature 20% of the beam. The model

was validated against two tests conducted in Group 4, with the results comparing closely at ambient and elevated temperatures. Also the failure mode of the connection was accurately predicted being governed by yielding of the reinforcement and deformation of the end-plate.

A component-based model developed by Leston-Jones[52] was modified to account for larger section sizes and connection details and then used to model the elevated temperature response of the flush end-plate bare-steel connections tested. The response of connections was closely predicted at both ambient and elevated temperatures.

Finite element modelling of the bare-steel and composite connection arrangements has been carried out by Liu[151], demonstrating the capability of accurately predicting elevated temperature connection characteristics.

It is apparent that the use of component-based models can provide a reasonable prediction of the connection response at both ambient and elevated temperatures similar to the results obtained from other forms of modelling based an understanding of the behaviour of the component parts.

8.9 RECOMMENDATIONS FOR FURTHER WORK

Future experimental research into the response of connections at elevated temperature should take into consideration the effects of structural continuity and restraint to thermal expansion which may change the behaviour considerably in the context of a complete framed building. This could be achieved by testing two- or three-dimensional sub-frames. Where isolated connection tests are unavoidable, possibly due to restrictions imposed by the testing furnace, an artificial restraint could be provided in order to restrict the horizontal expansion of the beams. Also when conducting further connection fire tests it is important to ensure the following:

- It is preferable to conduct an ambient temperature test prior to the fire tests in order to establish the ambient temperature connection response from which it would be possible to determine the levels of loading.

- In composite connection tests it is essential to provide (where possible) sufficient shear connectors in order to ensure composite action throughout the testing.

- For flexible end-plate connections experiencing two phases of response three elevated temperature tests are not adequate. In situations where a limited number of specimens is available it may be more appropriate to conduct the tests under constant temperature with increasing load levels.

Component-based models have demonstrated the capability of predicting the connection behaviour at elevated temperature with reasonable accuracy especially in the elastic range. The described model may easily be modified to model other forms of connection and arrangement at both ambient and elevated temperatures.

The use of commercial finite element programs such as ANSYS and ABAQUS in modelling the connection response at ambient temperature have becomes popular in

recent years. Results from such models have demonstrated the ability of these to provide good predictions of the connection response. It is possible to generate good prediction of the connection response at elevated temperature based on the rate with which the connection element properties degrade and the inherent nature of the connection. It is envisaged that the use of such programs would offer a cheap alternative to testing, providing improved understanding of the connection behaviour by studying the influence of various parameters. Results from such models can also enrich the database of connection behaviour at elevated temperature.

REFERENCES

1. Latter, R., "The European Market for Constructional Steelwork", *New Steel Construction* **2(5),** October 1995.

2. "*British Steel Report and Account 1997/98"*, British Steel, UK, 1998.

3. Desai, S. B., "Future Eurocodes and Structural Fire Design", *The Structural Engineer* **68**(22), Nov. 1990, pp. 451-453.

4. El-Rimawi, J. A., *"The Behaviour of Flexural Members under Fire Conditions"*, PhD. Thesis, Department of Civil and Structural Engineering, University of Sheffield, 1989.

5. Dowling, J., "Fire Protection Using Off-Site Applied Intumescent Coatings", *Proc. Intn Civ. Engrs Structs & Bldgs* **112**, May 1997, pp. 237-238.

6. Cooke, G., "Practical Fire Engineering-The Context", *National Structural Steel Conference*, London, Dec. 1984.

7. "*Steel Frames Continue Domination of UK Multi-storey Construction Market"*, Annual Survey, British Steel, UK, June 1998

8. Robinson, J., "Fire - A Technical Challenge and A Market Opportunity", *J. Construct. Steel Res.* **46**(1-3), 1998, paper No. 179

9. *"Investigation of Broadgate Phase 8 Fire"*, Structural Fire Engineering", Steel Construction Institute, June 1991, UK.

10. Lennon, T., "*Personal Correspondence"*, 1996.

11. *"BS 449: Specification for the Use of Structural Steel in Buildings"*, 1969, British Standard Institution, 1969.

12. Chen, W. F. and Lui, E. M., *"Stability Design of Steel Frames"*, CRC Press Inc., 1991. pp. 235.

13. Davison, J. B. and Nethercot D. A., "Overview of Connection Behaviour", *In the Structural Connection-Stability and Strength*", Ed. Narayanan, R., Elsevier Applied Science, 1989, pp. 1-22.

14. Lorenz, F. R., "A New Alternative in Steel Construction - Partially Restrained Connections", *Connection Flexibility and Steel Frames*, Ed. Chen, W. F., 1985.

15. Lawson, R. M., "*Design of Composite Slabs and Beams with Steel Decking"*, Publication 055, The Steel Construction Institute, London, 1989.

16. Price, A. M., and Anderson, D., "Composite Beams" *Constructional Steel Design: An International Guide*", Ed. Dowling, P. J., Harding, J. E., and Bjorhovde, R., Elsevier Applied Science, 1992, pp. 421-442.

17. Nethercot, D. A., "Towards a Standardisation of the Design and Detailing of Connections", *J. Construct. Steel Res.* **46**(1-3), 1998, Paper No. 58.

18. Robinson, J., "New Thinking on Multi-storey Building Fires: The Cardington Fire Test Programme - Initial Conclusions", *Fire Safety Engineering* **4**(6), Dec. 1997, pp. 25-26.

19. *"BS 5950 Structural Use of Steelwork in Building: Part 8: Code of Practice for Fire Resistance Design "*, British Standard Institution, London, 1990.

20. Wilson, W. M., and Moore, H. F., *"Tests to Determine the rigidity of Riveted Joints in Steel structures*", University of Illinois, Engineering Experimentation Station, Bulletin No. 104, Urbana, USA, 1917.

21. Barnard, P. R., "Innovation in Composite Floor Systems", *Canadian Structural Engineering Conference*, Canadian Steel Industries Construction Council, 1970, pp. 13.

22. Jones, S. W., Kirby, P. A., and Nethercot, D. A., "The Analysis of Frames with Semi-rigid Connections - A State-of-the-art Report" *J. Construct. Steel Res.* **3**(2), 1983, pp. 2-13.

23. Nethercot, D. A., *"Steel Beam-to-Column Connections: A Review of Test Data*", CIRIA, London, 1985.

24. Nethercot, D. A., "Design of Composite Connections", *The Structural Engineer* **73**(13), July 1995, pp. 218-219.

25. Anderson, D. A., Bijlaard, F., Nethercot, D. A., and Zandonini, R., "Analysis and Design of Steel Frames with Semi-Rigid Connections, IABSE Surveys, **S-39/87**, 1987.

26. Davison, J. B., Kirby, P. A., and Nethercot, D. A., "Rotational Stiffness Characteristics of Steel Beam-to-Column Connections", *J. Construct. Steel Res.* **3**, 1987, pp. 17-54.

27. Davison, J. B., Lam, D., and Nethercot, D. A., "Semi-Rigid Action of composite Joints", *The Structural Engineer*, **68**(24), Dec. 1990, pp. 489-499.

28. Chen, W. F. (Guest ed.), "Joint Flexibility in Steel Frame", *J. Construct. Steel Res.* **8**, 1987, pp. 1-290.

29. Chen, W. F. (Guest ed.), "Steel Beam-to-column Building Connection", *J. Construct. Steel Res.* **10**, 1987, pp. 1-482.

30. Kishi, N., and Chen, W. F., *"Database of Steel Beam-to-Column Connections"*, Structural Engineering Report No. CE-STR-86-26, School of Civ. Engrg., Purdue University, West Lafayette, Ind., 1986.

31. Kishi, N., and Chen, W. F., "Semi-Rigid Steel Beam-to-Column Connections: Database and Modelling", *J. Struct. Engng, ASCE* **115**(1), Jan. 1989, pp. 105-119.

32. Kishi, N., and Chen, W. F., "Moment-Rotation Relationships of Semi-Rigid Connections with Angles", *J. Struct. Engng, ASCE* **116**(7), July. 1990, pp. 1813-1834.

33. Xia, Y., and Nethercot, D. A., *"Database for Composite Connections"*, COSTC1 Working Group, C1-WD4-94-1, Lausame Switzerland, Dec. 1993, pp. 1-4.

34. Aggarwal, A. K., "Comparative Tests on End Plate Beam-to-Column Connections", *J. of Construct. Steel Res.* **30**, 1994, pp. 151-175.

35. Xia, Y., Choo, B. S. and Nethercot, D. A., "Composite Connections in Steel and Concrete: Part 2 - Moment Capacity of End Plate Beam to Column Connections", *J. of Construct. Steel Res.* **37**(1), 1996, pp. 63-90.

36. Bjorhovde, R., Colson, A., and Zandonini, R. (Ed.) *"In Connections in Steel Structures: Behaviour, Strength and Design*", Elsevier Applied Science, London, 1988.

37. Narayanan, R.(Ed.), "*Structural Connections: Stability and Strength"*, Elsevier Applied Science, London, 1989.

38. Bjorhovde, R., Colson, A., and Zandonini, R.(Ed.) *"In Connections in Steel Structures III: Behaviour, Strength and Design"*, Elsevier Applied Science, London, 1995.

39. *"BS 5950 Structural Use of Steelwork in Building: Part 1: Code of Practice for Design in Simple and Continuous Construction "*, British Standard Institution, London, 1985.

40. *"EC3: Design of Steel Structures, Part 1.1: Revised Annex J Joints and building Frames*", (Draft), Document CEN/TC250/SC3 N419E, European Committee for Standardisation, 1994.

41. *"Joints in Simple Construction Vol. 1: Design Methods*", SCI-P-105, The Steel Construction Institute and BSCA, 1992.

42. *"Joints in Simple Construction Vol. 2: Practical Application*", The Steel Construction Institute and BCSA, 1993.

43. *"Joints in Steel Construction: Moment Connections"*, The Steel Construction Institute, 1995.

44. *"Moment Connections in Composite Construction: Interim Guidance for End-Plate* Connections", Technical Report SCI-P-143, The Steel Construction Institute, 1995.

45. Kruppa, J., *"Resistance on feu des assemblage par boulous"*, Centre Technique Industrial de la Construction Metallique, St. Remy Chevzuese, France, 1976, CTICM Report, Document No. 1013-1, English translation available entitled *"Fire resistance of Joints with High Strength bolts"*.

46. *"The Performance of Beam/Column/Beam Connections in the BS 5950: Part 8 Fire Test"*, British Steel (Swindon labs), Reports T/RS/1380/33/82D and T/RS/1380/34/82D, Rotherham, 1982.

47. Lawson, R. M., "Behaviour of Steel Beam-to-Column Connections in Fire", *The Structural Engineer* **68**(14), 1990, pp. 263-271.

48. Lawson, R. M., *"Enhancement of Fire Resistance of Beams by Beam-to-column Connections"*, Technical Report, SCI Publications 086, Steel Construction Institute, 1990.

49. Lennon, T., and Jones, L. C., *"Elevated Temperature Moment Rotation Tests"*, Internal Report N135/94, Building Research Establishment, 1994.

50. Lennon, T., and Jones, L. C., *"Elevated Temperature Composite Connection Moment Rotation Tests"*, Internal Report N65/95, Building Research Establishment, 1995.

51. Leston-Jones, L.C., Lennon, T., Plank, R. J., and Burgess I. W., Elevated Temperature Moment-Rotation Tests on Steelwork Connections, *Proc. Instn Civ. Engrs Structs & Bldgs*. **122**, 1997, pp. 410-419.

52. Leston-Jones, L. C., *"The Influence of Semi-rigid Connections on the Performance of Steel Framed Structures in Fire"*, Ph.D. Thesis, Department of Civil and Structural Engineering, University of Sheffield, 1997.

53. Girardier, V., "Construction Led - Chapter 4: The Role of Standardised Connections", *New Steel Construction*, Feb. 1993, pp. 16-18.

54. Bailey, C. G., *"Simulation of the Structural Behaviour of Steel-Framed Buildings in Fire"*, Ph.D. Thesis, Department of Civil and Structural Engineering, University of Sheffield, 1995.

55 Goddard, G., "Fire Statistics United Kingdom Estimates 1996", Home Office Statistical Bulletin, UK, 1999.

56 *"Steel and Fire Engineering: A Global Approach"*, Steel Promotion Committee of Eurofer, Belgium, 1990.

57 *"BS 4422: Glossary of Terms Associated with Fire, Part: Miscellaneous Terms"*, BSI, London, 1976.

58 *"The Building Regulations 1991: Approved Document B, B2/3/4/5 Fire Safety"*, Department of Environment and the Welsh Office, HMSO, 1992.

59 "*EC3: Design of Steel Structures, Part 1.2: General Rules Structural Fire Design*", (Draft), ENV 1993-1-2, European Committee for Standardisation, 1995.

60 *"BS 476: Fire Tests on Building Materials and Structures, Part 20: Method of Determination of the Fire Resistance of Elements of Construction (General Principles)"*, BSI, London, 1987.

61 *"ISO834: Fire Resistance Tests - Elements of Building Construction"*, International Organisation for Standardisation, Switzerland, 1975.

62 "*ASTM-E.119: Standard Methods of Fire Tests of Buildings Construction and Materials"*, American Society for Testing and Materials, Philadelphia, USA, 1983

63 *"JIS A 1304: Method of Fire Resistance Test for Structural Parts of Buildings"*, Japanese Standard Association, Japan, 1976.

64 Smith, C., "Structural Steel Fire Protection for Multi-storey Buildings- Recent Developments", *Steel Construction*, **20**(2), 1986

65 *"BS 476: Fire Tests on Building Materials and Structures, Part 21: Method of Determination of the Fire Resistance of Load Bearing Elements of Construction"*., BSI, London, 1987

66 Newman, G. M., *"The Behaviour of Simple Structural Elements in Fire"*, Lecture Notes, Fire Engineering - Design of Steel Structures, University of Sheffield, 2-4 March 1998.

67 Law, M., "A Basis for the Design of Fire Protection of Building Structures", *The Structural Engineer*, **61A**(1), 1983, pp. 25–33.

68 Badoo, N., "Stainless Steel in Fire", *The Structural Engineer*, **77**(19), 1999, pp. 16-17.

69 Uddin, T. and Culver, C. G., "Effects of Elevated Temperature on Structural Members", *Journal of Structural Division, ASCE*, **101**(ST7), 1975, pp. 1531-1549.

70 Cooke, G. M. E., "An Introduction to the Mechanical Properties of Steel at Elevated Temperature", *Fire Safety Journal,* **13**, 1988.

71 Kirby, B. R., and Preston, R. R., "High Temperature Properties of Hot Rolled Structural Steels for Use in Fire Engineering Design Studies", *Fire Safety Journal,* **13**, 1988, pp. 27-37.

72 Mäkeläinen, P., Outinen, J., and Kesti, J., "Fire Design Model for Structural Steel S420M Based upon Transient-State Tensile Test Results", *J. Construct. Steel Res.*, **48**, 1998, pp. 47-57.

73 Mäkeläinen, and P., Outinen, J., "*Results of the High Temperature Tests on Structural Steels S235, S355, S352GD+2 and S420*", Compilation of Research Reports TeRT-95-03, TeRT-95-07, TeRT-96-02, Helsinki University of Technology, 1998.

74 Sakumoto, Y., and Saito, H., "Fire-safe Design of Modern Steel Buildings in Japan", *J. Construct. Steel Res.* **33**, 1995. pp. 101-123.

75 *"Fire Safety of Structures - Technical Committee 3 -European Convention for Constructional Steelwork",* European Recommendations for the Fire Safety of Steel Structures (ECCS), Elsevier, 1983.

76 Jorgensen, J. and Sorensen, A. *"Mechanical Properties of Structural Steel at Elevated Temperatures",* Institute of Building Technology and Structural Engineering, Report No. 8010, July 1980.

77 Kirby, B. R., "The Application of BS5950: Part 8 on Fire Limit State Design to the Performance of "Old" Structural Mild Steels", *Fire Safety Journal*, **20**, 1993, pp. 353-376.

78 Schneider, U., "Concrete at High Temperatures- a general review", *Fire Safety Journal*, **13**, 1988, pp. 55-68.

79 Khoury, G. A., "Compressive Strength of Concrete at High Temperatures: A Reassessment", *Magazine of Concrete Research*, **44**, No. 161, Dec. 1992, pp. 291-309.

80 Bǎzant, Z. P., and Kaplan, F. M., *"Concrete at High Temperature: Material Properties and Mechanical Models"*, 1st Edition, Longman Group Limited, 1996.

81 Idorn, G. M. "Expansive Mechanisms in Concrete", *Cement Concrete Research*, **22**, 1992, pp. 1039-46.

82 Chang, W., Wang, C., and Huang, C., "Concrete at Temperatures above 1000°C", *Fire Safety Journal*, **23**, 1994, pp. 223-243.

83 "*EC4: Design of Composite Steel and Concrete Structures, Part 1.2: Structural Fire Design*", (Draft), European Committee for Standardisation, 1992.

84 Jau, W. C. and Wu, G. G., "Performance of Lightweight Panels Subject to Fire", *International Symposium on Structural Lightweight Aggregate Concrete*, Sandefjord, Norway, 20-24 June 1995, pp. 180-192.

85 *"BS 8110 Structural Use of Concrete: Part 2: Code of Practice for Special Circumstances"*, British Standard Institution, London, 1985.

86 Sakumoto, Y., Keira, K., Furumura, F., and Ave, T., "Tests of Fire-Resistant Bolts and Joints", *J. Struct. Engng, ASCE*, **119**(11), Nov. 1993, pp. 3131-50.

87 Kirby, B. R., *"The Behaviour of High-Strength Grade 8.8 Bolts in Fire", J. Construct. Steel Res.* **33**, pp. 3-38,1995.

88 *"Fire Resistance Design of Steel Structures: A Handbook to BS 5950: Part 8"*, The Steel Construction Institute, 1990.

89 Holmes, M., Anchor, R. D., Cook, G. M. E., and Crook, R. N., "The Effects of Elevated Temperatures on the Strength Properties of Reinforcing and Prestressing Steels", *The Structural Engineer,* **60B**(1), 1982, pp. 7-13.

90 *"Design and Detailing of Concrete Structures for Fire Resistance*", IStructE and the Concrete Society, April 1978.

91 Twilt, L., and Kruppa, J., "European Research into the Fire Behaviour of Composite Floors and Beams", *3rd International Conf. on Steel-Concrete Composite Structures*, Fukuoka, Japan, September 1991.

92 Twilt, L., and Kruppa, J., "Current Research on Fire Resistance of Composite Floors and Beams", *International Conf. on Materials and Design Against Fire,* London, United Kingdom, October 1992.

93 Davison, J. B., *"Strength of Beam-Column in Flexibly Connected Frames"*, PhD Thesis, Department of Civil and Structural Engineering, University of Sheffield, 1987.

94 Gere and Timoshenko, *"Mechanics of Materials*", 3rd Edition, Chapman and Hall, 1994.

95 Lennon, T., *"Elevated Temperatures testing Facility: A Feasibility Study"*, BRE Internal Note N48/92, 1992.

96 Lennon, T., "Portable Furnaces", *New Steel Construction*, **3**(11), 1995, pp 21-24.

97 Haynes, P. A., *"Full-Scale Steel Frame Tests: Calibration of Rotation Devices*", N56/87, Building Research Establishment, 1987.

98 Al-Jabri, K. S., Burgess, I. W., and Plank, R. J., *"Behaviour of Steel and Composite Beam-to-Column Connections in Fire-Volume 2: Appendices*", Research Report DCSE/97/F/7, Department of Civil and Structural Engineering, University of Sheffield, Nov. 1997.

99 Horne, M. R. and Morris, L. J., *"Plastic Design of Low Rise Frame"*, Granada Publishing Ltd, 1981.

100 Boreman, J., Kirby, P. A., and Davison , J. B., *"Cardington Steel Frame Building: Tests on Nine Additional Isolated Bare Steel Connections*", Preliminary Report to BRE, Department of Civil and Structural Engineering, University of Sheffield, October 1995.

101 Kennedy, D. J. L. "Moment-Rotation Characteristics of Shear Connections", *American Institute of Steel Construction, Engineering Journal*, **6**(4), Oct. 1969, pp. 105.

102 Owens, G. W., and Moore, D. B., "Steelwork Connections: The Robustness of Simple Connections", *The Structural Engineer*, **70**(3), 1992, pp. 37-46.

103 *"Compendium of UK Standard Fire Test Data on Unprotected Structural steel"*, British Steel Corporation, Contract Report for Department of Environment, 1987.

104 Nethercot, D. A., Davison, J. B., and Kirby, P. A., *"Connection Flexibility and Beam Design in Non-sway Frames"*, American Society of Civil Engineers, Structural Convention, New Orleans, Sept. 1986.

105 Baker. J. F., *"Second Report"*, Steel Structures Research Committee, Department of Scientific and Industrial Research, HMSO, London, 1934.

106 Rathburn, J., "Elastic Properties of Riveted Connections", *Trans. Amer. Soc. Civil Engr*, **101**, 1936, pp. 524-63.

107 Nethercot, D. A., and Zandonini, R., "Methods of Prediction of Joint Behaviour: Beam-to-Column Connections", *Structural Connections: Stability and Strength*, Narayanan, R.(Ed.), Elsevier Applied Science, London, 1989, pp. 23-62.

108 Jones, S. W., Kirby, P. A., and Nethercot, D. A., "Effect of Semi-rigid Connections on Steel Column Strength" *J. Construct. Steel Res.*, **1(1)**, Sept. 1980, pp. 38-46.

109 Lionberger, S. R., and Weever, W., "Dynamic Response of Frames with Non-Rigid connections", *J. Engng Mech. Div.*, ASCE, **95**(EM1), 1969, pp. 95-114.

110 Romstad, K. M., and Subramanian, C. V., "Analysis of Frames with Partial Connection Rigidity", *J. Struct. Div.*, ASCE, **96**(ST11), 1970, pp. 2283-2300.

111 Moncarz, P. D., and Gerstle, K. H., "Steel Frames with Non-Linear Connections", *J. Struct. Div.*, ASCE, **107**(8), 1981, pp. 1427-1441.

112 Poggi, C., and Zandonini, R., "Behaviour and Strength of Steel Frames with Semi-Rigid Connections", *Connection Flexibility and Steel Frames*, W. F. Chen(Ed.), Proc. ASCE, 1985, pp. 57-76.

113 Sommer, W. H., *"Behaviour of Welded Header Plate Connection"*, MS Thesis, University of Toronto, Canada, 1969.

114 Fry, M. J., and Morris, G. A., "Analysis of Flexibly Connected Frames", *Can. J. Civ. Engng.*, **2**(3), 1975, pp. 280-291.

115 Sherbourne, A. N., and Bahaari, M. R., "Finite Element Prediction of End Plate Bolted Connection Behaviour. I: Parametric Study", *J. Struct. Engng.*, ASCE, **123**(2), Feb. 1997, pp. 157-164.

116 Richard, R. M., and Abbott, B. J., "Versatile Elastic-Plastic Stress-Strain Formula", *J. Engrg. Mech. Div.*, ASCE, **101**(4), 1975, pp. 511-515.

117 Ang, K. M., and Morris, G. A., "Analysis of Three-Dimensional Frames with Flexible Beam-Column Connections", *Can. J. Civ. Engng.*, **11**(2), 1984, pp. 245-254.

118 Ramberg, W., and Osgood, W. R., "*Description of Stress-Strain Curves by 3 Parameters*", Technical Report 902, National Advisory Committee for Aeronautics, 1943.

119 Jones, S. W., "Semi-Rigid Connections and Their Influence on Steel Column Behaviour", Ph.D. Thesis, Department of Civil and Structural Engineering, University of Sheffield, 1980.

120 Chen, W. G., and Lui, E. M., "Column with End Restraint and Bending in Load and Resistance Factor Design", *AISC Journal*, Third Quarter, 1985, pp. 105-132.

121 Lui, E. M., and Chen, W. G., "Analysis and Behaviour of Flexibly Jointed Frames", *Engrg. Struct.*, 8(2), 1986, pp. 107-118.

122 Attiogbe, E. and Morris, J., "Moment-Rotation functions for Steel Connections", *J. Struct. Engrg.*, ASCE, **117**(6), Jan. 1991, pp. 1703-1718.

123 De Stefano, M., De Luca, A., and Astaneh-Asi, A., "Modelling of Cyclic Moment-Rotation Response of Double-Angle Connections", *J. Struct. Engrg.*, ASCE, **120**(1), 1994, pp. 212-229.

124 El-Rimawi, J. A., Burgess, I. W., and Plank, R. J., "The Influence of Connection Stiffness on the Behaviour of Steel Beams in Fire", *J Construct. Steel Res.*, **43**(1-3), 1997.

125 Allam, A. M., Fahad, M. K., Liu, T. C. H., Burgess, I. W., Plank, R. J., and Davies, J. M., "Effects of Restraint on the Behaviour of Steel Frames in Fire", ", *Proc. 2nd European Conference on Steel Structures (EUROSTEEL99)*, Prague, May 26 – 29 1999.

126 Bose, S. K., McNeice, G. M., and Sherbourne, A. N., "Column Webs in Steel Beam-to-Column Connections, Part 1, Formulation and Verification", *Computers and Structures*, **2**, Feb. 1972, pp. 253-72.

127 Patel, K. V., and Chen, W. F., "Nonlinear Analysis of Steel Moment Connections", *J. Struct. Engng*, ASCE, **110**(8), 1984, pp. 1861-75.

128 Bathe, K. J., Wilson, E. L., and Iding, R. H., "*NONSAP: A Structural Analysis Program for Static and Dynamic Response of Nonlinear Systems*", Struct. Eng. Lab., University of California, Berkely, 1974.

129 Atamiaz Sibai, W., and Frey, F., "Numerical Simulation of the Behaviour up to Collapse of Two Welded Unstiffened One-Side Flange Connections", *In Connections in Steel Structures: Behaviour, Strength and Design*, R. Bjorhovde *et al.*(Ed.), Elsevier Applied Science, London, 1988, pp. 85-92.

130 Krishnamurthy, N., and Graddy, D. E., "Correlation between 2- and 3-Dimensional Finite Element Analysis of Steel Bolted End-plate Connections", *Computers and Structures*, **6**, 1976, pp. 381-89.

131 Krishnamurthy, N., "A Fresh Look at Bolted End-plate Behavior and Design", *Engrg. J.*, AISC, **15**(2), 1978, pp. 39-49.

132 Krishnamurthy, N., Huang, H. T., Jeffrey, P. K., and Avery, L. K., "Analytical M-θ Curves for End-plate Connections", *J. Struct. Div.*, ASCE, **105**(1), 1979, pp. 133-45.

133 Lipson, S. L., Hague, M. I., "Elasto-Plastic Analysis of Single-Angle Bolted Welded Connections using the Finite Element Method" *Computers and Structures*, **9**(6), 1978, pp. 533-45.

134 Richard, R. M., Gillet, P. E., Kriegh, J. D., and Lewis, B. A., "The Analysis and Design of Single Plate Framing Connections", *Engrg. J.*, AISC, **17**(2), 1980, pp. 38-52.

135 Richard, R. M., Rabern, D. A., Hornby, D. E., and Williams, G. C., "*Analytical Model for Steel Connections", In Behaviour of Metal Structures (Proc. W. H. Munse Symposium)*, Hall, W. J., and Gaus, M. P. (Ed.), ASCE, May 1983.

136 Krishnamurthy, N., "Modelling and Prediction of Steel Bolted Connection Behaviour", *Computers and Structures*, **11**, 1980, pp. 75-82.

137 Murray, T. M., and Kukreti, A. R., "Design of 8-Bolt Stiffened Moment End Plates " *Engrg J.*, AISC, 2nd Quarter, 1988, pp. 45-53.

138 Bursi, O., and Leonelli, L., "Semi-Analytical and Finite Element-Based Models for the Rotational Behaviour of Endplate Steel Connections", *Giornate Italiane Della Costruzione in Acciaio*, 1993, pp. 1-14.

139 Sherbourne, A. N., and Bahaari, M. R., "3-D Simulation of End-Plate Bolted Connections", *J. Struct. Engng*, ASCE, **120**(11), 1994, pp. 3122-36.

140 Choi, C. K., and Chung, G. T., "Refined Three-Dimensional Finite Element Model for End-Plate Connection ", *J. Struct. Engng*, ASCE, **120**(11), 1996, pp. 1307-16.

141 Troup, S., Xiao, R. Y., and Moy, S. S. J., "Numerical Modelling of Bolted Steel Connections", *J. Construct. Steel Res.*, **46**(1-3), 1998, Paper No. 362.

142 Leon, R., and Lin, J., "*Towards the Development of an Analytical Model for Composite Semi-Rigid Connections*", Report to AISC, Structural Engineering Report No. 86-06, University of Minnesota, Minneapolis, 1986.

143 Leon, R., and Lin, J., Ammerman, and MacCauley, "Semi-Rigid Composite Steel Frames", *Engrg J.*, AISC, **24**, 1987, pp. 147-55.

144 Puhali, R., Smotlak, I., and Zandonini, R., "Semi-Rigid Composite Action Experimental Analysis and a Suitable Model", *J. Construct. Steel Res.*, **15**, 1990, pp. 121-51.

145 Ahmed, B., and Nethercot, D. A., "Numerical Modelling of Composite Flush End Plate Connections", *Journal of Singapore Structural Steel Society*, **6**(1), 1995, pp. 87-102.

146 Liu, T. C. H., and Morris, L. J., "Theoretical Modelling of Steel Bolted Condition Under Fire Exposure", *Proc. of Int. Conf. on Comp. Mech.*, Vol. 1, Hong Kong, Dec. 1994.

147 Liu, T. C. H., "Finite Element Modelling of Behaviour of Steel Beams and Connections in Fire", *J. Construct. Steel Res.*, **35**(3), 1996, pp. 181-199.

148 Liu, T. C. H., and Morris, L. J., "The Development of A Shear Hinge and the Effect on Connection Flexibility", *Proc. Asian Pacific Conf Comp. Mech.*, Vol. 1, Hong Kong, Dec. 1991.

149 Liu, T. C. H., "Effect of Connection Flexibility on Fire Resistance of Steel Beams", *J. Construct. Steel Res.*, **45**(1), 1998, pp. 99-118.

150 Liu, T. C. H., "Three-Dimensional Modelling of Steel/Concrete Composite Connection Behaviour in Fire", *J. of Construct. Steel Res.*, **45**(1-3), 1998, paper No. 361.

151 Liu, T. C. H., *Personal Correspondence*, 1999.

152 El-Houssieny, O. M., Abdel Salam, S., Attia, G. A. M., and Saad, A. M., "Behavior of Extended End Plate Connections at High Temperature", *J. Construct. Steel Res.*, **45**(1-3), 1998, paper No. 172.

153 Moore, D. B., and Lennon, T., "Fire Engineering Design of Steel Structures", *Progress in Structural Engineering and Materials*, **1**(1), 1997, pp. 4-9.

154 Bailey, C. G., Lennon, T., and Moore, D. B., "The Behaviour of Full-scale Steel-Framed Buildings Subjected to Compartment Fires", *The Structural Engineer*, **77**(8), April 1999, pp.15-21.

155 El-Zanaty, M. H., and Murray, D. W., "Non-Linear Finite Element Analysis of Steel Frames" *J. Struct. Div.*, ASCE, **109**(ST2), 1983, pp. 353-368.

156 Saab, H. A., "*Non-Linear Finite Element Analysis of Steel Frames in Fire Conditions*", Ph.D. Thesis, Department of Civil and Structural Engineering, University of Sheffield, 1990.

157 Najjar, S. R., "*Three-Dimensional Analysis of Steel Frames and Sub-frames in Fire"*, Ph.D. Thesis, Department of Civil and Structural Engineering, University of Sheffield, 1994.

158 Bailey, C. G., Burgess, I. W., and Plank, R. J., "Computer Simulation of a Full-scale Structural Fire Test", *The Structural Engineer*, **74**(6), 1996, pp.93-100.

159 Bailey, C. G., Burgess, I. W., and Plank, R. J., "Analyses of the Cooling and Fire Spread on Steel-Framed Buildings", *Fire Safety Journal*, **26**, 1996, pp. 273-293.

160 Haung, Z., Burgess, I. W., and Plank, R. J. "Finite Element Modelling of Composite Frame Behaviour Subjected to Fire", *Proc. 2nd European Conference on Steel Structures (EUROSTEEL99)*, Prague, May 26 – 29 1999, pp. 611–614.

161 El-Rimawi, J. A., Burgess, I. W., and Plank, R. J., *"Modelling the Behaviour of Steel Frames and Sub-frames with Semi-Rigid Connections in Fire"*, Research Report DCSE/93/S/02, Department of Civil and Structural Engineering, University of Sheffield, April 1993.

162 Al-Jabri, K. S., Burgess, I. W., and Plank, R. J., *"Material and Geometrical Properties for Elevated-Temperature Beam-Column Connection Tests"*, Research Report DCSE/98/F/5, Nov. 1998, Department of Civil and Structural Engineering, University of Sheffield, UK.

163 Xiao, R. *"Behaviour of Connections in Steel and Concrete"*, PhD Thesis, University of Nottingham, UK, 1994.

164 O'conner, M. A., and Martin, M. D., "Behaviour of a Multi-storey Steel Framed Building subjected to Fire Attack" *J. Construct. Steel Res.* **46**(1-3), 1998, Paper No. 169.

165 Rose, P. S., Bailey, C. G., Burgess, I. W., and Plank, R. J., "The Influence of Floor Slabs on the Structural Performance of the Cardington Frame in Fire", *J. Construct. Steel Res.*, **40**(1-3), 1998, paper No. 181.

166 Al-Jabri, K. S., Burgess, I. W., and Plank, R. J., "Postulation of the Elevated-Temperature Moment-Rotation Characteristics of the Connections within the Cardington Frame", Research Report, Department of Civil and Structural Engineering, University of Sheffield, Dec. 1999.

167 Lennon, T.," *Cardington Fire Tests Survey of Damage to the Eight Storey Building"*, BRE Internal Report GD1286/86, July 1997.

168 Bailey, C. G., "Enhancement of Fire Resistance of Beams by Beam-to-Column Connections", *New Steel Construction*, **4**(44), 1998.

169 Benussi, F., Nethercot, D. A., and Zandonni, R., "Experimental Behaviour of Semi-Rigid Connections in Frames", *Connections in Steel Structures III: Behaviour, Strength and Design, Proc. of 3rd International Workshop*, Italy, 1995, pp. 57-66.

170 Li, T. Q., Nethercot, D. A. and Choo, B. S., "Behaviour of Flush End Plate Composite Connections with Unbalanced Moment and Variable Shear/Moment Rotations: Part 1: Experimental Behaviour", *J. Construct. Steel Res.*, **38**(2), 1996, pp. 125-164.

171 Xiao, Y., Choo, B. S. and Nethercot, D. A.: Composite Connections in Steel and Concrete. I. Experimental Behaviour of Composite Beam-Column Connections, *J. Construct. Steel Res.*, **31**, 1994, pp. 3-30.

172 Wales, M. W., and Rossow, E. C., "Coupled Moment-Axial Force Behaviour in Bolted Joints", *J. Struct. Engng., ASCE*, **109**(5), 1983, pp. 1250-66.

173 Laurie Kennedy, D. J., and Hafez, M. A., "A Study of End-Plate Connections for Steel Beams", *Can. J. Civ. Eng.*, **11**, 1984.

174 Chielowiec, M., and Richard, R. M., "*Moment Rotation Curves for Partially Restrained Steel Connections*", Report to AISC, University of Arizona, 1987, pp.127.

175 Tschemmernegg, F., "On the Non-Linear Behaviour of Joints in Steel Frames", *Connections in Steel Structures: Behaviour, Strength and Design*, Ed. R. Bjorhovde *et. al.*, Elsevier Applied Science Publishers, 1988, pp. 158-65.

176 Madas, P. J., *"Advanced Modelling of Composite Frames Subject to Earthquake Loading*", Ph.D. Thesis, Imperial College, University of London, July 1993.

177 Tschemmernegg, F., "A New Spring Model for Composite Joints", *Proc. COST C1 Workshop*, Strasbourg, 1992, pp. 356-368.

178 Anderson, D., and Tahir, M., M., "Economic Comparison Between Simple and Partial-Strength Design of Braced Steel Frames", *Connection in Steel Structures III: Behaviour, Strength and Design*, Ed. Bjorhovde, R., 1995, pp. 527-533.

179 Bravery, P. N. R. *"Cardington Large Building Facility: Construction Details for the First Building"*, Building Research Establishment, 1994.

180 "Semi-rigid Behaviour of Civil Engineering Structural Connections", *Composite Steel-Concrete Joints in Braced Frames for Buildings (Cost C1)*, Ed. Anderson, D., Luxembourg, 1996, pp. 3.16-3.23.

181 Jaramillo, T. J., "Deflections and Moments due to a Concentrated Load on a Cantilever Plate of Infinite Length", *Journal of Applied Mechanics, ASME*, **17**(1), 1950, pp. 67-72.

182 Ren, P., and Crisinel, M., "Prediction Method for Moment-Rotation Behaviour of Composite Beam to Steel Column Connection", In *Connections in Steel Structures III: Behaviour, Strength and Design*, Ed. Bjorhovde, R. *et al.*, Proc. of 3rd International Workshop, Trento University, Italy, 29-31 May 1995, pp. 33-46.

183 *"EC3, Design of Steel Structures, Part 1: General Rules and Rules for Building"*, Edited Draft, Issue 5, Nov. 1990.

184 Agerskov, H., "High Strength Bolted Connections Subject to Prying", *J. Struct. Div., ASCE*, **102** ST1, 1976, pp.161-175.

185 Yee, Y. L., and Melchers, R. E., "Moment-Rotation Curves for Bolted Connections", *J. Struct. Engrg.*, ASCE **112**(3), 1986, pp. 615-635.

186 Xiao, Y., Choo, B. S., and Nethercot, D. A., "Composite Connections in Steel and Concrete, Part 2 – Moment Capacity of End Plate Beam to Column Connections", *J. Construct. Steel Res.*, **37**(1), 1996, pp. 63-90.

187 Ahmed, B., Li, T. Q., and Nethercot, D. A., "Design of Finplate and Angle Cleated Connections", *J. Construct. Steel Res.*, **41**(1), 1997, pp. 1-29.

188 Walker, A. C., "The Post Buckling Behaviour of Simply-Supported Square Plates", The *Aeronautical Quarterly*, Vol. **XX**, 1969, pp. 203-222.

189 Aribert, J. M., and Lachel A., "Experimental investigation of Composite Connections in Global Interpretation." *Proc. of COST C1 Conference on Semi-rigid Joints,* Strasbourg, France, 1992, pp. 158-169.

190 Anderson, D., and Najafi, A. A., "Performance of Composite Connections: Major Axis End-Plate Joints", *J. Construct. Steel Res.*, **31**(1), 1994, pp. 31-57.

191 Ahmed B., and Nethercot, D. A., "Prediction of Initial Stiffness and Available Rotation Capacity of Major Axis Composite Flush End-plate Connections", *J. Construct. Steel Res.*, **41**(1), 1997, pp. 31-60.

192 Chapman, J. C., "Experiments on Composite Beams", *The Structural Engineer*, **42**(11), 1964, pp. 369-383.

193 Mottram, J. T., and Johnson, R. P., "Push Tests on Studs Welded Through Profiled Steel Sheeting", *Struct. Engr.*, **68**(10), 1990, pp. 187-93.

194 Lloyd, R. M., and Wright, H. D., "Shear Connection Between Composite Slabs and Steel Beams", *J. Construct. Steel Res.*, **15**, 1990, pp. 255-285.

195 Mistakidis, E. S., Thomopolos, K. T., Avdelas, A., and Panagiotopoulos, P. D., "Analysis of Composite Beams with Shear Connectors Allowing for Softening", *Steel Structures-Eurosteel '95*, ed. Kounadis, Balkema, Rotterdam, 1995, pp. 73-80.

APPENDIX A. MATERIAL PROPERTIES

A series of coupon tests was carried out to determine material properties for the steel members, reinforcing mesh and concrete at ambient temperature which were used in the series of bare steel and composite elevated-temperature beam-to-column connection tests. Coupon tests can provide very useful information when comparing the recorded material properties with the specified ones and for use in the validation of numerical modelling of structural behaviour. Two representative tensile coupons for the web and flange were tested for each of the member sizes. From these tests the modulus of elasticity and the yield and ultimate strengths of steel sections were determined. A summary of the results is presented in Tables A.1 and A.2.

Three specimens were cut from the A142 reinforcing mesh used in the composite connection tests in order to assess the actual material properties of the reinforcing bars and the results are shown in Table A.3. Compressive cube tests and tensile splitting tests were conducted in order to assess the strength of the lightweight concrete utilised in Group 4 and 5 tests. Results are tabulated in Tables A.4 to A.6.

Further detailed discussion and data concerning determination of material and geometrical properties of sections used in the beam-to-column connection fire tests may be found elsewhere[98,162].

Table A.1: Modulus of Elasticity (E) Values

Specimen Size:	***Web (kN/mm^2):***	***Flange (kN/mm^2):***
254x102UB	197.3	203.5
152x152UC	191.4	197.3
356x171UB	199.3	198.5
254x254UC	189.3	202.9
305x305UC	187.4	194.4
Av.	***196.1***	

Table A.2: Summary of Recorded Material Properties for Structural Steel

Specimen:	*Part:*	*A (mm^2):*	*σ_y (N/mm^2):*	*σ_{ult} (N/mm^2):*	*L_o (mm):*	*ΔL: (%):*
254x102UB22	Web	20x5.94	324	457	200	24.5
	Flange	20x6.58	310	448	200	26.7
	Av.	***125.2***	***317***	***452.5***	***200***	***25.6***
152x152UC23	Web	19.97x5.45	331	453	200	25.1
	Flange	19.95x6.38	321	458	200	25.5
	Av.	***118.06***	***326***	***455.5***	***200***	***25.3***
356x171UB51	Web	20.05x7.22	414	544	200	22.0
	Flange	25.03x11.98	417	560	80	28.9
	Av.	222.31	415.5	552	140	25.4
254x254UC89	Web	25x10.08	429	574	80	30.6
	Flange	40x16.23	423	572	200	24.9
	Av.	***450.6***	***426***	***573***	***140***	***27.7***
305x305UC137	Web	39.98x13.74	404	512	200	26.8
	Flange	39.95x20.11	386	506	200	29.7
	Av.	***676.36***	***395***	***509***	***200***	***28.2***

Table A.3: Summary of the Recorded Reinforcing Bars Properties

Specimen:	*A (mm^2):*	*σ_y (N/mm^2):*	*σ_{ult} (N/mm^2)*	*L_o (mm):*	*ΔL (%):*
No. 1	28.90	488	552	30	20.7
No. 2	28.65	489	555	30	19.4
No. 3	28.90	484	551	30	20.7
Av.	***28.82***	***487***	***552.67***	***30***	***20.27***

Table A.4: Summary of Recorded Concrete Compressive Material Properties for Group 4 Tests

Age at Test:	*Saturated Mass (g):*	*Density (kg/m^3):*	*Max. Load at Failure(kN):*	*Compressive Strength (N/mm^2):*
28 days (sat)	2082	2080	627.5	63.0
	2081	2080	636.0	63.5
	2084	2080	628.4	63.0
Av.	***2082.3***	***2082***	***630.63***	***63.17***
45 days (moist) FLC41	2071	2070	633.4	63.5
	2092	2080	614.6	61.5
	2073	2070	622.8	62.5
Av.	***2078.7***	***2073.3***	***623.6***	***62.5***
49 days (moist) FLC42	2089	2080	632.3	63.0
	2078	2060	628.1	63.0
	2075	2080	607.9	61.0
Av.	***2080.7***	***2073.3***	***622.8***	***62.3***
51 days (moist) FLC43	2080	2080	637.4	63.5
	2072	2070	628.6	63.0
	2070	2070	628.2	63.0
Av.	***2074***	***2073.3***	***631.4***	***63.2***
53 days (moist) FLC44	2077.3	2080	606.2	60.5
	2077.6	2080	607.4	60.5
	2078	2080	595.8	59.5
Av.	***2077.9***	***2080***	***603.1***	***60.2***
59 days (moist) FLC45 Amb.	2081	2080	618.9	62.0
	2080	2080	628.4	63.0
	2084	2080	621.4	62.0
Av.	***2081.7***	***2080***	***622.9***	***62.3***

Table A.5: Summary of Recorded Concrete Compressive Material Properties for Group 5 Tests

Age at Test:	*Saturated Mass (g):*	*Density (kg/m^3):*	*Max. Load at Failure(kN):*	*Compressive Strength (N/mm^2):*
21 days (moist) FLC51	1907	1910	476.6	47.5
	1919	1910	457.8	46.0
	1910	1910	453.7	45.5
Av.	*1912*	*1910*	*462.7*	***46.3***
23 days (moist) FLC52	1923	1910	462.9	46.5
	1929	1910	464.1	46.5
	1917	1910	473.5	47.5
Av.	*1923*	*1910*	*466.8*	***46.8***
25 days (moist) FLC53	1914	1910	464.6	46.5
	1918	1920	469.1	47.0
	1908	1910	466.9	46.5
Av.	*1913.3*	*1913.3*	*466.9*	***46.7***
28 days (sat.)	1954	1940	503.6	50.5
	1958	1940	510.5	51.0
	1954	1930	494.1	49.5
Av.	*1955.3*	*1936.7*	*502.7*	***50.3***
30 days (moist) FLC54	1914	1900	493.4	49.5
	1907	1910	479.8	48.0
	1912	1910	498.9	50.0
Av.	*1911*	*1906.7*	*490.7*	***49.2***

Table A.6: Summary of Recorded Concrete Tensile Splitting Properties for Group 4 Tests

Age at Test:	*Saturated Mass (g):*	*Density (kg/m^3):*	*Max. Load at Failure(kN):*	*Tensile Strength (N/mm^2):*
28 days(sat.)	3263.8	2080	127.8	4.05
	3287.9	2080	132.0	4.20
	3272.9	2080	114.9	3.65
Av.	***3274.9***	***2080***	***124.9***	***3.97***

APPENDIX B. TEMPERATURE DEPENDENT PARAMETERS

Table B.1: Temperature-Dependent Parameters for the Flush End-plate Bare-Steel Connections Tested

Temperature (℃):	*Group 1:*			*Group 2:*		
	A:	*B:*	*N:*	*A:*	*B:*	*n:*
20	8.000	5.55	4.800	21.500	27.500	4.900
100	6.800	5.385	4.800	15.000	27.300	4.900
200	6.150	5.150	4.800	13.000	27.000	4.900
300	4.500	4.665	4.800	10.000	26.800	4.900
400	3.225	4.486	4.800	8.325	25.500	4.900
500	1.875	3.668	4.800	5.000	18.650	4.900
600	0.885	2.000	4.800	2.500	10.200	4.900
700	0.118	1.350	4.800	-	-	-

Table B.2: Temperature-Dependent Parameters for the Flexible End-plate Bare-Steel Connection Tested

Temperature (℃):	*Group 3:*		
	A:	*B:*	*n:*
20	12.000	11.874	6.800
100	12.000	11.874	6.800
200	10.500	11.395	6.800
300	7.800	11.200	6.800
400	4.700	11.100	6.800
500	1.500	11.00	6.800

Table B.3: Temperature-Dependent Parameters for the Flexible End-plate Composite Connection Tested (Group 4)

Temperature (℃):	*Stage 1:*			*Stage 2:*				
	A:	*B:*	*n:*	ϕ_1*:*	M_1*:*	*A:*	*B:*	*n:*
20	24.5	26.1	9.000	64.70	68.7	1.550	27.100	40
100	24.5	26.1	9.000	64.70	68.7	1.550	27.100	40
200	22.0	24.7	8.825	65.51	66.5	1.520	26.267	40
300	20.0	22.0	8.450	66.52	62.0	1.520	27.600	40
400	18.0	18.1	7.34	68.63	59.9	1.48	26.951	40
500	16.0	13.0	5.885	70.03	58.0	1.38	25.365	40
600	15.0	10.319	5.885	73.52	46.5	0.500	12.35	40

Table B.4: Temperature-Dependent Parameters for the Flexible End-plate Composite Connection Tested (Group 5)

Temperature (℃):	*Group 5:*		
	A:	*B:*	*n:*
20	25.000	82.00	9.500
100	25.000	79.00	9.500
200	25.000	76.00	9.500
300	21.200	73.00	9.500
400	17.500	65.00	9.500
500	13.500	55.65	9.500
600	5.900	44.60	9.500

APPENDIX C DETERMINATION OF EFFECTIVE LENGTH l_{eff} FOR COLUMN FLANGE

In EC3: Part 1.1 the ultimate capacity of plate is calculated on the basis of assumed yield line patterns providing an upper bound estimation. The accuracy of the solution depends on the assumed yield line patterns. An acceptable prediction of the actual capacity is normally obtained when a small number of suitable yield-line patterns are used. It is suggested that yield-line patterns should consider the bolt row acting in isolation and in combination. The capacity of a bolt row $P_{cft.n}$, may be obtained assuming the column flange to act as an equivalent T-stub of l_{eff}:

$$P_{cft.n} = \frac{4M_{pt}}{m} \qquad \text{C.1}$$

where,

M_{pt} = the plastic moment capacity of an equivalent T-stub;

m = the distance the bolt centre to 20% into the column root radius

$$M_{pt} = \frac{l_{eff} t_{cf}^2 f_{ycft}}{4} \qquad \text{C.2}$$

t_{cf} = column flange thickness;

f_{ycft} = the yield strength of the column flange at a given temperature

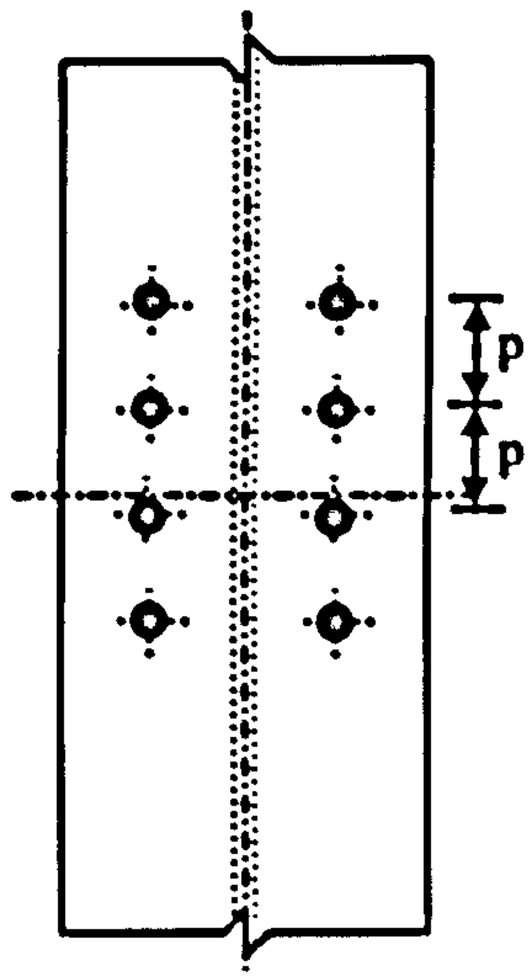

Figure C.1: Typical Column Flange

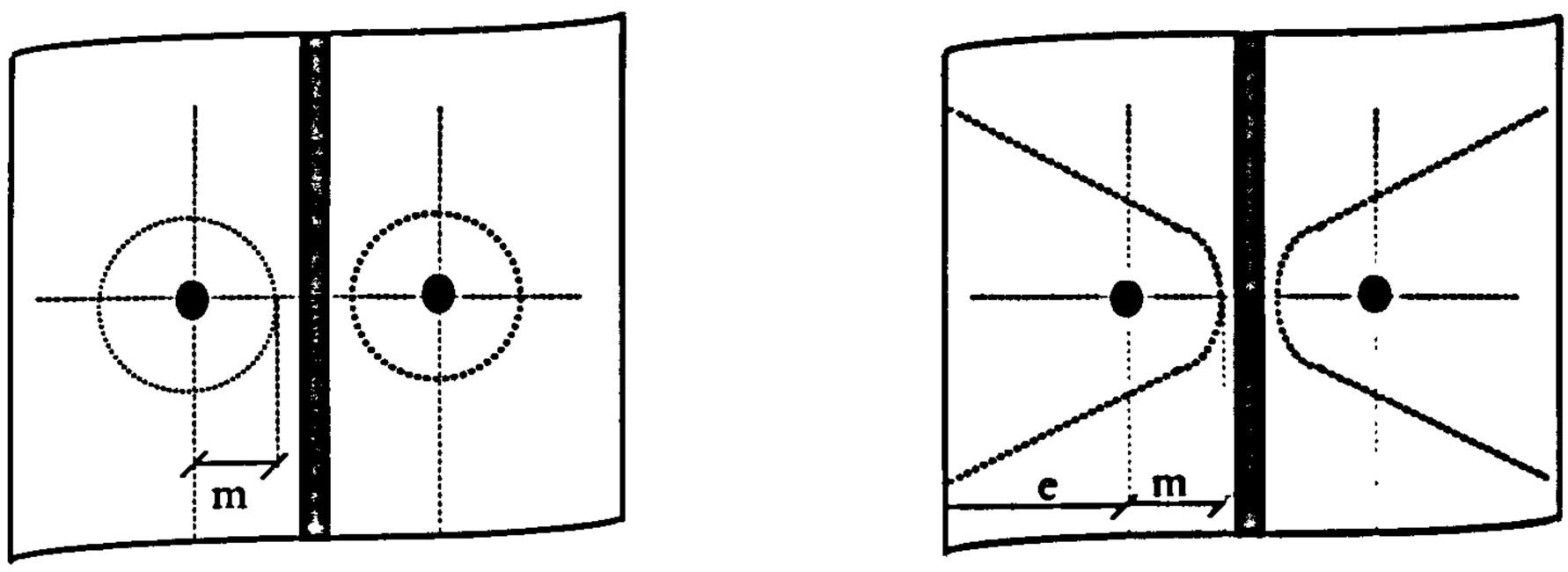

Pattern (i)
Circular yielding
$l_{eff} = 2\pi m$

Pattern (ii)
Side yielding
$l_{eff} = 4m + 1.25e$

Figure C.2: Assumed Yield Line Patterns for Column Flanges in isolation

In the case of bolts acting in isolation, the yield-line patterns shown in Fig. C.2 are assumed based on the standard patterns of circular and side yielding. The effective length should be taken as the minimum of patterns (*i*) and (*ii*). The effective yield line based on failure of a group of bolts acting in combination may be similarly assessed, where typical assumed yield line patterns are illustrated in Fig. C.3, the effective length being the minimum of patterns (*iii*) and (*iv*). It should be noted that each row may

firstly be considered in isolation, and then in combination with successive rows above, so as to ascertain the critical arrangement of yield lines:

$$P_{cft,1} = capacity\ of\ row\ 1\ alone;$$

$$P_{cft,2} = Min.\ of \begin{bmatrix} capacity\ of\ row\ 2\ alone \\ (capacity\ of\ rows\ 2+1) - P_{cft,1} \end{bmatrix}$$

$$P_{cft,3} = Min.\ of \begin{bmatrix} capacity\ of\ row\ 3\ alone \\ (capacity\ of\ rows\ 3+2) - P_{cft,2} \\ (capacity\ of\ rows\ 3+2+1) - P_{cft,2} - P_{cft,1} \end{bmatrix}$$

and so forth.....

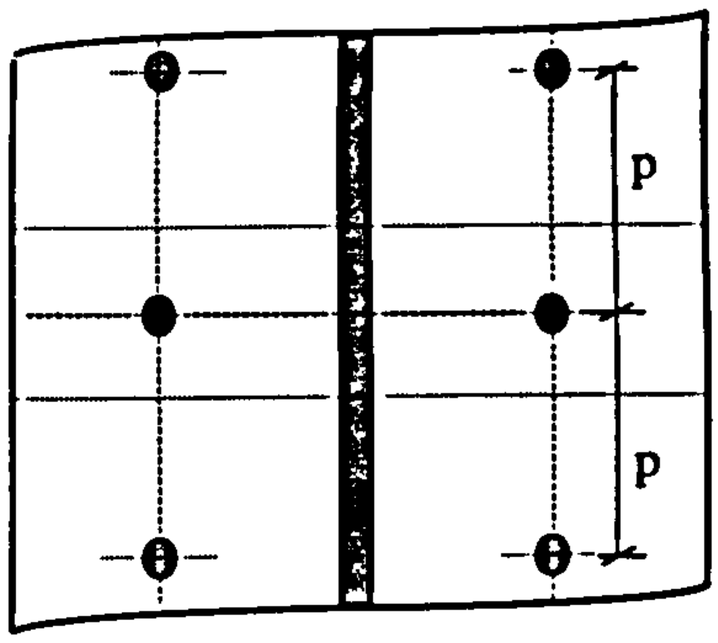

Pattern (iii)
Intermediate row
$l_{eff} = p$

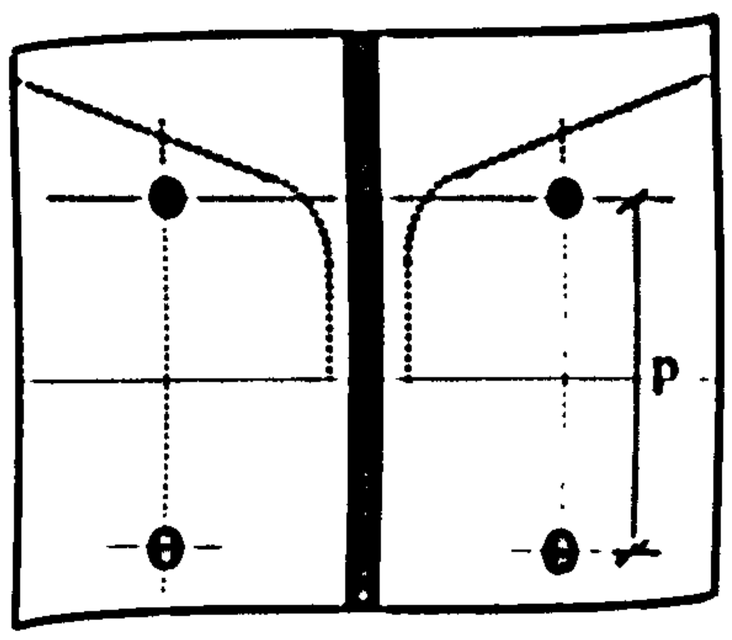

Pattern (iv)
Top and bottom row of a group along a clear length
$l_{eff} = 2m + 0.625e + 0.5p$

Figure C.3: Assumed Yield Line Patterns for Column Flanges Acting in Combination